U.S. DEPARTMENT OF COMMERCE
National Technical Information Service
PB-298 771

Self-Synchronous Propulsion System for Rapid Transit Railcars - Advanced Subsystem Development Program Volume II: Detailed Technical Discussion

General Motors Corp., Goleta, CA. Delco Electronics Div.

Prepared for

Urban Mass Transportation Administration, Washington, DC

Feb 78

UMTA-IT-06-0026-79-2

PB 298771

R78-14
FEBRUARY 1978

ADVANCED SUBSYSTEM DEVELOPMENT PROGRAM

SELF-SYNCHRONOUS PROPULSION SYSTEM FOR RAPID TRANSIT RAILCARS

FINAL PROJECT REPORT

Volume II - Detailed Technical Discussion

Prepared for
The BOEING VERTOL COMPANY
Philadelphia, PA 19142
Under P.O. No. CS 200955

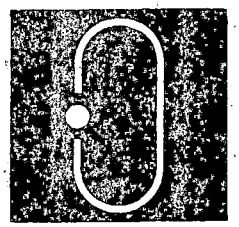

Delco Electronics

General Motors Corporation
- Santa Barbara Operations
Santa Barbara, California

Technical Report Documentation Page

1. Report No.	2. Government Accession No.	3. Recipient's Catalog No.
UMTA-IT-06-0026-79-2		PB298771

4. Title and Subtitle	5. Report Date
SELF-SYNCHRONOUS PROPULSION SYSTEM FOR RAPID TRANSIT RAILCARS - ADVANCED SUBSYSTEM DEVELOPMENT PROGRAM Volume II - Detailed Technical Discussion	February 1978
	6. Performing Organization Code
7. Author(s)	8. Performing Organization Report No. R78-14
9. Performing Organization Name and Address Delco Electronics* General Motors Corporation Santa Barbara Operations Santa Barbara, California 93102	10. Work Unit No. (TRAIS) IT-06-0026 11. Contract or Grant No. IT-06-0026
12. Sponsoring Agency Name and Address U.S. Department of Transportation Urban Mass Transportation Administration 400 Seventh Street, S.W. Washington, D. C. 20590	13. Type of Report and Period Covered Final Project Report 14. Sponsoring Agency Code UTD-30

15. Supplementary Notes *prepared for The Boeing Vertol Company, Philadelphia, PA 19142.
Volume I - Program Synopsis (UMTA-IT-06-0026-79-1) PB-298770
Volume III - Appendixes (UMTA-IT-06-0026-79-3) PB-298772

16. Abstract
Development of the Self-Synchronous Propulsion System was conducted under the Advanced Subsystem Development Program (ASDP), which is a part of the Urban Rapid Rail Vehicle and Systems (URRV&S) Program sponsored by the Urban Mass Transportation Administration. The Self-Synchronous Propulsion System was one of the advanced subsystems that had been identified during the Advanced Concept Train (ACT) proposal evaluation as showing outstanding merit, and was planned to be developed for evaluation by the Transit Authorities. The objective of the overall ASDP was to develop advanced subsystems suitable for application in existing or future transit cars. This report, Volume II, discusses the program technical effort, program scope, objectives, and background; summarizes the design and testing efforts and problem areas; contains conclusions and recommendations; discusses system functional characteristics, train performance characteristics, major component design, interfaces, and product assurance; covers developmental, major component and system level testing; contains a description of the changes made during system testing; discusses the status of the final configuration; and addresses unresolved problems. Volume I summarizes the content of Volume II, and follows essentially the same outline. Volume III contains appendix material which was considered either too bulky or too detailed to incorporate into Volume II. Appendixes A through G in Volume III are: Train Control Electronics (TCE) Flow Diagrams; Train Performance Analysis Computer Program; List of Drawings and Specifications; Diagostics Unit RAM Memory Code Identification; Diagnostics Unit Subroutine Flow Diagrams; Motor Power Supply System, U.S. Patent No.3,866,094; and Mapham Inverter and Analytic Model Description, respectively.

17. Key Words	18. Distribution Statement
tronic Vehicle Guidance; Propulsion Systems; Railcars; Rail Rapid Transit; Rapid Transit; Self-Synchronous Propulsion Systems; Train Performance; Transit Rail Cars - Propulsion Systems	Available to the public through the National Technical Information Service Springfield, Virginia 22161

19. Security Classif. (of this report)	20. Security Classif. (of this page)	22. Price
Unclassified	Unclassified	PC A18/MF A01

Form DOT F 1700.7 (8-72) Reproduction of completed page authorized

R78-14
FEBRUARY 1978

ADVANCED SUBSYSTEM DEVELOPMENT PROGRAM

SELF-SYNCHRONOUS PROPULSION SYSTEM FOR RAPID TRANSIT RAILCARS

FINAL PROJECT REPORT

Volume II - Detailed Technical Discussion

Prepared for
The BOEING VERTOL COMPANY
Philadelphia, PA 19142
Under P.O. No. CS 200955

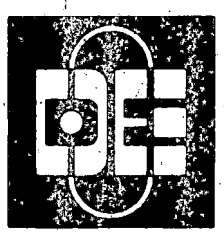

Delco Electronics

General Motors Corporation
- Santa Barbara Operations
Santa Barbara, California

PREFACE

The final documentation submitted under the ASDP Self-Synchronous Propulsion System contract consists of the following:

- Final Project Report – R78-14
  - Volume I - Program Synopsis
  - Volume II - Detailed Technical Discussion
  - Volume III - Appendixes
- Traction Motor Final Report – R78-15
  - Volume I - Technical Discussion
  - Volume II - Appendixes
- Gear Drive and Axle Coupling Final Report – R78-16
  - Volume I - Technical Discussion
  - Volume II - Appendixes
- Reliability Analysis Report – R78-17
- Safety Analysis Report – R78-18
- Maintainability Report – R78-19
- Drawing Package
- Specifications
- Miscellaneous Backup Data

The major report emanating from this program is the Final Project Report, Delco Electronics No. R78-14, which was prepared in three volumes, as shown above.

The program technical effort is discussed in detail in Volume II of this report. Contained in Volume II are the following sections:

I	Introduction	V	System Design
II	Summary	VI	Testing
III	Conclusions	VII	Developmental System-Final Status
IV	Recommendations		

Section I discusses the program scope, objectives, and background. Section II summarizes the design and testing efforts as well as problem areas uncovered. Sections III and IV contain the conclusions and recommendations respectively. Section V is a detailed discussion and description of the design including system functional characteristics, train performance characteristics, major component design, interfaces, and product assurance. Section VI covers the testing in detail, including developmental, major component and system level testing. Section VII contains a description of the changes made during system testing, the status of the final configuration, and a discussion of unresolved problems.

Volume I summarizes the contents of Volume II and follows essentially the same outline. Volume III contains appendix material which was considered either too bulky or too detailed to incorporate into Volume II. The appendixes included are as follows:

- Appendix A - Train Control Electronics (TCE) Flow Diagrams
- Appendix B - Train Performance Analysis Computer Program
- Appendix C - List of Drawings and Specifications
- Appendix D - Diagnostics Unit RAM Memory Code Identification
- Appendix E - Diagnostics Unit Subroutine Flow Diagrams.
- Appendix F - Motor Power Supply System, U. S. Patent No. 3,866,094
- Appendix G - Mapham Inverter and Analytic Model Description

This present report, Volume I of R78-14, summarizes the contents of Volume II and follows essentially the same outline.

TABLE OF CONTENTS

TABLE OF CONTENTS (continued)

TABLE OF CONTENTS (continued)

TABLE OF CONTENTS (continued)

TABLE OF CONTENTS (continued)

TABLE OF CONTENTS (continued)

TABLE OF CONTENTS (continued)

LIST OF ILLUSTRATIONS

LIST OF ILLUSTRATIONS (continued)

LIST OF ILLUSTRATIONS (continued)

LIST OF ILLUSTRATIONS (continued)

LIST OF TABLES

SECTION I
INTRODUCTION

1.1 PROGRAM SCOPE AND OBJECTIVES

The Self-Synchronous Propulsion System development was conducted under the Advanced Subsystem Development Program (ASDP) which is a part of the Urban Rapid Rail Vehicle and Systems (URRV&S) Program sponsored by the Urban Mass Transportation Administration (UMTA) and managed by the Boeing Vertol Company. The Self-Synchronous Propulsion System was one of the Advanced Subsystems that had been identified during the Advanced Concept Train (ACT-1) proposal evaluation that showed outstanding merit, and was planned to be developed for evaluation by the Transit Authorities. The objective of the overall ASDP was to develop advanced subsystems suitable for application in existing or future transit cars.

The ASDP propulsion system was planned to be incorporated into the two-car State-of-the-Art Car (SOAC) train for testing and evaluation at the Transportation Test Center (TTC) at Pueblo, Colorado. Other advanced subsystems to be evaluated concurrently with the propulsion system were an Improved Ride Quality Monomotor Truck and a Synchronous Brake System.

1.2 PROGRAM BACKGROUND

Direct current motors, primarily the series-wound type, have provided (and continue to provide) relatively good service in electric traction applications for rail transit cars. Their inherent torque-speed characteristics, excellent overload capabilities and relative insensitivity to fluctuations in line voltage make them well suited to these applications.

However, due to their disadvantages there has long been a desire by many users to replace them with commutatorless ac motors. These disadvantages include:

- Requirement for frequent inspection of commutator and brushes
- Brush replacement and commutator maintenance
- Large size and weight (low power density)
- Difficult to seal from the environment.

However, up to recently, only the dc motor was considered practical for traction applications because of the low starting torque and limited speed range of ac motors – unless controlled from a variable frequency, variable voltage source. This only became practical with the advent of high power capacity thyristors which have made possible the development of compact, reliable, and efficient static power converters.

Laboratory development conducted by Delco Electronics - Santa Barbara Operations (DE-SBO) beginning in 1972 under an in-house funded effort had indicated that an ac propulsion system based on a self-controlled synchronous motor would be well suited to transit car drive application. The lower weight and reduced size of the traction motor would permit easy integration with a monomotor truck, improving ride dynamics and eliminating slip-slide within a truck. The inherently good electrical braking capability of the synchronous machine would permit greater energy recuperation in the regenerative mode and reduces wear of the friction brakes. It was also expected that the brushless motor design and solid state controls, combined with liquid cooling, would result in higher reliability and reduced maintenance. (The features of the system which made it an attractive candidate for transit application are summarized in Table 1-I.)

In 1972 DE-SBO participated in the Phase I effort of the ACT-1 program with the LTV Corporation. As the culmination of this effort, a proposal was submitted to LTV for the ACT-1 program in late 1972. After a delay of over a year, Garrett was awarded the contract for ACT-1 in January 1974. Boeing Vertol and UMTA then started evaluating advanced subsystems from the "losing" proposals for the ASDP program (formerly ACT-2). In April 1974, Boeing Vertol issued a sole source RFP to DE-SBO for the ASDP propulsion system; a proposal was submitted in May 1974. After long delays due to funding limitations, a contract was finally awarded to DE-SBO in October 1975.

Contract-funded development effort on the propulsion system started in October 1975. The basic design and engineering effort was conducted essentially in accordance with the original schedule and within planned expenditures. PDR and CDR were successfully completed in February and June 1976, respectively. Fabrication of the Test Article to be used for system level qualification testing was started in July 1976 and completed in December 1976. During the checkout of the Test Article propulsion system, technical problems were uncovered requiring redesign and modifications, delaying the system level testing effort and resulting in significant cost overruns. By October 1977, all of the key technical problems

• Utilizes ac Synchronous Machine
– Inherent dc traction motor performance characteristics
– Brushless operation
– Low weight and compact size (1260 lb.)
– High reliability and reduced maintenance (100,000 Mile MDBF)
• Utilizes Solid State Power Converter
– Stepless control
– High efficiency (79% to 86% system efficiency)
– High reliability and reduced maintenance (100,000 Mile MDBF)
• Controlled Environment through Liquid Cooling
– Liquid cooling provides clean stable environment for motor and electric controller
• Provides Regenerative and/or Dynamic Braking
• Redundant Propulsion Systems Eliminate "Dead Car" in Service

Table 1-I. Salient Features of the Self-Synchronous Propulsion System

had been resolved except for the following:

- An inverter, cycloconverter, motor interaction problem in the motoring mode which resulted in loss of inverter SCR recovery time and inverter faulting.
- The over stressing of voltage surge protection (DSAS) devices in motoring mode at the moment of shutdown which results in ramdom DSAS failures.
- The voltage overstressing of the cycloconverter SCR's and voltage surge protection (DSAS) devices in the breaking mode at high motor speeds which results in SCR and/or DSAS failures.

Laboratory test results indicated that the propulsion system concept could be successfully developed. However, it was identified that substantial additional funds would be required to complete a full-scale engineering development. In addition, it appeared doubtful that the potential market was substantial enough to justify the additional required investment.

A decision was made in November 1977 by UMTA and Boeing Vertol to discontinue the development of the Self-Synchronous Propulsion System. It was decided to complete the development, fabrication, and delivery of all truck mounted equipment (traction motor,

gear drive, and axle coupling, etc.), but to stop the system laboratory testing of the propulsion electronics equipment after completion of "open loop" testing. The Test Article and residual material for the four planned prototype systems (partially completed) were to be delivered for final disposition by Boeing and UMTA. A comprehensive set of reports and general documentation comprise the balance of deliverables under this contract.

SECTION II
SUMMARY

2.1 DESIGN SUMMARY

2.1.1 FUNCTIONAL DESCRIPTION

In the Self-Synchronous Propulsion System the synchronous ac motor is caused to function as a commutatorless dc motor by phase-controlling its stator (armature) current by means of a rotor position sensor. This constitutes a direct analog of the dc commutator type motor, whereby a rotor position sensor, converter, and stationary armature perform the same function as the mechanical commutator and rotating armature.

A simplified functional block diagram of the propulsion system is shown in Figure 2-1. The capacitor-coupled-cycloconverter provides a current source output characteristic and a simple means of motor field excitation. This power converter, which basically consists of a high frequency inverter and cycloconverter, controls the motor current by frequency modulation of the interstage capacitive reactance. In effect, the reactance acts as a controlled lossless impedance in series with the motor terminals, and both controls motor current and provides the converter with a current source characteristic.

The machine terminal voltage has essentially a sinewave characteristic for efficient, constant flux operation. A high frequency interstage current transformer, which drives the motor field winding via the rotary transformer and rotating rectifier, provides field excitation with dc current proportional to armature current. Thus, the self-synchronous ac machine takes on the characteristics of a series dc motor.

The inverter stage of the propulsion system consists of three modified Mapham inverters which are gated to produce a three-phase output voltage over a 350 to 1,200 Hz frequency range. This sine wave series inverter provides simpler and more reliable commutation than force-commutated inverters.

The cycloconverter is an arrangement of six groups of three SCRs. At any instant of time two SCR groups, one for positive and one for negative current, are gated to form the equivalent of a full wave rectifier supplying current into one motor phase and out of another.

Brushless field excitation is provided by a rotary transformer and rotating rectifier. The primary of the rotary transformer is powered from a current transformer having primary windings in series with the cycloconverter input current. As a result, the current transformer provides motor field current proportional to armature current.

In braking, the traction motor is operated as a separately excited generator connected to phase delay controlled dynamic and regenerative brake rectifiers. Field excitation is provided by the same high frequency transformer used in motoring. Braking effort in dynamic and regenerative braking is controlled by a combination of field current control and rectifier phase control.

2.1.2 EQUIPMENT DESCRIPTION

The propulsion system provides one motor for each truck of a transit car, a separate gear drive and coupling assembly for each axle, separate power controls and cooling units, and miscellaneous equipment to interface with the car. This configuration provides redundant propulsion units whereby the car may continue to operate at a reduced performance level should one drive system become disabled (see Figure 2-2).

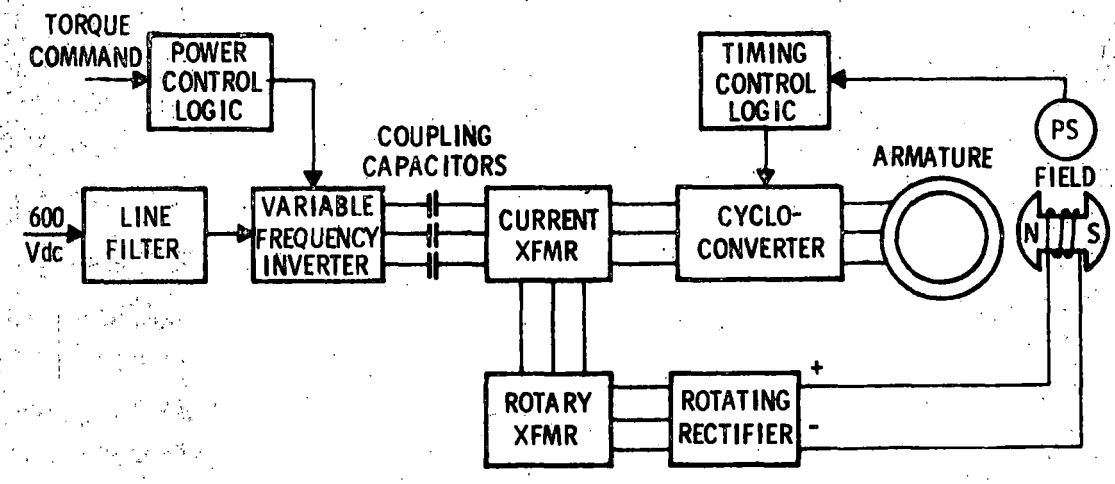

Figure 2-1. Propulsion System Functional Block Diagram

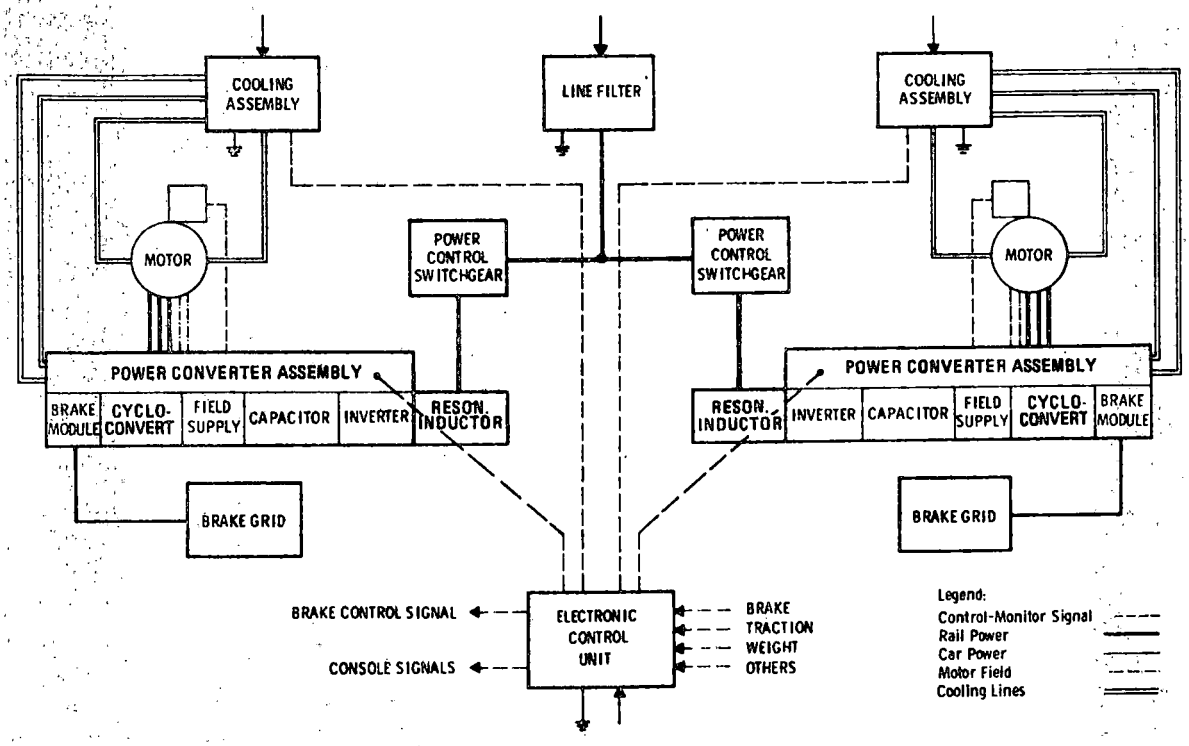

Figure 2-2. Propulsion System Block Diagram

The system obtains nominal 600 Vdc power from third rail shoes which is routed through a line filter to individual power control switchgear assemblies containing power contactors and over-current protection equipment. The filtered dc power provided to each drive system is then converted to 3-phase power by the power converter assembly to control the traction motors.

As shown in Figure 2-2, the traction motors are also connected to the brake modules of the power converter assemblies. During electrical braking, when the motor is functioning as a generator, power is directed back through the line filter for regenerative braking, or to the resistor grid for dynamic braking. A separate cooling assembly for each drive system routes liquid coolant through each traction motor and power converter. An electronic control unit containing the low level circuitry for both train control and propulsion control is mounted in the operator's cab and powered from the car battery. Diagnostic equipment is also provided for system checkout, monitoring, and fault isolation.

The overall arrangement of the propulsion system components on the SOAC car is illustrated in Figure 2-3.

The Delco propulsion system is based on the monomotor truck drive. In this drive concept, a single ac synchronous motor is used to drive both axles of one truck. With an output shaft at each end, the motor is centered longitudinally on the truck and drives each axle through a single-reduction hypoid bevel gear set designed for bi-directional service. Torque is transmitted from the gear drive output to the truck axle through a flexible coupling, which allows relative axle movements for the primary suspension motions.

As illustrated in Figure 2-4, the motor and gear drives together form a rigid assembly which, when mounted on the truck frame, significantly reduces the unsprung mass and truck mass moment of inertia. This reduces the shock loads and stresses on the motor, gears, and bearings while improving the ride characteristics. The elimination of slip-slide between the two axles of each truck provides improved traction. Use of a single drive for both axles reduces the overall complexity, maintenance, and cost of the propulsion system.

The ac traction motor is a four-pole, salient-pole self-synchronous machine designed to produce 490 hp (365 kW) from 1646 to 5642 r/min. The motor assembly, illustrated in Figure 2-5, consists of:

- A salient pole synchronous machine with a three-phase stationary armature and rotating field
- A three-phase rotating transformer and rectifier to provide dc field excitation
- A rotor position sensor to provide signals to control the switching of the commutating thyristors.

The monomotor truck drive concept depends on the use of a gear drive and coupling combination which allows play of the axle with respect to the truck mounted motor/gearbox subassembly. The gear drive and coupling shown in Figure 2-6 consists of a hollow shaft hypoid bevel gear axle drive and a flexible rubber joint cardan coupling developed by Brown-Boveri for high speed locomotives and transit cars.

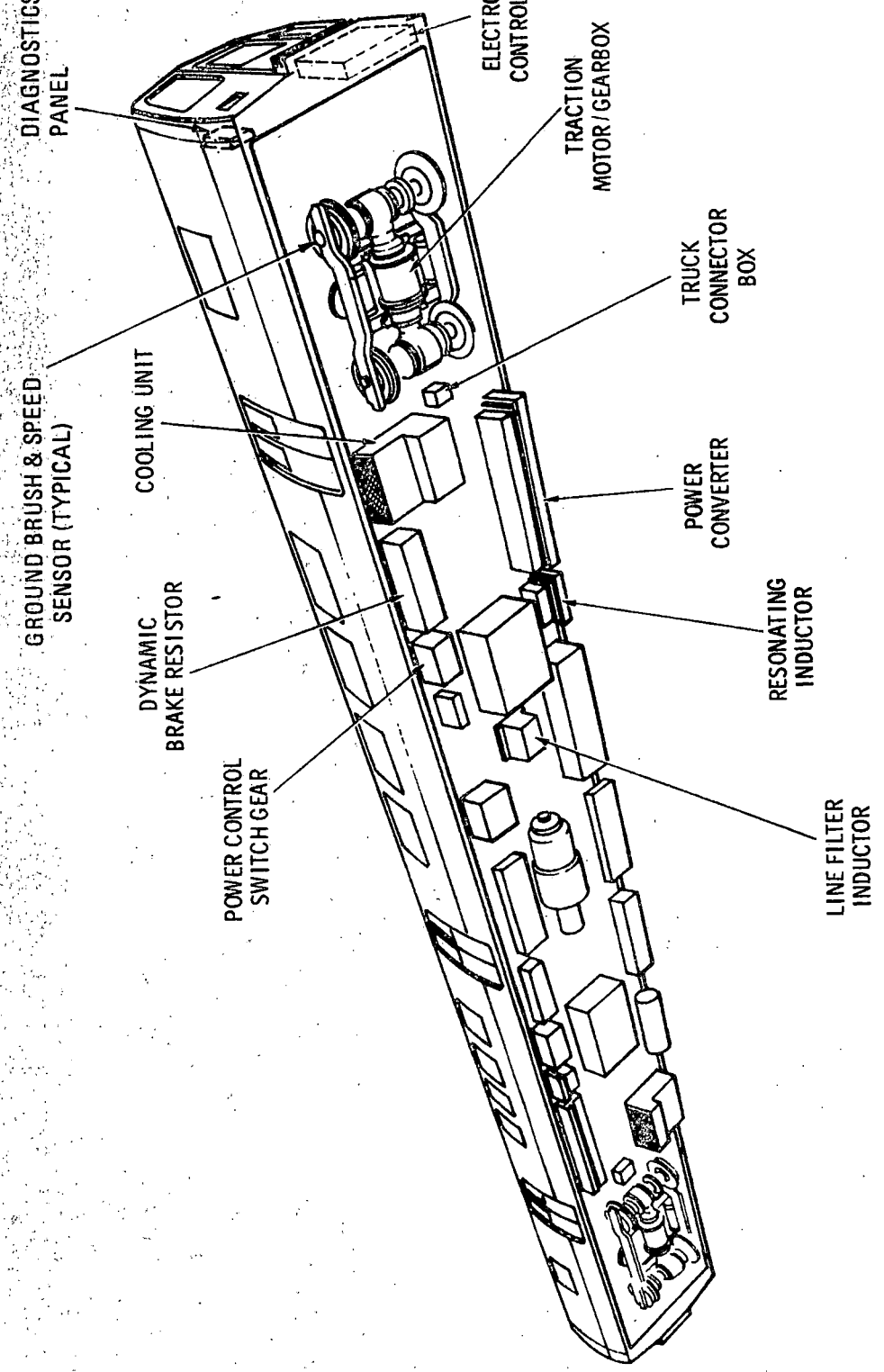

Figure 2-3. Propulsion Equipment Location

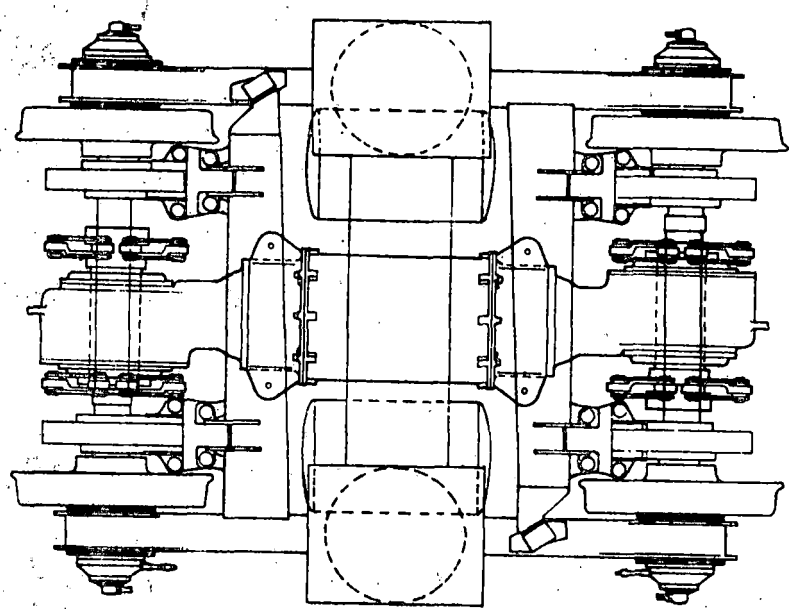

Figure 2-4. Monomotor Truck Drive

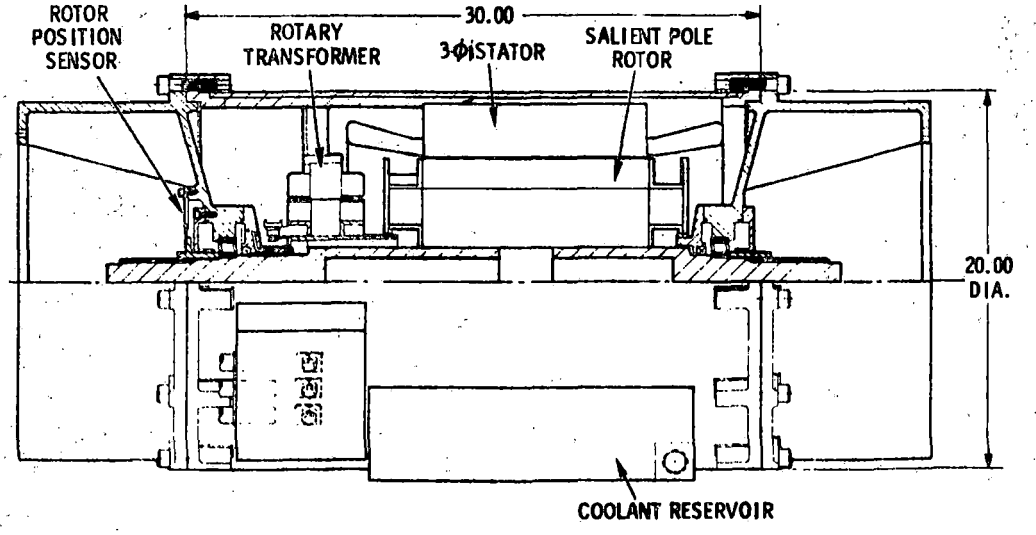

Figure 2-5. AC Traction Motor

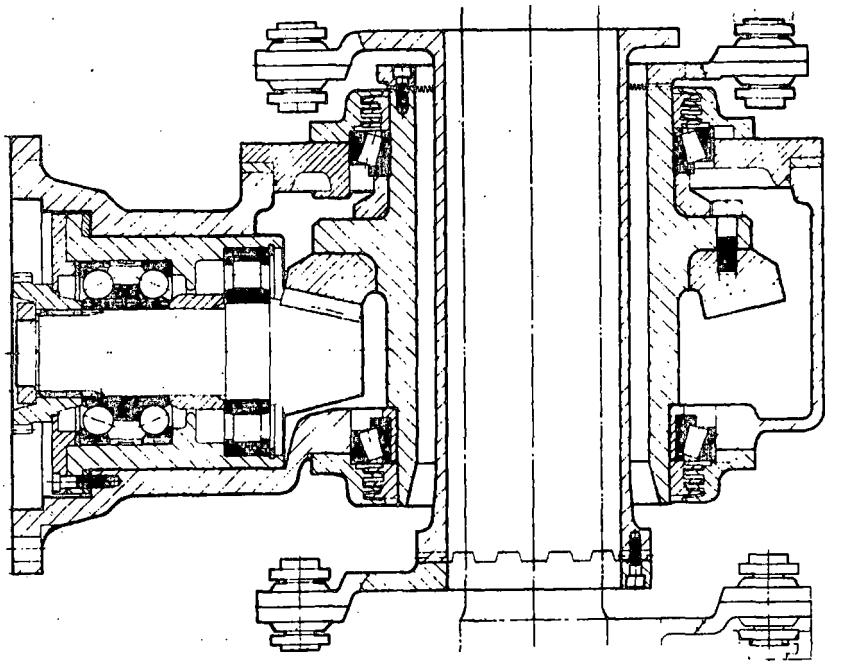

Figure 2-6. Gear Drive and Axle Coupling

The power converter assembly shown in Figure 2-7 contains the electrical power circuits and components required to control one traction motor. The assembly – consisting of a lightweight frame, slide-out modules, interconnecting cabling and coolant lines, and a hinged protective cover – is shock mounted to the car's underframe. The electrical components are packaged in replaceable subassemblies (modules) in accordance with the function they perform. The modular design employs slide-out modules and quick disconnect electrical and replacement at the subassembly level. The individual modules are sealed enclosures with liquid cooling provided for each module.

The cooling assembly contains two independent cooling loops, one for the traction motor and one for the power converter. Heat is transferred to the ambient air via fluid-to-air heat exchangers which used forced convection provided by a fan. The major components are: a two-section radiator cooled by a propeller type fan, two positive displacement pumps driven by a single motor, oil filters with replaceable filter elements, and transducers for pressure and temperature monitoring.

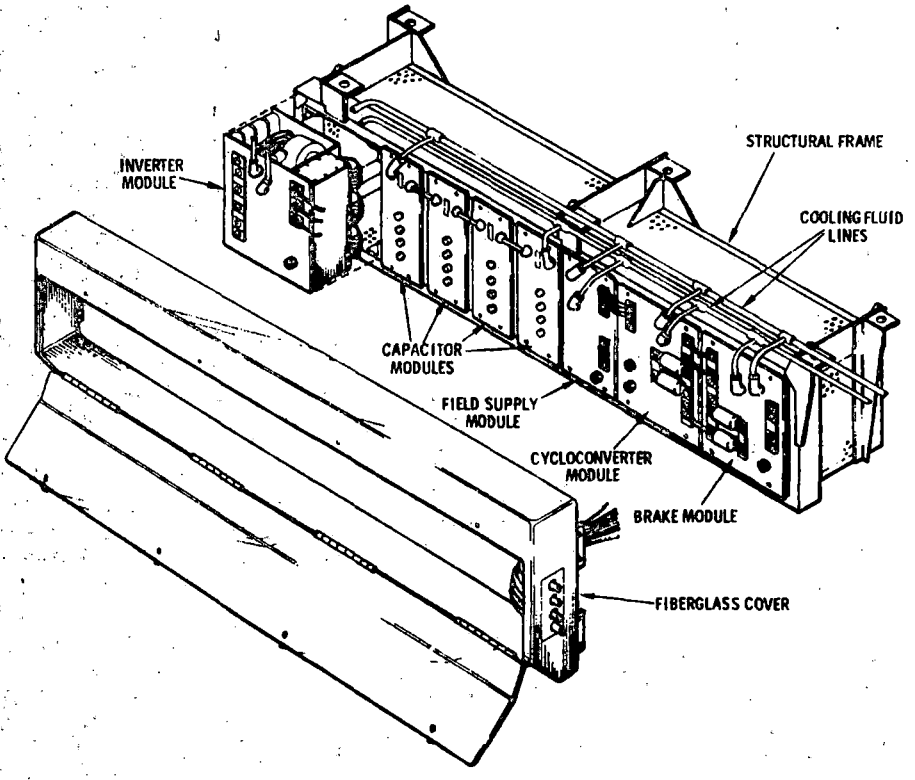

Figure 2-7. Power Converter Assembly

The remaining subassemblies not covered in this summary (line filter, power control switchgear, dynamic brake resistor, etc.) are of conventional design, similar to ones utilized in existing chopper controlled transit cars.

2.2 TESTING SUMMARY

2.2.1 DEVELOPMENTAL TESTING

Developmental tests in support of propulsion system design were conducted in the early stages of the program using breadboard test hardware from a pre-contract IR&D effort. The major development tests conducted are listed below:

- Cycloconverter gate drive development
- Brake control circuit development
- High frequency motor tests
- Cycloconverter output current capability tests
- Motor shock torque tests
- Coolant fluid testing
- Heat sink development.

The results of these early breadboard tests served as inputs to the propulsion system design to which the Test Article hardware was built.

2.2.2 MAJOR COMPONENT TESTS

These tests were conducted on the first item of each major component manufactured in order to establish its suitability for incorporation into the overall propulsion system for system level testing. A brief summary of the component level testing follows.

Power Electronics Components

All power electronics subassemblies (line filter, power control switchgear, power converter assembly, etc.) were subjected to component level checkout and verification tests. Typical tests included resistance, inductance, dielectric strength, capacitance, measurements, visual and continuity checks, and calibration. The thyristor modules were also tested for SCR and diode leakage current and voltage breakdown and the adequacy of the gate driver and dV/dt suppression circuits.

Traction Motor

Most of the traction motor testing was conducted by the supplier, Delco Products, Dayton, Ohio. The evaluation of motor performance in conjunction with the ASDP drive electronics, however, was performed at DE-SBO during system level testing.

Tests conducted at Delco Products included all routine insulation resistance, dielectric strength, resistance, no load saturation, inductance, etc., type tests. In addition, the moment of inertia was established, the overspeed capability verified, and the motor weighed. Major motor performance tests included a motoring test at 1800 rpm (60 Hz) at full power (489 hp), a test as an alternator at speeds up to 3000 rpm at full torque capability (1405 lb-ft) and thermal capability at the specified duty cycle. Based on the results obtained during these tests it was concluded that the traction motor met or exceeded all performance requirements specified in Design Verification Test Procedure T-688.

T . conducted with the motor at Delco Electronics as part of the system level testing covered both motoring and dynamic braking performance. Motoring capability was demonstrated throughout the complete torque/speed range specified. Dynamometer limitations did not allow braking tests to the full torque level at high speed. Analytical predictions made, however, projected full required braking capability for this untested area. It became apparent during

system level testing, that the axial load on the "fixed end" motor bearing exceeded the capacity of the roller bearing used. A replacement ball bearing was selected but its adequacy could not be verified prior to program termination.

Gear Drive and Axle Coupling

All performance testing on the gear drive and axle coupling was conducted by the subcontractor, Thyssen-Henschel of West Germany.

The qualification tests were conducted in two parts. The first series of tests included 27 hours of normal load tests in accordance with a simulated transit car operating profile, 100 hours of endurance test at constant speed and torque conditions, and shock torque tests at gradually increasing torque values. At the maximum specified shock torque (24,000 lb-ft), the axle coupling failed. A decision was made to redesign the failed component and requalify the complete gear drive and coupling assembly. The second series of qualification tests consisted of approximately 30 hours of endurance tests in accordance with a simulated operating profile, high speed tests up to the maximum overspeed requirements and shock torque tests up to the maximum axle shock torque specified.

On the basis of these tests, it was concluded that the Gear Drive and Axle Coupling satisfies the requirements of the specification and that it is suitable for incorporation into the ASDP cars.

2.2.3 SYSTEM LEVEL TESTS

System level tests were conducted using Test Article hardware representing one propulsion system of a transit car. Tests were performed on two different dynamometers. Due to their specific capabilities and limitations, one was used for low torque operation over the entire speed range; the other for high torque tests at speeds up to 2000 rpm. All system level testing was performed in an "open loop" mode of operation without the Train Control Electronics.

Motoring Tests

The motoring performance tests summarized here are based on the final sets of data taken after several circuit design changes were incorporated.

Figure 2-8 is a composite of test data taken in the two dynamometer laboratories. Comparing the data points obtained with the specification requirements (solid line) it can be seen that the power/torque/speed performance has been fully demonstrated. Overall system efficiency (from dc input to motor shaft output) ranged from 79.3% to 87.2% over the 1000 to 6000 RPM speed range. This compares favorably with the predicted values of 79% to 86% for the same speed range (proposal estimate).

Braking Tests

Dynamic braking tests were also conducted in an "open loop" mode of operation using two separate dynamometers. Here again only the final sets of test results are summarized. Figure 2-9 shows a composite set of test data taken in the two laboratories. The points plotted are the highest torque points tested, but they do not represent the maximum capability of the system. The absence of data in the high torque, high speed region of the plot was due to dynamometer limitations. Analysis and extrapolation of the data indicates that essentially the full braking torque specified for the system can be realized in the dyamic braking mode throughout the required speed range with additional circuitry changes and higher voltage SCRs.

2.3 MANUFACTURING SUMMARY

Fabrication of the Test Article hardware started in July 1976 immediately after completion of the Critical Design Review. In order to meet the prototype system delivery date of April 1977, fabrication of the four (4) production units had to be released essentially simultaneously with the Test Article. Based on the extensive development effort carried out both prior to and during the early stages of the ASDP program (as discussed in subsection 6.1) it had been assumed that the risk in releasing the production units for manufacturing prior to completion of system level testing with the Test Article was acceptable.

Due to the problems experienced during system integration and checkout of the Test Article it became apparent, however, that significant redesign and modification would be required. The fabrication of the production hardware was stopped at this time, pending solution of the technical problems uncovered during system level testing. The status of the production hardware at the time of this stop order is shown in Table 2-I.

2.4 PROBLEM AREAS

A series of problems frustrated initial attempts to operate and test the TA hardware at the system level. Some of these problems involved the motor and some involved the

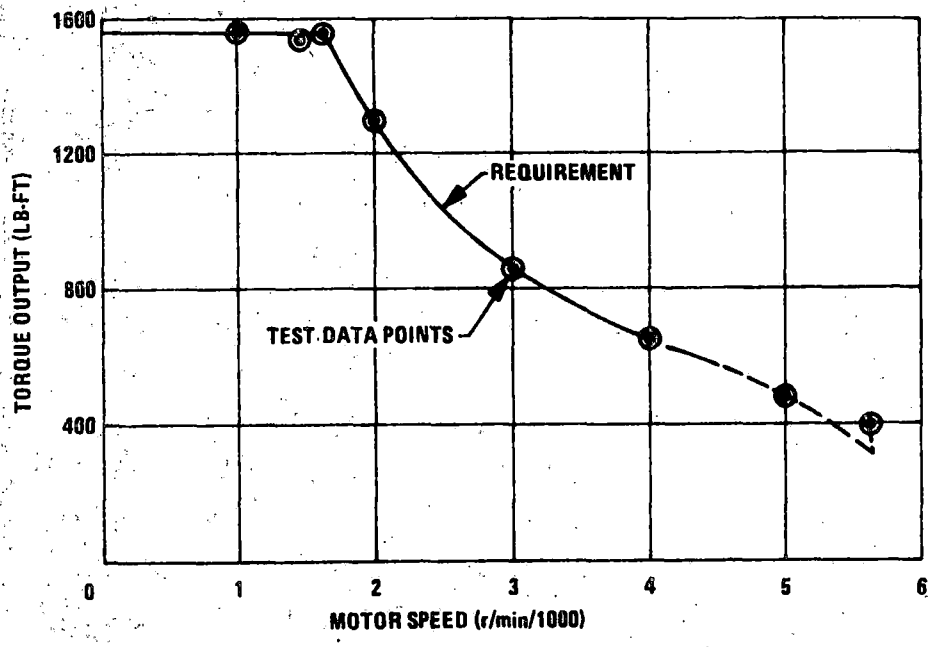

Figure 2-8. ASDP Propulsion System Motoring Performance

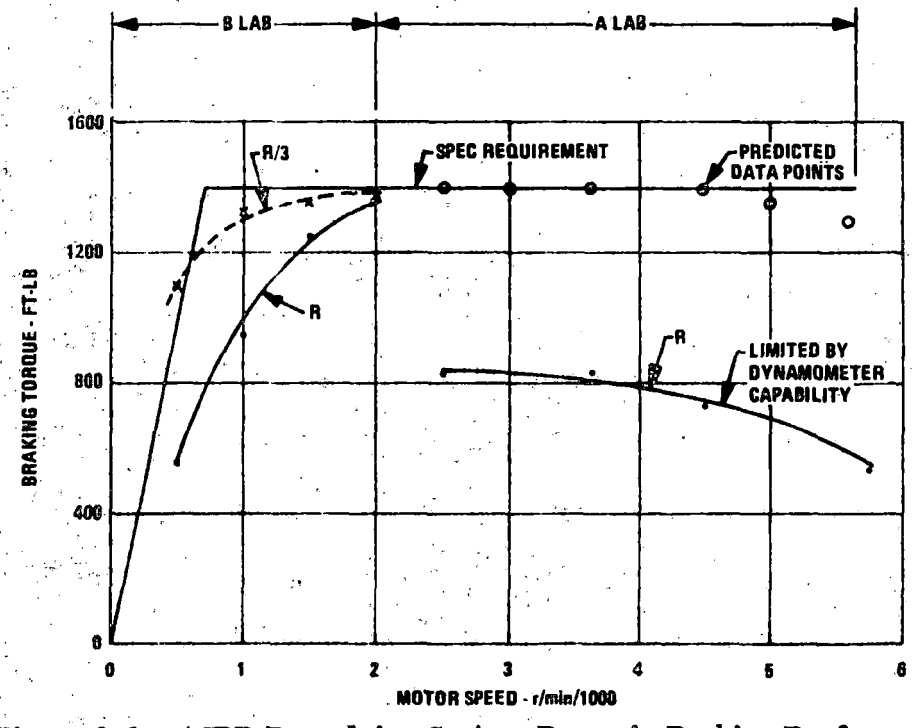

Figure 2-9. ASDP Propulsion System Dynamic Braking Performance

TYPE	STATUS	QUANTITY
Purchased Parts	Parts released	918
	Parts on order	162
	Parts received	756
Fabricated Parts	Parts released	340
	In process	112
	Painting and Plating	24
	Parts complete	204

Table 2-I. Production Hardware Status

power conversion and control electronics. To define, understand, and resolve these problems, a series of developmental investigations were undertaken.

The problems involving the motor are briefly as follows:

1. There was inadequate energy dissipation capacity in a voltage surge protection circuit intended to protect the motor field winding. This resulted in Zener diode failures.
2. The bearing seals were defective resulting in contamination of the bearing lubricant by coolant fluid.
3. The axial load on the "fixed end" motor bearing exceeded the capacity of the roller bearing used in the original design.

Modification or fixes were developed for all the motor problems except the bearing problem where the solution was to replace the roller bearing with a ball bearing. A replacement bearing was selected (SKF 6213 VAG) and will be incorporated into all deliverable motors. However, no further laboratory testing will be conducted to verify bearing suitability.

Of the major problems found in the power conversion and control electronics, some primarily affected motoring mode operation and some affected braking mode operation.

Those problems primarily affecting motoring mode operation were as follows:

1. The rise time and amplitude of the SCR gate drive for the cycloconverter, inverter and brake control modules was inadequate. This contributed to SCR failures.

2. The timing control of the SCR gate drive for the cycloconverter was inadequate. This also contributed to SCR failures.
3. There was an interaction between the inverter, cycloconverter, and motor. This resulted in insufficient inverter SCR recovery time which in turn caused inverter faulting.
4. The energy dissipation capacity of the surge protection circuit for the cycloconverter SCRs was inadequate. This resulted in protection circuit (DSAS device) failures.
5. There was excessive noise in the motor self control circuits, i.e., the RPS, CEMF, and PFA control circuits. This resulted in commutation and power factor advance control problems.
6. The supression of di/dt in the cycloconverter was inadequate. This resulted in potential cycloconverter SCR degradation or failure.
7. Motor field excitation was not adequate when the system operated at high speed and low torque. This resulted in cycloconverter faulting and automatic system shutdown (QSD).

The motoring mode problems were either completely solved or sufficiently alleviated to permit demonstration of the system in a self control mode throughout the specified torque-speed profile. In two areas the problems were not completely solved and as a result there was some degree of fragility to the system operation and reliability. One area involved that of inverter, cycloconverter, motor interaction (item 3 above). The other area involves the failure of the cycloconverter surge protection or DSAS devices (item 4 above). Additional development work and design refinement is required relative to both of these problems.

Those problems primarily affecting dynamic braking mode operation were as follows:

1. The voltage rating of the cycloconverter SCRs and DSAS devices was inadequate.
2. The voltage rating of the brake module SCRs was inadequate.
3. There is a noise problem in the brake module SCR gate drive circuit.
4. The dv/dt suppression circuits in the brake module were inadequate.

The problems of brake module SCR voltage rating (item 3) and dV/dt suppression (item 4) were solved as part of the developmental work performed. Time did not, however, permit resolving the problem of overvoltage on the cycloconverter during braking (item 1) and brake module SCR gate drive noise (item 3). These problems were circumvented in order to obtain dynamic braking performance data over the full speed range. Additional development work is required.

There was also a problem which involved both the motoring and braking modes. The input filter was found to have either insufficient inductance or insufficient damping or both. As a result, there was an inrush current at the instant of power application to the system. This inrush either exceeded fuze ratings or caused a transient which exceeded the voltage rating of the input filter capacitors. Fuze values were increased and limited attempts were made to improve, however, and to snub the overshoot transient. Lack of time prevented a complete investigation however and final performance was not acceptable. Additional development work is therefore required.

2.5 FINAL CONFIGURATION STATUS

Extensive modifications have been made to many parts of the propulsion system as a result of system level test effort. These modifications were made in electronic circuits, in electronics packaging, in the traction motors, and in the cooling system. Additional modifications are still required to make the system suitable for transit application.

Some of the changes, as in the case of the motors, have been developed to a point suitable for vehicle service tests. Other changes, such as those made to the inverter, cycloconverter, and brake control modules, are of a configuration adequate for continued laboratory development work but are not adequate, in terms of mechanical integrity, for vehicle service testing. In still other areas, such as circuit modifications to the motor control electronics (MCE), there are extensive make-shift modifications. In these cases, repackaging is recommended prior to any further development work.

status of the equipment drawings and specifications, like the status of the hardware, varies from component to component. It reflects the July 1976 CDR configuration and design changes instituted by ECO's between July 1976 and January 1977 when the fabrication effort was stopped.

The mechanical design drawings and specifications have not been updated to reflect changes to the Test Article configuration, except in the cases of the truck-mounted equipment. Electrical schematics, however, have been updated to incorporate the changes made during system level testing and do reflect the "final" configuration. A complete drawing list is included in Appendix C of Volume III of this report.

2.6 REMAINING DEVELOPMENT ACTIVITIES

The development of a production configuration requires, in general, the completion of the laboratory development and system qualification tests followed by a series of vehicle service tests. The remaining laboratory development tests consist of the following: (1) solving the previously discussed problems and completion of the open-loop characterization of the system for both the motoring and braking modes; (2) intregration of the MCE with the TCE and verification of closed loop control of the system including jerk limiting for both the motoring and braking modes; (3) verification of mode to mode transitioning; (4) verification of continuous motor control as opposed to discrete point operation, i.e., with car dynamic simulation model tied to control of the dynamometer; (5) verification of operation across simulated rail gaps; (6) resolution of previously identified cooling system and packaging problems; and (7) completion of simulation studies supportive to the development of a closed loop motoring and braking control, including a simulation based demonstration of slip/slide control.

Upon completion of laboratory development, qualification tests must be conducted to verify that the equipment meets established design and performance requirements and to provide a degree of assurance that it is suitable for integration into the modified-SOAC. Some of these tests would be conducted at the major component or assembly level; however, the primary means of qualification would be through system level tests of an integrated propulsion system.

The final phase of the required development activity involves the vehicle service tests. These would consist of engineering evaluation and acceptance tests of the equipment as installed in the modified SOAC. The tests, to be carried out at the TTC, at Pueblo, Colorado would serve (1) to confirm laboratory tests and simulations and (2) to demonstrate the readiness of the system for operational evaluation on a transit property.

SECTION III
CONCLUSIONS

Based on the experiences and results of the ASDP propulsion system program, several conclusions can be drawn. These can be grouped into two categories: program related conclusions and technical conclusions.

Program Related Conclusions

- In retrospect, it is obvious that the program was planned on an overly optimistic, success-oriented basis.

  The schedule from the start of design to delivery of qualified hardware was unrealistic for a new advanced system.

- Too much reliance had been placed on the results achieved during extensive IR&D effort carried out prior to the ASDP program.

  It had been assumed that a prototype system (called a Test Article in this report) based on the IR&D designs could be fabricated, checked out, and debugged expeditiously in a straightforward routine manner.

  However, the IR&D effort had been carried out using breadboard electronics and modified commercial motors, which fact, combined with some laboratory equipment limitations, had not permitted complete verification of all key operating concepts over the complete motoring and braking torque-speed profiles. In retrospect, it appears obvious that the IR & D effort was not as extensive as originally assumed.

- The program experienced several unforeseen problems during Test Article system integration, checkout, and testing resulting in schedule delays and cost overruns. Technical problems arose with the Test Article which were difficult to troubleshoot and diagnose and which, in some cases, required extensive circuit rework to correct. In retrospect, these problems were due primarily to an insufficient allocation of contingency time for the solution of possible technical problems.

- Deliverable hardware was prematurely committed to manufacturing. This was deemed to be necessary to meet schedules established for integration of equipment into the SOAC vehicles. As a result, there is a considerable amount of residual material.

- The propulsion system design turned out to be more complex than originally envisioned.

  To establish whether this was due to over-sophistication in the design approach, to overstated requirements, to the incorporation of too many "nice-to-have" features, or whether this is basic to the concept, would require extensive analysis and evaluation.

Technical Conclusions

Conclusions relative to the technical capabilities of the ASDP propulsion system can be discussed in relation to the expected advantages and benefits shown previously in Table 1-I.

- AC Synchronous Machine

  The traction motor development effort resulted in a successful self-synchronous machine design. Although some problems were encountered during testing, these have been resolved. The development cycle of this motor, however, cannot be considered complete until consistent high speed - high torque performance has been demonstrated and actual "in-service" experience has been accumulated.

  It has been demonstrated by testing and ayalyses that all major performance requirements (torque/speed, efficiency, electrical characteristics, etc.) are met or exceeded.

  - The inherent dc traction motor performance characteristics provided by field excitation proportional to armature current were demonstrated. The high torque required at low speeds for acceleration was achieved and maximum power operation over a 3.4:1 speed range was demonstrated.
  - Brushless operation was obtained by the successful development of a rotary transformer and rotating rectifier for field excitation. A problem relative to the transient protection of

the rotating rectifier diodes was resolved by incorporating a crowbar circuit and fast recovery diodes.

- Low weight and compact size of the motor have resulted partly from high speed operation and partly by the use of liquid cooling. Although the original weight goal was not met, the ASDP traction motor still shows a 2 to 1 weight advantage over most transit dc motor designs such as the SOAC motors. A comparison of the original weight estimate and the final motor weight is given in the following. The 2 to 1 weight advantage of the ASDP traction motors over the SOAC dc motors is supported as follows: the present SOAC transit cars are utilizing 4dc motors, one for each axle. Each motor weighs 1,560 lbs for a total motor weight/car of 6,240 lbs. The ASDP propulsion system uses two traction motors per car (monomotor truck design), with each motor delivering twice the power of a SOAC motor. For weight comparison purposes the basic motor weight of 1,569 lbs was considered, which does not include the weight of the transition (end) frames required to connect the motors to the gearboxes and to mount the motor/gearbox subassembly to the truck frame. The total motor weight/car for ASDP is then 3,136 lbs which is approximately half of the SOAC motor weight/car.

	Basic Motor	Transition Frames	Total
Original Weight (PDR), lb	1261	214	1475
Final Weight (Actual), lb	1568	340	1908

An additional weight saving of 350 lbs is possible by using aluminum for the main frame and for the transition (end) frames.

- High reliability and reduced maintenance cannot be demonstrated without actual operation in a transit car environment. The elimination of brushes and commutators, and the provision of a completely sealed design due to liquid cooling, however, promises significant improvements.

- Solid State Power Converter

Extensive system level dynamometer testing indicates that the overall design approach is sound. Test results obtained in the motoring mode demonstrated that the power/torque/speed characteristics can be met throughout the full torque-speed regime. Futhermore, system efficiency measured exceeds the predicted values. All performance verifications testing was performed in an "open loop" mode of operation. No conclusions can be made, therefore, relative to "closed loop" system operation using the microprocessor based train control electronics.

- Smooth stepless control of the solid state power controller was verified by testing. Control is accomplished by simply varying the inverter frequency.
- System efficiency (from dc power input to motor shaft output) at full power level was measured at 79.3% to 87.2% over a wide speed range. This compares favorably with the predicted values of 79% to 86% for the same speed range.
- Reliability and maintenance advantages cannot be demonstrated without operation in the transit environment. The use of solid state components with liquid cooling and the elimination of most mechanical contactors used in other propulsion systems, however, promises potential for improvements in these areas.

- Liquid Cooling

A unique feature of the Delco propulsion system is the liquid cooling of the motor and the power electronics using a fire resistant coolant (silicone). The effectiveness of the liquid cooling concept was verified during the extensive system level testing. Temperatures monitored inside the traction motor were below predicted levels and no high power solid state device failures could be attributed to inadequate cooling during testing. The only temperature related failure identified (a field supply transformer) is easily corrected by modifications to the transformer and cooling loop designs.

- Electrical Braking

  The test data obtained during systems testing in the dynamic braking mode of operation indicated that the full braking torque specified for the system can be realized throughout the speed range. Test data obtained demonstrated the maximum required capability below 2000 rpm. At higher speeds, full torque test data could not be obtained due to dynamometer and SCR voltage limitations. Analytical predictions correlated with test data indicate, however, that full dynamic braking capability can be provided essentially over the full torque/speed range.

  Regenerative braking capability was not verified prior to the termination of the program.

- Propulsion System Redundancy

  Provision was made in the design for redundant propulsion systems. Each truck is provided with an independent propulsion system to allow continued transit car operation (at reduced capability) after a failure in one of the drive systems.

Summary

Although development is incomplete, the self-synchronous propulsion system concept is considered a good potential for transit car application.

The status of the Test Article hardware and documentation is considered to be such that continuing development can be undertaken, if so desired.

SECTION IV
RECOMMENDATIONS

It is felt that the self-synchronous propulsion system represents a major advance in the state of the art, and that development should be re-initiated. However, the point to which the development is carried out should be established based on two economic factors:

(1) Life-cycle costs
(2) The potential market.

Since the potential market is highly dependent on the costs, both first and recurring costs, the development should be carried at least to the point that enables the life-cycle costs to be estimated with a reasonable degree of confidence in their accuracy. This can be done only with respect to a specific, well-defined design. Thus a two-phase program is recommended.

Phase I

- Continue dynamometer evaluation of the Test Article system by completing the "open loop" testing. One of the remaining major areas of investigation is the regenerative braking system performance.
- Based on the recommended design changes made in Section VII of this report and any additional modifications required resulting from further system testing, update the design and incorporate these design changes into the Test Article hardware.
- Include the Train Control Electronics in the system test setup and conduct "closed loop" testing in motoring and braking. It is anticipated that a system simulation effort will be required to support the "closed loop" testing.
- Validate the propulsion system design by a comprehensive dynamometer test program that fully qualifies the system with respect to specification requirements and the operating advantages of self-synchronous ac drives.
- Conduct a comprehensive analysis to establish system life-cycle costs and the operating advantages of self-synchronous ac drives.

Before initiating the Phase I effort recommended here, a preliminary life cycle cost analysis should be done on the basis of existing information to establish the economic viability of this ac propulsion system. In addition, a survey should be conducted to assess the potential market and the transit properties plan to introduce advanced concept transit cars.

Phase II

- Complete fabrication of the prototype equipment for one or two transit cars in accordance with the changes recommended earlier.
- Install propulsion system equipment on one or two SOAC cars along with new trucks and brakes.
- Conduct engineering testing at Pueblo with the SOAC car(s) to evaluate performance of the propulsion system, monomotor trucks, and brakes under simulated transit car operating conditions.
- Conduct a 10-car demonstration program in revenue service after successful engineering evaluation at Pueblo.

Phase II should not be initiated until all Phase I efforts are completed. This includes demonstration of compliance with all technical objectives under laboratory conditions and the establishment of favorable life-cycle costs and operating advantages.

A supplemental series of tasks correlated with the two-phase program is also proposed. This series of tasks would investigate and develop more radical changes to the system which could lead to a more cost effective, lower weight, higher reliability, or more efficient configuration. Examples of changes which offer the potential of considerable benefit are as follows:

- Self-Contained Cooling of Traction Motors.
  Preliminary studies indicate that a self-contained liquid cooling system for each traction motor might be practical. This would greatly simplify the cooling system and reduce size, weight, cost, and noise.
- Use of the Cycloconverter for Braking Control.
  The addition of a contractor assembly as discussed in paragraph 7.3 would permit use of the cycloconverter SCR's for braking control. This offers the potential of removing the braking module, 9 SCR's, and related SCR gate drive electronics from the system.

- A microprocessor for motor commutation and power factor control.
  Motor power factor control at intermediate and high speeds is based on the use of CEMF, a signal which is noisy and difficult to interpret due to cycloconverter commutation. Use of a microprocessor would permit use of RPS as the motor commutation timing reference for armature currents at all speeds with power factor advance (PFA) being added at intermediate and high speeds based on an a priori estimate of desired PFA.
- A Separate Inverter for Motor Field Excitation
  A separate field excitation inverter although more complex and costly than the existing transformer, might offer sufficient benefits in performance. It would also obviate the SCR over-voltage problems as discussed in paragraph 7.2.

SECTION V
SYSTEM DESIGN

5.1 OVERALL SYSTEM DESCRIPTION

This subsection provides an overview description of the ASDP self-synchronous propulsion system. Detailed descriptions are provided in ensuing sections of this report.

5.1.1 GENERAL

The ASDP propulsion system consists of the following major elements: train control electronics (TCE), motor control electronics (MCE), power control electronics, traction motor, gearboxes, cooling unit, and dynamic brake resistor. Duplicate independent propulsion systems (except for the line filter inductor) are provided for each truck of the transit car. A simplified block diagram of the dual propulsion systems is shown in Figure 5.1-1. A hardware family tree for a two-car train is shown in Figure 5.1-2.

The TCE is implemented with a digital computer utilizing microprocessor elements and conventional input/output interface devices. The MCE is a hard wired assembly of combinatorial and sequential logic elements, operational amplifiers, comparators, and passive components. The power control electronics portion of the propulsion system contains a line filter inductor, a power control switchgear assembly, a resonating inductor module, and a power converter assembly. The latter contains five liquid cooled modules: inverter, cycloconverter, capacitor, field supply, and brake control.

Input signals to the TCE are derived from the motorman's console and various car subsystems and sensors. The motorman's train-lined tractive effort command, or P-signal, is a zero to 1.0 ampere current where 0.55A to 1.0A represents zero to maximum motoring effort and 0.45A to 0.0A represents zero to maximum braking effort. The TCE interprets the P-signal, develops the appropriate system mode commands, and computes a desired ' ue based on the P-signal tractive effort command. The computation compensates for items such as speed, car weight, coolant temperature and pressure, and wheel diameter. The TCE also monitors motor current, voltage, speed, etc., and based on these inputs computes the actual torque being developed by the motor. Based on a comparison of the actual and desired torque levels, the TCE then modifies the motoring or braking mode torque command signals sent to the MCE.

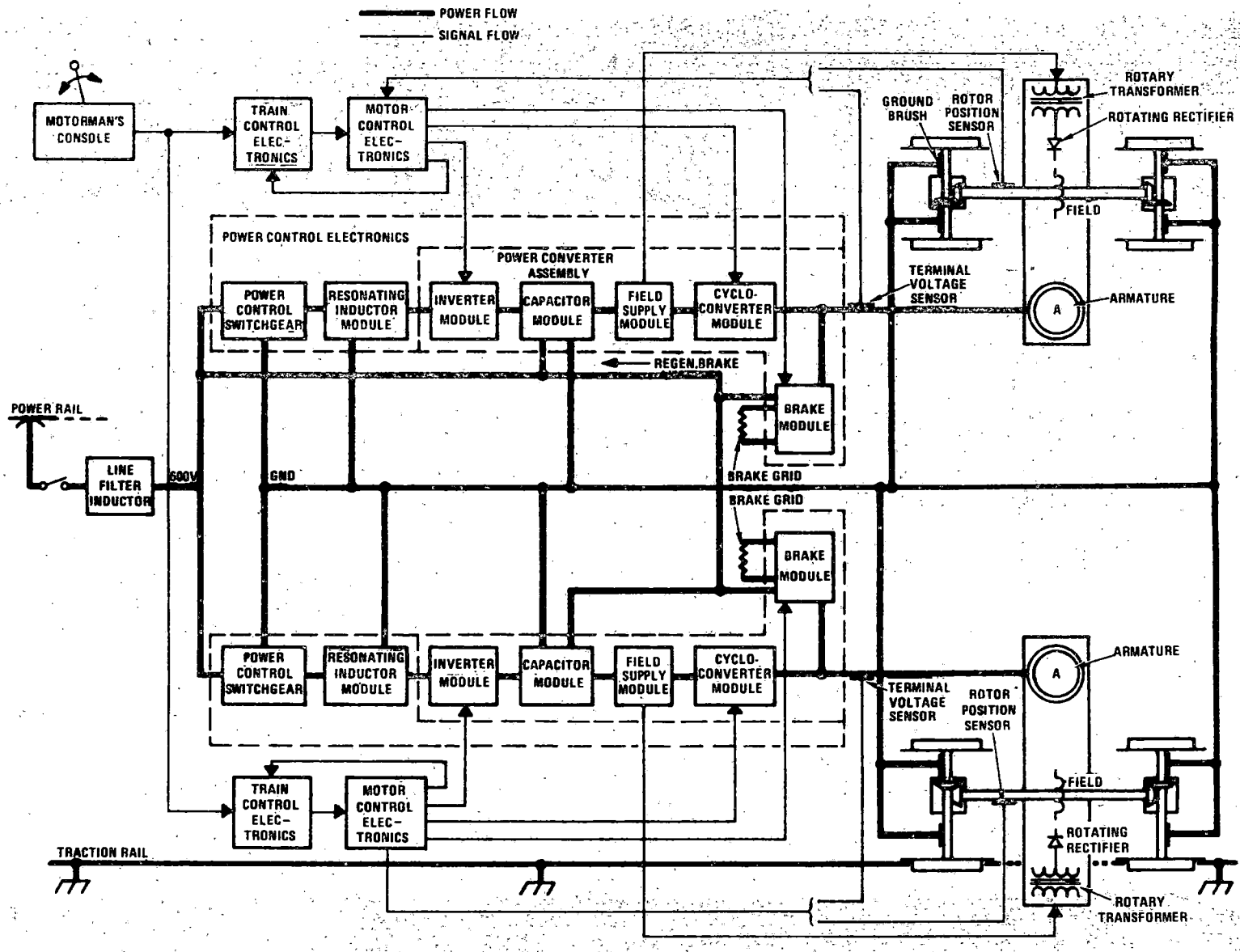

Figure 5.1-1. Propulsion System Block Diagram

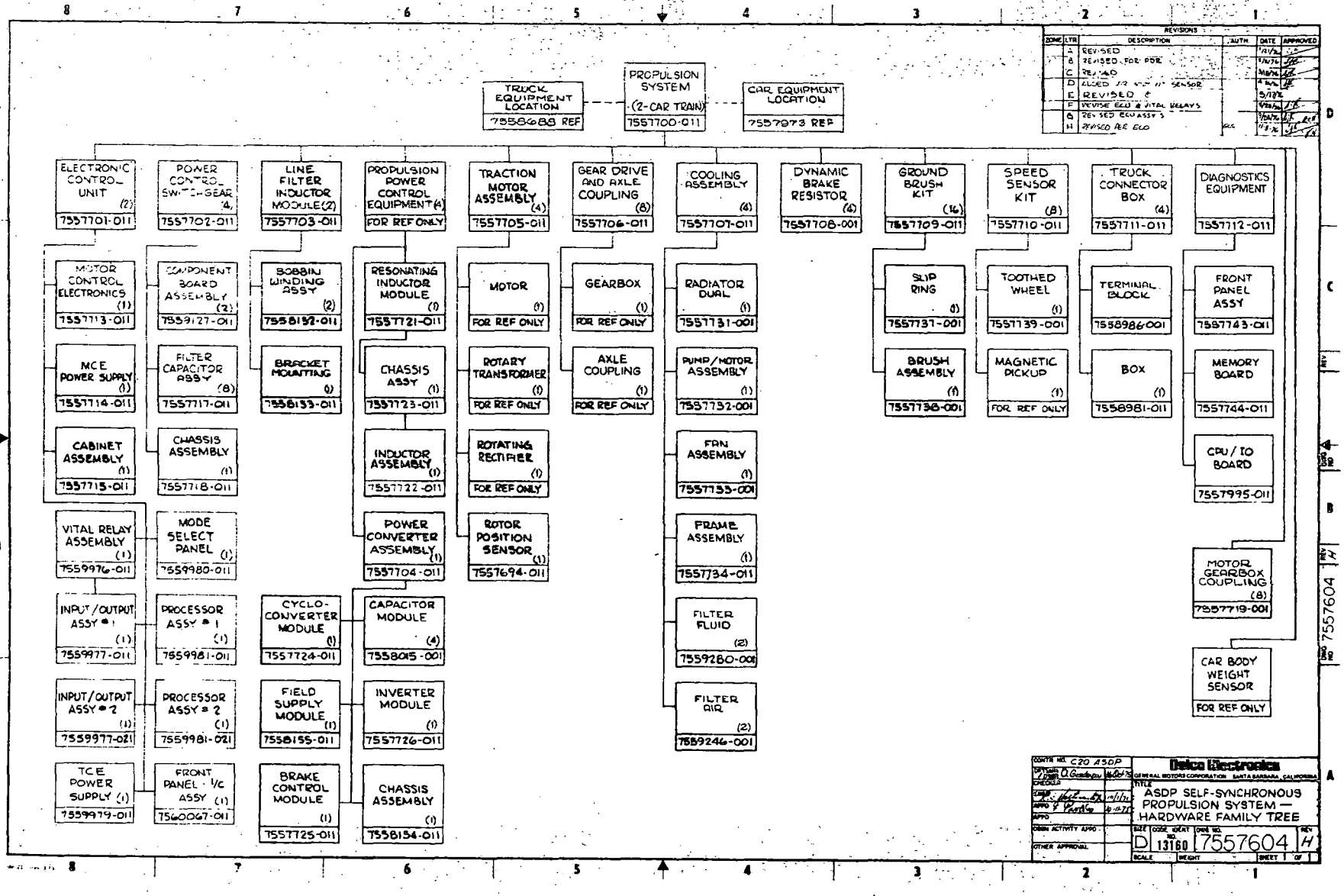

Figure 5.1-2. Hardware Family Tree

The MCE input command signal is applied to a voltage controlled-oscillator (VCO) to form the variable frequency clock pulses to time the firing of the SCR's of the inverter stage of the power control electronics. In motoring, the cycloconverter stage converts the inverter output current into motor current of the same amplitude but of lower frequency. This current level is determined by the frequency of the inverter stage. The frequency and phase of the motor current is determined by Rotor Position Sensor (RPS) and Terminal Voltage Sensor (TVS) signals processed in the MCE to form cycloconverter SCR gate pulses. In braking, cycloconverter gating is removed and the brake rectifiers in the brake module are gated for dynamic and/or regenerative brake control. As in motoring, field current is derived from a transformer in the field supply module.

The MCE develops several signals used by the TCE to compute the proper VCO command signal. These include motor phase current, motor voltage, and motor frequency. In addition, a drive shutdown signal is sent to the MCE in the event of an abnormal condition in the inverter, brake, or cycloconverter module.

A line filter inductor serves as an input line filter element for both propulsion systems. The projected reliability of the single inductor permitted its use with the otherwise redundant propulsion systems with a negligible effect on overall reliability.

The power control switchgear unit contains the main contactor and blocking diode, electrolytic capacitor bank, and overcurrent relay.

The traction motor (one per truck) is a brushless four-pole synchronous machine with forced convection liquid cooling. In motoring it has an output capability of 1560 lb-ft of torque from 0 to 1646 r/min and 489 hp from 1646 to 5642 rpm (80 mph). In dynamic braking it has an output capability of 1405 lb-ft from maximum speed to about 600 rpm. It can regenerate from maximum speed down to about 25 mph. The machine is fitted with a rotary transformer-rotating rectifier in lieu of the usual exciter-rotating rectifier found in constant speed synchronous motors. A rotor position sensor is installed in one end of the motor. The double ended motor drives two hypoid gear sets (5.875 to 1 reduction), having output shafts coupled to the axles by a rubber bushed flexible linkage.

Each of two independent cooling units consists of a double ended ac motor driving separate pumps for cooling of the power electronics and motor with a fire resistant silicone fluid. Heat is extracted from the coolant by a single two-section liquid-to-air heat exchanger. Air flow is provided by an ac motor and propellor fan.

Power supply current is collected from a nominal 600 Vdc third rail by means of a pickup shoe and returned to earth through the contact between the wheels and the traction rails. Ground brush assemblies on each axle complete the rotating connection between the vehicle power ground and the wheels.

The salient characteristics of the propulsion system major components are listed in data sheet format in Table 5.1-I.

5.1.2 MOTORING MODE OPERATION

In the motoring mode, (Figure 5.1-3), filtered dc power is converted to variable frequency ac power by the three-phase inverter. The inverter frequency is varied over a range of 350 to 1200 Hz by the tractive effort signal to control the reactance of, and hence the current through, the coupling capacitors. This current is converted to a lower frequency motor stator current by the action of the cycloconverter. The reactance of the coupling capacitors also gives the cycloconverter a current source output characteristic.

A functional description of the power converter, termed the capacitor coupled cycloinverter, is provided in the following subsections. A more detailed discussion is given in Appendix F, which is the patent description of the power electronics used for the ASDP propulsion system (U.S. Patent 3,866,099).

5.1.2.1 Inverter Stage

Figure 5.1-4 shows the simplified circuit of the three phase inverter. This unit consists of three single-phase series inverters gated to produce three-phase output voltage and current. The inductors and capacitors are key elements of the inverter since they largely determine its efficiency. The inductors have been optimized for high efficiency and power density. The multi-section combination resonating and coupling capacitors, developed originally for use in induction heating equipment, have been significantly upgraded in volt-ampere rating in recent years by a change from paper to composite paper-polypropylene dielectric. The use of these low-loss inductors and capacitors yields an inverter efficiency of approximately 95% over a relatively wide frequency range.

Line Filter Inductor

Type: Dual Iron Core Inductor	
Number Required per Car	1
Nominal Inductance	2.5 mH
Resistance	0.0022 ohm
Nominal Inductor Loss	790 watts
Cooling	Free air convection
Iron Core	E-I Laminations
Conductor	46 turns of sheet copper
Insulation	Nomex paper
Weight	775 lb
Manufacturer	Delco Electronics - SBO

Power Control Switchgear

Number Required per Car	2
Line Contactor	Single pole, normally open overcurrent hold-in (2000 A)
Overcurrent Sensor	900 A
Filter Capacitor Bank	8800 mF
Weight	230 lb
Manufacturer	Delco Electronics - SBO

Resonating Inductor

Type: Shell type laminated iron core linear inductors (6 per assembly)	
Number Required per Car	2
Inductance	150 μ H
Winding Resistance (dc)	0.00236 ohm
Quality Factor (Q) at 100 Hz (free space)	180
Lamination	4 mil silicon steel
Conductor	10 turns of Litz wire
Weight	675 lb
Manufacturer	Delco Electronics - SBO

Dynamic Brake Resistor

Type: Coil type resistor grid	
Number Required per Car	2
Maximum Power Dissipation	1150 kW
Average Power Dissipation	110 kW
Resistance Value (one tap)	0.78/0.26 ohms
Cooling	Self-Ventilated
Weight	265 lb
Manufacturer	Guyan

Motor/Gearbox Coupling

Type: Gear Coupling	
Number Required per Car	4
Maximum Normal Speed	5645 r/min
Maximum Normal Torque	1050 lb-ft
Maximum Shock Torque	4250 lb-ft
Maximum Misalignment	0.5°
Maximum Offset	0.040 in
Gear Pitch Diameter	6 in
Weight	32 lb
Manufacturer	Renold Ajax

Power Converter Assembly

General

Type: Capacitor Coupled Cycloinverter	
Power Rating - peak	430 kW
- average	237 kW
Output Voltage	850 V
Output Current	550 A
Cooling	Active Liquid cooling
Weight	910 lb
Manufacturer	Delco Electronics - SBO

Inverter Module

Frequency Range		350 to 1200 Hz
Power SCR's (6 ea)	- Blocking voltage	1800 V
	- Current rating (half sine at 1200 Hz)	300 A
	- Turn-off time	150 μ S
	- Type	GE C441 PN
Power Diodes (6 ea)	- Blocking voltage	1800 V
	- Current Rating	450 A
	- Type	West. RT 722
Associated Circuitry		- Gate drive circuit - dv/dt circuit - Current sensing circuit

Capacitor Module

Commutating Capacitors (6 sections)	40 μ F (ea)
Coupling Capacitors (3 sections)	80 μ F (ea)
RMS Voltage	780 V
RMS Current	700 A
Dissipation Factor	0.3% at 1000 Hz

Field Supply Module

Transformer primary windings - motoring	3 turns
Relay controlled dual primary - braking	144 turns
Transformer secondary windings	36 turns
Turns ratio in motoring mode	1/12
Turns ratio in braking mode	12/1

Cycloconverter Module

Input frequency		350 to 1200 Hz
Output frequency		0 to 200 Hz
Power SCR's (18 ea)	- Blocking voltage	1800 V
	- Current rating (half sine at 1200 Hz)	300 A
	- Turn-off time	200 μ S
	- Type	GE C441 PN
Associated Circuitry		- Gate drive circuit - dv/dt circuit - Surge suppression circuit

Brake Control Module

Type: Dual Phase Delay Rectifier		
Power SCR's (9 ea)	- Blocking Voltage	1800 V
	- Current rating (half sine at 1200 Hz)	300 A
	- Turn-off time	200 μ S
	- Type	GE C441 PN
Associated Circuitry		- Gate drive circuit - dv/dt circuit - CEMF sensing transformer

Table 5.1-I ASDP Propulsion System Major Components - Salient Characteristics (Sheet 1 of 2)

Cooling System

Type: A- e liquid cooling with radiator	
Number ired per Car	2
Coolant	Silicone, DC 200-50
Cooling Capacity - Motor Loop	19.5 kW
- Power Electronics Loop	12 kW
Coolant Flow rate - Motor Loop	20 gal/min
- Power Electronics Loop	20 gal/min
Radiator	Plate/fin brazed aluminum
Fan	1.5 hp, 6 blade, 22 in. dia
Pump	Rotary gear, 20 gpm at 1200 rpm
Weight	645 lb
Manufacturer	Delco Electronics - SBO

Electronic Control Unit

General

Type: Microprocessor based control electronics	
Packaging: Augat wirewrap circuitboards mounted on horizontal pullout drawers (11 boards)	
Cooling	Filtered, forced air cooling
Size	46 in x 12 in. x 30 in.
Weight	85 lb
Manufacturer	Delco Electronics - SBO
Number Required per Car	1

Train Control Electronics

Type of Microprocessor	8 bit Intel 8080
Number of I/O Channels	101
PROM Storage	8 k
RAM Storage	2 k
Main Loop Cycle Time	26 m sec
Number of interrupt input	8
Buffered test points (analog)	12
Fault indicators	15
Operational status lights	30

Ground Brush Assembly

Type: Spring Loaded Copper-Graphite Brush	
Number Required per Car	8
Current Rating	
- Continuous	250 A
- Intermittant (5 min)	400 A
Maximum Voltage	750 V dc
Weight	10 lb
Manufacturer	BBC-Secheron

Gear Drive and Axle Coupling

General

Number Required per Car	4
Maximum Axle Speed	960 r/min
Maximum Normal Axle Torque	6,120 lb-ft
Maximum Axle Shock Torque	24,975 lb-ft
Weight (actual)	1,093 lb
Manufacturer	Brown Boveri/Henschel

Gearbox

Type: Single reduction, Hypoid Bever Gear	
Reduction Ratio	5.875 to 1
Efficiency (min.)	96%
Lubrication	Oil Splash

Axle Coupling

Type: Flexible Rubber Joint Cardan Coupling	
Axle Displacement - Radial	± 0.75 in.
- Axial	± 0.50 in.
- Angular	± 1.3°

Traction Motor

Type: Self Controlled Synchronous Machine	
Number Required per Car	2
Armature - Three phase stationary	
Field - Three phase, salient pole, four pole rotor	
Field Excitation - Rotary transformer and rectifier	
Cooling - Liquid spray cooling (silicone fluid)	
Continuous Duty Power	350 hp
Maximum Power	500 hp
Maximum Speed	5642 r/min
Maximum Torque	1600 lb-ft
Weight - Motor only	1568 lb
- Including transition frames	1908 lb
Manufacturer	Delco Products

Diagnostics Unit

Type: Microprocessor Based Electronics with Memory Storage	
Microprocessor Type	Intel 8080
Storage capability - EPROM (Diagnostic program)	8 k
- RAM (Scratch pad)	2 k
- RAM (memory)	16 k
Number of informations monitored	256
Length of diagnostics record	
- High speed data (24 parameters)	16 sec
- Low speed data (8 parameters)	30 min
Build-in printer available for permanent records	
Test connectors provided for external instruments	
Operational status indicators provided	
Size	15 in. x 4.5 in. x 23.5 in.
Weight	15 lb
Manufacturer	Delco Electronics - SBO

Table 5.1-I ASDP Propulsion System Major Components - Salient Characteristics (Sheet 2 of 2)

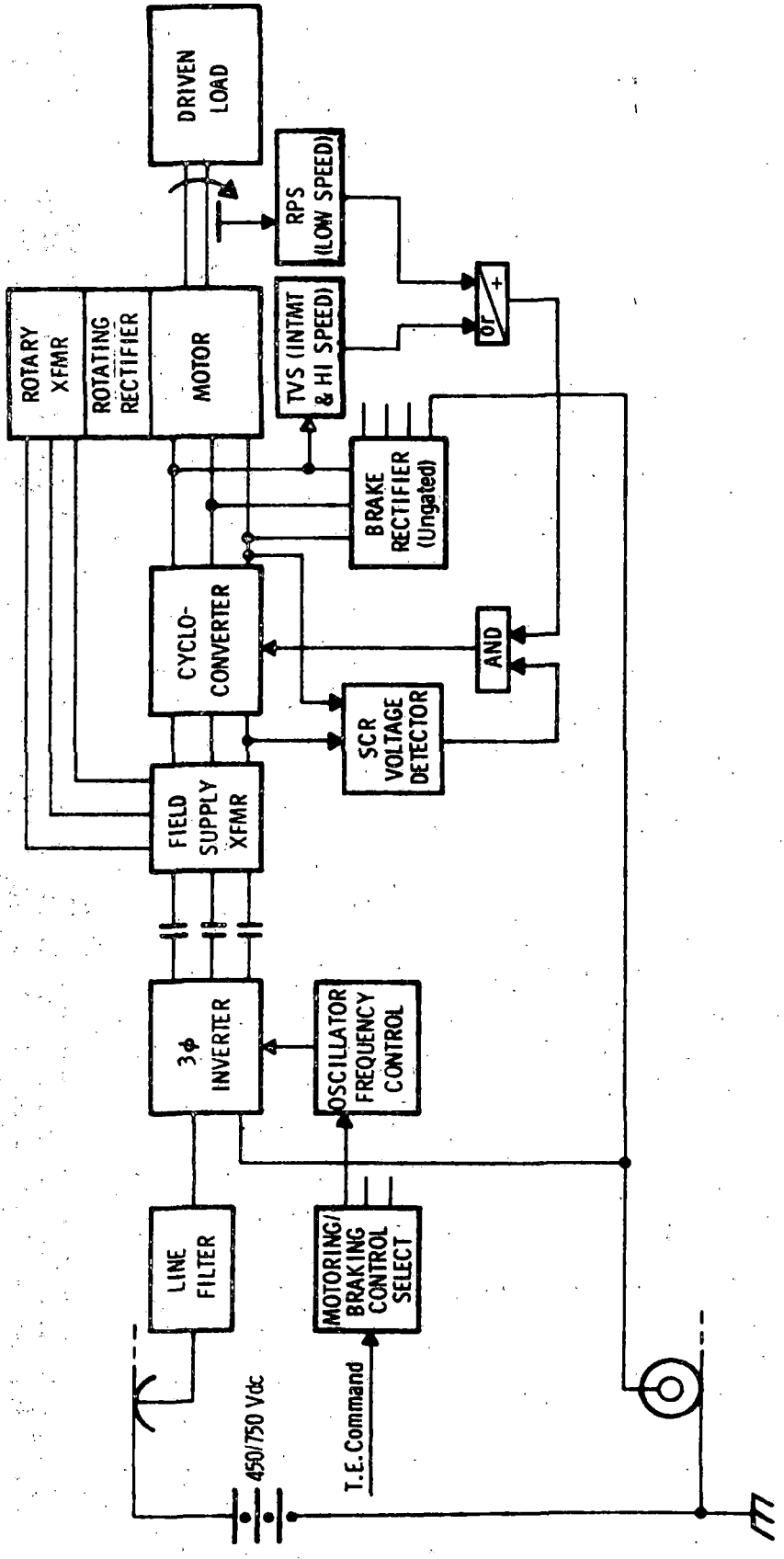

Figure 5.1-3. System Block Diagram – Motoring Mode

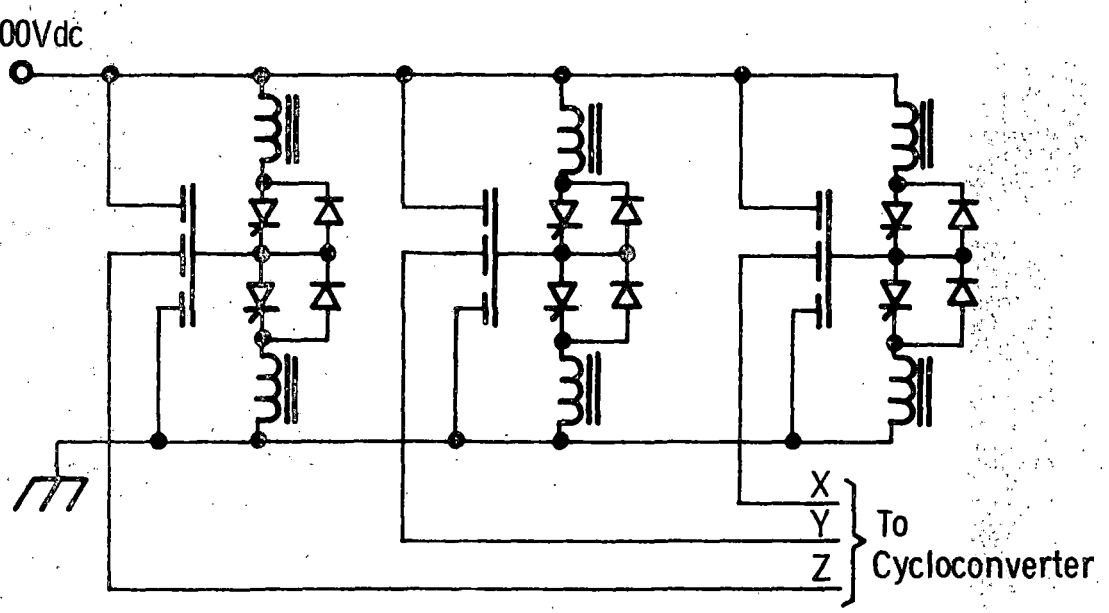

Figure 5.1-4. Input Inverter Stage

The inverter SCRs are150 μ s turn-off time devices with 1800 V blocking capability. The diodes anti-parallel to the SCRs are a fast recovery type with a recovered charge of 140 μ Q under normal operating conditions. The dV/dt suppression circuits connected across each SCR/diode pair prevent spurious SCR turn-on with a minimum of dV/dt circuit power loss. This is achieved through the use of a saturable inductor in series with each SCR/diode pair. The inductor stores a portion of the dV/dt circuit energy change in each inverter cycle, energy that would otherwise be lost in the dV/dt circuit resistance. An analytical simulation of this resonant inverter is presented in Appendix G.

The SCR/diode cooling method was a key element in achieving an inverter package size consistent with the space available. A heatsink arrangement consisting of externally oved cooling blocks, sealed by the SCR or diode being cooled, interconnected without the use of hoses or clamps, and exhausting into a coolant filled container was developed and patented. This method of cooling is further described in subsections 5.6 and 6.1.

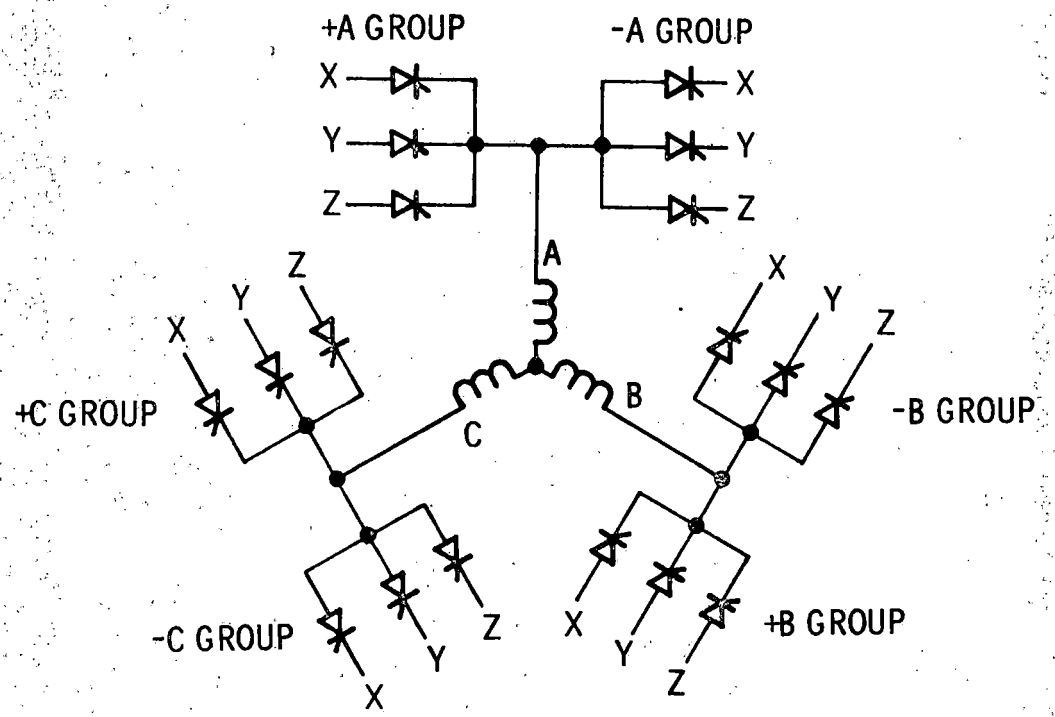

Figure 5.1-5. Cycloconverter Circuit

5.1.2.2 Cycloconverter Stage

The cycloconverter is an arrangement of six groups of three SCRs as shown in Figure 5.1-5. At any instant of time two SCR groups, one for positive and one for negative current, are gated to form the equivalent of a full wave rectifier supplying current into one motor phase and out of another. Again, at any instant of time (except for periods of commutation overlap), the voltage and current conditions in the external circuit cause conduction in two of the six gated SCRs. The current duty cycle per thyristor is thus (1/3) (1/3) = 1/9. This low duty cycle gives a relatively low total cycloconverter power dissipation. The modest SCR cooling requirements are handled with externally grooved heatsinks identical to those in the inverter module except for shallower coolant grooves to produce a lower flow rate.

Cycloconverter gate pulse timing is derived from three control signals. Two of the signals accomplish motor self control: at low speeds by the rotor position sensor (RPS), and at intermediate and higher speeds by the motor CEMF sensor (TVS). Use of the CEMF at intermediate and high speeds permits the desired power factor control. The composite RPS -TVS signal is ANDed with a signal which indicates the voltage across the cycloconverter

SCRs to produce an SCR gate pulse which is applied when individual SCR anode voltages become positive. (See Figure 5.1-3)

5.1.2.3 Motor Field Excitation

The synchronous traction motor makes use of a rotary transformer and a rotating rectifier for brushless field excitation. The primary of the rotary transformer is powered from a current transformer having primary windings in series with the cycloconverter input current. Two advantages result from this form of field power supply over the alternative use of a separate field supply inverter. First, the transformer supply is smaller and much less complex than an inverter. Second, the current transformer provides (except at low frequencies where rotary transformer magnetizing current is significant) motor field current proportional to armature current. This gives the traction motor a desireable motor speed-torque characteristic similar to a dc series motor and also maintains the motor torque angle approximately constant for stable operation and reliable commutation.

5.1.2.4 Motor Current Commutation

The commutation, or transfer, of current from one motor phase to another occurs in three modes: input line commutation, motor output line commutation, and mixed input/output line commutation. The commutation is initiated by the simultaneous removal of SCR gate pulses from the three SCRs in the phase to be turned off and the application of gate pulses to the three SCRs in the phase to be turned on. The one SCR of the three in the off-going group that was conducting is turned off by the application of reverse voltage from the external circuit.

At low motor speeds, where motor CEMF is much less than the inverter voltage, the SCR reverse voltage following gate current removal is derived from reversals of the cycloconverter input line voltage. At high motor speeds and accompanying high CEMF, the cycloconverter is timed to operate at a leading power factor. This produces a negative voltage on the off-going SCR when the on-coming SCR group is gated into conduction. At medium motor speeds, both input and output voltage provide commutation.

5.1.2.5 Motor Torque Production

The creation of rotor torque from stator current and field flux can be visualized with the aid of Figure 5.1-6. The field is depicted as a rotating magnet producing a flux Φ having north and south poles while the stationary armature (stator) is shown as three wye-

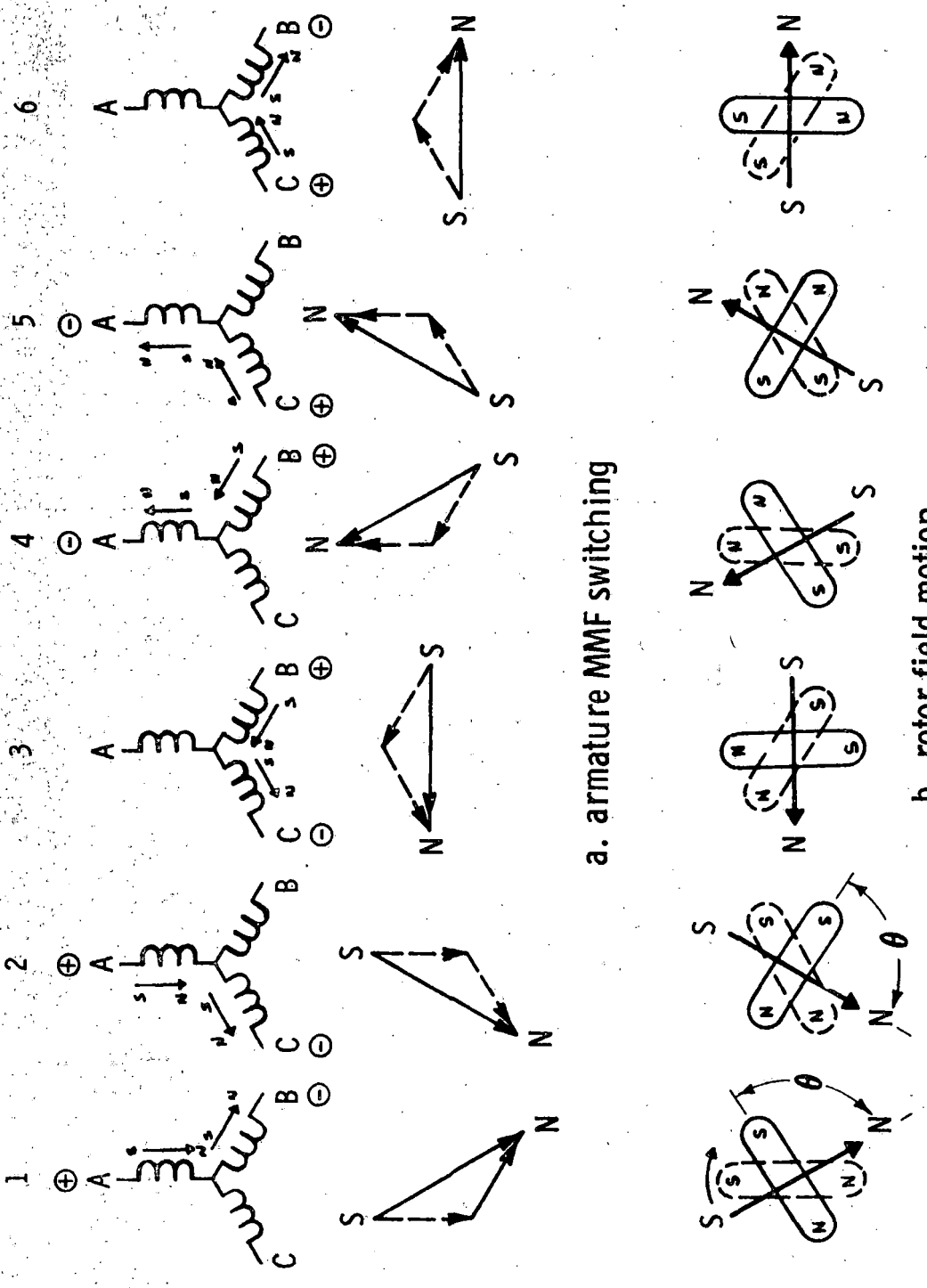

Figure 5.1-6. Generation of Self-Synchronous Rotating Stator Field

connected coils. With the rotor in position No. 1, the RPS signals, augmented by the CEMF sensor signals, direct the cycloconverter to inject current into phase A and remove it from phase B. The resultant A-B armature MMF vector lies at an angle θ with respect to the field magnet vector. Torque is produced according to the proportionality

$$T \alpha I\Phi \sin \theta .$$

Because of the high frequency of the cycloconverter rectification process and the armature inductance, current is relatively constant. Torque thus varies with $\sin \theta$. As the rotor turns against the load torque, the transition from position No. 1 to position No. 2 is made where the composite RPS/CEMF signal directs the cycloconverter to transfer (commutate) current from phase B to phase C. At the transfer point, the armature MMF steps ahead 60°. Once again, torque varies as $\sin \theta$, where θ is referenced 60° in advance of the original reference in position No. 1. The self-controlled torque production process described above continues indefinitely as long as motor torque is able to overcome the load torque.

5.1.3 BRAKING MODE OPERATION

In braking, the traction motor is operated as a separately excited generator connected to phase delay controlled dynamic and regenerative brake rectifiers (see Figure 5.1-7).

5.1.3.1 Field Excitation

Field excitation is provided by the same transformer used in motoring. The transformer circuit is reconfigured by de-energizing the low impedance primary windings (by removing the cycloconverter SCR gate signals) and by connecting high impedance primary windings through a relay to the inverter. Generator field current is then controlled by varying the inverter frequency over a range from 350 Hz to 1100 Hz. Inverter input power varies from approximately 1.0 to 30.0 kW over this frequency range. Braking effort in dynamic and regenerative braking is controlled by a combination of field current control and rectifier phase control.

.3.2 Braking Effort Control

The braking control modes available are:

1. Both trucks in dynamic braking
2. Both trucks in regenerative braking
3. One truck in dynamic and one truck in regenerative braking
4. Each truck in simultaneous dynamic and regenerative braking.

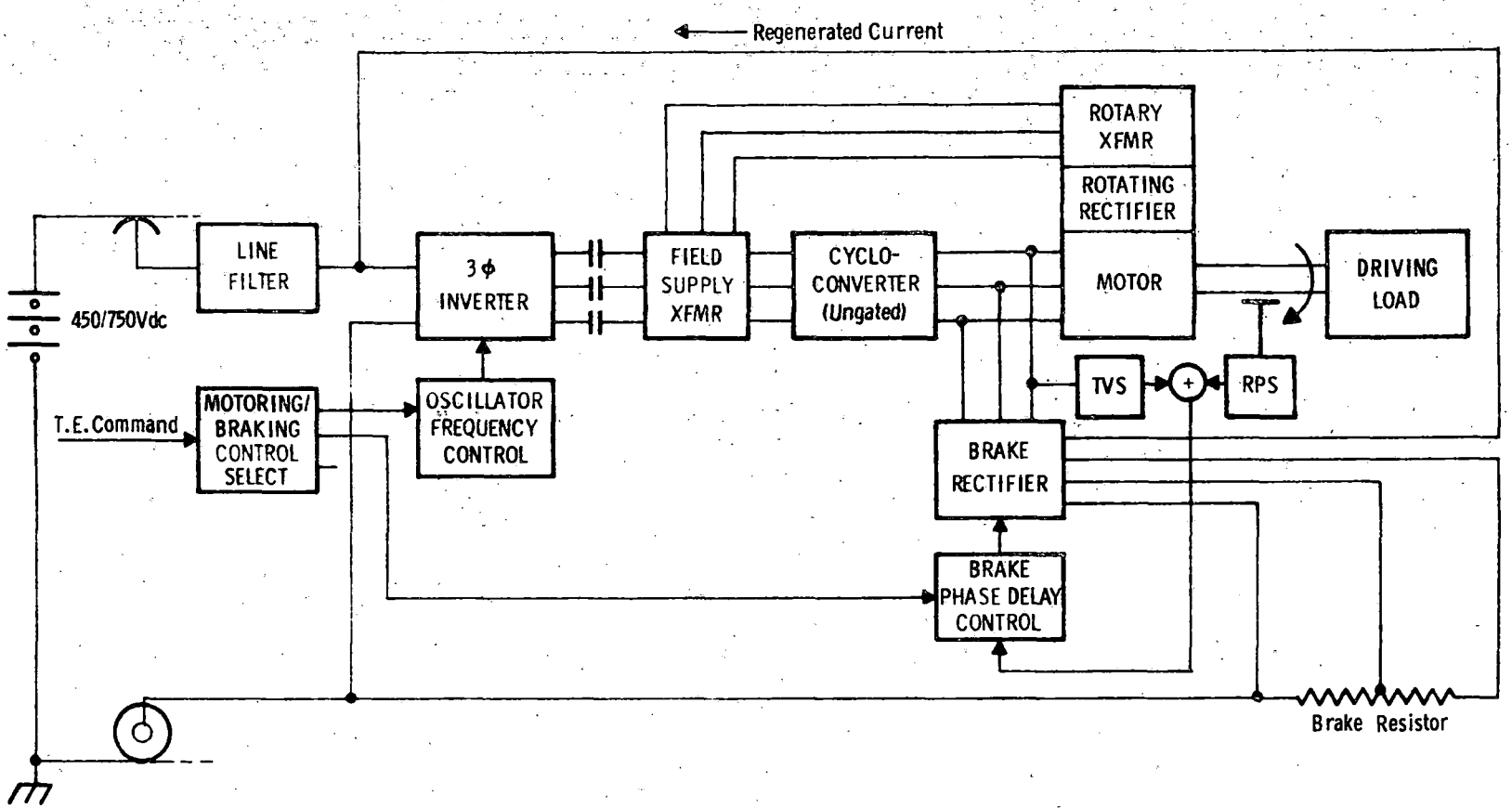

Figure 5.1-7. System Block Diagram – Braking Mode

In mode 1, tractive effort can be controlled by field current. This is desirable to minimize motor heating and torque pulsations. In modes 2-4, a combination of field and phase delay control is used. Phase control is also used for those control functions which require rapid modulation of tractive effort such as slide control, jerk control during mode transitioning, motor overvoltage control, and dc line overvoltage limit control during regenerative braking.

Dynamic braking is accomplished with only one brake resistance change to maintain full braking effort while slowing from 80 mph to approximately 7 mph. This single resistance change contrasts with the typically six resistance changes required for a dc motor propelled transit car. The greater range of high power operation with the synchronous motor propelled transit car is principally due to the use of a static rectifier external to the machine instead of a rotating mechanical commutator.

5.1.3.3 Brake Rectifier

The brake rectifier unit consists of nine SCRs in a dual semi-converter circuit with a tenth SCR used for brake resistor shunting. These are ungated in the motoring mode. These SCRs are cooled with externally grooved heatsinks identical to those used to cool the cycloconverter SCRs.

5.2 TRAIN CONTROL FUNCTIONAL CHARACTERISTICS

5.2.1 INTRODUCTION

There are two sets of Train Control Electronics (TCE) per railcar, one for each of the propulsion systems. The TCE is implemented with a digital computer utilizing microprocessor elements and conventional input/output (I/O) interface devices. The basic role of the TCE is to provide the interface control functions for the major subsystems of the railcar.

It monitors information in the form of analog and discrete signals from the trainlines (TL), m ..er controller, M/A set, and the synchronous brake system (SBS), and weight and speed sensors as well as from the propulsion system elements. In turn, it performs required calculations, makes logical decisions and produces the required control responses.

A summary of the TCE functional requirements is given in Table 5.2-I.

- Rate Adjustments
- Acceleration/Deceleration Open Loop Control
- Maximum Speed Control
- Jerk Limiting
- P-Signal Interpretation
- Brake Blending-Dynamic/ Regenerative/Friction
- Load Weight Compensation
- Wheel Spin-Slide Protection
- Friction Brake Transformation
- Roll Back Prevention
- Control Response (Dead) Time
- Speed Sensing (Velocity/ Acceleration/Jerk)
- Wheel Wear Compensation
- Quick Shutdown (QSD)
- Direction - Drive/Brake Control
- Emergency (Vital) and No Motion Relay
- Propulsion Trip/Reset
- Operational Status Lights
- Main Contactor, Control
- Coolant, Pressure and temperature
- Motor Current/Voltage/Power Monitor and Control
- Dynamic Resistor Select

Table 5.2-I. Summary of Train Control Requirements

Figure 5.2-1, Train Control Functional Mechanization, shows the role played by the TCE within the propulsion system. Most of the inputs, outputs and control functions are illustrated in this drawing. The large blocks on the right hand side show the inputs and outputs related to the motor controls. The outputs control tractive effort, speed, direction, QSD, drive, brake, etc. The large blocks on the left indicate inputs and outputs related to the master controller and train lines. Interconnections with the SBS are shown in the center of the figure.

5.2.2 TRAIN CONTROL OPERATION

The two TCEs of a car are identical, permitting one of the propulsion systems to keep functioning in case of failure of the other. However, some critical signals, such as axle speed, electrical braking effort, spin-slide indication, etc., are cross-coupled. This gives the TCE increased capability in decision making when both propulsion systems are operating properly.

Starting from a power-off condition, several signals must be present before the propulsion system can be operated. Cab mounted circuit breakers must be turned on prior to vehicle movement: control station, forward TL, reverse TL, motor-alternator control, hand brake,

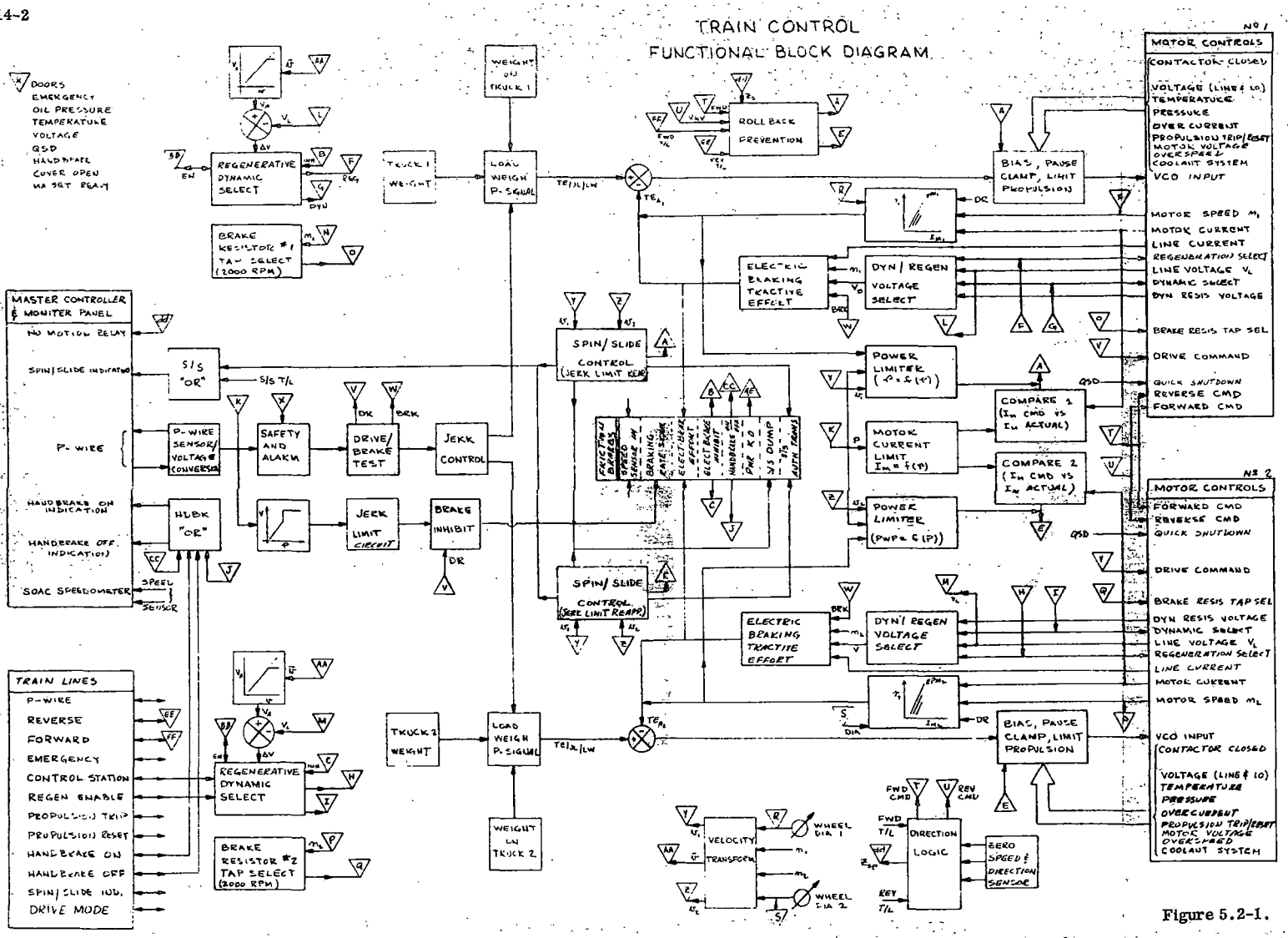

Figure 5.2-1.

Train Control – Functional Block Diagram

A

B

5.11

cutout control, propulsion control unit, brake control unit, door indicator, and door control. Other circuit breaker closures are optional and will probably be used, but are not required to move the car. The motor-alternator is normally started at this point in the start-up so that all systems using 60 Hz, 3 phase, 230 volts are supplied. Air pressure must be built up in the friction brake system. After the motorman has closed all doors, removed all parking brakes, and selected forward or reverse, the propulsion system should be ready to operate in the motoring mode upon a command initiated by the motorman moving the P-signal hand control forward. The TCE for each truck in the train monitors the P-signal command, as well as its own set of inputs (from its motor, cooling system, etc.), plus the trainlines, which all TCEs see. If a truck is not functioning properly, a trainline will indicate this to the motorman. However, this will not prevent him from proceeding to move the train. It is left to the judgment of the motorman (by sensing train response) to determine when too many trucks are inoperable to drive the train. No method was devised to provide (in the cab control station) information on the number and location of malfunctioning truck systems.

Safety and alarm signals consisting of cooling system indicators, QSD, etc., are fed from and to the TCE. Should a no-go condition be interpreted from any of these signals, the propulsion system would be automatically shut down and the vehicle brought to a controlled stop or allowed to coast, depending on the particular anomaly. Operational information consisting of signals required for normal car functioning, such as car weight, wheel speed, contactor closed, etc., all route through the TCE. These signals are used in scaling the propulsion and braking efforts, as well as for monitoring the car movement during a stopped or reversing condition.

The actual propulsion or braking command is fed into the system as a varying current level (P-signal) from zero to one ampere and is used to control the train over the complete range of full service brake to full tractive effort. A given P-signal commands a percentage of maximum motor current. This commanded level of motor current is compared with the actual measured motor current and the TCE adjusts the VCO command to achieve the desired current and tractive effort. In the drive mode, the tractive effort is a function of motor speed, motor current, and wheel diameter. The P-signal is conditioned by the jerk-limiting function such that the tractive effort commanded is limited to a maximum rate of change of 2.0 mphpsps in response to a step controller input. The level of command requested by the P-signal may be decreasedby correction factors introduced by car weight, coolant temperature and coolant pressure.

Preceding page blank

The propulsion system always maintains spin control authority. Slide control authority is divided between the synchronous brake system (SBS) and the propulsion system. The TCE senses velocity and monitors SBS events. Based on the information received, the TCE transfers authority and removes electric brake effort, or sends the SBS a slide dump signal and reduces electrical tractive effort.

The SBS monitors the electrical braking effort and the braking rate signal such that friction brake blending is provided as required. The SBS carries the burden of the total braking responsibility and must supply the difference between commanded braking and applied braking. The electrical brakes supply as much braking as is commanded or as much as the electrical braking capability allows.

When a braking command is received, regeneration of one motor is attempted to test receptivity of the line. If the commanded braking level is established, then the motor remains in regeneration and the second motor is enabled to attempt regeneration.

If less than 100% is established, then that motor is switched back to dynamic braking. Dynamic resistor tap selection is changed at about 2000 r/min. Below 2000 r/min the lower resistance value is in effect.

Rollback is prevented. When the P-signal indicates coast and the no-motion relays indicates movement, the VCO commands enough tractive effort to prevent rollback motion.

The TCE performs the operation of closing the main contactors. If, during operation, the main contactor opens, then a VCO clamp is initiated.

Line voltage is monitored by the TCE and corrective action taken for high or low voltage conditions. The TCE also protects itself against B+ anomalies by clamping the VCO for B+ values outside the 25-45 volt range.

A propulsion trip is initiated by the TCE in the event of overcurrent or differential current. Once the fault has been cleared, a manual reset is permissible unless it happens to be a non-resettable fault such as due to differential current.

Motor speed is montiored by the TCE and not allowed to exceed a predetermined maximum of approximately 6000 r/min. The TCE receives forward and reverse information from

trainlines. A zero speed must be sensed before a direction change command is allowed to be transmitted to the motors.

The occurrence of a rail gap may cause a loss of rail voltage and coolant pressure. Low coolant pressure will be ignored for 7.0 seconds before any action is taken. Loss of third-rail voltage for more than 2.0 seconds will cause the main contactor to open. Loss of third-rail voltage for more than 15.0 seconds will cause a QSD.

A step-by-step description of the flow through the Train Control is provided with detailed flow diagrams in Appendix A.

5.2.3 FAIL SAFE CONSIDERATIONS

Correct interpretation of the P-signal transformation to the friction brake system was an important design consideration. The design goals required it to be a reliable, fail safe, redundant circuit.

A simplified mechanization of the Fail-Safe Redundant P-Transform Circuit is shown in Figure 5.2-2. This mechanization shows the control functions necessary to establish fail-safe control. The requirements to satisfy fail-safe operation are as follows:

(1) Microprocessor P-Signal Input Requirements

$P_{1,0} = P_{2,0} \pm 2.15\%$.

If $P_{1,0} \leq 1V \pm 0.2V$,

then $P_{1,1} = 1V$.

When $P_{1,0} > 1V < 4.75V$,

$P_{T1,1} = 1.684\ P_{1,0}$.

If $P_{1,0} \geq 4.75V$,

then $P_{T1,1} = 10V$.

(2) P-Transform and Fail Detect Requirements

When $P_{TBB} \geq P_{T1,0} + 2\%$,

or $P_{TBB} \geq P_{T2,0} + 2\%$,

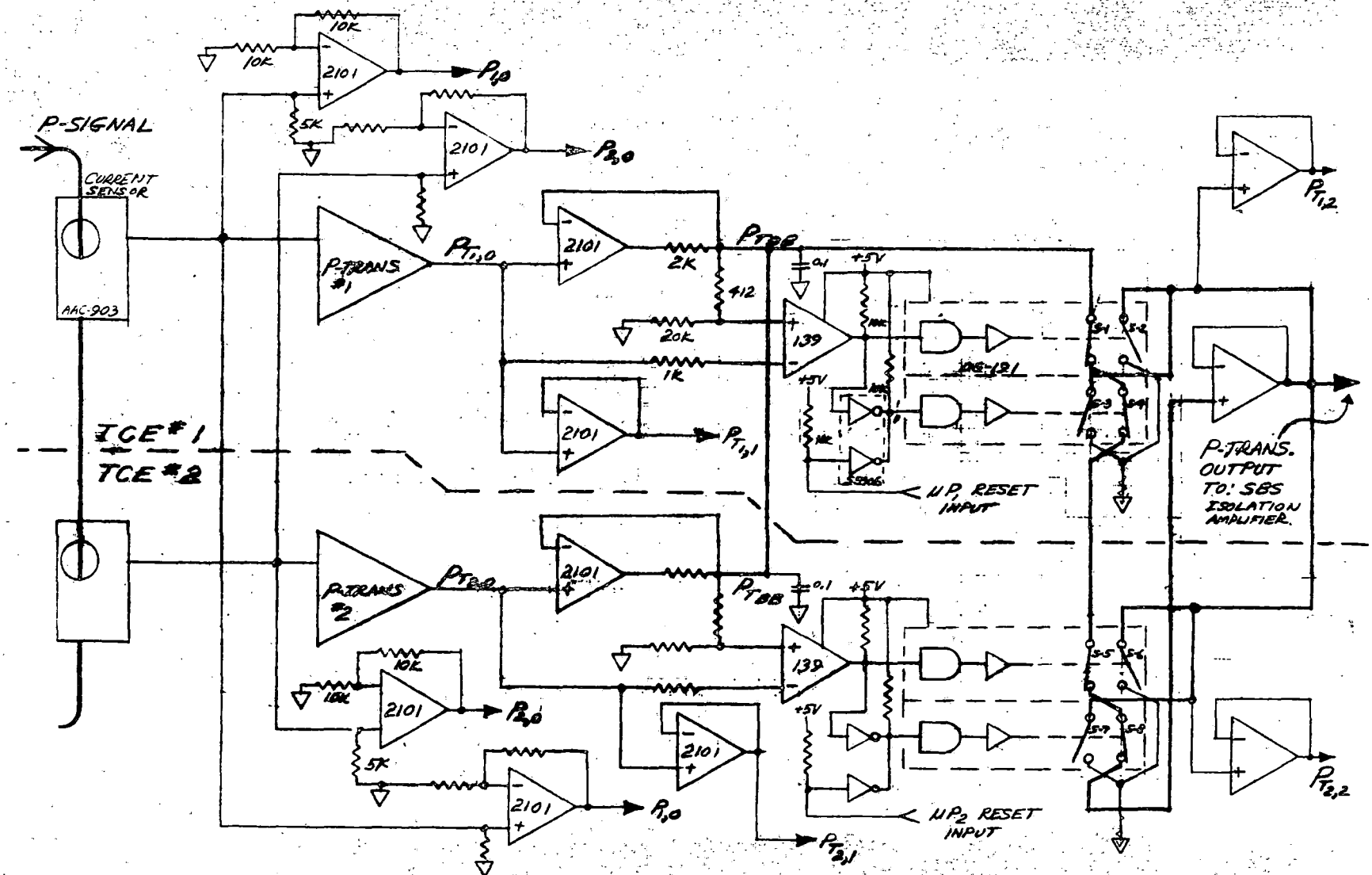

Figure 5.2-2. Fail Safe P Transformation Mechanization

P-TRANS output shall be equal to OV_{DC}(GND).

When $P_{T1,0} \leq P_{T2,0}$,

then $P_{TBB} = P_{T1,0}$,

Because if $P_{T2,0}$ fails to B+ or V+, then $V_{T1,2}$ inverting input becomes -V+.

$$\therefore P_{TBB} = P_{T1,2} + (V_+ - V_+)$$

$$= P_{T1,2} .$$

Since V_+ fail can be ± 12 Vdc and, with the output P-TRANS, output equals to $P_{T1,0} + P_{T2,0}$.

It can be seen that the failure of $P_{T2,0}$ in a hard positive (V+) condition limits the negative swing of P_{TBB} to

$$\frac{-2\ (V_{T1,0}) + V_+}{2} ,$$

where $V_{T1,0}$ represents the output dynamic range of the non-failed output.

Therefore, the range of the output

$$P_{TBB} = \frac{-2\ (12V) + 12V}{2}$$

$$= \frac{(-24 + 12)\ V}{2}$$

$$= -6V ,$$

or if the fail was V_-,

$$P_{TBB} = +6V \text{ range},$$

which would be lower than the maximum 10V signal and would represent no braking.

Conclusion: The redundant circuit, with the balanced compensating buffered output and buffer fail FET clamping override, plus redundant microprocessor override capability, can be considered FAIL-SAFE.

The flow diagram illustrating the microprocessor's contribution to this fail safe design is shown in Figure 5.2-3. Essentially the microprocessor is being used as a level comparison and glitch filter. For a given P_{10}, $P_{T\,11}$ must yield a predetermined value within a given tolerance or the brake rate command is clamped.

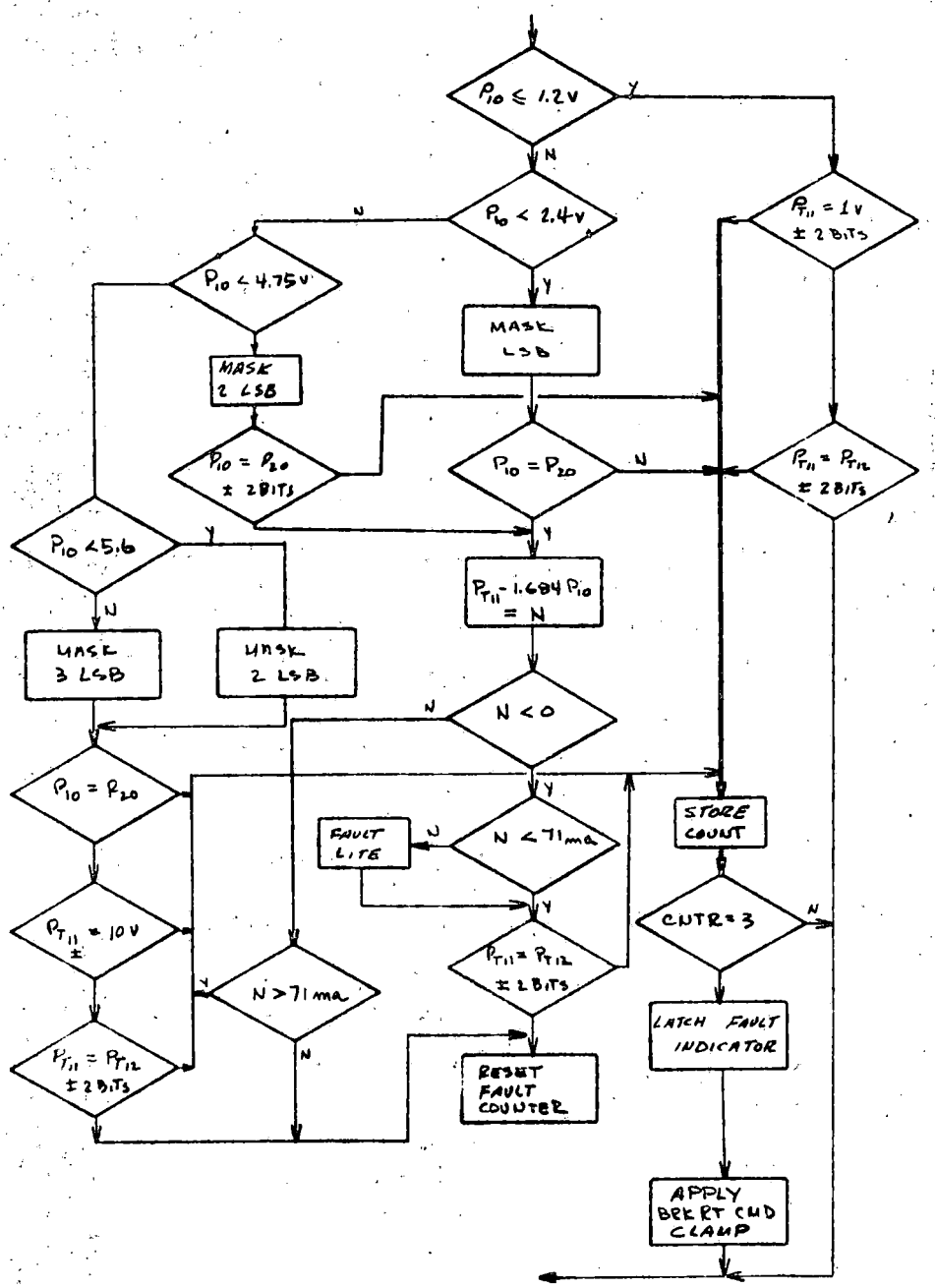

Figure 5.2-3. Microprocessor Failsafe Output Control

5.3 MOTOR CONTROL CHARACTERISTICS

5.3.1 MOTORING MODE

A simplified block diagram of the drive system in the motoring mode was shown in Figure 5.1-3. Motor stator current, equal in amplitude to the cycloconverter input current, is controlled by varying the three-phase inverter frequency over a range of 350 Hz to 1200 Hz. Current increases with frequency primarily because of the decrease in coupling capacitor reactance and also because of the increase in inverter output voltage with frequency. The cycloconverter stage converts the inverter frequency current into a lower frequency motor current. The phase of the motor current with respect to shaft position and line voltage is established by cycloconverter control signals derived from a rotor position sensor (RPS) and a counter EMF (CEMF) sensor. Motor torque reversal is accomplished at the logic level by inverting the RPS timing signals.

Motor field current is derived from a high frequency field supply transformer connected as a current transformer (CT) in the motoring mode. The low impedance winding of the transformer is in series with the cycloconverter input (the high impedance winding used in the braking mode is open circuited with a relay in motoring). The CT transformer secondary is connected to the primary of rotary transformer (RT) in the motor. The RT secondary is connected to the rotating rectifier which supplies dc current for the field winding. Because the field current is derived from a CT operating on a current approximately proportional to stator current, the traction machine operates in a manner similar to a dc series motor in the motoring mode.

The motor field and stator currents are not exactly proportional because of the CT and RT reactances and because of the RT speed sensitivity. The RT has an airgap which is large compared to that of a conventional transformer. Thus the magnetizing current is relatively large at the lower operating frequencies and this reduces the ratio of field to stator current. The RT is of phase-wound construction and thus is sensitive to shaft speed and direction of rotation. The sensitivty to speed is low because of the current source primary excitation supplied by the CT and also because of the high frequency of this excitation. The speed sensitivity of the RT is made equal in both directions of rotation by reversing the phase sequence of the inverter when the motor direction of rotation is reversed.

The motor power factor angle, θ, is held near zero below the motor base speed of 1646 r/min to maximize the torque-to-stator current ratio, and is programmed to vary with speed, N, above base speed approximately as

$$\theta = -12.4^{o} + 0.0075N \text{ for } 1646 < N < 5642 \text{ r/min}$$
$$\theta = 30^{o} \text{ at } 5642 \text{ r/min.}$$

This achieves the equivalent of field weakening, thus avoiding an excessive maximum motor voltage requirement. The power factor programming method utilizes the motor CEMF as a timing signal.

Motor voltage is proportional to speed and is a function of motor current and power factor angle.

The timing diagram in Figure 5.3-1 shows the response of the inverter, cycloconverter, and motor to a ramp increase in inverter frequency command. The resonant frequency of the inverter is 1500 Hz. For an inverter gating frequency of less than 1500/2 = 750 Hz, the inverter output voltage appears as a set of isolated half-sine pulses. For frequencies above 750 Hz, these pulses blend to form an approximate sine wave output.

The current through the coupling capacitors and field supply current transformer into the cycloconverter is a semi-trapezoidal wave at the lower inverter frequencies with oscillatory components at the transition points. At higher frequencies, the cycloconverter input current becomes a six-step square wave with amplitude increasing with frequency. The motor phase current is the rectified equivalent of the cycloconverter input current during motor current conduction periods. The low frequency motor current waveform is shown making the transition from positive current to zero current to negative current, then to zero and positive current again. The motor line to neutral voltage is shown retarded in phase from the motor current, indicative of leading power factor. The motor voltage has a ripple component at six times the inverter frequency caused by phase current undulation and motor leakage inductance. This ripple voltage decreases with increasing inverter frequency. The motor fundamental voltage component is shown increasing with inverter frequency, even though motor speed is shown as constant. This is due to the increase of flux resulting from the increasing series field current.

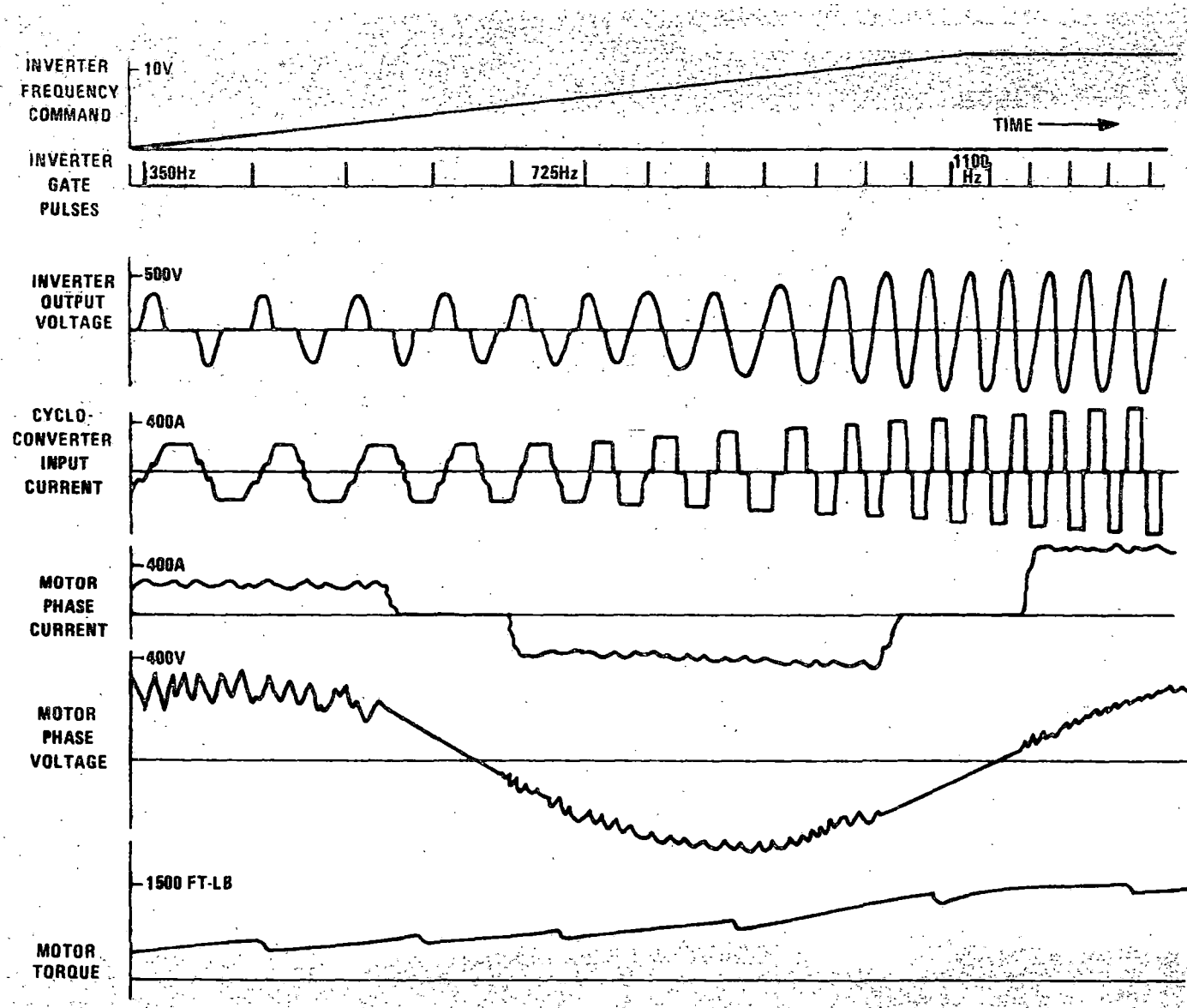

Figure 5.3-1. Timing Diagram, Motoring Mode

5.3.2 BRAKING MODE

Drive elements active in the braking mode were shown in the block diagram of Figure 5.1-7. The traction machine operates as a separately excited generator in braking. The high frequency field supply transformer is changed from a CT to a VT (voltage transformer) with a contactor, connecting the high impedance windings through a 3.0 μF coupling capacitor to the inverter. The cycloconverter gate signals are removed, de-energizing the CT primary winding of the transformer. Field current is controlled by varying the inverter frequency.

The traction machine is connected to a nine-SCR dual phase delay rectifier which is gated in the braking mode to provide dc dynamic brake resistor current or dc regenerative brake current to a receptive third rail. Braking effort is modulated by a combination of field current control and phase delay control. Simultaneous dynamic and regenerative braking can be obtained by operating one truck in dynamic and the other in regenerative braking, or by operating each truck in dynamic and regenerative braking simultaneously. The former method may be preferable because braking effort can be controlled primarily with field control, which gives lower inverter and machine losses and lower amplitude torque pulsations. The rapid torque control response available with phase delay gating is required to control wheel slide and to limit jerk.

At speeds below approximately 2000 r/min, a portion of the dynamic brake resistance is shunted with an SCR to extend dynamic braking tractive effort to a lower speed.

5.3.2.1 Phase Delay Braking Response

Figure 5.3-2 is a plot of normalized average dynamic brake rectifier output voltage and current as a function of phase delay angles for the idealized case of zero generator impedance. Figure 5.3-3 is a timing diagram showing the instantaneous dynamic brake current and torque response to a ramp increase in brake effort command. For delay angles less than 90°, current flows in discrete pulses at a fundamental frequency of three times the generator frequency.

The instantaneous airgap torque is found from the mechanical and electrical power equivalence as

$$T = \frac{i^2 R}{\omega} .$$

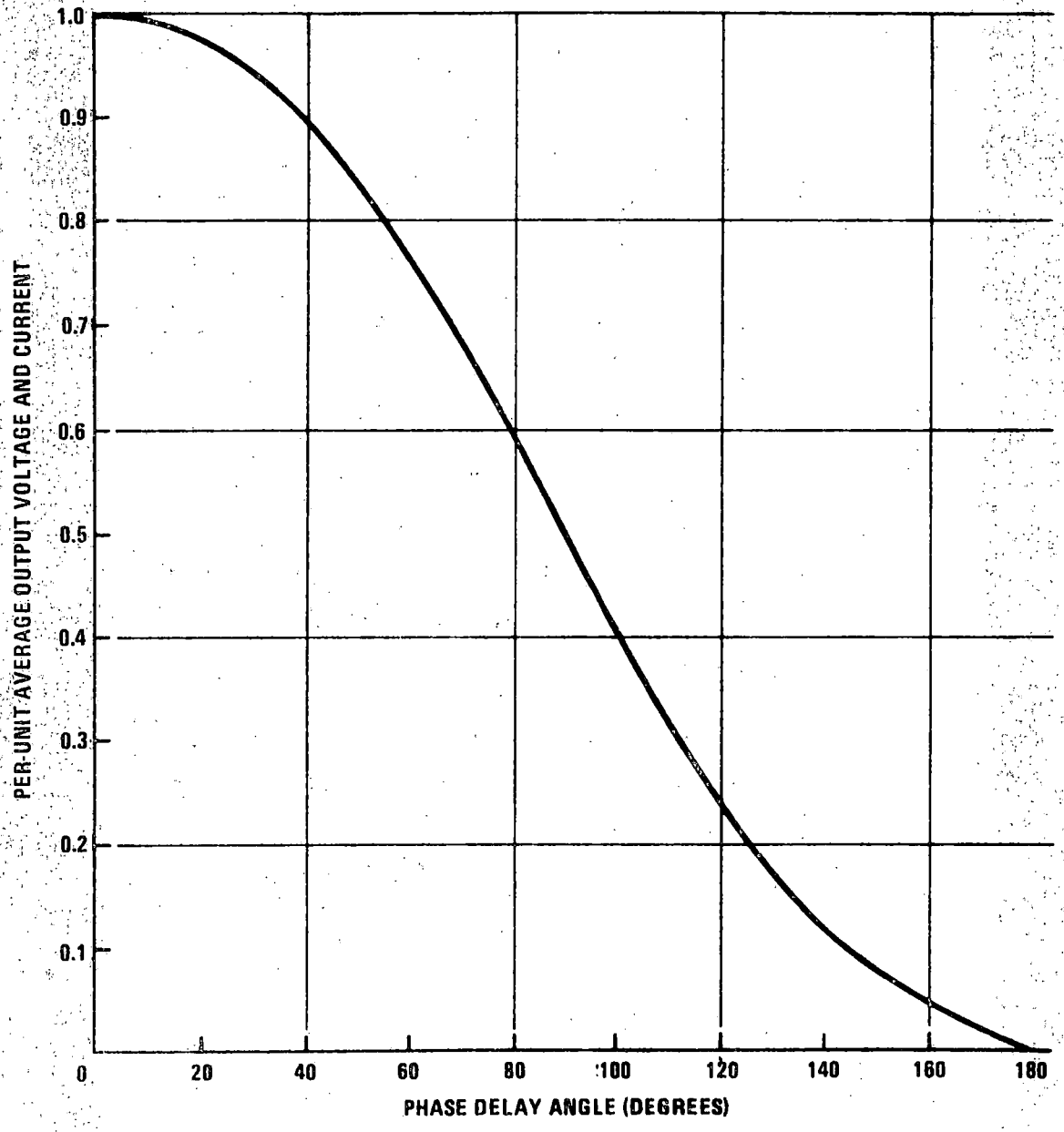

Figure 5.3-2. Dynamic Brake Rectifier Phase Control Characteristic

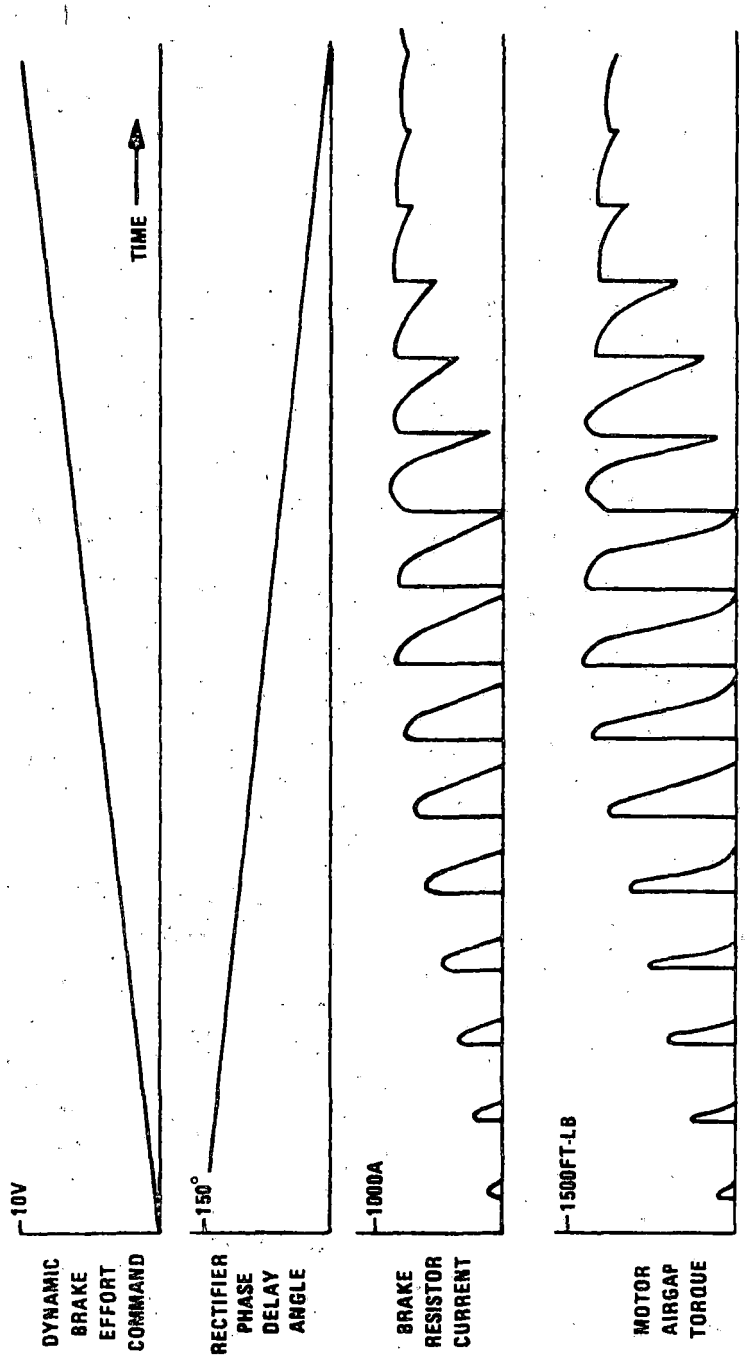

Figure 5.3-3. Timing Diagram, Dynamic Braking Phase Control

Since the generator velocity ω and brake resistance R are constant, instantaneous torque varies as the square of instantaneous current. The torque thus tends to have a higher peak to average ratio than the current. This peaking effect is shown in the sketch of torque versus time in Figure 5.3-3.

A timing diagram showing regeneration brake current and torque in response to a ramp braking effort command is shown in Figure 5.3-4. Again, by equating mechanical and electrical power, the airgap torque is

$$T = \frac{ei}{\omega} .$$

In regeneration, voltage as well as speed is constant so that the instantaneous airgap torque has the same waveform as current, as shown in Figure 5.3-4.

5.3.2.2 Field Control Braking Response

With field control only, the SCRs in the dynamic or regenerative brake rectifiers are gated as diodes with zero phase delay. Figure 5.3-5 shows how inverter frequency, generator field current, dynamic brake resistor current, and airgap torque respond to a ramp increase in braking effort command. The principal result of field controlled braking is a large reduction in torque pulsation compared to phase delay control.

Curves of regenerative brake rectifier response with field control would show current and torque profiles similar to that obtained in dynamic braking.

5.3.3 DRIVE RESPONSE TO LINE VOLTAGE VARIATIONS

Line voltage variations consist of low frequency components that are unaffected by the input line LC filter and higher frequency components which are attenuated by the filter.

For low frequency line voltage variations, the inverter input power varies as the square of the line voltage if inverter frequency and motor speed are held constant. In the operating system, the closed loop tractive effort control varies the inverter frequency to maintain tractive effort (and dc input power) approximately constant in response to low frequency line voltage variations.

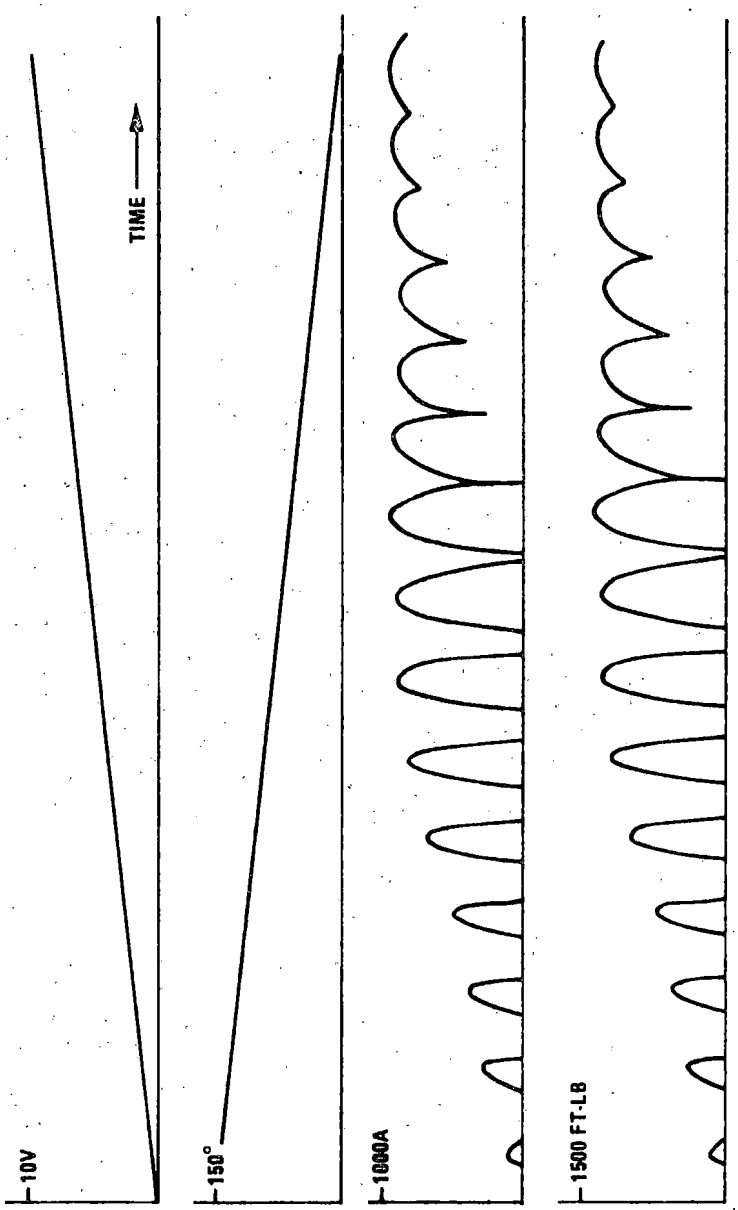

Figure 5.3-4. Timing Diagram, Regenerative Braking Phase Control

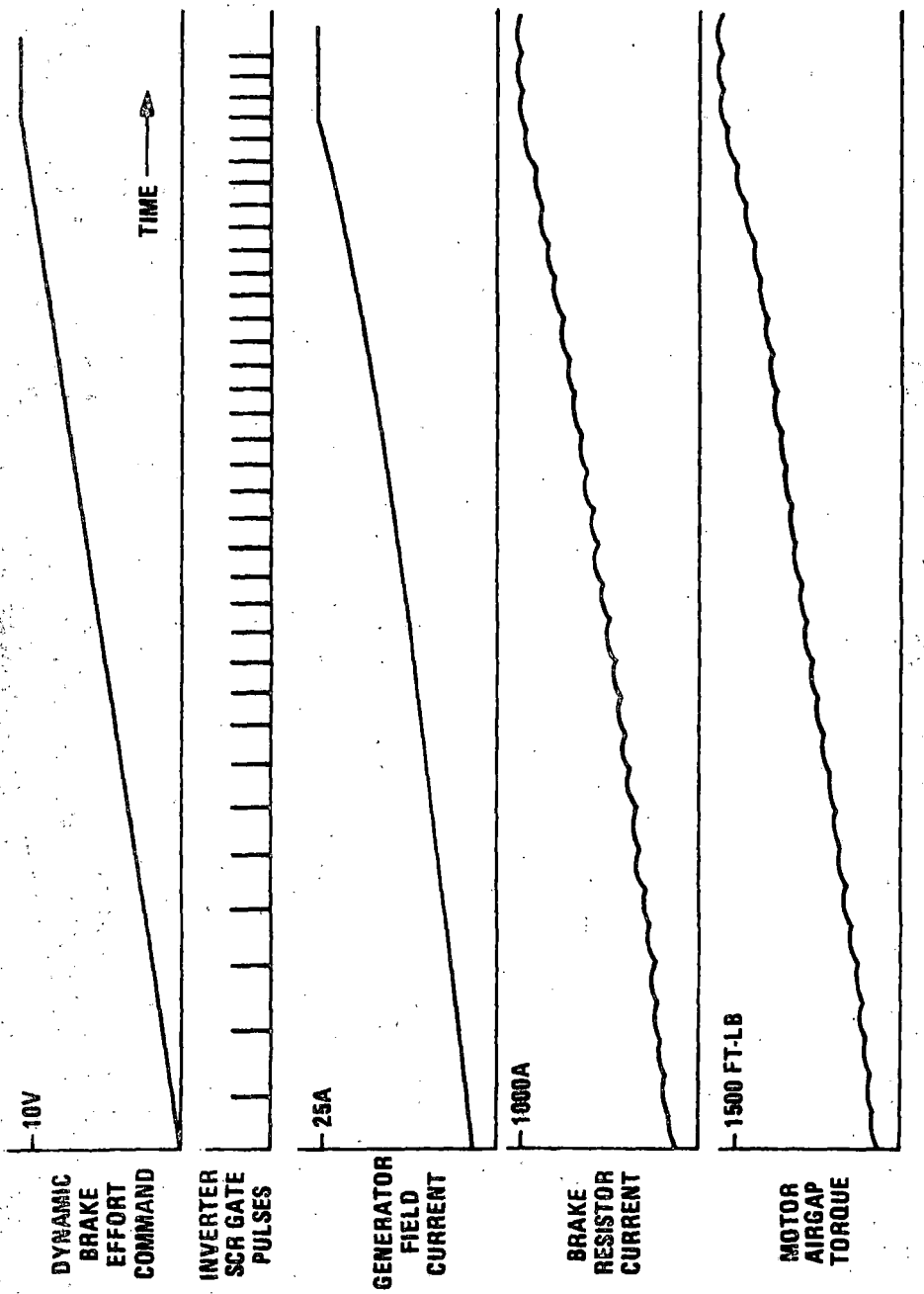

Figure 5.3-5. Timing Diagram, Dynamic Braking, Field Control

Rapid line voltage variations are attenuated by the input filter shown in Figure 5.3-6. The power source is modeled as a dc and ac voltage source, $E_{dc} + D_{ac}$, in series with resistive and inductive components which simulate the impedance characteristics of the 3rd rail. The ac voltage source represents power supply 360 Hz ripple voltage and the effect of intermittent loading of the supply by other transit cars. The third rail sliding contact is represented by switch S with the on-board contactors shown as S1 and S2.

The line filter consists of the dual inductor and the two capacitor banks at the input to the No. 1 and No. 2 power converters. The nominal inductance and capacitance (S1 and S2 closed) of the line filter are 0.0025H (for low current values) and 0.0176F. This yields a resonant frequency of 24.0 Hz and a resonant impedance of 0.377 ohm.

The damping resistance, R_d, is adjusted by inserting a metal sheet into the air gap. The sheet is equivalent to a resistive one-turn winding coupled to the inductor winding. As R_d is increased, damping is increased, and the voltage overshoot seen at the filter capacitor is reduced. A damping factor of approximately 0.4 (with both motor drive deenergized) is desired.

The capacitor bank voltage response to an applied step voltage is shown in Figure 5.3-7. The damping ratio of 0.4 gives a peak capacitor bank voltage overshoot of 25%. Figure 5.3-8 shows the input surge current transient for several damping factors. For $\zeta = 0.4$, it can be seen that

$$i_{smax} = 0.91E/Z_r.$$

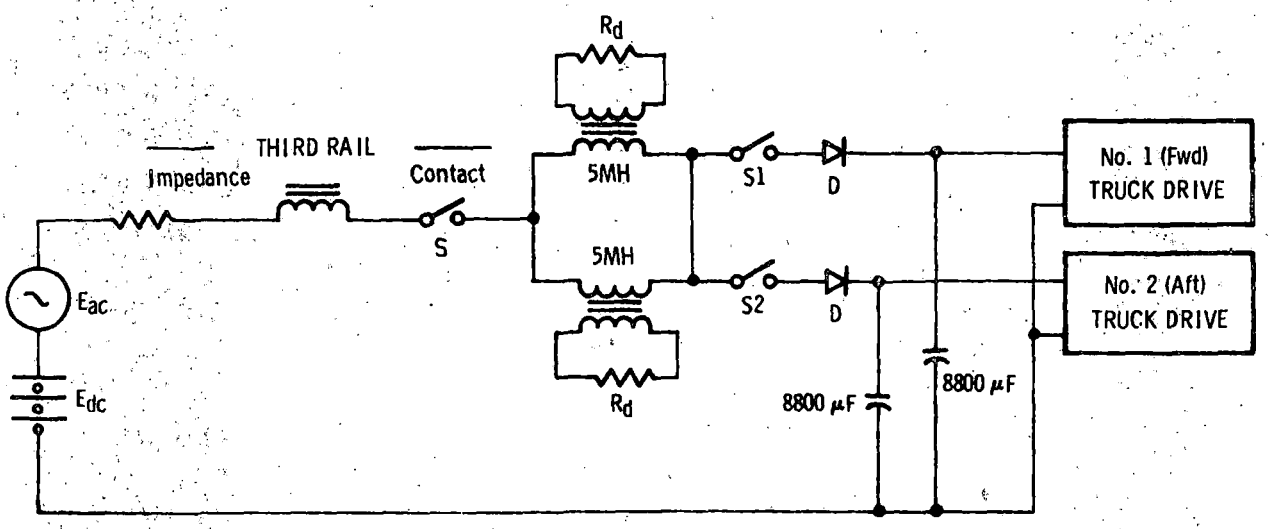

Figure 5.3-6. Power Supply and Line Filter Equivalent Circuit

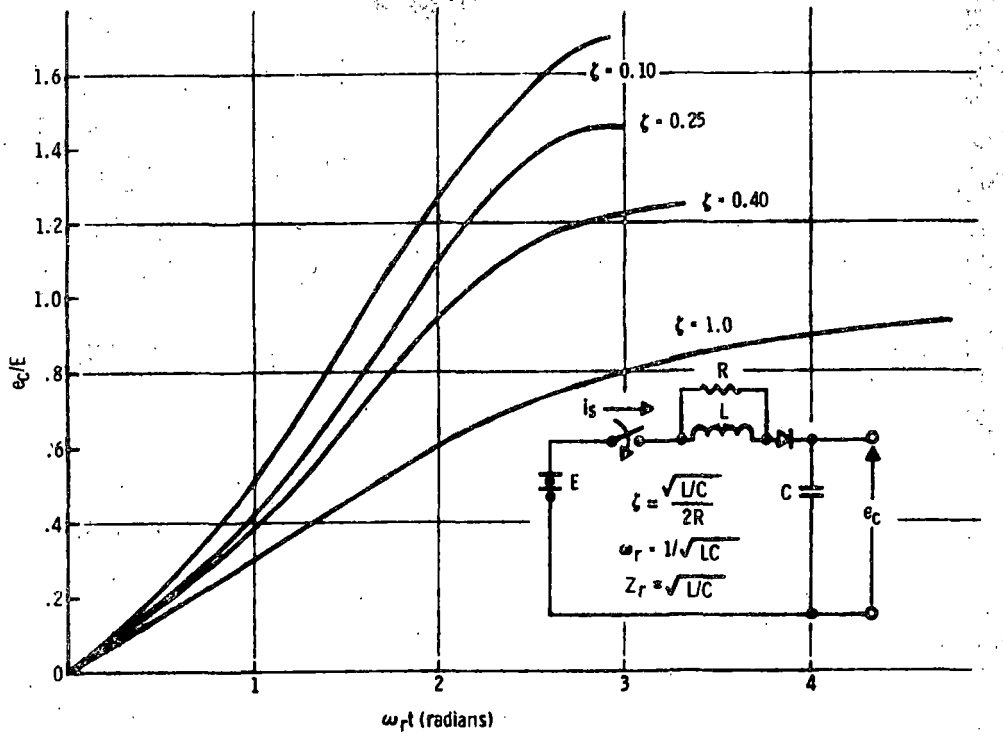

Figure 5.3-7. Capacitor Bank Voltage Response to Applied Line Voltage

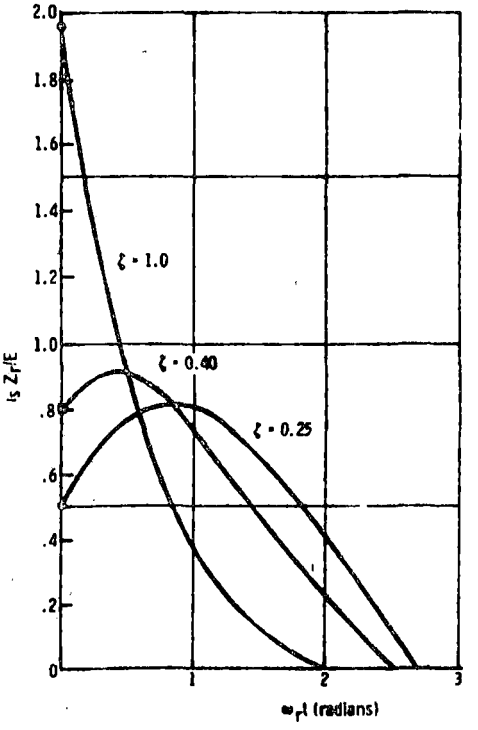

Figure 5.3-8. Line Filter Input Current Response to Step Applied Voltage

For L = 0.0025H and C = 0.0176F (both line contactors closed),

$Z_r = \sqrt{0.0025/0.0176} = 0.377$ ohm. For E = 600 Vdc,

$i_{smax} = 0.91 \times 600/0.377 = 1448$ A-peak.

5.3.4 OPERATION OVER RAIL GAPS

5.3.4.1 Motoring Mode

Operation over a rail gap is equivalent to an opening and subsequent reclosing of switch S, shown previously in Figure 5.3-6. During the opening of the switch, energy stored in the inductor is dissipated in an arc at the third rail contact shoe. Capacitor bank voltage drops rapidly at an initial rate of

$$\frac{de_c}{dt} = \frac{I_o}{C}$$

An alternative to dissipating the energy in the arc at the Contact shoe is to install a free wheeling diode across the line inductor. This permits the energy to momentarily remain stored in the inductor. The disadvantage of this approach is that decreases in the 3rd rail voltage due to other loads appear immediately at the ASDP inverter. The potential consequences of these voltage decreases have not been fully evaluated.

During acceleration the motoring current per car reaches approximately 1400 Adc, so that with C=0.0176F

$$\left.\frac{de_c}{dt}\right|_{t=0} \leq \frac{1400}{0.0176} = 79{,}500 \text{ V/sec} .$$

The capacitor bank voltage sensor and undervoltage control act to remove the inverter and cycloconverter gate signals and open the main contactors. The dynamic brake rectifier is momentarily gated to snub the motor overvoltage that results when the power converter is shut down at high speed. After the rail gap is crossed, the third rail contact is energized. The re-applied line voltage is sensed and the main contactors are re-closed to charge the capacitor bank as shown in Figure 5.3-7. If the railcar crosses a gap between a live and a dead third rail, the blocking diodes shown in Figure 5.3-6 prevent any remaining charge on the capacitors from being applied to the de-energized rail section. When the capacitor bank is re-charged to a normal operating level, typically 450 Vdc, the inverter and

cycloconverter gating is re-applied, with the inverter gating frequency ramped from a low frequency to the normal operating frequency.

5.3.4.2 Dynamic Braking Mode

The current drawn by the two inverters in dynamic braking does not normally exceed 80 Adc. The initial rate of decay of capacitor bank voltage is then

$$\frac{de_c}{dt}\Big/_{t=0} = \frac{80}{0.0176} = 4550 \text{ V/sec.}$$

When the capacitor bank voltage decays to the threshold level, inverter gate signals are removed and the main contactors are opened. The dynamic brake rectifier gate signals are maintained because the relatively slow decay of generator field current (time constant typically 1.0 second) permits significant braking effort while crossing the rail gap.

5.4 TRAIN PERFORMANCE ANALYSIS

This subsection describes a digital computer program developed as an aid in establishing propulsion system characteristics to meet specified performance criteria, and to calculate train performance parameters for given propulsion system characteristics.

The computer program can be used to evaluate performance over a single segment of track, or over a complete transit route consisting of many segments with station stops.

Also discussed are the primary performance requirements upon which the propulsion system design was based and the results of a computer analysis performed to verify adequacy of the system design.

5.4.1 PERFORMANCE ANALYSIS COMPUTER PROGRAM

The digital computer program developed for the evaluation of train performance has evolved into one which is moderately large and complex (about 2000 FORTRAN statements). A more detailed description of the program including the analysis used in deriving the necessary equations can be found in Appendix B.

The program simulates train motion under the various constraints imposed by input conditions, viz., segment distance, with profiles of grade, curve and tunnel, desired speed, maximum acceleration, minimum and maximum deceleration, and maximum absolute jerk (time rate of change of acceleration) while starting and stopping. Above a specified speed, friction braking to meet the minimum deceleration criterion is optional. Electrical braking (either regenerative or dynamic; i.e., resistive) is optional and governed by the motor torque specification when the motor is in the generating mode, i.e., negative torque applied to motor shaft. A motor speed may be specified to switch from regenerative to dynamic braking when the train is decelerating. However, regenerative and dynamic braking cannot be concurrent although the design of the system might permit this. Electrical braking is limited by the maximum deceleration criterion. The program also accounts for system dead times and specified station dwell times as well as head and tailwinds.

For purposes of this program, the propulsion system is considered to consist of three major elements: power controller, traction motor and gearbox.

Motor performance is specified in tabular form in both the motoring and generating modes wherein shaft torque is given as a function of shaft speed (rpm). The program is based on the assumption that both tables (motoring and generating) are, at most, double valued functions of shaft speed. The gearbox losses are also specified by similar tables of shaft speed. The gearbox losses are also specified by similar tables of motor shaft (counter) torque versus speed which, at the user's option, may be different for each operating mode. An additional degree of freedom allows specification of a maximum efficiency for the gearbox. The power losses for the motor are also tabular, the loss being given as a function of both torque and speed. Tables for each mode of operation must be provided. Power dissipation in the power control electronics is assumed to be independent of motor/generator speed, but a function only of torque. (In this system torque is approximately linearly proportional to motor current.) Again, tables for both motoring and generating modes must be provided. All tables are assumed to be polygonal functions, since the program is coded to interpolate linearly in the tables. Extrapolation has not been provided for within the program, so that adequate bounds must be included in all tables.

Rotary inertia, i.e., inertia of rotating parts, has been accounted for in the analysis by increasing the actual train mass, m, by a multiplicative factor, $\rho > 1$, so that the effective train mass is ρm. It can be shown that if the actual moment of inertia, I, with respect to the wheel speed, is known, $\rho = 1 + I/mr^2$, where r is the rolling radius of the wheel. Those parts which rotate at speeds different from the wheel must have their moments of inertia multiplied by the square of the speed ratio before summing to obtain the total effective moment of inertia.

Train resistance is the result of coulomb friction, viscous friction, and air resistance. The accepted formulation of train resistance, for purposes of analysis, is the Davis Equation or modifications of it. All forms differ only in the values of the empirical constants and are functions of train weight, (more precisely, the normal force on the track) numbers of axles and cars, and train frontal area, as well as train speed. For a given train configuration the train resistance is a quadratic function only of speed, provided the track is straight and level. If the track is on a grade, the train weight is easily resolved into the two forces which are parallel and normal to the track. The former force is algebraically added to the train resistance and the latter force replaces the train weight in the Davis Equation. Track curvature effects are not as easily resolved since these

effects are dependent on train speed and the track bank angle, as well as the track curvature. It has been assumed in the analysis that the bank angle of the track is precisely what is required to cancel lateral forces as the train negotiates the curve, i.e., a "coordinated turn." Even with this assumption the effect of track curvature is dependent on train speed in such a way that the total train resistance would no longer be a quadratic function of speed. Because the effect of track curvature is minor compared to other effects, it has been approximated so that the quadratic nature of the total train resistance is not disturbed. The analysis of this approximation appears in Appendix A.

Because propulsive and resistive forces are essentially functions of train speed, either directly or indirectly (as in the case of motor shaft speed), train speed was chosen as the independent variable and the format of the output data reflects this choice: All parameters are presented as functions of train speed, V, as can be seen in the excerpted sample run (see next four pages). For brevity, only the first page of input data is included here. All other inputs are tabular: torque-speed tables for motoring and generating and gearbox counter-torque; and power losses (both motoring and generating) in the traction motor as well as the power controller. Output data for the first 27 segments have been omitted; only the final segment output is reproduced. The output headings are, for the most part, self-explanatory. All values are instantaneous except for time, distance, and energy which are cumulative from the beginning of the segment. These three parameters are also totaled from the beginning of the first segment to the end of each succeeding segment of a transit route run. The interpretation of the signs attached to the numerical output may need clarification: negative ACC(eleration) is deceleration; negative JERK, similarly, is an acceleration rate opposing the direction of train motion. Negative (total train) RESIST(ance) implies a force tending to increase the train speed while (train tractive) EFFORT being negative implies a force that tends to decrease the train speed. Negative motor TORQUE indicates that the motor is acting as a generator. Since the column designated POWER is the power at the motor/generator shaft and calculated as the product of (motor) TORQUE and (motor rotational) SPEED, its sign must be necessarily the same as TORQUE. The last three columns are never negative since they represent power dissipations in the various components: CEPD in the power control electronics, MGPD in the motor/generator, and GBPD in the gearbox. The average values of these last three parameters are calculated analytically from the beginning of the transit route and printed at the end of each segment. However, the AVERAGE ABSOLUTE, ROOT MEAN SQUARE,

TRAIN TRANSIT ROUTE ANALYSIS PROGRAM II 13:28 FRI FEB 03,'78

PARAMETER INITIALIZATION

RESISTANCE COEFFICIENTS

R0 = ROLLING RESISTANCE COEFF	29.00000	LB/AXLE
R1 = ROLLING RESISTANCE COEFF	1.30000	LB/TON
R2 = ROLLING RESISTANCE COEFF	.04500	LB/TON/MPH
C0 = OPEN AIR RESIST COEFF	.002400	LB/FT**2/MPH**2
C1 = OPEN AIR RESIST COEFF	.000340	LB/FT**2/MPH**2/CAR
C0B = TUNNEL AIR RESIST COEFF	.002400	LB/FT**2/MPH**2
C1B = TUNNEL AIR RESIST COEFF	.000340	LB/FT**2/MPH**2/CAR

TRAIN PARAMETERS

A = TRAIN FRONTAL AREA	115.00000	SQ FT
RR = ROLLING RADIUS	15.00000	IN
M = TRAIN MASS	95200.0	LB
NA = NUMBER OF AXLES PER TRAIN	4	
NB = NUMBER OF GEARBOXES PER TRAIN	4	
NC = NUMBER OF CARS PER TRAIN	1	
NM = NUMBER OF MOTORS PER TRAIN	2	

PERFORMANCE LIMITATIONS

UD = MAX ACCELERATION LIMIT	3.200	MPH/S
XD = MIN DECELERATION LIMIT	3.000	MPH/S
YD = MAX DECELERATION LIMIT	3.200	MPH/S
UDD = MAXIMUM JERK LIMIT	2.000	MPH/S/S
RDS = REGEN/DYNAM CROSSOVER	8000.00	RPM
HSR = HIGH SPEED BRAKING LIMIT	.00	RPM

DRIVE TRAIN PARAMETERS

ETA = MAXIMUM GEARBOX EFFICIENCY	.9650
GAM = GEAR RATIO (MOTOR/WHEEL)	6.875
RHO = ROTARY INERTIA FACTOR	1.080
TLF = TORQUE LEVEL FACTOR	1.000

PHYSICAL PARAMETERS

GRAV = GRAVITATIONAL ACC	32.17405	FT/S/S
VW = HEADWIND VELOCITY	.000	MPH

STATION PARAMETERS

DEADT = STATION DEAD TIME	.50	S
DWELT = STATION DWELL TIME	20.00	S

I/O OPTIONS

INOPT = INPUT OPTION SELECTOR	2	
OUTOPT = OUTPUT OPTION SELECTOR	2	
VPRNT = VELOCITY INCREMENT (PRINTING)	5.000	MPH

LEGEND FOR KEY

A = ACCELERATION INITIATED
B = MAXIMUM ACCELERATION ATTAINED
C = MAXIMUM MOTOR TORQUE ATTAINED
D = ACCELERATION BLENDING INITIATED
E = PRESCRIBED SPEED ATTAINED
F = MAXIMUM CAPABLE SPEED ATTAINED
G = MOTOR/GENERATOR TORQUE NULLED
H = DECELERATION INITIATED
I = FRICTION BRAKING INITIATED
J = MAXIMUM DECELERATION ATTAINED
K = MAXIMUM GENERATOR TORQUE ATTAINED
L = MINIMUM DECELERATION ATTAINED
M = DECELERATION BLENDING INITIATED
N = FRICTION BRAKING TERMINATED
0 = SPEED INDEPENDENT RESISTANCE CHANGE(S) ENCOUNTERED

Excerpted Sample Run

```
                    T R A I N   T R A N S I T   R O U T E   A N A L Y S I S   P R O G R A M   I I      13:28 FRI FEB 03,'78

ANALYSIS FOR SEGMENT 28 HAVING THE FOLLOWING DESCRIPTION:

          AT DIST =       .00 FT = GRADE CHANGES TO    .5000 %
          AT DIST =       .00 FT = SPEED CHANGES TO  60.000 MPH (BEG)
          AT DIST =       .00 FT = ENTER CURVE (   .8333 DEG)
          AT DIST =  3335.00 FT = EXIT  CURVE (   .8333 DEG)
          AT DIST =  3335.00 FT = GRADE CHANGES TO  1.0171 %
          AT DIST =  3960.00 FT = SPEED CHANGES TO    .000 MPH (END)
```


Excerpted Sample Run

TRAIN TRANSIT ROUTE ANALYSIS PROGRAM II 13:28 FRI FEB 03,'78

DETAILED ANALYSIS FOR SEGMENT 28

	<-- PER TRAIN -->								<-- PER MOTOR -->					
KEY	SPEED (MPH)	TIME (S)	DIST, (FT)	ACC, (MPH/S)	JERK (MPH/S/S)	RESIST (LB)	EFFORT (LB)	ENERGY (W-HR)	SPEED (RPM)	TORQUE (LB-FT)	POWER (HP)	CEPD (KW)	MGPD (K_M)	GBPD (KW)
A	.000	.500	.00	.000	2.000	653.9	653.9	.0	.0	72.1	.00	1.197	.865	.000
C	2.071	1.939	1.46	2.878	2.000	659.5	14147.9	23.3	136.3	1560.0	40.48	25.896	16.254	1.062
	5.000	2.957	6.74	2.874	-.004	671.5	14144.0	77.7	329.1	1560.0	97.76	25.896	20.979	2.586
	10.000	4.699	25.90	2.866	-.006	702.9	14136.3	231.7	658.3	1560.0	195.52	25.896	26.327	5.247
	15.000	6.447	57.95	2.855	-.007	748.1	14127.6	461.4	987.4	1560.0	293.28	25.896	29.978	8.000
	20.000	8.203	103.02	2.840	-.009	807.1	14117.5	766.2	1316.5	1560.0	391.04	25.896	32.702	10.867
	25.000	9.969	161.31	2.822	-.011	880.0	14106.5	1146.8	1645.7	1560.0	488.80	25.896	35.083	13.857
	30.000	11.936	240.90	2.302	-.220	966.6	11765.0	1606.7	1974.8	1302.1	489.58	21.615	29.124	14.455
	35.000	14.323	354.91	1.919	-.129	1067.0	10061.5	2152.6	2303.9	1116.8	489.92	18.540	24.538	15.201
	40.000	17.165	511.57	1.620	-.082	1181.2	8772.1	2791.9	2633.1	976.1	489.37	16.209	20.785	16.050
	45.000	20.515	720.67	1.380	-.062	1309.2	7775.3	3535.0	2962.2	867.7	489.35	14.403	17.563	17.030
	50.000	24.440	994.49	1.179	-.043	1451.1	6978.6	4395.6	3291.3	781.0	489.46	12.965	15.546	18.058
	55.000	29.035	1348.75	1.006	-.031	1606.7	6319.8	5399.1	3620.5	709.6	489.13	11.779	14.279	19.146
D	59.816	34.218	1785.66	.859	-.025	1769.6	5794.6	6530.6	3937.6	652.7	489.30	10.834	17.181	20.255
	60.000	34.648	1823.40	.000	-2.000	1776.1	1776.1	6593.2	3949.6	209.7	157.70	3.481	11.451	11.644
F	60.000	34.648	1823.40	.000	-2.000	1776.1	1776.1	6593.2	3949.6	209.7	157.70	3.481	11.451	11.644
H	60.000	48.740	3063.52	.000	-2.000	1776.1	1776.1	7630.8	3949.6	209.7	157.70	3.481	11.451	11.644
	60.000	48.740	3063.52	-.000	-2.000	1776.1	1776.1	7630.8	3949.6	209.7	157.70	3.481	11.451	11.644
G	59.959	48.943	3081.36	-.406	-2.000	1774.7	-126.1	7638.6	3946.9	.0	.00	.000	.000	7.518
J	57.440	50.340	3202.32	-3.200	.000	1687.6	-13310.8	7638.6	3781.1	-1364.0	-974.76	22.476	45.632	33.292
	55.000	51.102	3265.19	-3.200	.000	1606.7	-13391.4	7638.6	3620.5	-1362.8	-939.41	22.622	43.669	31.787
B	52.157	51.991	3335.00	-3.200	.000	2008.6	-12989.6	7638.6	3433.3	-1322.1	-864.26	21.947	40.352	29.129
	50.000	52.665	3385.50	-3.200	.000	1943.2	-13054.9	7638.6	3291.3	-1329.3	-833.03	22.066	38.916	27.813
	45.000	54.227	3494.38	-3.200	.000	1801.4	-13196.7	7638.6	2962.2	-1345.0	-758.68	22.327	36.056	24.775
	40.000	55.790	3591.75	-3.200	.000	1673.4	-13324.7	7638.6	2633.1	-1359.4	-681.54	22.567	33.722	21.711
	35.000	57.352	3677.69	-3.200	.000	1559.2	-13438.9	7638.6	2303.9	-1372.5	-602.08	22.784	31.789	18.698
	30.000	58.915	3752.17	-3.200	.000	1458.8	-13539.3	7638.6	1974.8	-1384.2	-520.45	22.977	30.002	15.753
	25.000	60.477	3815.19	-3.200	.000	1372.2	-13626.0	7638.6	1645.7	-1394.3	-436.88	23.145	28.310	12.915
	20.000	62.040	3866.75	-3.200	.000	1299.3	-13698.8	7638.6	1316.5	-1402.9	-351.66	23.288	26.668	10.172
K	17.934	62.685	3884.71	-3.200	.010	1273.3	-13724.8	7638.6	1180.5	-1406.0	-316.03	23.340	25.806	9.066
	15.000	63.603	3906.88	-3.192	.008	1240.9	-13718.9	7638.6	987.4	-1406.0	-264.33	23.340	24.400	7.495
	10.000	65.173	3935.66	-3.180	.006	1198.1	-13710.3	7638.6	658.3	-1406.0	-176.22	23.340	21.541	4.910
LI	7.231	66.057	3946.81	-3.000	.000	1176.0	-12884.7	7638.6	476.0	-1321.7	-119.79	21.941	18.623	3.311
	5.000	66.800	3953.48	-3.000	.000	1163.7	-12897.0	7638.6	329.1	-1106.4	-69.33	18.366	13.294	1.909
M	2.250	67.717	3958.35	-3.000	2.000	1152.3	-12908.4	7638.6	148.1	-795.1	-22.42	13.198	6.405	.613

Excerpted Sample Run

TRAIN TRANSIT ROUTE ANALYSIS PROGRAM II 13:28 FRI FEB 03,'78

DETAILED ANALYSIS FOR SEGMENT 28

KEY	SPEED (MPH)	TIME (S)	DIST. (FT)	ACC. (MPH/S)	JERK (MPH/S/S)	RESIST (LB)	EFFORT (LB)	ENERGY (W-HR)	SPEED (RPM)	TORQUE (LB-FT)	POWER (HP)	CEPD (KW)	MGPD (KW)	GBPD (KW)
	PER TRAIN								PER MOTOR					
A	.018	69.084	3960.00	-.266	2.000	1146.1	-102.4	7638.6	1.2	-10.5	-.00	.174	.002	.000
C	.015	69.095	3960.00	-.245	2.000	1146.1	-.0	7638.6	1.0	.0	.00	.000	.000	.000
E	.000	69.217	3960.00	.000	2.000	1146.1	1146.1	7638.7	.0	126.3	.00	2.097	1.463	.000
TOTALS		2299.002	97680.00					181248.3						
					AVERAGE ABSOLUTE:		6710.9		1906.1	702.3	279.72	11.644	16.102	10.401
					ROOT MEAN SQUARE:		8829.2		2524.1	919.6				
					ROOT MEAN |CUBE|:		9954.9		2877.9	1036.5				
					FRICTION BRAKING:			1670.7						
										RMS LINE POWER:				288.516

Excerpted Sample Run

and ROOT MEAN CUBE of EFFORT, (MOTOR) SPEED, TORQUE, and POWER, as well as RMS LINE POWER are numerical averages of the printed values and depend on the print interval chosen – generally more accurate for smaller intervals.

The basic equation governing the motion of the train is:

$$\rho m\dot{V} = H - R, \tag{1}$$

where ρ is a factor to compensate for rotational inertia (discussed above), m is the mass of the train, $\dot{V}$ is the time rate of change of speed (acceleration), H is the total tractive effort, and R is the total train resistance. Since H and R are functions of V, equation (1) can be rewritten in the form

$$dt = \frac{\rho m}{H-R}\, dV \tag{2}$$

so that the time to change from say, speed, V_1, to speed, V_2, is found simply by integrating in closed form (since H is piecewise linear in V, and R is quadratic in V):

$$t_2 - t_1 = \rho m \int_{V_1}^{V_2} \frac{dV}{H-R} \cdot \tag{3}$$

If S is defined as the distance the train has moved, one has

$$\dot{V} = \frac{dV}{dt} = \frac{dV}{dS}\frac{dS}{dt} = \frac{dV}{dS}\, V, \tag{4}$$

so that combining equations (1) and (4) yields

$$dS = \rho m\, \frac{V}{H-R}\, dV\,. \tag{5}$$

Hence the distance covered in the time interval $t_2 - t_1$ is found by integration again:

$$S_2 - S_1 = \rho m \int_{V_1}^{V_2} \frac{V dV}{H-R} \cdot \tag{6}$$

Acceleration is given directly by equation (1).

$$\dot{V} = \frac{1}{\rho m} (H - R) \quad , \tag{7}$$

and jerk is found by differentiating this equation with respect to time:

$$\frac{d\dot{V}}{dt} = \dot{V} \frac{d\dot{V}}{dV} = \frac{H - R}{(\rho m)^2} \cdot \frac{d}{dV} (H - R) \tag{8}$$

The consumed energy is the integral of power over the appropriate time interval. This computation is made by evaluating an expression obtained by integration in closed form after changing the variable of integration from time to speed:

$$E = n_M \int_{t_1}^{t_2} P \, dt = n_M \int_{V_1}^{V_2} P \frac{dV}{\dot{V}} = n_M \rho m \int_{V_1}^{V_2} \frac{P(V)}{H-R} \, dV \, , \tag{9}$$

where E is the energy used by the train, n_M is the total number of motors per train, and P is the power (input for motoring, output for generating). Since the integrand in equation (9) is the quotient of two quadratics in V, the integral can be expressed in terms of elementary functions. The power losses in the various components must be accounted for in the expression for P, however. An analysis of these losses as it applies to the program is shown in Figure 5.4-1. Symbols not already defined are n_B: the total number of gearboxes per train; M: the motor/generator torque; $\bar{M}$: the gearbox counter torque; η: the gearbox maximum efficiency (limited at zero speed); ω: motor shaft speed in radians per unit time; EI: electrical power; and ΔP: power losses in components designated by the subscript. The gearbox loss is given by the expression below the appropriate box. It should be noted that the values under the column in the output format designated POWER (per motor) are precisely the values $M\omega$ in the figure.

Besides the limits on all the required integrals having to account for the "breaks" in tables, i.e., the tabular arguments, the specified limits on acceleration, deceleration, and jerk must also be considered when obtaining these integrals. The critical speeds at which the limits on these integrals must be supplied are defined in Figure 5.4-2. Notice that train acceleration ($\dot{V} > 0$, $\bar{\sigma} = +1$) does not necessarily imply motoring ($\sigma = +1$), nor does train deceleration ($\dot{V} < 0$, $\bar{\sigma} = -1$) imply generating ($\sigma = -1$).

Motoring Mode: $P_{in} = \frac{HV}{n_M} + \left[(1-\eta)M + \frac{n_B}{n_M}\bar{M}\right]\omega + \Delta P_{M/M} + \Delta P_{C/M}$

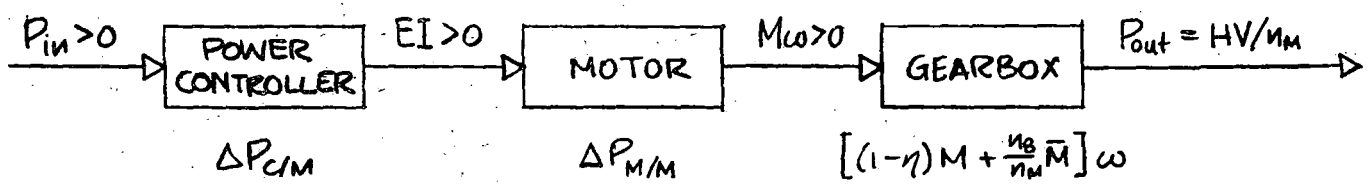

Generating Mode: $P_{out} = \frac{HV}{n_M} + \left[(1-\frac{1}{\eta})M + \frac{n_B}{n_M}\bar{M}\right]\omega + \Delta P_{M/G} + \Delta P_{C/G}$

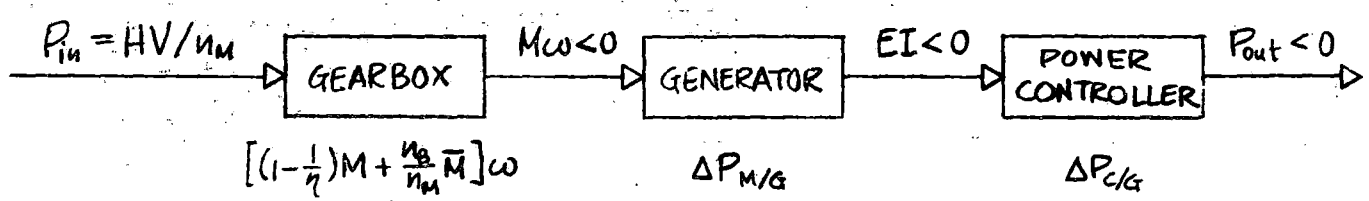

In general for $\left\{\begin{array}{l}\text{motoring},\ \sigma=+1\\ \text{generating},\ \sigma=-1\end{array}\right\}$: $P_{\{in\ out\}} = \frac{HV}{n_M} + \left[(1-\eta^{\sigma})M + \frac{n_B}{n_M}\bar{M}\right]\omega + \Delta P_{\{M/M\ M/G\}} + \Delta P_{\{C/M\ C/G\}}$

Figure 5.4-1. Analysis of Power Losses

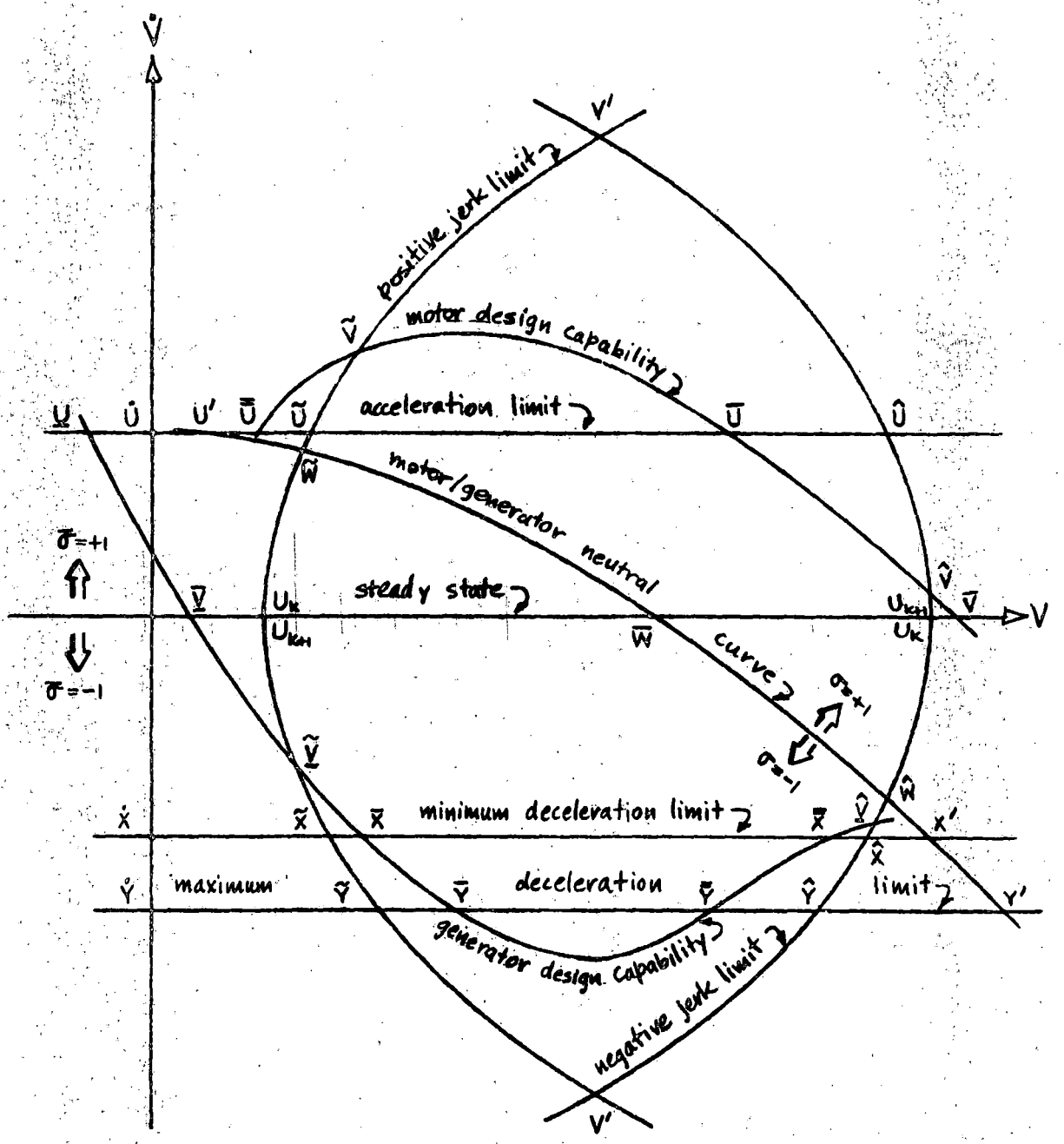

Figure 5.4-2. Depiction of Critical Speeds

For the hypothetical curves shown, the path followed by the computer program would be:

for acceleration,

U_k to $\tilde{U}$ along positive jerk limit curve

$\tilde{U}$ to $\overline{U}$ along acceleration limit line

$\overline{U}$ to $\hat{V}$ along motor design capability curve

$\hat{V}$ to U_{k+1} along negative jerk limit curve;

for deceleration:

U_k to $\hat{\underline{V}}$ along negative jerk limit curve

$\hat{\underline{V}}$ to $\overline{\overline{Y}}$ along generator design capability curve

$\overline{\overline{Y}}$ to $\overline{Y}$ along maximum deceleration limit line

$\overline{Y}$ to $\overline{\overline{X}}$ along generator design capability curve

$\overline{\overline{X}}$ to $\tilde{X}$ along minimum deceleration limit line

$\tilde{X}$ to U_{k+1} along positive jerk limit curve.

This deceleration path implies no high speed friction braking. For the case in which the high speed friction braking is desired, the first two steps should be replaced by the following three:

U_k to $\hat{X}$ along negative jerk limit curve

$\hat{X}$ to $\overline{\overline{X}}$ along minimum deceleration limit line

$\overline{\overline{X}}$ to $\overline{\overline{Y}}$ along generator design capability curve.

Because the expressions for the output parameters are dependent on the integration path, it is necessary to have a logical structure to determine the integration path so that the proper expressions will be implemented. Figure 5.4-3 depicts the program branching network to analyze the various possible cases for both the acceleration and deceleration states. The "primed" cases are those for which the torque-speed curves are double valued. Not shown is the dichotomy for the high speed friction braking option. A more complete logic diagram, given in Appendix B, depicts this branching. For clarity, the

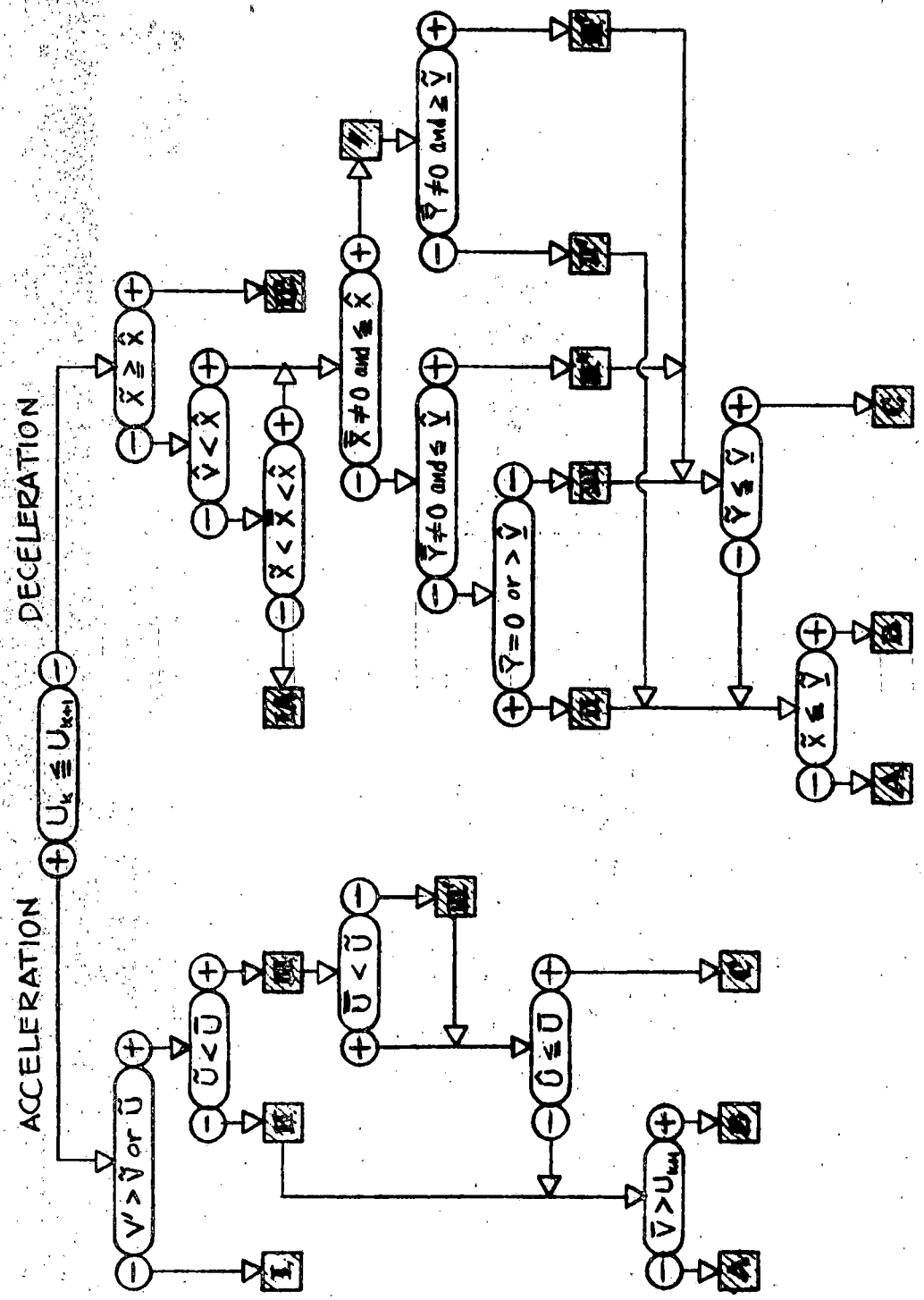

Figure 5.4-3. Logic for Analysis of Cases

various cases are delineated in Figures 5.4-4 and 5.4-5, as speed-acceleration diagrams. The shaded areas in Figure 5.4-5 indicate friction braking. It can be seen that the breakdown of cases by Roman numerals is governed chiefly by the relative magnitude of the limiting acceleration or decelerations, while the limiting speeds influence the designations by the Roman letters.

5.4.2 PERFORMANCE REQUIREMENTS

The major performance requirements affecting propulsion system design characteristics were based on an AW1 car weight of 95,200 lb and operation of a single car at a 600-volt nominal 3rd rail voltage.

Two sets of requirements were postulated: one for operation over the ACT-1 Synthetic Transit Route (characteristics of this route are tabulated in Appendix B) of the HSGTC at Pueblo, Colorado; the other was a set of discrete requirements. These can be summarized as follows:

Synthetic Transit Route

- For the conditions of new wheel diameter (30 in.) and no wind, propulsion system energy consumption over a round-trip shall not exceed 10.2 kW-hr/car mile when regenerative braking is not used. With regenerative braking and a fully receptive line, consumption shall not exceed 6.4kW-hr/car mile.
- With no time allowance between clockwise and counterclockwise runs, total round trip time for the 18.5 mile distance shall not exceed 39 minutes.

Discrete Requirements

- Under the conditions of no wind and level tangent track, the railcar shall be capable of maintaining a speed of 80 mph continuously with either new (30 in.) or worn (28 in.) wheels.
- Under the conditions of level tangent track and a 15 mph headwind, and with either new or worn wheels, the railcar shall be capable of intermittent 80 mph operation.

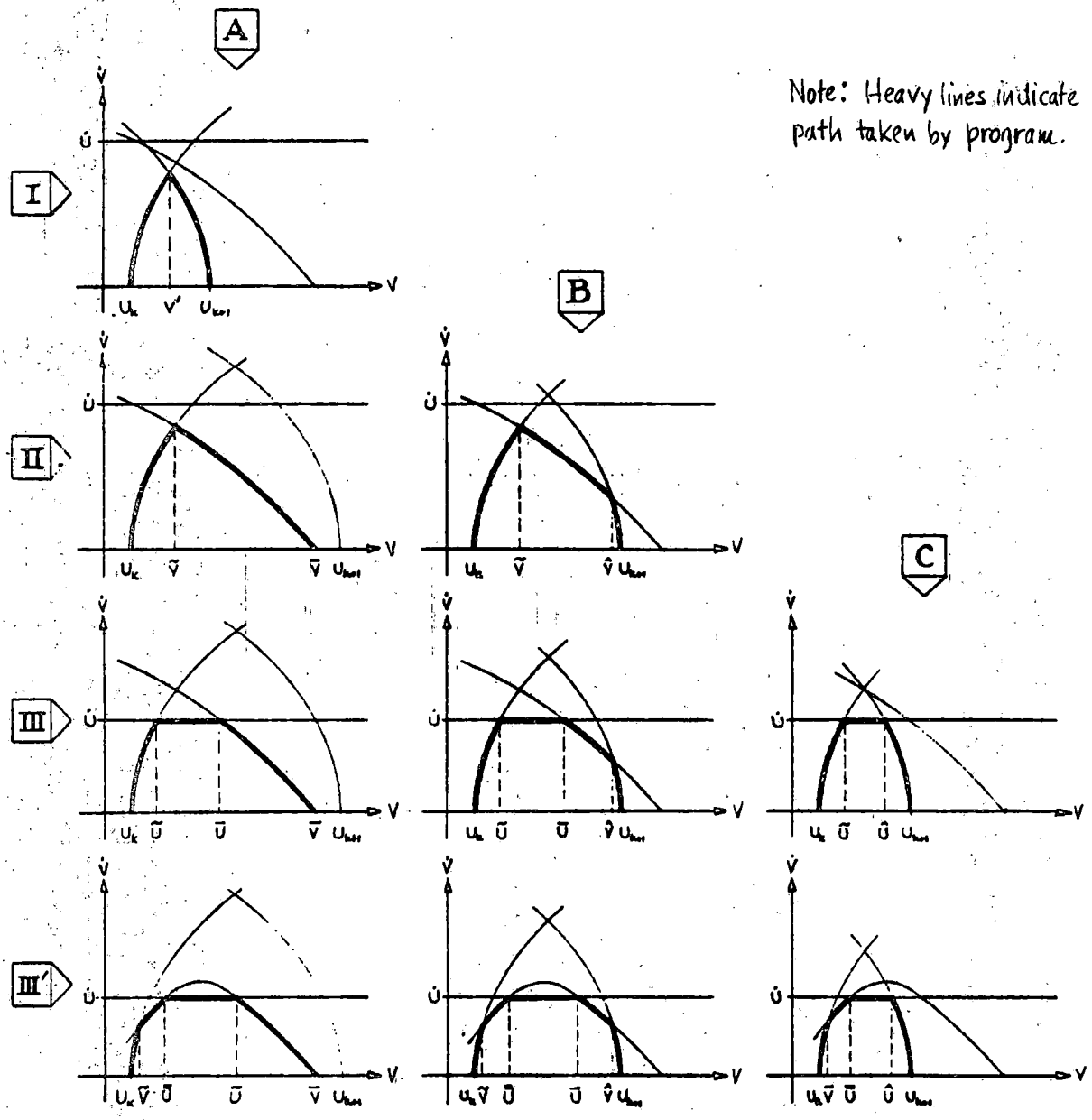

Figure 5.4-4. Diagrammatic Definition of Cases in Accelerating State

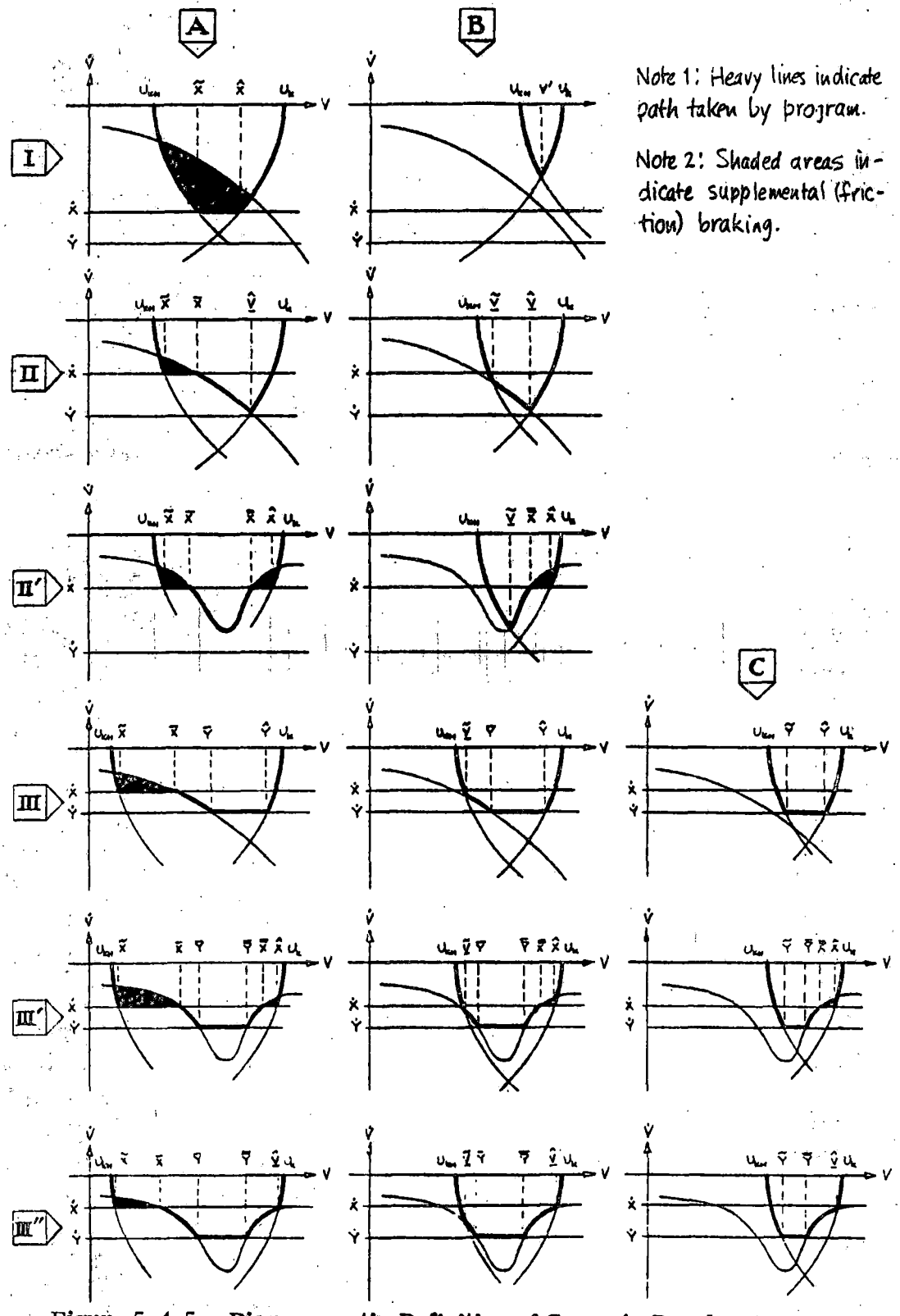

Figure 5.4-5. Diagrammatic Definition of Cases in Decelerating State

- With no wind, and with either new or worn wheels, the railcar shall be capable of maintaining a speed of 70 mph on a positive 3% grade for a distance of 6,000 ft.
- Under the conditions of level tangent track and no wind, and with new wheels, the railcar shall be capable of meeting the following acceleration requirements:
  - 3.0± 0.2 mphps to 25 mph
  - From stop, travel 700 ft in 20 sec (from input signal to the controller)
  - From stop, reach a speed of 60 mph in less than 38 sec.
- Under the conditions of level tangent track, no wind and new wheels, dynamic braking alone shall provide a deceleration level of -3.0 ± 0.2 mphps from 80 mph to 10 mph.
- For the case of new wheels, regenerative braking shall be available from 80 mph to 25 mph.
- Jerk rate shall not exceed 2 mphpsps.

In addition to the above, thermal design criteria for the propulsion system equipment were specified as follows:

- The continuous thermal rating and design shall be based on operation over the Synthetic Transit Route.
- The maximum capability thermal design shall be based on a duty cycle consisting of full power acceleration to 80 mph followed immediately (no steady-state) by full dynamic braking (supplemented at low speed with friction braking) from 80 mph to zero, rest for 20 sec., and then repeat over a 30 min. period. (This assumes that operation is within the acceleration, deceleration, and jerk constraints previously stated.)

5.4.3 ANALYSIS RESULTS

Two types of computer runs were made to evaluate train and propulsion system performance characteristics:

(1) Round-trip runs over the ACT-1 Synthetic Transit Route consisting of 28 segments

(2) Runs over single segments to verify "discrete" performance requirements.

In the motoring mode, motor torque-speed characteristics as verified by laboratory testing were used. In the braking mode, similar test results were not available for the full torque-speed range; therefore, braking capabilities as calculated by the motor designers were used.

Synthetic Transit Route

One car at AW1 weight (95,200 lb) was operated over the ACT-1 Synthetic Transit Route while using dynamic braking supplemented with friction braking at low speed. System dead times, station stops of 20 sec., and jerk, acceleration, and deceleration constraints were included.

The results indicated a round-trip time of 38.3 min. for the 18.5 mile run and an energy consumption rate of 9.80 kW-hr/car mile. Both these values meet specified requirements.

Other results of interest, particularly for system thermal design, were as follows:

- Average motor power output - 280 hp
- Average power dissipation (each)
  - Gearbox - 10.4 kW
  - Power Control Electronics - 11.6 kW
  - Motor - 16.1 kW.

In the case of a 2-car AW1 weight train, energy consumption is reduced to 9.20 kW-hr/car mile while round trip time remains essentially the same.

For the case of a 2-car AW3 (130,000 lb/car) train, round trip time is 40.2 min. while energy consumption is 11.78 kW-hr/car mile.

In the case of regenerative braking and a fully receptive line, energy consumption is 6.07 kW-hr/car mile for single car AW1 operation and 5.41 kW-hr/car mile for a 2-car train – again within specification.

Thus it appears that all Transit Route related performance requirements would be met by the system design.

Single-Segment Runs

Results from these runs can be summarized as follows:

- Under conditions of level tangent track, 28-inch wheels and no wind, a motor output (each) of 254 hp is required in order for a single AW1 car to maintain 80 mph.
- Under conditions of level tangent track, 28-inch wheels and a 15 mph headwind, a motor output (each) of 334 hp is required in order for a single AW1 car to maintain 80 mph.
- Under conditions of tangent track, 28-inch wheels and a +3% grade, a motor output (each) of 455 hp is required in order for a single AW1 car to maintain 70 mph.

For all the above cases, the power output requirements would be slightly less for the case of 30-inch wheels.

Since power outputs exceeding the above values have been demonstrated in the laboratory, speed capability requirements are considered to have been met.

Acceleration capabilities were analyzed for a single AW1 car for the conditions of level tangent track, 30-inch wheels, and no wind. Dead time (0.5 sec), jerk, and acceleration/deceleration limits were included.

Speed and distance as functions of time are shown in Figure 5.4-6. It can be seen that a speed of 60 mph is attained in 32.4 sec, and that a distance of 705 ft is covered in 0 to 20 sec. Both values exceed specified requirements.

The acceleration/deceleration profile for this case is shown in Figure 5.4-7. It can be seen that acceleration varies from about 3.0 mphps at start to about 2.9 mphps at 25 mph. In the case of braking, the motor output is adequate to maintain the required deceleration level from 80 mph to below 10 mph. Thus friction braking is required only at low speeds.

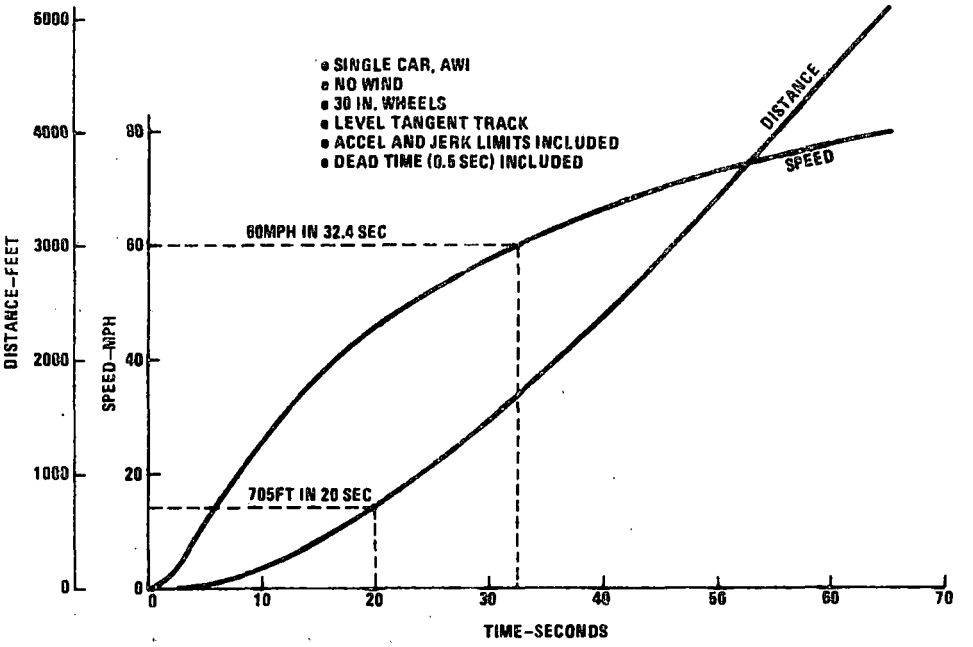

Figure 5.4-6. Speed and Distance as Functions of Time

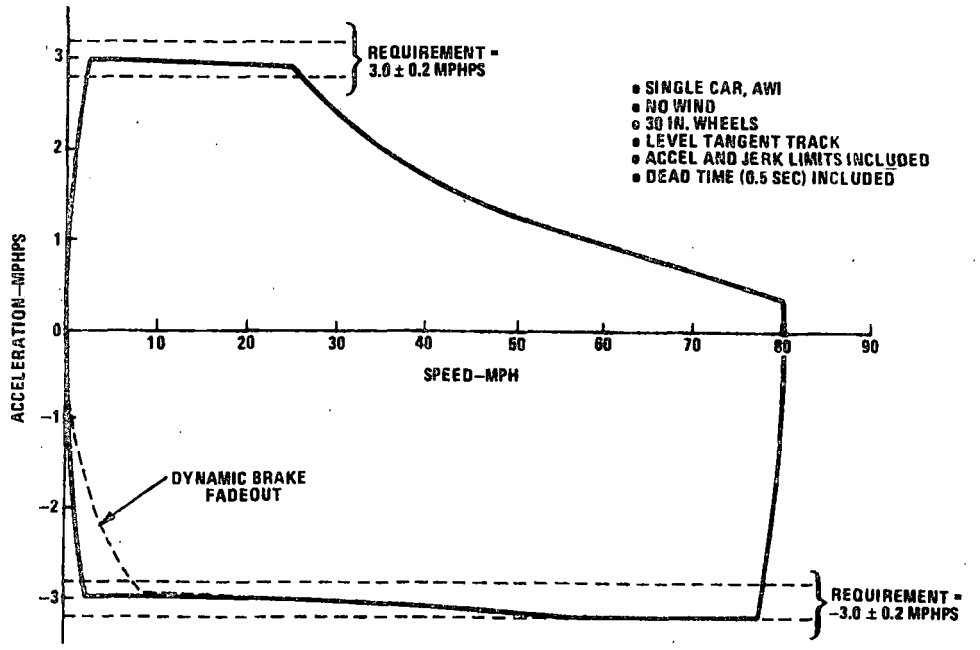

Figure 5.4-7. Acceleration/Deceleration Performance Profile

The vehicle operating profile and motor duty cycle corresponding to the maximum capability thermal design are also plotted. In Figure 5.4-8, acceleration and deceleration levels and vehicle speed are plotted as a function of time. It can be seen that the rail car can reach the maximum speed of 80 mph in about 65 sec. Braking from maximum speed to a stop takes about 27.5 sec. The corresponding motor duty cycle is shown in Figure 5.4-9 in which torque and power output and motor speed are plotted versus time.

Other results derived for this case were as follows:

- Distance to reach 80 mph from zero – 5,118 ft
- Distance to brake from 80 mph to zero – 1,5 87 ft
- Average motor output over complete cycle – 408 hp
- Average power dissipation (each)
  - Gearbox – 15.8 kW
  - Power Control Electronics – 12.6 kW
  - Motor – 20.1 kW.

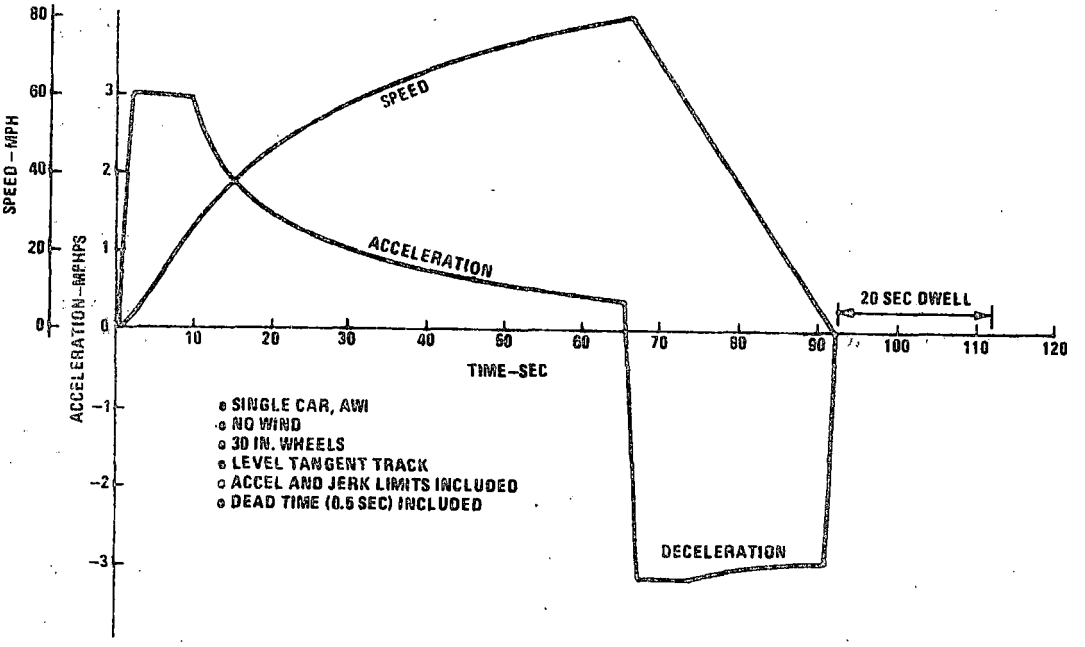

Figure 5.4-8 Vehicle Operating Profile

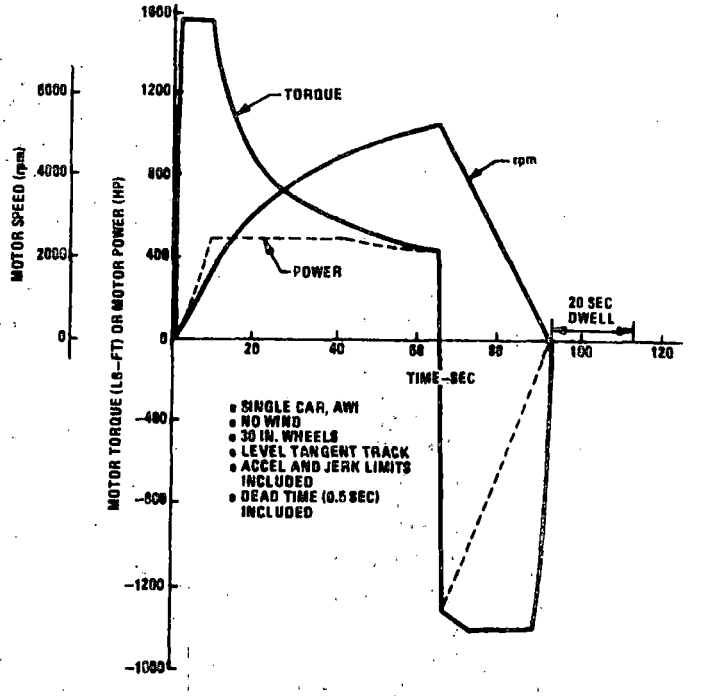

Figure 5.4-9. Motor Duty Cycle

5.5 SYSTEM SIMULATION ACTIVITIES

5.5.1 INTRODUCTION

Early experience with the ASDP propulsion system revealed development work in the laboratory to be time consuming. Further evaluation indicated that much future development work, especially that involving the verification of closed loop control functions, could usefully be performed by means of a computerized simulation of the system. In addition, it was observed that certain functions, such as spin-slide control, could not be directly tested in the laboratory but could be evaluated in a simulation. This led to the initiation of an effort to develop a computerized model of the system and to interface this model with the ASDP train control microprocessor in a hybrid system simulation.

5.5.2 SIMULATION EFFORT OBJECTIVES

The simulation effort was planned in two phases. The initial or short range phase comprised all development tasks directly supportive to the laboratory development, integration, and test of the ASDP propulsion system. The second or long range phase comprised those tasks supportive to the operational development of the system at the Pueblo test site and/or transit system properties. These tasks are summarized as follows:

Simulation Objectives – Short Range

1. The verification of closed loop stability and control characteristics in response to input commands. This included separate verifications of the motoring, dynamic braking and regenerative braking modes.

2. The development of microprocessor software and control algorithms by performing the initial development in a Sigma 7 computer using Fortran language. This development was planned for both braking modes. It is a simpler task for the motoring mode and was accomplished prior to initiating the simulation effort by using the microprocessor to verify the analytical formulation of the control algorithms.

3. The verification of microprocessor software for all modes of operation and for transitioning between modes.

Simulation Objectives – Long Range

1. The evaluation of motoring mode spin control characteristics.

2. The evaluation of regenerative and dynamic braking mode slide control characteristics.

3. The evaluation of system characteristics when interfaced to a simulation of a "real world" 3rd rail voltage source having complex impedance characteristics and experiencing representative voltage transients. Evaluation would include:

   a. Stability evaluation of both the motoring and regenerative braking modes

   b. Mode sequencing and system shut-down when operating voltage limits are exceeded.

5.5.3 SIMULATION DESCRIPTION

5.5.3.1 Simulation Configuration

The approach employed in the development of the simulation was to use a microprocessor identical in hardware and software to that used in the ASDP propulsion system. As illustrated by Figure 5.5-1 this microprocessor was interfaced at the analog and discrete signal level via a hybrid coupler to a XEROX Sigma 7 digital computer. The hybrid coupler is actually the A/D and D/A converter portion of an EAI 8800 Analog Computer. The latter and the Sigma 7 are the nucleus of a general purpose hybrid simulation computer facility at Delco Electronics. Some of the desirable features of a simulation in the above configuration are:

1. The need to emulate microprocessor computation in the general purpose computer are obviated.
2. The microprocessor software employed in the simulation, including that portion involving the I/O, is identical to that for the operational system.
3. It is possible to record, via a strip chart, the analog signal representation of the key vehicle parameters.

Figure 5.5-2 complements Figure 5.5-1 by showing a complete tabulation of signals as found at the microprocessor I/O and Sigma 7 computer I/O interface. The pointers not ..cended to the Sigma 7 I/O interface indicate these signals were not used in the simulation.

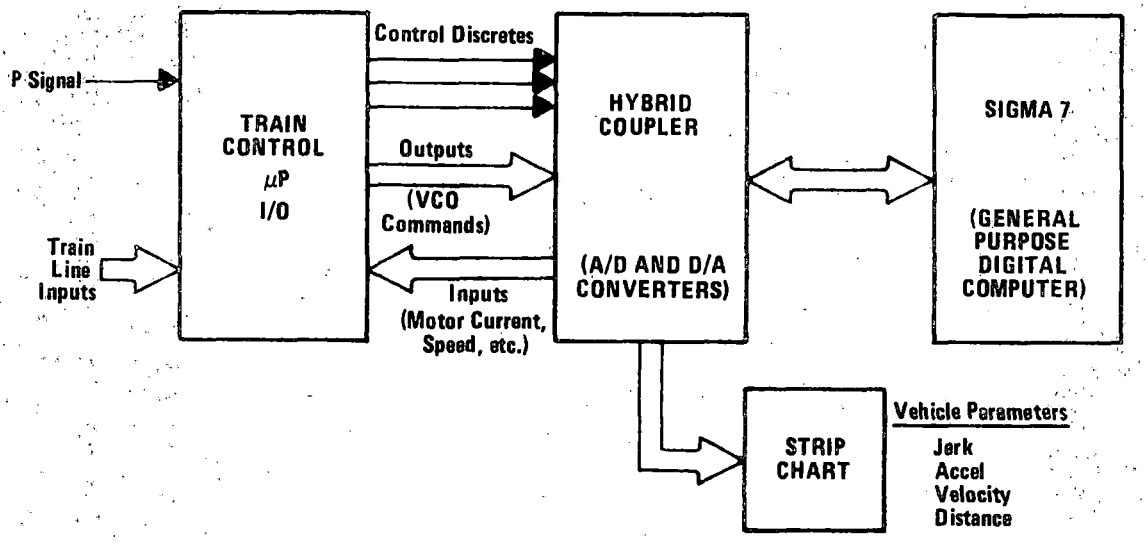

Figure 5.5-1. ASDP Hybrid Simulation

5.5.3.2 System Model Description

In the ASDP system, the primary control "P" signal is a tractive effort command that is related to a desired acceleration/deceleration level and to the propulsion system torque-speed output capabilities. The velocity loop is not closed other than through manual control of the "P" signal by the operator. By multiplying the tractive effort command by a vehicle weight factor and wheel radius, a computation performed in the microprocessor, a torque command is obtained. Also if motor current and either motor voltage or motor speed is properly interpreted, developed torque can be calculated. The error signal resulting from the comparison of commanded versus developed torque is the primary control signal in the ASDP system. In the motoring mode, this signal controls the VCO (Voltage Controlled Oscillator) frequency and in the braking mode the signal controls either the level of field excitation (via the VCO) or the phase gating angle of the braking SCR's.

Figure 5.5-3 provides a simplified illustration of the previously described calculations and of closed loop control of the system in the motoring mode. Although not illustrated in the figure, the system model simulated in the Sigma 7 computer did include the inertia

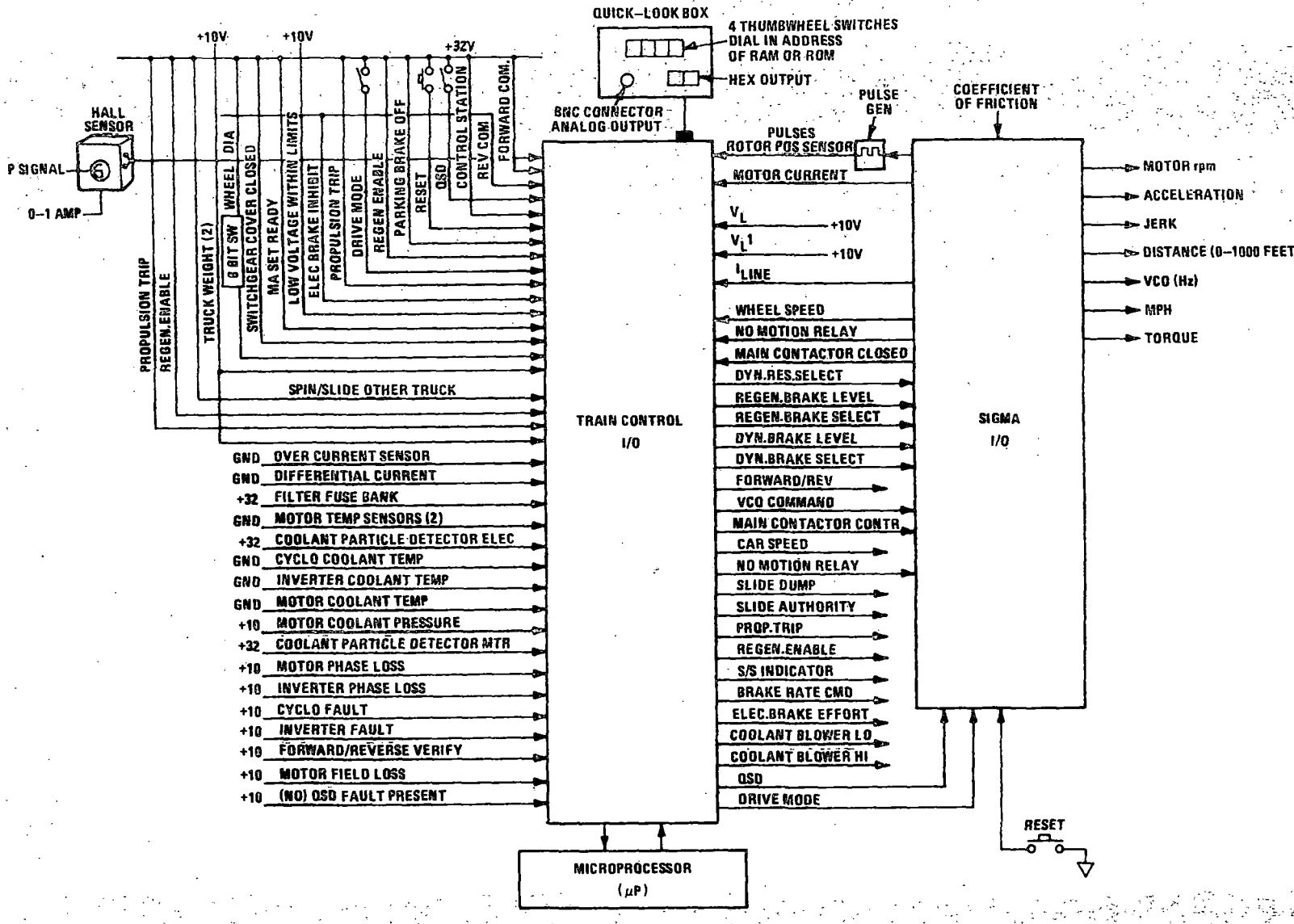

Figure 5.5-2. Simulation Interface Diagram

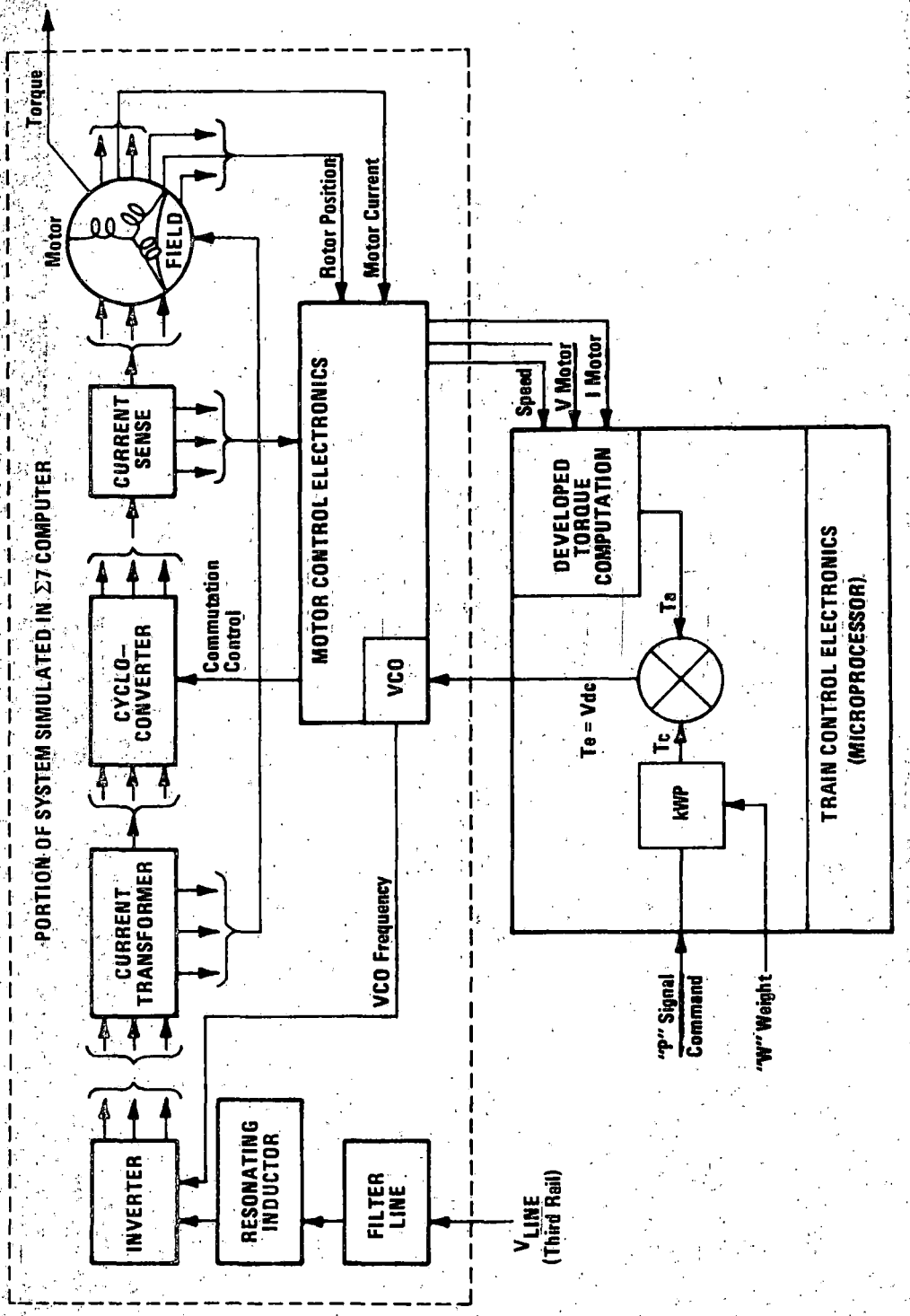

Figure 5.5-3. Motoring Mode Control

of the motor-gear train and other truck rotating components and the drag of the vehicle. Thus, open-loop computation of the velocity profile was possible. No consideration was given to closing the velocity loop through the manual operator. Models for the braking modes are not illustrated but are similar, although more complicated.

The simulation of the system in the Sigma 7 computer was being developed as an empirical rather than an analytic model. Also, the static and dynamic characteristics of the model were being developed separately. This approach is convenient since a vigorous analytical description of the inverter, cycloconverter, and motor would be extremely difficult to develop and verify. The static portion of the model programmed in the Sigma 7 computer is depicted by tables of motor torque versus VCO frequency at various speeds as shown in Figure 5.5-4. This figure is based on laboratory data obtained with the system operated open loop. A planned but not completed task was the development of additional sets of curves for all line voltages of interest. It was further planned to model the dynamics of the system by sinusoidally modulating the VCO command to the motor control electronics in the system test laboratory and observing the response gain and phase shift in generated torque.

It was felt that a model of the empirical dynamic response characteristic was not needed to pursue the short range simulation objectives as previously described. This is because it is expected that there is one predominant lag in the loop and it is determined by a design controlled lag in an electronic circuit. This is the lag in frequency change versus command in the VCO. This lag can be analytically described and simulated.

A second, possibly significant lag in the system involved the motor flux lag due to the field inductance. It was felt that the open loop phase-gain response data would be needed to evaluate the significance of this lag.

5.5.4 ACHIEVEMENTS AND STATUS

At the time of ASDP program termination, the simulation effort had progressed to the point where the Sigma 7 computer had been programmed as discussed in paragraph 5.5.3 and the program verified. The verification was accomplished prior to interfacing the Sigma 7 computer with the train control microprocessor. It was accomplished on an open loop basis by simulating the inverter VCO command signal and substituting it for the signal normally furnished by the microprocessor.

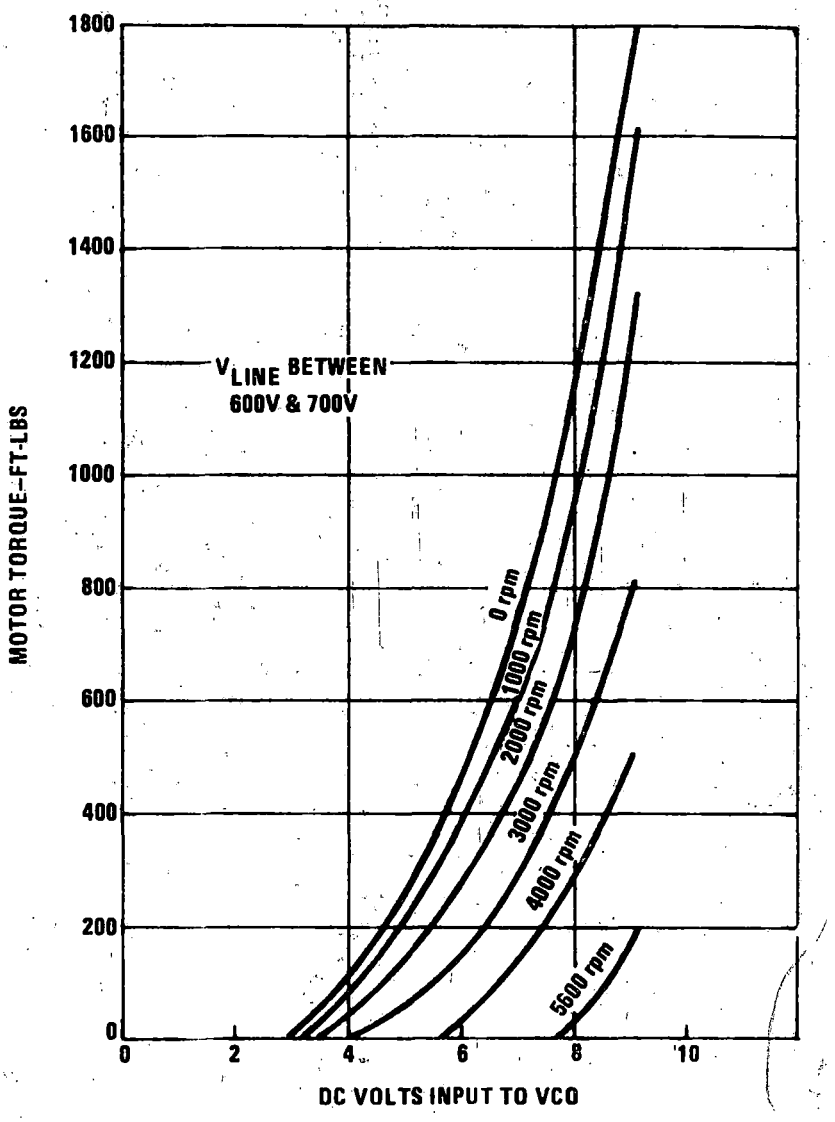

Figure 5.5-4. VCO Volts vs Motor Torque

The open loop response of the system when subjected to a simulated linear VCO ramp command is demonstrated by the chart recording of Figure 5.5-5. The ramp, to saturation, of the VCO command is shown by channel 5 of the recording. The response of the system is shown in terms of generated torque (channel 6), jerk (channel 1), acceleration (channel 2), velocity (channel 3), and distance traveled (channel 4). The plot of distance traveled is reset every 1,000 feet to enhance the granularity of the display. The drag torque (channel 7), as derived from the Davis drag equation, was subtracted from the generated torque in the implementation of the computations. This simulation was not expected to show specified system response characteristics in terms of acceleration and jerk rate because nonlinearities in torque versus VCO voltage and speed were not incorporated into the model. The compensation for these nonlinearities would ultimately be made in the microprocessor.

An effort was initiated to simulate the compensation on the Sigma 7. An algorithm derived from the graph of Figure 5.5 -6 was programmed on the Sigma 7 so as to control the rate of VCO frequency change as a function of VCO voltage and vehicle speed. This graph is based on empirical system performance data. It was planned to verify this part of the computation on the Sigma 7 and then to reprogram it in the microprocessor.

In an effort which paralleled the simulation work, a train control microprocessor was fabricated, verified at the unit level, and interfaced to the Sigma 7 as illustrated previously by Figures 5.5-1 and 5.5-2. Operational verification of the interface was initiated but did not progress to the point of significant results.

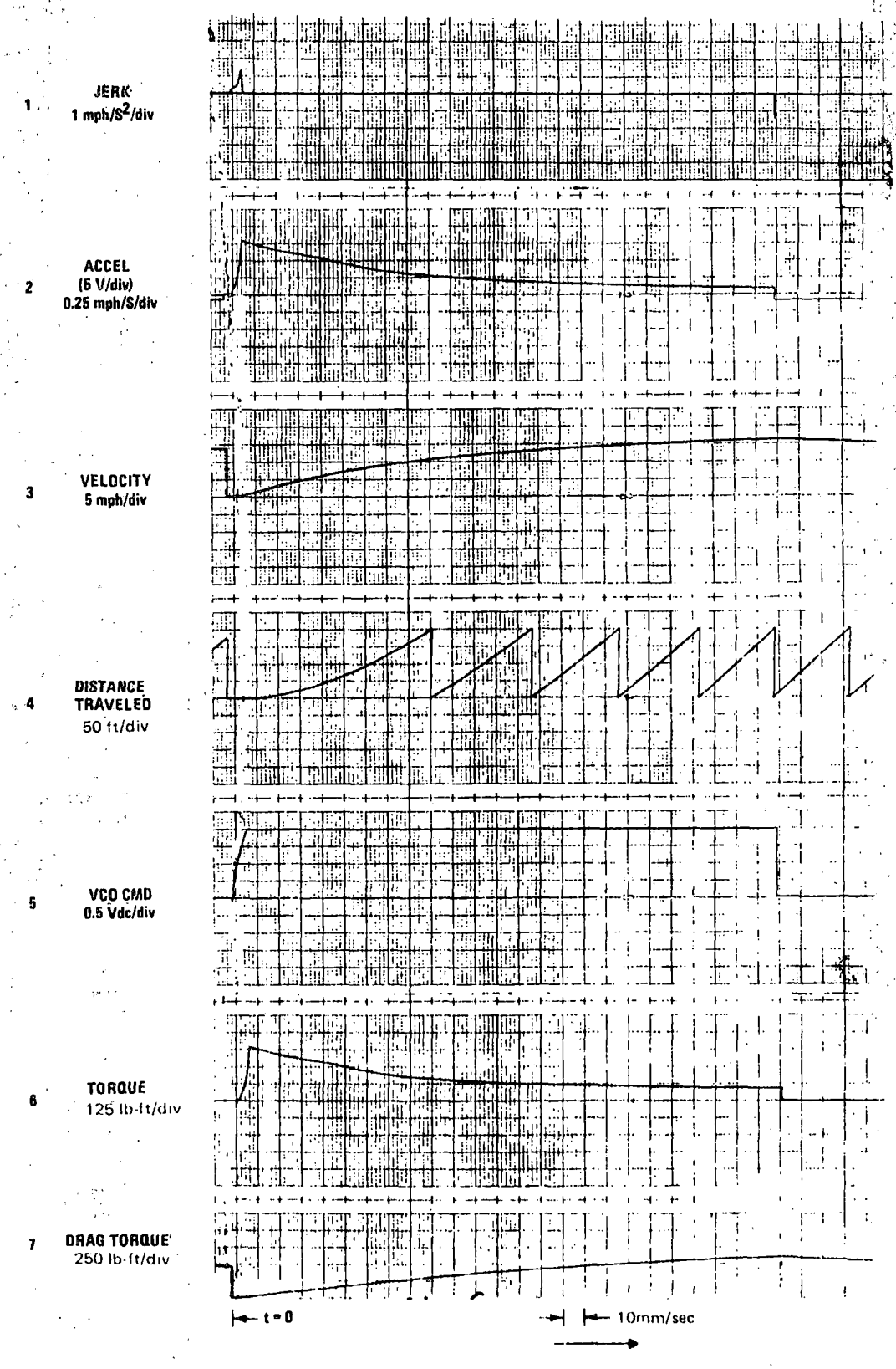

Figure 5.5-5. Open Loop Response

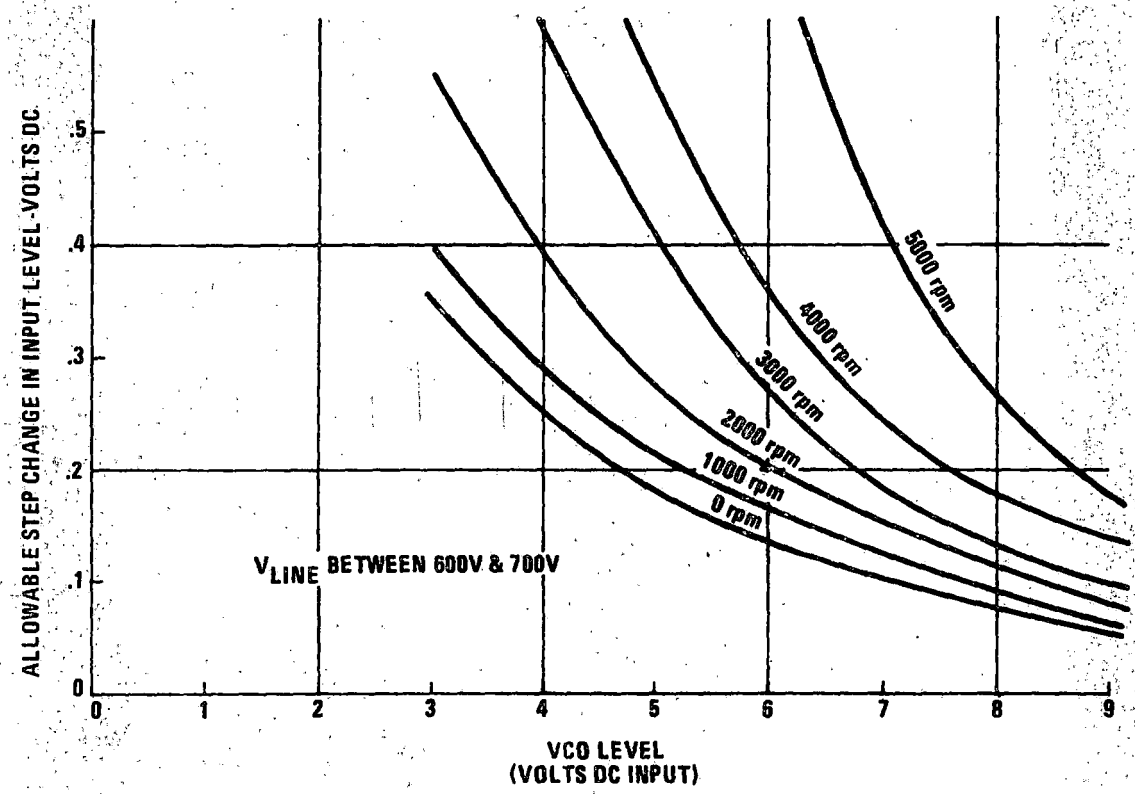

Figure 5.5-6. Jerk Rate vs VCO Control Change Rate

5.6 MAJOR COMPONENT CHARACTERISTICS

5.6.1 GENERAL

This section describes the characteristics of the major components of the propulsion system. A hardware family tree of this equipment, along with the applicable assembly drawing numbers, was shown in Figure 5.1-2. Lists of the complete drawing package and of the applicable specifications can be found in Appendix C.

Discussed are the functional requirements for the equipment, the design approach taken and the functional and physical descriptions.

The climatic, shock and vibration, load and acoustic noise requirements for the equipment are given below.

Climatic Conditions

- Maximum free stream ambient air temperature: 125°F
- Maximum undercar ambient air temperature/humidity: 150°F/10%
110°F/50%
- Minimum ambient temperature: -25°F
- Humidity: 2% to 100%
- Salt: Coastal air environment (20% salt-laden mixtures)
- Altitude: Sea level to 5,000 ft
- Water spray: Conditions associated with car washing and steam cleaning
- Fungus: Exposure to moist fungus
- Sand and Dust: Exposure to a sand and dust density of approximately 0.05 gram per cubic foot.

Vibration and Shock Requirements

- Car Body Equipment: 0.4g Vibration at up to 100 Hz
6g Longitudinal Shock
3g Lateral and Vertical Shock
- Truck Frame Equipment: 6g Vibration at up to 100 Hz in all directions
15g Vertical Shock
10g Longitudinal and Lateral Shock
- Axle-Mounted Equipment: 8g Vibration at up to 100 Hz in all directions
100g Vertical, Lateral, and Longitudinal shock.

Furthermore, car body-mounted equipment support structure shall be designed to avoid the first and second body bending frequencies of 8 Hz and 15 Hz.

Load Requirements (Car-Body Mounted Equipment)

- Normal Operation

The equipment shall withstand, without permanent deformation, the following independent loads:

Longitudinal:	6g
Vertical:	3g
Lateral:	3g

- Loss of One Support

The equipment support shall be capable of withstanding the following independent loads after the loss of any single support. The deflection of the equipment shall not violate the clearance envelope:

Longitudinal:	6g
Vertical Load:	3g
Lateral Load:	3g

Noise Requirements

Equipment noise measured prior to installation shall not exceed the levels specified below at a distance of 15 ft and under any operating condition:

Traction Motor:	75 dBA
Gear Drive:	82 dBA
Other Components:	65 dBA

5.6.2 ELECTRONIC CONTROL UNIT

The electronic control unit (ECU) contains the train control electronics (TCE), motor control electronics (MCE) and the associated power supplies and system vital relays.

5.6.2.1 Train Control Electronics

5.6.2.1.1 Requirements

The ASDP TCE provides the interface control for the propulsion system of the railcar. It receives information from the master controller, train lines, synchronous brake system

(SBS), MCE and the propulsion system power control elements, cooling system, and the traction motor. In turn, it provides the control functions required to operate the railcar.

The specific TCE functional requirements were summarized in paragraph 5.2.1. Detailed requirements can be found in TCE Design Specification EE-75-S-294.

5.6.2.1.2 Design Approach

A tradeoff study was conducted during the early stages of the program to evaluate the use of a microprocessor versus hard wired logic for the ASDP TCE. As a result of this trade study the microprocessor approach was recommended. The rationale for this selection is discussed below.

Advantages of the Microprocessor Approach

- Increased flexibility – Changes can be accomplished by reprogramming the microprocessor. With the availability of portable (suitcase type) programming equipment, this can be done at the test site (Pueblo) or at the various transit properties.
- Reduced amount of low level electronics – The use of a microprocessor results in a significant reduction in integrated circuit package count. This produces a simpler design, a smaller package, and eventually a lower manufacturing cost.
- Increased reliability – Reduced number of devices and interconnections results in higher reliability and lower maintenance.
- Reduced engineering/design time – Circuit design, breadboarding, and hardware debugging effort can be reduced. The availability of developmental systems can assist in this.
- Diagnostic techniques are easy to implement – Monitoring and fault locating can be simply implemented and simulator can be incorporated into the software.

Disadvantages of the Microprocessor Approach

- New approach – Microprocessors have not been applied previously in this application. Different engineering and technician skills are required to implement and maintain this equipment. Additional training will be required for support personnel.
- Major programming effort required – The software development effort may offset the engineering time saved in hardware development.
- Reprogramming requires special equipment – To make use of the flexibility to make software field changes, special portable (suitcase type) equipment is required with appropriately trained personnel.

Summary

On the basis of the trade study conducted, the use of microprocessors appeared to be an attractive solution for the ASDP TCE. The potential advantages for transit car production programs in terms of equipment cost, size, reliability, and maintainability are even more pronounced.

5.6.2.1.3 TCE Design Description

The TCE consists of I/O circuits, a microprocessor, power supplies and vital relays.

Input/Output Mechanization and Characteristics

The mechanization for the TCE I/O is shown in Figure 5.6-1.

The basic hardware design for inputs consisted of 32 multiplexed, differential, A/D converter (8-bit) analog inputs; 32 multiplexed, discrete inputs; 2 A/D converters (8 and 10 bits); 14 discrete inputs; and 2 digital clocked inputs.

The basic hardware for outputs consisted of six 8-bit D/A outputs and 30 digital-open lector outputs. Total I/O, descriptions and signal response times are shown in Table 5.6-I.

Circuits within the I/O which required special consideration were the synchronous brake system (SBS)/P-signal transformation and the No Motion relay which had to be Fail Safe.

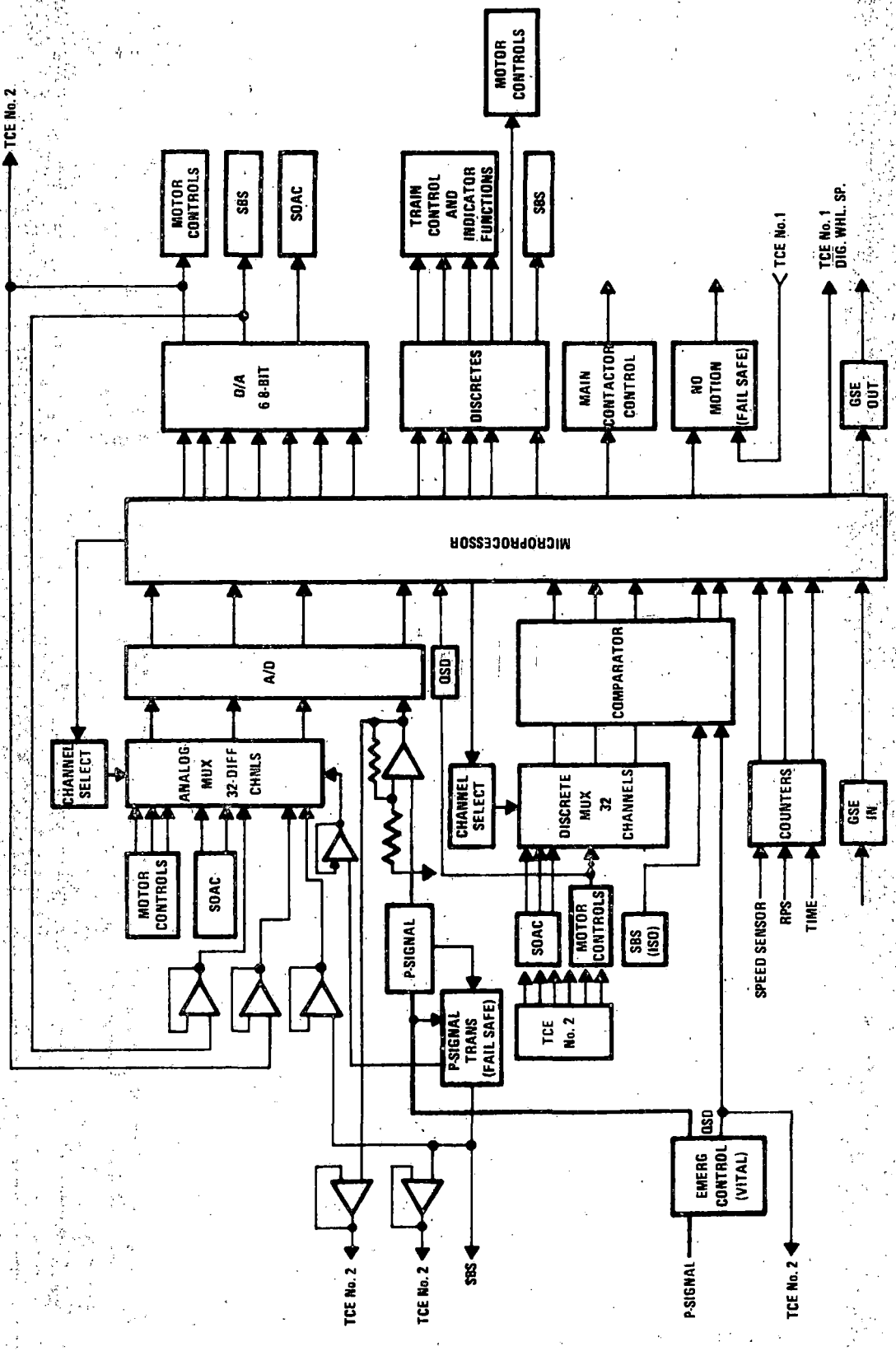

Figure 5.6-1. TCE Input/Output Functional Mechanization

I/O Chan Available	I/O Chan Used	Description	Response Time
32	24	Multiplexed, differential, A/D converter - channel inputs (8 Bits)	Select, slew and settling time <30μs/input
32	28	Multiplexed, discrete - channel inputs	Select and slew time <4μs/input
2	1	A/D converter - channel inputs (8 &10 Bits)	Settling time <27μs/input
14	11	Discrete - channel inputs	Response time <2μs/input
2	2	Digital clocked inputs	Response time 0.5μs/input
6	5	8-bit D/A converter output	Select and settling time ≤25μs/output
	5	8-bit feedback output	Select and settling time ≤25μs/output
30	17	Digital-open collector hex inverter output	Select and switching time ≤1μs/output
	8	Digital-open collector feedback output	Select and switching time ≤1μs/output
TOTAL I/O AVAILABLE = 118 TOTAL I/O USED = 101			<1.5 ms (1.351 ms) required to service 118 I/O ports. ~1 ms (1049 μs) required to service 101 I/O ports.

Table 5.6-I. TCE I/O Design Capability

The mechanization and circuit design of QSD signals, Main Contactor Drive, Cross-Coupled signals, and high voltage isolation also were given special attention.

The total I/O capability of the TCE as designed was 118 analog/discrete signals of which a total of 101 were used.

Input and output signal characteristics of the TCE I/O are described in Design Specifications EE-75-S-295 and EE-75-S-296. These are summarized in Tables 5.6-II and 5.6-III.

Included in the tables are the characteristics of the T/L, SBS, feedback, cross-coupled, motor and motor control, and interrupt (QSD) signals.

Shown are signal function, signal type, signal scaling, analog scale factor, digital/discrete scaling, response and setting time, tolerance, multiplexer number and channel, and the RAM memory storage location.

Microprocessor Mechanization and Characteristics

The processor used in the TCE is the Intel 8080 8-bit microprocessor. The 8080 microprocessor has 111 instructions in its instruction set. An Intel 8224 chip provides the basic system clock and reset. The clock is a crystal controlled oscillator. An 18 MHz crystal is used to result in an output clock of 2 MHz. A 8228 chip is utilized to generate all signals required to directly interface with RAM, ROM and I/O. Due to the large number of I/O, however, additional drivers are used on the address and data lines. The basic block diagram is shown in Figure 5.6-2.

The memory is comprised of 2k RAM and 8k EROM. The EROM used is the Intel 2708. This is a 1k × 8 unit and they are used to store the program and conversion tables. Address decode for the memory is provided by three 74154 4 to 16 line decoders.

There are 18 digital input ports and 16 digital output ports. Each of these ports is an Intel 8212 which is an 8-bit input/output device. In addition there are 6 DAC connected to the output bus. Analog device 7552 chips are used for the D/A conversion. There are also 6 ADC. The A/D converters interface with the CPU through input ports 00-06. Ports 00-04 are for five 8-bit A/D. Ports 05 and 06 are used for a 10-bit A/D. Analog Device 7570 chips are used for the A/D conversion. Six 74154, four-to-sixteen line decoders are used for multiplexer and input/output selection.

Interface signal characteristics	Signal Type	Signal Scaling	Analog Scale Factor	Digital/Discrete -Scaling/Phase	Response & Setting Time	Tolerance	MUX. No. & Channel	Memory Storage Location
*								
3.2.1 T/L Inputs								
3.2.1.1 P-Signal	Analog	0-10Vdc	10V/amp	4mA/Bit	≤ 30 μ sec	±1%	--	216E, 216D
3.2.1.2 Forward command (FWD CMD).	Discrete	0→5Vdc		1-FWD			4-1	201F
3.2.1.3 Reverse command (REV CMD).				1-REV			4-2	2037
3.2.1.4 QSD/P-signal inhibit.				1-QSD			--	
3.2.1.5 Control station				1-control			4-3	204F
3.2.1.6 Propulsion-reset.				1-reset			4-4	2057
3.2.1.7 Parking brake ON/OFF				1-OFF			4-5	207F
3.2.1.8 Regeneration enable.				1-regen			4-6	2097
3.2.1.9 Friction brake on.				1-brk on			4-7	20AF
3.2.1.10 Mode control.		0→5Vdc		1-drive			4-11	21DF
3.2.1.11 Propulsion trip.	Discrete	5Vdc→0		0-trip			5-12	2138
3.2.2 Synchronous brake system (SBS) inputs.								
3.2.2.1 Electric brake-inhibit.	Discrete	0→5Vdc		1-inhibit			--	--
3.2.3 Other train equipment and function inputs.								
3.2.3.1 Low voltage ($B+_{LO}$).	Discrete	5Vdc→0		0-lo volt			--	--
3.2.3.2 Motor alternator (MA) set ready.		0→5Vdc		1-ready			4-8	20C7
3.2.3.3 Switch gear cover-closed.		5Vdc→0		0-open			4-9	20DF
3.2.3.4 Wheel diameter.	Discrete	28 - 30"		0.008"/Bit			--	2182
3.2.3.5 Truckweight. AWO~ 86,000#	Analog	0-10V	4.4k#/volt	173#/Bit	≤ 30 μ sec	±5%	0-0	2018, 2048
3.2.3.6 Wheel speed.	Discrete	0→5Vdc		1-pulse			--	
3.2.3.7 Low voltage DC Power (LVDC)	Analog	0-10V	215mV/volt	0.2V/Bit	≤ 30 μ sec	±5%	0-2	20A8

* Paragraph numbers refer to design specification EE-75-S-295 unless otherwise specified.

Table 5.6-II (Sheet 1 of 2). μP - I/O Interface Signal Characteristics

Interface signal characteristics	Signal Type	Signal Scaling	Analog Scale Factor	Digital/Discrete -Scaling/Phase	Response & Setting Time	Tolerance	MUX. No. & Channel	Memory Storage Location
*								
3.2.4 TCE FDBK and cross coupled FDBK								
3.2.4.1 Electric brake effort (EBE) 3.2.7.1	Analog	0-10V	100mV/%	0.4%/Bit		± 10%	3-2 & 3	207B, 30AB
3.2.4.2 Braking rate CMD SIG. 3.2.7.2	Analog	0-10V	1V < X 1.684 <4.750V				3-4, 5 & 6	20DB, 216B, 213B
3.2.4.3 Slide authority transition. 3.2.7.3	Discrete	0-5Vdc		1-slide auth			4-12	2127
3.2.4.4 No motion.		5Vdc→0		0-no motion			4-13	213F
3.2.4.5 S/S (spin/slide) indication.		5Vdc→0		0-S/S			4-14	2157
3.2.4.6 Regeneration enable.		0→5Vdc		1-regen			4-15	217F
3.2.4.7 Main contactor closed.		5Vdc→0		0-closed			4-10	20F7
3.2.4.8 Propulsion trip.	Discrete	5Vdc→0		0-trip			5-0	2008
3.2.4.9 Truck weight. AWO ~ 86,000# 3.2.3.5	Analog	0-10V	4.4k#/volt	173#/Bit	≤ 30 μsec	± 5%	0-1	2018
3.2.4.10 Wheel speed.	Analog	0-10V	100mV/mph	0.4mph/Bit		± 5%	3-7	216B
3.2.5 MTR and MTR control inputs. Ref. EE-75-S-296								
3.2.6 T/L outputs.								
3.2.6.1 S/S (spin/slide) indication	Discrete	5Vdc→0		0-S/S			--	270B, B7
3.2.6.2 Regeneration enable.	Discrete	0→5Vdc		1-regen en.			--	270B, B6
3.2.6.3 Propulsion trip.	Discrete	5Vdc→0		0-trip			--	270B, B0
3.2.7 Synchronous Brake System (SBS) outputs.								
3.2.7.1 Electric Brake Effort (EBE). 0-100%	Analog	0-10Vdc	100 mV/%	0.4%/Bit	≤ 25 μsec	±1%	--	2712
3.2.7.2 Braking rate command signal.	Analog	0-10Vdc	1.0V<X 1.684 <4.750V			±1.5%	--	--
3.2.7.3 Slide authority transition.	Discrete	0 5Vdc		1-slide auth			--	270B, B3
3.2.7.4 Slide dump signal	Discrete	5Vdc 0		0-dump			--	270B, B2
3.2.8 Other train equipment and function - outputs								
3.2.8.1 No motion (zero speed).	Discrete	0→5Vdc		0-no motion			--	270B, B5, 4
3.2.8.2 Wheel speed (car speed) 0-100 mph	Analog	0-10Vdc	100 mV/mph	0.4mph/bit	≤ 25 μsec	± 1%	--	2713
3.2.8.3 Main power contactor	Discrete	5Vdc→0		0-closure			--	270C, B4
3.2.9 MTR and MTR control outputs. Ref EE-75-S-296								

* Paragragh numbers refer to design specification EE-75-S-295 unless otherwise specified.

Table 5.6-II (Sheet 2 of 2). μP - I/O Interface Signal Characteristics

Interface signal characteristics	Signal Type	Signal Scaling	Analog Scale Factor	Digital/Discrete -Scaling/Phase	Response & Setting Time	Tolerance	MUX. CH & Port No.	Memory Storage Location
*3.2.1 Motor and motor control inputs								
3.2.1.1 Rotor Position Sensor (RPS). 70.5 P/REV.	Discrete	0-5Vdc		12 pulses/Rev	1.5 μsec		8212	218D, 218C
3.2.1.2 Motor Current (I_M). 0-750	Analog	0-10V	13mV/Amp	3A/Bit	≤ 30 μsec	±5%	0-4	20D8
3.2.1.3 Motor Voltage (V_M). 0-850		0-10V	12mV/Volt	3.3V/Bit		± 15%	0-5	2108
3.2.1.4 Line Voltage (V_L). 0-1020		0-10V	4mV/Volt	4V/Bit		± 3%	1-0	2019
3.2.1.5 Line Voltage Filtered (V_L^1). 0-1020		0-10V	4mV/Volt	4V/Bit		± 3%	1-1	2049
3.2.1.6 Line Current (I_L). 0-1000	Analog	±10V	10mV/Amp	4.0A/Bit	≤ 30 μsec	± 2.5%	1-2 & 3	2079/20A9
3.2.1.8 Overcurrent sensor.	Discrete	0-5Vdc		1-overcurrent	1.5 μsec	>1200 amp	5-1 & 8212	2020
3.2.1.9 Differential overcurrent sensor. Δ125 A dc	Discrete	0-5Vdc		1-Diff.		~125 amp	5-2 & 8212	2038
3.2.1.10 Filter capacitor bank fuse indication.	Discrete	5Vdc→0		0-blown fuse		≥ 1 cap.	8212	2184
3.2.1.11 Motor temperature sensor. Δ284° F	Analog	0-10V	35 mV/° F	1° F/Bit	<30 μsec	± 5%	1-4 & 5	2108,2138
3.2.1.12 Coolant Particle Detector Elect.	Discrete	5Vdc→0		0-particle		PPM	5-3	2030
3.2.1.13 Cycloconverter coolant outlet temperature.	Analog	0-10V	31mV/° F	1.25° F/Bit	<30 μsec	± 5%	1-7	2169
3.2.1.14 Inverter coolant outlet Temp. Δ380° F			31mV/° F	1.25° F/Bit			2-0	201A
3.2.1.15 Motor coolant temperature.			31mV/° F	1.25° F/Bit			1-6	2139
3.2.1.16 Motor coolant pressure. 0-100 PSI			100mV/PSI	0.4 PSI/Bit			2-2	207A
3.2.1.17 Motor control electronics coolant pressure.	Analog	0-10V	100mV/PSI	0.4 PSI/Bit	< 30 μsec	± 5%	2-3	20AA
3.2.1.18 Coolant particle detection. Motor	Discrete	5Vdc→0		0-particle		PPM	5-4	2068
3.2.1.19 Motor phase loss.				0-Ø loss			5-5 & 8212	2080
3.2.1.20 Inverter phase loss				0-inv. Ø loss			5-6 & 8212	2098
3.2.1.21 Cycloconverter fault				0-fault			5-7 & 8212	20B0
3.2.1.22 Inverter fault				0-fault			5-8 & 8212	20C8
3.2.1.23 FWD/REV CMD verify				0-FWD/REV			5-9	20E0
3.2.1.24 FWD/REV direction verify				0-REV			5-10	20F8
3.2.1.25 Mtr. field current loss	Discrete	5Vdc→0		0-field loss			5-11	2110
3.2.1.26 Mtr. Control QSD	Discrete	5Vdc 0		0-QSD			5-15	2180
3.2.2 TCE motor control FDBK and cross coupled FDBK								
3.2.2.1 Voltage Controlled Oscillator (VCO)	Analog	0-10V	2mV/Hz	40mV/Bit	<25 μsec	± 20 Hz	3-0 & 1	201B, 204B
3.2.2.2 FWD. CMD.	Discrete	0-5Vdc		1-FWD			5-13	2140
3.2.2.3 REV. CMD.	Discrete	0-5Vdc		1-REV			5-14	2158

* Paragragh numbers refer to design specification EE-75-S-296.

Figure 5.6-III (Sheet 1 of 2). μP - Motor Control I/O Interface Signal Characteristics

Interface signal characteristics	Signal Type	Signal Scaling	Analog Scale Factor	Digital/Discrete -Scaling/Phase	Response & Setting Time	Tolerance	MUX. CH & Port No.	Memory Storage Location
*3...3 Motor and motor control outputs.								
3.2.3.1 Voltage Controlled Oscillator (VCO)	Analog	0-10V	2mV/Hz	21Hz/Bit	<25 μsec	±20 Hz	--	270F
3.2.3.2 Forward/Mtr Command	Discrete	5Vdc→0		0-FWD			8212	270A, B7
3.2.3.3 Reverse/Mtr Command	Discrete	5Vdc→0		0-REV			8212	270A, B6
3.2.3.4 Dynamic/regenerative brake select	Discrete	5Vdc→0		0-Dyn/Regen			8212	270A, B5, 4
3.2.3.5 Dynamic/regenerative level	Analog	0-10V	100mV/%	0.4%/Bit	<25 μsec	±1%	8212	2710 & 2711
3.2.3.6 Dynamic resistor select	Discrete	5Vdc→0		1 = 0.78 Ω			8212	270A, B3
3.2.3.7 Coolant blower (off, 2 speed)	Discrete	5Vdc→0		0-ON			8212	270D, B7, 6
3.2.3.8 Motor control - QSD	Discrete	0→5Vdc		1 = QSD			8212	270A, B2
3.2.3.9 Drive Mode CMD	Discrete	5Vdc 0		0-drive			8212	270A, B1
Interrupt inputs								
Line voltage filtered (V_L^1)	Discrete (Interrupt)			0-V_L^1 Lo	1.5 μsec	± 5%	8214	--
Overcurrent, Diffcurrent, Mtr. Phase loss, Inv. Phase loss, Cycloconverter Fault, Inverter Fault — OR'd Interrupt	↓ Discrete (Interrupt)			0-Fault	1.5 μ sec	± 5%	8212/ 8214	2813-B5 ↓ B0, B4, B3, B2 2813-B1

* Paragraph numbers refer to design specification EE-75-S-296.

Figure 5.6-III (Sheet 2 of 2). μP - Motor Control I/O Interface Signal Characteristics

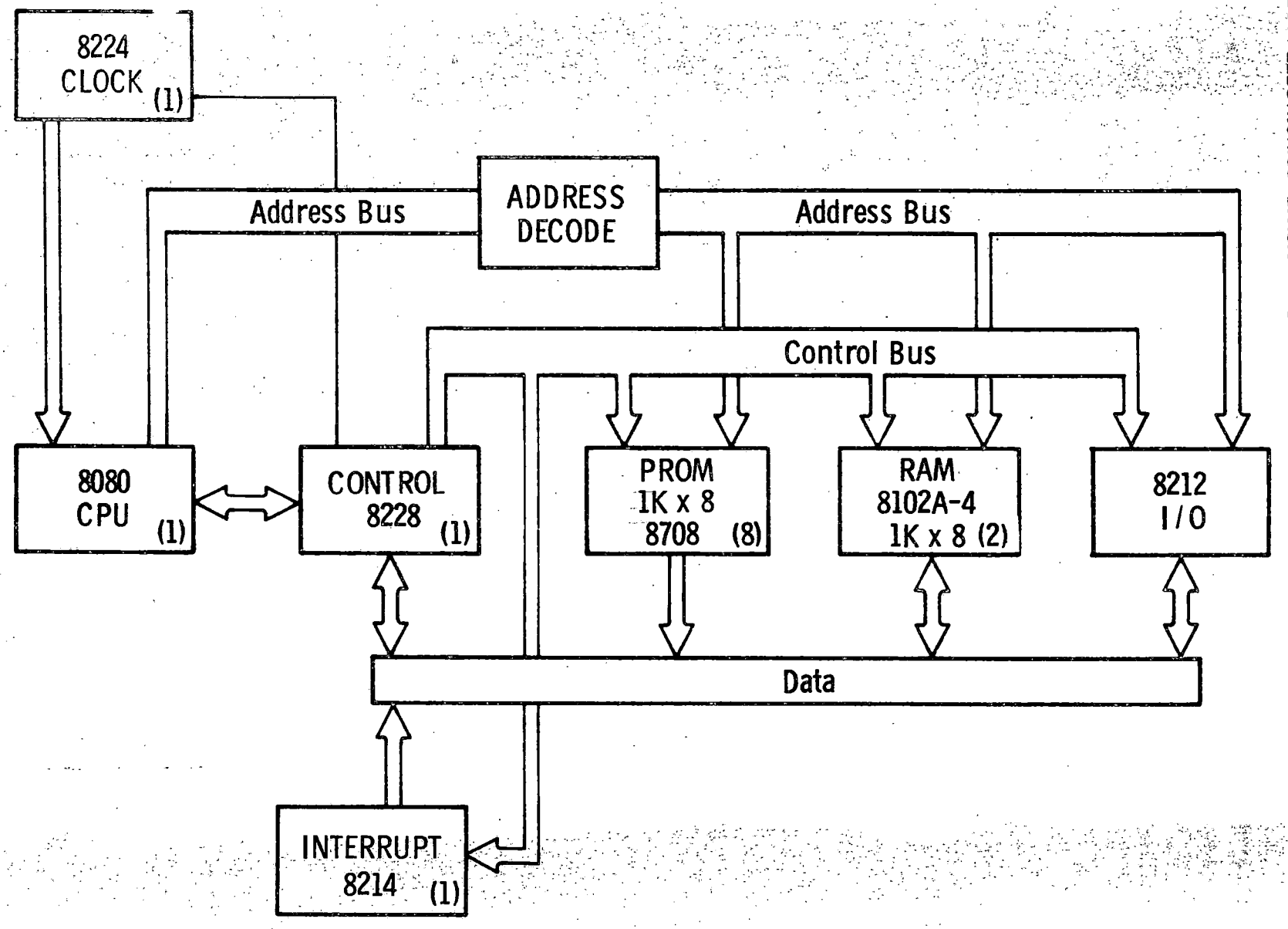

Figure 5.6-2. Microprocessor Functional Block Diagram

For diagnostics, input and output ports are assigned to a teletype interface. The supervisor subroutine provides the software required for the serial TTY data. This data is TTL and requires a modified teletype for this.

A "quick-look" display and associated software are also included. The display consists of two hexidecimal LEDs and four hexidecimal digit switches. Each time the program calls the output routine (at least once per loop) the four digit switches are read by the CPU. This data is used to read any location of memory. The contents of the specified memory location are then output to the LED display.

Memory storage and I/O port assignments, and program listings including subroutines are presented in a data package separate from this report. The software flow diagrams are contained in Appendix A.

TCE Board Descriptions

Each TCE is comprised of four augat universal wire wrap boards (8136-U series). These boards have 54 rows of 50 pins each. The boards are organized in six (A, B, C, D, E, F) groups of 9 rows. Associated with each group are provisions for three connectors of 28 pins each. These pins are for interconnection of signals external to the board. Power and ground are hardwired to the power and ground plane of the augat board.

Board #1 – Digital I/O Board: Board 1 contains A/D's, D/A's, input ports, output ports, and associated decode and conditioning circuits. The layout is shown in Drawing 7560072, pages 6 to 11. Pages 12 through 14 of this drawing show the functional flow of the I/O and pages 15 through 25 are the detailed schematics.

Board #2 – CPU Board: This board contains the CPU, memory, and control elements. Physical layout of the CPU board is shown in pages 6 through 11 of Drawing 7560073. Pages 15 through 21 are the logic diagrams for this board.

Board #3 – AUX Input/Output Board: This board contains analog circuits to condition external signals for interface to the digital processor. This includes circuits for QSD, filter caps, B+ and V_L. There are also counters to determine wheel speed, rotor position sensor speed, and real time. The physical layout is given in pages 6 through 11 of Drawing 7560074. Pages 15 through 27 are schematics for these circuits.

Board #4 – Analog Board: This board contains the analog condition circuits for most of the signals required by the TCE. Multiplexers for these signals are also on this board. Drawing 7560075 gives the complete physical description of this board. Pages 8 through 13 are the physical layout and pages 17 through 56 are the detailed schematics.

Interconnection Cabling

Delco Electronics Design Specification EE-75-S-380 contains I/O pin assignment lists for each of the four TCE boards: CPU Board, I/O Board, Auxiliary I/O Board, and Multiplexer Board. Shown are the from/to conditions for all TCE signals power, and grounding.

Regulators and Power Supply

The TCE power supply was designed and built to Delco Electronics Specification 75-S-303. The power supply design for the TCE has a source voltage from the SOAC M/A Set/Battery power of 28 to 44 Vdc and had to be designed to withstand transients or surges of 50 joules. The TCE as designed required ±5V, +12V, ±15V and +28 Vdc for some interface hardware. Mechanization of the power supply includes a Delco-designed transient protection input and preregulator (pulse width modulation-switching regulator), four commercial supplies (+5 Vdc - Abbott, +28 Vdc Technetics, ±15 Vdc, and -5 Vdc Abbott), one +12 Vdc post regulator, and two ±15 Vdc overvoltage protection circuits. Schematic representation of the power supply is shown in Figure 5.6-3.

Vital Relays

Two vital relays are incorporated in each railcar. These are the Emergency Relay, which is a trainline and shuts down total train propulsion and causes emergency braking to be applied, and the No Motion Relay, which is energized when car speed is below about 2 mi/h. This permits car doors to be opened and the brake charging valve to be energized. This relay is not a trainline, but operates on a per car basis.

Grounding

The Train Control grounding philosophy is depicted in Figure 5.6-4. Signal interface with the SBS is strictly handled through optical isolators. Good solid car grounds are provided at the junction boxes, motor and motor controls, and battery. Other units tie to these junction boxes and battery low in an effort to provide a single point grounding philosophy.

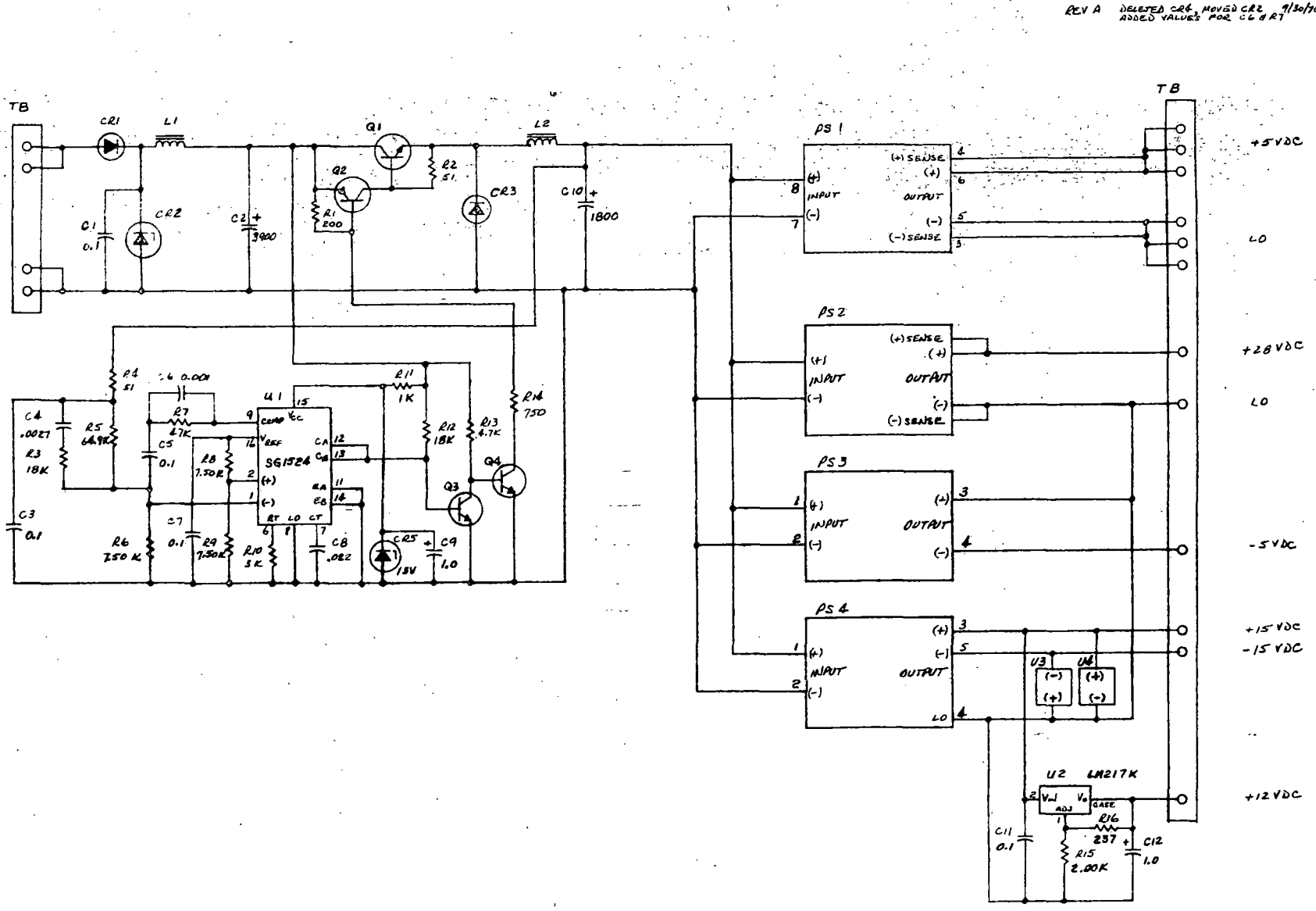

Notes:

1. UNLESS OTHERWISE NOTED ALL RESISTANCE VALUES ARE IN OHMS AND ALL CAPACITANCE VALUES ARE IN MICROFARADS.

Figure 5.6-3. Preregulator and Commercial Power Supplies

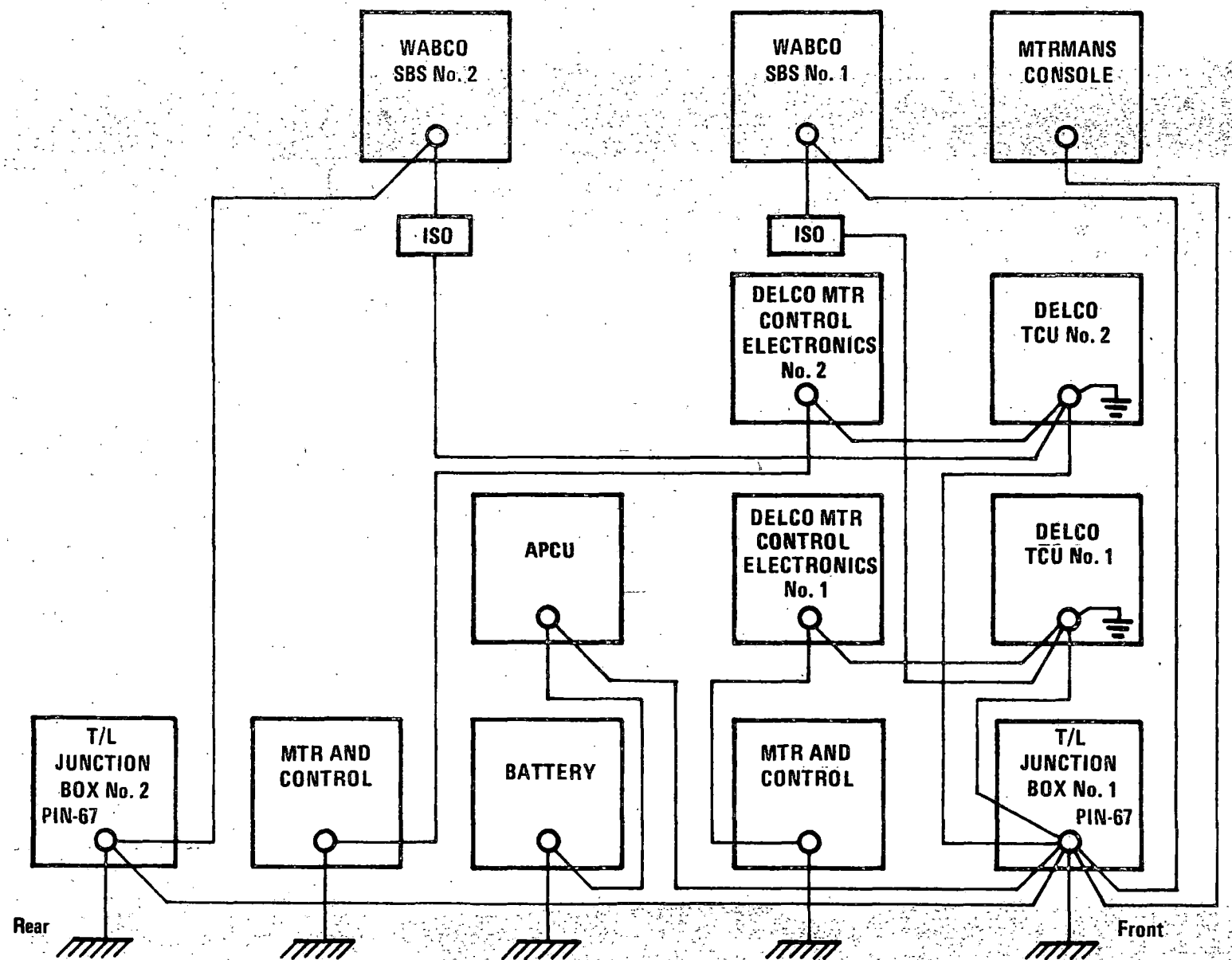

Figure 5.6-4. Grounding Philosophy (one car)

5.6.2.2 Motor Control Electronics (MCE)

5.6.2.2.1 MCE Functional Requirements

The MCE translates TCE generated Voltage Controlled Oscillator (VCO) tractive effort command analog signals, as well as various discrete signals, into inverter gate timing and mode control signals. The mode control signals place the motor in the motoring or dynamic braking, motoring or regeneration braking, and forward or reverse modes. The discrete signals from the MCE also shutdown and reset the SCR gate drive to the inverter, cycloconverter, and brake rectifier modules.

The MCE also processes the motor rotor position sensor (RPS) and Counter EMF (CEMF) signals to form cycloconverter and brake rectifier SCR gate pulses. This self-controlled SCR gate timing produces operation equivalent to that of a dc motor in the motoring mode and phase delay rectifier operation in the braking mode. The RPS/CEMF derived signals are also sent to the TCE as a pulse train indicating motor speed.

The MCE processes inverter diode current signals to obtain protection against operation with insufficient inverter SCR turn-off time. It also processes motor phase current signals to issue a drive QSD command in the event of a cycloconverter fault. The motor current signals are also rectified and sent to the TCE as an indication of tractive effort.

5.6.2.2.2 MCE Design Approach

The MCE was designed using combinatorial logic elements (NAND, NOR, etc., gates), sequential logic elements (flip-flops, monostables, etc.), analog comparators, and operational amplifiers. At the beginning of Test Article (TA) system level testing in January 1977, all logic elements, operational amplifiers, comparators, resistors, capacitors, and diodes were packaged in dual-in-line package (DIP) modules.

During the early phases of the previously mentioned IR&D program (1971-1973) the MCE circuits were packaged on printed circuit boards with connections completed with soldered wires. In 1974, the MCE circuits for one motor were repackaged on a single wirewrap panel because of the greater reliability and flexibility of the wirewrap approach. In the 1975-1976 period, during the ASDP system development, the logic type was changed from High Noise Immunity Logic (HiNIL) to Complementary Metal Oxide Semiconductor (CMOS) because of the better availability and variety of CMOS devices. The individual MCE

circuits were changed to CMOS during periods of system down time to minimize the impact on the development program schedule. Also in this period, multiple resistor, capacitor, and diode assemblies became available in dual-in-line (DIP) packages. These passive component assemblies were incorporated in the MCE, replacing discrete components soldered to component carriers. The ease of modifying the wirewrap panel permitted these changes to be made with no effect on the performance or appearance of the panel.

During the design integration of the MCE and TCE it became necessary to add one-half of a wirewrap panel for each MCE to accommodate TCE interface circuitry, making a total of three panels for the two MCE units of a railcar.

Numerous circuit changes were made during the TA test program as discussed in paragraphs 6.3.3 and 7.1.1. These circuit changes were implemented with discrete components soldered to component carriers. Trimpots for changing resistance values were installed on component carriers. These replaced the plug-in DIP assemblies used for making resistance or capacitance changes in the original TA MCE. Several small auxiliary wirewrap panels containing modified circuits were attached to the main wirewrap panels.

Because the MCE wirewrap panels must be reworked to be suitable for installation on a railcar, the following discussion groups the MCE functional circuits as they would be installed on the reworked panels.

5.6.2.2.3 MCE Wirewrap Panel Design Description

Board I

Board I contains most of the control circuitry for the forward propulsion system of the railcar, with the balance of the control circuitry contained on Board II.

- Panel Group A (drawing No. 7559411, Sheet 2) contains the voltage controlled oscillator (VCO), ring counter, inverter phase reverser, and motor phase loss sensing circuit.

  The VCO is an integrated circuit with external resistor-capacitor timing components operating over a frequency range of 2100 Hz to 7200 Hz in response to the 0 to 10 Vdc tractive effort control signal from the Train Control Electronics (TCE).

The ring counter, formed from a shift register integrated circuit, produces the six-phase inverter SCR gate timing signals.

The inverter phase reverser is an arrangement of logic gates which reverses the inverter gating phase sequence when the motor direction of rotation is reversed. This gives the rotary transformer in the motor the same sensitivity to speed in both directions of rotation.

The motor phase loss sensing circuit consists of several logic gates operating on the motor phase current logic signals. The circuit issues a quick shutdown (QSD) signal if one or more of the six motor current logic signals is missing.

- Panel Group B (Drawing No. 7559411, Sheet 3) contains inverter fault protection, inverter phase loss protection, and frequency limiting circuits.

The inverter fault protection circuit operates on three phase (x, y, z) signals originating from CTs in the inverter module. The x signal phase, for example, represents the pulse widths of the currents in the pair of power diodes which are anti-parallel to the two SCRs in the x inverter phase. Diode current pulse width is interpreted as SCR turn-off time. In the event of an actual or incipient inverter fault, one or more of the six diode current pulse widths will fall short of the pulse width established by reference monostables, and a QSD command will be issued.

The inverter phase loss circuit operates on the inverter diode signals described above and issues a QSD command if one or more of these signals are missing.

The inverter frequency limit circuit reduces the inverter frequency, and hence the drive power level, in the event of excessive motor speed, voltage, or current or inadequate inverter turn-off time.

- Panel Group C (Drawing No. 7559411 Sheet 4) contains latch circuits and light emitting diode (LED) drivers. The latches issue, and hold until reset, a master QSD command in response to the individual QSD commands: inverter

fault, inverter phase loss, motor phase loss, cycloconverter fault, or manual QSD. The LED drivers energize the appropriate MCE front panel LED to indicate the cause of the shutdown.

- Panel Group D (Drawing No. 7559411 Sheet 5) contains the rotor position sensor (RPS) synchronous demodulator, the counter EMF (CEMF) phase advance circuitry, three-phase/six-phase logic, and the forward/reverse logic.

The motor RPS produces three-phase, four-wire suppressed carrier signals. These 30 kHz signals from the high impedance RPS source are clipped with diodes and buffered with integrated circuit unity gain operational amplifiers. The signals are then full wave synchronously demodulated, using six CMOS bilateral switches. The demodulated RPS signals are then RC filtered and added to the phase advanced CEMF signals to form the input to the three RPS/CEMF comparators. Operation of the RPS and CEMF circuitry is further discussed in References 1, 2, and 3.

The three-phase RPS/CEMF comparator outputs are processed by a group of logic gates to form the six-phase cycloconverter SCR gate timing signals. Additional logic gates change the phase sequence of these signals for reverse operation.

- Panel Group E (Drawing No. 7559411 Sheet 6) contains the cycloconverter synchronous gating logic. The cycloconverter gate timing signals are synchronized with both the cycloconverter input voltage at the inverter frequency (350 Hz to 1200 Hz) and with the 30 kHz cycloconverter RF gate rectifier supply voltage.

Synchronizing the cycloconverter timing signals with cycloconverter input voltage prevents a weak gate SCR turn-on due to the random premature removal of gate current that occurs with non-synchronized gating. It also prevents the application of gate current to an SCR when the anode-to-cathode voltage is highly negative.

The cycloconverter gate timing signals are also synchronized with the 30 kHz RF gate drive in order to avoid a random weak gate SCR turn-on. This synchronization is accomplished with 18 Flip-Flops having the 18 cycloconverter gate timing signals as data inputs. The Flip-Flops are clocked by th 30 kHz RF gate rectifier supply voltage to effect synchronization.

- Panel Group F (Drawing No. 7559411 Sheet 7) contains cycloconverter fault protection circuitry and motor voltage and current signal rectifier circuits. The group also contains drivers for LEDs that indicate which two of the six cycloconverter SCR triples are being gated.

The cycloconverter fault protection circuitry consists of six comparators which operate on the motor current sensor outputs to produce logic signals that indicate the presence or absence of motor currents of plus and minus polarity in each of the three motor phases. Each motor current signal is extended in time and ANDed with a current command signal of the same phase but at opposite polarity. A coincidence of the actual current signal and the commanded current signal, which indicates a real or an incipient fault, produces a QSD command. Additional information on the fault protection method is contained in Reference 4.

Board II

Board II contains Operate/Test and TCE interface circuitry and brake control circuitry for both propulsion systems of a railcar.

- Panel Group A (Drawing No. 7559412 Sheet 1) contains Operate/Test interface circuitry. This circuitry permits operation of the MCE from either the TCE or from the MCE control panel.

- Panel Group B (Drawing No. 7559412 Sheet 2) contains the TCE interface circuitry.

- Panel Group C (Drawing No. 7559412 Sheet 3) contains the brake phase control circuitry. This circuitry consists of ramp generators (reset integrators) operating from the cycloconverter RPS/CEMF timing signals. The integrator drive voltage level is derived from a tachometer circuit. This serves to maintain the ramp amplitude constant as the frequency of the generator changes. Voltage comparators operate on the ramp voltages to give logic signals delayed in proportion to the comparator threshold levels which are derived from the tractive effort command signal. Three comparators each are provided for control of the dynamic brake rectifier and the regenerative brake rectifiers operating as a dual semi-converter. The three uncontrolled rectifiers in the semi-converters are gated to act as diodes using undelayed RPS/CEMF timing signals.

  DC gate control for the dynamic brake resistor shunting SCR is also contained in Panel Group C.

- Panel Group D (Drawing No. 7559412 Sheet 4) is functionally identical to Panel Group A. It provides the same functions for the no. 2 (aft) propulsion system as Group A provides for the no. 1 system.
- Panel Group E (Drawing No. 7559412 Sheet 5) is functionally identical to Panel Group B. It provides the same functions for the no. 2 (aft) propulsion system as Group B provides for the no. 1 system.
- Panel Group F (Drawing 7559412 Sheet 6) is functionally identical to Panel Group C. It provides the same functions for the no. 2 (aft) propulsion system as Group C provides for the no. 1 system.

Board III (Drawing No. 7559413 Sheets 1 – 6)

Board III contains control circuitry for the No. 2 (aft) propulsion system and is functionally identical to Board I.

5.6.2.3 Electronic Control Unit Packaging

The Electronic Control Unit (ECU) contains the train control and motor control electronics, related power supplies, and vital relays required for control of the two propulsion systems of a car. For ease of maintenance the major subassemblies are packaged in slide mounted horizontal pullout drawers with tilt-up and tilt-down capability. Figures 5.6-5 and 5.6-6 show the overall assembly.

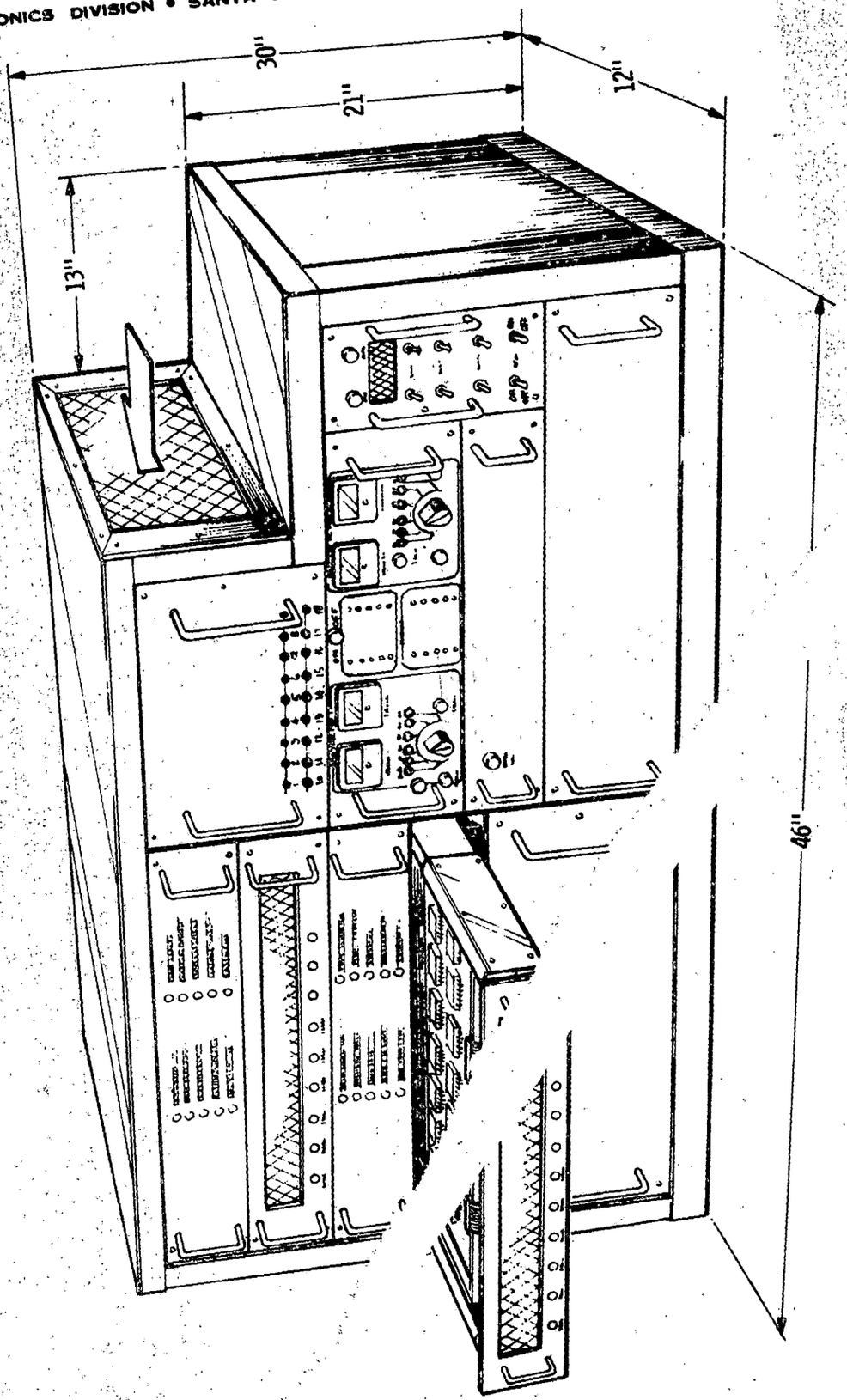

Figure 5.6-5. Electronic Contr

R78-14-2

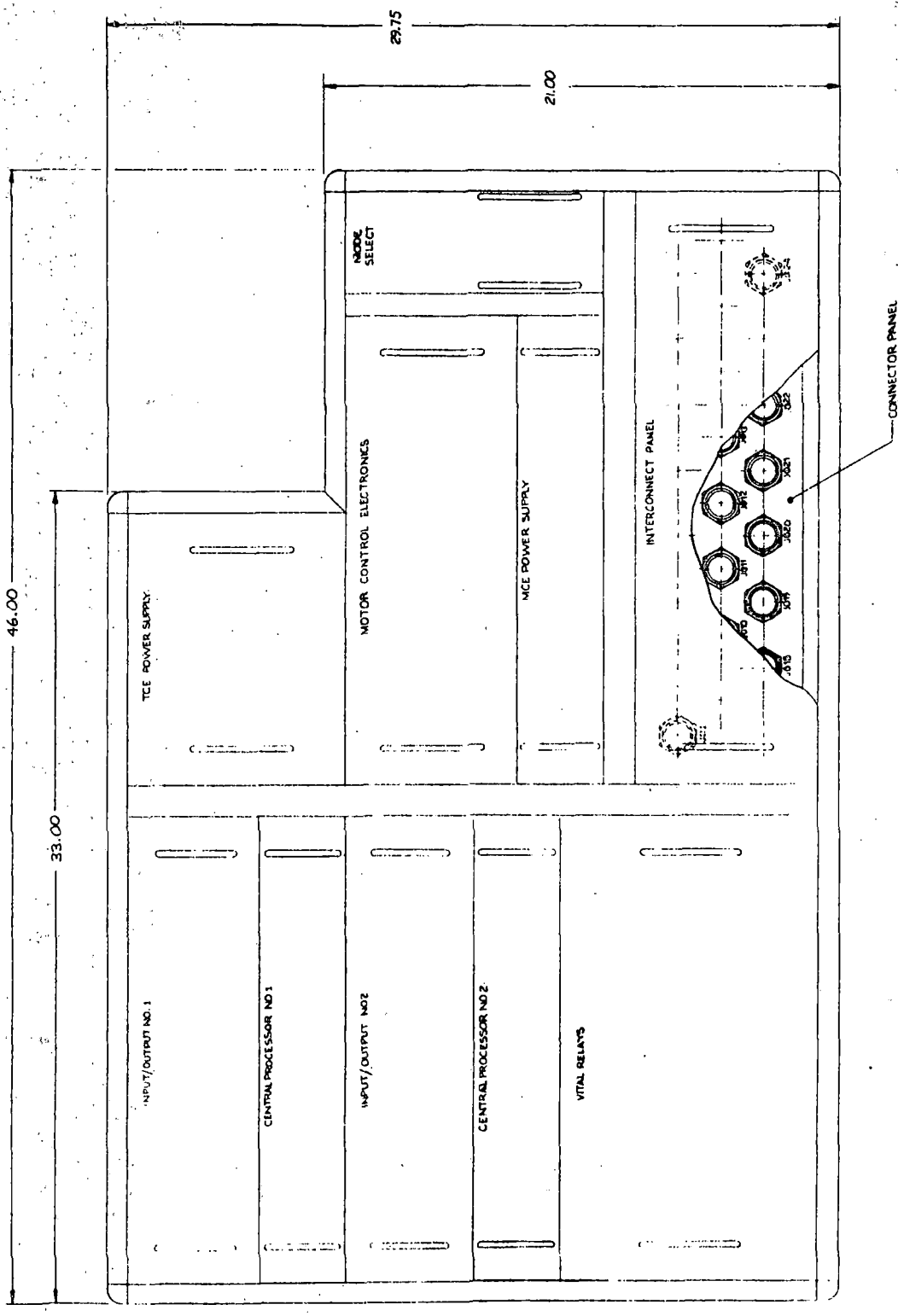

Figure 5.6-6. ECU Assembly – Front View

The unit enclosure is a modularized cabinet made from commercially available aluminum end caps and extrusions. The side and rear panels are also aluminum and are welded to the extrusions to provide a solid unitized structure. The unit is customized to fit in the motorman's cab area under the front window. The lower surface along the top of the unit provides a step which allows the driver to leave through the SOAC car emergency window exit.

The unit is cooled by a forced air system. Conditioned air enters the unit through filtered inlets on the front panels and in the stepped area. It is then drawn directly across the components and through protective grilles by the backwall mounted exhaust fans.

A backwall harness assembly interconnects the individual drawers with one another and with the interconnect panel. This panel is located behind a blank panel in the lower right corner of the ECU cabinet (see Figure 5.6-6).

5.6.2.3.1 Train Control Electronics (TCE)

The complexity of the TCE electronics dictates the use of a computer type packaging approach. As a result, the TCE for each propulsion system is partitioned into an input/output (I/O) drawer and a central processor (CPU) drawer. Both drawers each contain two augat wirewrap assemblies which may be pivoted upward (for the top assembly) or downward (for the lower assembly). Harness interconnections are made along the rear of the augat board to minimize the service loop.

Since the majority of the system interface enters the TCE on the I/O boards, all indicators and test points are displayed on the I/O assembly front panel. This allows the CPU front panel to be fully vented for cooling of the higher heat dissipating components found in the CPU. A list of the assigned I/O test points and indicators is given in Table 5.6-IV. A lamp test switch is also located on the I/O front panel which activates all indicator lamps to assure their proper functioning.

Each connector is keyed such that it cannot mate with the bulkhead connector of the incorrect unit. The space between the connector interface panel and the blank panel provides a feedthrough for cable assemblies which interface with the ECU assembly. As a result this area of the ECU is environmentally sealed from the rest of the ECU hardware.

	TEST POINTS		INDICATORS
1.	P-Signal	1.	Electronics Coolant Pressure
2.	Line Voltate Cap	2.	Mtr Coolant Pressure
3.	Line Current	3.	Diff Current
4.	Mtr Current	4.	Over Current
5.	Mtr Voltage	5.	Mtr Temp Hi
6.	Line Voltage	6.	Cycloconverter Coolant Temp Hi
7.	Brake Rate CMD	7.	Inverter Coolant Temp Hi
8.	Electrical Brake Effort	8.	Mtr Overspeed
9.	Brake Level	9.	QSD/P-Signal Inhibit
10.	Brake Mod.	10.	Mtr Phase Loss
11.	Truck Weight	11.	Inverter Phase Loss
12.	Wheel Speed	12.	Cycloconverter Fault
		13.	Inverter Fault
		14	Blown Fuse
		15	Field Current Loss
		16.	LOB +
		17	Fail Safe Clamp

Table 5.6-IV. TCE Front Panel Test Points and Indicators

The TCE power supply assembly extends back into a doghouse area at the rear of the ECU assembly. Redundant power supplies assure that power is provided to the TCE logic in case of a single-point failure. The decision to use redundant power supplies was based on the premise that a failure of the TCE logic to identify an out of tolerance train condition could result in an undetected hazardous condition. Electronic components in the power supply mount directly to an aluminum chassis which acts as a conductive heat sink. Air is drawn over the components through an air inlet mounted in the stepped portion of the ECU chassis adjacent to the power supply.

5.6.2.3.2 Motor Control Electronics (MCE)

The MCE as packaged in the ECU services two propulsion systems (one for each truck). Quick shutdown capability to prevent the possibility of further system damage is provided. The MCE is packaged into the major subassemblies located in the right ECU bay. These

are the MCE logic assembly, the MCE power supply, and the mode select panel. The MCE logic assembly has three frame mounted wirewrap-type augat boards capable of hinging up or down. The center board mounts forward of the top and bottom panels to permit full 90^{o} rotation about the pivot point. All interconnect is accomplished at the rear of the panels.

The MCE power supply contains two driver circuit card assemblies which provide the power electronics with gate drive information. The power electronics involved are controlled by inputs from the logic unit mentioned above. Interface with the circuit cards is accomplished using augat board type connectors which in this case plug into IC adapter style receptacles mounted in the middle of the board.

The MCE input power supply mounts on an aluminum chassis behind the mode select panel. This allows the assembly to use the ECU chassis as a conductive heat sink. The mode select panel provides the emergency shutdown capability as well as mode selection. In general, a series of switches provide various combinations of system operation. For a given set of switch positions the particular group of propulsion system performance characteristics may be investigated.

5.6.3 LINE FILTER INDUCTOR

5.6.3.1 Functional Requirements

The line filter inductor, in conjunction with the line filter capacitors located in the power control switchgear assembly, buffers the power converter from third rail voltage variations and attenuates line current undulation caused by the input inverter.

5.6.3.2 Design Approach

The inductor was sized to provide a dc resistance that would produce less than 1000 watts average loss over the ACT-1 Synthetic Transit Route. Inductance was based on that required to limit the line surge current. The inductor damping resistance was selected to limit the line filter capacitor bank overvoltage to an acceptable level.

The ASDP inductor design is based on experience gained during the IR&D program discussed in subsection 6.1 and uses copper sheet conductor and standard E-I laminations. Damping is provided by a metal sheet placed in the airgap. Material and dimensions of

this sheet were determined empirically to give the desired inductor transient response. The mechanical design of the inductor mounting structure is based on the need to protect the inductor from impact with flying objects and to prevent the inductor from dropping off the car in the event of failure of the mounting bolts.

5.6.3.3 Design Description

The line filter inductor assembly is a single unit containing two filter inductors, one for each of two propulsion systems per car. It consists of two parallel windings on two separate laminated silicon steel E-cores which share a common I section (see Figures 5.6-7 and 5.6-8). The windings are 46 turns of sheet copper having a combined (two windings in parallel) resistance of 0.0022 ohm. Turn-to-turn insulation is 5 mil Nomex paper. The inductor assembly is vacuum dipped and baked with solvent-less epoxy varnish. The nominal inductance is about 2.5 mH with a saturation current of 800A. The saturated inductance is approximately 340 μH. The line filter is designed as a swinging choke and hence has a relatively large air gap. The nominal inductance (per coil) is 5 mH at low current values and 2.5 mH at 400 A/coil or 50% of rated current. This is the point where a relatively soft transistion into saturation occurs. By permitting saturation at high currents, the weight of the inductor is reduced by approximately 50% over that otherwise required. The use of a swinging choke is feasible because at input current levels of 800A and above, the input impedance of the inverters is low. This provides, in conjunction with the power source impedance, an additional degree of line transient filtering. In addition, at high inverter input current levels, the inverter frequency is high, so that inductor reactance is high even with inductance reduced by saturation.

Damping is provided to limit peak inductor current and peak capacitor voltage when the filter is energized by closing the main contactors or by contact of the rail shoe with an energized third rail. The damping resistance is obtained by means of a metal sheet in the airgap. The sheet is equivalent to a resistive one turn winding coupled to the inductor winding.

The inductor steady-state rms current is estimated from the ACT-1 Synthetic Transit Route duty cycle as 600A. Inductor loss is essentially due to the dc resistance and is

$$P = 600^2 \times 0.0022 = 792W.$$

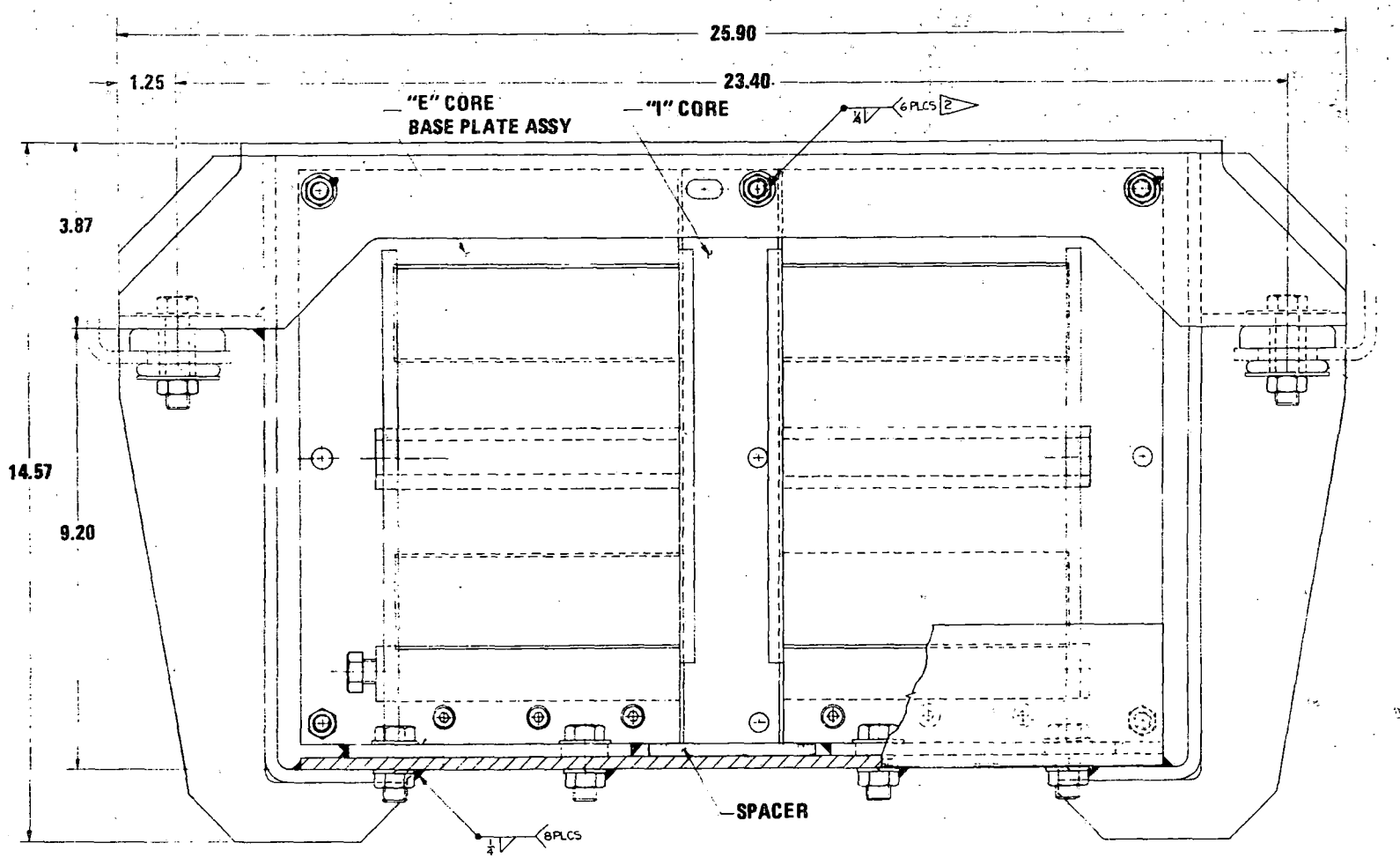

Figure 5.6-7. Line Filter Inductor – Front View

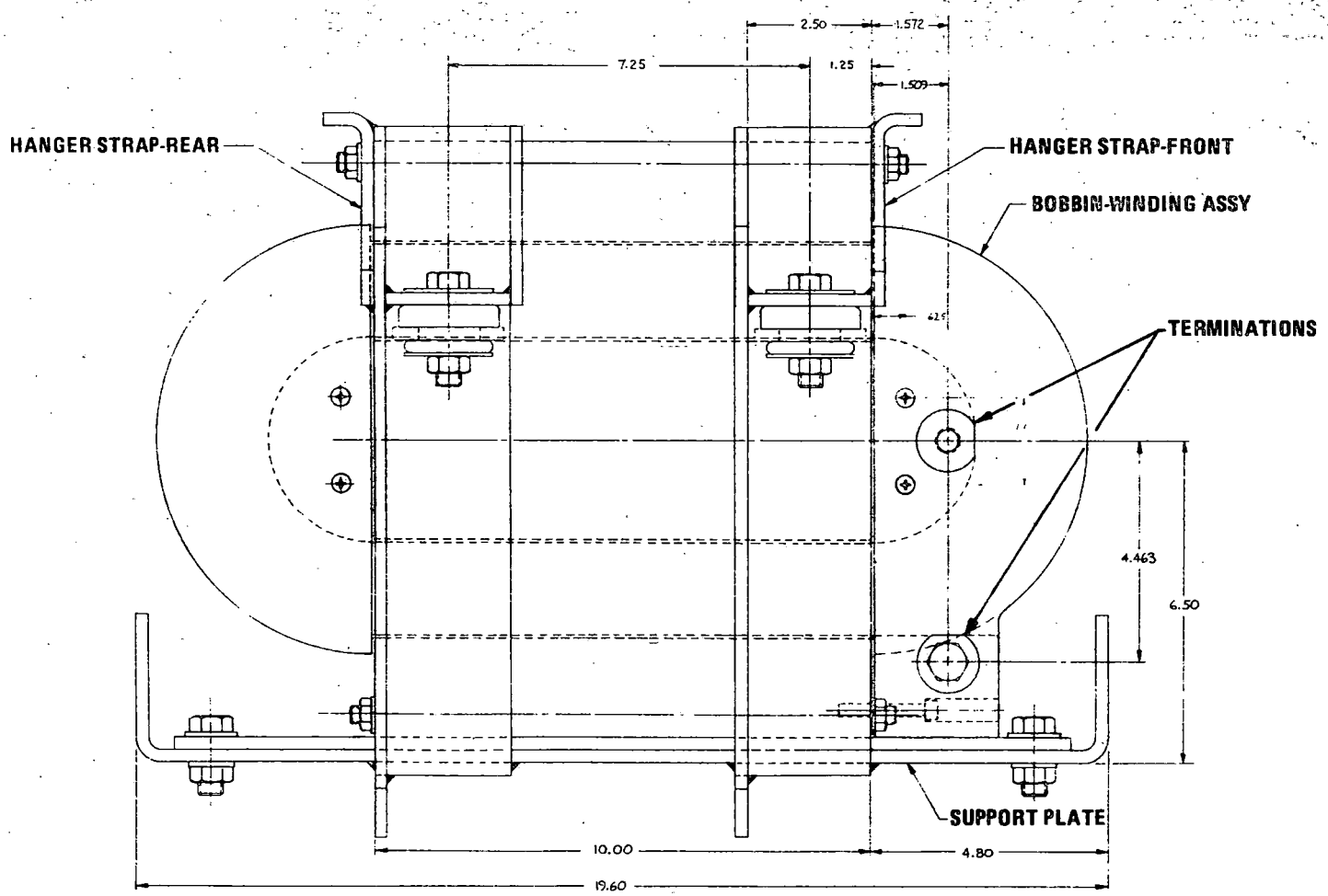

Figure 5.6-8. Line Filter Inductor – Side View

The inductor surface area is approximately 2200 $in.^2$, for a surface power density of 792/2200 = 0.36W/$in.^2$. This results in a surface temperature rise above a 35°C ambient in still air of 40°C. For a typical hotspot-to-surface temperature rise of 40°C, the hotspot temperature is 35 + 40 + 40 = 115°C. This is well below the Nomex insulation temperature rating of 250°C. Cooling is by free air convection.

The inductor chassis and the laminations are welded together to form a unitized construction. Copper bar terminals are silver soldered to the end of the copper sheet. The terminals are electrically isolated from the chassis and laminations by means of fiberglass insulators. Steel plates located across the faces of the inductor windings provide protection against airborne rocks and other debris.

A photograph of the line filter inductor is presented in Figure 5.6-9.

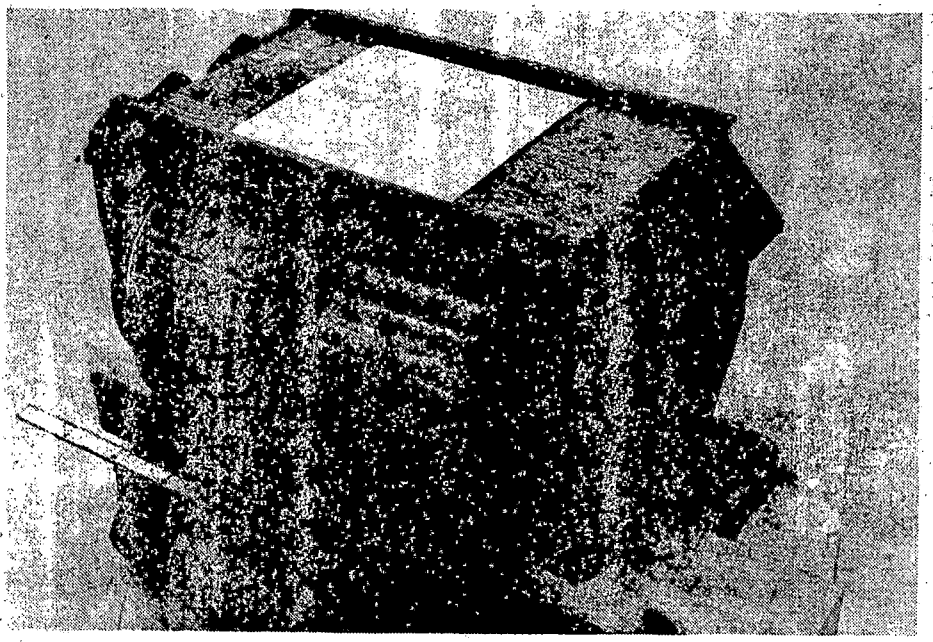

Figure 5.6-9. Line Filter Inductor

5.6.4 POWER CONTROL SWITCHGEAR

5.6.4.1 Functional Requirements

The power control switchgear (PCS) assembly provides filtered 3rd rail power to the propulsion power control equipment, protects against overcurrents, provides a means of quickly disconnecting the load from the source and prevents current flow back into the 3rd rail except during regenerative braking.

5.6.3.2 Design Approach

Two identical PCS assemblies are provided per railcar. Each operates in conjunction with a propulsion system driving one truck.

5.6.3.3 Design Description

This assembly contains a line contactor and some auxiliary contactors, current and voltage sensors, a capacitor bank which in conjunction with the line filter inductor provides filtering of the 3rd rail power, diodes, and fuses.

A schematic of the PCS circuit is shown in Drawing 7558198 (Figure 5.6-10).

The line contactor is a single pole, normally open contactor. This contactor provides the means to electrically disconnect the system from the line when necessary. Rail experience has shown that a contactor cannot open fast enough to protect a semiconductor from a line-line short (as can occur in the inverter). Therefore, a contactor was selected that has over-current hold-in (OCHI) characteristics that magnetically prevent the armature from releasing if the fault current exceeds 2,000 amps. Faults can far exceed this value. When the fault current has decreased to less than 2,000 amps (because of a fuse clearing) the contactor will open. If this feature were not incorporated in the design, the contactor would have to be physically many times larger in order to be able to contain the arc. This contactor weighs less than 25 pounds.

When the contactor coil is opened, a high voltage (exceeding 400 volts) will be present on the B+ line. This must be snubbed or clamped. In this system a simple diode is used across the coil which keeps the transient very low. Logic circuits are also protected from contactor coil inductive kicks by this diode (CR2). Although suppressing the transient extends the drop-out time of the armature, it is felt that this results in more dependable operation.

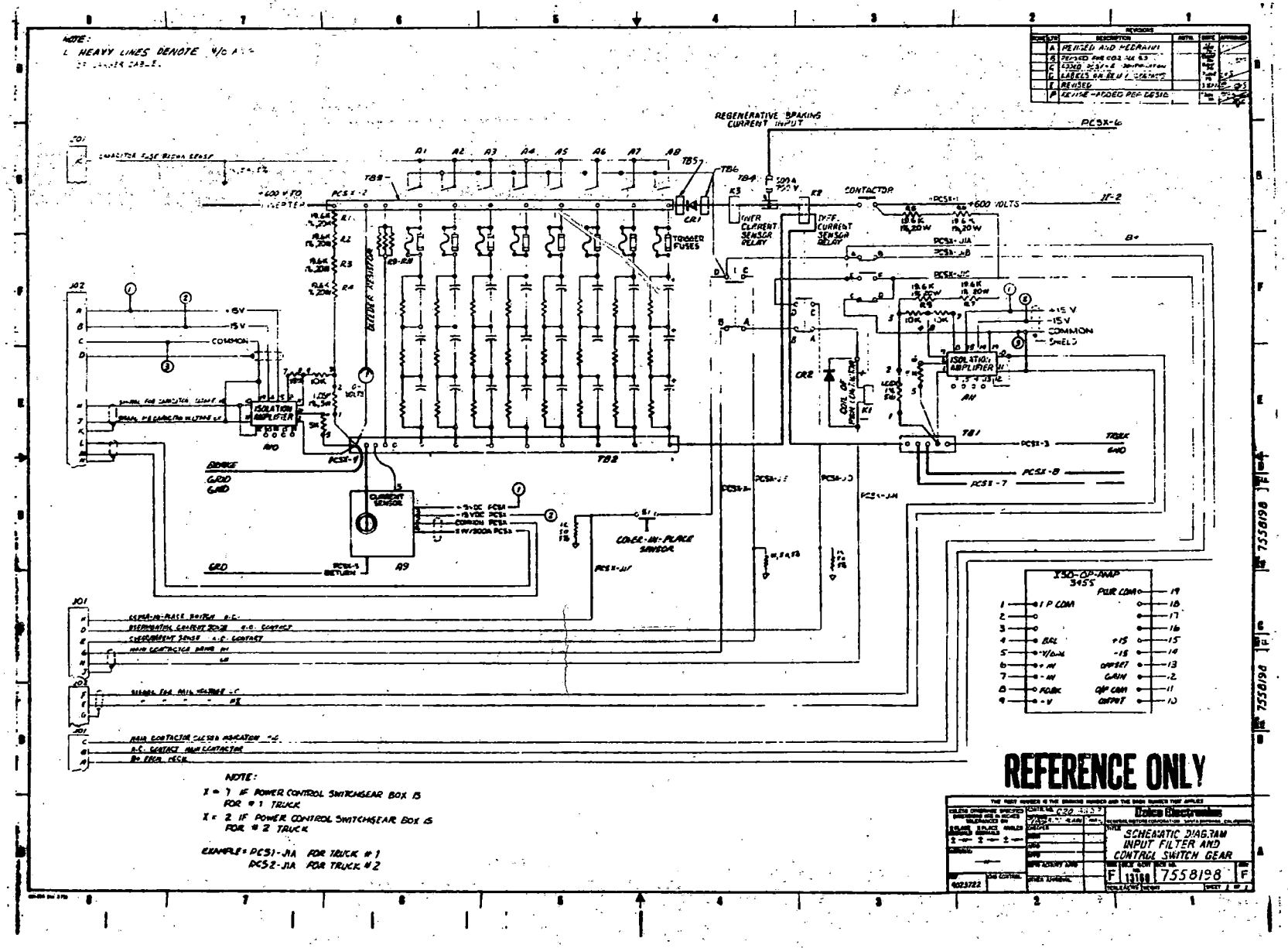

Figure 5.6-10. Schematic Diagram of PCS Circuit

The differential current sensor is a relay which permits the positive and negative power cables to pass through the magnetic circuit side-by-side. If the current in the negative cable equals the current in the positive cable, their mmfs cancel and there is no net ampere-turn result to produce flux. The relay does not operate in this case. If the ground (negative) cable current is less than the positive cable current, a failure in insulation is signified. The mmfs no longer balance and, at approximately 125 amps difference, the relay will actuate, signalling the microprocessor to QSD, and will not permit reset until the problem has been corrected.

The overcurrent sensor is a relay which is similar to the differential relay. It contains only the positive polarity cable. This sensor is to shut off the system when the input current is 900 amps or more, well over rated value (600 amps), but is not in a fault situation. The auxiliary contacts signal the train control microprocessor which QSD's the system and latches. In this case, however, a reset is permitted.

Blocking diode CR1 prevents the capacitor bank from discharging back into the source in the event the source voltage is low, shorted, or grounded.

The filter capacitor bank consists of 8 parallel strings with 3 capacitors per string. Nominal capacitance is 3300 microfarads per capacitor or 8800 microfarads for the assembly. The capacitor voltage rating is 350 volts dc. Voltage divider-resistor/bleeder resistors are across each capacitor and an additional bleeder resistor is across the entire assembly in order to discharge the capacitor bank to 50 volts or less within 30 seconds. Each capacitor string is fused for 60 amps. This value permits the charging current inrush to occur without blowing a fuse, but is low enough to enable the fuse to blow if a capacitor string shorts. When a 60 amp fuse blows, the parallel, high-resistance, trigger fuse clears also and a spring-loaded plunger pops out and actuates a leaf switch, indicating a shorted capacitor string to the microprocessor. A panel meter which indicates the dc voltage across the capacitor bank is also included in the PCS in order to provide a visual indication to help protect anyone working on this assembly.

Two high quality isolation amplifiers to sense voltage, which can operate properly over the expected temperature range, and a Hall sensor (1000/0/+1000 amps) are also contained in the PCS.

The chassis is a welded aluminum structure which provides a high strength lightweight housing. Front and rear panels and cable stuffing tubes seal the enclosure against dirt, dust, and moisture. Modules were developed within the PCS wherever possible for ease of maintenance and repair.

The only high heat dissipation component in the unit is the blocking diode. This diode was mounted such that it is electrically but not thermally isolated from a heatsink which protrudes through the rear panel of the unit into ambient air. Cooling of the PCS is by free air convection.

An arc chute was built to direct any arcing in the line contactor down and away from the unit. This eliminates the possibility of an arc sustaining itself internally and resulting in the potential destruction of the unit.

A cover switch is actuated when the cover is closed indicating to the train control that the cover has been replaced. If this cover is left off, a warning light warns the motorman.

Figure 5.6-11 a photograph of the PCS unit, and Figure 5.6-12 shows a view of the mechanical arrangement.

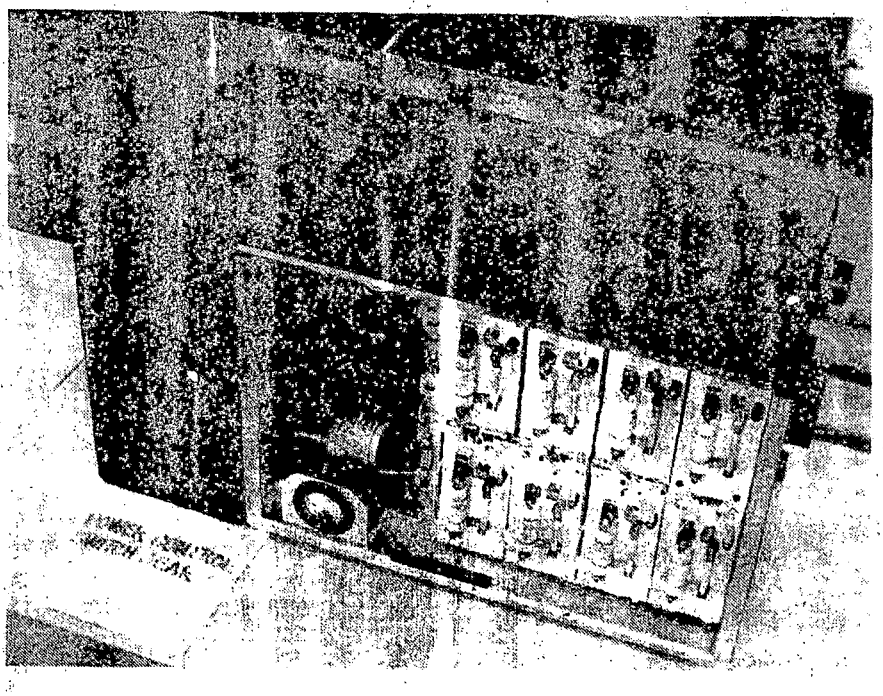

Figure 5.6-11. Power Control Switchgear Assembly

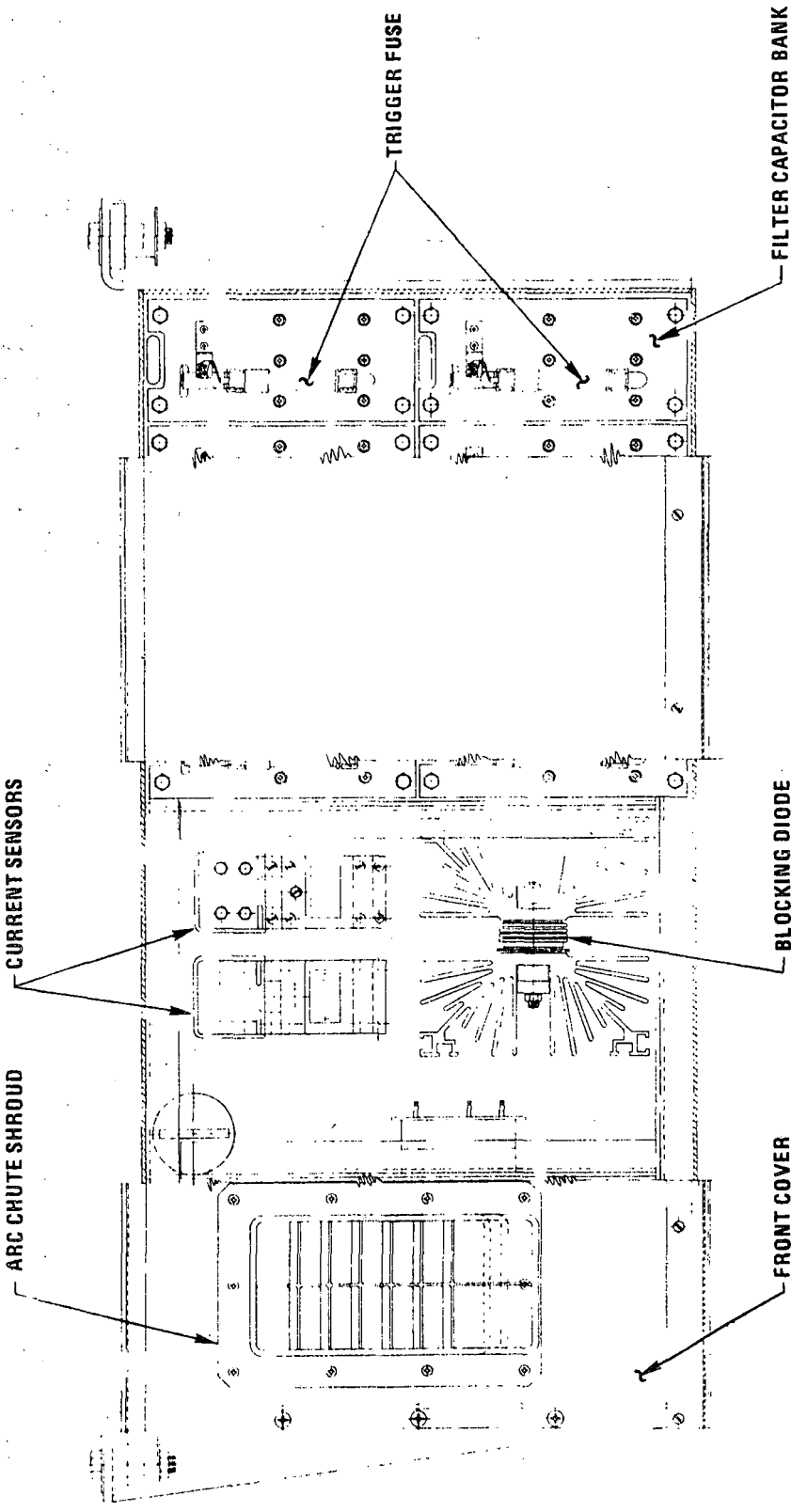

Figure 5.6-12. Power Control Switchgear Assembly

5.6.5 RESONATING INDUCTOR MODULE

5.6.5.1 Functional Requirements

The resonating inductor module contains linear and saturating inductors that, in conjunction with the resonating capacitors in the power converter capacitor module (paragraph 5.6.6.2) and the SCR's and diodes in the inverter module (paragraph 5.6.6.1), convert filtered third rail dc supply voltage into variable frequency three-phase ac voltage for input to the cycloconverter module. The resonating inductor module also contains three current limiting fuses which protect the SCR's, diodes, and resonating capacitors.

The inductor elements of the module are sized to carry the current demands of the power converter.

5.6.5.2 Design Approach

The value of the linear inductance needed to satisfy the drive current and power requirements was established through an analog computer simulation of the propulsion system. To achieve minimum loss within the inductor weight budget, various conductor types and core configurations were evaluated. A combination of AWG 30 Litz wire and grain-oriented silicon steel I-shape laminations arranged in a shell-type structure was selected.

The resonating inductor was optimized for minimum loss (highest Q) at the maximum power level by making core loss equal to copper loss at the highest operating frequency. Under this condition, the maximum achievable Q is given in terms of the ac winding resistance, R_{ac}, inductance, L, and radian frequency, ω, as

$$Q_{max} = \frac{\omega L}{2 R_{ac}} .$$

For Litz wire at frequencies of less than 20 kHz, the ac and dc winding resistances are approximately equal. Thus at 1000 Hz,

$$Q_{max} = \frac{2 \pi \times 1000 \times 0.00015}{2 \times 0.00236} = 200$$

The size and material of the saturable inductors were selected with the aid of dV/dt circuit theory supported by tests of the breadboard hardware from a previous IR&D development program.

5.6.5.3 Design Description

A circuit diagram of the resonating inductor module is shown in Figure 5.6-13. A photograph is shown in Figure 5.6-14.

5.6.5.3.1 Linear Inductors

Six linear inductors, in conjunction with the resonating/coupling capacitors and SCR/diode switching elements, form the three-phase inverter input stage of the motor drive power converter.

Each shell type inductor is wound with 10 turns of 1444 strand AWG 30 insulated magnet wire on a laminated core. The dc winding resistance at room temperature is 0.00236 ohms. The core is formed from epoxy impregnated 4 mil grain-oriented silicon steel laminations having dimensions of 0.75 in. × 2.50 in. with a stack length of 16 in. Horizontal segments of the laminations are shared by two inductors, as shown in the cross-sectional view of Figure 5.6-15.

Tests of the Test Article inductors in free space gave Q = 180 at 1000 Hz, indicating close to optimum inductor design.

The proximity of the welded aluminum inductor mounting frame to the inductors proved to be a source of loss, however, reducing Q to values as low as 110. This frame was later redesigned in fiberglass (see Section VII) to give Q = 172 for an inductor in the middle of the stack to Q = 130 for an inductor next to the aluminum cover.

5.6.5.3.2 Saturable Inductors

Each of six saturable inductors is connected in series with one of the linear inductors. The saturable reactor snubs the reverse recovery current of the associated inverter power diode. This reduces the power loss in the inverter dV/dt suppression circuits. Each saturable inductor is made up of three tape-wound Deltamax cores with dimensions c OD = 2.0 in., ID = 0.75 in., Ht = 2.0 in. The three toroids are housed in insulated aluminum cases and installed on a round copper buss bar. The bar serves both as a mounting structure and as a one-turn winding.

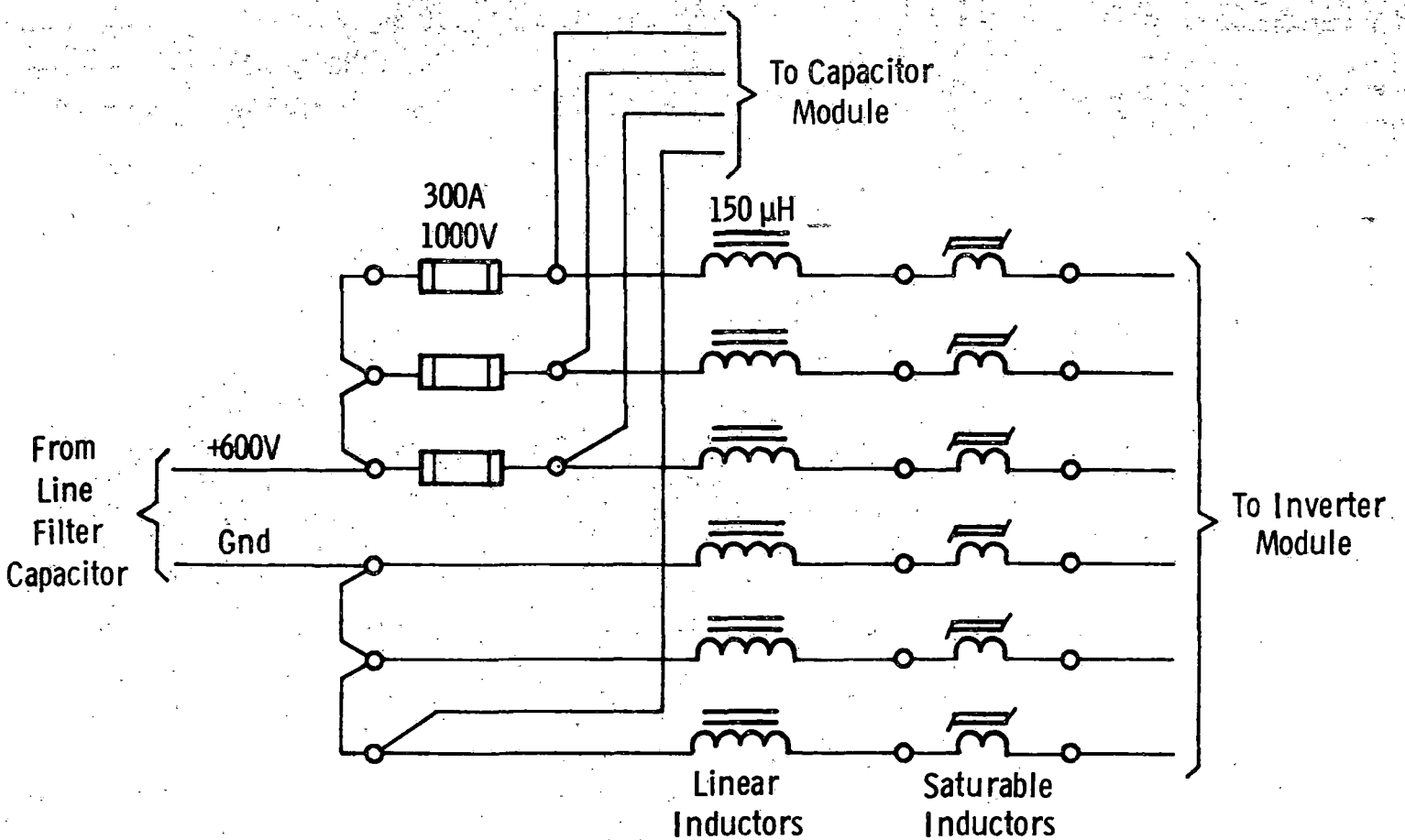

Figure 5.6-13. Resonating Inductor Circuit Diagram

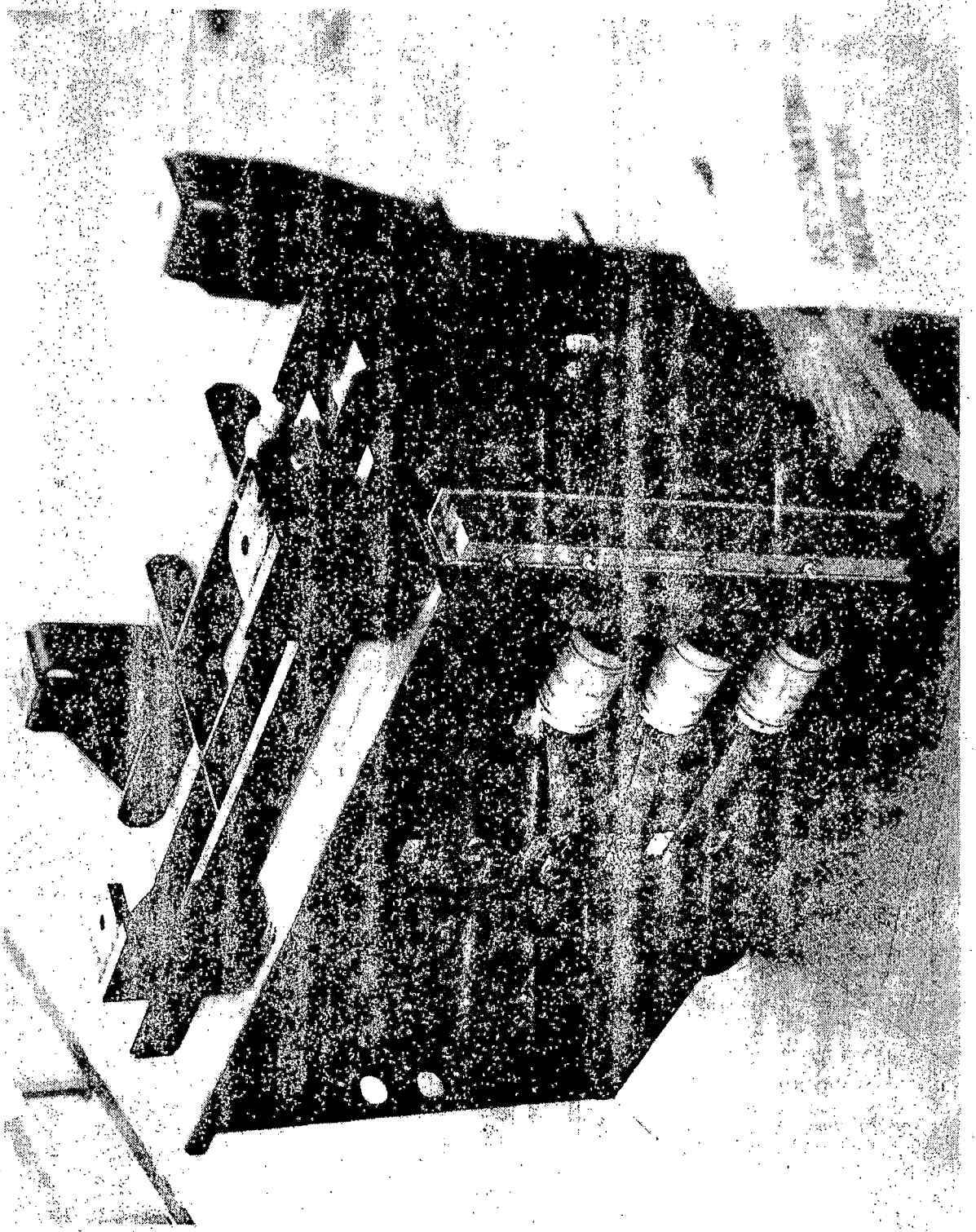

Figure 5.6-14. Resonating Inductor Module

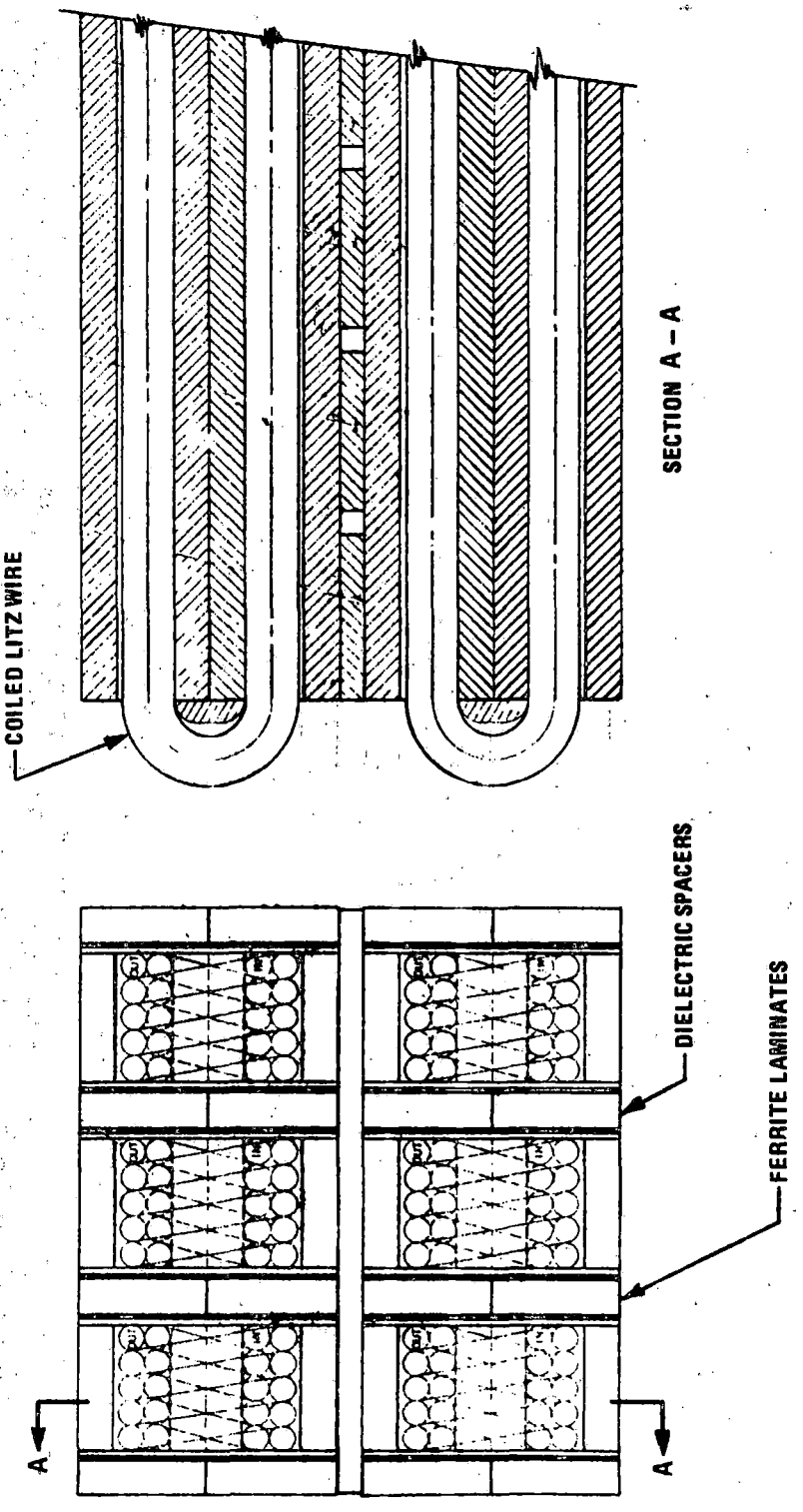

Figure 5.6-15. Resonating Inductor Component Assy.

5.6.5.3.3 Mechanical Arrangement

The module housing is a welded, structurally ribbed, aluminum enclosure which, together with the front panel, provides a seal against dirt and moisture contamination and coolant leakage.

A chassis assembly, which is interior to the enclosure, supports the stacked inductor assemblies shown in Figure 5.6-15. The inductors consist of coiled Litz wire wound on bobbins and sandwiched between stacks of steel laminations. Electrical gaps between lamination stacks are provided by fiberglass spacers. The lamination stacks are pinned to eliminate axial misalignment and compressed with a rubber pad to secure them against lateral movement. At one end the inductor assembly end cap also acts as the coolant manifold directing liquid through the coils and out the opposite end into the enclosure. (A further discussion on the cooling of the unit is found in paragraph 5.6.7.) The fuses and reactors mount external to the enclosure in a cover assembly area which is also protected from the environment. These can be seen in the photograph of Figure 5.6-14.

5.6.6 POWER CONVERTER ASSEMBLY

The power converter assembly (PCA) shown in Figure 5.6-16 consists of five major modules: inverter, capacitor, field supply, cycloconverter, and brake control. All are liquid cooled by means of a silicone fluid.

5.6.6.1 Functional Requirements

The PCA, in conjunction with the resonating inductor module, serves two primary purposes. In motoring, it converts filtered third rail dc power from the power control switchgear assembly into three phase ac motor power. In braking, it converts the filtered dc power into the traction generator field power and rectifies the generator output for application to a dynamic brake resistor or for regenerative feedback to the third rail dc line. There are two PCA's per car, one for each propulsion system.

The control signal inputs to the PCA consist of inverter, cycloconverter, and brake rectifier SCR gate signals, and motor/brake mode control signals. Signal outputs from the PCA consist of inverter diode signals, motor CEMF and current signals, cycloconverter input voltage reference signals, and a contact closure indicating integrity of the connections between the field supply transformer and the rotary transformer in the motor.

The PCA input power rating was derived from the motor power requirements and the estimated converter efficiency. The peak input power rating of 430 kW is limited by SCR voltage and current ratings and inductance and capacitance values in the input inverter stage. The average power rating of 237 kW is established by the cooling system heat rejection capability and is based on operation over the ACT-1 Synthetic Transit Route at the HSGTC in Pueblo, Colorado.

5.6.6.2 Design Approach

The design of the dc to three phase ac power converter was based on the capacitor-coupled cycloconverter approach (Reference 5). This concept was devised during the IR&D program described in subsection 6.1 to achieve a naturally commutated power converter with a current source output characteristic and a passive field supply suitable for driving a salient pole synchronous motor.

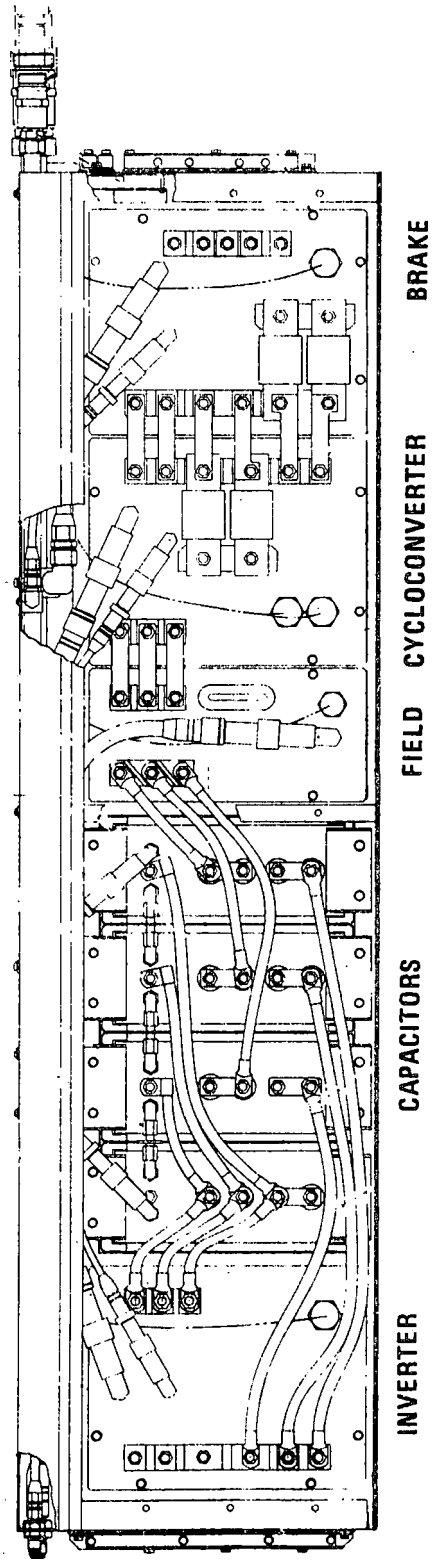

Figure 5.6-16. Power Converter Assembly

The power converter output voltage and current capabilities of 850 V and 550 A were established during this IR&D phase and were based on the electrical characteristics of the low speed "workhorse" motor described in 6.1. The ASDP motor was then to be designed to produce the required power and torque versus speed characteristics within the pre-existing envelope of available voltage and current. An early ASDP motor design was not able to meet the performance requirements while staying within the motor weight limit. This problem was corrected by modifying the MCE and PCA to produce a leading power factor that increases with speed.

A forced convection liquid cooling method was developed for the SCR's, capacitors and inductors. This considerably reduced the size of the PCA.

5.6.6.3 Circuit/Component Descriptions

The circuitry and components of the inverter, capacitor, field supply, cycloconverter and brake control modules are described in the following paragraphs.

5.6.6.3.1 Inverter Module

The inverter module contains the inverter power SCRs, power diodes, diode current sensors, dV/dt suppression circuitry, gate drive circuitry, SCR/diode cooling elements, and high current busswork. The circuit diagram of the module is shown in Figure 5.6-17.

Power SCRs

The power disc SCRs are equivalent to General Electric type C441PN or International Rectifier type 750PB. SCRs were purchased from these firms under Delco Specification Drawing No. 7559111-001. Pertinent parameters are:

$T = -40^{\circ}C$ to $+125^{\circ}C$
$V_{DRM} = 1800V$
$I_{T(AV)} = 300A$ half sine at 1200 Hz
$I_{TSM} = 10,000A$
$I^2t = 400,000\ A^2\text{-s}$
$di/dt = 15A/\mu s$
$t_q = 150\ \mu s$
gate drive = 14V, 20Ω, 1.0 μs rise time
mounting force = 3,000, +500, -000 pounds.

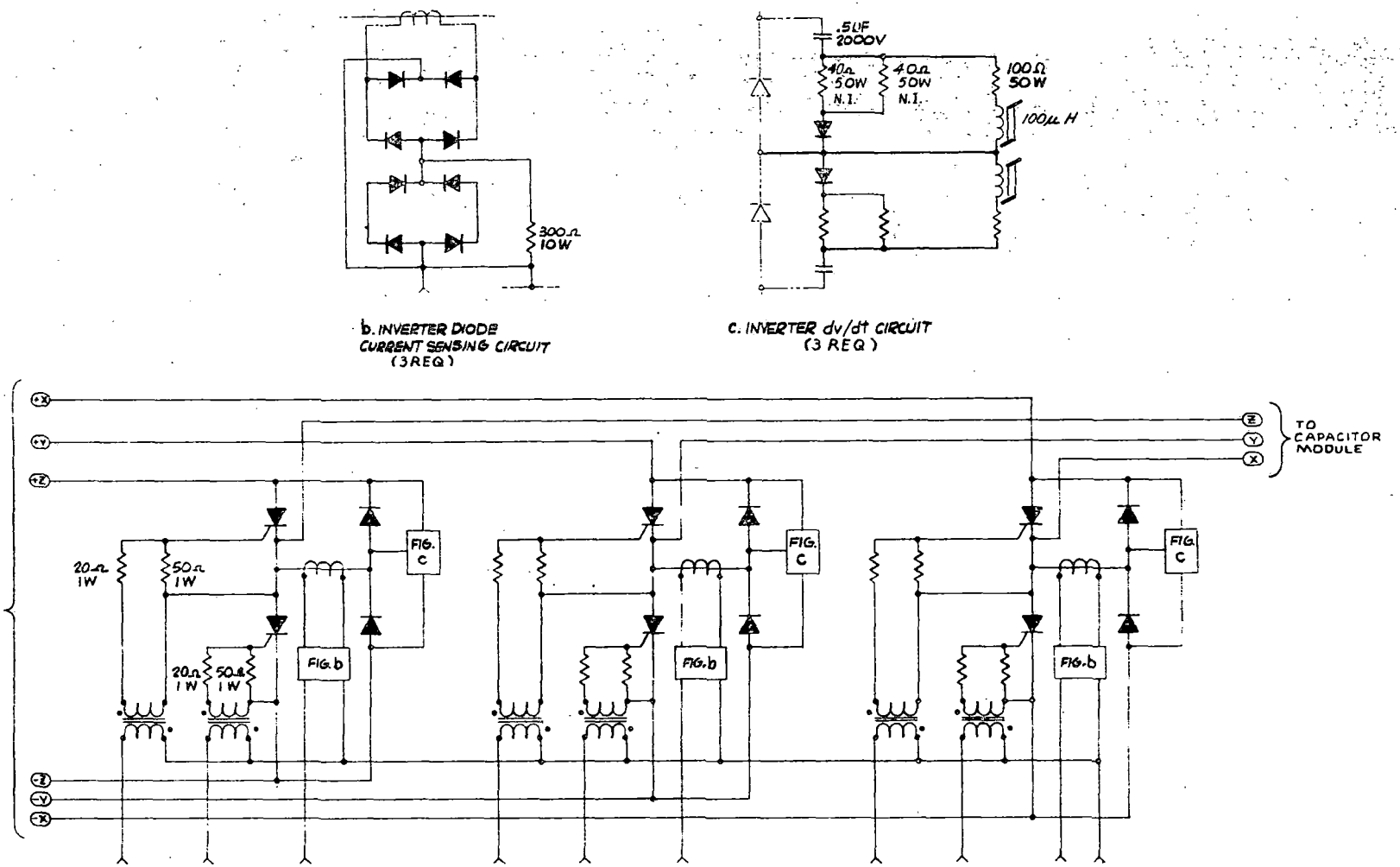

b. INVERTER DIODE CURRENT SENSING CIRCUIT (3 REQ)

c. INVERTER dv/dt CIRCUIT (3 REQ)

a. OVERALL SCHEMATIC

Figure 5.6-17. Inverter Module Schematic Diagram

Power Diodes

The power disc diodes are equivalent to Westinghouse type RT722 or International Rectifier type 651PDL. Diodes were purchased from these firms under Delco Specification Drawing No. 7559112. Pertinent parameters are:

$T_j = -40^oC$ to $+125^oC$

$V_{RRM} = 1800V$

$I_{F(AV)} = 450A$

$I_{FSM} = 6000A$

$I^2t = 200,000\ A^2\text{-}s$

$Q_r = 140\ \mu C$

Diode Current Sensors

Each of the diode current sensors consists of a current transformer with the secondary winding supplying current pulses which are a replica of the inverter diode current pulses to a nonlinear load circuit. This circuit, shown in Figure 5.6-17, consists of a rectifier which supplies unidirectional current pulses to a load consisting of two diodes and a parallel resistor. The diodes convert the rectified quasi-half sine current pulses into quasi-square wave voltage pulses. The load resistor removes distortion in the output waveform due to transformer magnetizing current. The diode current sensor output signals are processed in the MCE to provide control signals which:

- Reduce the inverter frequency and power level if the diode current pulse width (SCR turn-off time) is marginally short.
- Issue a QSD command if the pulse width is very short (incipient or actual inverter fault).
- Issue a QSD command if one or more of the diode current signals is missing.

dV/dt Suppression Circuitry

The dV/dt circuit serves to reduce the rate-of-rise of SCR forward blocking voltage. The forcing function for the dV/dt circuit has two components.

The first is due to the sudden drop in resonating inductor voltage when the inductor current rate-of-change goes from a finite value to zero. The second is due to the abrupt collapse of the reverse recovery current of the SCR's anti-parallel diode. Saturable inductors are used in series with the linear inductors in the resonating inductor module to limit the magnitude and slope of the diode recovery current.

The dV/dt suppression circuit, shown in Figure 5.6-17b, functions in two modes. First, when the SCR forward blocks, the diode in the circuit conducts placing a relatively low 20 Ω resistance in series with the 0.5 μF capacitor and the linear and saturating inductors. This yields a dV/dt at the maximum power level of approximately 150V/μs. Next, when the SCR is gated into conduction, the dV/dt circuit diode blocks, placing the 100 Ω resistor and a 100 μH saturating inductor in series with the 0.5 μF capacitor discharge path. The 100 μH inductor limits the rate-of-rise of the discharge during the first two microseconds. The 100 Ω resistor limits the peak discharge current during the following 10 μs to a value less than the normal SCR load current.

Gate Drive Circuitry

The gate drive circuits, shown in Figure 5.6-17a, consist of a pulse transformer and secondary series and shunt resistors. The circuit provides an SCR gate pulse of 16 μs width and a gate current exceeding 1 amp in 0.5 μs.

5.6.6.3.2 Capacitor Module

The schematic diagram of the capacitor module is shown in Figure 5.6-18a. This module contains four liquid cooled capacitors of a type developed for use by the induction heating industry. Each of the capacitors contains two 20μF and two 40μF sections. The four capacitors are connected to form the equivalent three-capacitor circuit shown in Figure 5.6-18b. The 80μF segments linking the inverter module to the field supply module are termed the coupling capacitors. The 40μF segments connecting to the ground return and to the resonating inductor module are termed the commutating capacitors.

The capacitors are constructed with a common aluminum plate. The edges of the plate are bent to form a surface to which a copper coolant tube, wound in a serpentine pattern, is soldered. This construction allows heat to be extracted from the center of the capacitor through a metallic path instead of through the dielectric, as in conventional capacitor construction.

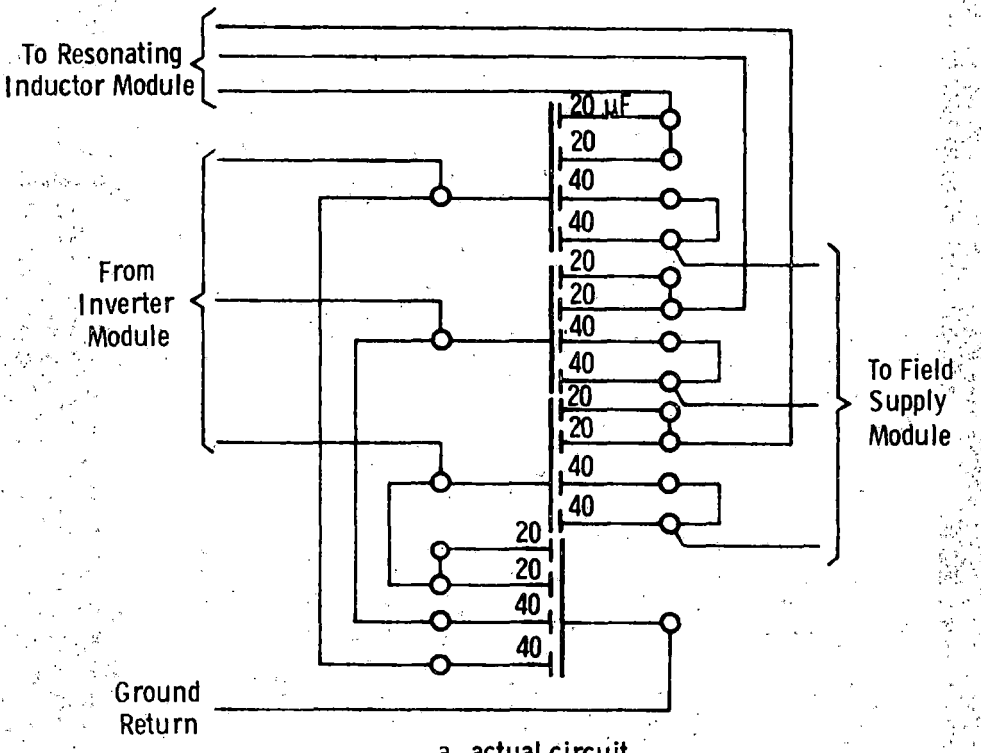

a. actual circuit

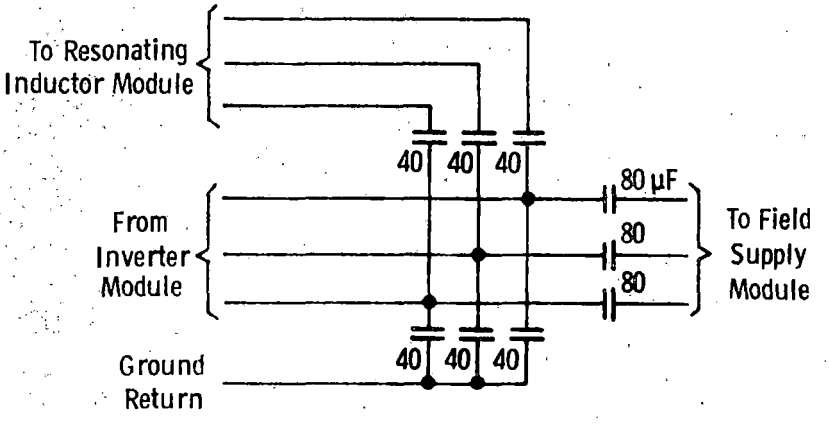

b. equivalent circuit

Figure 5.6-18. Capacitor Module Circuit Diagram

A dielectric formed of kraft paper and polypropylene film separates the common plate from the output plates. The wound assembly of capacitor plates and dielectric, with attached coolant tube, is installed in an aluminum can which is then welded shut, leaving a fill hole for the dielectric fluid. The capacitor is then vacuum impregnated with dielectric fluid, wetting the entire surface area of the capacitor plates and polypropylene film. This improves heat conduction and minimizes corona discharge.

Midway in the procurement of the ASDP capacitors, the conventional PCB dielectric fluid became unavailable because of a production ban by the U. S. Government stemming from public health and environmental concerns over the non-biodegradability of PCB fluid. Accordingly, the capacitor design was modified to incorporate non-PCB dielectric fluid for the remainder of the procurement.

The 80 μF and 40 μF values of the coupling and commutating capacitances were determined with the aid of an analog computer simulation prior to the ASDP contract. These values were used in the IR&D breadboard drive system and in the ASDP Test Article drive system. Capacitors for the ASDP Test Article were designed for the application by the General Electric Co., to Delco Specification Drawing No. 7558015.

Pertinent parameters for the ASDP four-section capacitors are:

Capacitance:

40μF sections, 40 μF ±6%
20μF sections, 20μF ± 6%
} measured at 60 Hz

Voltage:

dc bias = 400V
peak working voltage = 1450V
rms voltage = 780V
dc test voltage = 2000V for 10 seconds

rms Current:

40μF sections, 245A
20μF sections, 105A
total, 700A

Dissipation Factor:

0.3% at 1000 Hz

Shock:

6g longitudinal axis

3g lateral and vertical axis

Coolant:

Dow Corning, DC-200-50CS

Flow rate, 2 ± 0.3 gal/min

5.6.6.3.3 Field Supply Module

The field supply module, shown schematically in Figure 5.6-19, provides motor field excitation by entirely passive means. A three-phase transformer derives voltage and current for the motor's rotary transformer from the three-phase inverter operating over a frequency range of 350 to 1200 Hz.

Motoring Mode

In motoring, the motor/brake relay de-energizes the 144 turn windings of the transformer. Current into the cycloconverter passes through the three turn primary windings producing a corresponding current reduced in amplitude by 3/36 = 1/12 in the 36 turn secondary winding. This mode is termed current transformer operation because the impedance presented by the rotary transformer, which changes with inverter frequency and motor speed, has negligible effect on the primary and secondary transformer currents.

Braking Mode

In braking, the motor/brake relay is energized, placing the 144 turn windings of the transformer, and the 3.0 μF coupling capacitors, in series with the 80 μF coupling capacitors of the capacitor module. Also in braking, gate drive to the cycloconverter SCRs is removed so that current goes to zero in the three turn windings. The transformer then operates as a voltage transformer with a ratio of 144/12 = 12/1. The 3.0 μF capacitors serve to increase the rate-of-change of transformer primary voltage with frequency, and also prevent saturation of the transformer core during inverter turn-on.

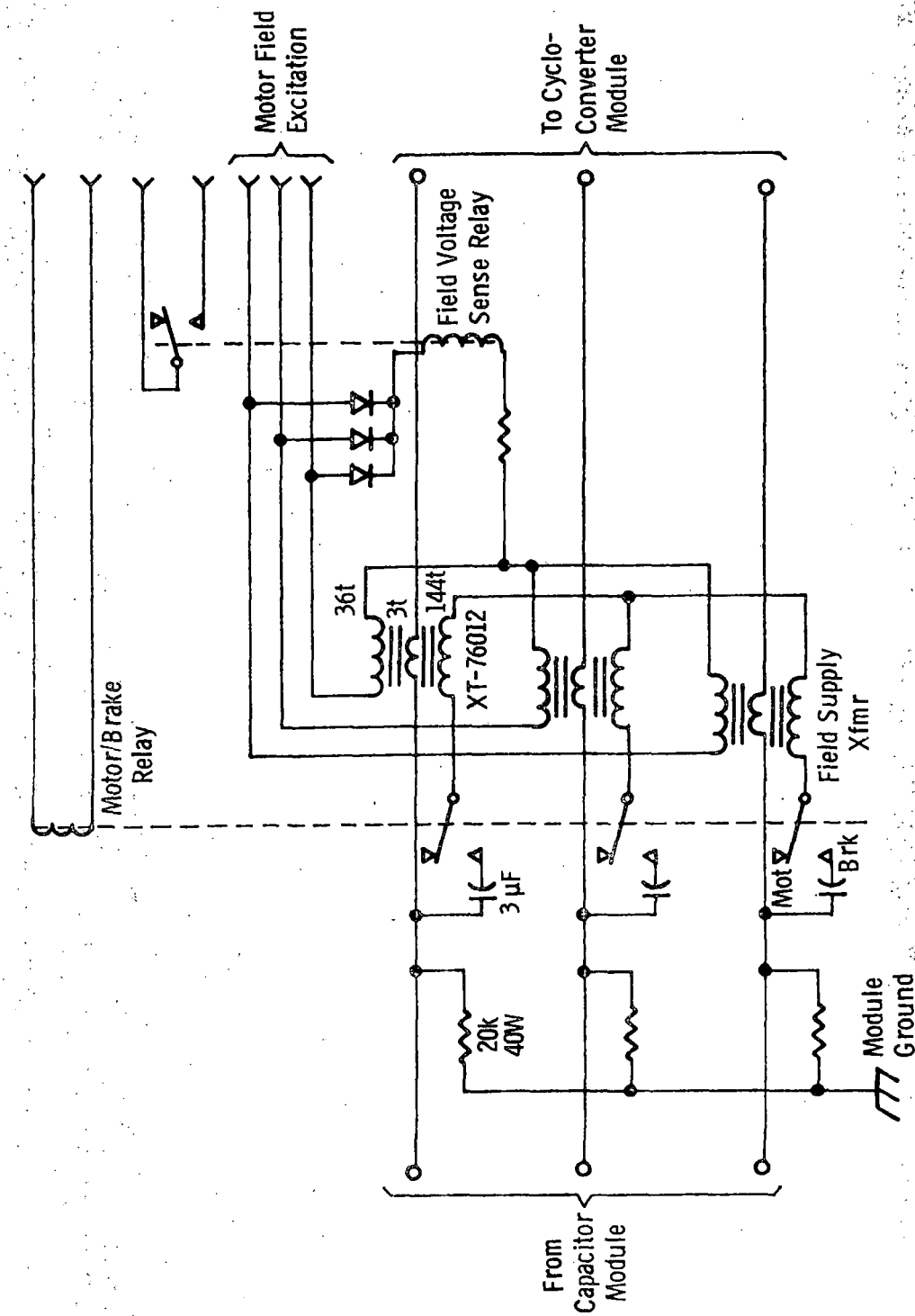

Figure 5.6-19. Field Supply Module Schematic Diagram

Voltage Sense Relay

The field voltage sense relay provides a contact closure if the secondary connection to the rotary transformer is interrupted. A three-phase half wave rectifier converts the transformer secondary ac voltage to a dc voltage for the relay coil. Loss of the secondary load results in a voltage on the relay coil in excess of the pull-in voltage.

Cooling System Equalization

The field supply module is intended to serve as an equalizing chamber for the power converter liquid cooling system. The module inlet is unrestricted and connected to the low pressure rail of the cooling system and also vented to the atmosphere. Expansion or contraction of the system coolant is accommodated by a rise or a fall in the level of fluid in the module.

5.6.6.3.4 Cycloconverter Module

The cycloconverter module contains the power SCRs, dV/dt and surge suppression circuits, and gate drive circuits which comprise the cycloconverter circuit. The circuit diagram of the module is shown in Figure 5.6-20. External to the module, three tape wound torroid cores of Deltamax material are threaded onto the cycloconverter input cables. These cores serve to reduce the magnitude and slope of the cycloconverter SCR reverse recovery currents.

Power SCRs

The power disc SCRs are equivalent to General Electric type C441PN or International Rectifier type 750PB. SCRs were purchased from these firms under Delco Specification Drawing No. 7559111-002. Pertinent parameters are:

$T = -40^{\circ}C$ to $+125^{\circ}C$

$V_{DRM} = 1800V$

$I_{T(AV)} = 300A$ half sine at 1200 Hz

$I_{TSM} = 10,000A$

$I^2t = 400,000\ A^2\text{-}s$

$di/dt = 15A/\mu s$

$t_q = 200\ \mu s$

gate drive = 14V, 20Ω, 1.0 μs rise time

mounting force = 3,000, +500, -000 pounds.

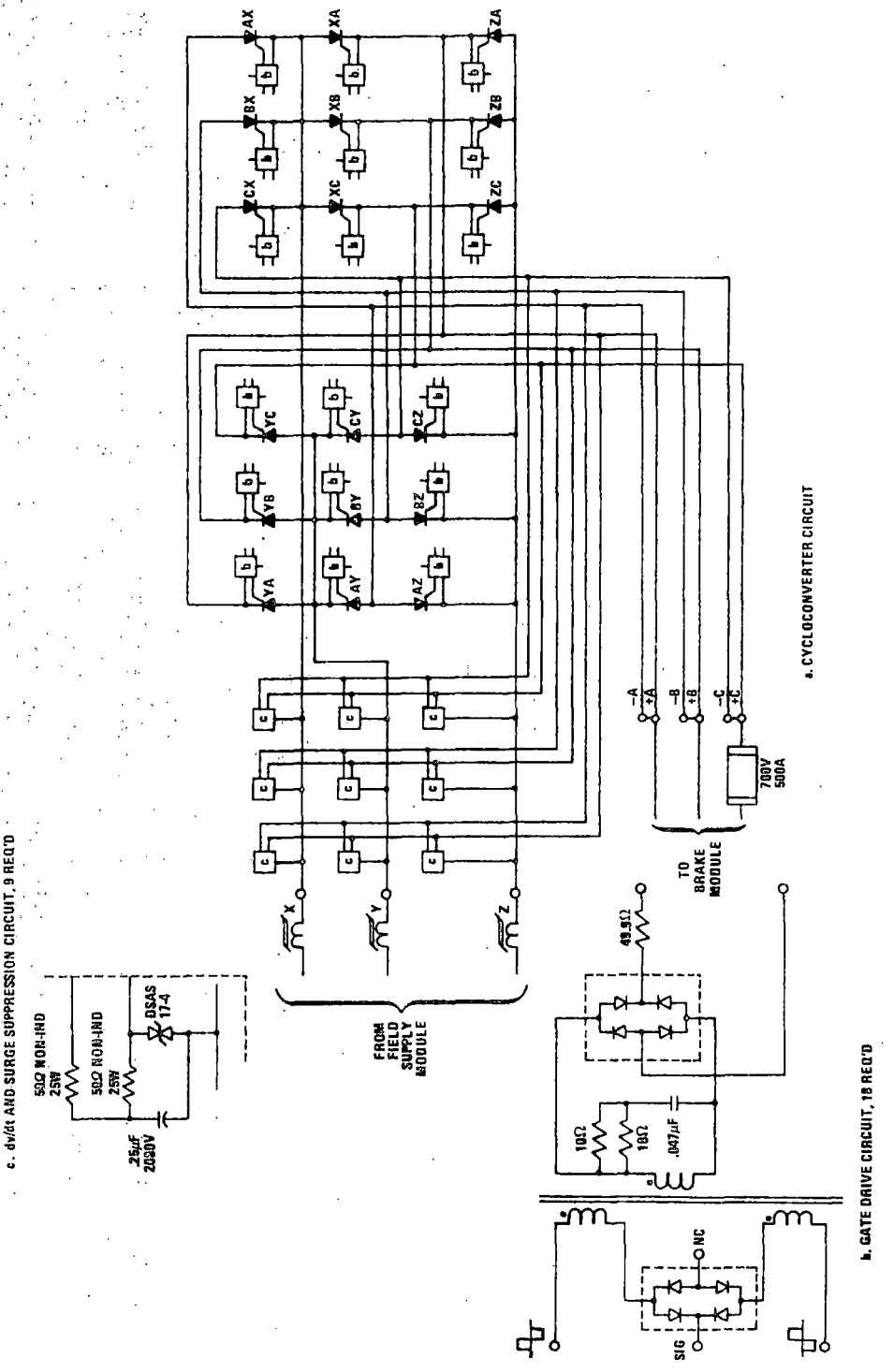

Figure 5.6-20. Cycloconverter Module Schematic

dV/dt and Surge Suppression Circuitry

The dV/dt circuit consists of a pair of 25 Ω resistors and an 0.25 μF capacitor across each of the 18 SCRs. In the cycloconverter, a high rate of change of SCR anode-to-cathode voltage can occur in either a positive or a negative going direction in the presence of either a positive or negative blocking voltage. These four conditions are shown in Figure 5.6-21.

Of the blocking voltage conditions shown, only the case of simultaneous positive voltage and rate-of-change of voltage (dV/dt) (Figure 5.6-21d)can cause spurious SCR conduction. This condition can arise from three sources.

The first occurs as a result of gating the SCRs in synchronism with the cycloconverter with a phase delay angle α. The voltage waveforms across the gated and anti-parallel ungated SCRs are shown in Figure 5.6-22. The voltage applied to the cycloconverter input is assumed to be sinusoidal.

In Figure 5.6-22a, the SCR is gated at a delay angle of $\alpha = 30^{\circ}$. This angle is much larger than that occurring in the ASDP cycloconverter. When the gate pulse is applied, SCR voltage falls in a period of 1.0 to 2.0 μs from a level of $\hat{E} \sin 30^{\circ} = \hat{E}/2$ to the typical ON voltage of 1.2V. The positive blocking voltage prior to conduction is termed the "finger voltage." In the anti-parallel SCR, the turn-on of the gated SCR is reflected as a change in negative blocking voltage from $-\hat{E}/2$ to -1.2V. Note that even though dV/dt. is positive, the blocking voltage is negative, so that the SCR cannot spuriously turn on from the finger voltage even with high dV/dt. When the conducting SCR ceases conduction at $\omega t = 180^{\circ}$, its voltage falls from +1.2 to $-\hat{E}/2$ V while the voltage on the ungated anti-parallel SCR rises from -1.2 to $\hat{E}/2$ V. The anti-parallel SCR is thus subject to spurious turn-on from simultaneous positive dV/dt blocking voltage. The value of the dV/dt at $\omega t = 180^{\circ}$ is determined by the conducting SCR's reverse recovery current characteristic and by the dV/dt suppression circuit. This circuit consists of a 25 Ω resistance and a 0.25 μF capacitance across each of the nine inverse parallel connected SCRs and the cycloconverter source loop inductance. This inductance consists of the inductance of two of the three cables connecting the inverter, coupling capacitors, field supply module, and cycloconverter, the stray inductance of the capacitor, and the field supply transformer winding inductances. The saturable reactor in series with the cycloconverter input cables is normally saturated during the dV/dt transient.

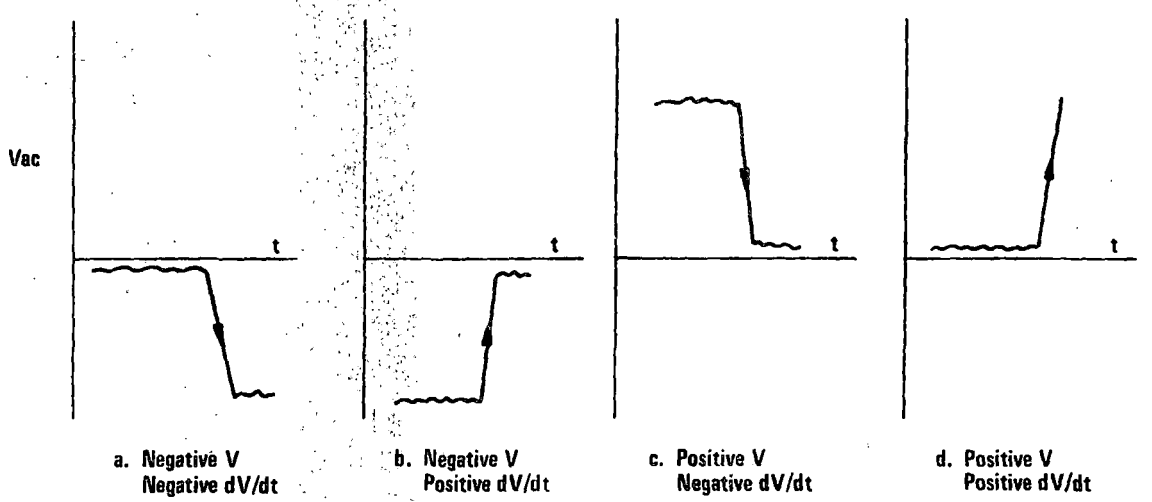

Figure 5.6-21. Cycloconverter Blocking Voltage Conditions

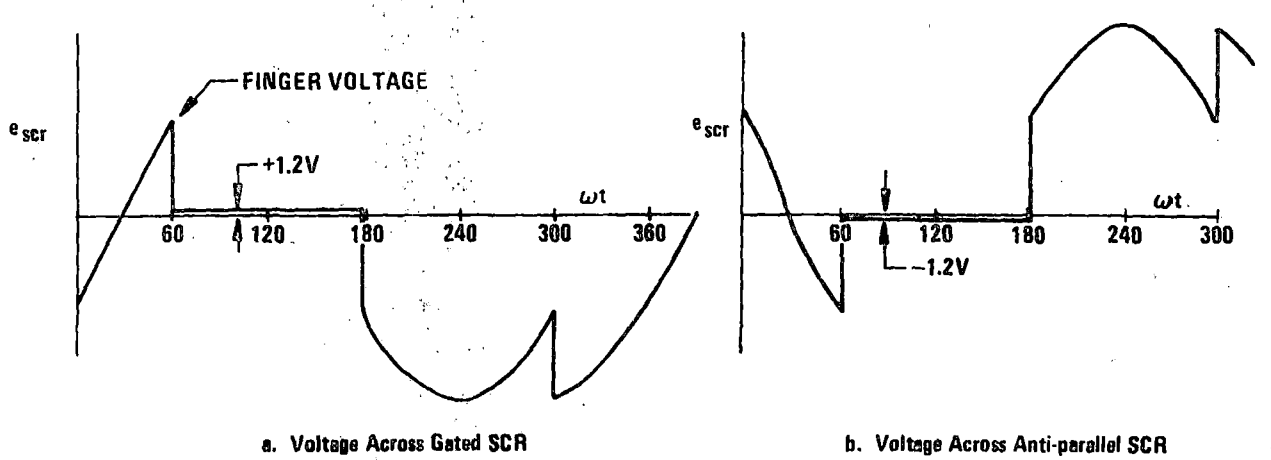

Figure 5.6-22. SCR Voltage with Synchronous Gating ($\alpha = 30^{o}$)

An additional positive dV/dt-positive voltage condition occurs at $\omega t = 300^{o}$, as seen in Figure 5.6-22b. The magnitudes of the voltage step and the dV/dt are the same as those occurring at $\omega t = 180^{o}$.

The second source of positive dV/dt-positive voltage occurs when a motor phase is gated into conduction with leading power factor. Thus, for example, if current is to be commutated from motor phase +a to phase +b, and commutation is initiated by gating SCR XB at a leading trigger angle of, say, 30^{o}, a step voltage of $\sin 30^{o} = 1/2$ of the peak motor line voltage is impressed across SCR BZ and its paralleled RC circuit when the latter SCR is blocking positive voltage. The dV/dt suppression circuit active at the instant that this commutation is initiated contains the BZ RC circuit and the cycloconverter source loop inductance.

The third forcing function for positive dV/dt-positive V occurs at the end of the motor phase current commutation interval. In this case, the voltage drop in the motor leakage inductance suddenly goes to zero at the instant that phase current flow ceases. This drop in motor voltage appears as a rise in voltage across the SCR and its RC circuit. The loop inductance in this circuit is the relatively large motor inductance. Thus the rate-of-rise of SCR voltage is much less than that occurring at the beginning of commutation, as described in the paragraph above.

The surge suppressor, incorporated in the dV/dt circuit of Figure 5.6-20 c, is a bi-directional avalanche diode rated at approximately 15 Joules. Suppressor conduction commences at approximately 1590V.

Gate Drive Circuit

The cycloconverter gate drive circuit provides an SCR gate pulse having a width equal to that of the gate current command logic signal produced in the MCE. This is accomplished with the transformer-rectifier circuit of Figure 5.6-20 b. Square wave voltage at approximately 30 kHz is applied to the outer terminals of the primary windings. Primary current flows when the cathodes of the diodes connected to the inner terminals of the primary windings are grounded by turn-on of a drive transistor in the MCE in response to a motor current command logic signal. The resulting secondary current is then rectified and applied through the 49.9 Ω resistor to the SCR gate.

The series 5 Ω-0.047 μF RC network connected across the transformer secondary provides a path to prevent capacitively coupled spikes coming through the transformer from activating the SCR gate.

The SCR gate current pulse waveform is characterized by a pulse of current that rises to at least 1 amp in 0.5 μsec, overshoots to about 2 amps, and decays to a steady state value of approximately 0.5 amp.

5.6.6.3.5 Brake Control Module

The brake module contains the power SCRs, dV/dt circuits, and gate drive circuits which comprise the dynamic and regenerative brake rectifiers and the dynamic brake shunt SCR switch. The nine rectifier SCRs are operated as a dual semi-converter, with the ground-connected SCRs gated as diodes and carrying current for both the dynamic and regenerative brake rectifiers. The module also contains the motor CEMF voltage sensing transformer. A circuit diagram of the dual phase delay rectifier and the auxiliary circuits is shown in Figure 5.6-23.

Power SCRs

The power disc SCRs are equivalent to General Electric cype C441PN or International Rectifier type 750PB. SCRs were purchased from these firms under Delco Specification Drawing No. 7559111-002. Pertinent parameters are:

$T = -40^{o}C$ to $+125^{o}C$

$V_{DRM} = 1800V$

$I_{T(AV)} = 300A$ half sine at 1200 Hz

$I_{TSM} = 10,000A$

$I^2t = 400,000\ A^2\text{-s}$

$di/dt = 15A/\mu s$

$t_q = 200\ \mu s$

gate drive = 14V, 20Ω, 1.0 μs rise time

mounting force = 3,000 - 3,500 lb.

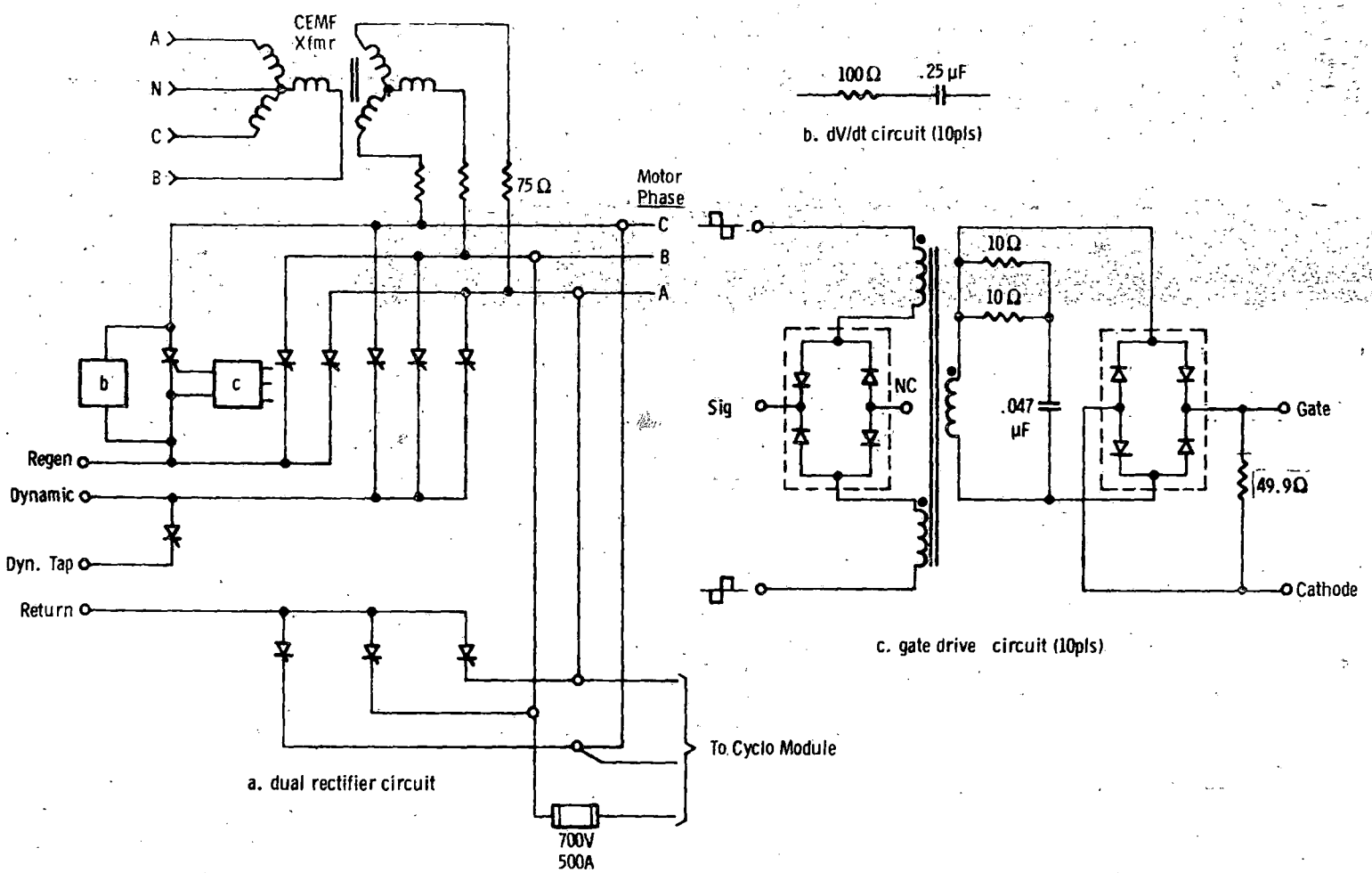

Figure 5.6-23. Brake Control Module Schematic

dV/dt Suppression Circuitry

The dV/dt circuits consist of a 100 Ω resistor and a 0.25 μF capacitor across each SCR. These circuits serve to suppress voltage transients arising principally from reverse recovery currents in the rectifying SCRs. This suppression requirement is less severe than in the cycloconverter because the SCRs are not connected anti-parallel and are not operated in the inverting mode.

Gate Drive Circuit

The brake module SCR gate drive circuits are identical to those in the cycloconverter module, as described in paragraph 5.6.6.3.4.

CEMF Sensing Transformer

The CEMF transformer primary is connected to the motor terminals via the power wiring connections from the motor to the brake module. The transformer steps down the motor line voltage having a maximum level of approximately 1000 Vrms to a level compatible with the signal comparators and operational amplifiers in the MCE. The transformer also serves to isolate the MCE logic ground from the power system ground.

The transformer is wound on a three-phase E-core. An electrostatic shield connected to logic ground is placed between the primary and secondary. A resistance of 75 Ω is placed in series with the primary windings to limit primary heating from dc current when the motor is operated with locked rotor for extended periods.

5.6.6.4 Packaging Description

The power converter assembly (PCA) is shown in Figure 5.6-16 and in the photograph of Figure 5.6-24. It contains the electrical power circuits and components required to control one traction motor. The assembly – consisting of a lightweight frame, five slide-out modules, interconnecting cabling, coolant lines, and a hinged protective cover – is shock-mounted to the car's underframe. The electrical components are packaged in replaceable subassemblies (modules) in accordance with the function they perform. The modular design employs slide-out modules and quick-disconnect electrical and cooling fluid connections for ease of maintenance and replacement at the subassembly level.

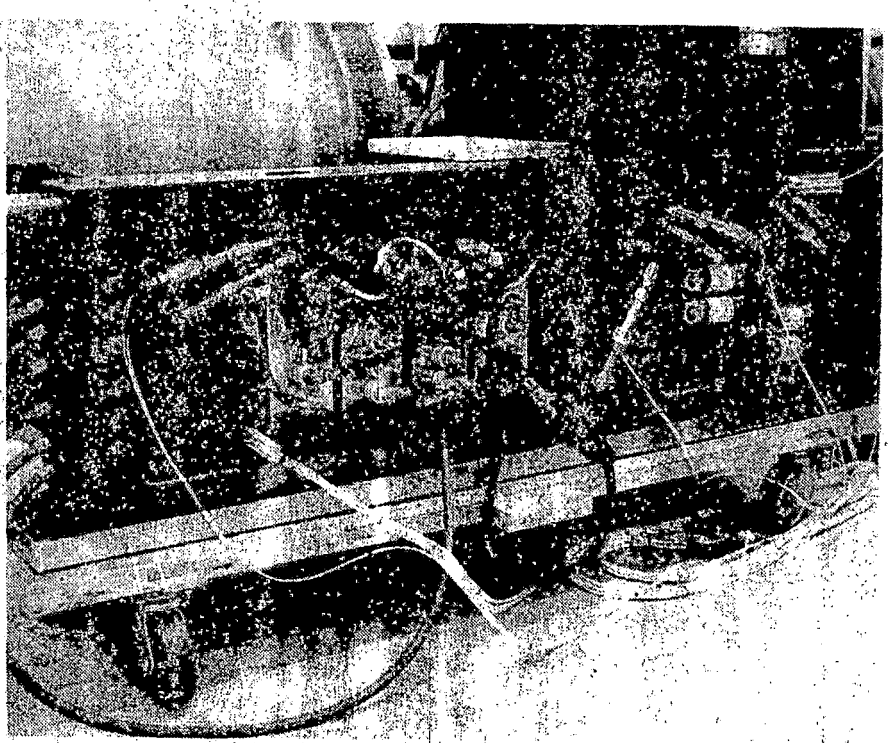

Figure 5.6-24. Power Converter Assembly

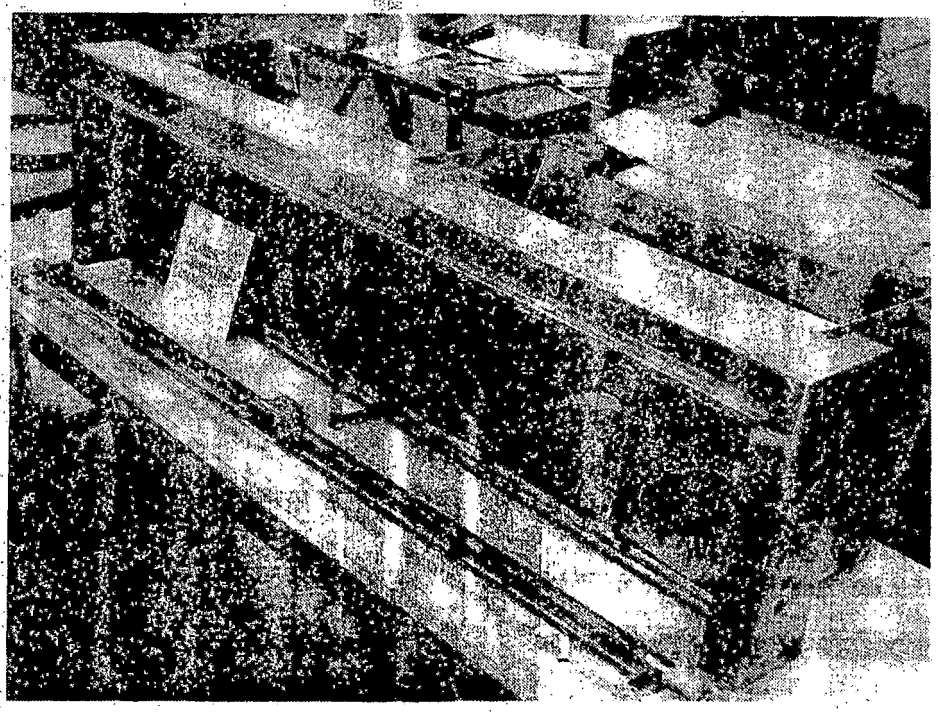

Figure 5.6-25. Power Converter Assembly Chasis

The PCA chassis shown in Figure 5.6-25, is a welded aluminum enclosure. A front cover encloses the assembly power terminations. The cover provides a safety barrier for personnel as well as protection against dirt and moisture contamination. For ease of maintenance the covers mount with quick release fasteners.

As can be seen in Figure 5.6-16, hard plumbed inlet and outlet coolant manifolds are mounted to the structure above the modules. This allows the modules to be installed or removed without interference with the plumbing. To prevent coolant leakage or contamination, fluid interconnects are made through wrenching, self-sealing disconnects. Each module slides into the enclosure on guides and is bolted into place. Locking inserts are used wherever possible to minimize the amount of hardware required.

The PCA contains the inverter, capacitor, field supply, cycloconverter and brake control modules. Due to the similarity of their componentry, packaging of the inverter, cycloconverter and brake control modules is based on similar conceptual approaches. The capacitor and field supply modules required somewhat different treatments.

Inverter Module

The inverter module packaging is illustrated in Figures 5.6-26 and 5.6-27. The module contains power SCR's and diodes and the associated gate drive circuits, dV/dt circuits, and current sensors.

The gate drive and dV/dt circuitry assembly is supported by the structure behind the SCR's. This assembly consists of two terminal boards, one fabricated from sheet metal and the other from fiberglass. Terminations are accomplished at the board terminals. As a result the module harness assembly is pigtailed and installed as a part of this assembly.

The module is enclosed within a deep drawn aluminum can attached by a flanged lip. This lip forms a fluid tight seal with the baseplate such that the enclosure becomes a return manifold for the coolant fluid. The SCR stacks are supported by a shear panel open box structure as shown in Figure 5.6-27.

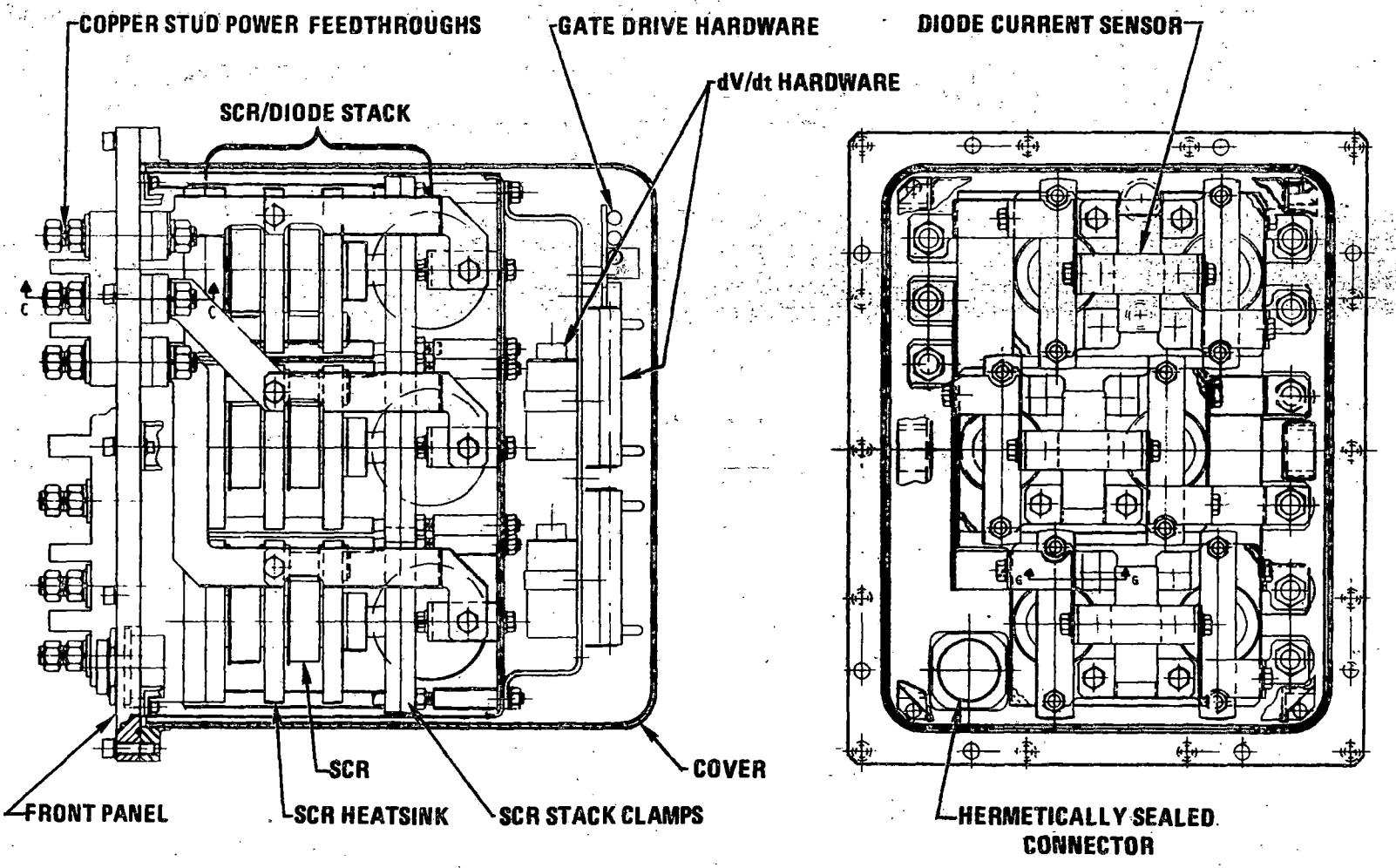

Figure 5.6-26. Inverter Module

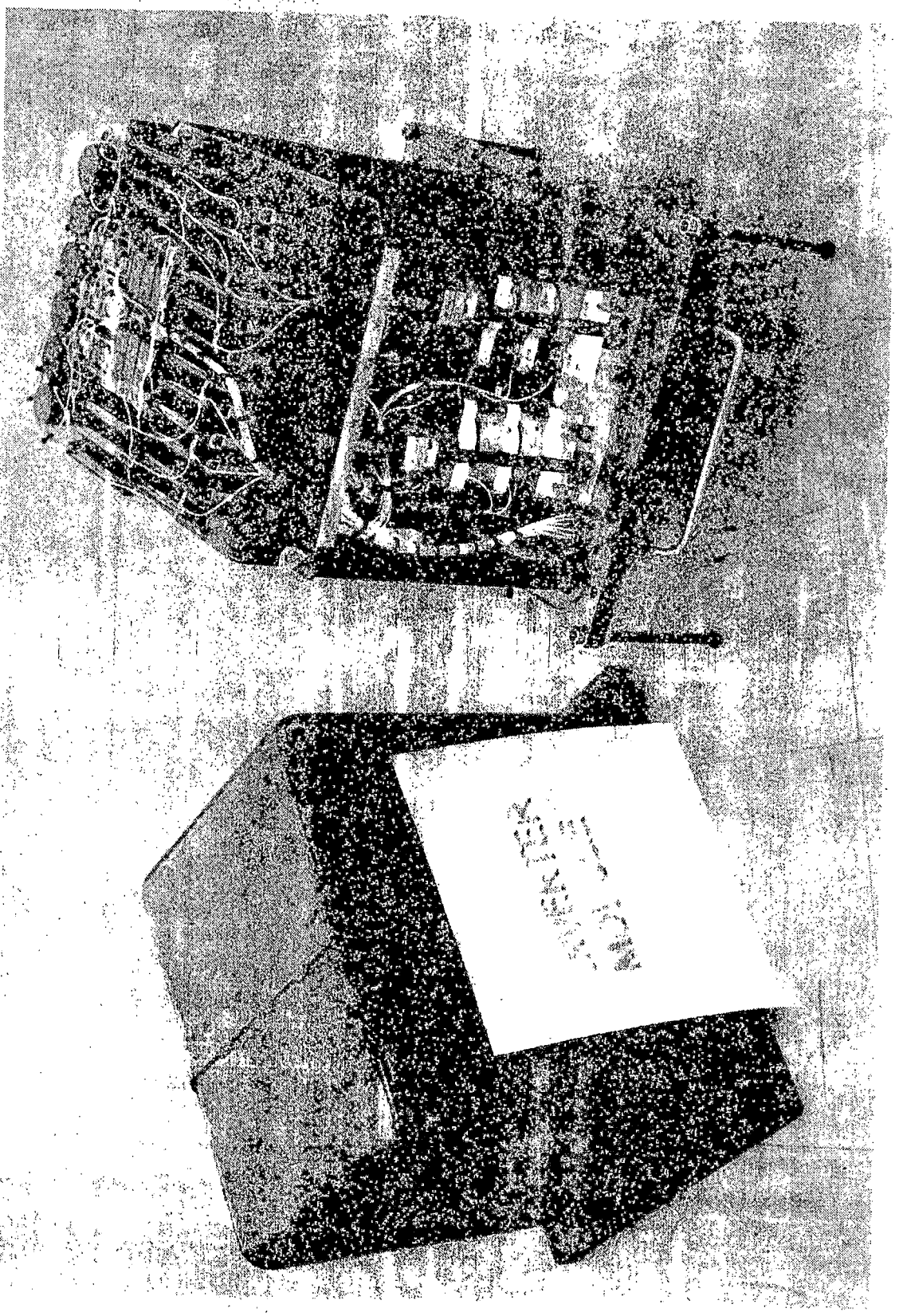

Figure 5.6-27. Inverter Module

The cooling fluid enters the module through an inlet port on the front panel. From there is fills a manifold which distributes the fluid through the various SCR stacks. A typical SCR stack is shown in Figure 5.6-28. The fluid enters each SCR heatsink and is channeled through a spiral groove which provides direct fluid contact to the SCR pole face. Figure 5.6-29 shows an exploded view of the SCR to heatsink interface. A tail at the outermost edge of the spiral groove allows the fluid to dump into the sealed module enclosure. The integration of the SCR stacks into the assembly can be seen in detail in Figure 5.6-26.

The fluid-filled enclosure provides additional SCR cooling by acting as an SCR fluid bath. Fluid is drawn out of the enclosure and into the power converter return manifold by the cooling assembly pump.

The heatsink development began as an IR&D effort prior to the ASDP contract. Initial development work in this area resulted in Patent 4,010,489. Further analysis and testing was performed to accommodate the selected coolant, DC200-50CS (see subsection 6.1 of this report). The final heatsink design is defined in DESBO Drawings 7558927 and 7558928.

System electrical interconnections are located on the front panel for ease of assembly. Feedthroughs include hermetically sealed connectors for the signal interfaces and large copper stud feedthroughs for the power terminations. Power terminations within the module are made by bolting the bus bars to the SCR heatsinks.

With the enclosure removed and the front panel face down as shown in Figure 5.6-27, the unit can be efficiently serviced. The side panels can be unscrewed and slide out providing easy access to the SCR power and gate terminations.

In general, it is felt that the design provides excellent servicing access to nearly all module hardware.

Capacitor Modules

The capacitor modules shown in Figure 5.6-30 mount in the PCA chassis on fiberglass guides. The capacitor cases are at some electrical potential other than ground and therefore are isolated from one another and from chassis ground by fiberglass insulation barriers.

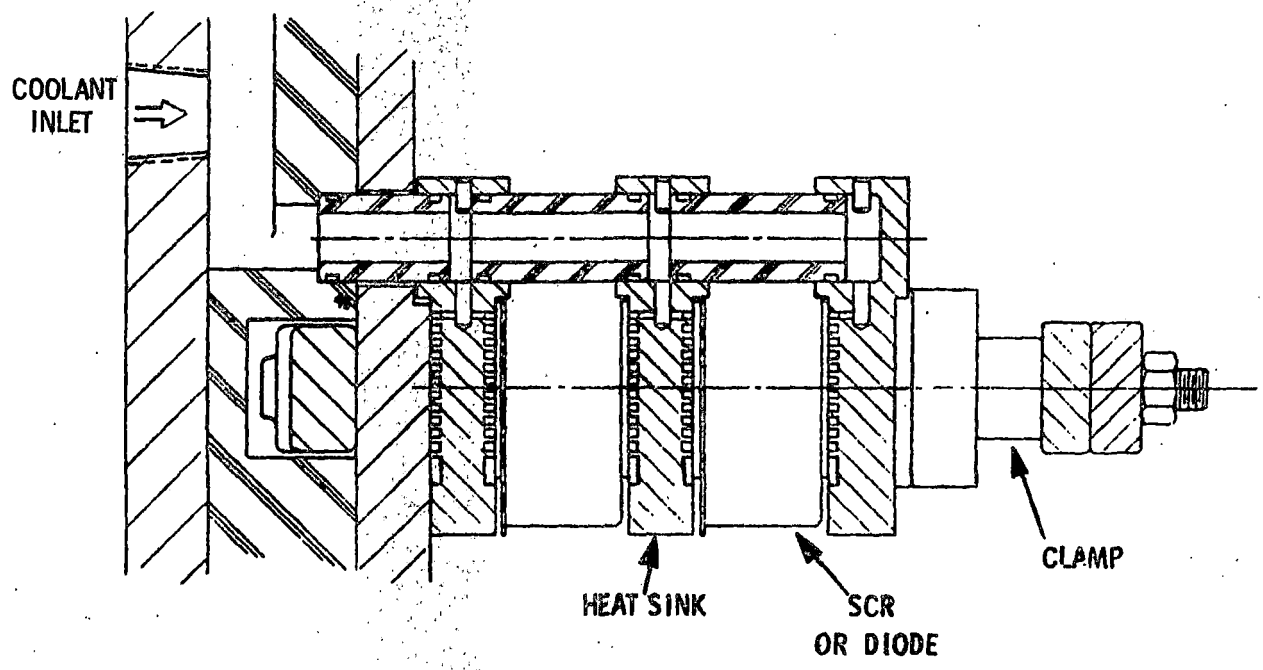

Figure 5.6-28. Diode and SCR Cooling

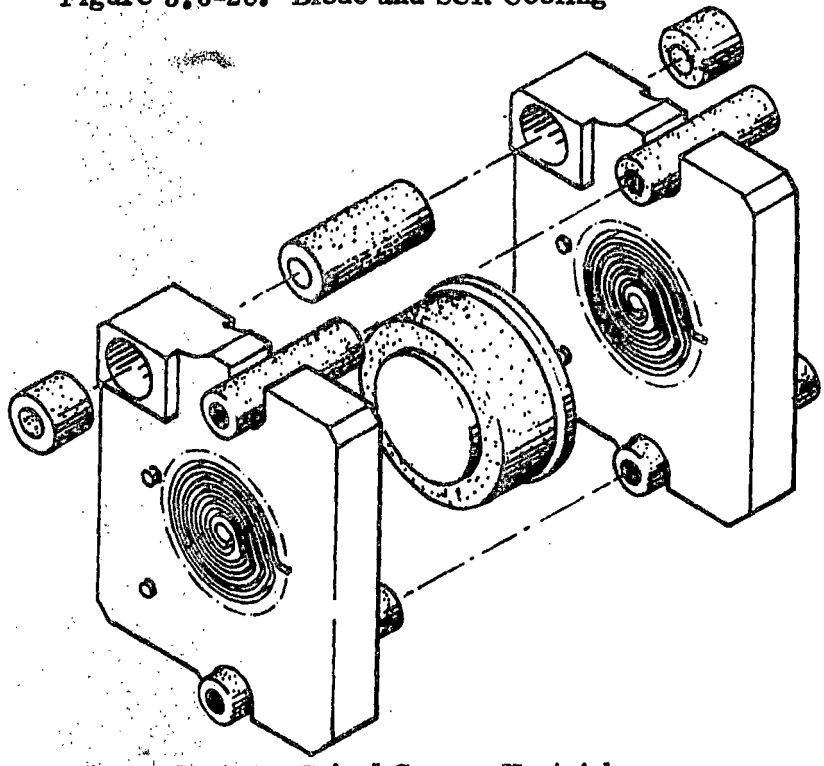

Figure 5.6-29. Spiral Groove Heatsink

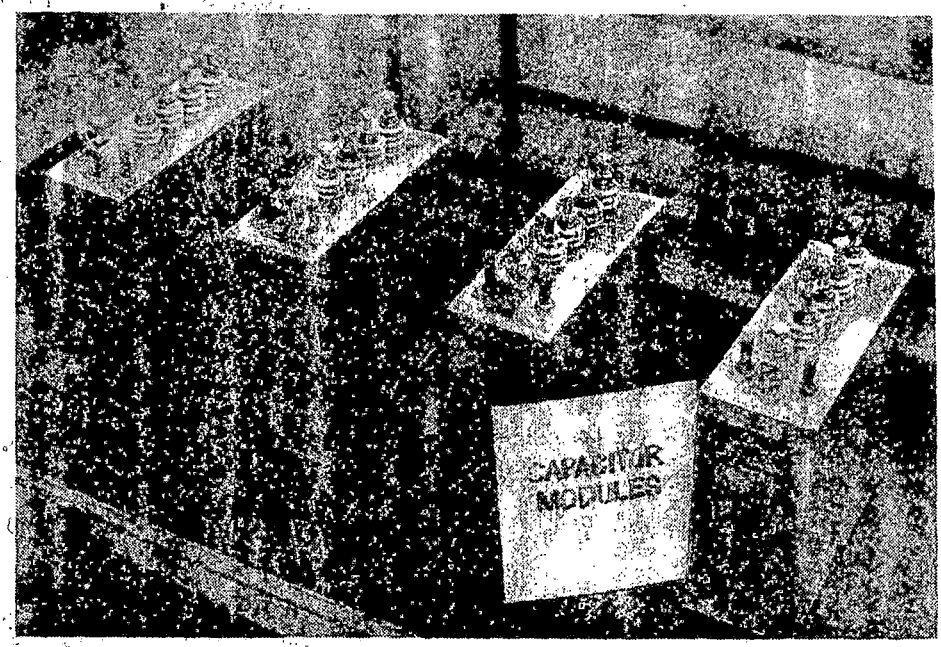

Figure 5.6-30. Capacitor Module

Coolant interconnects are in series between the four capacitors. The coolant is directed through each capacitor in a copper tube. The capacitor case contains a sealed heat transfer fluid which provides efficient heat removal from the module. Power interconnect terminations on the front of each unit have a permanent seal around the base of the stud.

Field Supply Module

The field supply module shown in Figure 5.6-31 contains the field transformer and its associated circuitry. The module is enclosed within a deep drawn aluminum can similar to the inverter module. The unit acts as a standpipe for the cooling system and thus has a differential pressure vent to maintain the slight pressure head necessary to eliminate draining of the return manifold back into the unit. All system power and signal interconnect terminations are made in the same manner as in the inverter module.

Capacitors, resistors and relays within the unit are mounted on sheet metal brackets. Harness assembly termination interconnections to these components are made using pressed-in terminals located on the brackets.

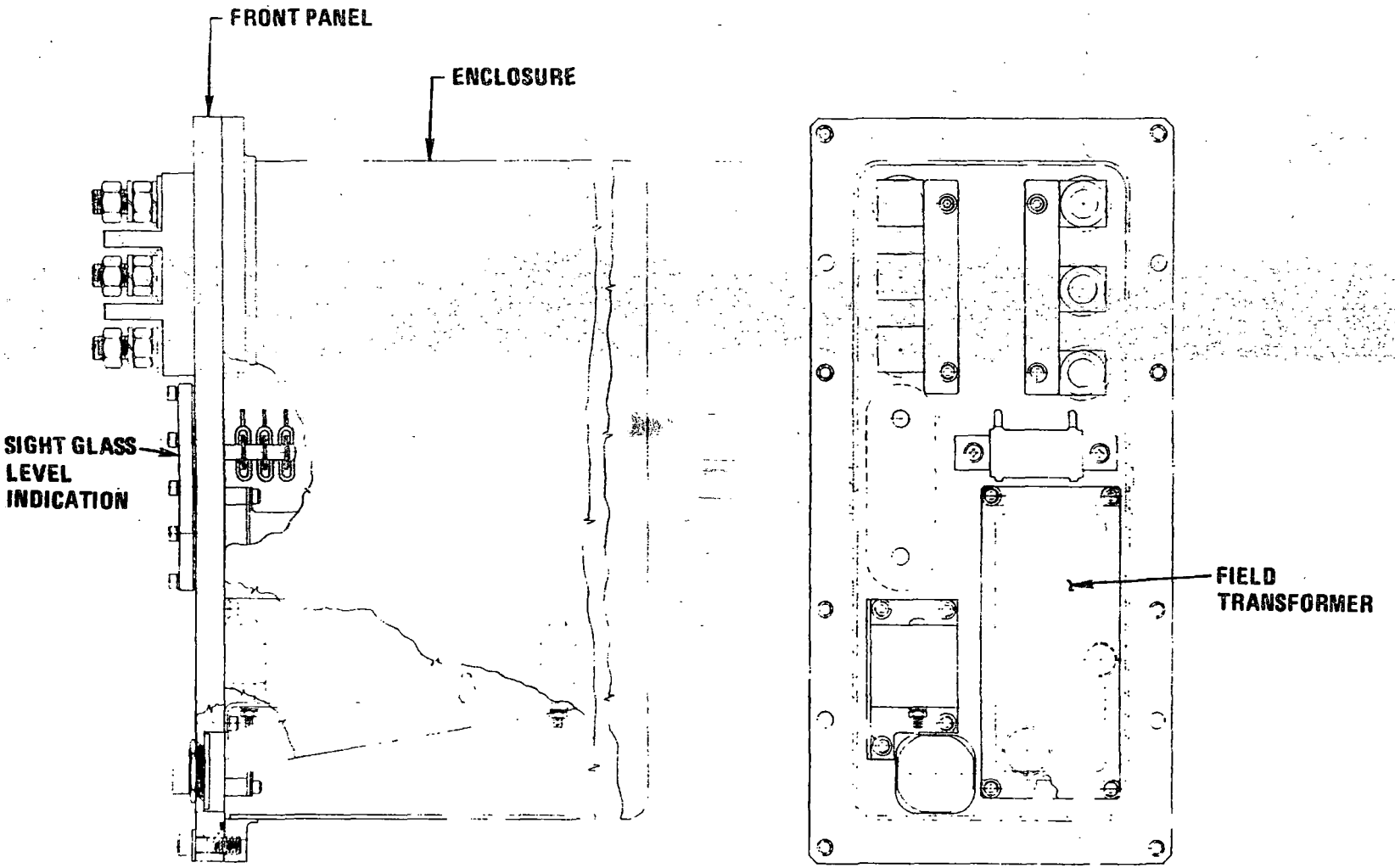

Figure 5.6-31. Field Supply Module

Cycloconverter Module

The cycloconverter module shown in Figure 5.6-32 contains power SCR's and their associated over voltage protection, dV/dt, and gate drive circuits. The packaging and cooling of this module is similar to the inverter module discussed earlier. The primary difference is that the gate drive circuit subassembly is a circuit card assembly instead of a terminal board. This was necessary in order to achieve the density requirements dictated by the large amount of gate drive circuitry. The harness assembly interfaces with this card through terminal blocks located in rows as shown in Figure 5.6-33.

Brake Control Module

The brake module shown in Figure 5.6-34 contains the CEMF transformer as well as power SCR's and their associated dV/dt, and gate drive circuits. This unit uses the same conceptual packaging approach described for the inverter module. However, the brake module uses the same gate drive circuit card (with fewer driver circuits assembled) as the cycloconverter.

The counter-EMF transformer is also housed in the brake module. Since the unit contains only five SCR stacks compared to the normal six, the transformer was mounted to the base in place of an SCR stack. The transformer can be seen in Figure 5.6-35 through the left hole in the side structure.

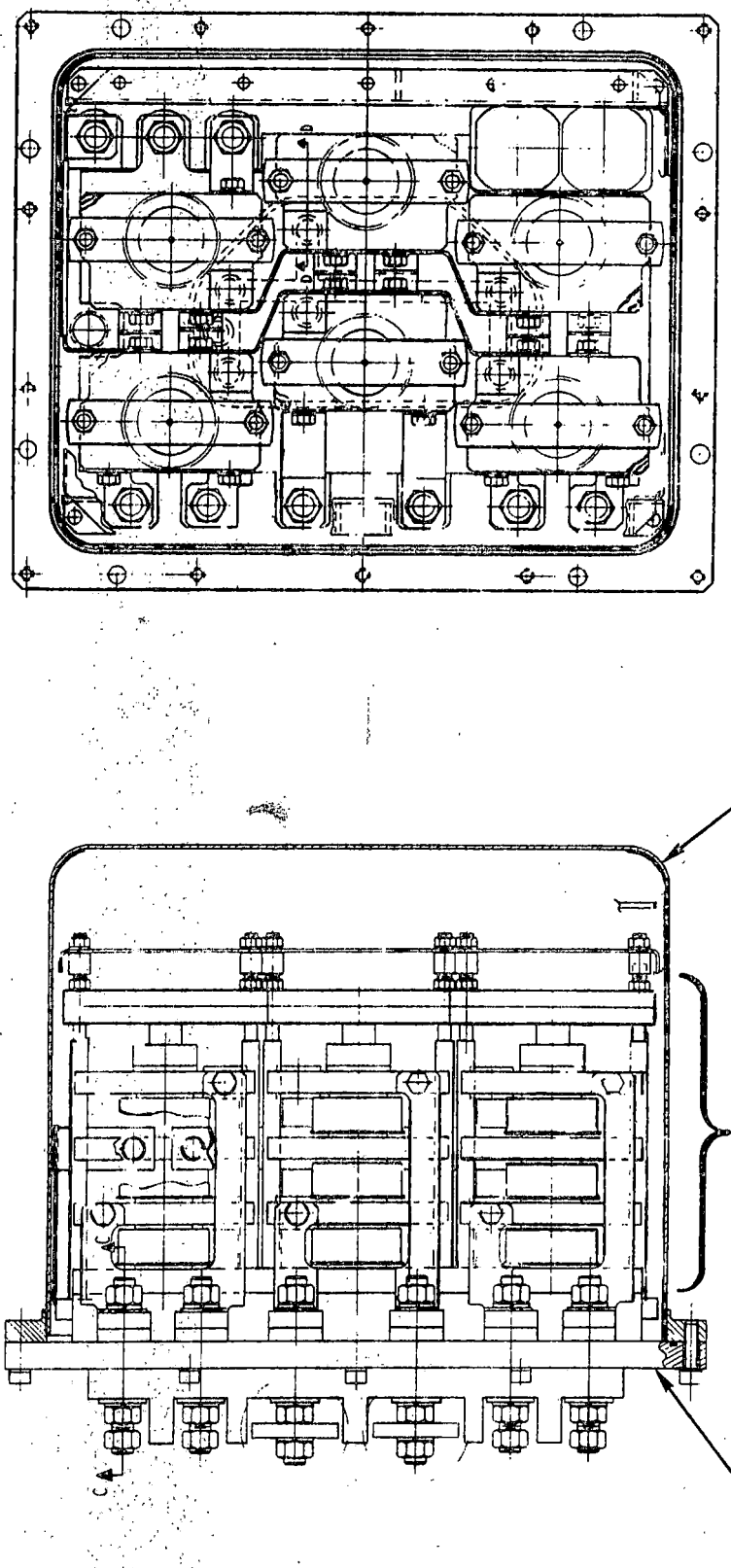

Figure 5.6-32. Cycloconverter Module

Figure 5.6-33. Cycloconverter Module Assembly

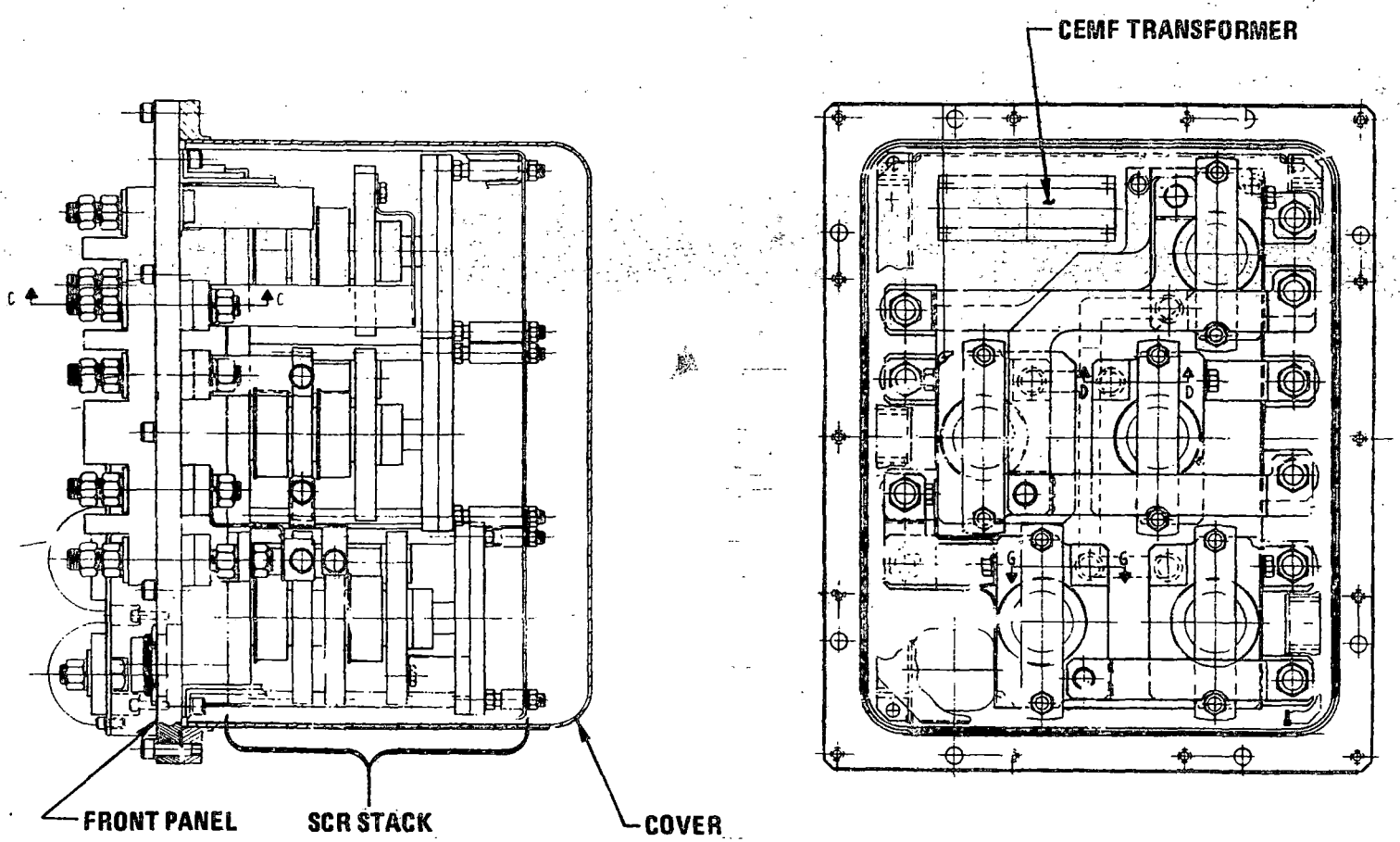

Figure 5.6-34. Brake Control Module

Figure 5.6-35. Brake Module

5.6.7 COOLING SYSTEM

5.6.7.1 Functional Requirements

The liquid cooling system provides the means for removal of heat from the high power dissipation elements of the ASDP propulsion system; the resonating inductor module, the power converter assembly (PCA), and the traction motor. This must be accomplished under the environmental conditions stated in paragraphs 5.6.1 and for one or two car operation over the ACT-1 Synthetic Transit Route as described in subsection 5.4.

5.6.7.2 Design Approach

The design approach taken is based on the use of two independent forced convection liquid cooling systems per car, one for each of the propulsion systems. This redundant feature was considered to be essential since adequate cooling is critical to the performance of the ASDP propulsion system. Furthermore, two independent cooling loops within each system were postulated: one for the traction motor, the other for the power electronics.

Another important consideration in the design was the choice of coolant fluid. Early in the ASDP program a search was made for fluids with properties suitable for ASDP application. Fire resistance and lubrication qualities were considered to be of primary importance.

Information received from vendors on several candidate fluids was condensed and compared as shown in Table 5.6-V. As can be seen, only a phosphate ester-petroleum oil mix (Pydraul MC) and a fluor-silicone fluid (Krytox 143 AB) were considered suitable from a fire resistance standpoint. However, not only was Krytox not in large scale production at that time, but its cost was estimated to be at least an order of magnitude greater than that of Pydraul. Therefore, the Pydraul MC was tentatively selected although there was some question about the acceptability of its performance at low temperatures.

Subsequent to this selection, it was decided to use grease lubricated bearings in the tr- on motor rather than rely on the use of the coolant fluid for lubrication. This decision made it possible to consider an additive-free silicone fluid. Therefore, evaluations and tests were conducted and a comparison was made between Pydraul MC and Dow Corning DC200-50CS fluids. The specific tests conducted are discussed in subsection 6.1.

Properties	COOLANT FLUID					
	Pydraul MC Phosphate Ester/Oil	Skydrol 500C Phosphate Ester	Coolanol 45 Silicate Ester	SF-96(mod) Silicone	F-50 Chlor Silicone	Krytox 143 AB Fluor Silicone
Cost/Gallon	~$5	~$10	~$20	~$15	~$60	High
Fire Resistance	Yes	No 410°F Fire	No 430° Fire	No 575°F Fire	No 550°F Fire	Yes
Non Toxic	Yes	Skin/ Irritant	Yes	Yes	N/A	Yes
Good Lubricant	Yes	Yes	Yes	Yes* (with Additives)	Yes	Yes
Compatibility	Yes	Attacks Copper	Yes	Yes	Yes	Yes
Low Pour Pt	No (-10°F)	Yes	Yes	Yes	Yes	Yes
Viscosity	Yes	No(3.8cs)	No (4 cs)	Yes	Yes	Yes
Thermal Stability	Yes	Yes	Yes	Yes	Yes	Yes
Low Dielectric Constant	Yes	No (8.6 at 77°F)	Yes	Yes	Yes	Yes
Low Dissipation Factor	No, 5.8% at 77°F	No, 2% at 77°F	Yes	Yes	Yes	Yes
Hi Dielectric Strength	Yes	Yes	Yes	Yes	Yes	Yes
Hi Insulation Resistance	Yes	Yes	Yes	Yes	Yes	Yes
Low Volatility	Yes	No	Yes	Yes	Yes	Yes

* Additives may degrade electrical properties

Table 5.6-V. ASDP Coolant Tradeoff

The results of this comparison are summarized in Table 5.6-VI. Based on these results, it appeared obvious that the silicone fluid was superior with respect to nearly all properties of interest. Therefore, the DC 200-50CS fluid was selected as the propulsion system coolant, even though its cost is about 2-1/2 times that of Pydraul.

Following this selection, analyses were conducted to help establish cooling system design and performance requirements. These and experience gained during previous breadboard testing established the power dissipation and flow requirements shown in Table 5.6-VII for operation over the HSGTC ACT-1 Synthetic Transit Route. Subsequent additional analysis indicated that the dissipation levels shown were somewhat conservative.

Additionally, the design was based on maintaining semiconductor junction temperatures well below maximum rating. For example, the SCR's and power diodes were derated from 125°C to 85°C.

5.6.7.3 Design Description

5.6.7.3.1 General

A schematic of the liquid cooling system is shown in Figure 5.6-36. It shows two independent flow loops: one for the traction motor, the other for the propulsion power control equipment (PPCE) which is comprised of the resonating inductor, inverter, capacitor, cycloconverter, brake control, and field supply modules. The field supply module serves as a standpipe and reservoir for this cooling loop; the other five modules are connected for parallel flow.
Maximum fluid operating temperature is 145°F in the PPCE loop and 165°F in the traction motor loop. Both loops have a flow rate of 20 gpm.

(Flow tests were conducted on the Test Article modules to determine actual flows. Differences between actuals and the goals shown in Table 5.6-VII were deemed to be acceptable. These tests are discussed in subsection 6.2.)

PROPERTIES	COOLANT FLUID	
	DC 200 (50 CS)	Pydraul MC
Viscosity	350 SSU @ 40° F 185 SSU @ 100° F	5800 SSU @ 40° F 320 SSU @ 100° F
Flash Point	535° F	475° F
Fire Point	670°F	525° F
Nontoxic (compared to oil)	Yes	Yes
Lubricity	Poor	Good
Material Compatability	Good	Good
Pour Point	-67° F	-10° F
Thermal Stability	300° F	200° F
Dielectric Constant (@ 25° C)	2.71	4.6
Dissipation Factor (@ 25° C)	0.00002	0.058
Dielectric Strength (volts /0.1 inch)	35 kV Initial	22 kV Initial
Insulation Resistance	10^{14} ohm-cm	$> 10^{8}$ ohm-cm
Low Volatility	Yes	Yes
Specific Heat @ 77° F	0.39	0.39
Thermal Conductivity	0.0871	0.0728

Table 5.6-VI. Comparison between Pydraul MC and DC 200-50CS

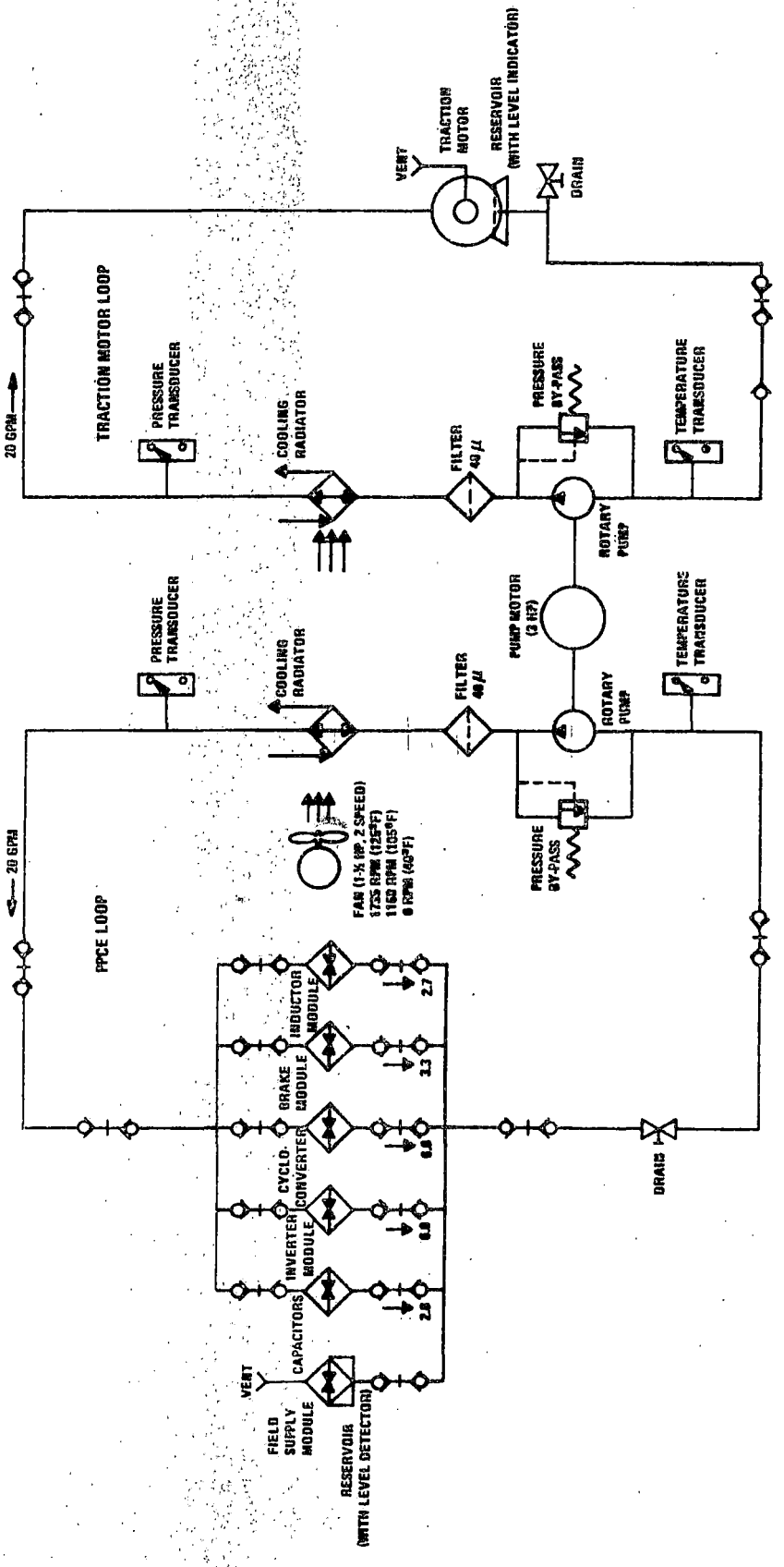

Figure 5.6-36. Cooling System Schematic

Module	Nominal Dissipation (kW)	Coolant Flowrate (gal/min)
Inverter	3.6	6.0
Cycloconverter	2.0	6.0
Capacitor	1.0	2.0
Resonating Inductor	3.6	2.7
Brake	1.2	3.3
Field Supply	0.6	0.0
Power Control Electronics Loop Total	12.0	20.0
Traction Motor Loop Total	19.5	20.0

Note: Based on the average computed power losses over the ACT-1 Synthetic Transit Route

Table 5.6-VII. Power Dissipation and Cooling Requirements per Truck

5.6.7.3.2 Cooling Assembly

A cooling assembly (see the drawings in Figures 5.6-37 and 5.6-38 and the photograph in Figure 5.6-) contains the following major hardware components:

- Two radiators cooled by a single propeller type two-speed fan
- Two rotary positive displacement pumps driven by a single motor
- Two oil filters with replaceable filter elements, one in each cooling loop
- Two air intake filters
- Pressure and temperature transducers for monitoring fluid operating conditions.

A detailed list of the cooling assembly components is provided in Table 5.6-VIII.

The unit is designed to be attached to the undercar body by four shock mounts. The structure is of welded aluminum angle with gussets and braces as necessary to ensure continued operation should one of the mounts fail. Aluminum panels enclose most of the assembly. Sound dampening panels are mounted to the frame interior to reduce noise generated by the pumps and fan.

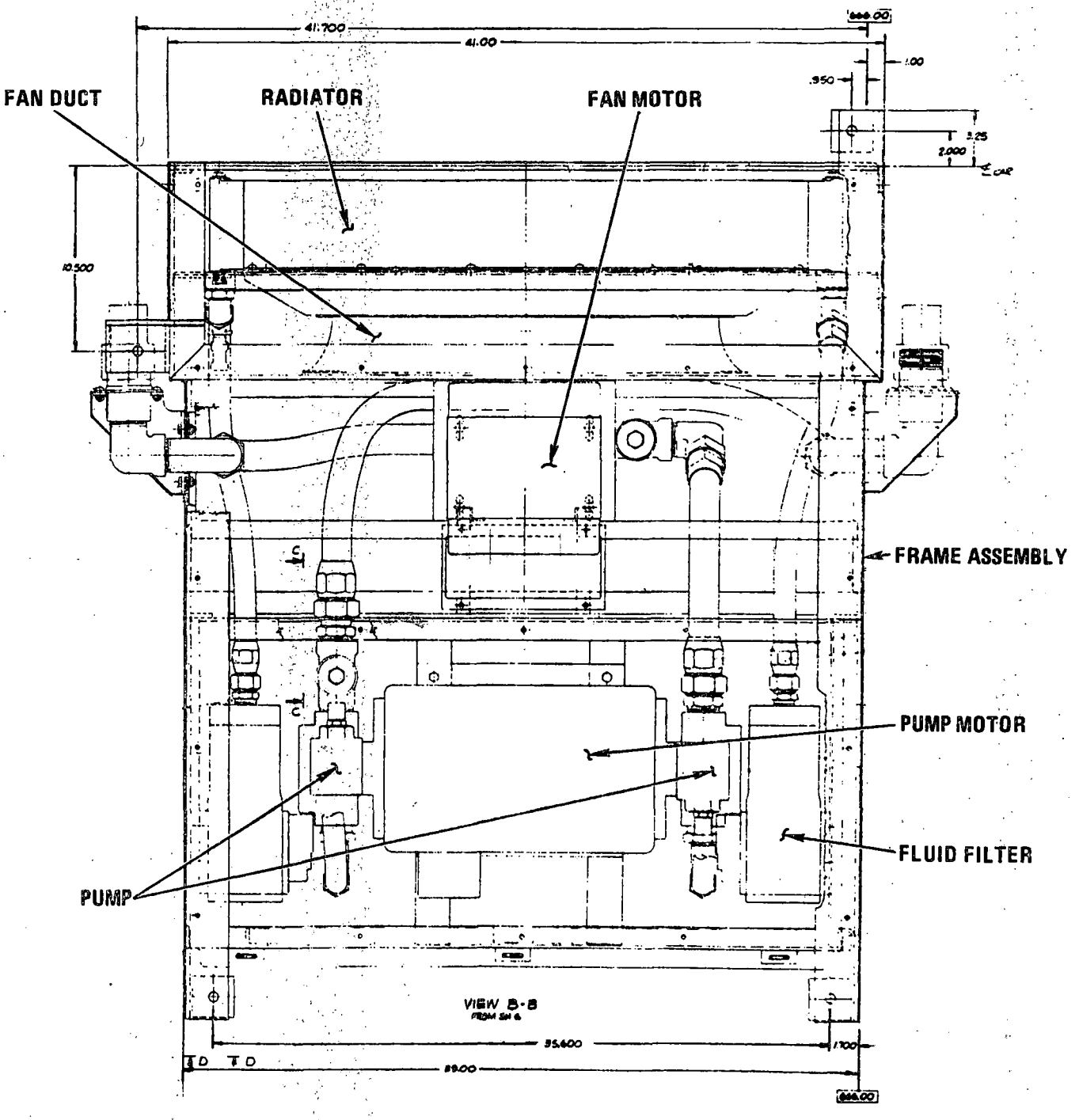

Figure 5.6-37. Cooling Assembly – Top View

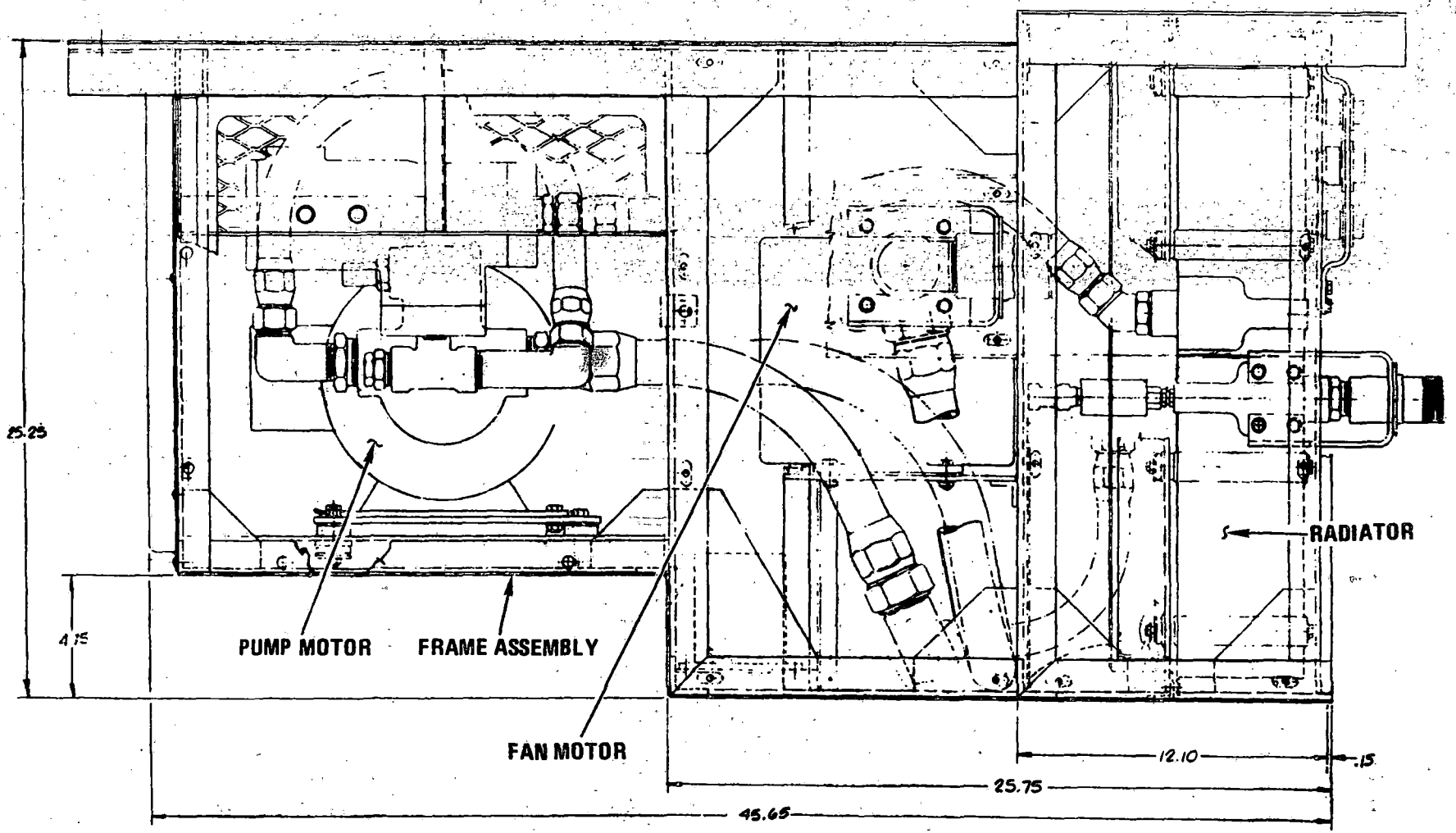

Figure 5.6-38. Cooling Assembly – Side View

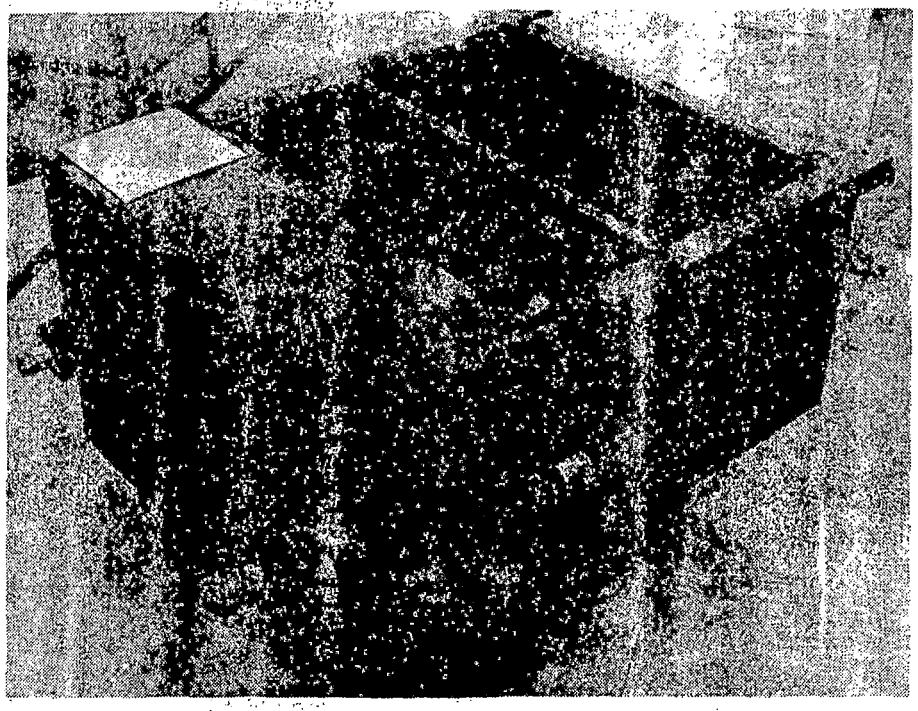

Figure 5.6-39. Cooling Assembly

Component	Qty	Description	Vendor
Pump Motor	1	3 hp, 230 Vac, 3 Phase, frame 213 TC (modified)	Delco Products
Pump	2	Rotary, 20 gpm at 1200 rpm, integral pressure relief valve	Viking Model HL475
Radiator	2	Plate/fin brazed aluminum	Modine
Fan	1	1.5 hp, 6 blade, 22" dia	Hartzell Type C (high-pressure)
Fluid Filter	2	40μ nominal, wire cloth	Parker Model 20S
Pressure Transducer	2	Linear type (0 to 100 psi)	Consolidated Controls Model 41SG30
Temperature Transducer	2	Linear type (-70^{o} to 300^{o}C)	Lewis Engineering P/N 56B17 (MS 28034-3)
Fluid Coupling	4	Self-sealing, wrenching type	Aeroquip 5100 series
Magnetic n Plug	2	Self-sealing	Tech. Development Co. P/N M-109
Air Filter	2	Expanded alum (<2"WG ΔP)	Aluminum Filter Co.
Hoses	AR	1" pressure hose, 1.5" suction hose	Aeroquip Type FL350
Check Valve	1	O-ring sealing, low cracking pressure	Circle Seal P/N 259B-12PP-15

Table 5.6-VIII. Cooling Assembly Components

The radiators, located at one end of the enclosure, are structurally isolated by rubber mounts and flexible coolant hoses. Ambient air is forced through the radiators by a fan. Air intake filters are located at the fron and one side of the unit. Removal of the front air filter provides access to the horizontally mounted fluid filters for element replacement.

Fluid flow is generated by one of two identical pumps driven by a common double-ended 3 hp motor. The coolant flows through a 40 micron filter, past a pressure transducer and via flexible hose, and into the radiator. From the radiator the fluid flows to the traction motor (or PPCE). Self-sealing, wrenching-type couplings interconnect the radiator hoses with the coolant lines to and from the motor (or PPCE). A transducer measures the temperature of the returning fluid before entering the suction side of the pump. A magnetic drain plug is located between the pump and the filter which allows draining of the filter housing prior to element removal.

5.6.7.3.3 PPCE Loop

This loop comprises the cooling system for the resonating inductor module and the power converter assembly modules. It contains a total of approximately 22 gallons of coolant fluid with 5 gallons in the reservoir.

Each module in the power converter assembly has rigid plumbing running across the top, which manifolds the coolant fluid into the modules through flexible tubing. In the case of the resonating inductor module, fluid enters the unit through hoses which connect to the power converter assembly manifolds.

A self-sealing wrenching-type disconnect coupling is installed at the inlet and outlet ports of each module. This permits module removal without coolant leakage. The field supply module acts as a standpipe and reservoir for the loop. This module is vented to the atmosphere and has only a self-sealing, wrenching disconnect outlet port. It contains a slight glass which indicates the fluid level.

Each module has a bleeder valve at the top of the unit to insure that air entrapment does not occur.

The cooling fluid enters a typical SCR module through an inlet port on the front panel. From there is fills a manifold, which distributes the fluid to the various SCR stacks. The fluid enters each SCR heatsink, is channeled to the SCR pole face, and dumps into the sealed module enclosure. Fluid is drawn out of the enclosure and into the power converter return manifold by the cooling assembly pump.

Fluid entering the resonating inductor passes into a manifold which encloses one end of the resonating inductor coils. The fluid then is expelled through windings and dumps into the module enclosure. An orifice is used to obtain the desired pressure drop versus flowrate characteristic.

5.6.7.3.4 Traction Motor Loop

A separate cooling loop is provided for the traction motor containing approximately 9 gallons of coolant fluid with 5.25 gallons in the reservoir. The fluid reservoir is part of the traction motor housing.

The inlet and outlet ports to the motor are SAE internal straight thread bosses with O-ring sealing. A check valve is located in the coolant fluid outlet line near the sump outlet port. This prevents coolant fluid from seeping back into the motor sump and giving an erroneous fluid level indication.

A slight glass is located on the side of the motor sump and indicates a fluid level range over which the traction motor will operate. The 5-1/4 gallon maximum allowable fluid level is marked "full"; the 5 gallon minimum allowable fluid level is marked "add."

The motor may be filled by removing the hex head plug located on the upper slope of the sump just above the sight glass from the upper angular surface of the motor sump and pumping in coolant fluid. The motor is drained by removing a hex plug from the lower side wall of the motor sump.

B\ . fittings are located near the sight glass to provide maintenance personnel with the ability to coordinate the sump fluid level with the fluid input and removal.

The internal cooling of the traction motor is described in detail in the Traction Motor Final Report, R78-15.

5.6.8 TRACTION MOTOR

5.6.8.1 Requirements

The design and performance requirements for the traction motor were derived from the overall propulsion system requirements. Delco Electronics Specification ES 11372, included in Appendix A of the ASDP Traction Motor Final Report R78-15, defines motor requirements in detail.

The motor performance characteristics curves for motoring and braking are shown in Figures 5.6-40 and 5.6-41, illustrating the maximum requirements established for the motor design. The continuous duty rating of the motor (350 hp) is based on a duty cycle derived from the ACT-1 Synthetic Transit Route operation as defined in Boeing Vertol Specification D239-10000-1 (see paragraphs 5.4.2 and 5.4.3 of this report). The continuous thermal design is based on the repetitive duty cycle shown in Figure 5.4-9 for a 30-minute duration.

5.6.8.2 Design Approach

The overall design concept for the traction motor was established on the basis of Delco IR&D effort prior to ASDP contract award. Some of the major considerations in the concept selection are discussed below.

Rotor Construction

The two basic synchronous motor concepts initially considered were: (1) homopolar inductor machine and (2) wound rotor salient pole machine. The homopolar inductor machine has a solid steel rotor with high speed capability and does not require field excitation. It lacks, however, the efficient materials utilization obtainable with wound rotors and the flexibility of separately excited machines. Furthermore, the high inductance of homopolar inductor motors makes commutation more difficult at high frequencies. Based on these considerations and the more mature technology behind the wound rotor design, the salient pole wound rotor concept was selected for ASDP.

Field Excitation

Excitation of the wound rotor can be accomplished through slip-rings or by means of a rotary transformer and rectifier. The advent of the reliable silicon diode rotating rectifier, coupled with a rotary transformer makes the brushless wound rotor machine a

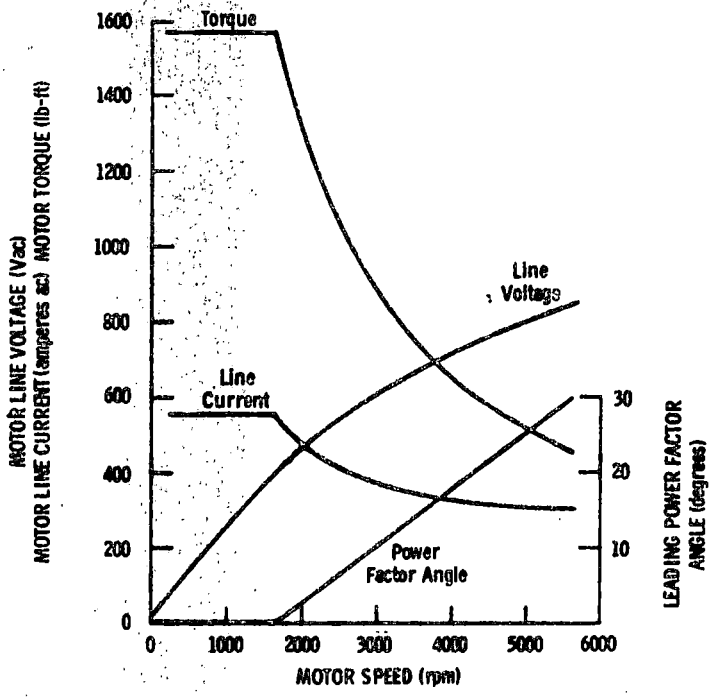

Figure 5.6-40. Characteristic Curves During Motoring for E-6497 Synchronous Motor Final Design

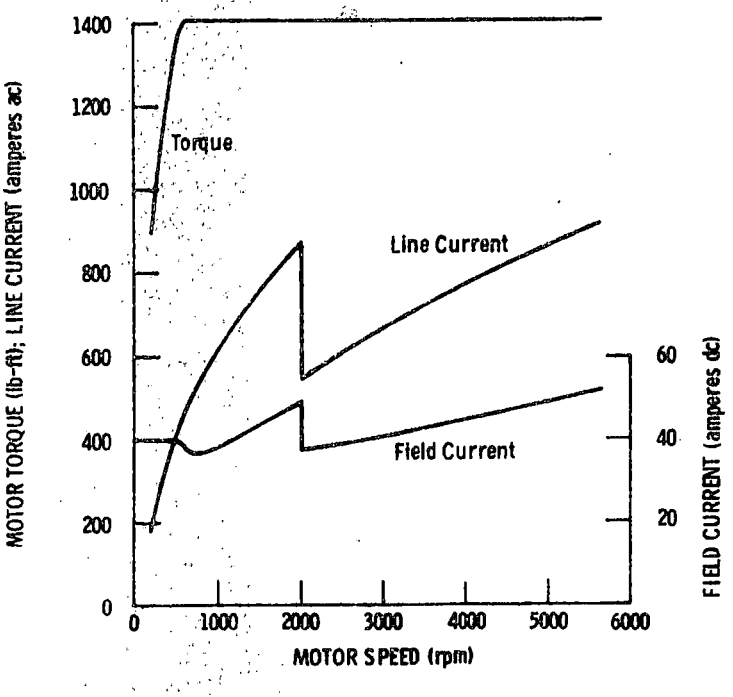

Figure 5.6-41. Characteristic Curves during Dynamic Braking for E-6497 Synchronous Motor Final Design

practical reality. Rotating rectifiers have been used successfully for commercial brushless alternators. The high frequency (350 - 1200 Hz) source for field excitation allows a light weight rotary transformer design without penalizing motor size. In addition, brushless operation permits liquid cooling, which raises the permissible current density.

Motor Cooling

The tradeoff between air-cooled and liquid-cooled motor designs resulted in the selection of a liquid cooled configuration. Liquid cooling significantly reduces weight and size and permits a completely enclosed construction, thereby providing isolation from the environment. Motor insulation life is also improved because the coolant reduces moisture penetration and oxidation of the insulation.

Motor Speed

During the initial tradeoff studies maximum motor speeds of 4500 and 8000 rpm were considered. Higher maximum speed reduces motor size and weight but requires a higher gear reduction ratio and increases stresses on rotor components. The 5600 rpm maximum speed selected represents a compromise. It can be accommodated with a single step gear reduction and state-of-the-art rotor construction and bearing technology.

5.6.8.3 Design Description

The ASDP traction motor shown in Figure 5.6-42 is a four pole, salient pole, self-synchronous machine designed to produce 490 hp (365 kW) from 1642 to 5642 r/min. The motor assembly consists of:

- A salient pole synchronous machine with a three-phase stationary armature and rotating field
- A three-phase rotating transformer and rectifier to provide dc field excitation
- A rotor position sensor to provide signals to control the switching of the commutating thyristors.

The motor design, including overall dimensions and a sectional view, is illustrated in Figure 5.6-43. A photograph of the motor rotor is shown in Figure 5.6-44.

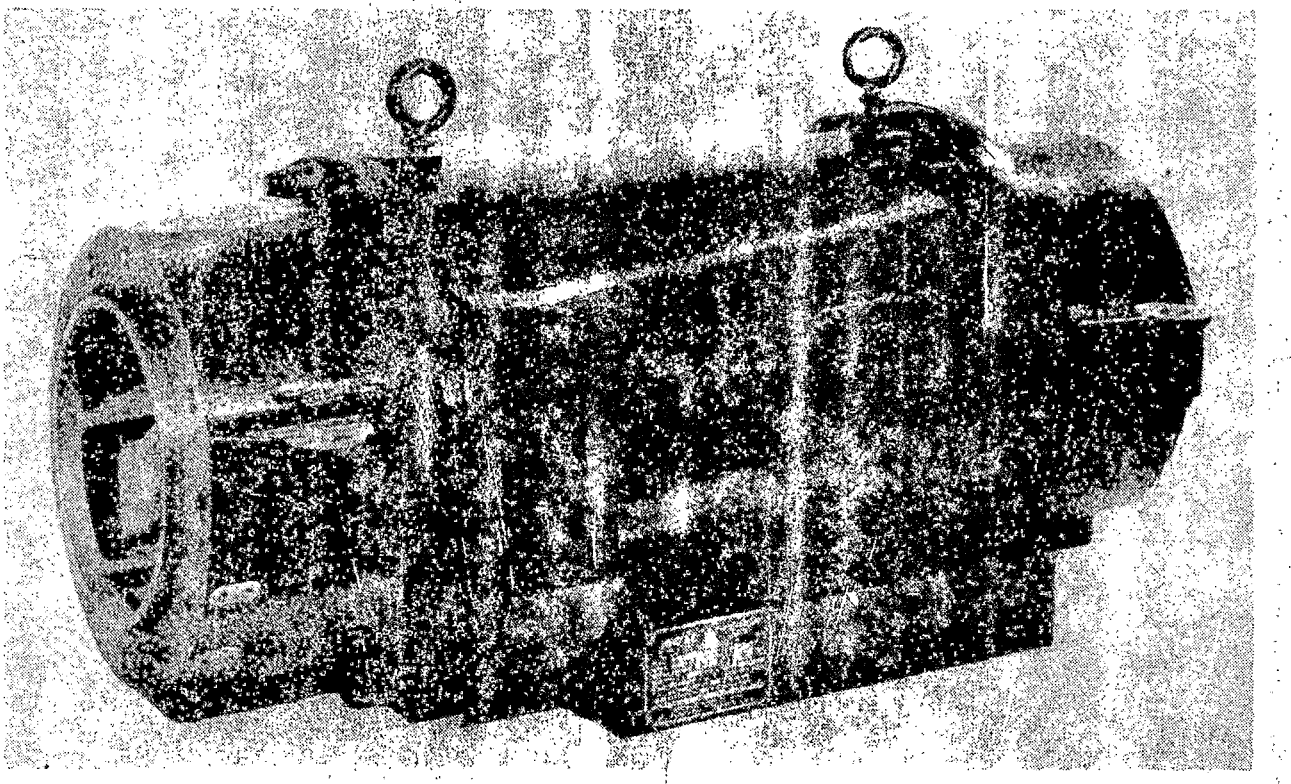

Figure 5.6-42. ASDP Traction Motor

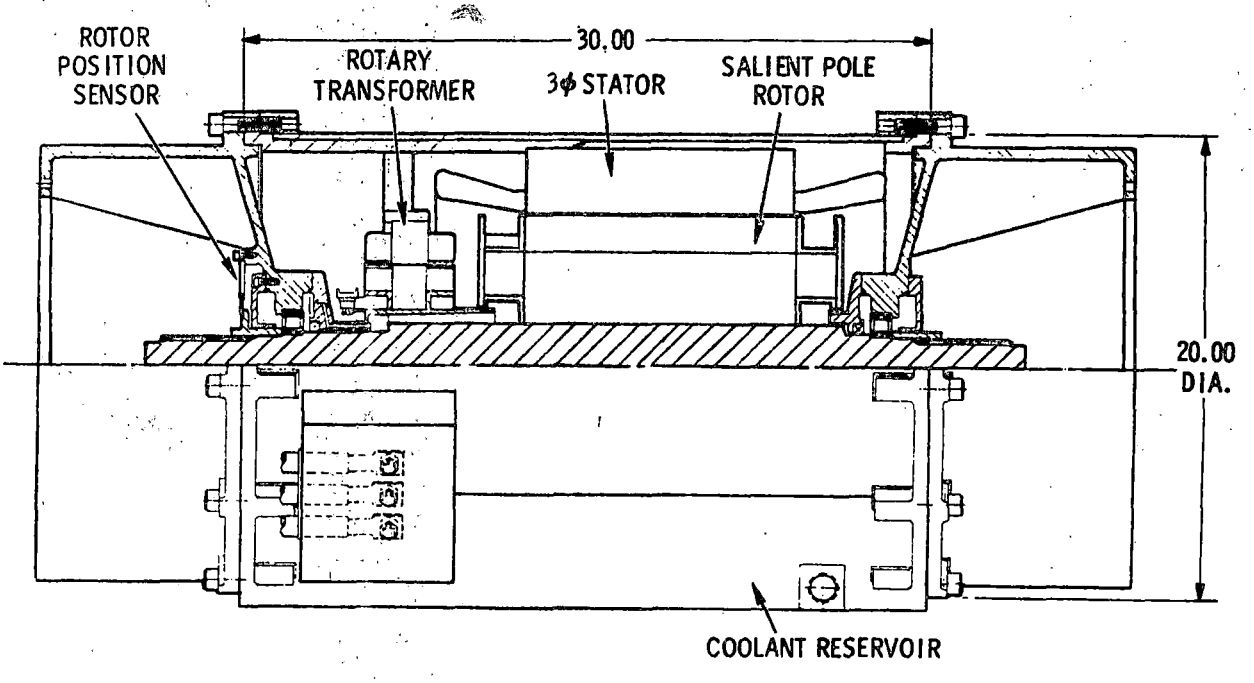

Figure 5.6-43. Traction Motor Sectional View

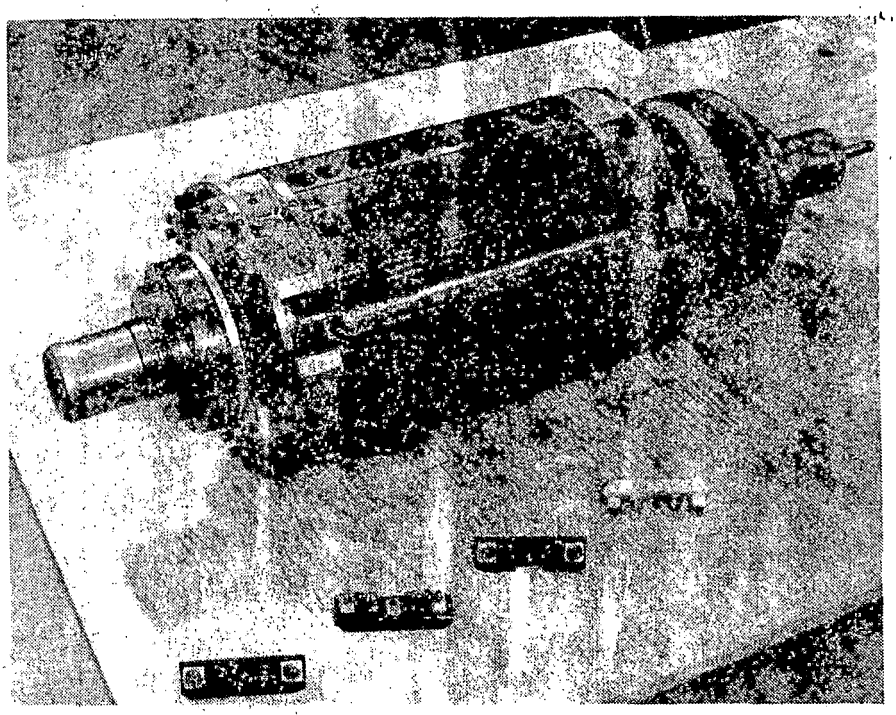

Figure 5.6-44. Motor Rotor

The stator laminations are conventional with semi-closed slots. The winding is made of multiple strands of round wire in parallel using Class "H" insulation. The rotor is a one-piece forging with four poles. Laminated pole head assemblies are bolted to each of the four poles of the rotor forging to hold the prewound coils in place. Damper bars are also incorporated in the pole head.

The rotary transformer is designed using conventional three-phase laminations. A four-pole winding is used. Since the transformer primary is fed from a high frequency current source, the output of the rotary transformer is nearly constant from zero to maximum speed. The rotating rectifier consists of six diodes in a full wave three-phase bridge between the rotary transformer secondary and the main rotor windings.

The rotor position sensor provides information concerning the rotor angular position relative to the stator windings. It consists of a laminated magnetic assembly with nine coils on the stator and two lobes on the rotor. Null points are accurately detected to provide signals to the thyristor triggering circuits.

The motor is liquid cooled with fire resistant silicone fluid which is sprayed on both the stator conductors and the end turns of the rotor windings. Coolant is also directed to the rotating transformer/ rectifier. A sump is provided at the bottom of the motor frame collecting the coolant which is pumped back to the cooling assembly.

The motor shaft is shrunk into the rotor forging and has a splined extension on each end. Grease lubricated bearings are used with face seals preventing the cooling fluid from entering the bearing housing. Temperature sensors are provided for diagnostic monitoring.

5.6.9 GEAR DRIVE AND AXLE COUPLING

5.6.9.1 Requirements

The performance and design requirements for the gear drive and axle coupling assembly were derived from the overall propulsion system performance requirements (Boeing Specification D239-10000-1). Delco Specification ES 11366 defines the requirements in detail. A summary of the major requirements is shown in Table 5.6-IX.

5.6.9.2 Design Approach

The design approach was selected to accommodate the monomotor truck drive concept which is a key design feature of the Delco self-synchronous propulsion system (see subsection 5.7). In this concept a single traction motor is used to drive both axles of one truck. The motor is centered longitudinally on the truck and drives each axle through a single reduction bevel gear set (right angle drive). Torque is transmitted from the gear drive output to the truck axle through a flexible coupling, which allows axle movement for the primary suspension motions. This allows the mounting of the heavy motor-gearbox assembly directly to the truck frame thus reducing the unsprung mass for improved ride dynamics. Figure 5.6-45 illustrates how the axle motions are accommodated by the flexible axle coupling.

The gear drive and axle coupling design originally proposed by Brown Boveri and Company (BBC) was based on an adaption of an existing design used in the Munich subway system.

• Wheel Size	28 to 30 in.
• Maximum Axle Load	32,500 lb
• Maximum Axle Speed	960 r/min
• Maximum Normal Axle Torque	6120 lb-ft
• Maximum Axle Shock Torque	24,975 lb-ft
• Cubic Mean Axle Torque	3850 lb-ft
• Cubic Mean Axle Speed	535 r/min
• Gear Life	1,000,000 Miles
• Bearing Life	500,000 Miles
• Acoustic Noise	82 dBA at 15 ft
• Axle Displacement Radial	± 0.75 in.
Axial	± 0.50 in.
Angular	± 1.3°

Table 5.6-IX. Gear Drive and Axle Coupling Assembly Design Requirements

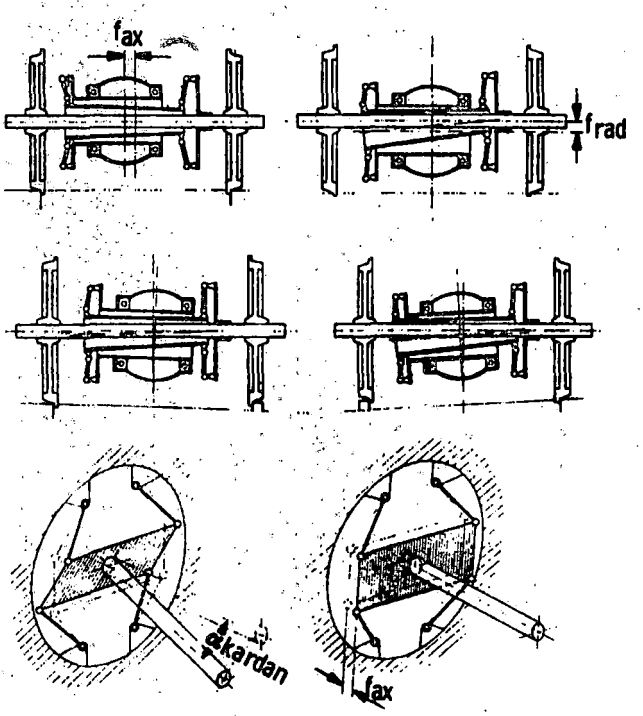

Figure 5.6-45. Double-sided Flexible Coupling Axle Deflections

5.6.9.3 Design Description

The gear drive and axle coupling, shown in Figure 5.6-46 consists of a hollow shaft hypoid bevel gear axle drive and a flexible rubber joint cardan coupling developed by BBC for high speed locomotives and transit cars. Salient features of the design are summarized in Table 5.6-X .

The gear drive unit is bolted directly to the traction motor flange. Motor torque is transmitted to the pinion shaft through a gear coupling capable of accommodating small misalignments. A single-stage hypoid gear set provides a 5.875 to 1 reduction between the motor and axle. A ring gear mounted on a hollow shaft transmits torque to the axle through a rubber joint cardan drive. There is a small offset (0.8 in.) provided to minimize gear sliding losses at high speed. The gear teeth are case hardened and lapped for minimum wear. The axle bearings are tapered roller bearings to take both radial and axial loads. The pinion bearings are a combination of roller and ball bearings. A cylindrical roller bearing is provided to take the large radial load of the pinion gear, while a pair of angular contact ball bearings are provided for taking the axial loads.

GEAR DRIVE

- Single reduction Hypoid gear drive (5, 875 to 1)
- Oil splash lubrication
- Aluminum housing

FLEXIBLE COUPLING

- Double sided coupling with hollow quill shaft
- Produces very low unbalanced forces
- Rubber joints used to provide flexibility
- Coupling spring rate: Radial 363 lb/in.
  Axial 435 lb/in.
  Torsional 4670 ft-lb/deg

Table 5.6-X. Gear Drive and Axle Coupling Assembly Salient Features

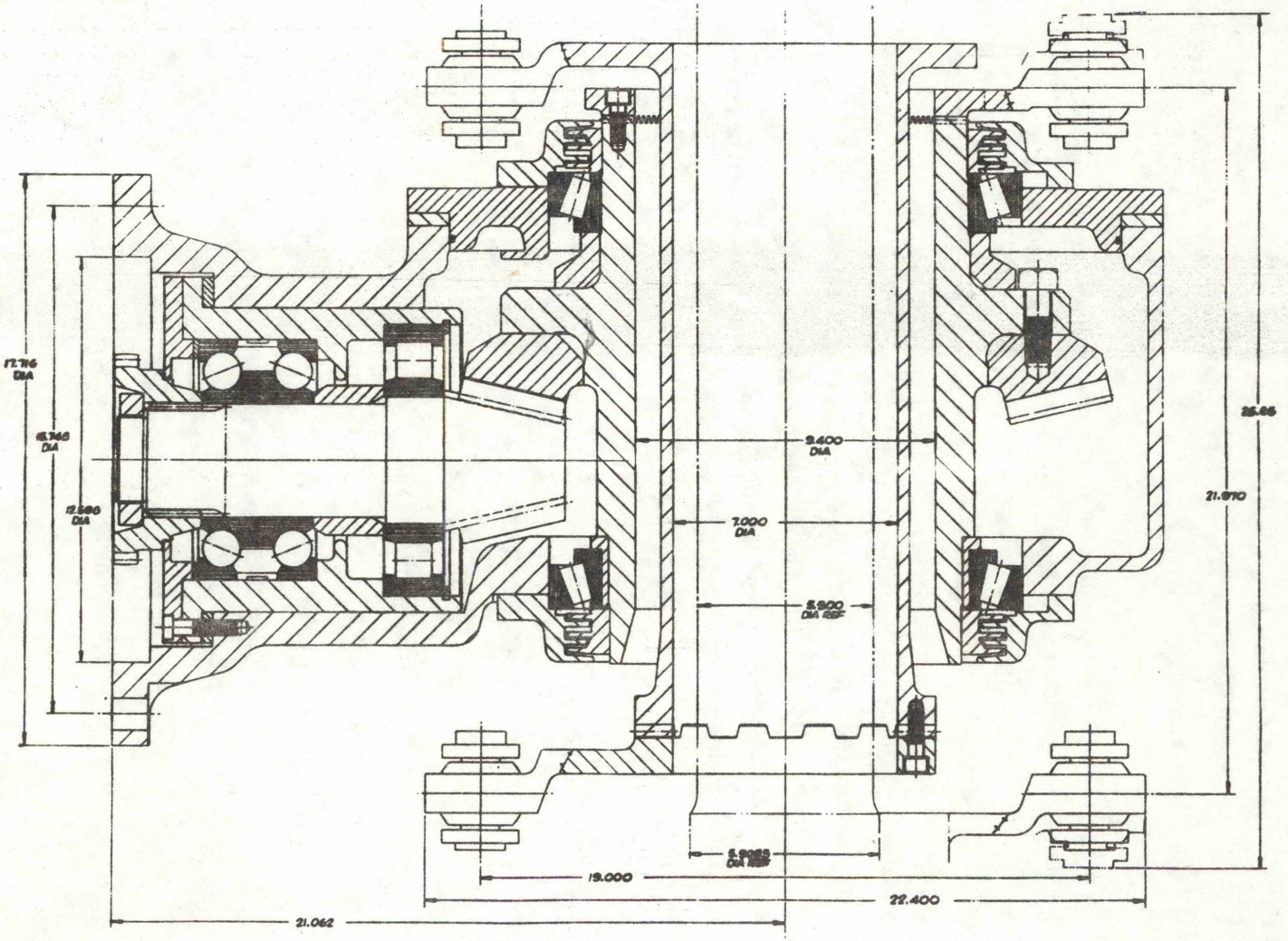

Figure 5.6-46. Gear Drive and Axle Coupling

The gears and bearings are oil splash lubricated. Labyrinth seals are provided to retain the oil in the gearbox. Breathers, magnetic plugs, sight gages, and inspection openings are provided for maintenance and servicing.

The rubber joint cardan coupling is designed for high speed operation and permits combined axle motions of ±0.75 inches radial, ±0.50 inches axial and ±1.3 degrees angular. In the tangential direction (torque transmission) the coupling is rigid to preclude angular vibrations between the coupled axles and the monomotor drive.

The cardan drive consists of two rubber joint link-type couplings connected with a quill shaft through the hollow shaft of the gearbox. The approximate symmetry of the overall drive assembly allows a disc brake to be located on each side.

5.6.10 MOTOR/GEARBOX COUPLING

5.6.10.1 Requirements

The motor/gearbox coupling connects the traction motor output shaft to the gearbox input shaft. Delco Specification Control Drawing 7557719 defines the coupling requirements in detail. A summary of the major performance and design requirements is shown in Table 5.6-XI.

Nominal (average) Power	140 hp
Nominal (rms) Torque	455 lb-ft
Nominal (rms) Speed	2525 rpm
Maximum Normal Power	245 hp
Maximum Normal Torque	1050 lb-ft
Maximum Shock Torque	4250 lb-ft
Maximum Normal Speed	5645 rpm
Maximum Overspeed	6130 rpm
Direction of Rotation	50% CW; 50% CCW
Maximum Misalignment	0.5 deg
Maximum Parallel Offset	0.040 inches

Table 5.6-XI. Motor/Gearbox Coupling Requirements

5.6.10.2 Design Approach

Due to possible misalignment between the motor and gearbox shafts due to machining tolerances, structural deflections, and thermal expansion, only flexible types of couplings were considered. The requirement for quick coupling disengagement eliminated all but the gear coupling type. All proposals received recommended the use of gear couplings with minor differences in design approach. Vendor selection was made on the basis of cost and delivery schedule.

5.6.10.3 Design Description

The coupling, shown in Figure 5.6-47, consists of two hubs with external teeth engaging internal teeth on a one-piece sleeve that fits over both hubs.

The hubs are splined to the shafts with a slight interference fit to prevent loosening in this bidirectional application. The gear teeth on the hubs are crowned, providing major diameter piloting for good dynamic balance and optimum crowned flank for maximum load capability under misaligned conditions.

Lubrication is provided by Anderol 786 grease pumped into the gear contact area through a standard Alemite fitting. A lube discharge hole is provided for venting the coupling cavity. The grease is retained inside the coupling by O-ring seals.

The coupling is made of A151 4140 steel alloy heat treated and case hardened for increased wear resistance by nitriding.

The coupling gear data is as follows:

Pitch Diameter	6 inches
Number of Teeth	48
Pressure Angle	20^{o}
Face Width	0.75 inches.

A unique feature of this coupling design is the capability for disengagement by simply separating the gearbox from the motor as shown in Figure 5.6-48.

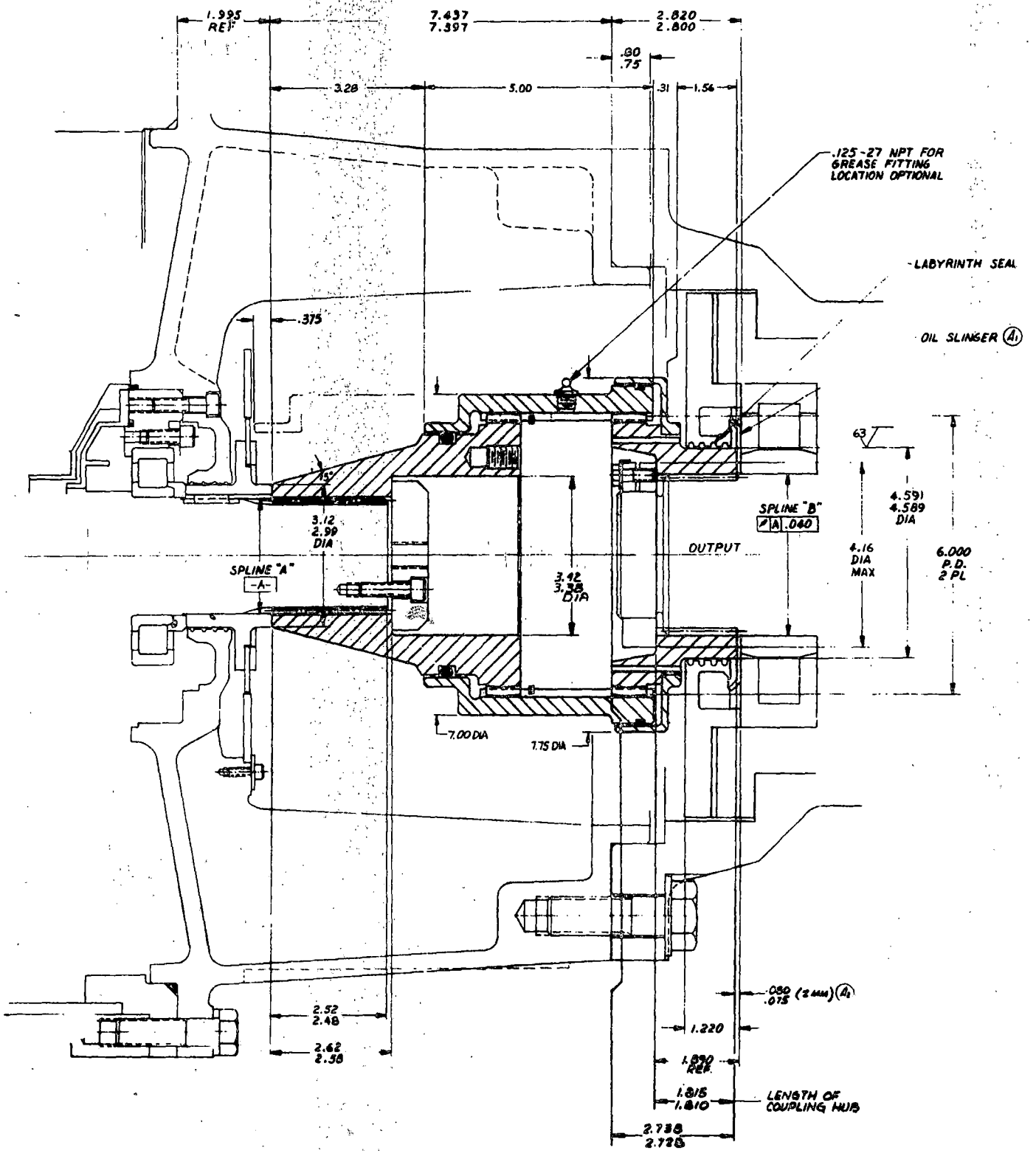

Figure 5.6-47. Motor/Gearbox Coupling

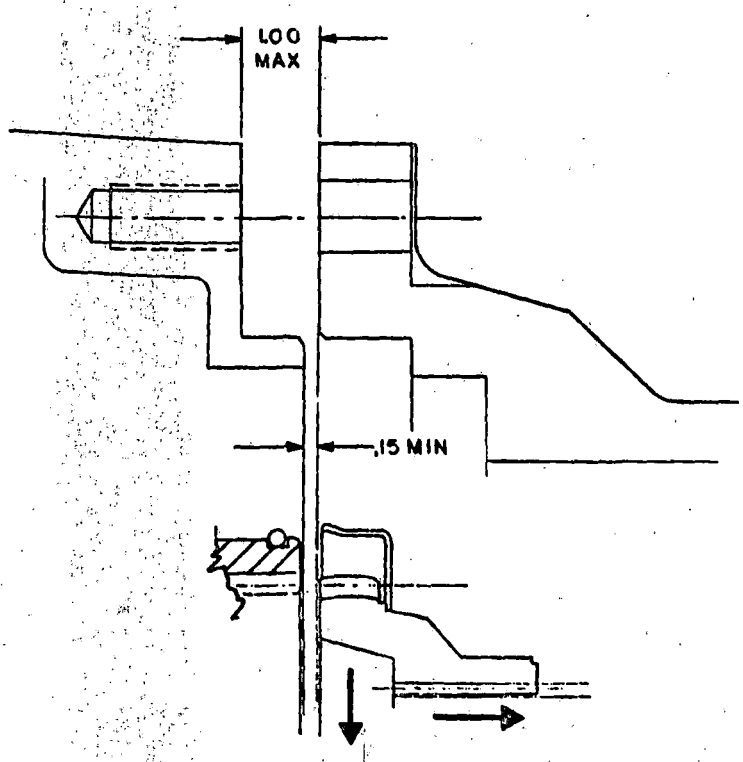

Figure 5.6-48. Coupling Disengagement

5.6.11 DYNAMIC BRAKE RESISTOR

5.6.11.1 Functional Requirements

The brake resistor is required to dissipate railcar kinetic energy during the dynamic braking mode of operation in accordance with the deceleration requirements and the maximum thermal capability repetitive duty cycle specified in paragraph 5.4.2 of this report.

5.6.11.2 Design Approach

Two resistors are used per rail car, one for each of the two propulsion systems. Analysis showed that motor braking torque of 1405 lb-ft (required for a nominal deceleration of -3 mphps for a car of AW1 weight) could be maintained from maximum speed (80 mph) to approximately base speed (23 mph) with a resistor value of 0.78 ohms. It was decided to maintain this torque level down to about 10 mph, requiring the resistor to be tapped at 0.26 ohms.

This, combined with the requirements stated above, resulted in the power dissipation versus time repetitive duty cycle shown in Figure 5.6-49. This is equivalent to an average dissipation of 110 kW over the cycle.

5.6.11.3 Design Description

Motor current is supplied to the brake resistor through a 9-SCR phase delay brake rectifier as discussed previously in subsections 5.1 and 5.3. Motor current, and therefore braking effort, is modulated by a combination field current control and phase delay control. Below base speed, another SCR in the brake control module shunts out about two-thirds of the brake resistance.

The brake resistor assembly is shown in the sketch and photograph of Figures 5.6-50 and 5.6-51, respectively.

The dynamic brake resistor consists of several controlled impedance coils which are bussed to provide the two desired resistance values. The coils are captivated at regular intervals in high temperature ceramic feedthrough tubes which are in turn supported by insulator blocks. The coils are attached to threaded copper alloy terminations which feed through insulator end plates. The terminations are then connected in a bussing arrangement with taps at the appropriate impedances. A typical system connection is accomplished by bolting the interconnect cable to the tap, using a hole provided in the right angle portion of the resistor tap.

The structure consists of steel extrusions designed to provide structural integrity at elevated resistor temperatures. The coils are enclosed in protective perforated diamond pattern sheet metal panels to permit the passage of air in and around the coil assembly. These panels also provide protection against the possibility of maintenance personnel coming in contact with the heated coils.

The mounting interface consists of a two-hole pattern in each of the four support arms. The holes are oriented such that the resistor assembly can be mounted in only one orientation.

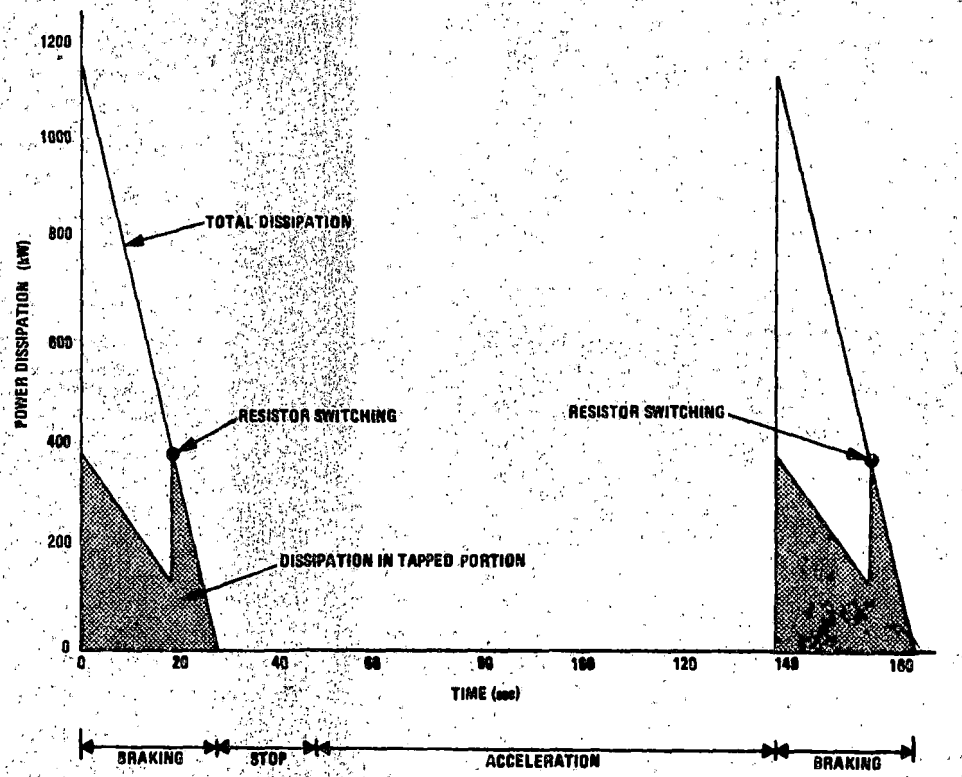

Figure 5.6-49. Dynamic Brake Resistor – Repetitive Duty Cycle

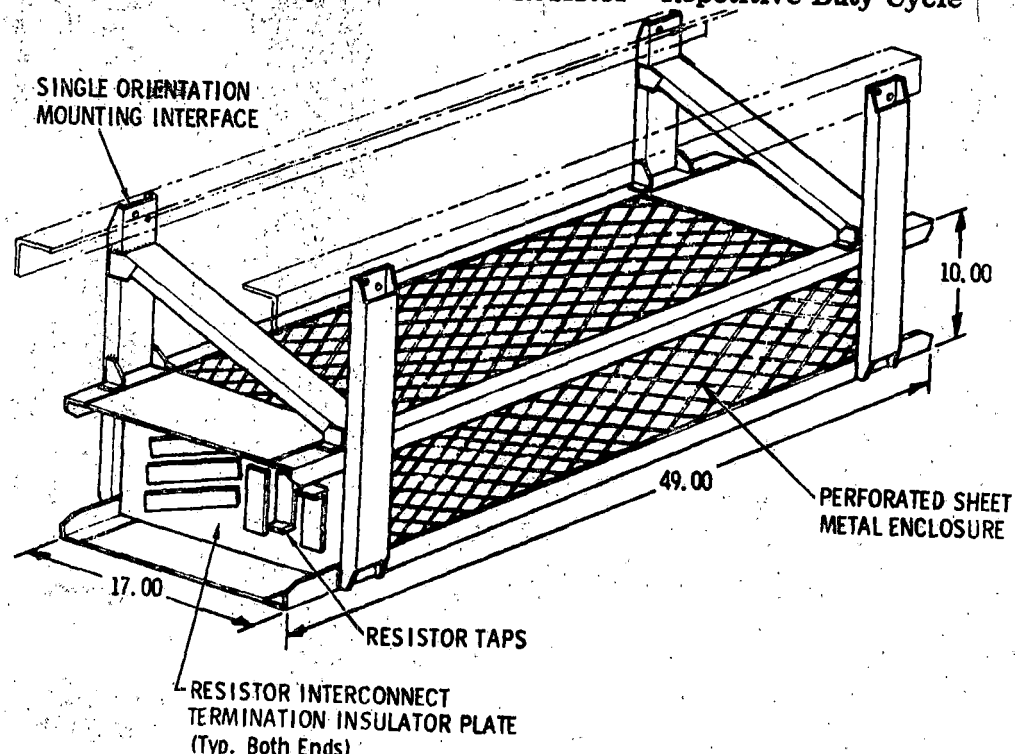

Figure 5.6-50. Dynamic Brake Resistor

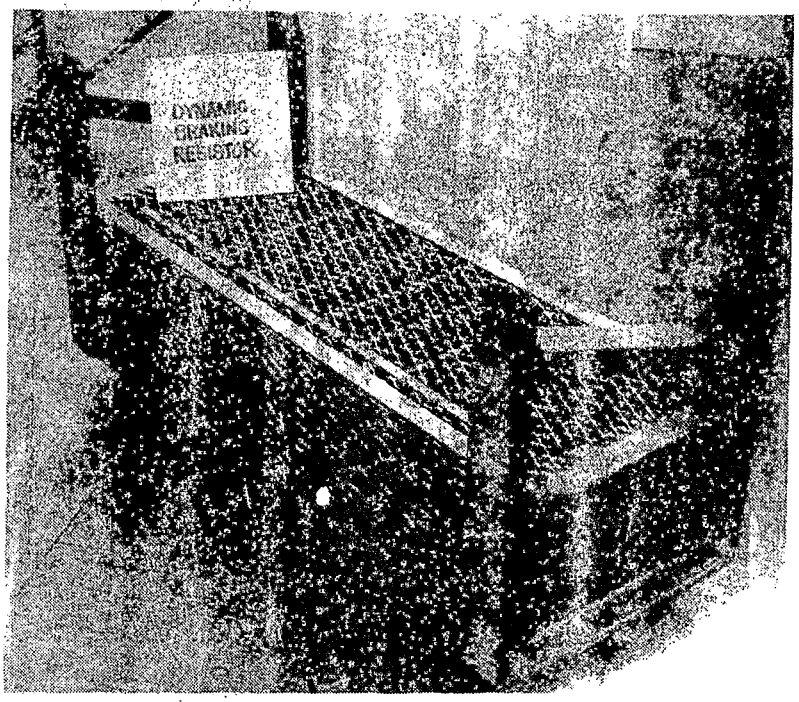

Figure 5.6-51. Dynamic Braking Resistor

5.6.12 TRUCK CONNECTOR BOX

5.6.12.1 Functional Requirements

The truck connector box shown in Figure 5.6-52 serves as a junction point for cables between carbody mounted equipment and the power source, and between truck-mounted equipment and its associated carbody equipment. This allows truck cabling and 3rd rail power to be easily disconnected from the car during maintenance and repair activities.

5.6.12.2 Design Description

There are two connector boxes per car, one for each propulsion system.

e housing is a split aluminum weldment. When the cover and cable interconnect hardware are removed, one-half of the housing may be separated with the truck. This maintains the cable interconnect keying and prevents the possibility of incorrectly reconnecting cables. During initial assembly the interconnect cables are adjusted to a fixed depth, then secured in the sealing tubes. During engagement, the cable terminations which are mounted

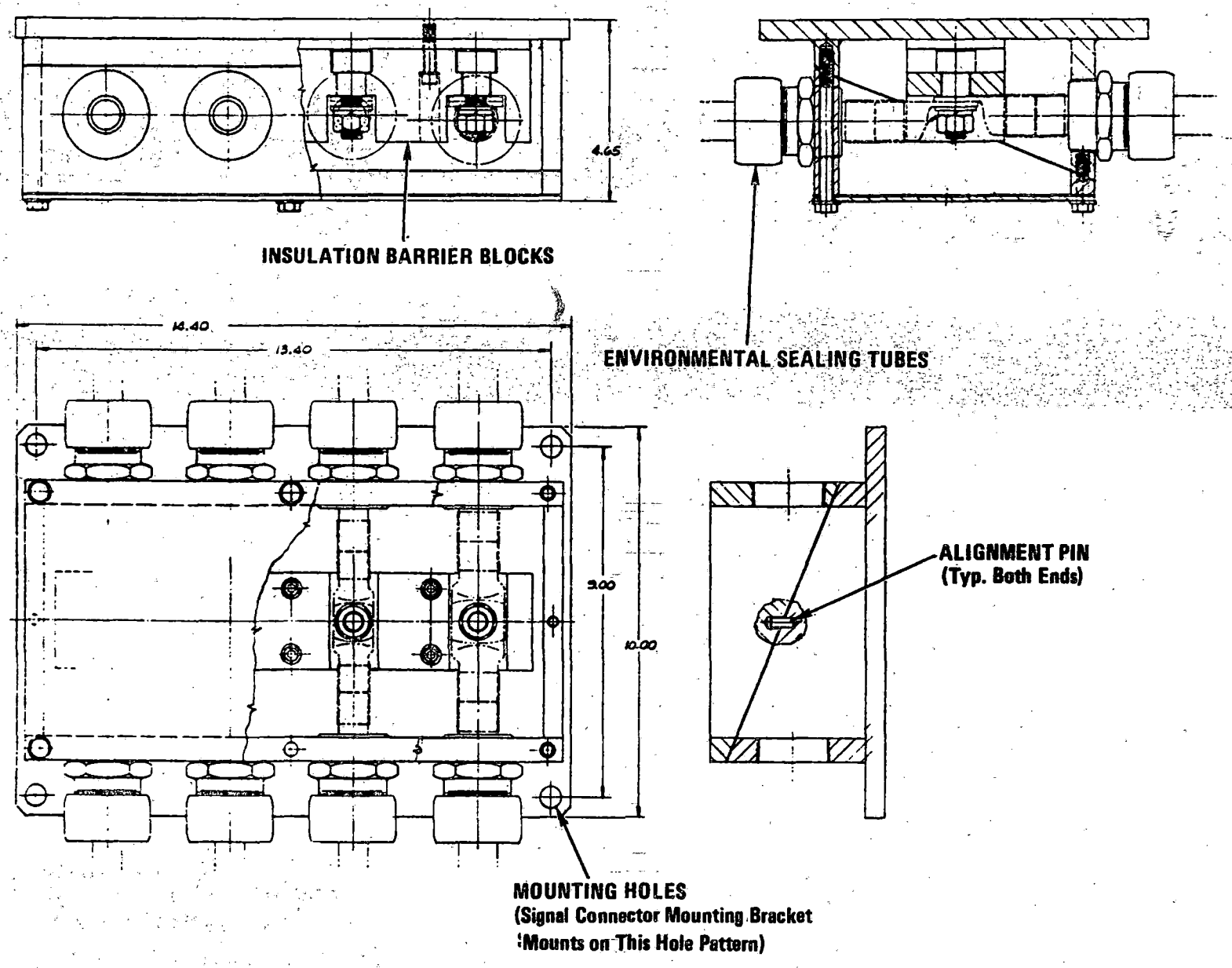

Figure 5.6-52. Truck Connector Box Layout

in the upper half of the truck connector box slide down over the interconnect bolts. Pins provide precision alignment between housing bolt patterns and the cable termination bolt pattern. Flat gaskets, as well as the sealing tubes, are used at the various interfaces to seal against dirt and moisture contamination.

5.6.13 GROUND BRUSH

5.6.13.1 Functional Requirements

The ground brush provides a low resistance return path to the truck axle, and thence to ground, for the line current, bypassing the axle bearings.

The current load consists of that required for auxiliaries such as the M-A set and heaters as well as the propulsion current.

5.6.13.2 Design Approach

There are eight ground brushes per car, one at each end of all four axles. The current capability was established such that any four brushes on a car can safely handle the total line current.

5.6.13.3 Design Description

The ground brush assembly is shown in Figure 5.6-53. It consists of a copper/graphite brush, a spring loaded brushholder, and a housing which protects the ground brush components from mechanical injury, dirt, and oil. The assembly is mounted on the axle bearing cover and the brush is held securely by means of spring loading against a brass disc mounted on the end of the axle. The brush shunt is connected to the truck frame. Thus the bearings are protected against pitting and wear.

Each brush is rated for 250A dc continuously and 400A dc for 5 minutes.

5.6.14 SPEED SENSORS

5.6.14.1 Functional Requirements

Sensors are required to provide car speed information to the motorman and for overspeed and spin-slide detection and control. Thus, both axle speed and motor speed must be sensed and the information transmitted to the cab.

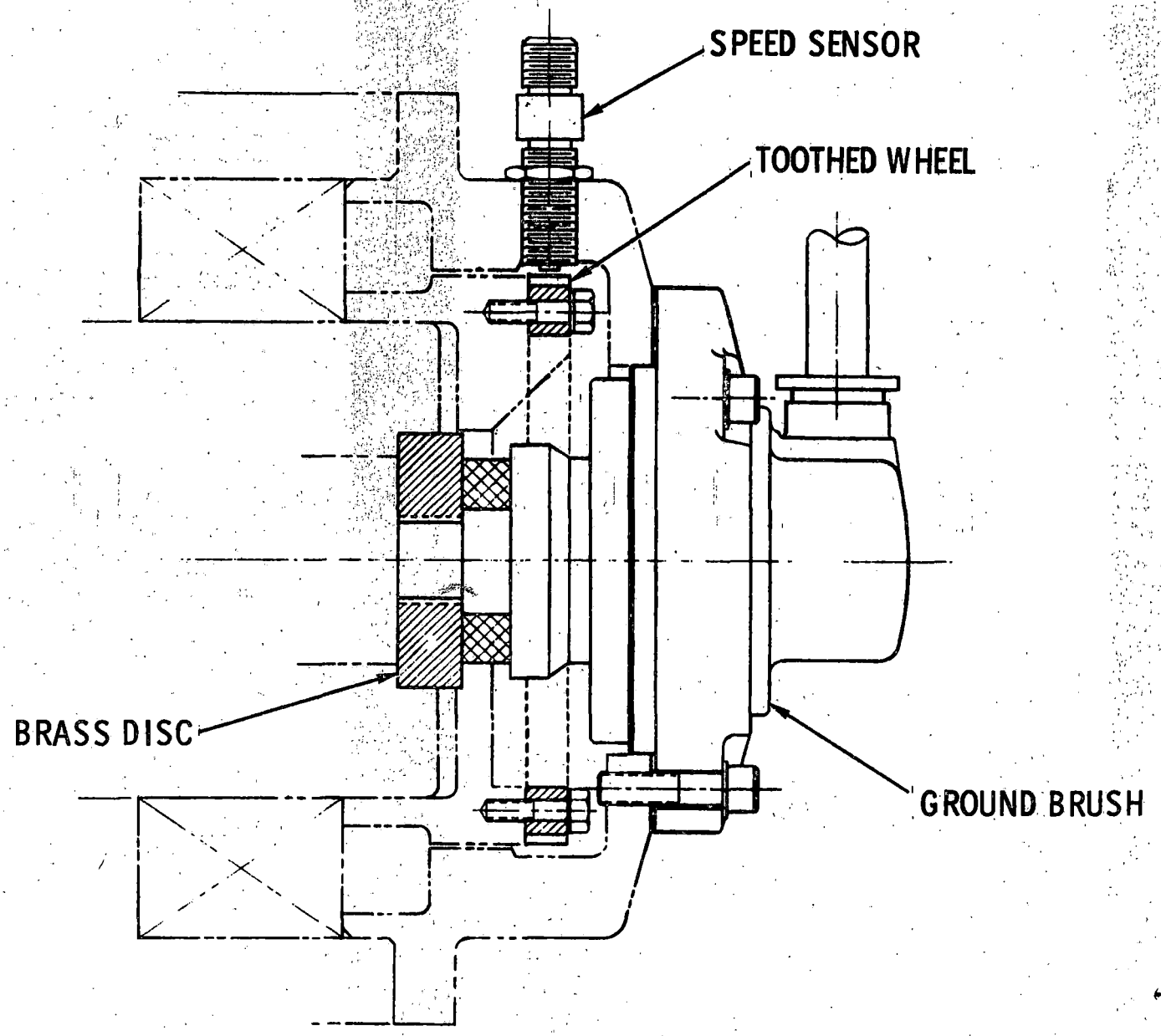

Figure 5.6-53. Ground Brush and Speed Sensor Installation

5.6.14.2 Design Approach

A sensor consisting of a magnetic transducer activated by a toothed wheel is incorporated in one of the ground brush assemblies on each axle of the car (see Figure 5.6-53). In addition, each traction motor contains a shaft-mounted rotor position sensor (RPS) whose chief purpose is to provide signals to control switching of the propulsion system SCR's, but is also used as a speed sensor.

5.6.14.3 Design Description

The magnetic pickup is a standard unit used by the synchronous (friction) brake system (SBS) supplier, WABCO. The 100-tooth wheel is of cold rolled steel, fabricated to fit in the ground brush assembly. One magnetic pickup from each truck is connected to the train control, the other to the SBS.

The RPS signals from the motors are both fed to the train control. The RPS is of the variable reluctance type, consisting of a laminated magnetic assembly having nine coils (3 primary, 6 secondary) on its stator and two lobes on its rotor (Figure 5.6-54). It produces about 72 pulses per axle revolution down to zero speed. Because of this superior low speed capability, it is the primary speed signal used by the train control. The axle speed signals are available for backup in case of RPS failure.

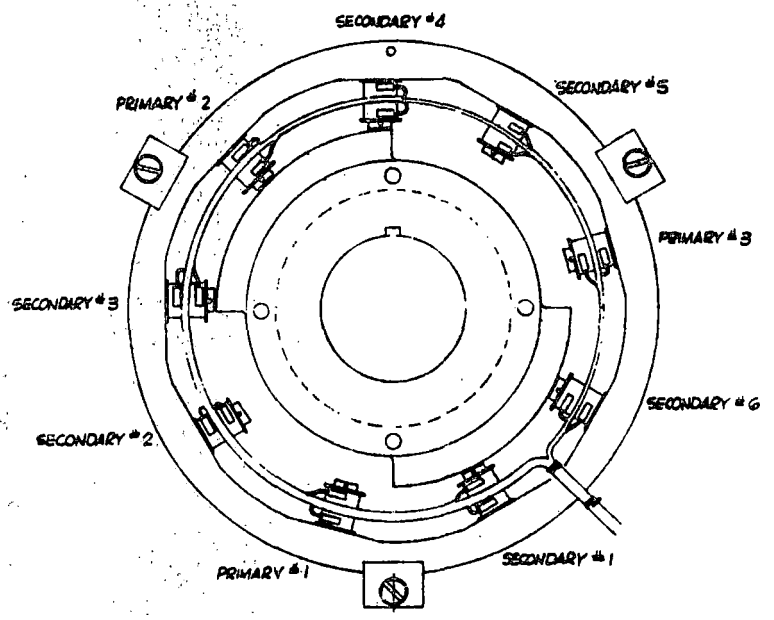

Figure 5.6-54. Rotor Position Sensor

5.6.15 DIAGNOSTICS UNIT

The diagnostics unit was inteded to be used during test and evaluation of the modified SOAC at the HSGTC, Pueblo, Colorado and during demonstrations on transit properties in various major U.S. cities.

5.6.15.1 Requirements

The ASDP diagnostics unit shall display status data, indicate the occurrence of a fault, display the location code of the fault, and provide sufficient historical data to reconstruct the cause of the malfunction.

5.6.15.2 Design Approach

The initial diagnostics concept consisted of a hard-wired monitor panel with buffered test points; analog meters with which to display particular outputs; and an array of selected fault indicators.

Once the decision was reached to design a microprocessor-based train controller, it became apparent that the initial diagnostics concept was lacking in many important areas. The microprocessor train controller opened an entirely new concept for diagnostics. It now became feasible for the diagnostics unit to possess an "on board" solid state memory, a capability the hard-wired concept did not have. The display capability would be expanded to include an LED digital word readout, Hex location and data readout, and an alpha-numeric printer for hard copy. Isolation of a QSD producing signal would be accomplished by freezing the "on board" memory at QSD and displaying the location code of the QSD source.

This alternative approach allowed all signals and intermediate solutions, within the Train Control, to be candidates for recording or display. The hard-wired system only provided for display of the signals previously wired into the panel. The microprocessor designed diagnostics unit provided for a TCE Self-Test and Preoperational Checkout. The hard-wired system provided only limited discrete information.

For all these reasons, the microprocessor approach was considered vastly superior to the hard-wired approach and was therefore selected for implementation.

Several different microprocessor concepts were proposed before a final selection was made. Basically these involved systems with 8000 and 16,000 bytes of data storage and a system incorporating an endless loop digital tape recorder. The primary concern involved the length of real time for which data would be recorded. The system that was decided on had 14,336 8-bit bytes of data storage. This allowed for 14 seconds of storage for the fast varying parameters, such as currents and voltages, and 30 minutes of storage for slowly varying parameters such as temperature and pressure. A QSD signal would allow data to continue to be recorded for 7 seconds. Therefore, data memory would contain 7 seconds of data before the fault occurred and 7 seconds after the fault.

The 14,336 bytes of data storage was divided into 256 cells of 56 bytes. Each cell would contain TCE1 and TCE2 data. The memory locations would be written into, in order, zero through 14,335, and then be written over again. Each 28-byte cell would contain fast varying parameters in as many of the lower locations as required and these locations would be written into on every cell, every cycle. The high order locations would be written into on a one cell per cycle basis until all were filled. At that point a refresh would begin and the old data would be written over. Therefore, the slowly varying parameters would be recorded for a period 256 times the loop cycle time of the memory, or approximately 30 minutes.

Safety requirements of the train control demanded that the diagnostics be noninteracting; i.e., the diagnostics must, under no condition, interfere with train control. An explanation of the manner in which this interface is mechanized can be found in paragraph 5.6.15.6.

5.6.15.3 Diagnostics Operating Concept

During operation the diagnostic system displays and stores data. The operator selects the data to be displayed, and also selects the data to be stored. Several standard data storage lists are available. Typical lists are shown in Table 5.6-XII. Up to 256 locations are available which can be included in each of the standard lists, and three standard lists

	A	B	C
1.	Motor Current	P Signal P20	Prop Trip
2.	Motor Voltage	P Signal LSB	Overcurrent
3.	Line Voltage	P Signal MSB	Diff Current
4.	Filtered Voltage	Drive Mode T/L	Cool Particle Elect
5.	Line Current	Line Amps (Braking)	Cool Particle Motor
6.	Overcurrent	Line Amps (Motoring)	Motor Ø Loss
7.	Diff Overcurrent	S/S Indication	Inverter Ø Loss
8.	Motor Temp	Elec Brk Effort	Cyclo Fault
9.	Cycle Cool Temp	Brk Rate Cmd	Inverter Fault
10.	Inverter Cool Temp	Slide Auth	Prop Trip T/L
11.	Motor Cool Temp	Friction Brk On	Loss Field Current
12.	Motor Cool Press	Parking Brk off	QSD Discretes
13.	MCE Cool Press	Reg Enable	Emergency
14.	P-Signal	Wheel Speed	For T/L
15.	QSD	VCO Feedback	Rev. T/L
16.	Prop Trip	Rotor Position Sensor	Control Station
17.	Low Voltage	Time LSB	Prop Reset
18.	Truck Weight	Time MSB	MA Ready
19.	-	Truck Weight	Sw. Gear Cover
20.	-	No Motion	Contractor Closed
21.	-	-	Drive Mode T/L
22.	-	-	No Motion
23.	-	-	For/Rev Verify
24.	-	-	Cap Fuse

Table 5.6-XII. Standard Monitor Lists

are planned. If no operator selection is made, a "default" list is used. If the operator desires, he can change any of the data lists to include any of the 256 parameters which are available. Appendix D contains the RAM memory location identification for all signals presently available for display. These may include either standard input, output data from the TCE, intermediate (calculated) data from train control calculations in the TCE, or data from the synchronous brake system.

The data which has been selected is stored in a solid-state memory. After the memory is filled, old data is sequentially replaced by new data. If a system malfunction is detected, or if the operator commands it, data is "frozen" in memory. This data can then be played back to help determine the cause of the malfunction. Data may be played back from the memory at any time by sacrificing recording or it may be played back in real time while recording is in process. The printer can be used to provide a hard copy of data. Two analog meters may be used to display information, and digital data can also be read out on two data displays. Indicators are provided on the front panel of the diagnostics unit to display crucial operational status data. In addition, two test jacks are located on the front panel (paralleling data on the panel meters) so that external meters, scopes, recorders or other instrumentation can be used to monitor selected data if desired.

Another desirable feature of the diagnostic equipment is that it provides a preoperational test capability. The status of critical system parameters (voltages, temperatures, pressures, currents, or other crucial information) can be automatically checked for satisfactory condition and a permanent record printed out. In addition, test signals can be displayed on the indicators and meters to check their proper operation. The printer is also tested, and provides a hard copy of desired check-out information (this could include system gains, operating conditions, or any other selected data.

A keyboard is available on the front panel to allow the operator to control the system. The keyboard is used to select data for display and may also be used to select data for storage in the main memory. The keyboard can also be used to change data baud rate. If red, the operator can use the keyboard to "freeze" data in memory and play it back for analysis.

5.6.15.4 Diagnostics Design Concept

5.6.15.4.1 Equipment Concept

A front view of the diagnostics equipment is shown in Figure 5.6-55. Side and rear views are given in Figures 5.6-56 and 5.6-57.

Two analog meters are shown in the upper left section of the front panel. The signal which is being displayed on the left-hand meter is also available at test jack M1, located at the lower-right corner of the panel. Similarly, data on the right-hand analog meter is available at test jack M2. Immediately beneath the analog meters are two displays which provide a code indicating the signals which are being shown on the meters.

The location codes shown on the hex displays correspond to those listed on the code callup placard. A sample code callup placard is shown in Table 5.6-XIII. The entire signal list is included in Appendix A. As an example, if the scale code shown in the display were 10, the analog meter would be indicating the weight of the number one truck with full scale corresponding to 200,000 pounds.

Digital data displays are located near the left center portion of the diagnostics panel. The two left-hand digits indicate the display code of the data (as shown on the code callup placard). The four right-hand digits represent the data. Any data available on the code callup placard (up to 256 variables) can be displayed, and the digital displays can operate in real time or can display stored data.

The Display/Program Control keyboard allows the operator to control the diagnostics system. The keyboard has the hexidecimal characters zero through F and auxiliary keys for RESET, ENTER, RECORD, and CLEAR. The keyboard is utilized to call up data for displays, select data for main memory storage, modify RAM, and control the printer. The keyboard operations are summarized in Table 5.6-XIII.

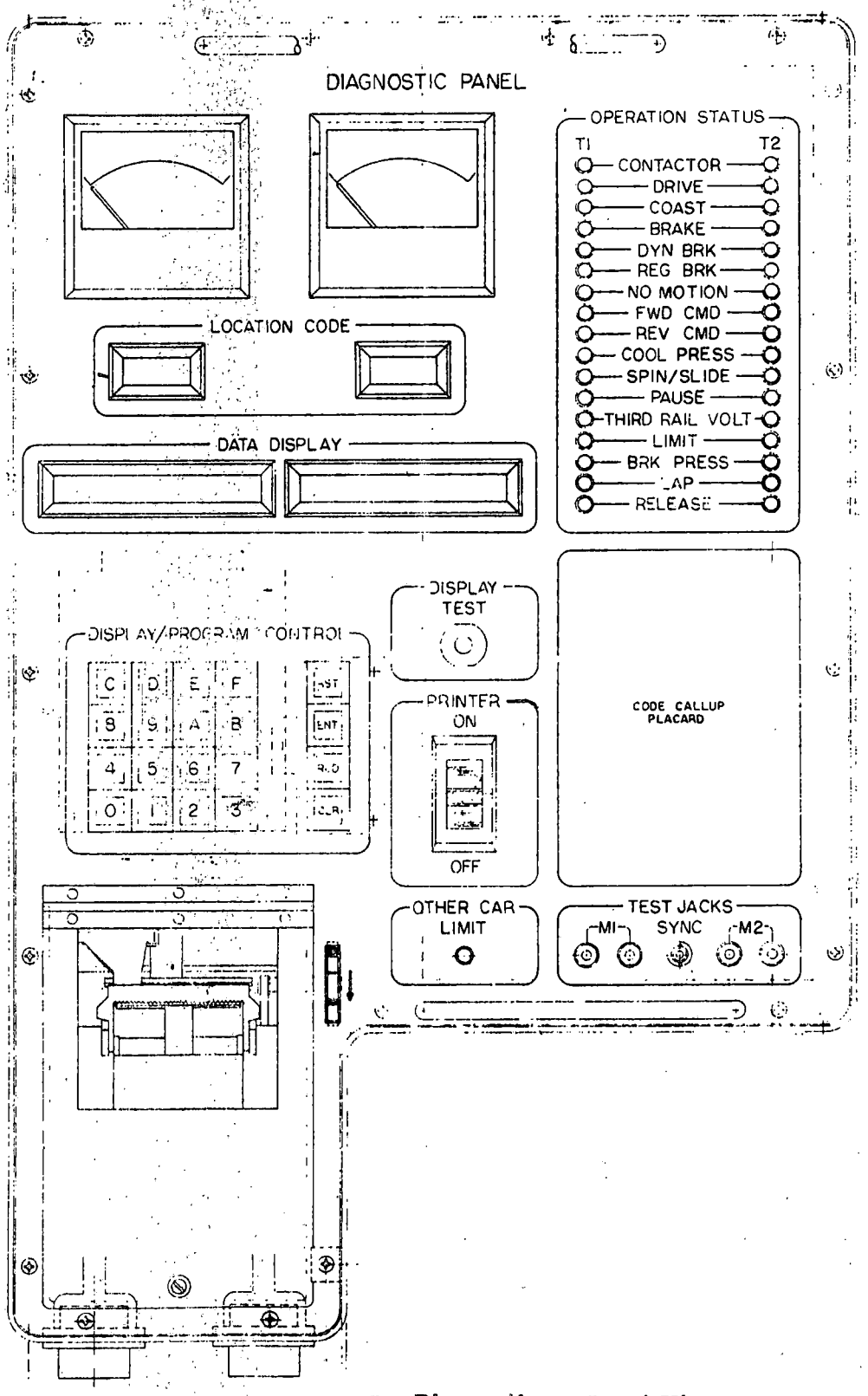

Figure 5.6-55. Diagnostics - Front View

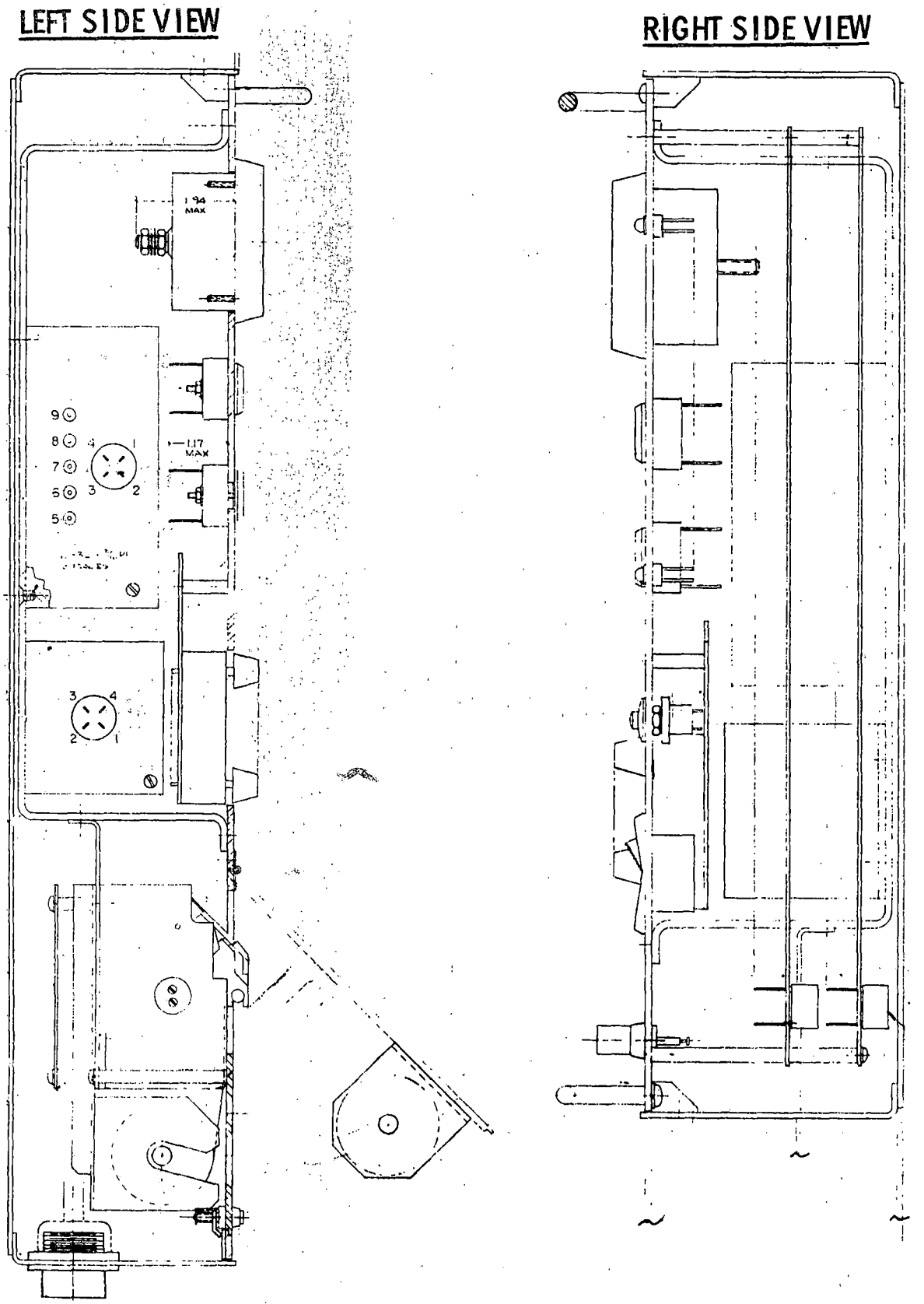

Figure 5.6-56. Diagnostics

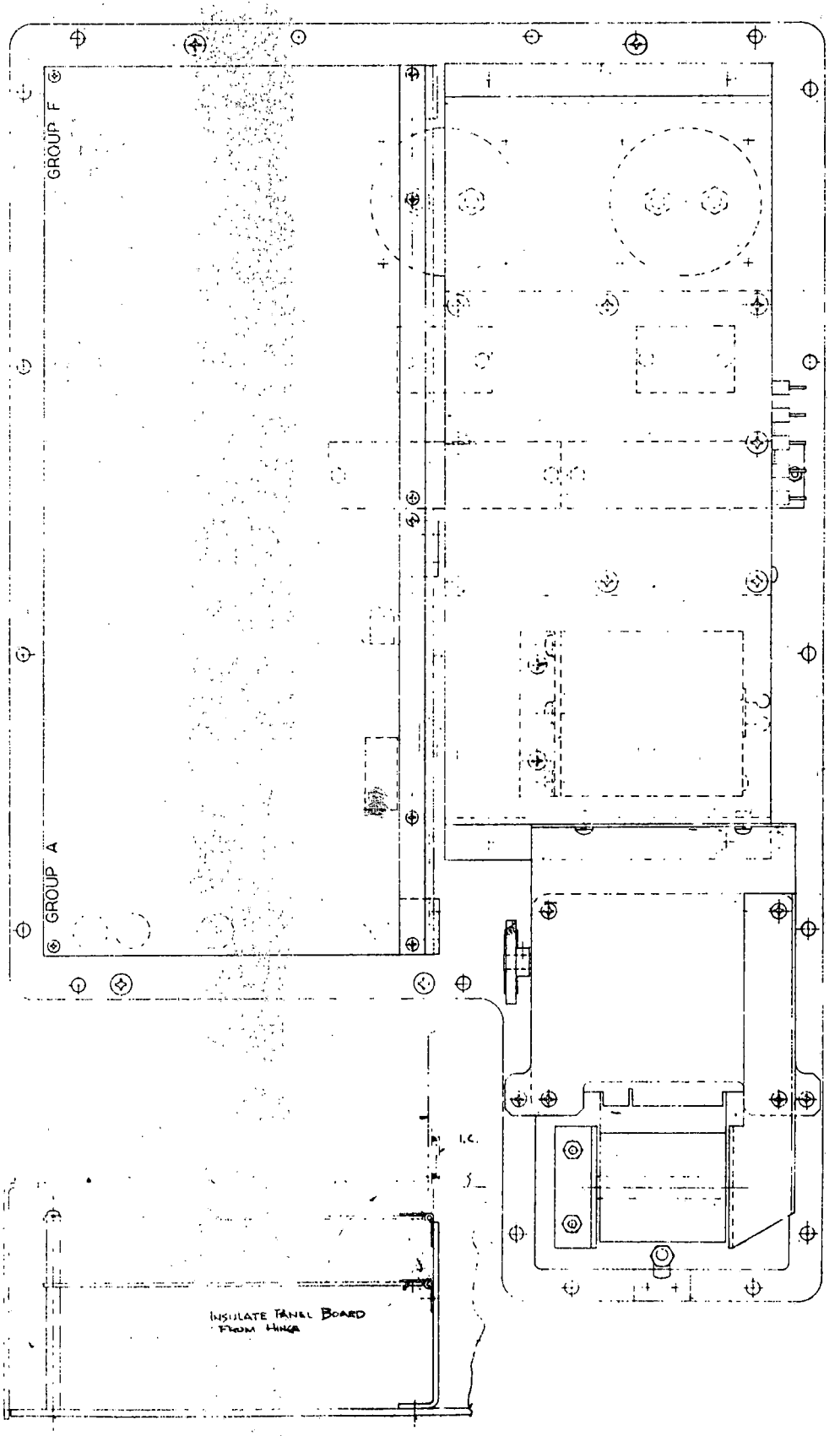

Figure 5.6-57. Diagnostics - Rear View

TCE1 LOC IDENT	TCE 2 LOC IDENT	TCE RAM LOC	SIGNAL	SCALE FACTOR (Full Scale)
10	90	2000	Truck Wt 1	200,000 pounds
11	91	2030	Truck Wt 2	200,000 pounds
12	92	2123	P-signal P_{20}	1.0 amp
13	93	2005	P-signal LSB P_{10}	100 mA
14	94	2006	P-signal MSB P_{10}	1.0 amps
15	95	200A	Wheel Dia (this truck)	50 inch
16	96	2153	Wheel speed (other)	100 mph
17	97	200E	GSE	–
18	98	2016	Time LSB	–
19	99	2017	Time MSB	–
1A	9A	2014	RPS LSB	–
1B	9B	2015	RPS MSB	–
1C	9C	2012	Wheel speed LSB	100 mph
1D	9D	2013	Wheel speed MSB	100 mph
1E	9E	2003	VCO Feedback (this)	10V
1F	9F	2033	VCO Feedback (other)	10V

Table 5.6-XIII. Code Callup Placard Example

As an example, if the operator wishes to display the number one truck's weight on the left-hand digital meter (Meter 3) he would use the keyboard to enter 3, 1, 0 and ENTER. These four keystrokes would be recognized by the diagnostics as indicated in Table 5.6-XIV. Similar operations are used to display information on any of the four meters.

Standard storage lists are also easily selected. For example, to select list A, the operator would use the kayboard to stroke in 5, A, A and ENTER. Similar actions by the operator allow the data storage list to be modified. If the operator decides to "freeze" the data, he does so by keying in F, C, C and ENTER . To return to data sampling, he "enables" the data storage using E, C, C and ENTER

Memory printout can be accomplished in several ways, as indicated in Table 5.6-XIV. For example, a sequence of memory can be printed; lists A, B, or C can be printed; and all memory or selected portions can be printed out after shut-down.

The diagnostics control panel also has a switch to turn the printer on or off, and an indicator labeled "other car limit." When illuminated, this indicates that the propulsion system on the other car is being limited due to low line voltage, or unsafe temperature or coolant pressure conditions.

Discrete operational status indicators are provided in the upper right section of the panel. There are two LED's for each status parameter, one for each truck of a car. All LED's are green except those for THIRD RAIL VOLT and LIMIT, which are red. These displays provide the following information:

CONTACTOR - is a discrete indication of the status of the main power contactor. When the LED is illuminated the contactor is closed.

DRIVE - is a discrete indication of the status of the microprocessor control. When the microprocessor is experiencing a drive propulsion command (and is responding properly) the DRIVE LED is illuminated.

COAST - is a discrete indication of the status of the microprocessor control. When the microprocessor is experiencing a coast propulsion command (and is responding properly) the COAST LED is illuminated.

FUNCTION						
METER 1	1	X	X	ENT	-	Displays the data whose location code is xx on Analog Meter 1
METER 2	2	X	X	ENT	-	Displays the data whose location code is XX on Analog Meter 2
METER 3	3	X	X	ENT	-	Displays the data whose location code is XX on Digital Meter 3
METER 4	4	X	X	ENT	-	Displays the data whose location code is XX on Digital Meter 4
STORE LIST A	5	A	A	ENT	-	Selects Standard list A for Storage in Main Memory
STORE LIST B	5	B	B	ENT	-	Selects standard list B for storage in Main Memory
STORE LIST C	5	C	C	ENT	-	Selects standard list C for storage in Main Memory
MODIFY LIST	5	E	E	ENT	-	Modify the selected list as shown by the following keystrokes
DATA LINE & LOCATION	X_3	X_2	X_1	X_0	ENT	X_3X_2= line of data list, X_1X_0= Data location code
	-	-	-	-	ENT	After last print out list modification ENT-ENT terminates command.
BAUD RATE	6	X_1	B	ENT	-	X_1Selects desired BAUD rate X_1 = 1, BR = 300; X_1=2, BR = 1200
ENABLE	E	C	C	ENT		Enable data sampling
FREEZE	F	C	C	ENT		Disable data sampling
PRINT MEM	7	1	X	ENT		Print out memory according to the following sequence
FROM/TO	X_7 X_6	X_5 X_4	X_3 X_2	X_1 X_0	ENT	Memory printed out from $X_7X_6X_5X_4$ to $X_3X_2X_1X_0$
PRINT LIST DATA	7	2	X			The present data corresponding to the selected list A, B, or C is printed out
PRINT MEM AFTER SHUTDOWN	7	4	4	ENT		Print all memory after shutdown according to the following
FROM/TO	X_7 X_6	X_5 X_4	X_3 X_2	X_1 X_0	ENT	From memory location $X_7X_6X_5X_4$ to location $X_3X_2X_1X_0$
PRINT MEM AFTER SHUTDOWN	7	6	6	ENT		Print out selected data after shutdown according to the following
SELECT DATA	X_1	X_0	ENT			Data to be printed
			ENT			After print data is selected a double enter, "ENT,ENT" stops sequence.

Table 5.6-XIV. Keyboard Operations

BRAKE - is a discrete indication of the status of the microprocessor. When the microprocessor is experiencing a brake propulsion command (and is responding properly) the BRAKE LED is illuminated.

DYN BRK - is a discrete indication that dynamic braking is occurring. During the time that the microprocessor is providing the motor control electronics (MCE) with a dynamic brake select command the DYN BRK LED shall be illuminated.

REG BRK - is a discrete indication that regenerative braking is occurring. During the time that the microprocessor is providing the MCE with a regenerative brake select signal the REG BRK LED is illuminated.

NO MOTION - is a discrete indication that "zero speed" has been reached and the NO MOTION relay has pulled in. When this occurs the NO MOTION LED is illuminated.

FWD CMD - is a discrete indication that the microprocessor is providing the motor control electronics (MCE) with a forward motor command. During the time thst the forward command is being issued the FWD CMD LED shall be illuminated.

REV CMD - is a discrete indication that the microprocessor is providing the motor control electronics (MCE) with a reverse motor command. During the time the reverse motor command is being issued the REV CMD LED shall be illuminated.

COOL PRESS - is a discrete indication that both the electronics and motor coolant pressures are in a safe range. During the satisfactory pressure performance the COOL PRESS LED's shall be illuminated.

SPIN/SLIDE - is a discrete indication that a spin/slide condition exists and a correction is being performed. During the time that a correction is being made the SPIN/SLIDE LED is illuminated. The minimum on time for the LED is 0.5 seconds.

PAUSE - is a discrete indication that a particular command has been issued but the necessary response has not occurred (e.g., main contactor closure has been requested but has not yet occurred). The PAUSE LED will be illuminated during the time that PAUSE occurs.

BRK PRESS - is a discrete indication from the WABCO synchronous brake system to the diagnostics system which shows the status of the Brake Cylinder Pressure. The BRK PRESS LED is illuminated during the high pressure condition.

LAP - is a discrete indication from the WABCO SBS to the diagnostic system which shows the status of the wheel slip valve. The LAP LED is illuminated when the valve is energized.

RELEASE - is a discrete indication from the WABCO SBS to the diagnostics system which provides the status of the wheel slip valve. The RELEASE LED is illuminated when the wheel slip valve is energized.

THIRD RAIL VOLT - is a discrete indication of the status of the line voltage. The THIRD RAIL VOLT LED will be illuminated during the time that the line voltage is outside the normal range. Both LED's indicate the same THIRD RAIL VOLT, but operate from separate sensors on each truck.

LIMIT - is a discrete indication of the status of the microprocessor controller. The LIMIT LED will be illuminated during the time that the propulsion system's output is being limited due to low line voltage, temperature, pressure, etc.

5.6.15.4.2 Diagnostics Software Concept

The flow diagram for the main loop of the diagnostics program is shown in Figures 5.6-58 and 5.6-59. As can be seen, the main loop is relatively simple, with most of the detailed programming consisting of subroutines. Flow diagrams for the subroutines are presented in Appendix E. The diagnostics program coding which has been completed is given in Delco's Engineering Exhibit EE-75-S-377.

5.6.15.5 Diagnostic Hardware

The heart of the diagnostics unit is an Intel 8080 microprocessor. The microprocessor controls the operation of the printer, the keyboard, memory storage, playback and all displays. The system's design, layout, and wire wrap board for this portion of the circuitry, including program memory, is identical to the TCE CPU board. This includes the central processing unit, system controller, interrupt control, bus drivers, random

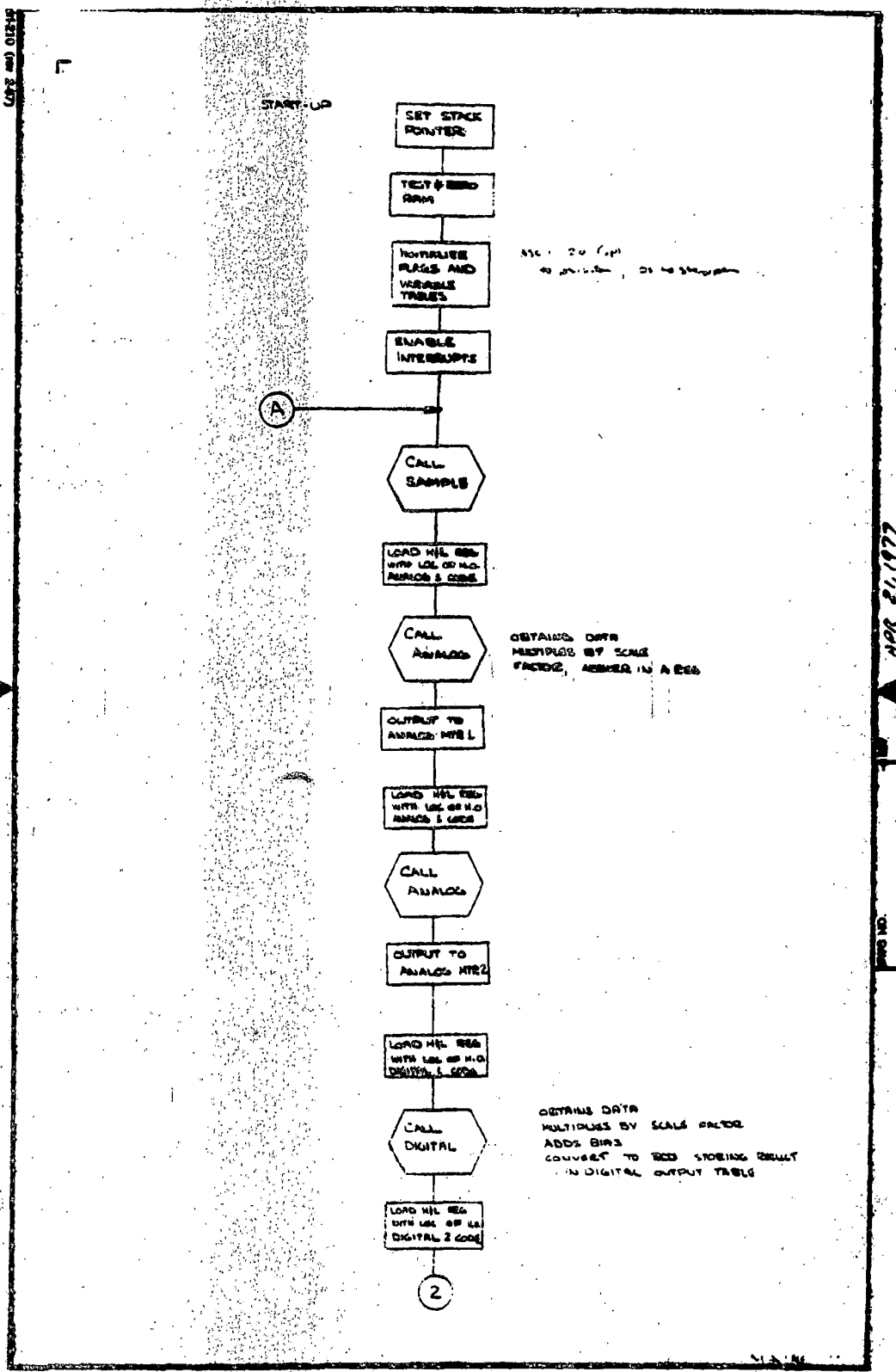

Figure 5.6-58. Main Loop

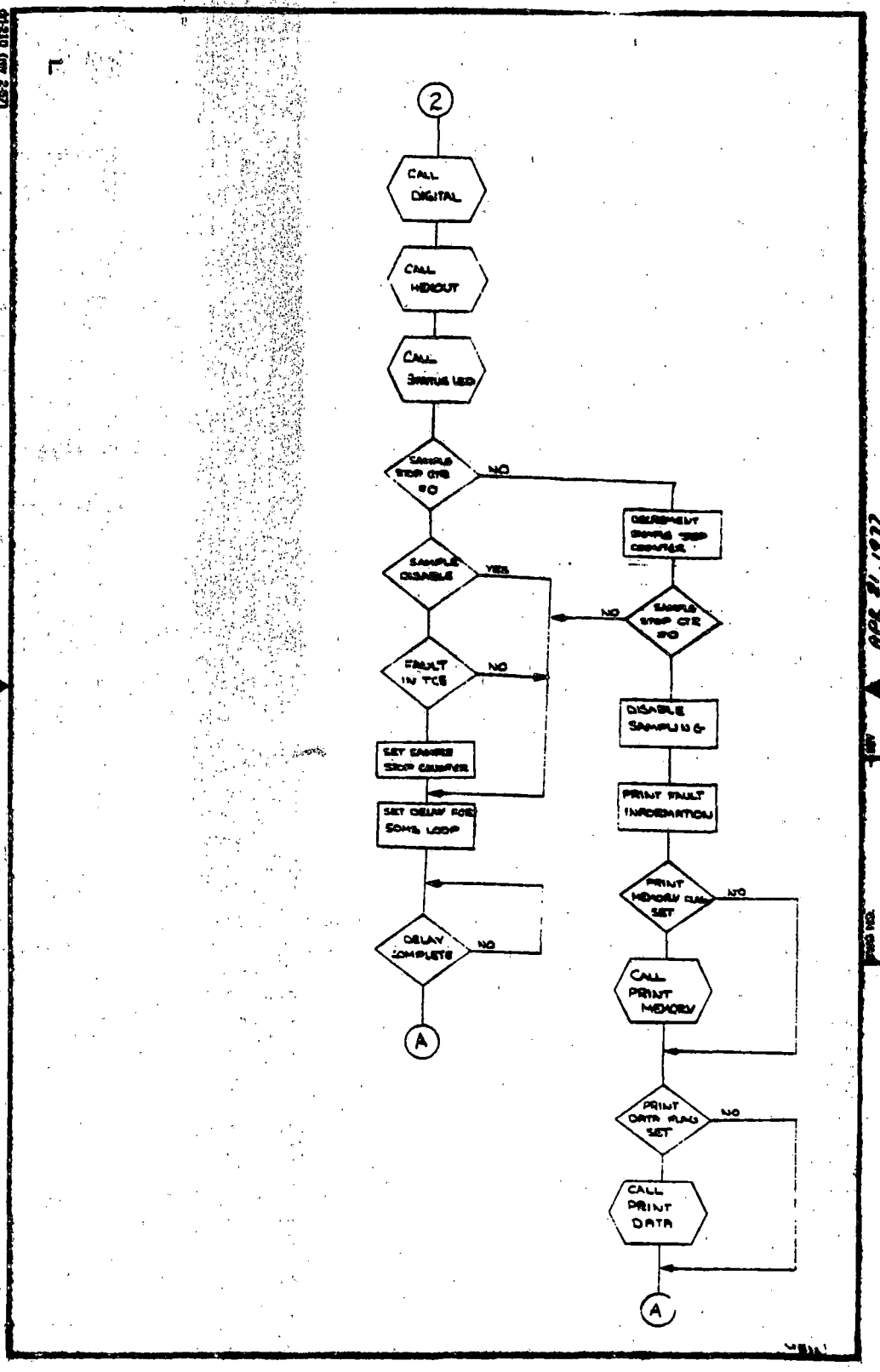

Figure 5.6-59. Main Loop

access, and Read Only Memory. The circuitry unique to the diagnostics is the operational status drivers (Display Drivers), analog circuitry, GSE control, and Read/Write control. Read/Write control is discussed in detail in 5.6.15.6. Wire lists for the diagnostic circuit boards are included in Delco specifications EE-75-S-378 and EE-75-S-379.

The operational status drivers (Figure 5.6-60) illuminate the required LED's on the display panel upon receipt of the necessary TCE or Wabco discrete information. Circuitry is provided to monitor a Limit train line so that a discrete indication is given if the other car goes into a shutdown or reduced power condition. The display panel is provided with a pushbutton which will initiate a software controlled preoperational test sequence.

When the push to test button is depressed the Operational Status LED's are illuminated from the lower LED's through the upper in a ripple fashion to test the operation of the circuitry and the LED's. Next, the data display and location code are set to zero and counted sequentially through to F. The analog meters are exercised by deflecting to 100%, then 50% and zero. The printer completes the test by recording a message and all displays are returned to their original condition.

The analog circuitry (Figure 5.6-61) consists of two digital to analog converters, two multiplexers and required filtering and buffering circuits. TCE data, stored in memory or read real time, may be selected through multiplexer and displayed on the panel meter. The other multiplexer channels are dedicated to the Synchronous Brake System analog signals. The system is designed to allow any two signals to be displayed on either meter or even the same signal displayed on both meters at the same time for comparison. The panel meters are equipped with parallel connected test points, which allows external connections to be made at the front panel for monitoring or recording purposes.

The drawing titled GSE Control (see Figure 5.6-62) illustrates an external communications link with the outside world. Baud rate control is keyboard selectable so that there is a capability of communicating with different types of externally connected equipment. The 8251 programmable communications interface provides serial in, serial out transforms. This USART is used as a peripheral device and is programmed by the CPU to operate using virtually any serial data transmission technique presently in use. The USART accepts data characters from the CPU in parallel format and then converts them

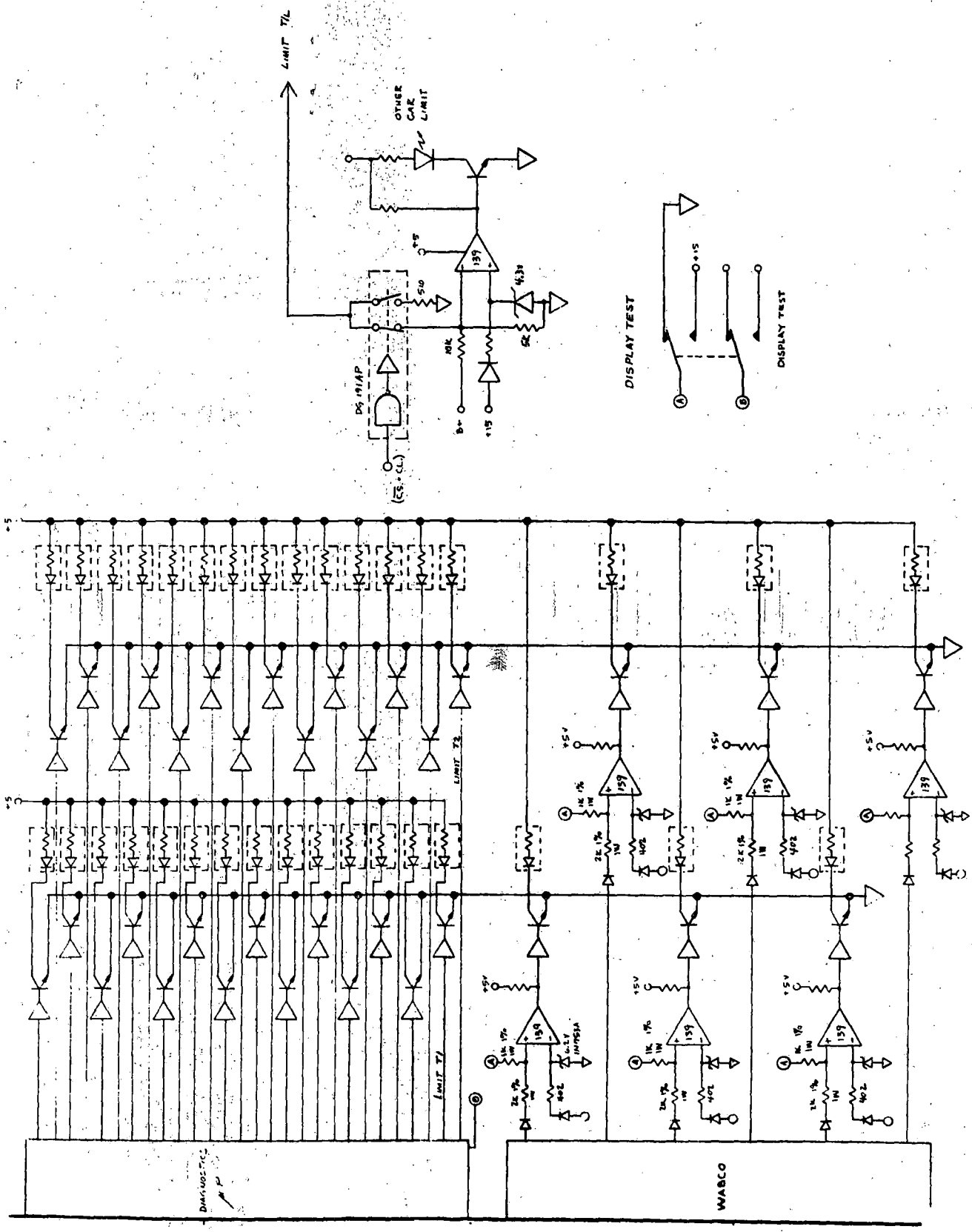

Figure 5.6-60. Diagnostics Operational Status

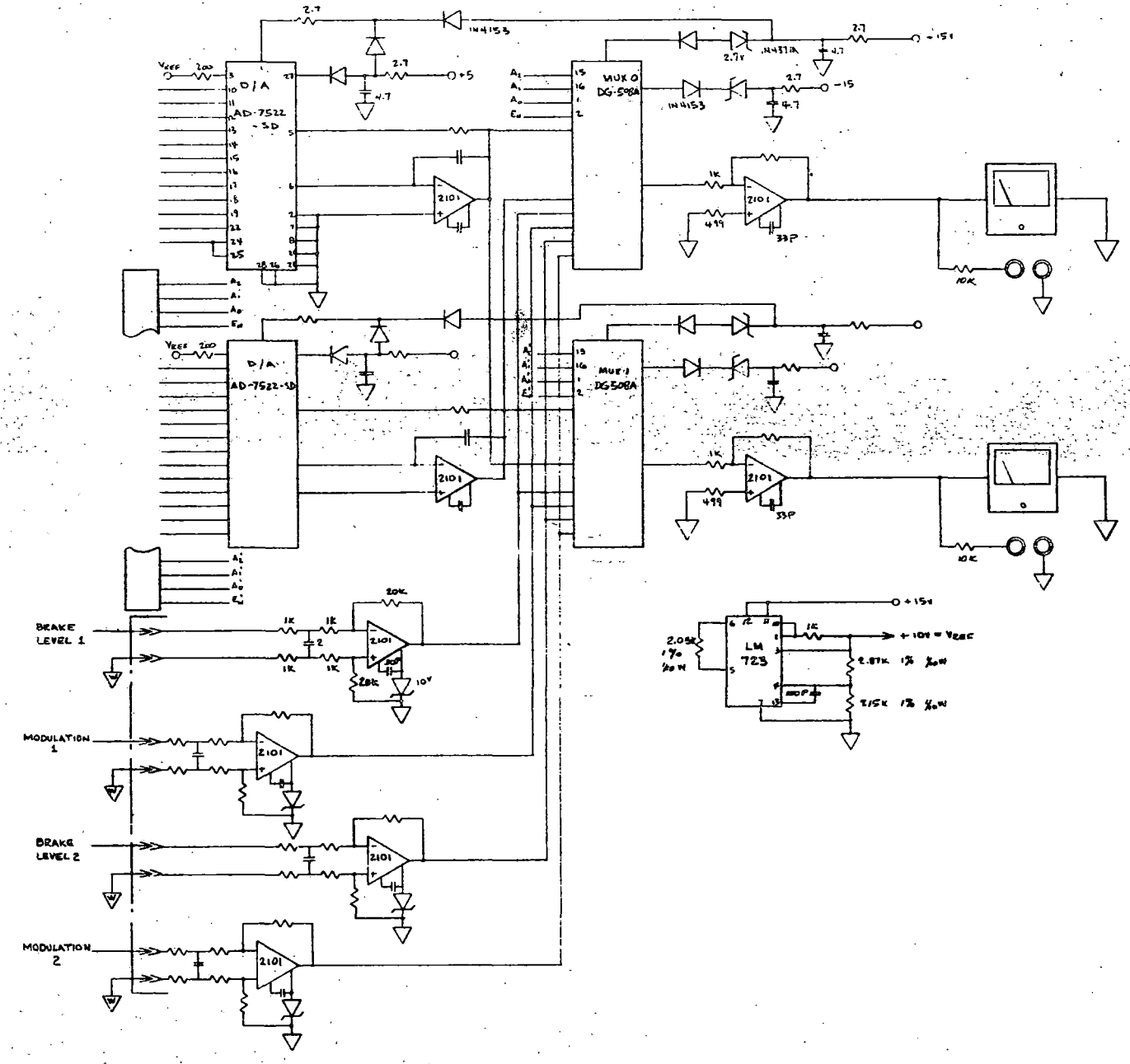

Figure 5.6-61. Diagnostic Analog Circuit

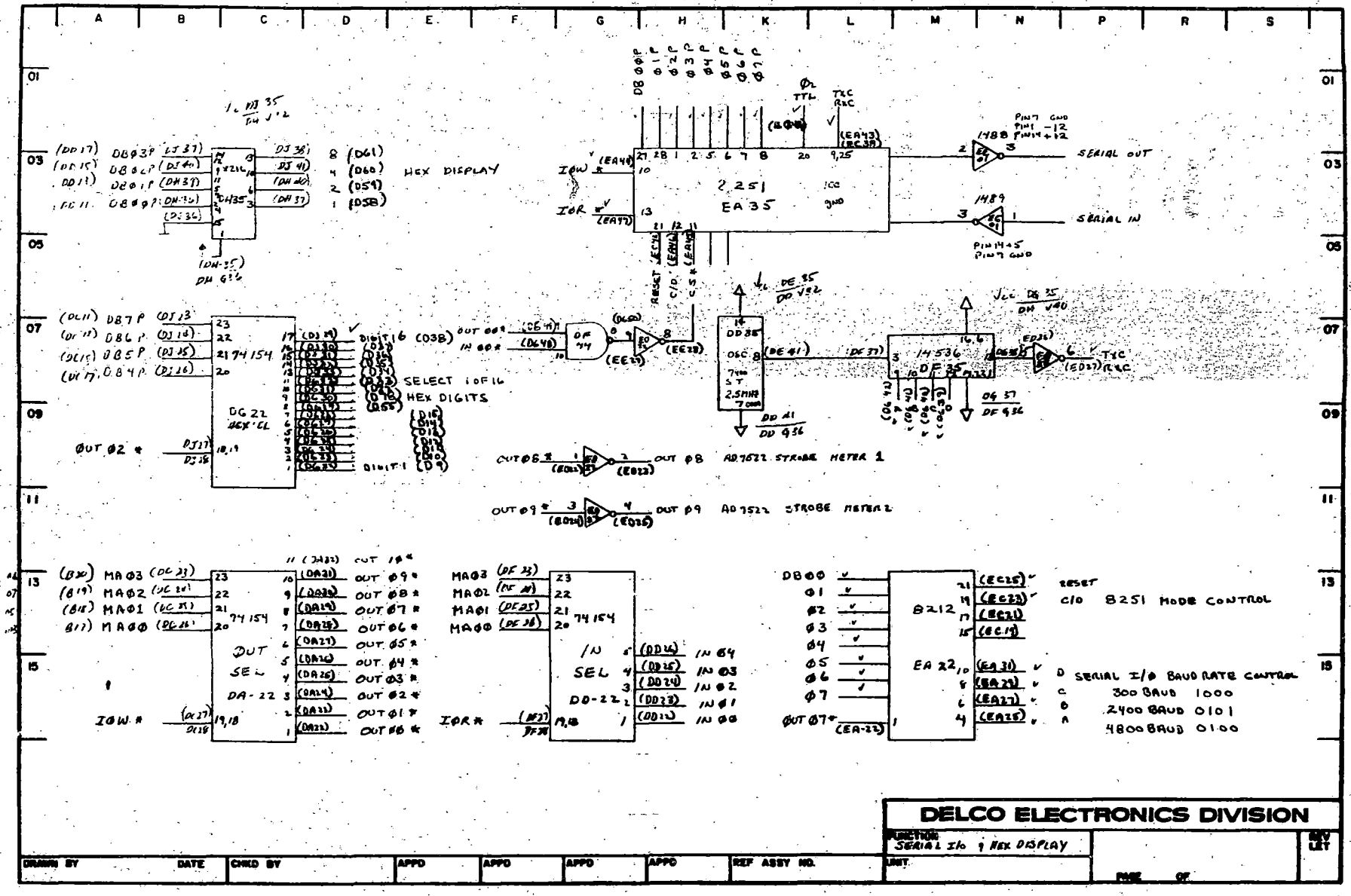

Figure 5.6-62. GSE Control

into a continuous serial data stream for transmission. Simultaneously, it can receive serial data streams and convert them into parallel data characters for the CPU. Thus, external instruments such as teletypes and digital tape recorders can be connected to this interface.

5.6.15.6 Diagnostics/TCE/SBS Interfaces

The system block diagram is shown in Figure 5.6-63. The diagnostics interfaces with both Train Controls (TCE 1 and TCE 2) on the car. The Train Control data bus and Address bus are sampled by the use of a reliable, high input impedance latch driver, as discussed below. The data and address information are then written into the RAM Buffer to provide a mirror image of the Train Control scratchpad memory. The Read/Write Controls, 1, and 2, allow this to occur. After the first Write Cycle, RAM Buffer data may be routed as desired to the display and storage devices. A standard data list (Table 5.6-) or modified list will be stored in data main memory. Data may be read out in real time or from data memory.

The diagnostics unit interfaces with the TCE, the TCE power supply and selected signals from the Wabco Synchronous Brake System (SBS). The Wabco signals do not exist within the TCE and are therefore brought separately into the Diagnostics. Six of the Wabco signals are discretes and four are analog. One set of signals is displayed for each track of the car. The analog signals, brake level and modulation, can be displayed on the analog meters and are selectable from the keyboard through a multiplexer. The status of the discrete signals, Brake Pressure, LAP and Release, are indicated on the display panel LED's.

TCE WRITE

During a TCE processor write, the address and data bus used by the 2k RAM memory is strobed into three octal latching drivers (74LS374) (Figure 5.6-64). This "one word" address and data memory is used to hold the address and data in case the address and ta bus for the "2k Buffer RAM" is being used for a read by the diagnostic processor. At the same time the data and address information is strobed into the 74LS374's a WRITE flip flop is set, indicating that a word of data is to be stored in the 2k Buffer RAM when the address and data bus is free. If the diagnostic processor is not using the address and data bus, BMEMR (Buffer Memory Read) will be low and the 74221 will be enabled.

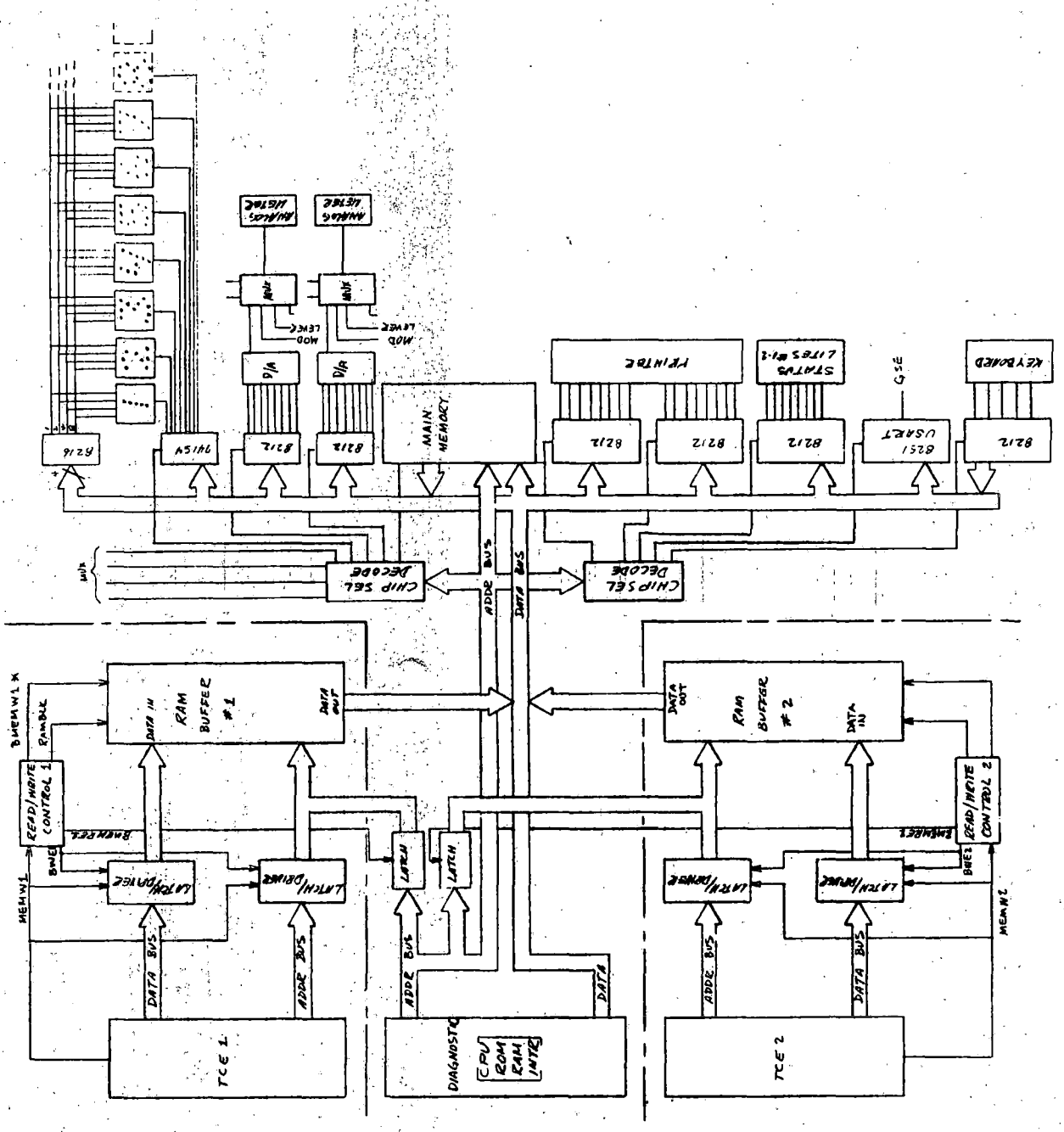

Figure 5.6-63. ASDP Diagnostics System Block Diagram

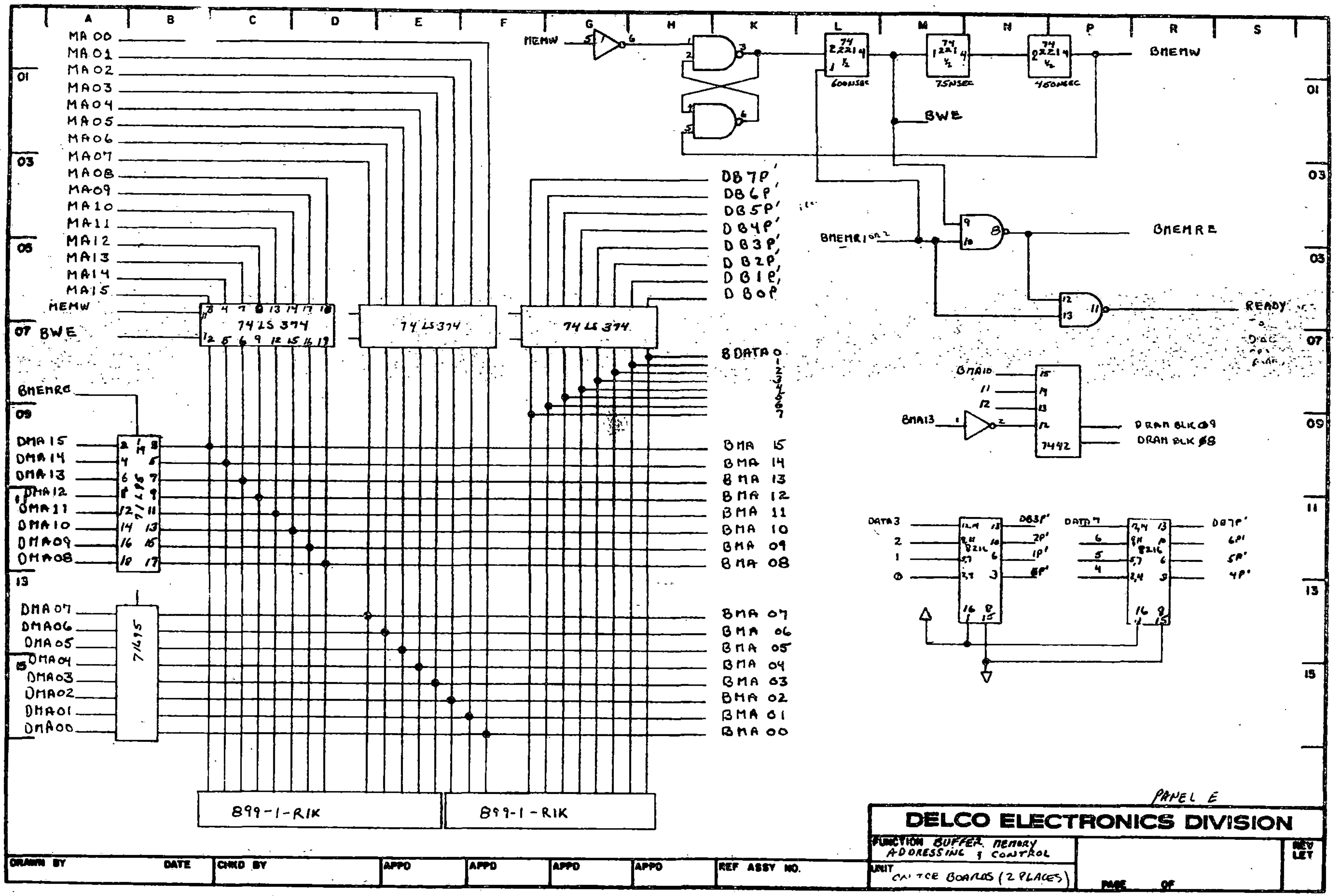

Figure 5.6-64. Read/Write Control

This allows starting of the write process whereby the output of the 74LS374's will be enabled and a write pulse generated by another 74221. The generation of this write pulse (Buffer Memory Write) (BMEMW) resets the WRITE flip flop. Upon completion of the write process the address and data bus will again be available for read operation by the diagnostic processor. At no time is the TCE processor aware of this write into the 2k Buffer RAM and therefore no slow-down or halting of the TCE processor is experienced.

If during a write by the TCE processor the diagnostic processor was in process of reading from the 2k RAM Buffer, and thus had control of the address bus (BMAOO-BMA15) (Buffered Memory Address), the first 74221 would not be enabled and the write process would not start until BMEMR goes low indicating the diagnostic processor has completed the read.

Diagnostic READ

When the diagnostic processor attempts to read from the 2k Buffer RAM, BMEMR will go high. If a write by the TCE is not in process the output of the write flip-flop will go low. This signal BMEMRE (buffer memory read enable) is used to enable the diagnostic processor's address bus onto the buffer memory address bus. If a write by the TCE were in progress the "READY" line will go low and cause the diagnostic processor to enter a void state.

Power Supplies

The diagnostic unit shares the +12 Vdc and ±15 Vdc train control power supplies (see Figure 5.6-65). They are connected in a diode OR'd configuration to assure continued operation of the diagnostics in the event of a power supply failure. These supplies are also resistor isolated from the diagnostics to prevent train control disruption in the event of a diagnostics fault. The shared +12 Vdc and ±15 Vdc are low current, well regulated supplies and can easily accommodate the addition of the diagnostics. The +15 Vdc and +5 Vdc are required within the diagnostics to supply power to the thermal printer and the diagnostics memory. The high current pulsed load of the printer could not be coupled with the highly regulated low bias current +15 Vdc supply. Similarly, the +5 Vdc diagnostics memory current was beyond the capability of the existing +5 Vdc TCE supply. Therefore +15 Vdc and +5 Vdc power supplies are incorporated within the diagnostic enclosure.

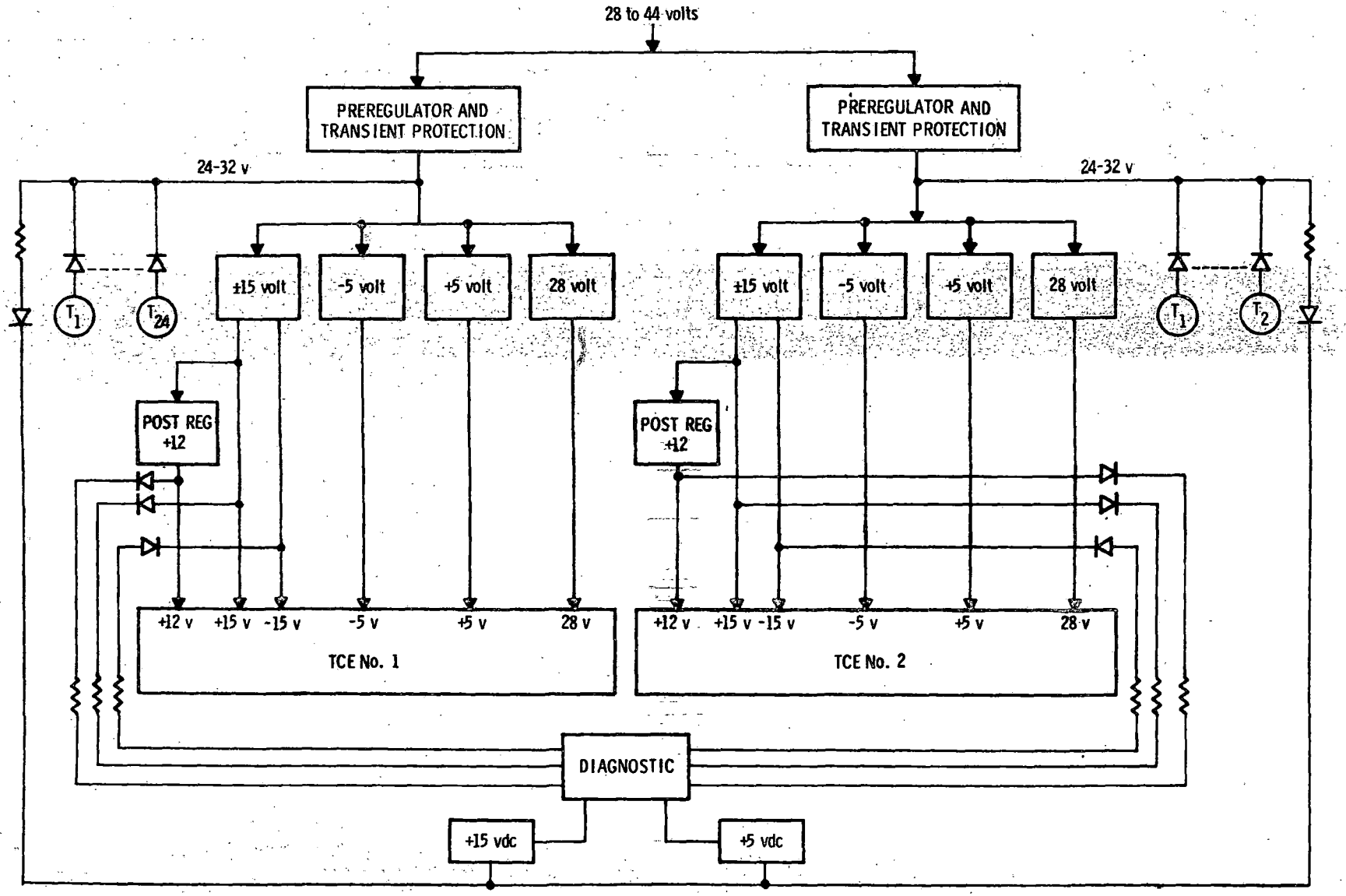

Figure 5.6-65. Train Control Electronics Power Supply System

Alternate Applications

The diagnostics unit is actually a "stand alone" system. It has its own CPU, ROM, RAM and I/O. It could therefore be programmed to perform many alternate tasks. One such task that has previously been considered is that of monitoring acceptance tests. Since wheel speed pulses are present within the TCE, both time averaged velocity and acceleration could be monitored, stored and displayed and a hard copy printed out.

In this way all of the time, speed and distance profiles could be very accurately measured and recorded. The same is true for plots of motor current, voltage torque, line voltage, etc.

5.6.15.7 Final Status of Diagnostics System Unit (or Equipment)

The documentation and software for the diagnostics system were well advanced when further effort was halted. The status is summarized below:

Documentation/Software	Percentage Completed
Design Specification	95
System Flow Diagram	95
Program Main Loop	100
Program Subroutines	75

The diagnostic hardware fabrication was nearing completion but check-out was still to be done. Table 5.6-XV summarizes the hardware status.

5.6.16 EQUIPMENT SIZE AND WEIGHT SUMMARY

The sizes and weights of the ASDP propulsion system components are shown in Table 4.5-XVI. Also shown are the quantity per car of each component and the Delco Electronics envelope drawing number applicable to each item.

The equipment is grouped according to its mounting location on the railcar: truck, undercarbody, or cab.

ITEM	DIAGNOSTICS CPU BOARD	DIAGNOSTICS RAM BOARD	TCE CPU BOARD (DIAGNOSTICS ADD ON)	DISPLAY
Design Concept	Complete	Complete	Complete	Complete
Circuit Design	100%	Complete	Complete	90% Complete
Board Layout	100%	Complete	Complete	100% Complete
Wire List	Complete	Complete	Complete	-
Punched Cards	Complete	Complete	Complete	-
Parts Procurement	Complete	Complete	Complete	98% Complete
Components Received	Complete	Complete	Complete	98% Complete
Board Fabrication	In Process	In Process	Complete	N. S.
Board Checkout	N. S.	N. S.	Complete	N. S.

N. S. - Not Started

Table 5.6-XV. Diagnostic Hardware

ITEM	DESCRIPTION	QTY/ CAR	ENVELOPE DRAWING NO.	APPROXIMATE SIZE (L × W × H) (inches)	WT (WET) - lb	
					UNIT WT	TOTAL WT/CAR
1	Traction Motor	2	7558253	48 × 22 × 21.2	1905	3810
2	Gear Drive and Axle Couplings	4	7557706	37 × 27.2 × 24	1093	4372
3	Motor/Gearbox Coupling	4	7557740	7.75 dia × 10.2	32	128
4	Ground Brush and Speed Sensor Assembly	8	7557738	6.3 dia × 5.1	10	80
	Sub Total Truck Mounted					8390
5	Truck Connector Box	2	7559843	17.6 × 11.2 × 5.3	50	100
6	Power Converter Assy	2	7559837	78 × 24.3 × 21.3	910	1820
7	Resonating Inductor Module	2	7559835	30.1 × 22.6 × 19.6	675	1350
8	Cooling Assembly	2	7557707	45.7 × 41.0 × 26.5	645	1290
9	Power Control Switchgear	2	7559867	41.1 × 24 × 18.1	230	460
10	Line Filter Inductor	1	7559836	19.6 × 25.9 × 14.6	775	775
11	Dynamic Brake Resistor	2	7557708	49 × 20 × 10	265	530
	Sub Total Car Mounted					6325
12	Electronic Control Unit	1	7557736	46 × 13.5 × 29.8	85	85
13	Diagnostic Panel Assy	1	N/A	15 × 4.5 × 23.5	15	15
	Sub Total Cab Mounted					100
	Total Propulsion System					14,815

Table 5.6-XVI. Propulsion System Weight and Size Summary

5.7 EQUIPMENT INTERFACES

5.7.1 EQUIPMENT LOCATION

The locations of the propulsion system equipment on the modified SOAC railcar are shown in a general manner in the artist sketch of Figure 5.7-1. Components for one system are annotated. Under-carbody components of the second propulsion system are mounted in reverse orientation from the first. Detailed location information for the under-carbody components, such as station numbers and specific mounting locations, can be found in Figure 5.7-2 (Delco drawing 7557973). The truck-mounted equipment is shown in Figures 5.7-3 and 5.7-4.

5.7.2 MECHANICAL INTERFACES

5.7.2.1 Under-Carbody Equipment

All under-carbody mounted components were designed to be shock mounted in accordance with Figure 5.7-5 except the dynamic brake resistor assembly and the truck connector box which were to be hard-mounted to the car. These were designed to bolt directly to support plates which are welded to the car frame.

5.7.2.2 Truck Equipment

In this design, a single traction motor drives each axle of the truck (Figures 5.7-3 and 5.7-4) through a gear drive and axle coupling assembly. The geardrives are bolted directly to the motor flanges and motor torque is transmitted to the pinion through a gear coupling. Gear drive output torque is then transmitted to the axle through a flexible coupling which permits some axle movement. The entire motor-gear drive-coupling assembly is mounted to the truck frame.

A ground brush is bolted to the bearing cover at both ends of each axle. The spring loaded brush rides on a brass disc mounted on the end of the axle (see Figure 5.6-53).

.3 ELECTRICAL INTERFACES

All interface wiring falls into one of three categories:

- Power (600 Vdc and 230 V, 3Ø, 60 Hz)
- Low Voltage (32 Vdc)
- Signal.

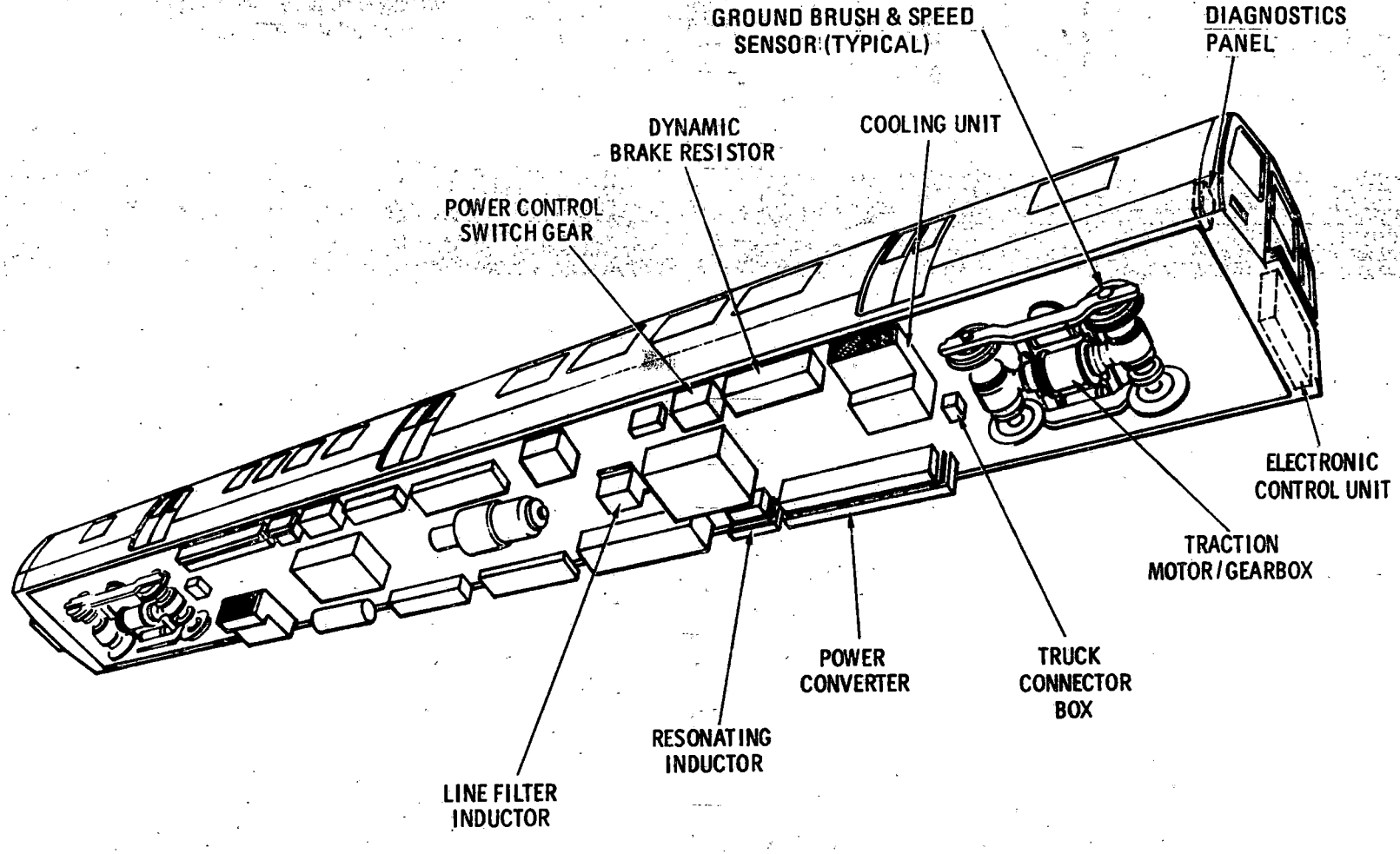

Figure 5.7-1. Propulsion Equipment Location

NOTES:

1. EACH ASSEMBLY SHOWING AN ASTERISK (*) HAVE A 4/0 GROUND STRAP FROM THE METAL OF THE ASSEMBLY TO THE CAR BODY.

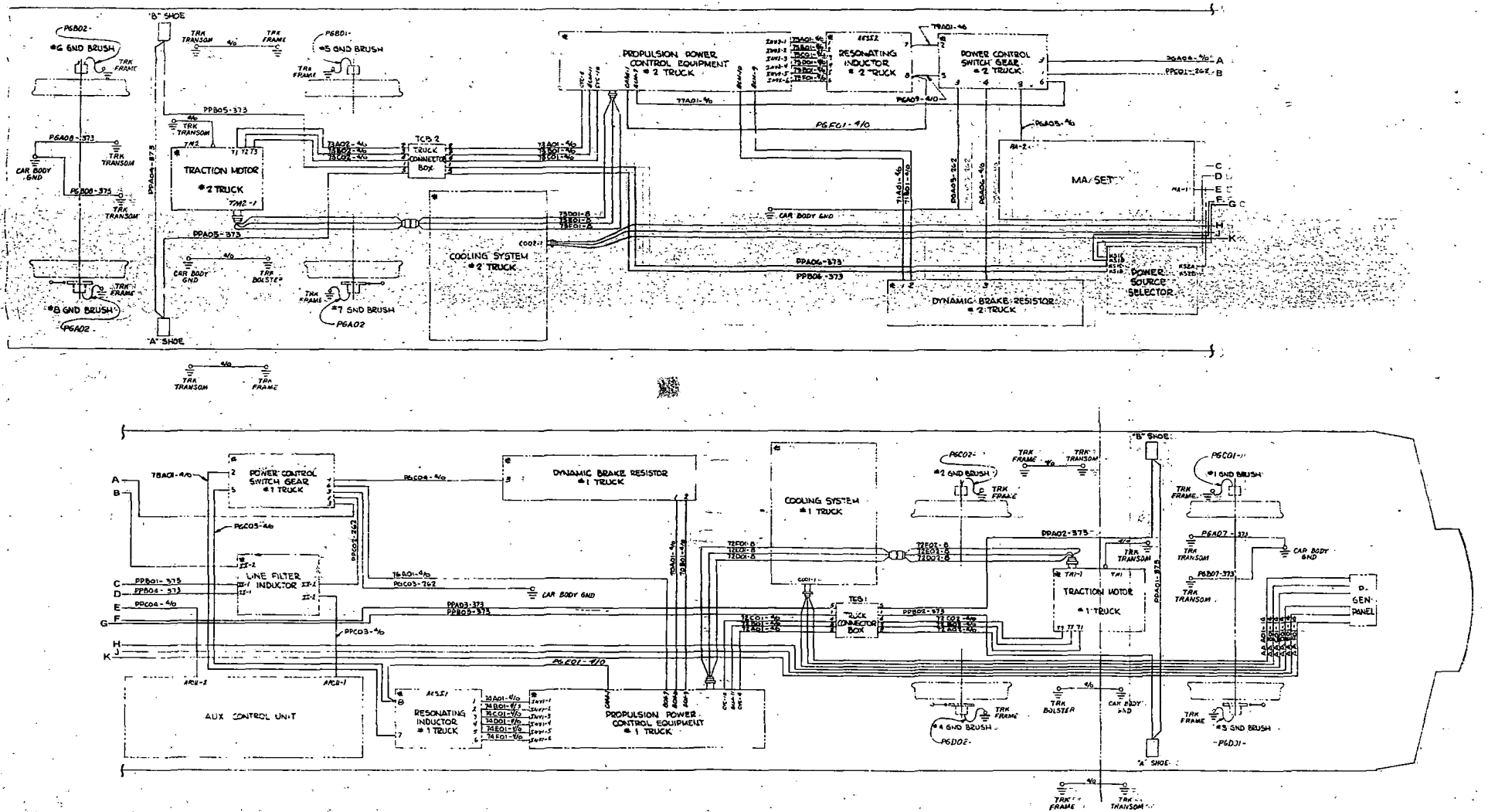

Figure 5.7-2. Car Equipment Location

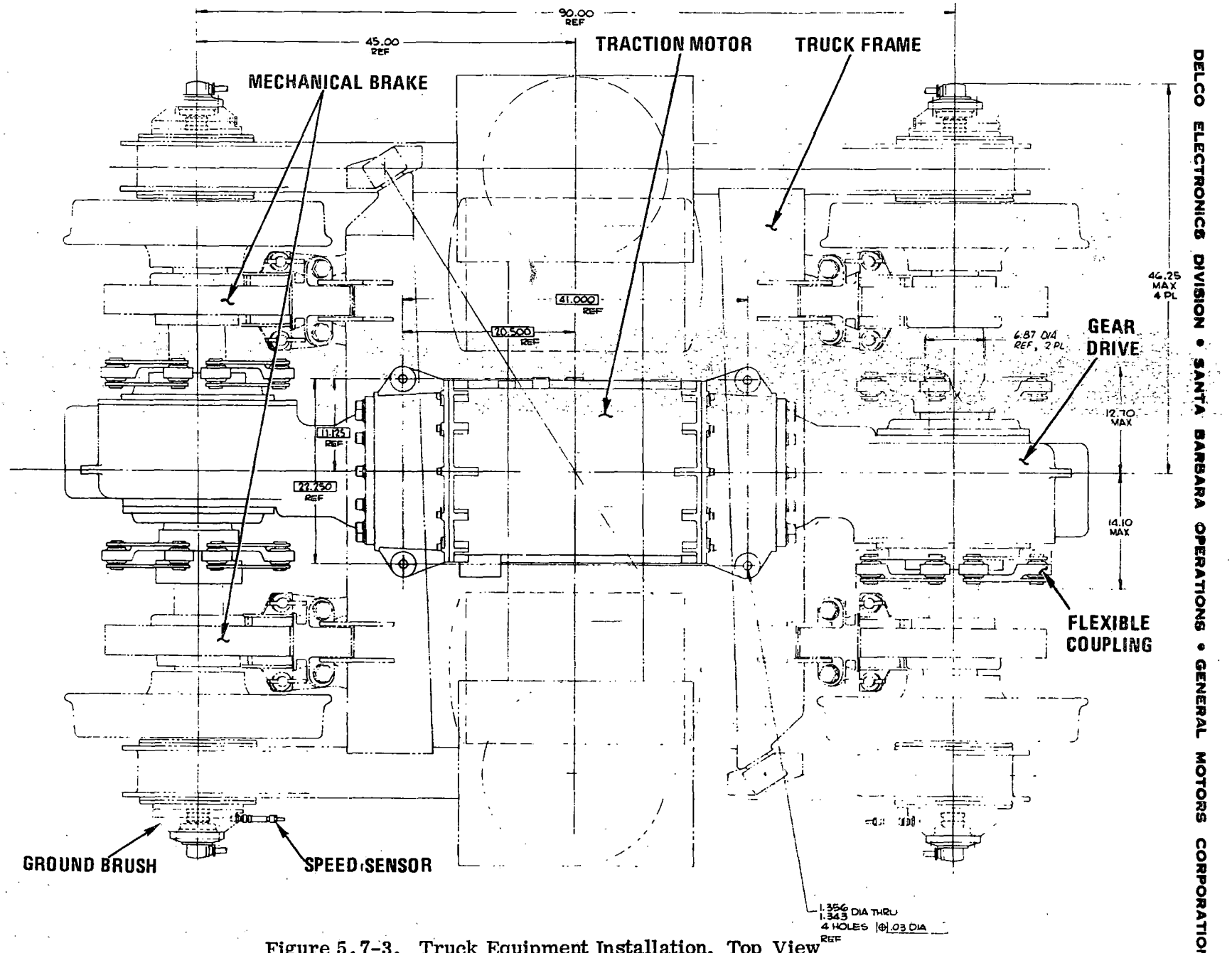

Figure 5.7-3. Truck Equipment Installation, Top View

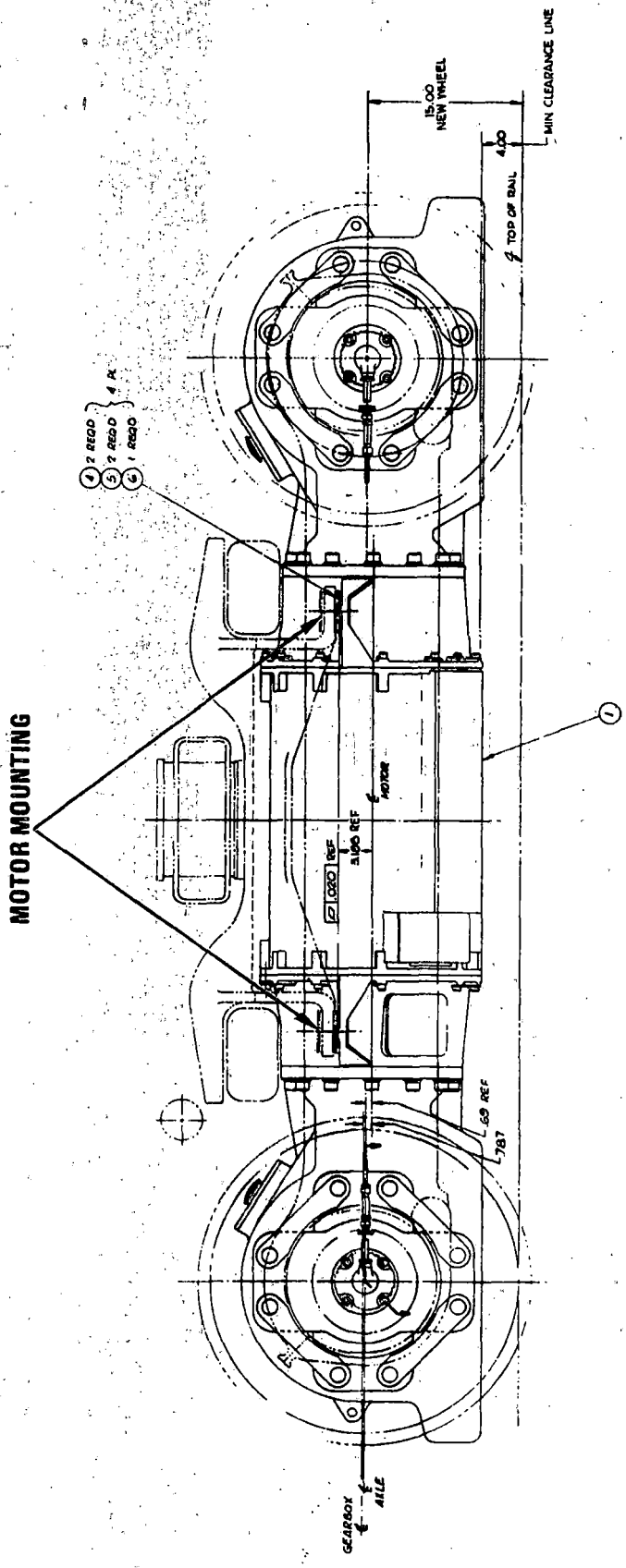

Figure 5.7-4. Truck Equipment Installation, Side View

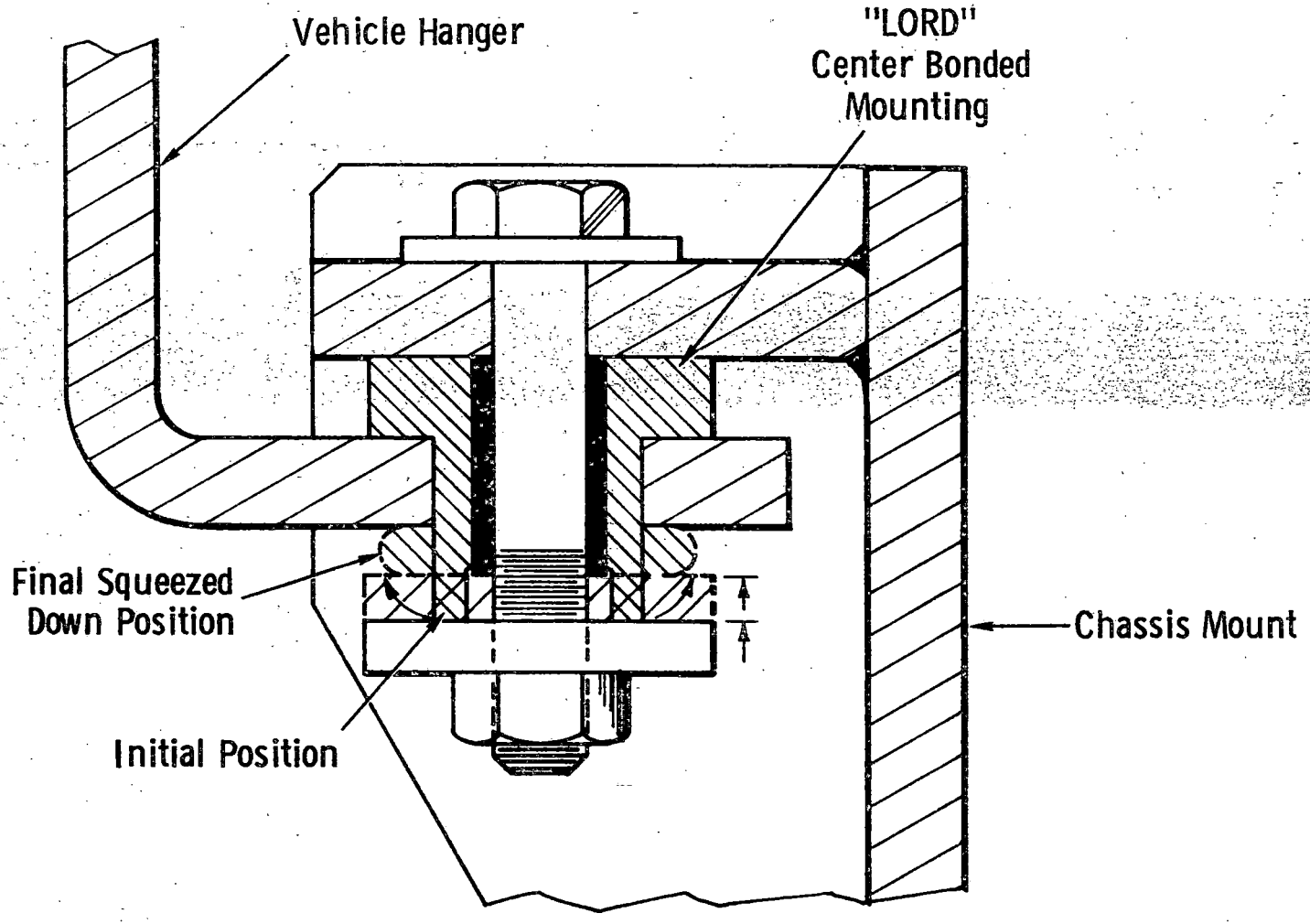

Figure 5.7-5. Typical Shock Mount Installation

The controlling document for all propulsion system wiring is a computerized wire list (Delco drawing 7557720). It identifies each wire separately, even if part of a cable assembly.

It contains the following types of information:

- Abbreviations used for connector/terminals (labels or connectors and boxes).
- Abbreviations used for wire circuits (labels on wires/cables).
- A list of all terminals for crimping on cables, with an identifying symbol, description, wire size, stud size, and vendor part numbers (usually more than one source for each terminal)
- A breakdown of a terminal on a subassembly, such as the power control switchgear, giving all connector pins and the use of each pin in that connector.
- A complete list of all box-to-box and box-to-car wiring, including gage, voltage, estimated length, beginning and ending terminal and connector identification, plus a word description function of the wire.

An example of the wire list (for low voltage wiring) is shown in Table 5.7-I.

Box-to-box and box-to-car power wiring is shown in Figure 5.7-6 (Delco drawing 7558575). Low voltage wiring (box-to-box) is shown in Figure 5.7-7 (Delco drawing 7558949).

Cable/Connector interfaces can be found on drawing 7559876 while detailed interfaces between train control electronics (TCE) and the rest of the ASDP propulsion system (including the synchronous friction brake system) are contained in the following Delco Electronics specifications:

EE-75-S-295	TCE Input/Output Interface
EE-75-S-296	TCE Motor and Motor Control Interface
EE-75-S-330	ASDP Diagnostics System

WIRE NUMBER	VOLTAGE LEVEL	ESTIMATED LENGTH,FT.	FROM BOX/ CONNECTOR/ TERMINAL	WIRE TERMINAL TYPE	TO BOX/ CONNECTOR/ TERMINAL	WIRE TERMINAL TYPE	FUNCTION	
26MC1-14	LV DC	70.	PECU-8	161M	C00L2-5	157D	+24 VOLTS DC	
26NC1-16	LV DC	70.	PECU-8	161N	C00L2-5	157C	POWER RETURN	
26PC1-14	LV DC	70.	PECU-8	161P	C00L2-5	157A	+ SIGNAL FOR PSL21	
26RC1-16	LV DC	70.	PECU-8	161R	C00L2-5	157B	SIGNAL RETURN	
26SC1-14	LV DC	70.	PECU-8	161S	C00L2-5	157E	SHIELD FOR D & C	
26TC1-16	LV DC	70.	PECU-8	161T	C00L2-5	157F	SHIELD FOR A & B	
26UC1-14	LV DC	70.	PECU-8	161U	C00L2-6	157D	+24 VOLTS DC	
26VC1-16	LV DC	70.	PECU-8	161V	C00L2-6	157C	POWER RETURN	
26WC1-14	LV DC	70.	PECU-8	161W	C00L2-6	157A	+ SIGNAL FOR PSL22	
26XC1-14	LV DC	70.	PECU-8	161X	C00L2-6	157B	SIGNAL RETURN	
26YC1-16	LV DC	70.	PECU-8	161Y	C00L2-6	157E	SHIELD FOR D & C	
26ZC1-16	LV DC	70.	PECU-8	161Z	C00L2-6	157F	SHIELD FOR A & B	
27AC1-16	LV DC	25.	PECU-1	1C1A	PCS1-7	1C3A	B+ FROM PECU TO #1 PCS	
27BC1-16	LV DC	25.	PECU-1	1C1B	PCS1-7	1C3B	NC CONTACT ON MAIN CONTACTOR	
27CC1-16	LV DC	25.	PECU-1	1C1C	PCS1-7	1C3C	NO CONTACT ON MAIN CONTACTOR	
27DC1-16	LV DC	25.	PECU-1	1C1D	PCS1-7	1C3D	NO CONTACT ON DIF. CURRENT RELAY	
27EC1-16	LV DC	25.	PECU-1	1C1E	PCS1-7	1C3E	NO CONTACT ON OVERCURRENT RELAY	
27FC1-16	LV DC	25.	PECU-1	1C1F	PCS1-7	1C3F	NC CONTACT ON COVER-IN-PLACE SW.	
27GC1-16	LV DC	25.	PECU-1	1C1G	PCS1-7	1C3G	+ LEAD TO MAIN CONTACTOR COIL CK	
27HC1-16	LV DC	25.	PECU-1	1C1H	PCS1-7	1C3H	- LEAD TO MAIN CONTACTOR COIL CK	
27JC1-SH	LV DC	25.	PECU-1	1C1J	PCS1-7	1C3J	SHIELD FOR G & H	
27KC1-16	LV DC	25.	PECU-1	1C1K	PCS1-7	1C3K	SIGNAL ON BLOWN CAP. BANK FUSE	
27LC1-16	LV DC	25.	PECU-1	1C1L	PCS1-7	1C3L	SPARE	
27MC1-16	LV DC	25.	PECU-1	1C1M	PCS1-7	1C3M	SPARE	
27NC1-16	LV DC	25.	PECU-1	1C1N	PCS1-7	1C3N	SPARE	
27PC1-16	LV DC	25.	PECU-1	1C1P	PCS1-7	1C3P	SPARE	
27RC1-16	LV DC	25.	PECU-1	1C1R	PCS1-7	1C3R	SPARE	
27SC1-16	LV DC	25.	PECU-1	1C1S	PCS1-7	1C3S	SPARE	
27AAC1-16W	LV DC	50.	PECU-2	1C5A	PCS1-8	1C7A	+15 V FROM PECU	WHITE
27ABC1-16B	LV DC	50.	PECU-2	1C5B	PCS1-8	1C7B	-15 V FROM PECU	BLUE
27ACC1-16G	LV DC	50.	PECU-2	1C5C	PCS1-8	1C7C	COMMON FROM PECU	GREEN
27ADC1-SH	LV DC	50.	PECU-2	1C5D	PCS1-8	1C7D	SHIELD FOR A,B,&C	
27AEC1-16W	LV DC	50.	PECU-2	1C5E	PCS1-8	1C7E	SIGNAL FOR RAIL V	WHITE
27AFC1-16B	LV DC	50.	PECU-2	1C5F	PCS1-8	1C7F	SIGNAL FOR RAIL V	BLUE
27AGC1-SH	LV DC	50.	PECU-2	1C5G	PCS1-8	1C7G	SHIELD FOR E & F	
27AHC1-16W	LV DC	50.	PECU-2	1C5H	PCS1-8	1C7H	SIGNAL FOR CAP. V	WHITE
27AJC1-16B	LV DC	50.	PECU-2	1C5J	PCS1-8	1C7J	SIGNAL FOR CAP. V	BLUE
27AKC1-SH	LV DC	50.	PECU-2	1C5K	PCS1-8	1C7K	SHIELD FOR H & J	
27ALC1-16W	LV DC	50.	PECU-2	1C5L	PCS1-8	1C7L	SIGNAL FOR DC AMPS	WHITE
27AMC1-16B	LV DC	50.	PECU-2	1C5M	PCS1-8	1C7M	REFERENCE FOR L	BLUE
27ANC1-SH	LV DC	50.	PECU-2	1C5N	PCS1-8	1C7N	SHIELD FOR L & M	
27APC1-16	LV DC	50.	PECU-2	1C5P	PCS1-8	1C7P	SPARE	
27ARC1-01	LV DC	50.	PECU-2	1C5R	PCS1-8	1C7R	SPARE	
27ASC1-16	LV DC	50.	PECU-2	1C5S	PCS1-8	1C7S	SPARE	
28AC1-16	LV DC	25.	PECU-3	1C9A	PCS2-7	1C3A	B+ FROM PECU TO #2 PCS	
28BC1-16	LV DC	25.	PECU-3	1C9B	PCS2-7	1C3B	NC CONTACT ON MAIN CONTACTOR	
28CC1-16	LV DC	25.	PECU-3	1C9C	PCS2-7	1C3C	NO CONTACT ON MAIN CONTACTOR	
28DC1-14	LV DC	25.	PECU-3	1C9D	PCS2-7	1C3D	NO CONTACT ON DIF. CURRENT RELAY	
28EC1-16	LV DC	25.	PECU-3	1C9E	PCS2-7	1C3E	NO CONTACT ON OVERCURRENT RELAY	
28FC1-16	LV DC	25.	PECU-3	1C9F	PCS2-7	1C3F	NC CONTACT ON COVER-IN-PLACE SW.	
28GC1-16	LV DC	25.	PECU-3	1C9G	PCS2-7	1C3G	+ LEAD TO MAIN CONTACTOR COIL CKT	
28HC1-16	LV DC	25.	PECU-3	1C9H	PCS2-7	1C3H	- LEAD TO MAIN CONTACTOR COIL CKT	
28JC1-SH	LV DC	25.	PECU-3	1C9J	PCS2-7	1C3J	SHIELD FOR G & H	
28KC1-16	LV DC	25.	PECU-3	1C9K	PCS2-7	1C3K	SIGNAL ON BLOWN CAP. BANK FUSE	
28LC1-16	LV DC	25.	PECU-3	1C9L	PCS2-7	1C3L	SPARE	
28MC1-16	LV DC	25.	PECU-3	1C9M	PCS2-7	1C3M	SPARE	
28NC1-16	LV DC	25.	PECU-3	1C9N	PCS2-7	1C3N	SPARE	
28PC1-16	LV DC	25.	PECU-3	1C9P	PCS2-7	1C3P	SPARE	
28RC1-14	LV DC	25.	PECU-3	1C9R	PCS2-7	1C3R	SPARE	
28SC1-16	LV DC	25.	PECU-3	1C9S	PCS2-7	1C3S	SPARE	

Table 5.7.I. Example of Wire List - Low Voltage Wiring

5.8 PRODUCT ASSURANCE

This subsection contains brief summaries of the Product Assurance Engineering efforts carried out in support of the ASDP propulsion system development. As used here, the term Product Assurance encompasses the following disciplines:

- Reliability
- Safety
- Maintainability.

Detailed discussions are contained in individual reports prepared on each of the above subjects: Delco Electronics Report Nos. R78-17, R78-18, and R78-19, respectively.

The reliability and maintainability analyses summarized herein reflect the propulsion system design as of January 1977, that is, the Test Article configuration. In the case of the safety analyses, in accordance with customer direction, the final design of the truck-mounted components was taken into consideration.

5.8.1 RELIABILITY ANALYSIS

The primary topics included in this effort were a failure modes, effects and criticality analysis (FMECA) and predictions of mean distance between failures (MDBF) and of schedule reliability.

5.8.1.1 Failure Modes, Effects and Criticality Analysis

A total of 414 failure modes were analyzed and graded as to their criticality in accordance with the following designations:

Criticality

0	No discernible effect on performance
1	Minor degradation of performance, such as limited acceleration, braking or top speed capability ($<25\%$ degradation)
2	Moderate degradation of performance ($\approx 50\%$)
3	Severe degradation of performance (car can barely move or can be operated for only short periods of time)
4	Complete failure (car is incapable of self-propulsion)
5	Catastrophic failure (entire train is immobilized).

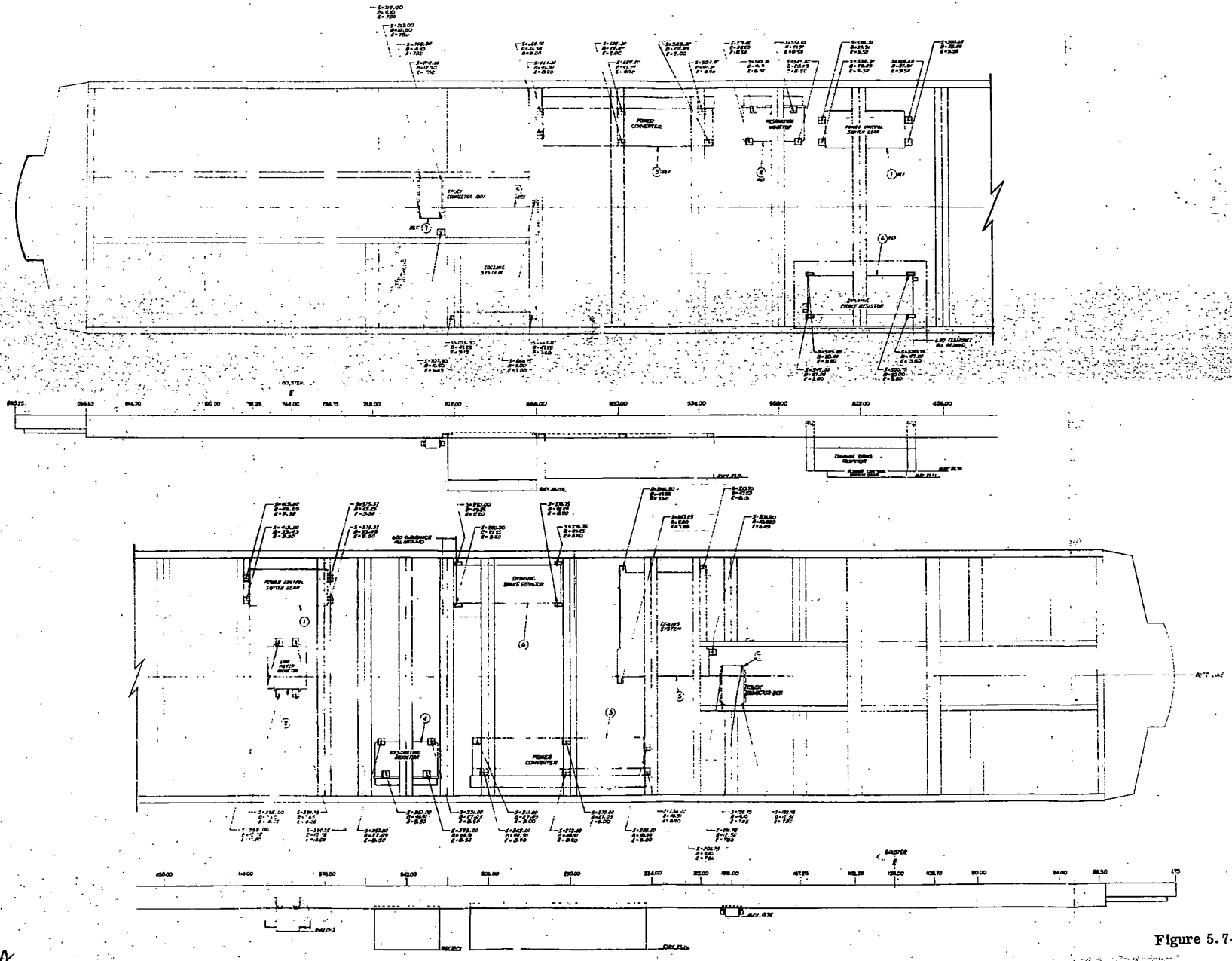

Figure 5.7-6. Wiring Installation

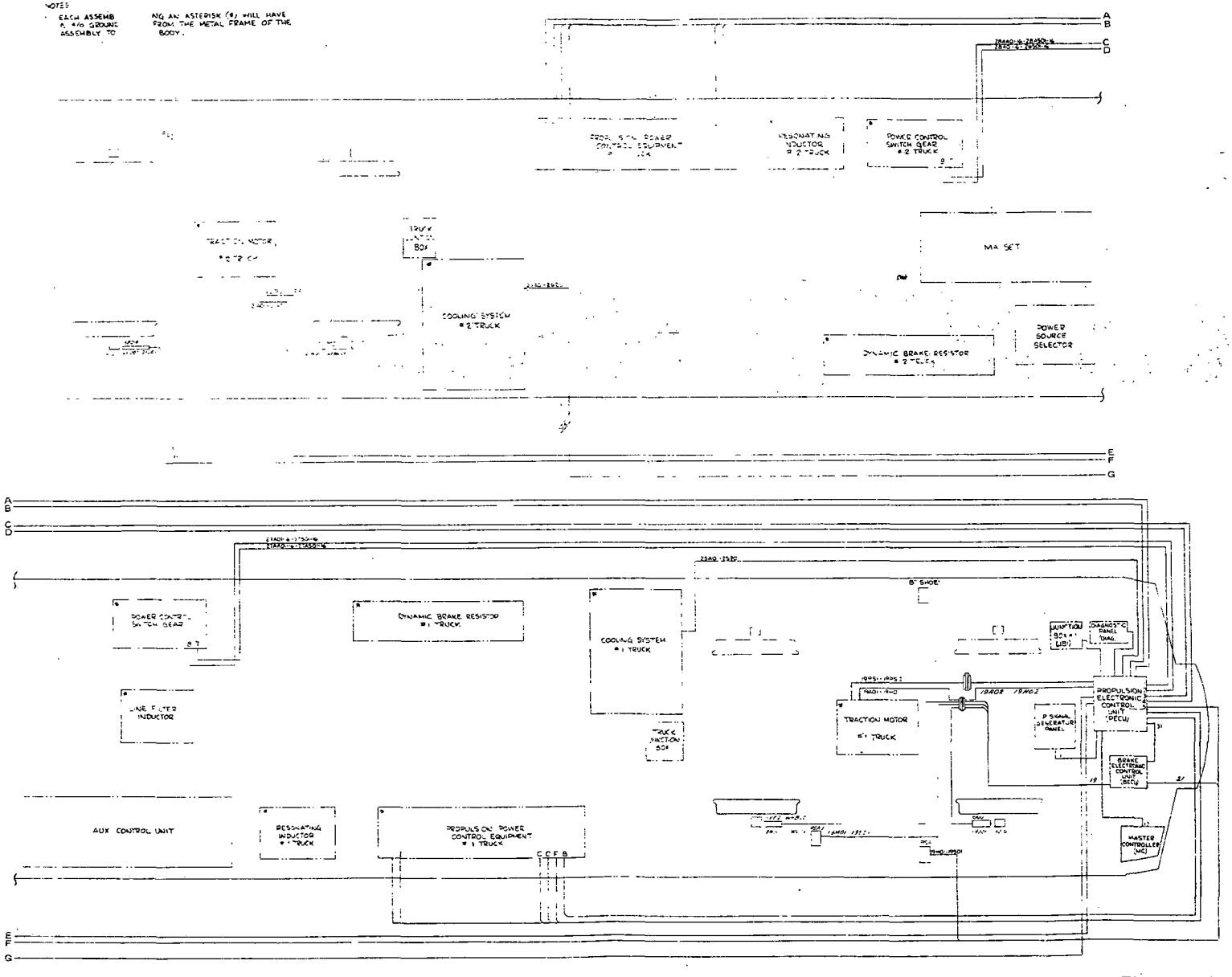

Figure 5.7-7. Wiring Installation

Preceding page blank

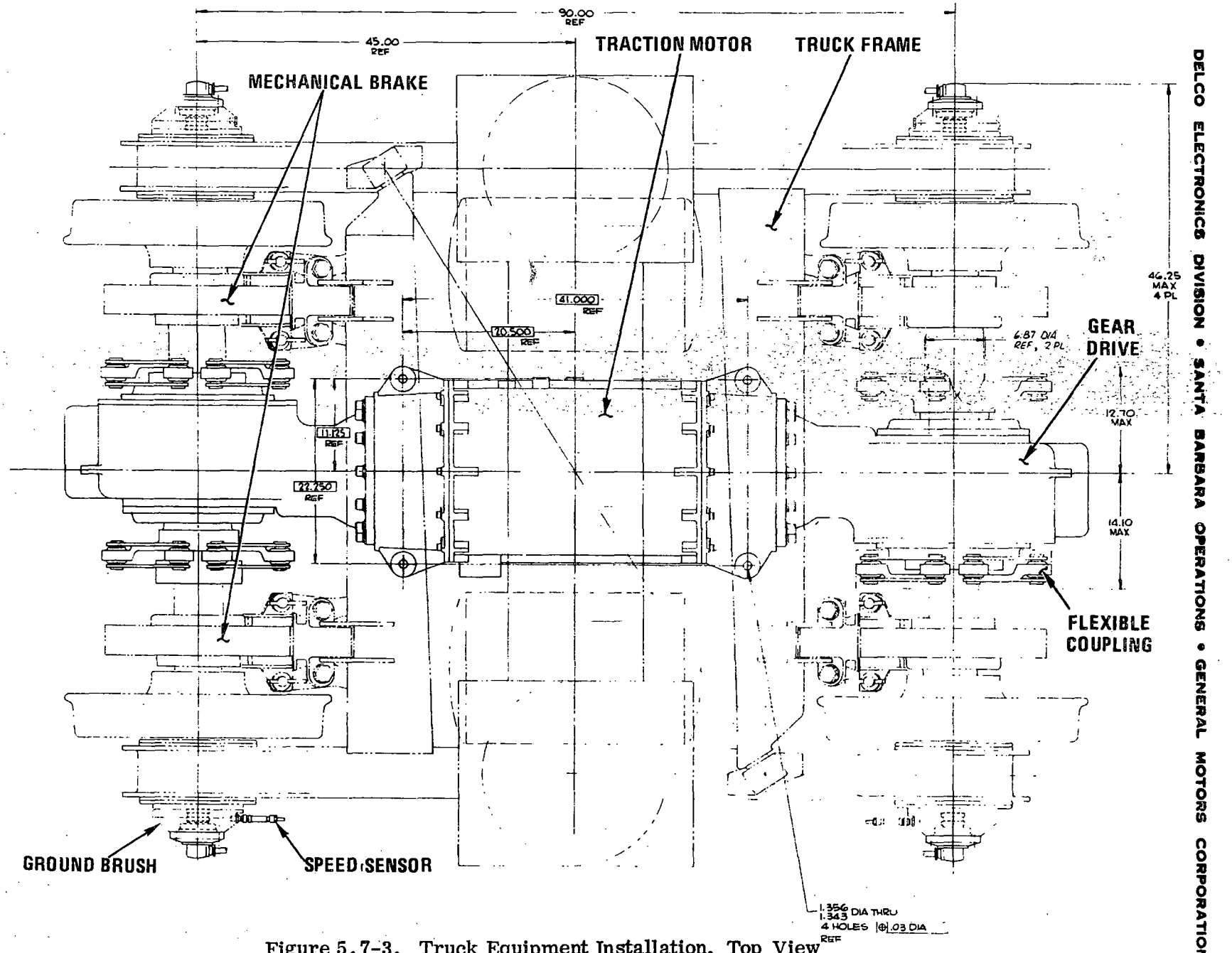

Figure 5.7-3. Truck Equipment Installation, Top View

A breakdown by major subassembly is given in Table 5.8-I.

Of these, it can be seen that 287 (failures rated at 1 or higher) will cause some degradation of performance and therefore affect schedule reliability. However, only 6 (rated at 3 or higher) are considered to be "critical."

5.8.1.2 Reliability Predictions

The ASDP self-synchronous propulsion system is predicted to achieve a schedule reliability of 0.999892 in simulated revenue service. This prediction gives the probability of a two-car train completing one round-trip traverse (CW and CCW) of the ACT-1 Transit Route at the HSGTC at Pueblo, Colorado with the loss of not more than one-half of the headway under simulated rush-hour conditions. The prediction assumes that the propulsion system(s) are fully operational prior to the start of the run and is further based on the projected reliability of a mature system. The predicted mean-distance-between failures (MDBF) for the propulsion system components of a single car is 100,000 miles, calculated by using the method of MIL-HDBK-217B, and assuming, in many cases, parts and components of the highest military quality procurable. A system configured in this manner may not be the most desirable from a cost-effectivity standpoint (a life cycle cost analysis is required to determine this), but would be required to meet the specified design goal of 100,000 miles MDBF. Only independent random failures of components of a single car installation (essentially two complete propulsion system sets) were considered and an average train speed of 27 mph was assumed in computing the MDBF given above.

5.8.2 SAFETY ANALYSES

The following safety related analyses were carried out during the ASDP propulsion system development:

- Fire Hazard Analysis
- Fault Tree Analysis
- Subsystem Hazard Analysis.

It was concluded that, in general, no hazards are associated with the ASDP system that are not present to some degree in existing rail rapid transit systems.

Results of the individual analyses noted above are summarized in the following paragraphs.

Item	Total Failure Modes Analyzed	Criticality Rating					
		0	1	2	3	4	5
Power Control Switchgear	19	9	3	7	-	-	-
Cycloconverter Module	10	1	-	9	-	-	-
Brake Control Module	7	-	3	4	-	-	-
Inverter Module	13	2	-	11	-	-	-
Field Supply Module	3	1	2	-	-	-	-
Capacitor Module	3	-	2	1	-	-	-
Inductor Module	3	-	1	2	-	-	-
Traction Motor	10	1	1	7	1	-	-
Ground Brush	1	1	-	-	-	-	-
Speed Sensor	1	1	-	-	-	-	-
Gear Drive and Axle Coupling	5	-	1	1	2	-	1
Motor Coupling	2	-	1	1	-	-	-
Cooling System	7	-	4	3	-	-	-
Motor Control Electronics							
• VCO Frequency Control	35	7	-	28	-	-	-
• Inverter Frequency Limit	78	40	11	27	-	-	-
• Brake Control	39	2	25	12	-	-	-
• RPS/CEMF Detector	29	1	5	23	-	-	-
• Cycloconverter Gate Logic	12	-	-	12	-	-	-
• Cycloconverter Fault Protection	26	11	-	15	-	-	-
Train Control Electronics							
• Input Circuits	73	33	12	26	-	2	-
• Output Circuits	38	17	6	15	-	-	-
TOTALS	414	127	77	204	3	2	1

Table 5.8-I. Failure Modes Analysis Summary

5.8.2.1 Fire Hazard Analysis

An examination of the ASDP Propulsion System was made to assess the degree of fire hazard inherent in the system due to design, materials, and operational considerations. It is concluded that no significant fire hazard exists for several reasons, one or more of which applies to each subassembly of the system.

1. Most of the subassemblies are entirely enclosed by metal cases or cabinets which will contain any fire initiated within the enclosure.
2. Relatively small, in some cases insignificant quantities of combustible material are present in the system. In addition, electrical insulating materials are, in general, relatively incombustible and do not support combustion.
3. Several of the subassemblies are liquid cooled by silicone fluid. Although the fluid is itself a combustible material, having a flash point of 375 ^{o}C, it restricts oxygen access and cools other materials so that combustion cannot occur.

5.8.2.2 Fault Tree Analysis

A Fault Tree Analysis was conducted to identify combinations of operational conditions, system states and equipment malfunctions that can cause injury to passengers or serious damage to the train. In general, the level of analysis was adequate either to verify the existence of a hazard or confirm that no single point failure would result in a hazard. Specific hazardous conditions identified by the analysis which were further analyzed consisted of:

- Excessive speed
- Inadequate braking capability
- Excessive acceleration/deceleration
- Rollback
- Excessive jerk
- Wheel slide.

Conclusions derived from the analysis relative to each of these hazards are discussed in the succeeding paragraphs.

Excessive Speed

The ASDP Propulsion System contains sufficient safeguards that no single point failure can cause this hazard to exist. In general, a combination of failures coupled with inattention or negligence on the part of the motorman would be required.

Inadequate Braking Capability

There is no single point failure mode associated with this hazard. This conclusion is based on Delco Electronics understanding of the capabilities of the Synchronous Friction Brake System when used in conjunction with the ASDP Propulsion System.

Excessive Acceleration/Deceleration

The degree of hazard existing with respect to these factors is marginal and depends on the track grade. It was estimated that acceleration/deceleration would exceed specification limits only on grades exceeding 10%. Since the maximum grade specified is 6%, this hazard is not considered critical.

Rollback

The ASDP Propulsion System adequately protects against rollback in that no single point failure can result in the occurrence of this hazard.

Excessive Jerk

It is concluded that certain malfunctions and/or operating conditions, notably an emergency stop situation, can cause jerk levels to exceed the specified level of 2 mphpsps. It is felt, however, that the level of jerk attainable due to propulsion system failure would not exceed this value by an amount sufficient to present an undue hazard.

Wheel Slide

No single point failure mode was identified which would result in this hazard.

5.8.2.3 Subsystem Hazard Analysis

All potential hazards defined by this analysis were classified in accordance with the following categories:

A - safety features are considered to be adequate
N - safety features are considered to be inadequate
RA - risk accepted.

It was originally required that by completion of the development program there were to be no "N" category hazards in the system. Furthermore, all "RA" category items were to be reviewed with Boeing Vertol to determine that the risks were acceptably low.

However, safety engineering effort was terminated early in 1977. Therefore, review of the "RA" category hazard has not taken place and several "N" hazards still remain in the analysis, although some may have been removed by design changes made during the system level tests discussed in paragraph 6.3.3.

Thus, the analysis still identifies several hazards that require additional consideration relative to design changes required and/or risk acceptability. These are:

- A potential hazard exists during regenerative braking operation if the train were to enter a section of track in which the third rail has been isolated, such as for repair purposes. Momentarily, in such a situation the third rail voltage may be raised to a potential in excess of 100 volts.
- Undercar equipment mountings have been designed to withstand the specified shock and vibration requirements and to retain the equipment even if the attaching bolts fail. However, the mounting arrangements have not been tested in service.
- Cab mounted equipment mountings have been designed to withstand the specified shock and vibration requirements. However, the mounting arrangement have not been tested in service.
- Charge buildup on the individual components contained within the propulsion system modules may constitute a safety hazard to maintenance personnel.
- Failure of the blocking diode located in the power input line in the shorted mode will permit an unenergized third rail to be momentarily raised to a potential in excess of 600 volts.
- Bearing seizure or gear lockup in the traction motor or gear drive may result in a sudden deceleration of the car which could be hazardous to the passengers.

- Several different modes of failure of the brake control circuits have been noted which could cause maximum electric braking effort to be developed. This is considered to be a safety hazard in that deceleration/jerk levels in excess of the maximum specified would result.
- Various failures in the Train Control Electronics could result in hazards such as loss or delay of electrical braking effort, or loss of slide control at moderately low speeds.
- A number of areas were noted where safety placards or warning notes in the maintenance manuals are considered advisable. These have been indicated as hazards in the analysis with the intention of changing their classification as soon as the required action was taken.

5.8.3 MAINTAINABILITY ANALYSIS

The maintainability engineering effort carried out during the ASDP propulsion system development included preparation of the following:

- Maintenance Concept
- Maintainability Demonstration Plan.

Summaries of these efforts follow.

5.8.3.1 Maintenance Concept

Development of the Maintenance Concept considered the ASDP propulsion system both as an experimental system and as a system in transit revenue operation.

The experimental phase was to consist of test and evaluation at the HSGTC at Pueblo, Colorado and of demonstrations over transit properties in various major cities of the United States. The Maintenance Concept was to be revised as experience was gained during this phase.

Included in the Maintenance Concept are the following plans:

- Inspection Plan
- Component Repair Plan
- Overhaul Plan
- Preventive Maintenance Plan.

Inspection Plan

This plan covered two separate inspections, to take place at intervals of every 5,000 and 15,000 miles, based on typical transit service. It was recommended that a "walk-around" inspection plus some simple checkouts be carried out on a daily basis during the experimental phase.

Component Repair Plan

This plan identified the components and associated repairs that would be accomplished at the operating site and at the propulsion system contractor's facilities. In general, repair of components requiring extensive troubleshooting, special equipment for checkout and recertification, and highly skilled personnel would be accomplished at the contractor's facilities. Items in this category would include the Power Converter modules and various elements of the Electronic Control and Diagnostics Units. Other components in most cases would be repaired at the operating site – perhaps with the aid of contractor or vendor personnel.

Overhaul Plan

Only two major components were identified as requiring overhaul: the Traction Motor and the Gear Drive and Axle Coupling Assembly. This would be accomplished at either the contractor's or vendor's facility.

Preventive Maintenance Plan

Preventive maintenance is to be performed in accordance with the following:

• Replace the gear drive lubricant first time after new unit is installed	5,000 miles
• Replace gear drive bearings	500,000 miles
• Grease motor-gear drive coupling	12 months or 30,000 miles
• Clean coolant unit air filter	6 months or 15,000 miles
• Clean coolant unit radiator	6 months or 15,000 miles
• Replace coolant unit filters	12 months or 30,000 miles
• Grease blower motor bearings	24 months or 60,000 miles
• Grease pump motor bearings	24 months or 60,000 miles

• Replace blower motor bearings	500,000 miles
• Replace pump motor bearings	500,000 miles
• Replace pump bushings	500,000 miles
• Replace traction motor bearings and seals	500,000 miles
• Measure wheel diameters and adjust value in train electronics	6 months or 15,000 miles
• Analyze the coolant fluid for acidity and viscosity	24 months or 30,000 miles.

5.8.3.2 Maintainability Demonstration Plan

A maintainability demonstration test had been planned to be conducted during the test and evaluation phase at the HSGTC at Pueblo, Colorado.

The demonstration was to be conducted by Delco Electronics personnel on the ASDP-Modified SOAC vehicles to verify the maintenance manhours goals stated in the Self-Synchronous Propulsion System Specification (Boeing Vertol Document D239-10000-1). These goals are:

Maintenance Task	Direct Manhours/Task
Basic Inspection	3.0 manhours/car
Remove and Reinstall	
a. Traction Motor Assembly	2.0 manhours/unit
b. Cycloconverter Module	1.0 manhours/unit
c. Capacitor Module	1.0 manhour/unit
d. Field Supply Module	2.0 manhours/unit
e. Inverter Module	1.0 manhour/unit
f. Brake Control Module	1.0 manhour/unit

A detailed step-by-step procedure was established for each of the above items. Analysis indicated that the above goals could be met provided that all tools, fixtures and equipment were readily available.

SECTION VI
TESTING

This section describes the testing that was performed relative to the ASDP self-synchronous propulsion system. Discussed are the following types of tests:

Developmental Tests - These encompass tests performed both prior to and following ASDP contract award in support of self-synchronous propulsion system design and development.

Major Component Tests - These were conducted on the first item of each major component manufactured in order to establish its suitability for incorporation into the overall propulsion system for system level testing. These tests generally consisted of visual inspections, continuity checks, resistance, dielectric and inductance measurements, and simple functional tests. Exceptions were the Gear Drive and Axle Coupling Assembly, which was fully qualified as a separate entity apart from the rest of the propulsion system, and the Traction Motor, whose performance could only be partially verified prior to system level testing.

System Level Tests - These were tests conducted in a dynamometer laboratory with a complete Test Article propulsion system (less Gear Drive and Axle Coupling Assembly). Covered are descriptions of the laboratory equipment and test setups and discussions of the motoring and braking tests conducted – the problem areas encountered and the results achieved.

6.1 DEVELOPMENTAL TESTING

This paragraph discusses the testing that was conducted in support of development and design of the self-synchronous propulsion system. Development of such a system for railcar application started in 1971 and can be considered to have continued through fabrication of the Test Article and its installation in the dynamometer laboratory for system level testing in February 1977.

Development during the time period from 1971 through ASDP contract award in October 1975 was carried out as an IR&D effort.

During early IR&D development effort, the concepts of the capacitor-coupled cycloconverter, current transformer field excitation, and counter EMF power factor control were developed. Later, a 90 kW liquid cooled Bendix aircraft alternator was modified by the installation of a rotor position sensor and rotary transformer to serve as a drive motor and a 1Ø/3Ø 150 kW power converter was designed and fabricated using commercial SCR heat sinks.

Major improvements in the laboratory facility and in drive technology were made during the final phases of the IR&D program. An air cooled synchronous motor (the "workhorse" motor) and a locomotive traction motor were purchased for use as a drive motor and dynamometer, respectively. The drive concept was changed from 1Ø/3Ø to 3Ø/3Ø conversion and major advances in SCR cooling techniques and inductor design were made to achieve a compact and efficient power converter.

The laboratory test setup from the start of the contract in October 1975 to April 1976 consisted of the Delco Products conventional four-pole air cooled machine ("workhorse motor") directly coupled to the EMD D-79 dc motor/generator. The power converter was the breadboard unit from the pre-contract IR&D program. From April until the first ASDP motor became available, the drive motor used was a standard 10-pole synchronous motor modified for high speed-high frequency operation.

In February 1977, the ASDP Test Article propulsion system was installed in the dynamometer laboratory and checkout was started in preparation for system level testing.

The major development tests conducted prior to this point in time are discussed in the paragraphs following.

6.1.1 CYCLOCONVERTER GATE DRIVE DEVELOPMENT

The cycloconverter gate drive circuitry originally installed in the Test Article represented the fourth generation of circuit development. These generations were:

- 1st generation – August 1971 to September 1973. dc group fired gating. No synchronism with inverter. Breadboard system.
- 2nd generation – September 1973 to December 1975. dc group fired gating with gate current stretched by SCR voltage sensor to avoid random weak gate pulses. Breadboard system.
- 3rd generation – December 1975 to March 1976. "One shot" narrow pulse gating to avoid random weak gate pulses and cycloconverter faulting. Breadboard system.
- 4th generation – March 1976 to June 1977. dc group fired gating with gate current stretch programmed for constant phase angle. Test Article system.

The first generation cycloconverter was designed with group fired SCR gating with no synchronism between the gate timing and the cycloconverter input voltage. It was found that this type of gating produced a weak gate – di/dt failure mode due to the occasional removal of gate current just prior to the SCR becoming conductive. To counter this problem, a circuit was developed and patented (Reference 6) which utilized sensed SCR voltage to stretch the gate current in time beyond the point where the SCR became conductive. However, subsequent testing with a high speed aircraft alternator showed that the gate current stretch of the second generation circuit produced a tendency for the cycloconverter to produce a fault across the motor at the higher ASDP motor frequencies (up to 200 Hz).

Thus, near the start of the ASDP contract, development of a third generation "one-shot" pulsed gating technique was commenced which eliminated the random weak gate problem

while avoiding the faulting tendency at high motor frequencies. The pulsed gate circuit produced 10 μs wide gate pulses timed with signals derived from voltage sensors across each SCR. In addition to eliminating the cycloconverter random weak gate problem, pulsed gating also eliminated the problem of applying gate current to SCR blocking negative voltage. Further, it required considerably less circuitry than the former dc gating method. However, a fatal flaw in the pulsed gating approach was found in March 1976. The flaw resulted from irregularities and discontunuities in the reverse or blocking voltage across the cycloconverter SCR's. They occurred at low inverter frequencies as the capacitively coupled inverter, operating well below resonance, tends to produce pulses of output current with a large component at the 2nd harmonic frequency. Occasionally, due to the finite threshold of the SCR voltage sensor and the irregular nature of the SCR blocking voltage, a gate pulse would be skipped. This resulted in nonconduction of the cycloconverter SCR and a transient change in the load on the inverter. The inverter SCR's would then experience a momentary short turn-off time with resulting drive shutdown.

The pulsed gate circuitry was replaced with the fourth generation gate circuit in March 1976. In this dc gate circuit, gate current was stretched by a constant phase angle to avoid the random weak gate problem. The circuit was tested using a standard 10-pole 60 Hz motor modified by banding the rotor and reconnecting the stator windings for operation to 133 Hz. The motor was not fitted with a rotor position sensor and thus could not operate at high torque at frequencies below 20 Hz. The fourth generation gate circuit performed satisfactorily at high cycloconverter current levels in the frequency range of 20 Hz to 133 Hz but was not tested in the 0 to 20 Hz and 133 Hz to 200 Hz ranges prior to Test Article system level testing due to equipment limitations. (During system level testing problems were discovered with this circuit which led to a 5th generation design. This is discussed in paragraph 6.3.3.3.2.)

6.1.2 BRAKE CONTROL CIRCUIT DEVELOPMENT

A 10 SCR brake control unit, with a power circuit identical to that of the Test Article unit (Figure 5.6-23), was fabricated using conventional liquid cooled heat sinks. The traction machine was the 10-pole synchronous motor modified for overspeed operation. Motive power was furnished by the D-79 dc machine operating as a motor from either constant voltage diode rectifier power or variable voltage SCR rectifier power. Field excitation was supplied by a three winding - three phase transformer, identical to that later used in the Test Article unit. The high impedance windings of the transformer were energized from the three phase 350 Hz to 1200 Hz inverter.

The phase delay rectifier (PDR) SCR control differs from conventional PDR control of 60 Hz utility power in that both the voltage and the frequency of the three phase rectifier input voltage vary as the transit car decelerates. In general, PDR control utilizes an ac reference signal voltage derived from the rectifier input voltage. This reference signal is compared to a dc control signal to produce delayed SCR gate signals. With variable voltage systems, it is necessary to use integrators to form ramp type reference signals derived from the zero crossings of the rectifier input voltage. When frequency as well as voltage is variable, the ramp generating integrators must be modified to produce ramp wave shapes which are independent of frequency. To accomplish this, a closed loop ramp waveform control loop was developed and tested with the breadboard brake control unit.

The brake control rectifier is a dual semi-converter. That is, the three dynamic brake SCRs and the three regenerative brake SCRs share a common group of three ground return SCRs. The latter group is gated with zero delay to make the SCRs perform the role of semi-converter diodes. A tenth SCR is provided to shunt a portion of the dynamic brake SCR at low speed. This latter SCR is commutated off by removing the gate signals to the other SCRs.

Tractive effort can be controlled by varying the input voltage to the dual rectifier through motor field control with either the dynamic brake or the regenerative brake rectifier operated with zero phase delay. Tractive effort can also be controlled with constant motor field excitation by phase delay gating of either the dynamic brake or the regenerative brake rectifier or both rectifiers simultaneously. In the latter mode, regenerative braking is given first priority with dynamic braking blended in to prevent the dc third rail voltage from exceeding its limit level.

The brake control rectifier was tested with both separate dynamic and regenerative and combined braking. A semi-receptive source was simulated by using the dc dynamometer machine as a voltage source, with the generator resistance increased by the addition of an external resistor. Power levels to 163 kW, limited by the laboratory 60 Hz power supply, were achieved in dynamic braking. Regenerative braking power to 347 kW with 1940 ft-lb of torque was also achieved.

6.1.3 HIGH FREQUENCY MOTOR TESTS

High frequency - high power tests were performed to evaluate motor commutation performance and component stress at motor frequencies in the upper range of the ASDP motor frequency band. To accomplish this, a GE 10-pole machine having a normal operating speed of 720 r/min was used. The machine was disassembled and a structural analysis was performed to determine the speed capability of the rotor laminations, windings, and damper bars. The damper bar end connections proved to be the limiting elements. Accordingly, the damper bar projections were wound with epoxy impregnated cord under tension and cured at an elevated temperature. The stator windings were also reconnected for lower volts/Hz.

For high speed testing, the dc machine dynamometer was connected to regenerate through a series diode to the 600V supply. This allowed high power operation without overloading of the 150 kVA 60 Hz isolation transformer. To expedite the test program, no torque transducer or rotor position sensor was installed. Cycloconverter timing was by means of CEMF only, with the power factor advance circuitry described in Reference 1* operative. The test motor was started with a V-belt connected auxiliary motor.

Figure 6.1-1 shows motor torque (computed from dc input power, estimated efficiency and speed) plotted versus inverter frequency at three motor speeds. The data represents power and torque levels in excess of 500 hp and 2000 ft-lb, respectively.

Figure 6.1-2 shows representative oscillograms of inverter SCR voltage and current and motor line voltage and phase current for operation at 1400 r/min with 655 Vdc, 439 kWdc inverter input power. Mechanical output power is approximately 386 kW (518 hp).

The key inverter stress parameters are peak SCR voltage, peak SCR current, and SCR turn-off time (duration of anti-parallel diode current). Figure 6.1-2a shows these values to be 1400 V-peak, 920 A-peak, and 245 μs.

Cycloconverter commutation is shown in the motor voltage and current waveforms of Figure 6.1-2b. The peak motor voltage and current are 1000V and 540A. The commutation overlap angle (indicated by the duration that line-to-line voltage is clamped to zero) is 27^{o}. This is also the value of the commutation advance angle. The commutation is

* References are listed on page R-1 at the rear of this document.

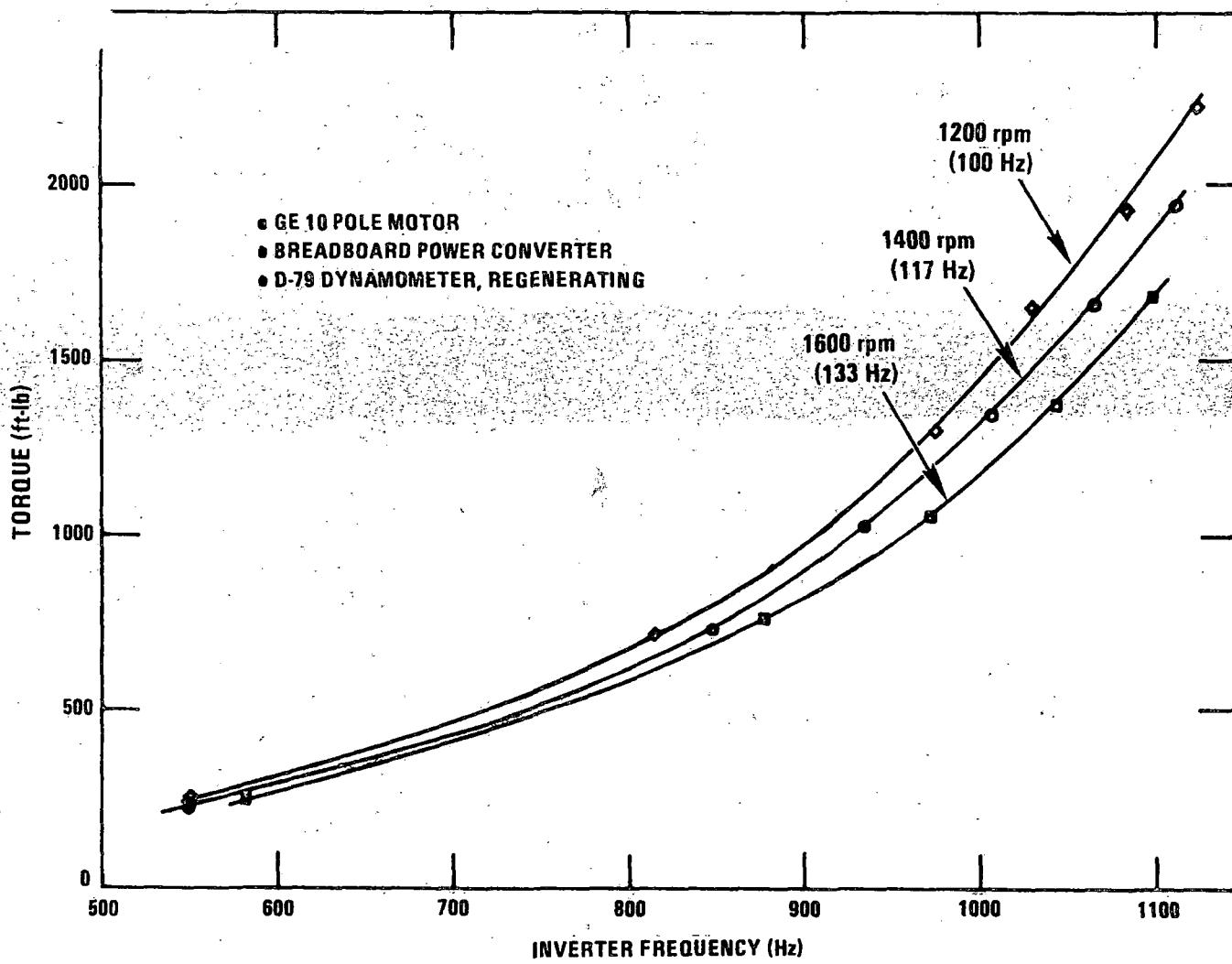

Figure 6.1-1. Torque Versus Inverter Frequency Developmental Test

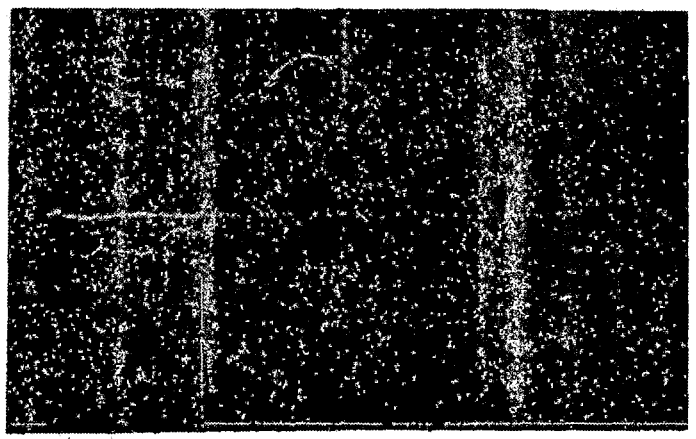

a. Inverter SCR/Diode Voltage and Current

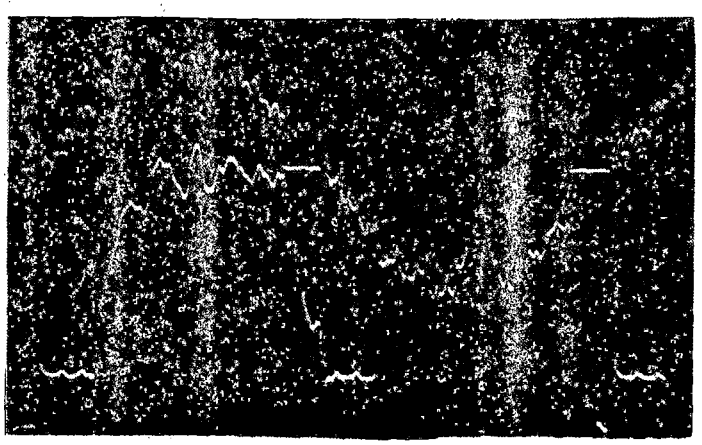

b. Cycloconverter Output Voltage and Current

Figure 6.1-2. High Frequency Motor Test Waveforms

being effected by the leading power factor of the cycloconverter load with reserve commutation from the cycloconverter input line.

6.1.4 CYCLOCONVERTER OUTPUT CURRENT CAPABILITY TEST

The cycloconverter output current capability was measured to verify the correctness of the values of inductance and capacitance of the three-phase resonant inverter. This capability had not been demonstrated earlier because a motor capable of absorbing the rated cycloconverter current had not been available. To simulate a stalled motor, an inductor was connected across two of the cycloconverter output phases. The resulting dc current was then converted to an equivalent ac rms current by multiplying by $\sqrt{2/3}$. Figure 6.1-3 shows the equivalent rms cycloconverter output current and the inverter input power as a function of inverter frequency. The data showed that the required 550 A rms low speed motor current could be achieved with an inverter frequency of 1080 Hz. This frequency produces a peak SCR blocking voltage of approximately 1500V and a peak SCR current of 700A. The net result of this test was to establish that sufficient current was available at low speed to produce the required motor torque of 1560 ft-lb.

6.1.5 MOTOR SHOCK TORQUE TESTS

The presence of a fault across the terminals of a traction motor operating under power produces a current surge and a shock torque on the drive train. The magnitudes of the current and torque pulses are determined by the motor speed, field current, and the characteristics of the current-limiting fuse in the fault circuit.

Fault conditions on the Delco Products four pole "workhorse" motor were simulated by closing a contactor in series with a fuse across the motor terminals, with the motor operating as a generator.

Operating the machine at 1130 r/min and 260 V_{ll} produced a peak current of 1300A and a peak torque of 2000 ft-lb when the machine was shorted through a 250A fuse. Torque transducer limitations prevented testing with a larger fuse, higher speed, or higher field current.

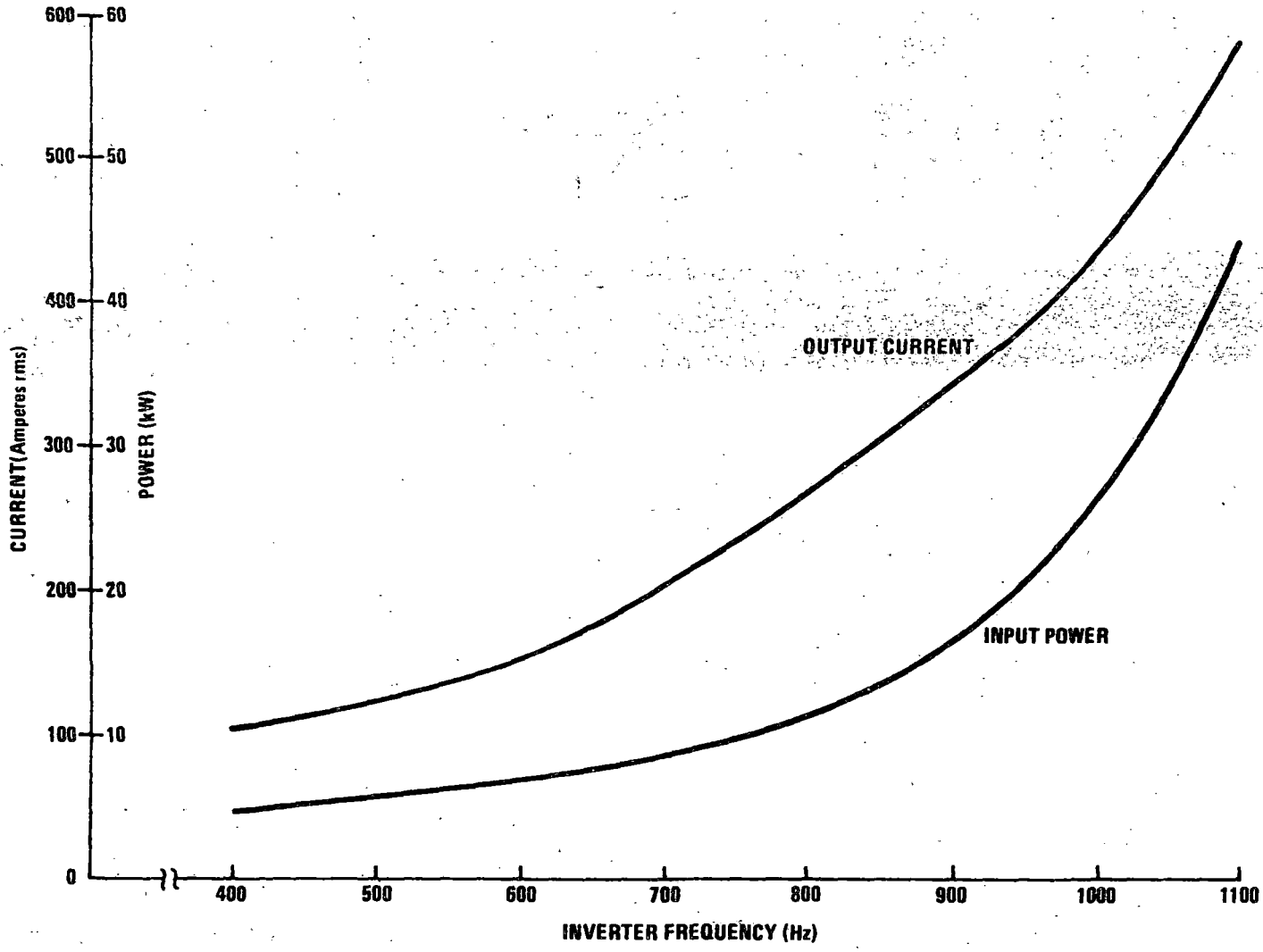

Figure 6.1-3. Cycloconverter Output Current and Inverter Input Power at Very Low Speed, 600 Vdc Supply

6.1.6 COOLANT FLUID TESTING

Following an extensive survey of available synthetic fluids and a study of their properties relative to their potential use as a cooling fluid in the ASDP propulsion system, the choice was narrowed down to two candidates:

- Dow Corning 200 series, 50 centistokes viscosity silicone fluid (DC 200-50CS)
- Monsanto phosphate ester-petroleum oil mix (Pydraul MC).

These fluids were then subjected to a series of tests, the results of which, combined other comparative evaluations, formed the basis for selection of the fluid considered most suitable for ASDP application (see paragraph 5.6.7).

6.1.6.1 Flash and Fire Point

This test measures the temperature at which the fluid vapors are sufficiently concentrated to flash or burn when ignited directly by a source of ignition. The more volatile a fluid is, the lower its flash and fire points.

The flash and fire points for Pydraul MC were determined to be 255°C and 290°C, respectively. For DC 200-50CS the corresponding readings were 316°C and 365°C.

Burning behavior was markedly different. Pydraul burned fiercely with a bright yellow-orange flame and dense black sooty smoke. The fluid also tended to spatter out of the container, thus spreading the fire. The silicone fluid burned quietly with a luminous flame and a relatively small amount of light gray smoke with entrained gray "soot." A gray ash formed on the liquid surface which apparently reduced flame severity.

Both fluids were self-extinguishing after removal of the heat source.

6.1.6.2 Autogeneous Ignition Temperature (A.I.T)

Th st establishes the minimum temperature necessary to effect ignition of the fluid without an ignition source applied directly to the fluid surface. Both DC200-50CS and Pydraul MC pass the Bureau of Mines Schedule 30, A.I.T. requirement of 600°F (316°C). However, the A.I.T's for DC200-50CS and Pydraul MC were found to be 590°C and 750°C, respectively.

6.1.6.3 Compatibility

A test program was conducted to evaluate compatibility of various candidate coolant fluids with certain electrical insulation components to be used both in the construction of the traction motor and of the power converter modules. It was found that the proposed insulation materials were not compatible with Pydraul MC. Equivalent tests were not run with DC200-50CS because of its known compatibility characteristics.

6.1.6.4 Pour Point and Viscosity

Tests were conducted to evaluate the low temperature pumping characteristics of Pydraul MC and DC200-50CS. It was determined that, in order to pump Pydraul MC at ambient temperatures down to -25°F, heaters would be required which together with the pumps would have to operate continuously whether the overall propulsion system was operating or not. By contrast, this test showed that silicone fluid can perform satisfactorily down to a temperature of -35°F. Both fluids exhibit acceptable high temperature pumping properties.

6.1.6.5 Electrical Properties

Tests of Pydraul MC indicated that increased temperatures markedly increased fluid dielectric constant and dissipation factor. In general, it was concluded that electrical properties were poor compared to materials generally classified as dielectric fluids.

6.1.7 HEAT SINK DEVELOPMENT

Since adequate and reliable cooling of the power control elements is a basic requirement in the Delco self-synchronous propulsion system, a substantial effort was devoted to the development of a suitable heat sink for the SCR and diode devices.

Tests and analysis conducted prior to ASDP contract award had established that commercially available heat sinks were not suitable for parallel flow operation because their flow resistance is too low. Their use in this manner would result in an excessive flow rate requirement for the hydraulic pump. Connecting them for series flow would penalize cooling performance due to the increased coolant temperature presented to the last heat sink of a string. The use of commercial heat sinks would also result in unacceptably large package size for the power converter modules and would require complex plumbing. Thus, it was decided that a high impedance parallel flow system was necessary.

To this end, development of a grooved heat sink which would be clamped to the SCR pole face and immersed in an oil bath was undertaken. Heat sink blocks of various groove configurations and groove dimensions were fabricated and tested for pressure drop and thermal resistance at various flow rates.

The test results obtained (References 7 and 8) during the pre-ASDP contract phase generally established the superiority of the externally grooved heat sink over conventional designs and, furthermore, indicated that varying thermal dissipation requirements could be met by simply varying the groove depth. However, the results obtained could not be directly used for ASDP system design because the fluid used, Diala AX, has properties considerably different from the ASDP coolant DC 200-50CS.

Thus, additional heat sink tests were conducted during the ASDP design/development phase based on ASDP flow rate requirements and using the selected DC 200-50CS.

The objective of these tests was to determine the groove depths that would provide the desired pressure drop at the two ASDP design flow rates of 0.33 and 0.67 gpm per thyristor device. (The 0.67 gpm rate applies to the inverter module SCR's which must dissipate significantly more power than the devices in the other power converter modules.)

As a result of these tests, two groove depths were established for the ASDP design: 0.066 in. for 0.33 gpm and 0.110 in. for 0.67 gpm. Groove width in both cases is 0.06 in. Thermal resistance was measured as 0.12°C/W for the 0.066 in. depth and 0.09°C/W for the 0.110 in. depth for the SCR heat sink assembly in air. Previous pre-contract test results have shown that these thermal resistance values would be reduced to approximately 0.10° C/W and 0.072° C/W by immersion of the heat sink assembly in the coolant filled module. Additional details of these tests can be found in Reference 9.

6.2 MAJOR COMPONENT TESTING

This subsection briefly discusses the tests performed on various major power control and electronic components prior to their incorporation into the overall propulsion system Test Article used for the system level testing discussed in subsection 6.3. Generally these tests consisted of visual inspections, dielectric and continuity checks, measurements of resistance and inductance, and basic functional tests. The purpose was to establish the suitability of these components for the planned system level tests. Additionally, the tests would

establish component characteristics for future reference. In the case of the propulsion power control equipment and line filter, one means of establishing suitability was to confirm that the characteristics of circuit elements did not differ significantly from those of the elements of the IR&D breadboard hardware previously determined to be acceptable during the developmental testing previously discussed in subsection 6.1.

In the case of the traction motor, tests conducted by the subcontractor, Delco Products, prior to shipment of the motors, are summarized. Since these tests could only partially verify required motor performance prior to integration with the rest of the propulsion system, motor test results obtained during system level testing at Delco Electronics are also described.

All performance testing of the gear drive and axle coupling assembly was performed by the subcontractor, Thyssen-Henschel of West Germany. Results of engineering, qualification, and acceptance testing are summarized.

6.2.1 RESONATING INDUCTOR MODULE

The Test Article resonating inductor module differed from the breadboard unit by the addition of an internal support structure to meet the shock and vibration loads of the rail-car installation. Initially, this structure was fabricated from aluminum. Testing showed that this structure degraded the inductor quality factor (Q) to an unacceptable degree. A second inductor module was therefore fabricated having an inert fiberglass internal support structure and retrofitted into the drive system after the start of the Test Article test program. At this time, an error in the design of the input fuse circuit was also corrected.

The final version of the resonating inductor module was tested prior to filling with coolant fluid and with the module cover installed. The inductance and quality factor (Q) of each of the six linear inductors in the module was measured at 100 mV, 1000 Hz excitation. Inductance ranged from 139.6 μH to 148.3 μH. This represents an inductance spread of ± 4.35 μH or $\pm 3.02\%$. The resulting spread in inverter resonant frequency is $\pm 1.51\%$. Inductor Q ranged from 129 for inductors next to the front panel or rear cover to 170 for inductors in the middle of the stack.

The dielectric strength of the inductor insulation was tested by applying 990 Vac between opposite inductors and 1500 Vac between inductors to the case. Insulation resistance was measured as greater than 500 MΩ at 500 Vdc.

6.2.2 INVERTER MODULE

The electrical elements of the inverter module consist of six gate driver circuits, six power SCR's, six power diodes, six dV/dt suppression circuits, and three diode current sensing circuits. These were tested with the module cover not installed.

6.2.2.1 Gate Driver Circuits

The gate driver circuits were checked for gate current rise time, peak current, and pulse width. Figure 6.2-1 below shows typical gate current and transformer output voltage traces. The waveforms show a rise to 0.4A in 1.0μs, a peak current at 0.5A, and a pulse width of 11μs.

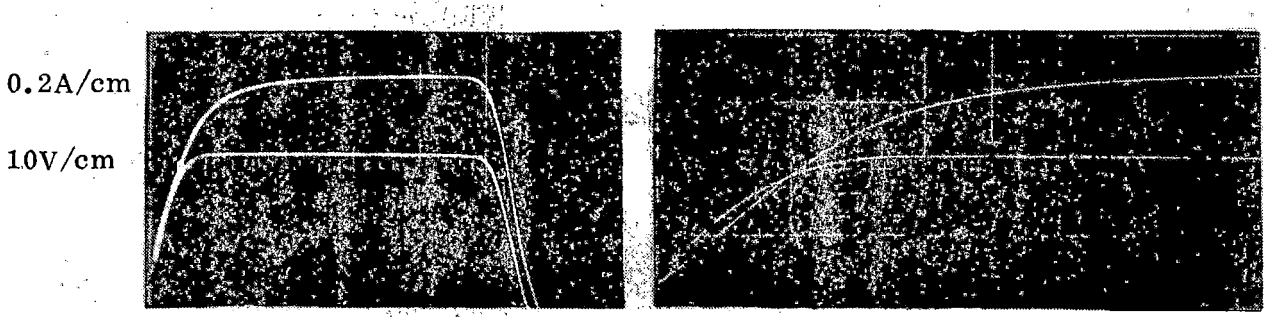

Figure 6.2-1. Typical Inverter SCR Gate Current and Voltage

Isolation between the gate pulse transformer primary and secondary windings was measured by applying 1600 Vdc between the SCR cathodes and logic ground. Leakage currents were less than 10μA.

6.2.2.2 SCR's and Diodes

SCR's and anti-parallel diodes were measured for leakage current at room temperature with 1600 Vdc applied. Leakage current ranged from 1.6 mA to 5.6 mA. Leakage currents between the SCR cathodes and the chassis were also measured at 1600 Vdc. In one instance, a voltage breakdown occurred at 1000 V. This took place between a front cover feedthrough terminal and the SCR support frame. The insulation between the frame and feedthrough was modified to correct the problem.

The minimum gate current to trigger each SCR was determined at room temperature by applying a variable amplitude gate current pulse with dc voltage applied between the SCR anode and cathode. The minimum gate current to trigger ranged from 58 mA to 130 mA.

6.2.2.3 dV/dt Suppression Circuits

The leakage current of the dV/dt capacitors was measured at 1620 Vdc. Leakage current was 1700 μA for the six capacitors. The volt-ampere characteristic of each dV/dt circuit was determined with the aid of a Tektronix 576 Curve Tracer. Figure 6.2-2 below shows a typical plot of current versus voltage.

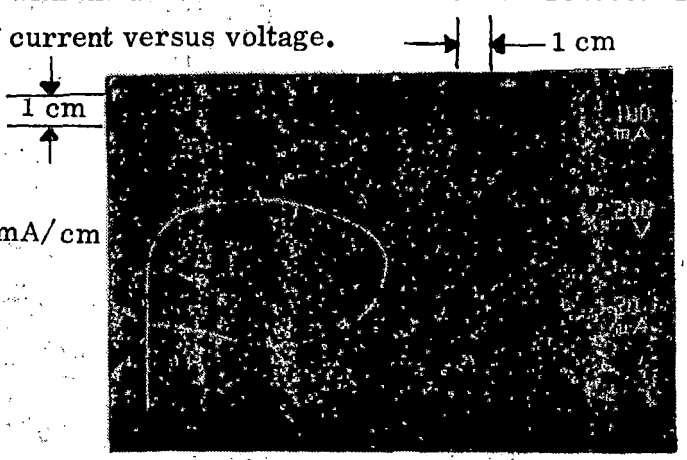

Figure 6.2-2. Typical dV/dt Circuit Characteristic

6.2.2.4 Diode Current Sensing Circuits

The diode current sensing circuits were checked with the inverter operating in air at 525 Vdc and 153 Hz. Figure 6.2-3 below shows typical traces of current in the power diode, the sensor output voltage, and the logic signal in the MCE representing the existence of diode current

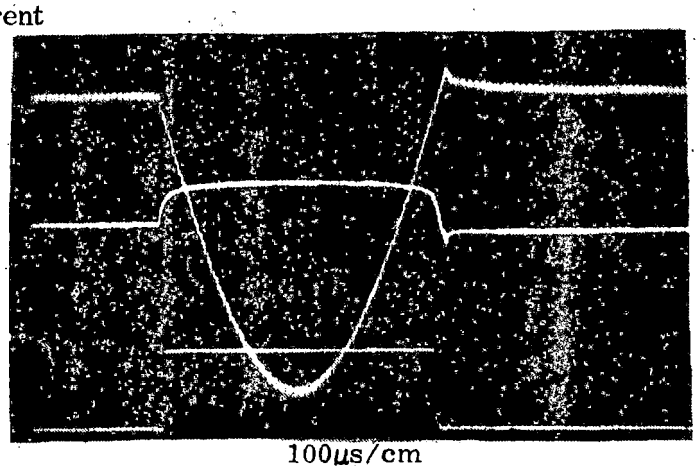

Figure 6.2-3. Typical Diode Current Sensor Signals

6.2.3 FIELD SUPPLY MODULE

The field supply module contains a field supply transformer, 3.0μF coupling capacitors, power control relay, signal rectifier and relay, and various resistors.

6.2.3.1 Field Supply Transformer

The field supply transformer consists of three sets of windings on a three-phase core. The turns ratio and phasing at the braking field windings (144t/36t) and the motoring field windings (3t/36t) were verified by applying a voltage of 14.4 Vrms at 1000 Hz to the 144 turn windings and measuring the amplitude and phase of the signal on the 3t and 36t windings.

6.2.3.2 Coupling Capacitors

The capacitance and dissipation factor of the 3.0μF capacitors which energize the 144 turn braking field windings was measured at 1000 Hz. Capacitance ranged from 2.85μF to 2.96μF with dissipation factor from 0.0045 to 0.005. Leakage current was 23.5μA at 600 Vdc for the three capacitors.

6.2.3.3 Power Control Relay

The power control relay connects the 144 turn braking windings to the inverter via the 3.0 μF capacitors in the brake module and the 80μF inverter-cycloconverter coupling capacitor sections of the capacitor module. The relay pull-in and drop-out voltages of 12.7 Vdc and 3.6 Vdc were measured and contact closures were verified.

6.2.3.4 Signal Relay

The signal relay provides a contact closure to indicate overvoltage on the secondary of the field supply transformer. A pull-in voltage of 11.25 V at 53 mA was measured and the contact closure was verified.

6.2.4 CYCLOCONVERTER MODULE

The cycloconverter module contains 18 SCR's with associated gate drivers and dV/dt and transient suppression circuits. SCR voltage sensing circuits were originally installed in the module but were later removed when a change to synchronous gating was made during system testing (see Section 6.3).

6.2.4.1 Gate Driver Circuits

The gate driver circuits were energized with a 30 kHz, 56 V-pp square wave and pulsed on by means of a pulldown transistor operating on the circuit signal input (see Figure 5.6-20.) The pulldown transistor was energized with a 50 Hz 1.4 ms pulse. Typical SCR gate current waveforms are shown superimposed in Figure 6.2-4. The waveforms show a risetime of 2.5 μs to 0.3 A. This risetime was adequate with the dc (unsynchronized) gating originally employed in the Test Article cycloconverter.

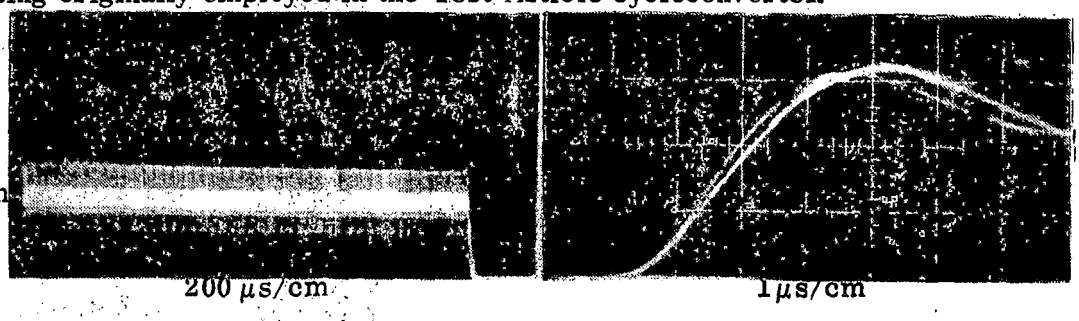

Figure 6.2-4. Cycloconverter Gate Current Waveforms

Isolation of the gate drive transformer secondaries from logic grounds was determined by applying 1600 Vdc from the cycloconverter power terminals to logic ground. Leakage current ranged from 58 μA to 60 μA. Isolation from the high voltage terminals to the chassis was also measured at 1600 Vdc. Leakage current ranged from 90 μA to 100 μA.

6.2.4.2 Cycloconverter SCR's

The forward and reverse SCR leakage currents were measured at room temperature with 1800 Vdc applied. Leakage currents ranged from 13 μA to 375 μA, following replacement of one SCR having excessive leakage current.

Gate current-to-trigger was measured at room temperature. This current ranged from 29.0 μA to 124 μA.

6.2.4.3 dV/dt Suppression Circuits

The dV/dt circuits were exercised with a curve tracer to ensure proper circuit connections and component characteristics. A typical volt-ampere characteristic is shown in Figure 6.2-5.

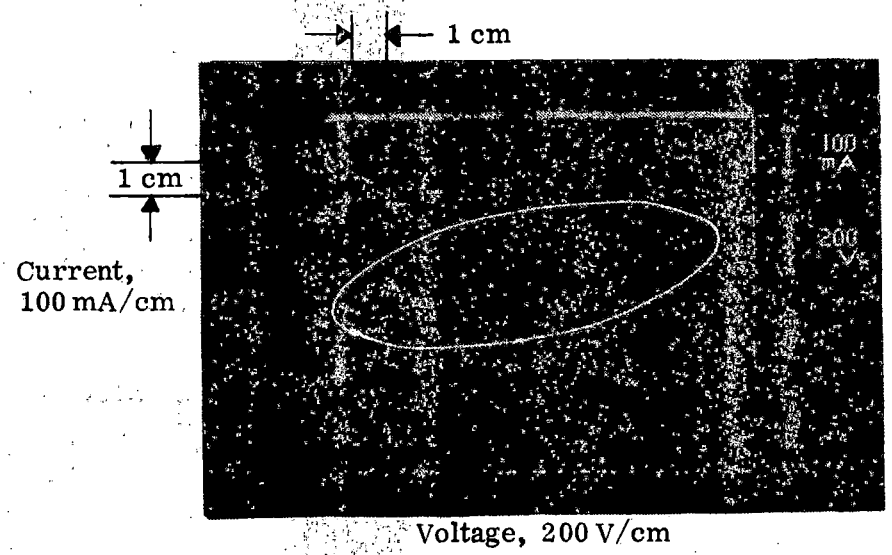

Figure 6.2-5. Typical Cycloconverter dV/dt Circuit Characteristic

6.2.4.4 Surge Suppressors

The surge suppressors are avalanche diodes having similar forward and reverse blocking characteristics. Avalanche current commences at approximately 1600 V. Because of circuit capacitance, the curve tracer was unable to provide adequate sweep voltage to reach the avalanche condition.

6.2.4.5 SCR Voltage Sensors

The nine voltage sensors are placed across the anti-parallel pairs of cycloconverter SCR's. Each sensor was tested for saturation threshold by applying variable dc voltage to the sensor input terminals, noting the voltage required to reduce the output logic signal from 12.0 V to 1.0 V. The saturation threshold ranged from 28.2 V to 58.2 V.

6.2.5 BRAKE MODULE

The brake module contains the 10 SCR's and associated gate driver circuits which comprise the dual brake rectifier and brake resistor shorting SCR. The original Test Article brake rectifier circuit did not contain dV/dt circuits (this was also the case for the breadboard brake rectifier circuit). The brake module also houses the motor CEMF sensing transformer which provides cycloconverter timing signals in the motoring mode and brake rectifier timing signals in the braking mode.

6.2.5.1 Gate Driver Circuits

The brake module gate driver circuits are identical to those in the cycloconverter module. (Refer to paragraph 6.2.4.1 for a description of the gate driver test waveforms.)

Isolation of the gate drive transformer secondaries from logic ground was determined by applying 1800 Vdc from the cycloconverter power terminals to logic ground. Leakage current was less than 0.2 μA. Leakage current from the high voltage terminals to the chassis was also measured as less than 2.1 μA at 1800 Vdc.

6.2.5.2 Brake SCR's

The forward and reverse leakage currents were measured at room temperature with 1800 Vdc applied. Leakage currents ranged from 7 μA to 3.5 mA.

6.2.5.3 CEMF Sensing Transformer

The turns ratio of the transformer was checked by applying 480 $V_{\ell-\ell}$ 60 Hz 3Ø to the primary and measuring the secondary voltage with a VTVM. Phasing was checked with an oscilloscope.

The primary-to-secondary isolation of the transformer was verified during the isolation test of the gate drive transformers, since the CEMF transformer was connected in its normal manner between the high voltage terminals and logic ground during the previous test.

6.2.6 POWER CONTROL SWITCHGEAR (PCS)

Power wiring and low voltage circuits were visually checked for conformance to the PCS schematic (drawing 7558198). Additional checks of the low voltage circuits were made by means of an ohmmeter across connector terminals and manually actuating relay and contactor contacts.

The overcurrent and differential current relays were calibrated. The former was adjusted to operate at a threshold of 900 amps dc and the latter to operate with 180 amperes.

The voltage indicator was checked and found to read line voltage correctly within 2% of full scale. At the same time, the time constant of the capacitor bank/shunting resistor circuit was measured. It was found that 37 seconds were required for the voltage to decay to 50 volts. Voltage across the contactor coil (with the free-wheeling diode across the coil) was checked to be sure that voltage transients were not induced on the B+ line when the circuit to the coil was interrupted. None were present.

In general, everything was determined to be in order except for a capacitor which had been installed with reverse polarity.

6.2.7 LINE FILTER INDUCTOR

The line filter inductor was checked for values of inductance and resistance. Readings for the two windings in parallel were 5.4 mH inductance and 2.2 milliohms resistance, which were considered acceptable based on previous experience with the IR&D breadboard line filter.

6.2.8 DYNAMIC BRAKE RESISTOR

The brake resistor assembly was checked for resistance, dielectric strength, and weight. Resistances measured were 0.76 and 0.26 ohms, which were within specification limits. Dielectric strength was determined to be adequate, withstanding 1700 volts rms referenced to the frame for one minute without any sign of breakdown.

6.2.9 ROTOR POSITION SENSOR

Functional tests were not performed on the rotor position sensor until installed on a Test Article motor, since a special fixture would have been required. However, as a result of dynamometer testing the design was changed to make the sensor more robust. This involved increasing the wire size to No. 24 AWG and decreasing the number of turns per coil to 125. This also had the effect of lowering the impedance, making the device less sensitive to noise.

6.2.10 COOLANT FLOW TESTS

Flow tests were conducted of the propulsion power control modules to determine the pressure drop as a function of flow rate for each module and to compare the results with the design flow rates.

The measured pressure drop characteristics are shown in Figure 6.2-6. The measured flows are compared to the design flows below:

Module	Design Flow - gpm	Actual Flow - gpm
Capacitor	2	1.55
Brake	3.3	2.35
Resonator Inductor	2.7	3.25
Cycloconverter	6	6.1
Inverter	6	6.8

Note: 20 gpm total, 60 psi drop, 80° flow temperature

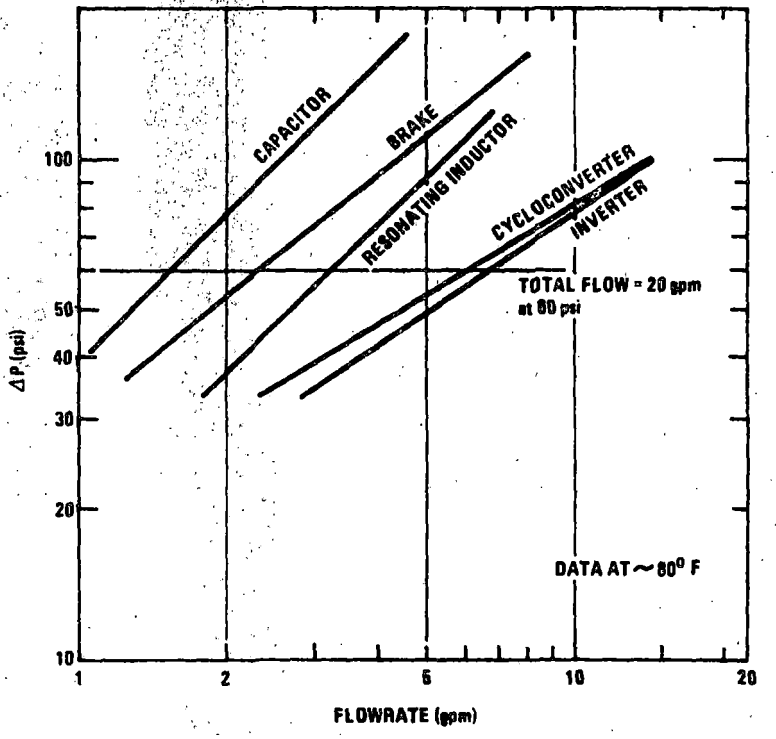

Figure 6.2-6. PPCE Module Pressure Loss Versus Flowrate

Differences from the predicted flows were attributed primarily to changes in the groove shape found necessary for fabrication purposes. In making these changes, care was taken to insure that the flow in the critical inverter module was at least 6 gpm. Flow in the brake module, which was the only module with sensitive components that had a reduced rate, was considered acceptable due to its relatively short duty cycle.

The Test Article equipment testing to date has verified that the actual flow rates are acceptable.

6.2.11 TRAIN CONTROL ELECTRONICS

6.2.11.1 TCE Component and Board Checkout

When the CPU and I/O boards were wired, parts were inserted and interconnect testing was begun. A short, simple program, shown below, was programmed in a 2708 and located at the power-up start point.

```
0000    3C          Start  INR A
0001    D3 00              OUT 0
0003    C3 0000            JMP START
```

Initial Test Program

A Pro-Log M800 system analyzer was utilized to insure that the program ran properly. The teletype was then connected to the GSE socket, forcing program operation (via interrupt) to jump to the supervisor subroutine. The teletype was not an active interface to the system. This was utilized to enter simple tests to allow checkout of all memory and I/O.

6.2.11.2 Software Checkout

When this procedure was completed the various routines of the operational program were entered. The READ routine was inhibited during this phase of the checkout. This allowed control of the input variables through the use of the teletype. To check a routine, known values of variables were entered and program operation verified with the analyzer. By controlling the variables in this manner, all subroutine operations were verified.

6.2.11.3 Test Console Testing and Operation

A test console was built to simulate a single TCE with train signal interfaces. A 36 Vdc inverter is used to supply power to the entire test console. The 36 Vdc is then converted down to ±5 Vdc, +12 Vdc, and ±15 Vdc by a dc-dc converter to power the TCE. Once the ac line cord is connected, power is applied to the console by placing the power supply switch in the "ON" position.

In order to apply dc power to the TCE, the switch labeled "BATTERY" on the Master Control Panel is placed in the "ON" position. The ±5 Vdc, +12 Vdc, and ±15 Vdc power

will then be applied to the TCE boards and the system placed in an operating condition ready to receive input signals from a simulated sensor and to produce outputs to their respective lines.

The simulator panel in the lab test console can be used to produce test signals and conditions as inputs to the microprocessor to check the software and hardware for proper operation. This panel is shown in drawing TF200206 (Figure 6.2-7). All inputs shown on the panel were checked with the train control for operation only.

The test panel consists of analog and discrete signals. It has the capability of individually switching each of the panel controls to act as an input to the train control or switching to the actual system parameter. As an example, V sub L is the input voltage to the power control switchgear contactor. If it is not within 400--700 volts dc the train control will not permit the power transistors to turn on the main contactor. By switching the V sub L switch to Var/Cal position (variable-calibration) the panel can simulate any desired voltage (read on the meter in the center of the panel), if the toggle switch under the meter is in Sel-2 position and if the rotary switch is set to V_L. Then, by sweeping from 330--800 volts it can be seen whether contactor pick-up occurs at 400 volts and if drop-out occurs at 700 volts. Similar tests are possible with all the discrete switches.

6.2.12 TRACTION MOTOR

Most of the traction motor testing was conducted by the supplier, Delco Products, Dayton, Ohio. The evaluation of motor performance in conjunction with the ASDP drive electronics, however, was performed at Delco Electronics during the system level testing described in subsection 6.3. In addition, all high speed testing was conducted at Delco Electronics due to dynamometer equipment limitations at Delco Products. The traction motor testing is discussed in detail in the "Traction Motor Final Report," Delco Electronics Report No. R78-15.

6.2.12.1 Tests Conducted at Delco Products

One traction motor was subjected to extensive testing to demonstrate compliance with requirements and to establish various performance characteristics for future reference.

The tests were conducted in accordance with Delco Products Design Verification Test Procedure T-668. Results indicated that all requirements were met. The tests conducted and the significant results obtained are summarized in the following paragraphs.

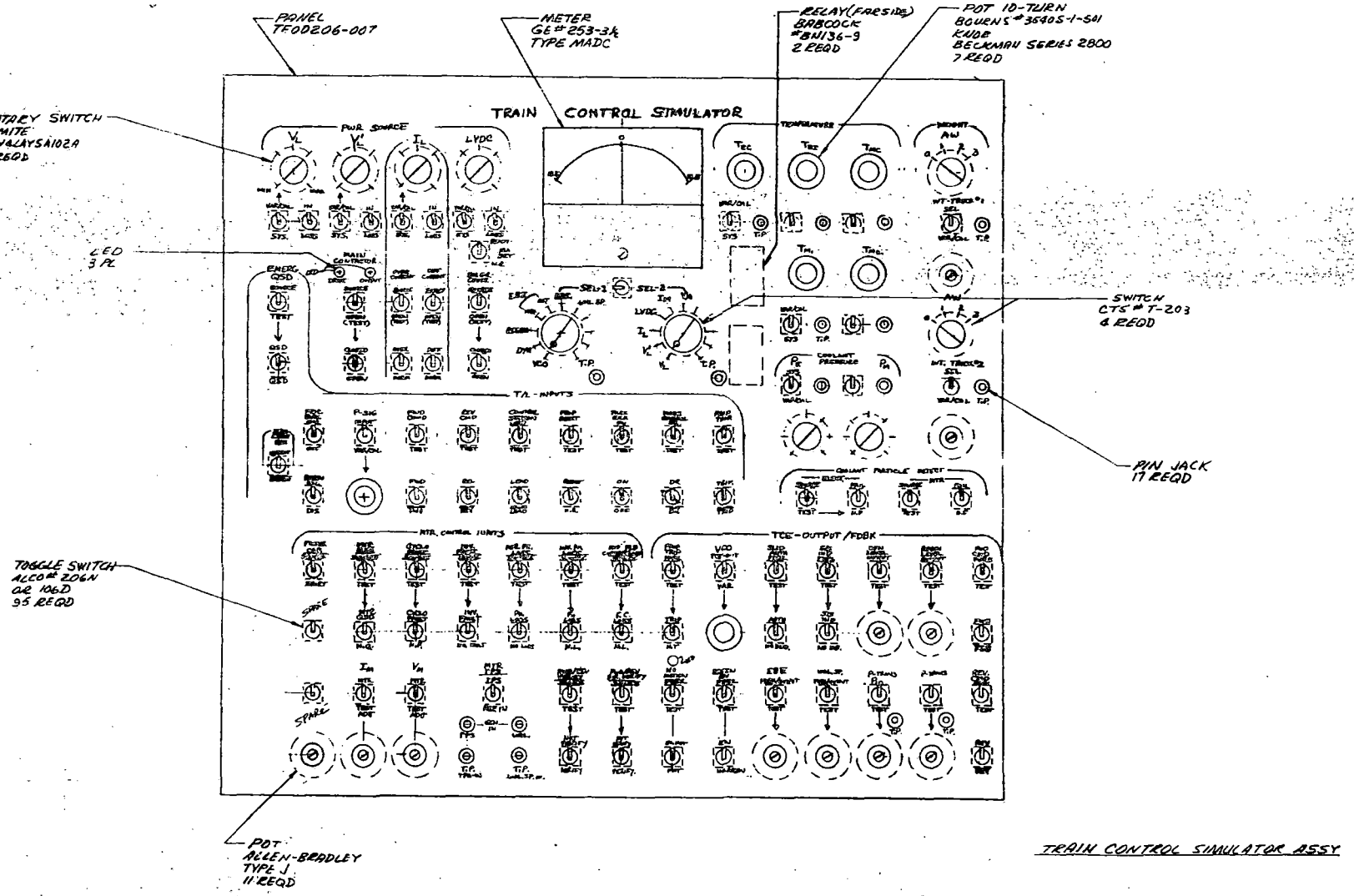

Figure 6.2-7 Simulator Panel

Summary of Motor Tests Conducted at Delco Products

- Insulation Resistance
  - Rotating transformer primary tested infinite.
  - Rotating transformer secondary tested infinite.
  - Rotating field coils tested infinite.
  - Motor stator tested infinite.
- Dielectric Strength
  - Rotating transformer primary passed 2750 volt test.
  - Rotating transformer secondary passed 1250 volt test.
  - Rotating field coils passed 1250 volt test.
  - Motor stator passed 2750 volt test.
- Resistance Measurements

- Rotary transformer primary	0.0202 - 0.0204 ohms
- Rotary transformer secondary	0.0162 - 0.0163 ohms
- Rotating field	1.99 ohms
- Motor stator	0.0227 - 0.0228 ohms

- Moment of Inertia

  The inertia was tested to be 2.465 lb-ft-sec^2.

- Overspeed

  The rotor successfully passed an overspeed test of 6720 rpm for 2 minutes at a temperature of 158^{o}F with no distortion of parts.

- Rotary Transformer and Rectifier

  Output voltage was measured as a function of input voltage and current at seven speeds between 0 and 6000 rpm. No load saturation data was obtained at 1646 rpm for two phase sequences.

- Motor Magnetic Circuit (Slip Ring Tests)
  - No load saturation data at 1000, 1646, 2000, 3000 rpm
  - Main stator voltage as a function of input amps at four speeds
  - Core loss data at three speeds
  - Generator load points at two speeds and four different loads

- Motor load points at 1800 rpm and four loads
- Temperature run at 1800 rpm, 1105 lb-ft and 428 volts.

• No Load Saturation Tests on Complete Motor

- Output voltage as a function of input voltage at four speeds
- Output voltage as a function of input current at four speeds
- No load saturation data for reversible operation
- Core loss data at four speeds
- Core loss data for reversible operation.

• Coolant Losses

Coolant losses were measured at 15 gpm for speeds up to 3000 rpm. No oil level change was noticed.

• Capability as an Alternator

- Load Point: 3000 rpm, 1405 lb-ft output fed into a 3-phase full wave rectifier connected to a 0.79 ohm resistor. Efficiency tested 94.5 percent.
- Load points at two speeds and several different loads
- With the machine at 1646 rpm and no load, 39.7 amps ac are required in the transformer primary to obtain 405 volts ac (600 volts dc) on the stator output.

• Thermal Capability

- The machine was operated at a speed of 1800 rpm and a torque output of 1105 lb-ft at 428 volts.
- Main stator temperature rise was 80.5°C.
- Primary transformer temperature rise was 7°C.

• Power Output and Efficiency

Motor load point: 1800 rpm, 489 hp. Efficiency tested 95.1 percent.

- Load points at several percent loads were also taken.

- Stator Inductance Measurements
  - Stator leakage inductance was tested to be from 400 microhenries up to 540 microhenries.
  - Primary transformer leakage inductance was tested to be from 550 microhenries up to 605 microhenries.
- Weight

  1908 pounds.

6.2.12.2 Tests Conducted at Delco Electronics

Validation of traction motor performance capability was completed at Delco Electronics - Santa Barbara Operations using the ASDP power electronics to drive the motor. These motor tests were part of the system level testing.

During the system level testing, a large number of data points were obtained at gradually increasing power level. The demonstrated test results for both motoring and braking modes of operation are illustrated in Figure 6.2-8.

Motoring Tests

The final series of system laboratory test data are summarized here to illustrate motor performance capability. The ASDP drive system was operated with the automatic power factor advance circuit. Due to the limitations in dynamometer capability, motoring tests were conducted on two separate dynamometers. The A laboratory tests covered the high speed (above 2000 rpm) operation, while the B laboratory tests evaluated high torque/ low speed performance.

A representative set of data points are plotted in Figure 6.2-9 comparing the test results with specification requirements.

Braking Tests

Dynamic braking tests were also conducted as part of the systems laboratory testing. Two basic data sets were taken. In one set, torque at each speed was controlled by varying motor field excitation which is accomplished by controlling VCO frequency. In the other, field excitation was maintained at a constant level and phase gating of the brake module SCR's was varied. No testing was accomplished in the regenerative braking mode.

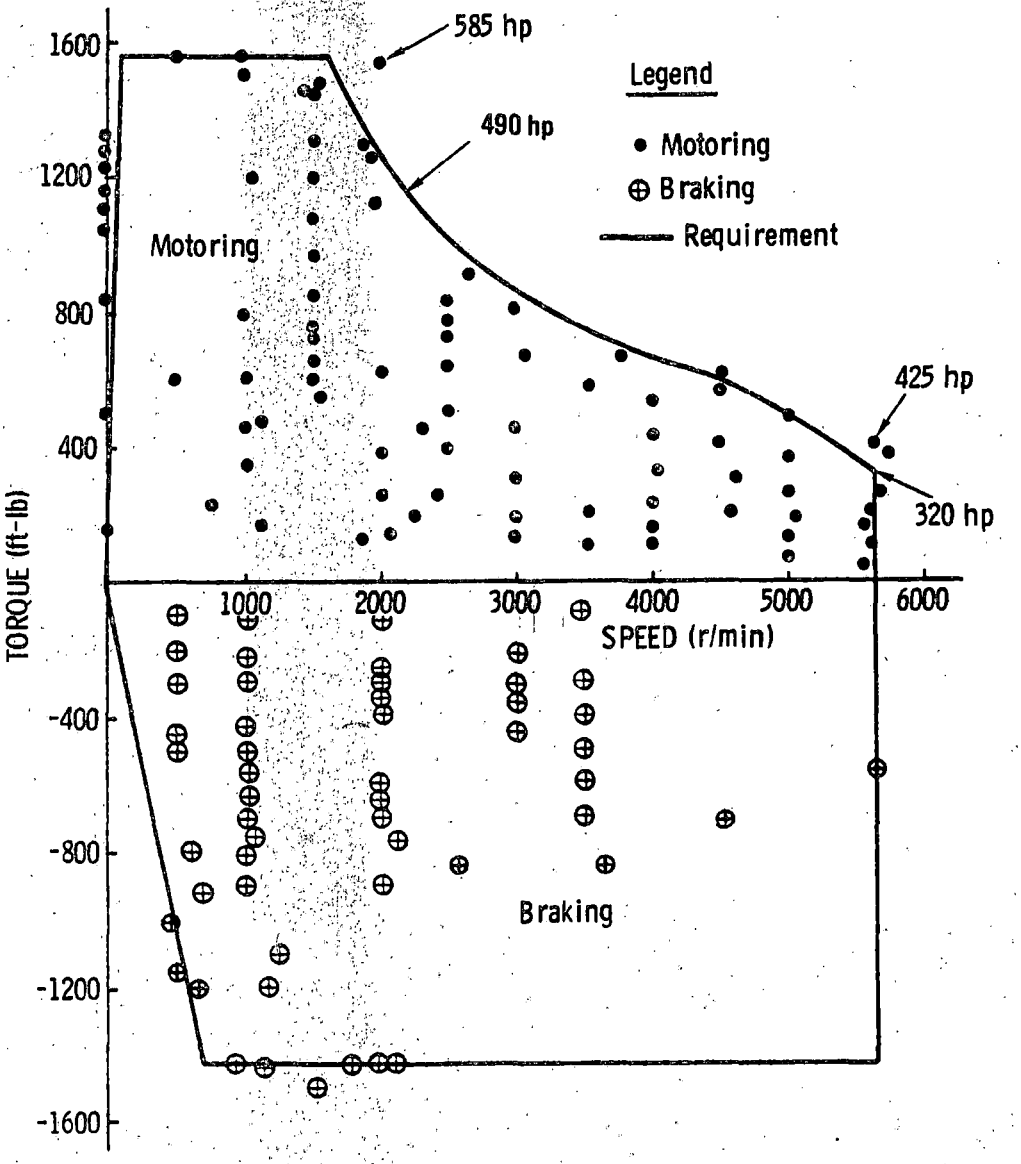

Figure 6.2-8. Demonstrated Motoring/Braking Test Results

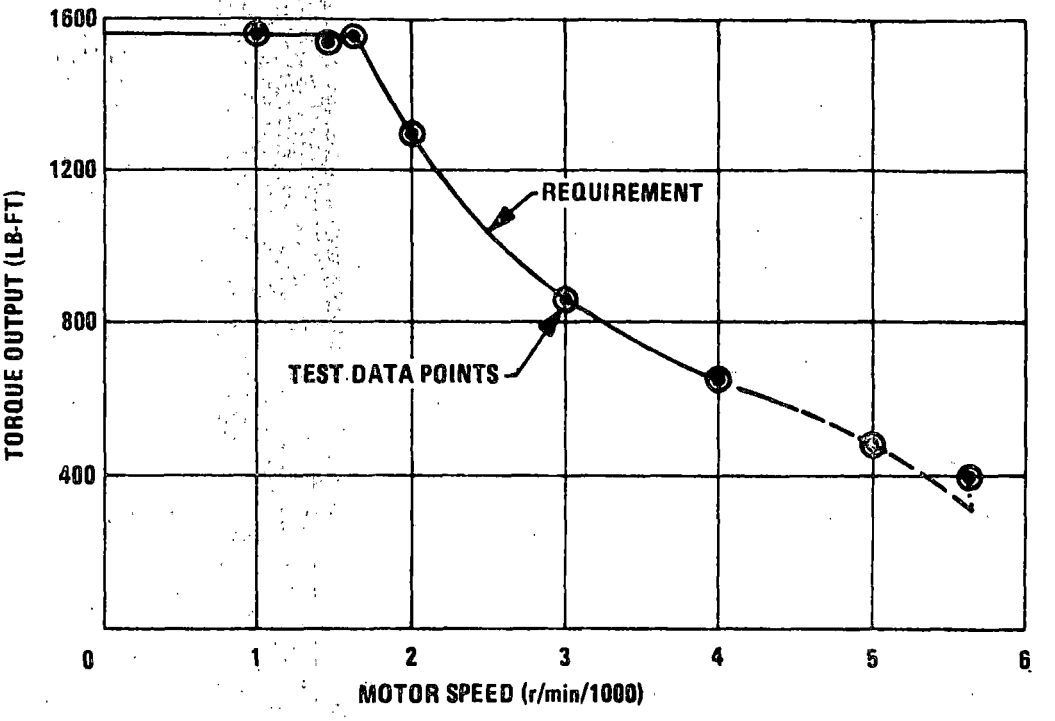

Figure 6.2-9. Motoring Torque Requirements and Capabilities

Dynamic braking test results included 491 separate data points. Recorded parameters were torque, speed, brake grid voltage, motor line-to-line voltage, phase current, SCR peak voltage, motor field excitation, etc.

A composite plot of the maximum dynamic braking torque achieved in laboratory system testing is shown in Figure 6.2-10.

The points plotted are the highest torque points tested, but they do not represent the maximum capability of the system. The absence of data in the high torque, high speed corner of the plot was due to A laboratory dynamometer limitations. Analysis and extrapolation of the data indicates that the full braking torque specified for the system can be realized in the dynamic braking mode throughout the entire speed range. As shown in Figure 6.2-10, full braking torque was not attained at the low and high speed corners of the envelopes. The field current used in these tests was limited to approximately 36 A; by increasing the field current to 50 A, which is within the capability of the traction motor for intermittent duty operation, the full braking torque could be obtained.

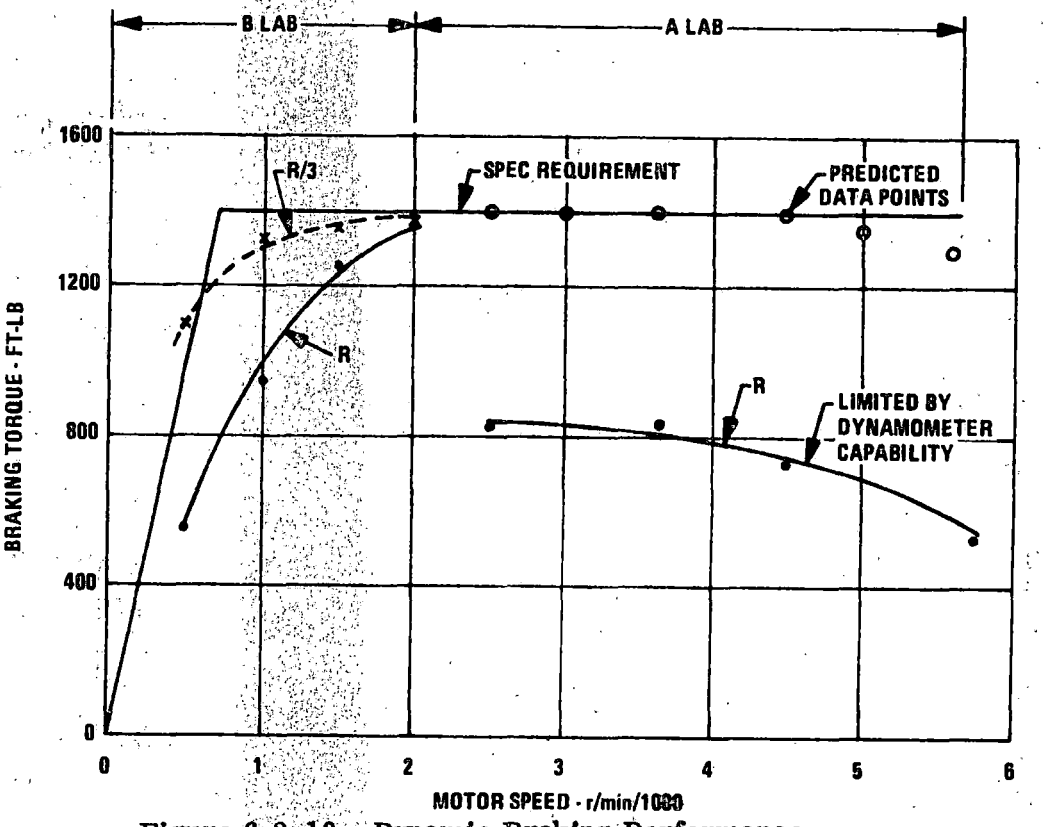

Figure 6.2-10. Dynamic Braking Performance

6.2.13 GEAR DRIVE AND AXLE COUPLING

All performance testing on the gear drive and axle coupling assembly was conducted by the subcontractor Thyssen-Henschel of West Germany. A simple test to assure compatibility of the gear drive with the traction motor and motor/gearbox coupling was performed by Delco - Santa Barbara Operations.

Detailed discussions of the complete test program are included in Delco Electronics Report R78-16, "Gear Drive and Axle Coupling Final Report."

A summary of the testing is given in the following paragraphs.

6.2.13.1 Engineering Tests

Engineering tests were conducted to support the design and to provide assurance that qualification test requirements would be met.

Prequalification tests were performed using the first two gear drive assemblies manufactured in a test simulating typical transit car duty cycle operation. After approximately 14 hours of test time some evidence of gear scoring was observed. As a result, the hypoid gear set was redesigned by increasing face width and optimizing tooth profile. Overspeed tests at 1045 rpm (as compared to a nominal 960 rpm maximum) axle speed were successfully completed at various axle displacements.

Acoustic noise tests conducted in an acoustically isolated chamber and also in the open laboratory indicated that the 82 dBA noise specification can be met.

Motor/Coupling/Gear Drive compatibility tests verified the proper fit and function of these three assemblies. A sweep through the full speed range indicated smooth, vibration-free operation.

6.2.13.2 Qualification Tests

Qualification tests were performed in two parts. The first series of tests conducted in March 1977 consisted of the following:

Normal load tests were conducted in accordance with a simulated transit car operating profile. A total of 27 hours of test time was accumulated at various axle displacements in both directions of rotation.

Endurance tests were conducted for 100 hours at constant speed and torque conditions representing the specified cubic mean axle speed and torque values.

Shock torque tests were conducted at gradually increasing axle torque values up to the maximum shock torque level specified (24,000 lb-ft). At this torque the axle coupling failed (permanent deformation and cracking of the torque tube).

A decision was made to redesign the failed component and requalify the complete gear drive and coupling assembly. The second series of qualification tests was conducted in June-July 1977 as follows:

Running-in tests (4 hours, 22 minutes)

Endurance tests (24 hours, 21 minutes) were conducted in a test program simulating a typical transit car operating profile.

High speed tests were run up to an axle speed exceeding the maximum overspeed requirements.

Shock torque tests were conducted up to the maximum axle shock torque specified.

After successfully completing above tests, the test units were disassembled and examined. All parts and components were found free from wear, deformation or cracks.

On the basis of these tests it is concluded that the ASDP Gear Drive and Axle Coupling Assembly satisfies the requirements of Delco Specification ES 11366 and that it is suitable for incorporation into the ASDP cars and will perform well in rapid transit operation.

6.2.13.3 Acceptance Tests

Each of the ten (10) deliverable gear drive assemblies was subjected to acceptance tests prior to delivery. These tests included an inspection, dimensional check and a functional run during which noise, temperature and oil seal tightness were observed. Acceptance data sheets were submitted for each of the deliverable units.

6.3 SYSTEM LEVEL TESTING

6.3.1 INTRODUCTION

6.3.1.1 Overview

The ASDP program experienced several problems during system integration and test resulting in schedule delays and cost over-runs. In retrospect, these problems were due primarily to an insufficient allocation of contingency time for the solution of possible technical problems.

Due to the extensive development effort carried out both prior to and during the early stages of the ASDP program (as discussed in subsection 6.1), it had been assumed that checkout and debugging of the prototype (Test Article) system would proceed expeditiously in a routine manner. Then formal qualification testing could proceed as planned. However, the development effort had been carried out using breadboard electronics and modified commercial motors, which fact, combined with some laboratory equipment limitations, had not permitted complete verification of all key operating concepts over the complete motoring and braking torque-speed profiles.

As a consequence, unforeseen problems arose which were difficult to troubleshoot and diagnose and which, in some cases, required extensive circuit rework to correct. This and the repair and replacement of failed components all proved to be extremely time-consuming.

6.3.1.2 Scope

The description of the laboratories facilities as discussed in the following subsection 6.3.2 is intended to provide the background and perspective essential to the subsequent discussion of system tests and problem investigations. Included is a general description of the overall facility and a general discussion of facility capabilities, limitations and test methods. Subsection 6.3.3 presents a chronological summary of motoring mode tests, related development work and problem investigation, followed by a summary of demonstrated performance characteristics. This in turn is followed by a detailed discussion of problems experienced and the status of problem solutions for the motoring mode of operation. Subsection 6.3.4 presents a discussion of braking mode testing in a manner similar to that previously outlined for the motoring mode.

6.3.2 LABORATORY FACILITIES

6.3.2.1 Equipment

The ASDP motor drive test facility consists of two dynamometer rooms isolated from a control room by reinforced concrete walls and shatter-proof windows. Figure 6.3-1 shows the facility layout.

Due to their specific capabilities and limitations, the A lab dynamometer was used for low torque operation over the entire speed range; the B lab dynamometer was used for high torque tests at speeds up to about 2000 rpm. The ASDP propulsion system control and power electronics were common to the two labs; however, separate ASDP traction motors were used in the two test setups to expedite testing.

The A lab contains a cycloconverter-controlled ac synchronous dynamometer machine connected through an in-line torque transducer and speed increasing gearbox to the motor under test, the dynamometer ac/ac power converter, and a 350 kVA multi-tap isolation transformer and rectifier to simulate a transit property dc supply. Additional A lab equipment includes ASDP propulsion system and dynamometer disconnect switches, a dynamometer field supply transformer and rectifier, and a 400 Hz m/g set control cabinet. The 500 kVA distribution transformer and the ASDP cooling assembly and brake grid, as well as the oil cooler for the dynamometer cycloconverter are installed in an open area next to the south wall. ASDP static equipment under test in the A lab consists of the line filter inductor, power control switchgear (PCS), resonating inductor, and the power converter assembly (PCA). A photograph of the A lab dynamometer machine, speed increaser, and ASDP motor under test are shown in Figure 6.3-2.

The B lab contains a dc machine dynamometer (Electro-Motive Division D-79 modified locomotive traction motor) connected through an in-line torque transducer to the motor under test, a 150 kVA isolation transformer, and dynamometer field and armature rectifiers. A photograph of the B lab dynamometer machine and an ASDP machine under test is shown in Figure 6.3-3.

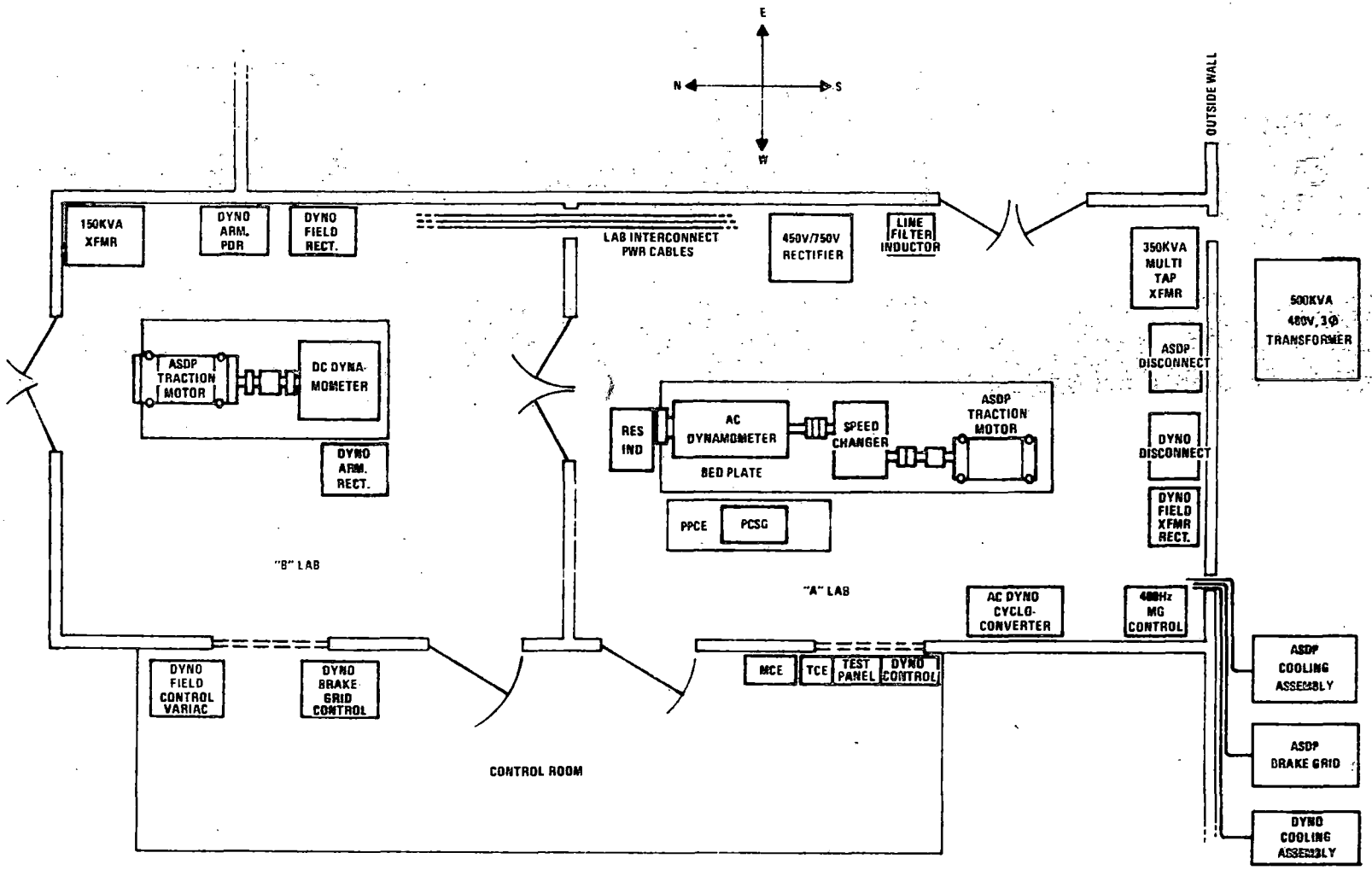

Figure 6.3-1. ASDP Laboratory Layout

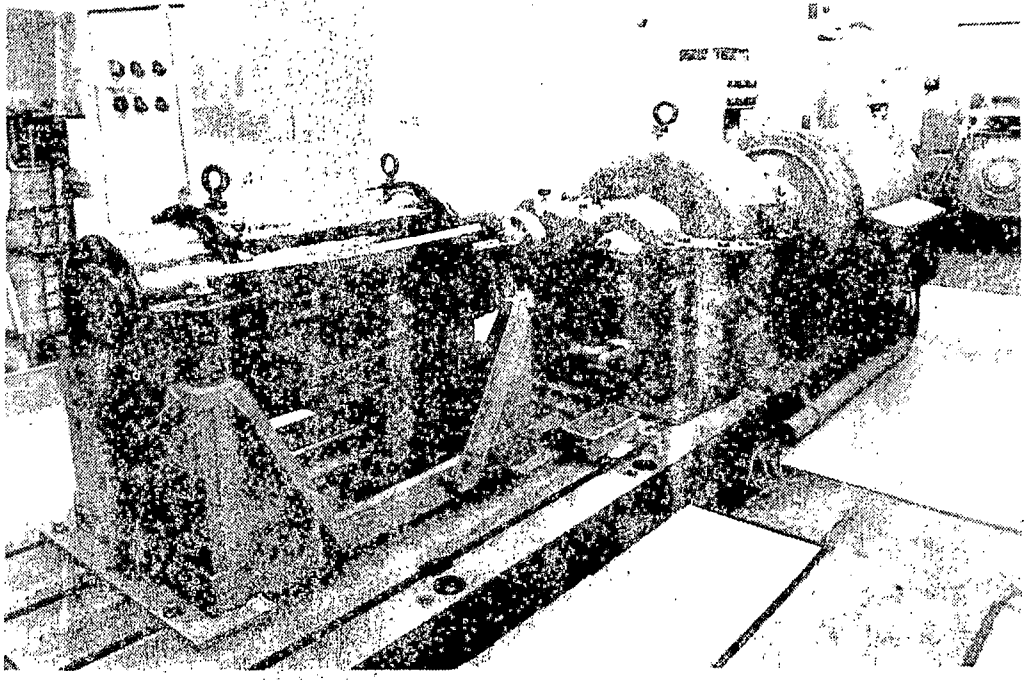

Figure 6.3-2. A Lab Rotating Equipment

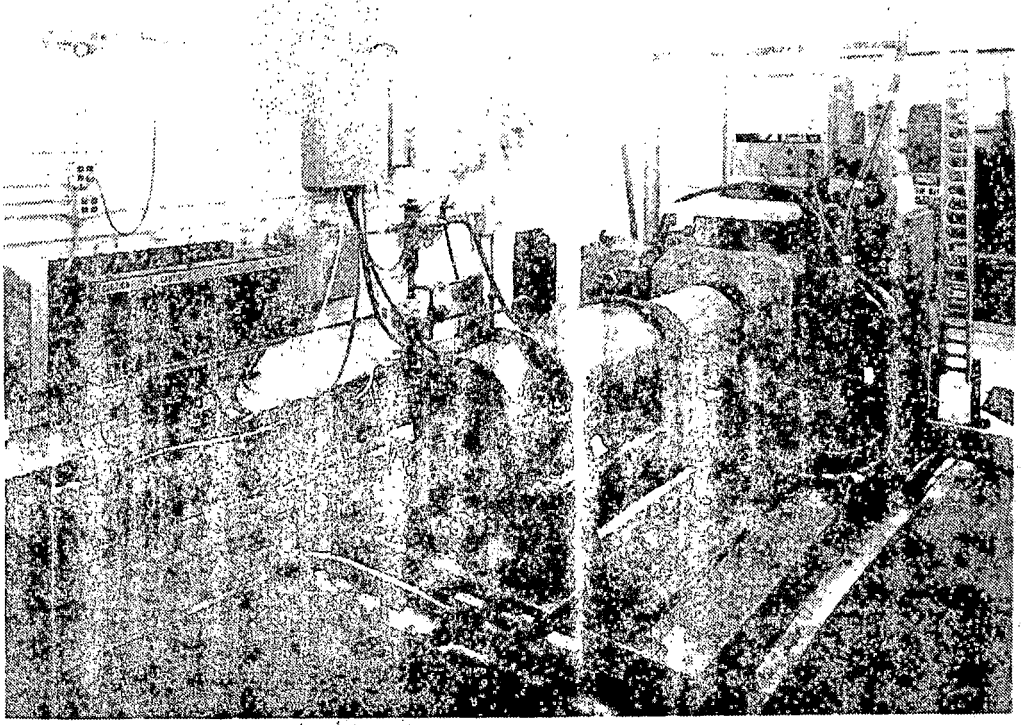

Figure 6.3-3. B Lab Rotating Equipment

The control room contains the motor control electronics (MCE) rack and a console incorporating the train control electronics (TCE) panel, the dynamometer remote control panel, and a test panel. The B lab dynamometer field supply Variac and a control panel for selecting the B lab dynamometer brake resistance are also installed in the control room. The dynamometer brake resistors with tap select relays are mounted in a weatherproof enclosure on the roof of the B lab.

6.3.2.2 A Lab Dynamometer

The A lab dynamometer is a 500 kW, 0.8 pf slip ring excited synchronous motor/generator operating from 480 V, 60 Hz power through a cycloconverter frequency changer. The dynamometer is a four-quadrant ac/ac drive with inherent regenerative braking capability. The cycloconverter-synchronous motor-utility frequency powered drive was developed with IR&D funding for application to commercial and military vehicles and industrial drives. The operation of the drive is described in Reference 10. Potential safety problems with a flywheel dynamometer approach originally proposed led to the selection of this ac/ac drive for use as a dynamometer. Key to selection of this drive approach was the ability to program torque to simulate railcar inertia, wind drag, rolling resistance, and grade. However, the ASDP propulsion system program was terminated before this capability was demonstrated.

The rated torque of the A lab dynamometer machine can be computed from its 500 kW, 1800 rpm rating as a generator. Thus

$$T_{rated} = \frac{7043\ P}{N} = \frac{7043 \times 500}{1800} = 1956 \text{ ft-lb.}$$

The presently installed speed increaser has a ratio of 3.2 so that the rated torque at the high speed shaft, assuming no gear losses is:

$$\frac{T_{rated}}{3.2} = \frac{1956}{3.2} = 611 \text{ ft-lb.}$$

The rated current of the dynamometer motor at its rated voltage of 480 V and power factor of 0.8 is:

$$i_{rated} = \frac{P}{\sqrt{3} E \cos\theta} = \frac{500}{1.73 \times 48 \times 0.8} = 753 \text{ A rms.}$$

The dynamometer was operated in motoring to a maximum torque of 1100 ft-lb on the high speed shaft, corresponding to an overload factor of 1100/611 = 1.80. The supply current required to produce this torque was approximately 1000A rms, a level that can be sustained for approximately five minutes before the input line breaker trips.

A second speed increaser was purchased to enable testing at higher traction motor torques but was not installed. This unit has a ratio of 2.373. The available peak torque at the high speed shaft with this ratio is

$$T_{max} = 1100 \left(\frac{3.2}{2.373} \right) = 1483 \text{ ft-lb},$$

which exceeds the ASDP braking torque requirement of 1405 ft-lb. With this lower ratio gearbox, the dynamometer speed at a maximum ASDP traction motor speed of 5266 r/min (corresponding to 80 mph with new wheels) is

$$N_{max} = \frac{5366}{2.373} = 2219 \text{ r/min.}$$

This represents a 23% overspeed. Discussions with the manufacturer, Delco Products Division, indicated that operating to 25% overspeed is acceptable.

The A lab ac/ac dynamometer was designed to regenerate into the 60 Hz lines. However, checkout of this braking function was not initiated until near the end of the program due to other testing priorities. Thus in the time available, it was possible only to demonstrate reliable regeneration capability to a level of a few hundred kilowatts.

6.3.2.3 B Lab Dynamometer

The B lab dynamometer equipment was installed as corporation funded capital equipment to permit high power development testing of the breadboard ASDP power converter and "workhorse" low speed synchronous traction motor previously discussed in subsection 6.1. The Electro-Motive Division D-79 dc motor/generator has a torque capability of 5000 ft-lb from zero to 1000 r/min decreasing to approximately 1500 ft-lb at 1600 r/min and to 700 ft-lb at the maximum speed of 2200 r/min. This torque capability permits testing of the ASDP machine in motoring with adequate absorption capability, but is deficient in torque from 1600 to 2200 r/min when testing the ASDP machine in braking where approximately 1400 ft-lb of torque is required at all speeds.

The D-79 machine can be operated from zero to maximum speed in motoring at restricted power levels by using the fully controlled six SCR phase delay rectifier (PDR) which is powered from the 150 kVA isolation transformer. For higher power testing, 3 phase 480 V power from the A lab 350 kVA multi-tap transformer is cabled over to an uncontrolled rectifier in the B lab. In this mode, the dc motor is started by means of a contactor controlled starting resistor. The motor speed is varied with field current control obtained from a Variac and rectifier.

As a braking generator, the D-79 can be operated into a resistor grid having a contactor controlled resistance value, or it can regenerate into the 600 Vdc ASDP bus, with a considerable savings in laboratory power.

6.3.2.4 Laboratory Instrumentation

Torque and speed in the A and B labs are measured with in-line Lebow model 1106 strain gage torque transducers, each equipped with a 60-tooth gear and an Airpax speed pickup. The torque transducer signal conditioners provide RF excitation to the strain gage bridges and synchronous detection of the bridge output signals. Speed in r/min is indicated by frequency counters operating on the speed pickup signals.

Direct current (dc) into the ASDP power control electronics and D-79 dynamometer is measured with a blade-type shunt and a digital voltmeter. Voltages are indicated with conventional 4-1/2-inch panel meters having d'Arsonval movements. For more accurate measurements, where required, dc voltage is measured with a digital voltmeter.

Alternating-current (ac) motor phase currents are measured with commercial current transformers rated for 5.0A secondary current. The response of these transformers is somewhat questionable below 10 Hz. The transformer secondary current is indicated by 4-1/2-inch panel meters having iron-vane movements. These meters indicate true rms and have reasonably wide bandwidth. Motor phase current readings are not used for power determinations; hence high absolute accuracy is not a requirement.

Alternating current motor line voltages were monitored on 4-1/2-inch panel meters having iron-vane movements. For accurate readings at frequencies other than 60 Hz, rectifier-d'Arsonval movement panel meters were utilized.

Torque transducers were calibrated by applying known torques to the locked transducer shaft. Offset and slope correction factors were computed to permit calculation of the corrected torque as

$$T_{corrected} = a + bT_{indicated}.$$

6.3.3 MOTORING MODE SYSTEM LEVEL TESTS

6.3.3.1 Introduction – Chronological Summary

Operation and checkout of the integrated ASDP propulsion system in preparation for motoring mode testing was initiated in February 1977. An early problem was the clearing (blowing) of fuses in series with the filter capacitors in the power control switchgear, due to the high surge current required to charge the capacitors. This problem was circumvented by using larger fuses and by clamping the line filter inductor by placing an SCR across it. System checkout continued and, by March 15, torque levels of 200 ft-lb at 3000 rpm and 320 ft-lb at 900 rpm were achieved. Operation was not reliable however. Inverter faults and QSD's (automatic Quick Shut Down's) were being experienced and there were failures of both inverter and cycloconverter SCR's. Evidence of cycloconverter faulting, i.e., the motor was not being properly commutated, was also seen. In addition, the first of three failures had occurred of a surge protection Zener diode, mounted in parallel with the motor field winding (located on the motor rotor), which was intended to protect the field winding from excessive voltage surges. On March 15, the first of several motor bearing failures was experienced. (Subsequent failures were not seen, however, until much later in the program.)

It was determined that the ultimate solution of providing adequate electrical surge protection for the motor would entail the installation of a "crowbar" circuit in the motor.

Due to the long lead time associated with this type of circuit modification, a decision was made to continue ASDP power electronics development work using the "workhorse" motor previously used in the development testing discussed in subsection 6.1. This motor is a 225 hp open frame motor. Electrically it is a very similar to the ASDP motor but field excitation is carried to the rotor through slip rings rather than through the rotary transformer. This motor was set up in the B lab since both the motor and the dynamometer had similar maximum speed limitations of approximately 2000 rpm.

In support of the crowbar circuit verification testing, the rotary transformer on one of the ASDP motors was replaced with a slip ring assembly. The motor was received by Delco Electronics in June and was used in various subsequent investigations.

Testing showed that the crowbar circuit was marginal, in that for some conditions of normal operation, the "crowbar" would trigger and short out the field resulting in a loss of field excitation. Solutions to this problem were developed and implemented in the traction motor.

The period of operation with the workhorse motor extended from early May to early August. Efforts were concentrated on the investigation of the previously mentioned inverter and cycloconverter problems which were preventing operation of the system at high speed and/or power levels. Table 6.3-I lists the more significant problems investigated and the solutions developed.

On August 6, the workhorse motor was replaced by an ASDP motor and tests to verify stall torque capability were initiated. While operating at stall for a period of one to two minutes at 1320 ft-lb torque and a motor current of 746 amps, the stator of the motor burned out. This was unfortunate since the motor is not, by specification or application, required to operate for extended periods of time at high levels of stall torque. It should also be noted that the motor protective circuitry normally available had been disconnected for this test. The motor was replaced and torque or time was limited procedurally in all subsequent stall tests, more realistically representing ultimate deployment. After demonstrating capability of maximum specified torque for all speeds up to 2200 rpm, the maximum speed for the dynamometer in the B lab, testing was transitioned in early August to the A lab and verification of operation at higher speeds was initiated. At higher speeds, additional problems with cycloconverter gating were experienced which led to further revisions to cycloconverter gate timing control. Furthermore, DSAS devices (high voltage, high energy Zener diodes) intended to protect the cycloconverter SCR's from voltage overstress would sometimes burn out at the instant of system shutdown from high speed operation. After this and other minor problems were circumvented or overcome, operation was demonstrated over the full specified torque/speed profile by mid-September.

ASDP COMPONENT		PROBLEM DESCRIPTION	REMARKS	SOLUTION
Cycloconverter	1)	Timing control was inadequate; permitted weak gates; permitted gating when SCR was blocking	Caused SCR failures	• Redesigned gating control to employ synchronous gating concept; gated SCR's on only after voltage on SCR was positive
	2)	SCR gate drive amplitude and rise time were inadequate	Caused SCR failures	• Redesigned gate drive electronics • Redesigned gate drive transformer and circuits • Redesigned interconnect cable • Synchronized gating with 30 kHz excitation source
	3)	120^{o} gating at low speed caused missing gate pulses	Caused SCR failures	• Inhibit 120^{o} gating at low speed
	4)	Excessive di/dt; dV/dt on SCR caused SCR failure	Caused SCR failures under "fault" conditions	• Added linear and saturating inductors between inverter and cycloconverter
Inverter	1)	SCR gate drive amplitude and rise time marginal	Potential cause of SCR failures	• Same as Item 2, for the cycloconverter
	2)	SCR recovery time was not adequate because of inverter-cycloconverter "beat" problem	Caused inverter QSD (Quick Shutdown) or inverter fault	• Changed to SCR's with devices having much faster recovery times

Table 6.3-I. Significant Problems and Solutions

With the resumption of high speed operation, additional motor bearing failures were experienced. The investigation of these bearing failures was conducted concurrently with the control and power electronic development work until late in November when a dedicated series of bearing and seal tests was initiated. (These are discussed in the ASDP Traction Motor Final Project Report, Delco No. R78-15.)

Although operation was demonstrated, as previously mentioned, over the specified torque and speed range, a number of problems, uncertainties or limitations remained. Many but not all of these remaining problems were resolved in the course of the development work that was conducted up to the point of system level test program termination on December 9. The most significant achievement of the final phase of work was the successful demonstration of operation over the complete torque/speed profile with automatic RPS ⟷ CEMF transitioning and automatic power factor advance.

Table 6.3-II presents a chronological summary relative to system development and integration as previously discussed. Also included are key events relative to the braking mode development work which will be covered in subsequent sections.

6.3.3.2 Summary of Demonstrated Motoring Performance Characteristics

6.3.3.2.1 General Description of Test Procedures

All performance verification or demonstration testing accomplished in the ASDP test laboratories was performed with the system operating "open loop." This means that data was recorded at fixed operating points defined in terms of motor torque and speed. Operating points were established by independent manual manipulation of two controls. One was a potentiometer which controlled the VCO frequency and thereby, as a rough approximation, system output power. The other control was a potentiometer which controlled dynamometer torque. Since the controls did interact, iterative pot trimming was required to arrive at a predetermined torque-speed operating point. Once an operating point was established, parameters of interest were observed and recorded, usually in a tabular log. Typical parameters included torque, speed, input voltage and current, motor voltage and current (usually one phase only), VCO frequency, motor field excitation current, motor power factor angle and inverter recovery time.

DATE	EVENT
2/8/77	Moved control electronics into ASDP motor-dynamometer lab.
2/24/77	First power-up of system
3/11/77	First rotating rectifier Zener diode failure
3/15/77	Achieved 3000 rpm, 200 ft-lb.
3/15/77	First motor bearing failure
4/18/77	Achieved 900 rpm, 320 ft-lb.
4/21/77	Second Zener diode failure (See 3/11/77 Item)
5/2/77	Third Zener diode failure (See 3/11/77 Item)
5/9/77	Initiated replacement of ASDP motor with 225 hp Delco Products Motor.
6/4/77	Initiated conversion to synchronous gating.
6/12/77	Discovered cycloconverter gate drive was inadequate; initiated redesign.
7/16/77	Added linear and saturating reactors between inverter and cycloconverter.
8/1/77	First DSAS failure (SCR overvoltage protection device)
8/2/77	726 ft-lb, 1140 rpm; 1140 ft-lb, 605 rpm } Achieved
8/2/77	Initiated testing/verification of dynamic braking mode
8/5/77	Completed braking mode SCR gate drive and control circuit modifications (similar to motoring).
8/5/77	Achieved specified motoring torque-speed to 2000 rpm using workhorse motor.
8/6/77	Replaced workhorse motor with ASDP motor.
8/28/77	1) Achieved specified dynamic braking torque to 2000 rpm and partial torque (dynamometer limited) to 3500 rpm. 2) Identified need for increased voltage rating on braking mode SCR's.
8/31/77	Installed improved motor bearing seal.
9/20/77	Achieved specified motoring torque-speed over full profile.
10/20/77	Installed fast recovery diodes in rotating rectifier circuit (to prevent false triggering of crowbar.
10/20/77	Motor bearing and seal failure analysis completed—corrections recommended
10/22/77	General requirements for power factor advance profile defined.
11/15/77	Completed dynamic braking tests to full speed and maximum torque limit of dynamometer: a. Cycloconverter overvoltage problem found and circumvented b. SCR gate drivenoise problem found and circumvented
11/15/77	Initiated installation of automatic power factor advance (PFA) control electronics.
12/8/77	Completed verification of automatic PFA.
12/9/77	Took final data set demonstrating: a. RPS <=> CEMF transitioning b. Automatic PFA control.
12/9/77	Terminated all laboratory development work.

Table 6.3-II. Chronological Summary of Events

Additional system controls were employed at various points in the development sequence either to support special investigations or to implement functions not yet automated. These included toggle switches to implement sub-modes of SCR gating control and to control RPS<->CEMF transitioning. The most significant of these was a manually set potentiometer which controlled system power factor advance (PFA). This was the last supplementary control to be eliminated by conversion to automatic PFA.

Forward planning called for "closed loop" testing but the program was terminated prior to initiation of this type of test. The planned testing required the use of a microprocessor to monitor motor current, speed and related parameters. Using these inputs the microprocessor would compute torque generated and derive an error signal from a comparison of torque generated versus torque required as commanded by the "P" signal. The error signal would then correct the VCO frequency, just as the manual potentiometer did in the open loop tests. An independent closed control loop operating through an analog representation of the railcar would have held the dynamometer to a predetermined torque or speed.

The motoring performance and system characterization data derived from open-loop testing is discussed in the following paragraphs. Only the final sets of data taken in each laboratory are presented.

6.3.3.2.2 Review of Final A Lab Performance Data

The Test Article drive system was operated in the motoring mode with the automatic power factor advance circuit operational. The motor speed was varied with the dynamometer load for each of several inverter frequencies. Quantities measured included the cycloconverter trigger angle, motor torque, and inverter SCR turn-off time. Motor output power at each inverter frequency level was computed from torque and speed.

Figure 6.3-4 is a plot of cycloconverter trigger angle β versus motor speed for inverter frequencies of 500, 800, and 1050 Hz. This angle, described in the waveform sketch in Figure 6.3-4, is the number of electrical degrees between the initiation of motor phase current and the zero crossing of the motor phase voltage, plus 30 degrees. The motor displacement power factor angle θ in terms of β and the commutation overlap angle μ (also shown in Figure 6.3-4) is

$$\theta = B - \mu/2.$$

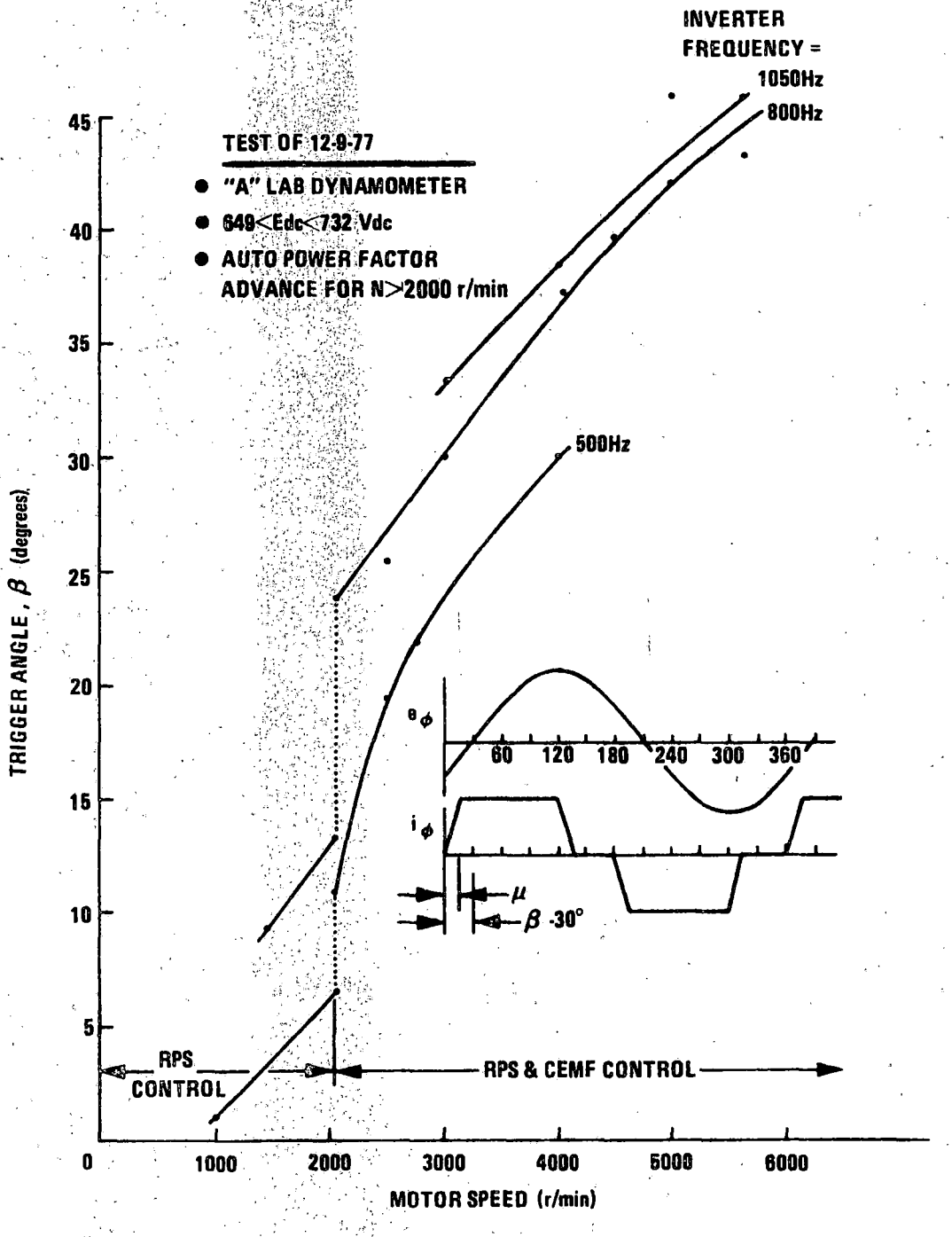

Figure 6.3-4. Cycloconverter Trigger Angle vs Speed

The power factor angle is advanced with motor speed using the polyphase CEMF signal processing technique described in Reference 7. Power factor angle advance avoids excessive motor voltage at high speed while maintaining a high torque per ampere ratio at low speed.

Problems with filtering the CEMF signals at low speed had previously arisen during high torque testing in the B lab. In this case, the CEMF noise problem was eliminated by switching out the CEMF and relying on RPS control only at speeds below 2000 r/min. This control transition was also used in the A lab and results in the discontinuities in β seen in Figure 6.3-4.

Torque versus speed is plotted for various inverter frequencies in Figure 6.3-5. Because the dynamometer machine was loaded with a rectifier and resistor load, it was not possible to maintain load torque to very low speed. At each inverter frequency, torque decreases approximately inversely with speed, with a torque discontinuity at the 2000 r/min CEMF switching point.

Shaft power versus speed is plotted in Figure 6.3-6. Power tends to be constant over a fairly broad speed range, especially for inverter frequencies below 900 Hz.

Overall system efficiency (shaft power out/dc power in) at inverter frequencies of 500, 900, and 1050 Hz is plotted in Figure 6.3-7. These frequencies represent low, medium, and high power settings. The data shows an efficiency of 80-81 percent at low power increasing to 84-85 percent at high power. Efficiency is reasonably independent of speed for speeds in excess of 2000 r/min.

6.3.3.2.3 Review of Final B Lab Performance Data

B lab motoring testing was performed for the purpose of problem diagnosis. Hence a consistent set of data taken with inverter frequency or other system parameters held constant is not available. Figure 6.3-8 shows four representative high power data points in the torque-speed plane as well as the ASDP torque versus speed requirement. The tabular data in Figure 6.3-8 also shows the inverter frequency, dc supply voltage and power, and overall efficiency for the four data points.

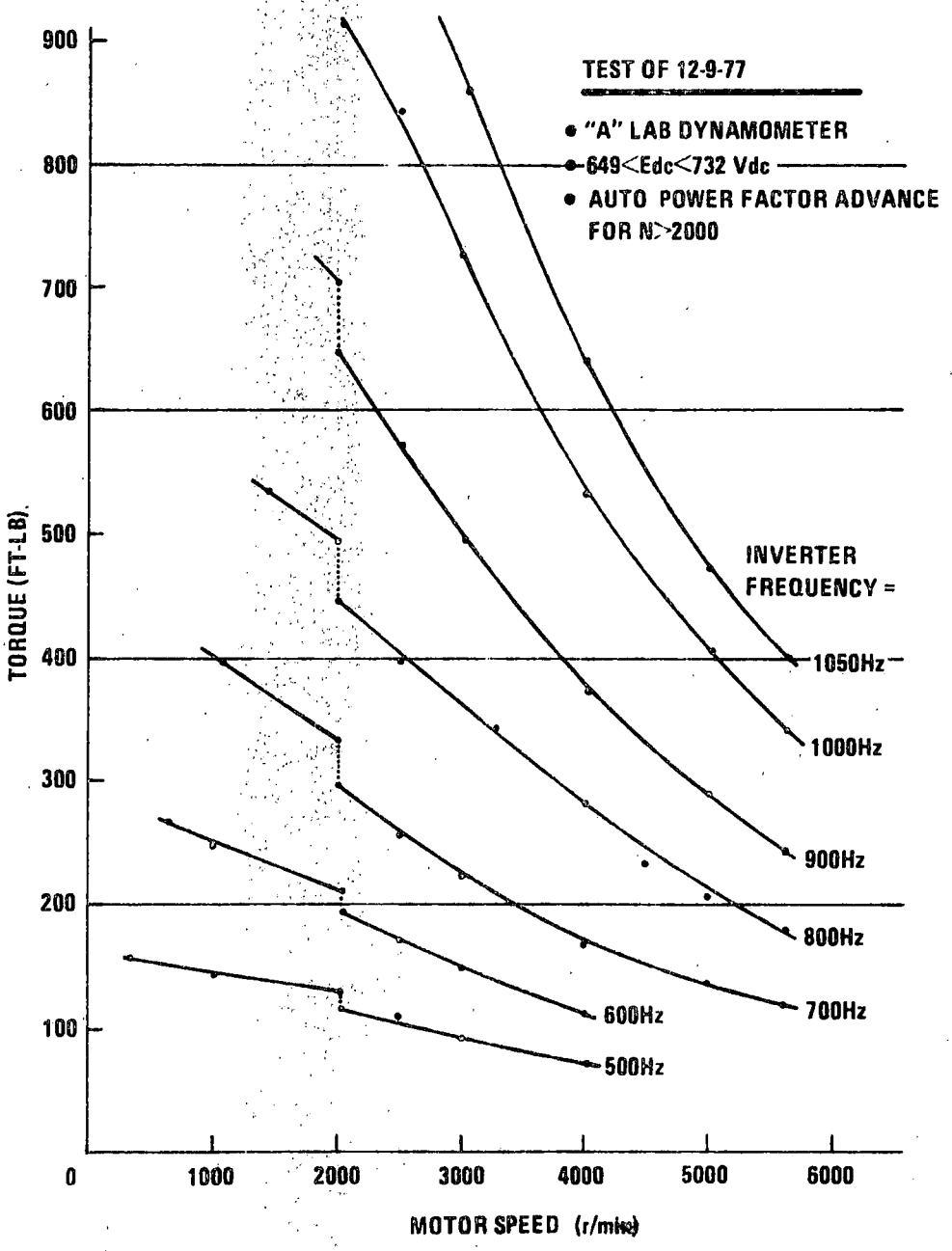

Figure 6.3-5. Torque-Speed Characteristics for Constant Inverter Frequencies

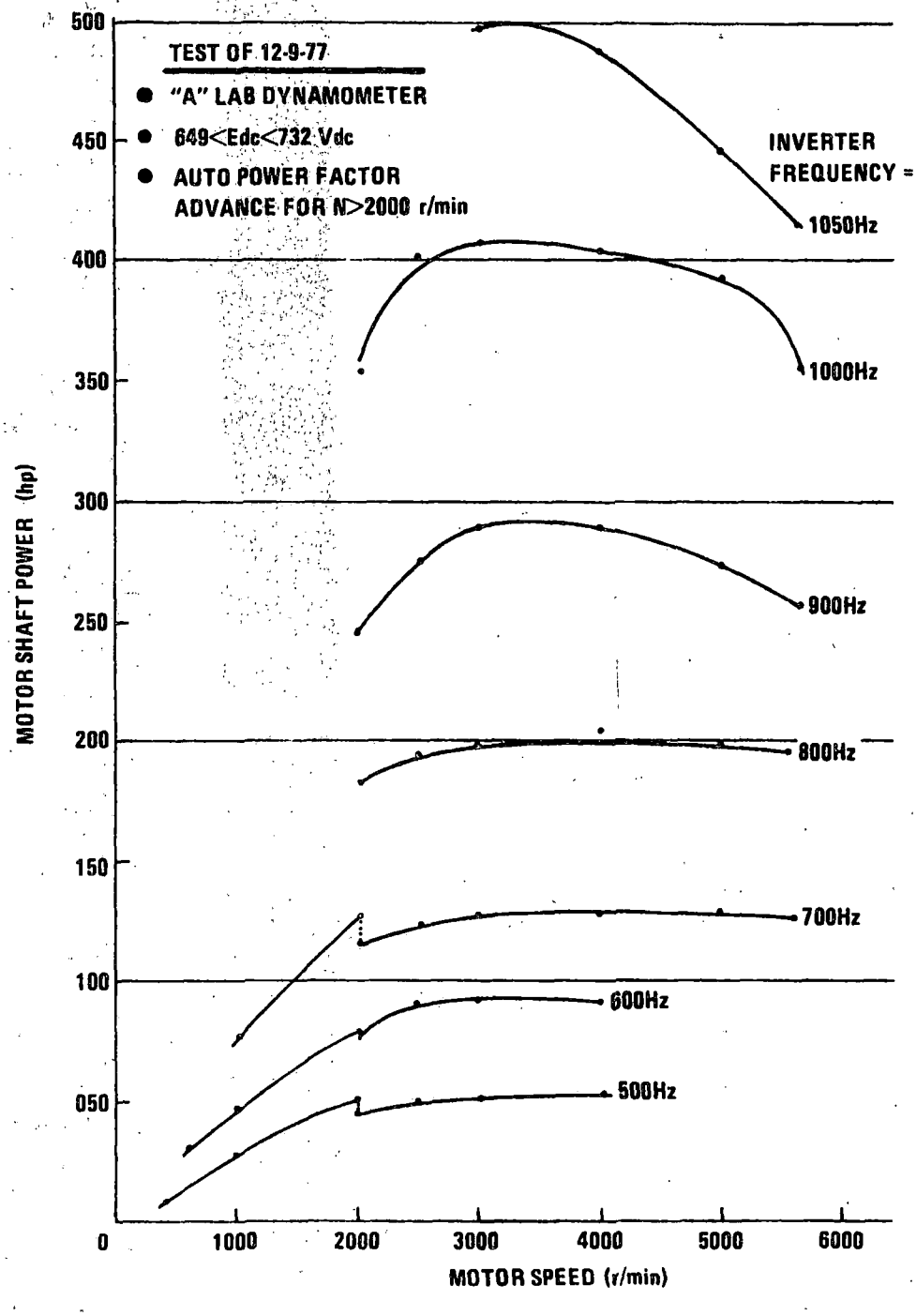

Figure 6.3-6. Power-Speed Characteristics for Constant Inverter Frequencies

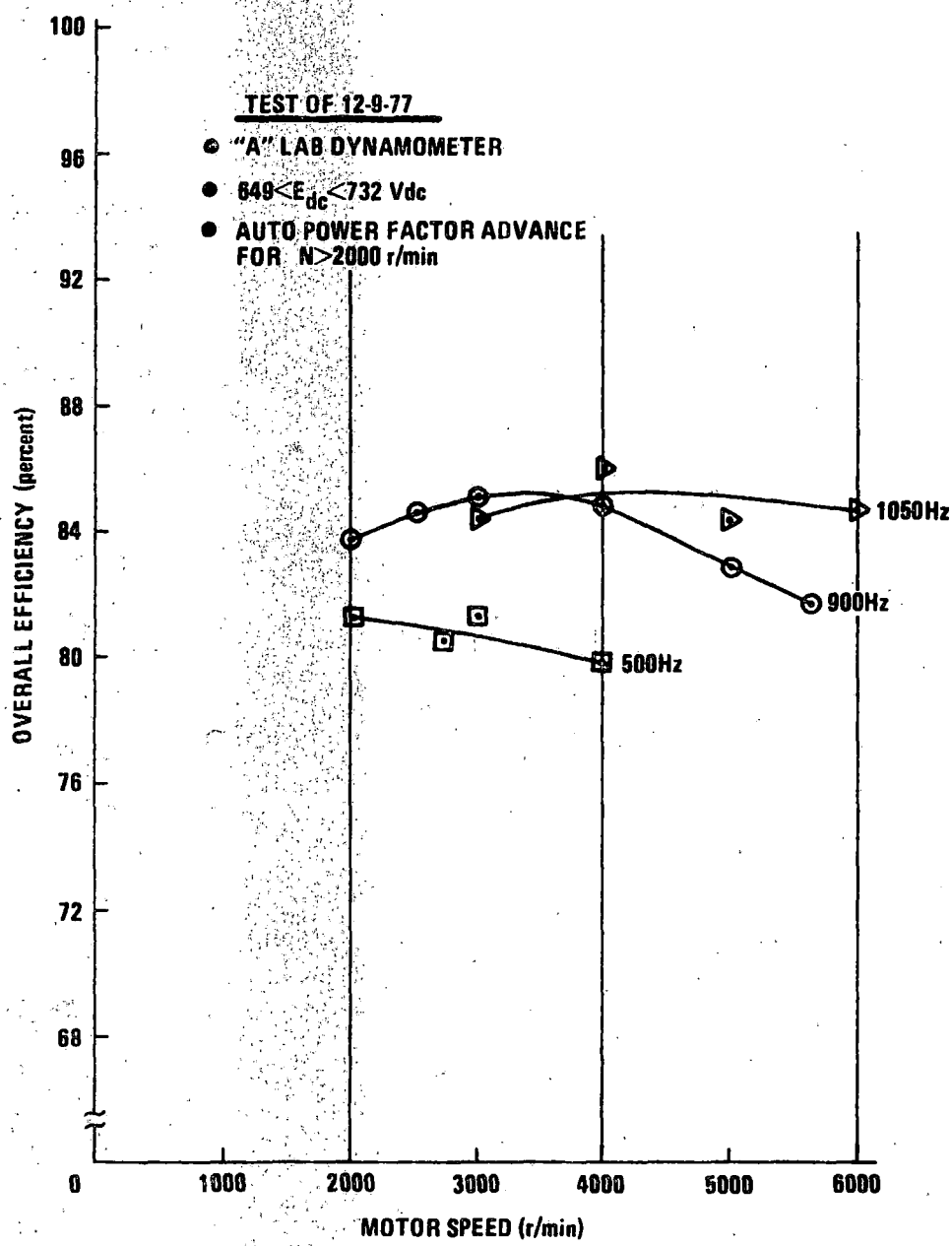

Figure 6.3-7. Overall System Efficiency Versus Speed

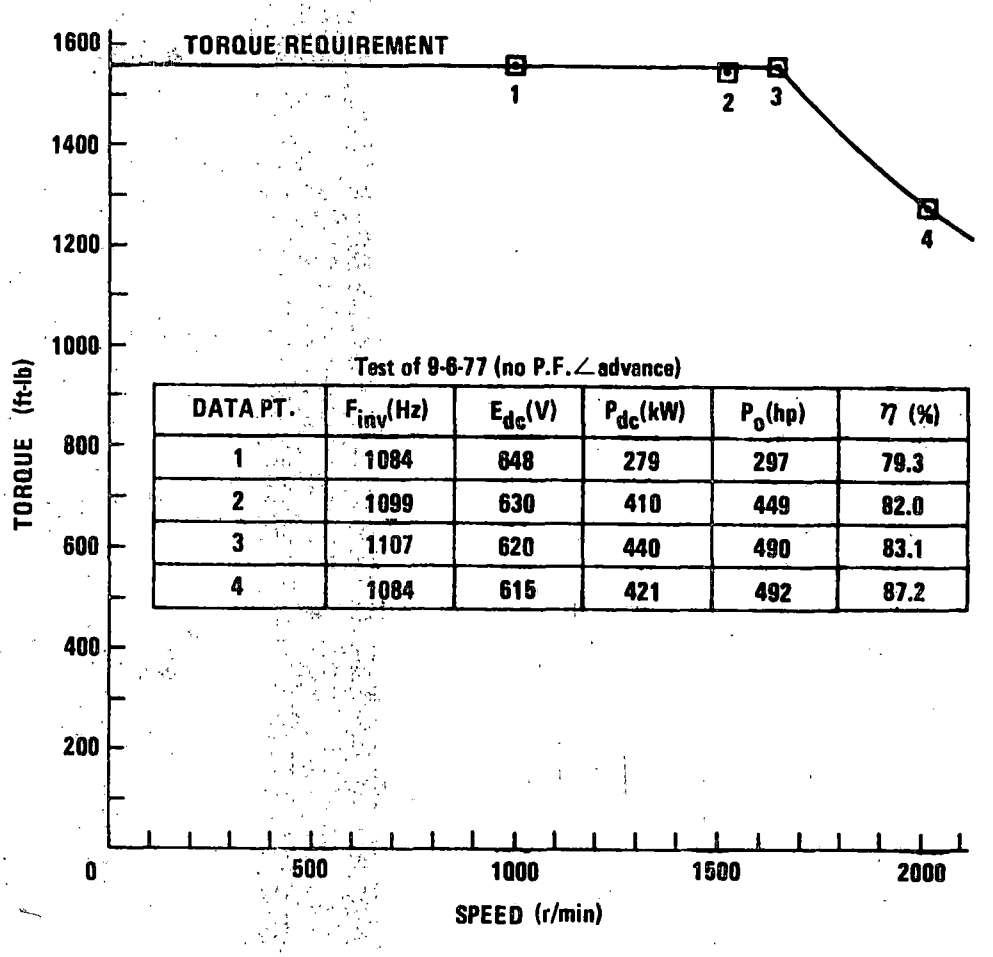

Test of 9-6-77 (no P.F.∠ advance)

DATA PT.	F_{inv}(Hz)	E_{dc}(V)	P_{dc}(kW)	P_o(hp)	η (%)
1	1084	648	279	297	79.3
2	1099	630	410	449	82.0
3	1107	620	440	490	83.1
4	1084	615	421	492	87.2

Figure 6.3-8. Representative B Lab High Power Data Points

The 1646 r/min base speed torque and power requirements of 1560 ft/lb and 490 hp are met in data point No. 3. Maximum torque is achieved with a motor current of 557 A rms. This is well within the maximum allowable current limitation of 600 A rms given in the motor specification. Drive overall efficiency increases with speed from 79.3% at 1000 r/min to 87.2% at 2016 r/min.

6.3.3.2.4 System Characterization Data

The system characterization data includes the voltage and current waveforms associated with key circuit elements. This data was taken during motoring tests in both labs.

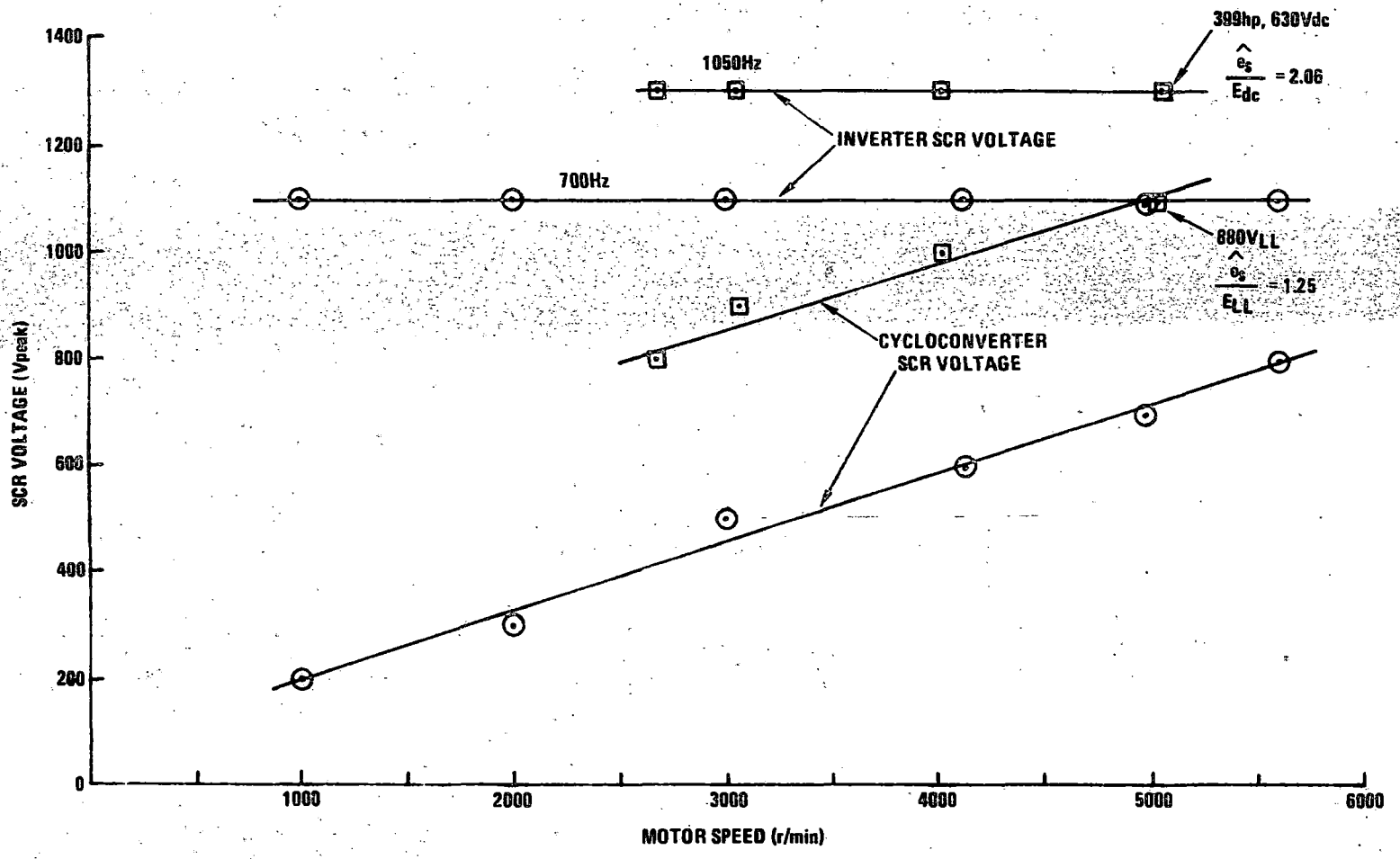

Figure 6.3-9. Peak SCR Voltage Versus Speed

SCR Blocking Voltage

Peak inverter and cycloconverter SCR blocking voltage is shown as a function of motor speed in Figure 6.3-9. The inverter SCR voltage increases with inverter frequency and is approximately independent of speed. The ratio of peak inverter SCR voltage to dc supply voltage is 2.06 at the maximum power point of 630 Vdc, 1050 Hz, 399 hp. The cycloconverter SCR voltage increases with both speed and inverter frequency. At the maximum power point, the ratio of peak SCR voltage to rms line-to-line motor voltage is 1.25.

A typical inverter SCR blocking voltage waveform is shown in Figure 6.3-10.

Motor Current and Voltage

The oscillosgrph of Figure 6.3-11 shows typical motor line voltage and phase current waveforms. The motor frequency is 116 Hz at an output power of 200 hp. The commutation overlap angle is 15^{o} and the cycloconverter trigger angle with respect to motor voltage is 21^{o}. The leading power factor angle therefore is $21 - 15/2 = 13.5^{o}$.

Cycloconverter SCR Current and Voltage

Figure 6.3-12 shows typical cycloconverter SCR voltage and current waveforms. The traces show conditions before and after the termination of conduction in a group of three SCR's. During the conducting interval, the small spike of positive SCR voltage, or finger voltage, caused by gating synchronized with the cycloconverter input voltage, is evident. Following removal of gating, the SCR first blocks reverse voltage and then blocks forward voltage. The SCR current pulse is 120^{o} on, 240^{o} off. A resonant oscillation is evident at the leading edge of the current pulse. This oscillation is due to resonance between the cycloconverter input coupling capacitance and the field supply transformer inductance, added linear inductance in series with the transformer and the motor leakage inductance. The oscillation vanishes at higher power levels.

Field Supply Transformer

In the motoring mode, the field supply transformer produces a secondary current proportional to the cycloconverter input current. The cycloconverter converts the transformer primary current into motor stator current of the same amplitude with lower frequency.

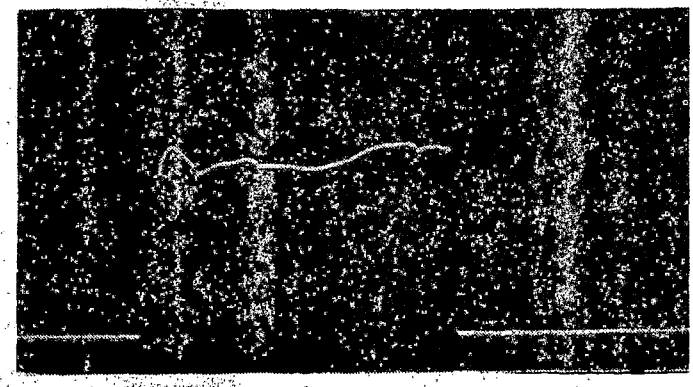

Figure 6.3-10. Typical Inverter SCR Blocking Voltage Waveform

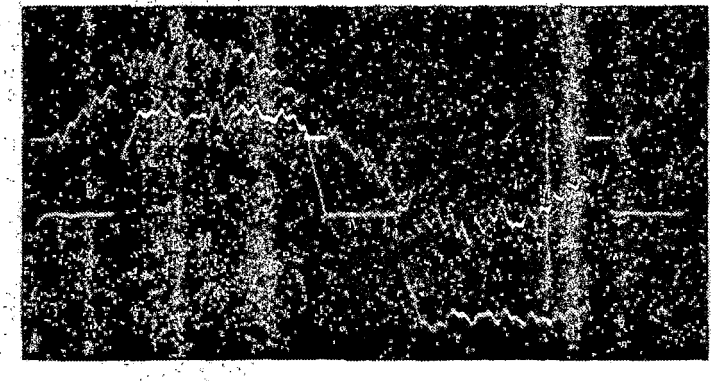

Figure 6.3-11. Typical Motor Current and Voltage Waveforms

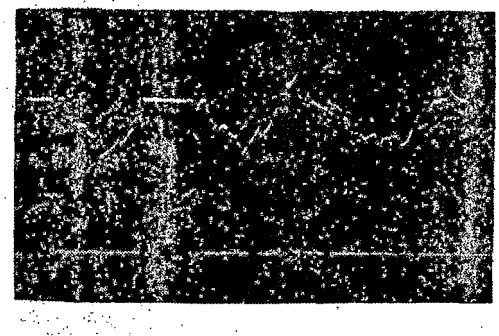

Figure 6.3-12. Typical Cycloconverter SCR Voltage and Current

The rotary transformer and rotating rectifier in the motor convert the secondary current into a dc field current which is, except for the effect of transformer leakage and magnetizing inductances, proportional to the field supply secondary and primary currents. Thus, the motor field dc current and stator ac currents are proportional.

Typical field supply transformer primary and secondary current waveforms are shown in Figure 6.3-13. The primary current is a six-step square wave showing the same characteristic oscillation at the leading edges of the current pulses as the cycloconverter SCR current pulses in Figure 6.3-12. The droop in the secondary current is due to transformer magnetizing current. Leakage inductance accounts for attenuation of the high frequency current component.

Rotating Rectifier and Field Winding

Figure 6.3-14 shows typical field rectifier input current and output voltage (field voltage) waveforms. These waveforms were obtained with the rotary transformer and rotating rectifier mounted outside of the motor. The rectifier output was applied to the field winding through slip rings.

The field winding voltage waveform of Figure 6.3-14 has four components. These are:

- The voltage drop of the dc resistance of the winding, equal to dc (average) field current × resistance.
- The transient voltage drop in the field winding inductance caused by the field supply transformer attempting to force a current waveform into the rotating rectifier with a shape different from that naturally required by the rectifier to produce constant field current.
- The counter EMF generated in the field winding as a result of square wave stator current. This voltage appears at the sixth harmonic of the motor frequency.
- Narrow voltage spikes (faintly visible in Figure 6.3-14) caused by the sudden change in rectifier reverse recovery current acting on the stray inductance of the rectifier circuit. These voltage spikes were greatly reduced by the change to fast recovery diodes.

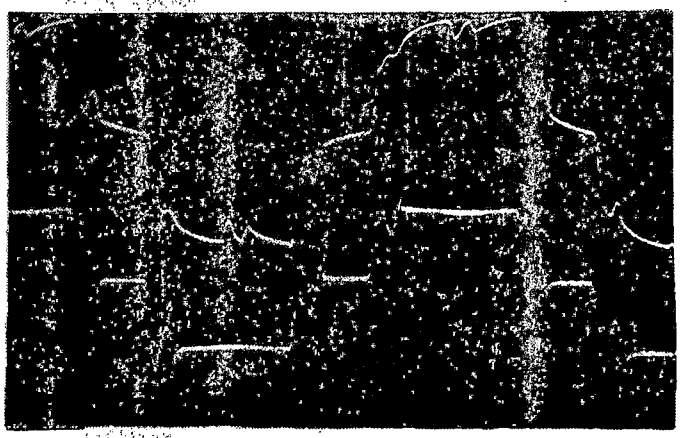

Figure 6.3-13. Typical Field Supply Transformer Primary and Secondary Waveforms

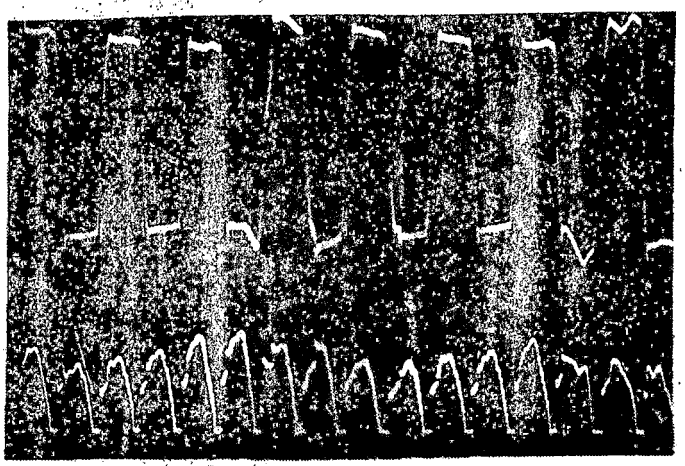

Figure 6.3-14. Typical Rotating Rectifier Input Current and Field Winding Voltage

6.3.3.3 Synopsis of Motoring Mode Developmental Problems and Solutions

Specific problems in the ASDP propulsion system frequently involved more than one of the major electrical power components, i.e., inverter, cycloconverter and the motor. They sometimes also involved other power components and they frequently involved both the power circuits in the major power components and the low level signal electronic control circuits in the motor control electronics (MCE).

One example is the inverter-cycloconverter interaction problem which results in loss of inverter SCR recovery time. The generic problem is discussed in paragraph 6.3.3.3.3. Aggravation of the condition by cycloconverter gate timing problems, and by the addition of capacitors to suppress transients in the motor field excitation circuits, is discussed in paragraph 6.3.3.3.2 and 6.3.3.3.7, respectively. Also covered in the latter paragraph are possible differences in the test motors and their potential effect on the interaction problem.

The following discussion, for the most part, is organized to associate specific problems with that major component where the symptom of the problem was noticed. The location of related corrective action (if taken) is explained in the detail discussions. Recommendations for further investigation and specific solutions are discussed in paragraph 7.4.1.

Another characteristic of the problem and solution discussions is that they are oriented in the direction of test, interpret, and evaluate. This follows from the complex modes of interaction between the power components and from the difficulty associated with developing representative analytical models.

6.3.3.3.1 Cycloconverter SCR Gate Drive and Rise Time

A previous discussion noted that early in the program, cycloconverter SCR's would fail if cycloconverter faulting occurred. These failures occurred at relatively low system power levels. A change in the cycloconverter gate timing control to a concept called "synchronous gate," which was made to avoid a "weak gate problem," resulted in an even higher incidence of SCR failures. The problem increased in severity to the point that it became difficult to operate the system at any power level long enough to conduct diagnostic tests.

Analysis of failed SCR's, a review of the SCR manufacturer's specification for SCR gate drive, and the observation of actual SCR gate drive current pulses led to the conclusion that the SCR gate drive was inadequate.

The manufacturer of the SCR (GE) specified as a minimum that the SCR gate current pulse rise to 0.5 ampere within 0.5 microsecond. If the di/dt of the SCR current at turn-on is high, it is further specified as desirable that the gate drive current pulse rise to 1.0 ampere within 0.5 microsecond. Figure 6.3-15 shows approximations of the pulse rise time and amplitude both before and after incorporating modifications to overcome the inadequate gate drive condition. Both normal and abnormal pulses are illustrated for the system as originally designed. The modifications greatly improved the rise time and amplitude of the normal pulse and completely eliminated the occurrence of the abnormal pulse.

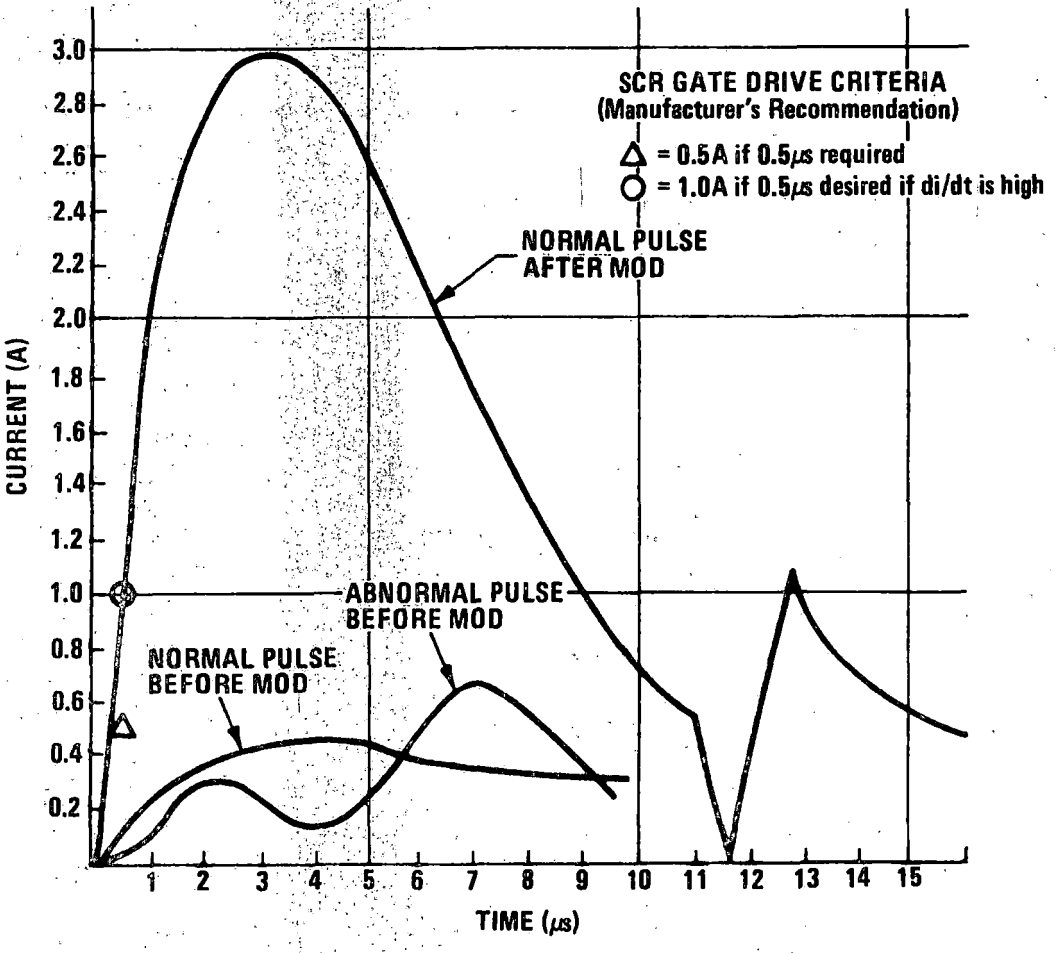

Figure 6.3-15. Cycloconverter SCR Gate Drive

A brief review of the gate drive circuit will illustrate why abnormal pulses could occur with the original design and how they were eliminated. First, it is noted that the cycloconverter requires what is referred to as "continuous gating." Continuous gating is required because conduction through the SCR's sometimes tries to reverse momentarily and a gate current is required for conduction to resume. The inverter, by comparison, is gated by the more conventional "pulse gating." The difference is that with continuous gating, a gate drive current is maintained for the complete intended period of SCR conduction whereas with pulse gating, the gate pulse is momentary and the maintenance of continuous forward SCR conduction current is required for the complete intended conduction period.

The "continuous gating" current pulse is generated by a drive circuit illustrated by the simplified schematic of Figure 6.3-16. This circuit incorporates all changes made to improve the gate drive.

In summary, it is a 30 kHz carrier system. Only one (1) each of eighteen (18) drive transistors, (Q_1), drive transformers (T_1), rectifier bridges ($CR_{1\rightarrow 4}$), and SCR's (SCR_1) are shown. A common 30 kHz square wave generator and interconnect cable is fanned out at the transformer primary to excite all 18 drives. By gating Q_1 "ON", a gate drive current as illustrated in Figure 6.3-15 is applied to SCR_1. T_1 serves to couple the 30 kHz source to the rectifying bridge, to match impedances and to isolate the high voltages on the SCR side from the control signals.

In the original design, "drive synchronization" circuitry as illustrated by Figure 6.3-16 did not exist. As a result, on a random basis, Q_1 would attempt to generate a gate pulse at the exact instant that the 30 kHz excitation source was reversing polarity. This random coincidence resulted in the "abnormal pulses" illustrated in Figure 6.3-15. This pulse is representative but not highly repeatable. Slight changes in gate drive timing relative to 30 kHz transitioning caused great variations. The extremely long rise time, and the tendency to start to turn-on, hesitate, and then continue was the most serious deficiency in the original gate drive circuit and is presumed to have been the principal cause of early SCR failures.

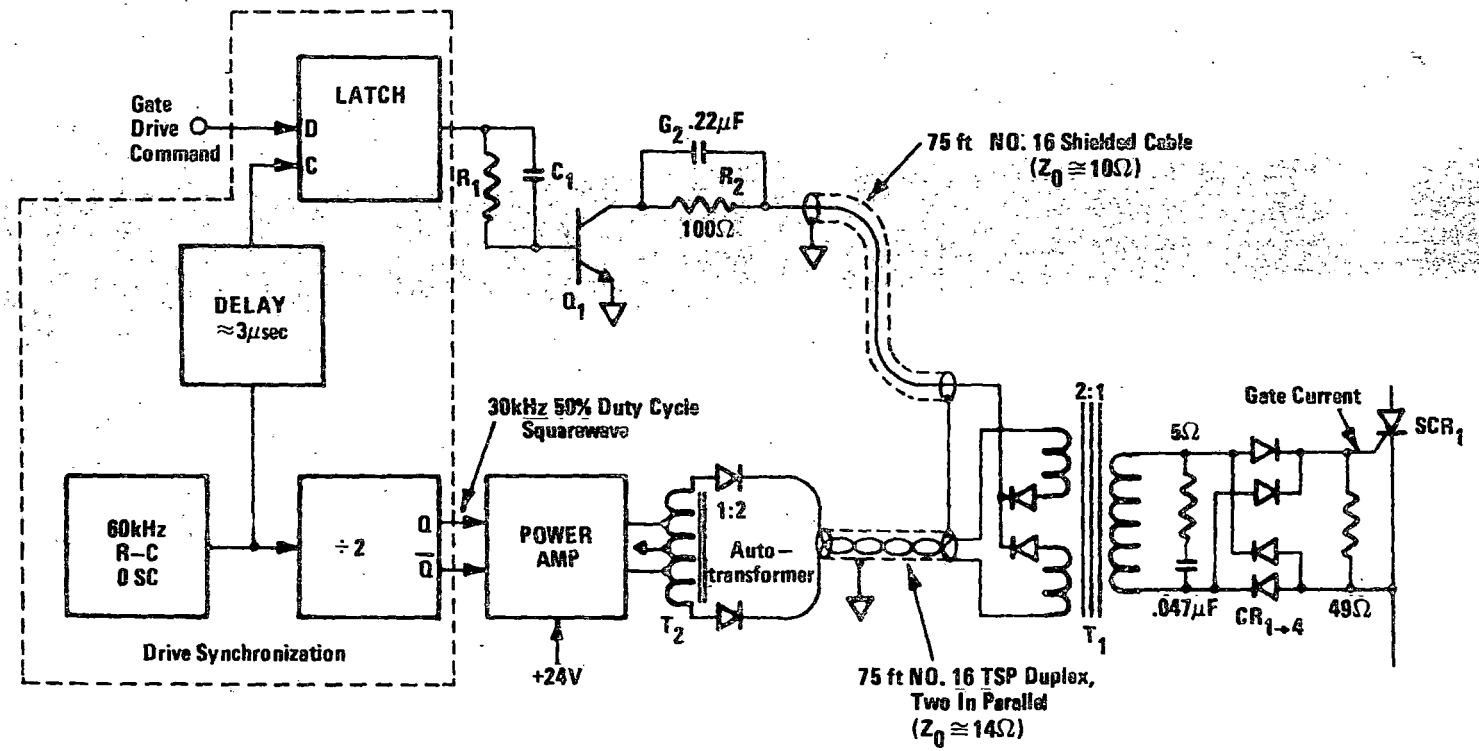

Figure 6.3-16. Cycloconverter Gate Drive Circuit

The rise time of the "normal pulse" in the unmodified design was well below that specified and considerably below that in previous developmental systems. There were several reasons for this but the most significant was attenuation and ringing in the long interconnect cable and losses due to leakage inductance in the transformer. A summary of the interconnect and other circuit changes made to improve the normal pulse rise time is shown in Table 6.3-III.

ITEM	DESCRIPTION	REASON
1.	Replace multi-conductor cable between Q_1 (18 ea) and T_1 (18 ea) with AWG No. 16 single conductor shielded cables	• To reduce characteristic impedance and permit matching
2.	Replace multi-conductor cable between 30 kHz power source and T_1 (18 ea) with parallel shielded twisted PR	• To reduce characteristic impedance and to minimize inductance. Note that polarity change of square wave excitation does not change net current in twisted PR.
3.	Added C_1 (18 ea)	• To speed-up turn-on of Q_1 (18 ea)
4.	Relocated R_2 (18 ea) from T_1 (18 ea) secondary to MCE end of 75 ft cable	• To reduce T_1 (18 ea) voltage and core size
5.	Added C_2 (18 each)	• To speed-up turn-on and provide initial large SCR drive current overshoot
6.	Changed T_1 (18 ea) core and detail construction	• To reduce leakage inductance and parasitic capacitor coupling between windings
7.	Changed turns ratio of T_1 (18 ea) and T_2 from 1:1 to 2:1	• To improve impedance match to cables and to provide harder (current source) gate drive

Table 6.3-III. Summary of Changes to Improve Cycloconverter Gate Drive

Figure 6.3-15 shows the normal pulse current going momentarily to zero at approximately 11.6 μsec. This results from reversing the phase on the excitation to the gate drive transformer. The momentary transient therefore continues to occur at twice the excitation frequency or every 16.7 μsec. This brief drop to zero in the current has no effect on SCR operation because recovery occurs well before any significant number of carriers can recombine in the SCR junction.

Following incorporation of the improved gate drive circuits, the failure rate of cycloconverter SCR's decreased dramatically, even with cycloconverter faulting occurring due to noise or gate timing control problems.

The changes made to increase the rise time and amplitude of the gate drive current to the cycloconverter SCR's were also incorporated into the brake module and the inverter SCR drives. Since the inverter gate drive is a pulse gate system, there was no need to synchronize the gate drive with the carrier excitation. Furthermore, SCR di/dt in the inverter is much lower due to the large series inverter inductance; therefore gate drive is not as critical. However, the change was made as a precautionary measure. The original circuit did not generate the specified level of rise time and amplitude but there was no evidence of inverter SCR failures due to this deficiency.

6.3.3.3.2 Cycloconverter Gate Timing Control Problems

The function of the cycloconverter is to commutate or switch, on a time sequenced basis, the interface between the inverter, a capacitively coupled 3-phase variable frequency (350 Hz to 1200 Hz) source, and the motor, a 3-phase variable frequency (0 Hz to 200 Hz) load. The cycloconverter input and output rms current levels are identical. The cycloconverter output frequency and phase of the output frequency with respect to output voltage are determined by gating the SCR's from signals obtained from a rotor position sensor (RPS) and a motor terminal voltage sensor (TVS). The discussion of this paragraph deals with problems experienced in correctly timing the application of the gate commands to the cycloconverter SCR's.

A simplified schematic diagram of the inverter, cycloconverter and motor is shown in Figure 6.3-17. This figure also illustrates the time sequence in which SCR's must be gated in order to commutate the currents in the motor stator and thereby create a rotating stator field. Not shown in the interests of simplicity is the change in sequencing required to reverse the motor direction. Also not shown is the excitation subsystem for the rotor field and the control subsystem which determines the phase position of the stator field relative to the rotor field. The latter, comprised of the rotor position sensor (RPS), the counter EMF (CEMF) monitor circuit and related signal processing circuits, will be discussed in a subsequent paragraph dealing with RPS $\leftrightarrow$ CEMF transitioning and power factor angle (PFA) control.

Cycloconverter Commutation Criteria

Conceptually, there are two functions the cycloconverter must accomplish and three conditions it must prevent in performing its commutation function. The functions to be performed are inverter or input line commutation and motor or output line commutation.

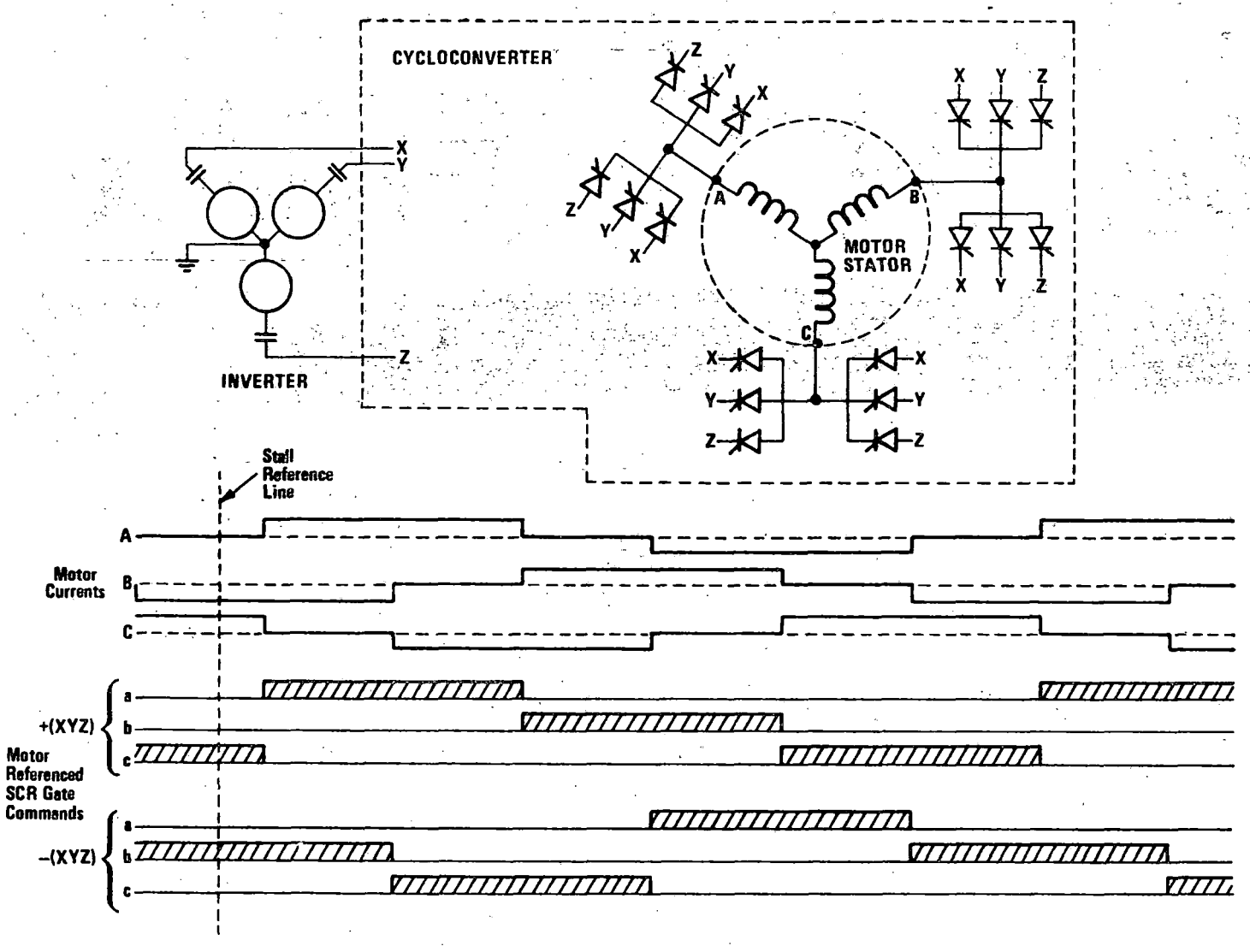

Figure 6.3-17. Cycloconverter Operation and Motor Stator Current Control

These functions, although performed concurrently, can be likened to two independent steps.

In the first step the inverter output can be considered to be converted to dc through a 3-phase full bridge rectifier. In the second step, the commutation of the output currents can be considered the exact inverse, i.e., converting the dc to a new frequency defined by the speed of the motor.

This oversimplification is deficient, however, in that it does not serve to illustrate de-commutation or the basis for current transfer from one SCR or motor phase to another on the output. This is effected by reversals of the input line voltage when motor or output line voltage is low, as at low speed or low current, or by leading power factor of the cycloconverter output line when this voltage is high. At intermediate output line voltages, a gradual transition occurs.

Concurrent with implementation of the input and output commutation, "weak gates" must be avoided, the SCR's must not be gated when a large negative voltage exists across them, and no combination of SCR's can be gated which will result in a phase-to-phase short circuit across either the inverter or motor. The criteria for proper commutation, the problems in achieving it, and the status of relevant solutions are the subjects of the following discussion.

Inverter Commutation, Motor Commutation

Inverter or input line commutation is most simply illustrated if a stalled motor (a fixed stator field) is assumed. Operation can then be interpreted with referenee to the "stall reference line" shown on Figure 6.3-17 and the simplified circuit can be reduced to that illustrated in Figure 6.3-18. Motor or output line commutation can be interpreted in terms of the timing diagram of Figure 6.3-17 if the stall reference line is assumed to propagate to the right at a rate proportional to motor speed. The phase angle of this time based propagating line, i.e., the phase angle of the stator field relative to the rotor field, determines the power factor of the motor.

The important criteria for inverter commutation is that the inverter always have a load and that it never be shorted. In terms of the illustration of Figure 6.3-18, one or more SCR's on the "+" side must be gated on, i.e., the one on the most positive inverter output (overlap on simultaneous conduction is permissible). The inverse must apply for the "-"

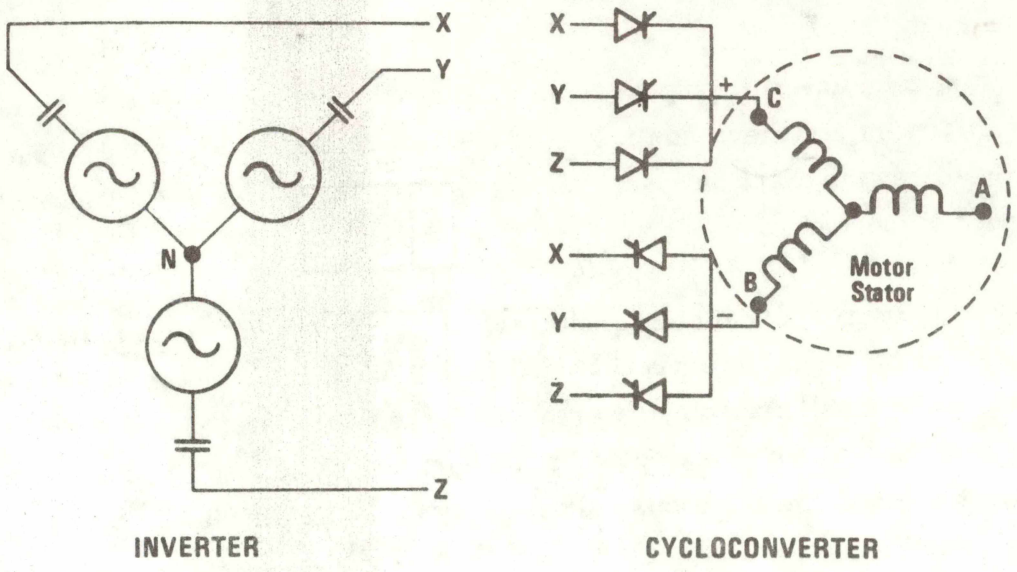

Figure 6.3-18. Cycloconverter Operation – Motor at Stall

side. No other SCR's should be gated and the active SCR's should not be gated when they are blocking with a large (>400 V) reverse voltage across them.

The important criteria for motor commutation is that the "stall reference line" propagate at the proper velocity and phase angle, thereby providing the desired power factor.

Weak Gate Control

Although an SCR "weak gate inhibit" circuit had been successfully demonstrated during circuit development effort conducted under the IR&D program discussed in paragraph 6.1.1, it did not prove to be adequate for the full speed range of required ASDP propulsion system operation. The weak gate problem relates to the timing of SCR gate pulses and is not related to the problem of inadequate SCR gate drive rise time and amplitude which was discussed in paragraph 6.3.3.3.1. Weak gates are possible if the gate timing control circuit applies a gating current to an SCR immediately prior to a conduction period, while the SCR is blocking current, and then removes the gate current before SCR conduction is fully established. This can occur on a random basis. The way it can happen can be seen from the commutation timing and signal processing illustration of Figure 6.3-19. Note that if a motor commutation command is present on a given SCR, the inverter commutation

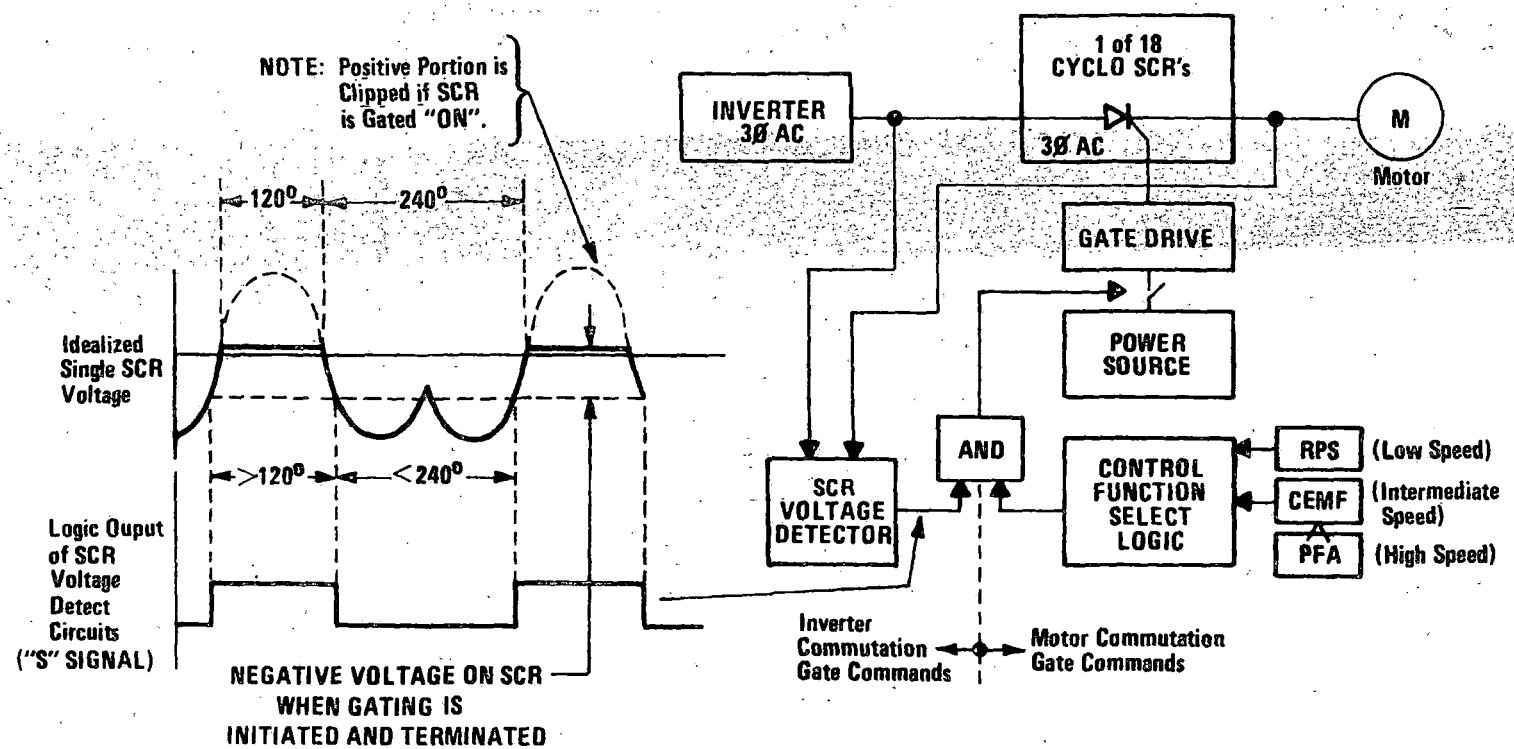

Figure 6.3-19. Illustration of Original Commutation Signal Processing

command can cause the SCR to receive gate current while the SCR is still blocking current. Normally, this is not a problem if the reverse potential across the SCR is not large. The gate is "flooded" with carriers or "soaked" and when the polarity across the SCR reverses, conduction occurs immediately. In effect, the SCR looks to the system like a diode. A weak gate occurs on the rare occasion that the motor commutation command is removed immediately after the inverter commutation command turns the gate on. This immediately terminates the gate drive current. A finite time is required for the carriers in the SCR to dissipate, however. If during this dissipation period the polarity reverses on the SCR, there may be sufficient residual carriers to initiate conduction. This will cause the SCR to be destroyed by a very high density current at a localized spot on the SCR surface.

The weak gate phenomena was identified during an early IR&D effort and circuits to prevent its occurrence were developed, tested, and in one case patented. The solutions, in concept, all depended on "stretching" the motor referenced commutation gate commands. As illustrated by Figure 6.3-20, this maintains gating and conduction in one motor phase (phase "A" as illustrated) until conduction is transitioned to the next motor phase (phase "B" as illustrated).

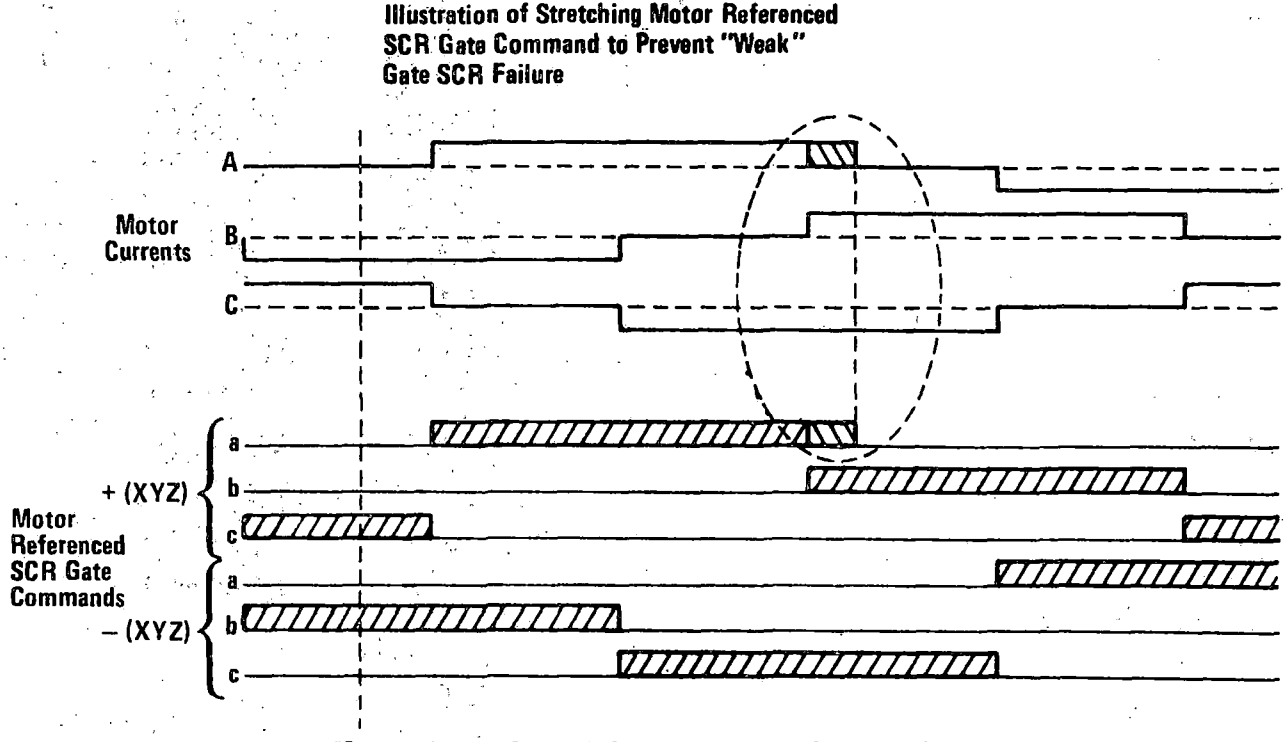

Figure 6.3-20. Illustration of Stretching Motor Referenced SCR Gate Command

Of the previously developed circuits, one worked well at low speeds, and one worked well at high speeds during ASDP testing. After spending a period of time on circuit refinement it became evident that to obtain the desired characteristics over the complete speed range would be difficult and that the resulting circuit would be quite complex. This led to a decision to change to a concept referred to as "synchronous gating."

Synchronous gating differs from the previous gating control approach by delaying the initiation of gating current until after a forward voltage of 100V to 200V has developed across the SCR. Conceptually, this is illustrated by Figure 6.3-21. The short positive voltage spike which appears across the SCR in this concept is referred to as the "finger voltage." Synchronous gating successfully obviated the "weak gate" problem. It also provided a second order, unexpected benefit of producing a slightly higher motor torque at a given inverter frequency. The reason for this improvement is not understood and was not investigated. On the negative side, the conversion to synchronous gating led to new and in some cases unanticipated developmental problems. These problems were experienced in the areas of gate drive and gate timing control.

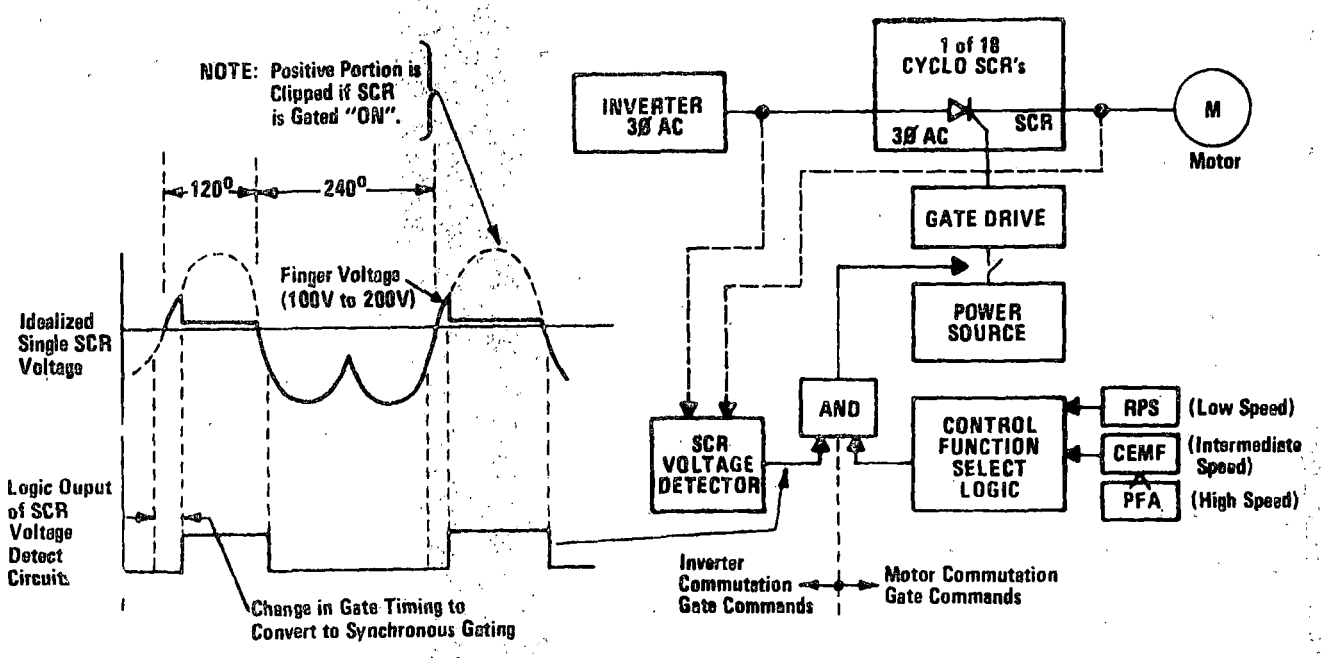

Figure 6.3-21. Synchronous Gating Commutation Signal Processing

The SCR gate drive requirements, in terms of gate current rise time and amplitude, were found to be much more critical with synchronous gating than they were with the previous approach. There are two primary reasons for this. One is that gate rise time is not critical if there is time for the drive current to "soak the gate" or saturate it with carriers prior to initiation of SCR current. This was the case with the original circuit. The other reason is that di/dt can be much higher if a forward voltage exists on the SCR at the time gate current is initiated. The significance of this was that the original gate drive circuit which was marginal to adequate in the developmental systems was inadequate in a system employing synchronous gating. This amplified the need for gate drive improvements as was discussed in paragraph 6.3.3.3.1.

Synchronous Gating Timing Control

A comparison of Figures 6.3-19 and 6.3-21 might suggest that the control circuit changes required for synchronous gating would be relatively simple. In reality, they were very extensive. During a 6-month period (June through November), approximately 50% of the laboratory time was devoted to their investigation and additional work remained at the time of test program termination.

One reason for these developmental problems was that signal waveshapes are not idealized sine waves. At low and intermediate inverter frequencies (well below resonance) distortion of the inverter output voltages is very high. The higher order harmonics frequently cause the SCR current to be interrupted within the idealized 120^{o} conduction period. They also cause conduction beyond the 120^{o} window. Failure to gate the SCR and allow resumption of conduction reflects back through the inverter and forces conduction in another inverter phase. This can lead to inverter faulting (due to inverter-cycloconverter interaction as discussed in paragraph 6.3.3.3.3) or to cycloconverter faulting. The other significant reason for the developmental problems was that an accurate, broadband SCR voltage detector did not exist. To design such a detector is difficult for two reasons. One is that the detector must isolate the very high SCR voltage levels from the signal level circuits. The other is that "common mode" rejection must be very high (>60 dB) to avoid dV/dt feedthrough.

The SCR voltage detector in the original design monitored the voltage directly across the SCRs as illustrated by Figure 6.3-19. It employed photo diodes for isolation and was deficient in that it had some spurious noise pulses at its output when there was high dV/dt

on the SCR. With the original gating control, the system was somewhat tolerant of noise, however, because the major function of the signal (referred to in the original design as the "S" signal) was to prevent gating the SCR when a large negative voltage was present. Some noise gates on a blocking SCR appeared to be acceptable. However, this had never been verified at the high power levels required for ASDP.

When the conversion to "synchronous gating" was made, a new SCR voltage detection circuit was used which did not monitor the SCR voltage directly across the SCR, as suggested by the simplified illustration of Figure 6.3-21. Instead, the new circuit indirectly determined the voltage across the SCR by monitoring the phase-to-phase voltages at the inverter output. Inverter voltages were coupled to the signal processing circuits by the CIRTS (Cycloconverter Input Reference Transformer System). A simplified schematic and timing diagrams of CIRTS gating control are shown in Figures 6.3-22 and 6.3-23, respectively.

These illustrations can be examined relative to the gating of SCR XA. It should be recalled that XA should be gated on any time a positive voltage is seen across it in excess of the "finger voltage," if inverter commutation is to proceed. Inverter terminal XZ will correctly show a positive voltage across XA if SCR AZ is conducting. Similarly XY will show the correct voltage if SCR AY is conducting. Continuing with the idealized assumption that sinusoidal voltages appear at the inverter output, it it illustrated that SCR XA will be correctly gated "ON" if the gating command is based only on inverter voltage XZ. This assumes there is sufficient hysteresis on the threshold of the -180^{o} gate detector to develop the "finger voltage." There is a problem with using a gate 180^{o} wide, however. The idealized SCR conduction period is only 120^{o} so the gate remains "ON" long after the SCR starts blocking. This gating, when the SCR is blocking a high potential, will increase the leakage current and may damage the SCR. To avoid this potential problem, logic was added to limit XA gating only to the time inverter voltage XZ was positive and inverter voltage YX was negative. As illustrated, the addition of this logic "AND" function provides an SCR gate nominally 120^{o} wide. For the idealized sinusoidal voltages, this eliminates the problem of gating the SCR's when they are blocking.

Initial attempts to operate the system using 120^{o} gating in the inverter commutation circuit resulted in cycloconverter faulting and SCR failures at low motor speeds. This occurred due to severe distortion of the YX inverter voltage which caused discontinuities

in the XY logic function. If XY was not present to "AND" with XZ at the beginning of the XZ period, the SCR XA gate command would be missing or delayed. A reasonable hypothesis for the SCR failures caused by missing gate pulse is as follows. The unfired SCR would allow coupling capacitor voltage to build to a high level. Subsequent SCR gating would discharge the capacitor, placing excessive dV/dt across an ungated SCR. This dV/dt would fire the SCR in a mode of low di/dt capability into a circuit producing high di/dt.

The solution to the low speed SCR failure problem was to employ 180° gating when the maximum SCR blocking voltage was below approximately 400V and 120° when the voltage

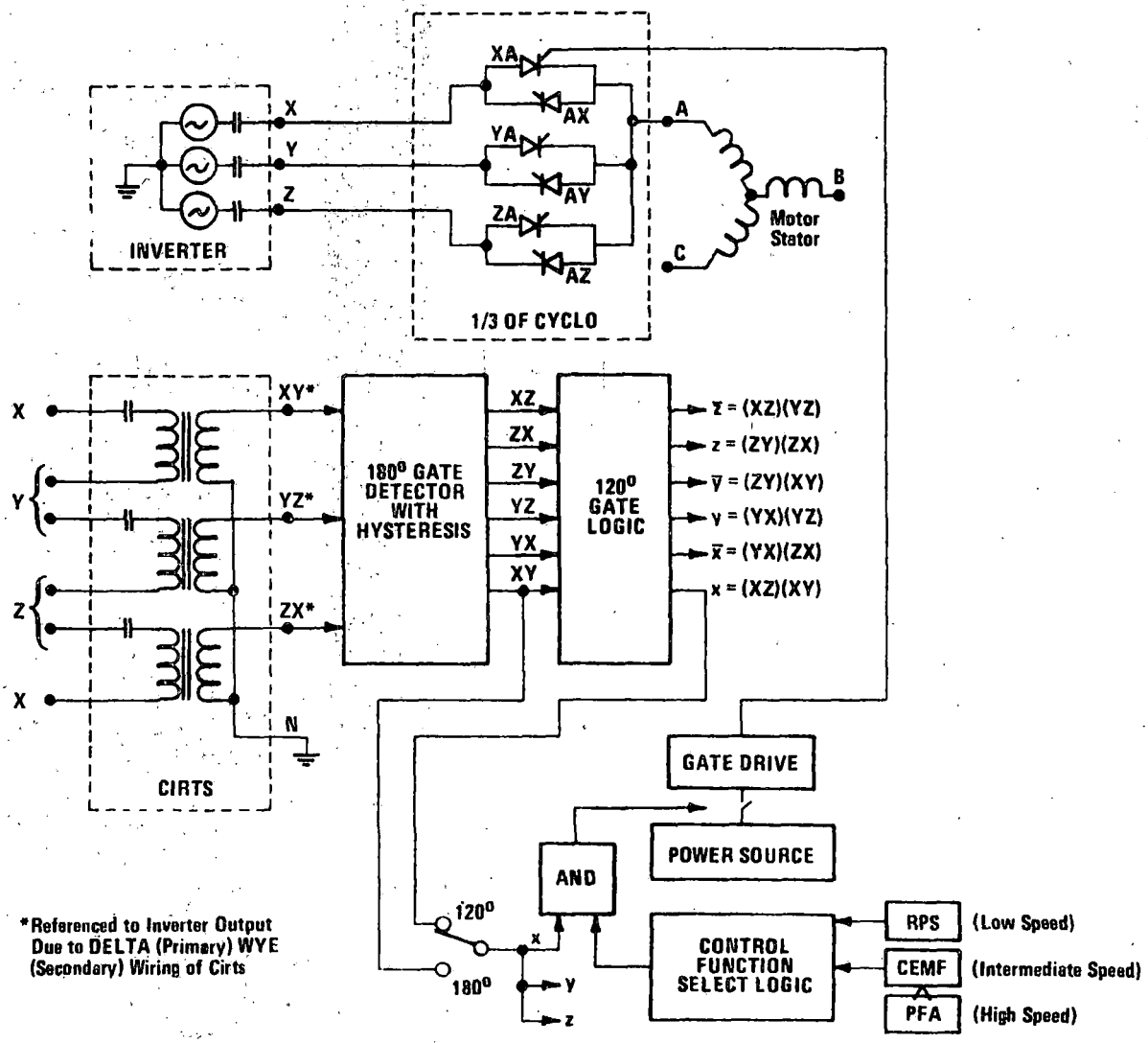

Figure 6.3-22. Illustration of CIRTS Gating Control

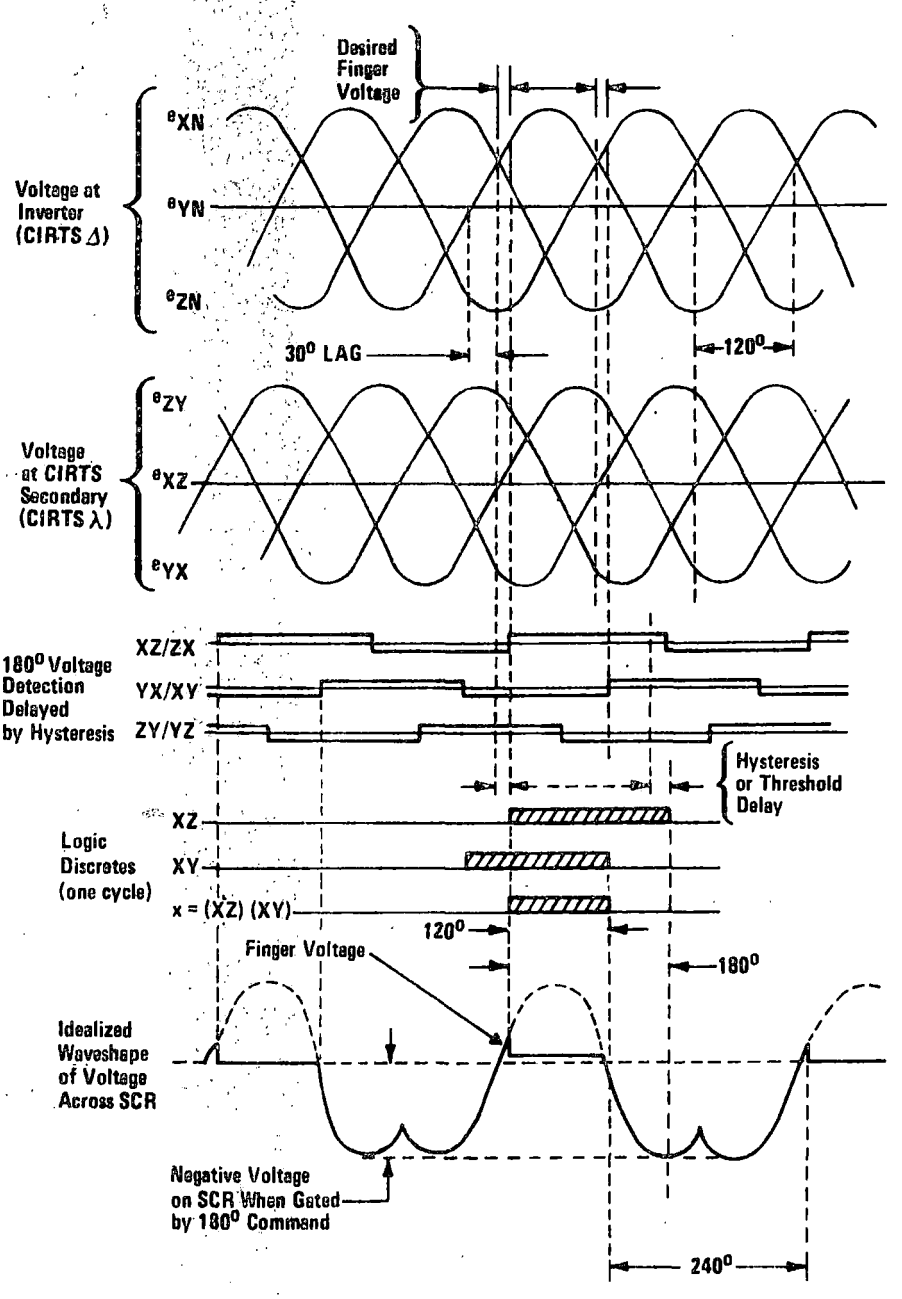

Figure 6.3-23. Timing Diagram of CIRTS Gating Control

was higher. The SCR blocking voltage is very close to the motor voltage, so motor CEMF is the signal monitored to determine the switch point. CEMF depends on motor speed and motor excitation. Since excitation depends on VCO frequency, the $180^{o} \leftrightarrow 120^{o}$ transition occurs at a composite of loci defined by high motor speed and high motor frequency. Above the transition point, the inverter waveshapes are much less distorted and the missing gate-dV/dt-di/dt SCR failure mode does not occur.

In a comparison of 180^{o} gating vs 120^{o} gating at high speeds, the use of 120^{o} gating resulted in higher dv/dt voltage changes across the cycloconverter SCR's and also an increase in inverter-cycloconverter interaction, especially at inverter-motor beat frequencies.

The higher dv/dt conditions appeared at times to approach the 200V/μsec rating of the SCR, but this could not be firmly established due to instrumentation and signal interpretation problems. Several discussions were held with the SCR manufacturer's application engineers relative to the instrumentation and interpretation technique employed. In these discussions it was pointed out that the 200 V/μ sec specifications without further definitions as to initial voltage and final voltage, is little more than a coarse figure of merit. The only clear indication of a rating being exceeded is the "after the fact" observation that the dv/dt conditions did cause the SCR to conduct. Improper conduction did not occur in the ASDP system when the higher dv/dt's were being observed. The condition could represent a latent failure mode, however, and should be alleviated.

Inverter-Motor Beat Frequencies

There is a generic inverter-cycloconverter interaction phenomenon which, if not controlled, can result in loss of inverter SCR recovery time and a consequent inverter derived QSD. The QSD command is generated by a monitor circuit in the inverter which measures available SCR recovery time. A QSD is commanded any time any inverter SCR has less than 50 microseconds available to recover from conducting forward current and begin blocking a severe voltage.

In this paragraph, the relationship of gate timing control to the interaction phenomenon is discussed. The related background is discussed in paragraph 6.3.3.3.3. In that discussion, it is noted that the tendency for interaction is most pronounced when:

1.) $F_{BEAT} = {}^{6}F_{MOTOR} - F_{INV}$, where ${}^{6}F_{MOTOR} > F_{INV}$.

2.) $F_{BEAT} = F_{INV} - {}^{6}F_{MOTOR}$, where ${}^{6}F_{MOTOR} < F_{INV}$.

Expressed in terms of motor speed, the equations become:

3.) $F_{BEAT} = N_{MOTOR} - 5F_{INV}$, where $N_{MOTOR} > 5F_{INV}$.

4.) $F_{BEAT} = 5F_{INV} - N_{MOTOR}$, where $N_{MOTOR} < 5F_{INV}$,

where N = Motor Speed in rpm.

The initial problem seen in system test occurred when F_{BEAT}, as described by Equation 3, was approximately equal to 50 Hz. The problem was seen at speeds of approximately 3750 rev/min and above.

An investigation followed to determine the reason for susceptibility at the unique 50 Hz beat frequency. The investigation revealed 50 Hz to be the frequency where the CIRTS coupling capacitors, as illustrated in Figure 6.3-22, resonated with the CIRTS transformer primary leakage inductance. The scope photograph of Figure 6.3-24, illustrating the resonance, was obtained by applying dc in place of the inverter referenced gate commands and employing motor commutation only. If inverter commutation had been operating, QSD would have occurred before the photo could be taken.

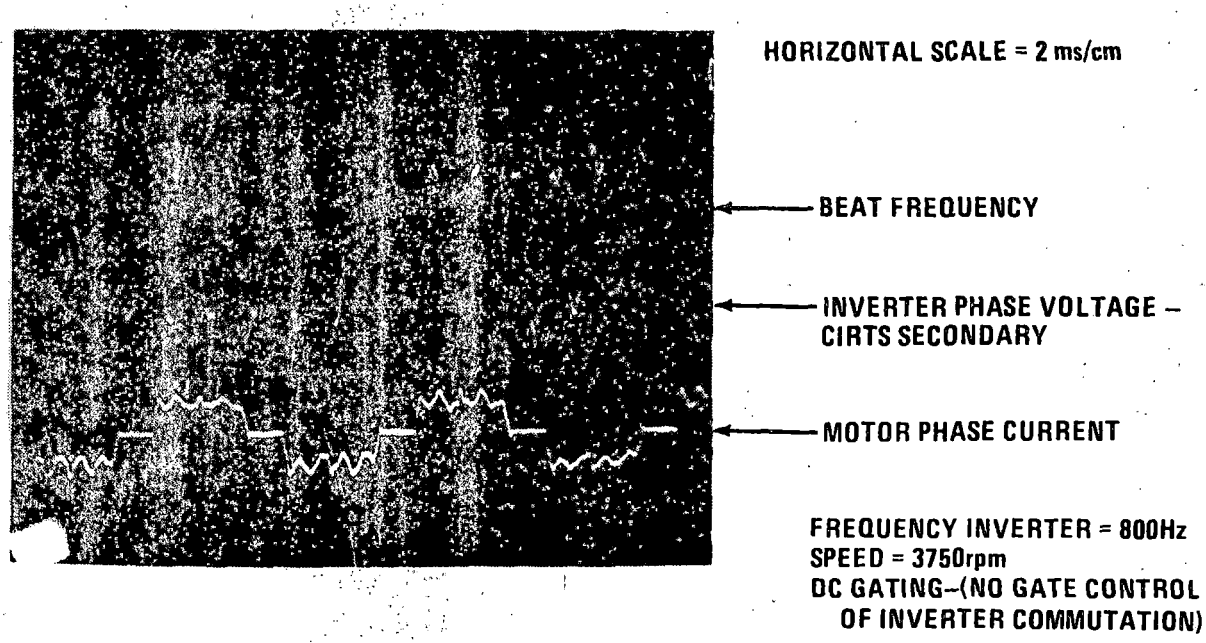

Figure 6.3-24. CIRTS Resonance at Beat Frequency

Design analysis plus several experimental tests failed to reveal a solution to the CIRTS input resonance problem. Additional damping (resistance) resulted in unacceptable phase shift, and removal of the capacitor resulted in transformer saturation from dc current. Changes in component values would change the resonant frequency but the same system problem, i.e., the inverter QSD would occur at the new beat frequency.

In an effort to obviate the input resonance problem, CIRTS was replaced by CIRPS (Cycloconverter Input Reference Photo Sensor). This change, as illustrated by Figure 6.3-25, replaced the CIRTS transformer and threshold detectors by photo-transistors and related components.

The pending test program termination prevented the complete development of CIRPS and a complete evaluation of the configuration at the system level. An experimental circuit was built and tested in the system. The results of limited tests showed the BEAT problem was successfully eliminated for all beat frequencies except $F_{BEAT} = 0$. At zero beat, degradation in inverter recovery and the related QSD problem was more acute that it was with the previous CIRTS circuit. The results were considered inconclusive, however, since there was some dV/dt related noise on the CIRPS output and the thresholds of the phototransistors may not have been matched.

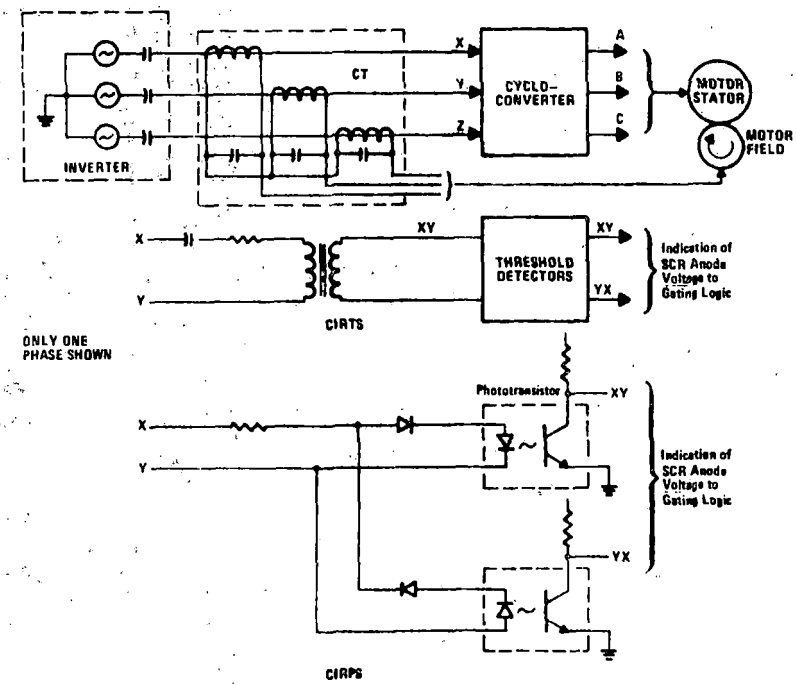

Figure 6.3-25. CIRTS Vs CIRPS Gating Logic

The vulnerability of the system to inverter recovery degradation and related QSD's was also adversely affected by the addition of capacitors across the secondary of the motor field excitation current transformer. These capacitors are illustrated in Figure 6.3-25. They were added on an experimental basis as discussed in paragraph 6.3.3.3.7 to prevent false triggering of the rotating rectifier "crowbar" circuit. The effect of this degradation is illustrated by the scope photographs of Figure 6.3-26. These photographs were taken on a memory scope which recorded many inverter cycles as system speed was slowly swept through the operating region needed to provide all beat frequencies. It, therefore, reflects a composite of the best and worst recovery conditions experienced.

Automatic RPS ↔ CEMF Transitioning and PFA Control

Motor commutation control requires a transition from RPS control at low speed to CEMF control at intermediate speeds. The original design was based on a gradual blended transition beginning at around 600 rev/min. The blending would have been accomplished by allowing the increasing CEMF voltage to override the fixed amplitude RPS voltage. A problem was experienced, however, which resulted in excessive noise on the CEMF signal at low speeds. The problem was that the commutation current noise rejection circuit did not perform as expected. The reason was that motor inductance changed as a function of stator current, whereas the noise rejection circuit was based on a single value of inductance. The solution employed was to delay transitioning until a motor speed of 2000 rev/min was reached and then to transition instantaneously. System experience showed the step transition to work well and all final motoring data was recorded employing the concept. An additional easily made control circuit modification which would reduce the size of the step change in power factor angle at the point of transition is discussed in paragraph 7.2.4.

High speed system operation requires increasing the PFA over that obtained by CEMF alone. Due to the previously discussed QSD problems, most testing was performed employing manual control of PFA by the use of potentiometers (having a common shaft) on each of the three phases. Late in the program, the automatic advance capability was im[illegible]ented and final demonstration data employed automatic PFA.

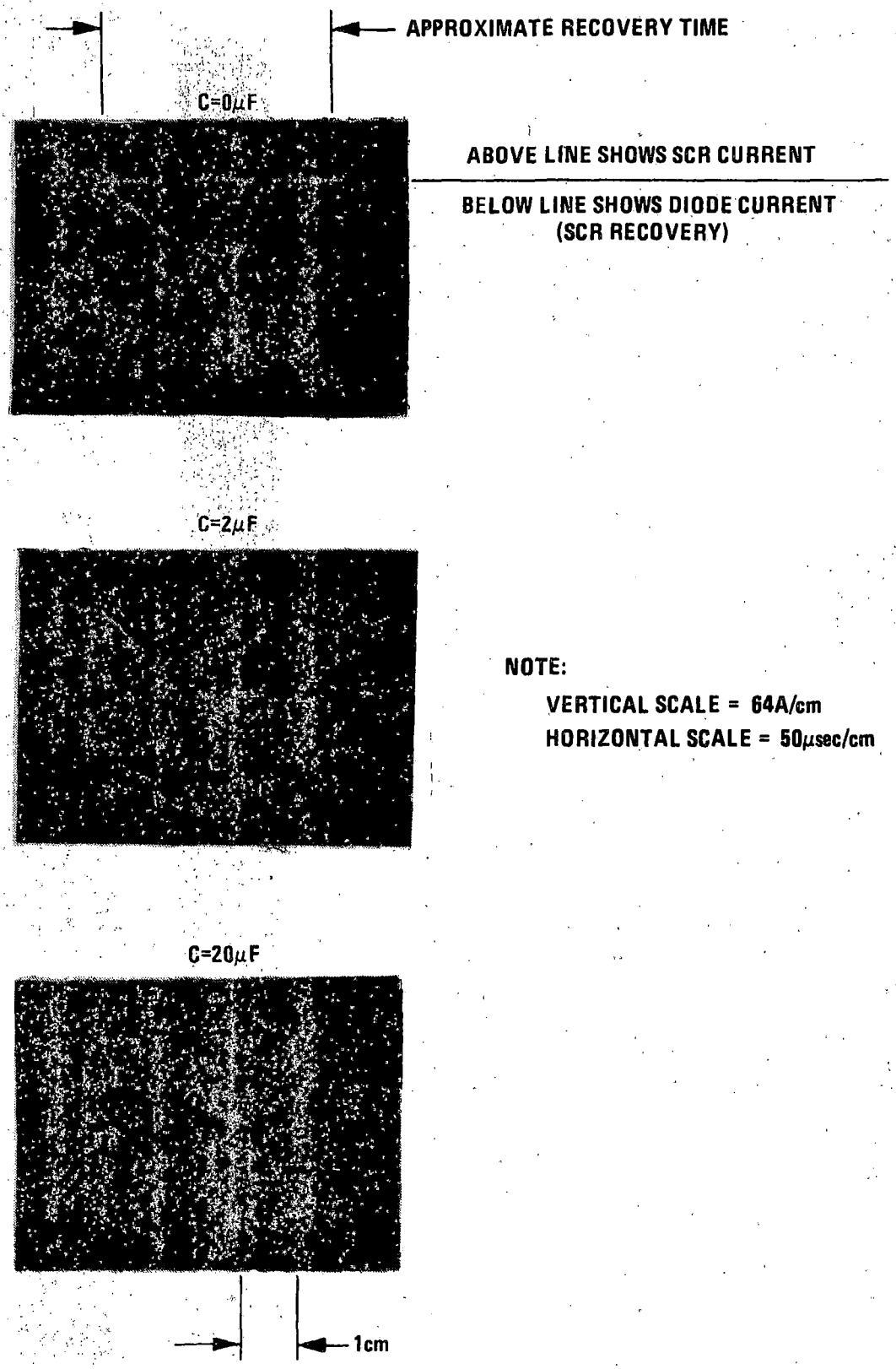

Figure 6.3-26. Inverter SCR Recovery Time with Added Capacitors

To optimize system operation for recording a final set of system demonstration data, the CIRPS gating control circuits were removed and the system was reconfigured back to operation with CIRTS. This represented the first time the system was operated with CIRTS and automatic PFA. System operation was solid and repeatable with very little degradation in inverter recovery time, even at the previously discussed CIRTS resonant frequency point. It is presumed this was due to improved balance in phase-to-phase power factor angles largely resulting from the use of automatic PFA. Another possible favorable factor was the use of traction motor 2B77 which, as discussed in paragraph 6.3.3.3.7, does not require noise suppression capacitors on the current transformer secondary to prevent false triggering of the rotary rectifier crowbar circuit.

6.3.3.3.3 Inverter-Cycloconverter Interaction Problem

The existence of a disturbance in the inverter SCR and diode currents due to cycloconverter output current commutation was noted at the inception of the IR&D program in August 1971. During this initial phase of the development the power converter consisted of a single phase inverter capacitively coupled to a 1Ø/3Ø cycloconverter. The inverter-cycloconverter interaction was especially severe when the inverter frequency was close to six times the motor frequency. Under these conditions, the inverter SCR and diode currents showed a cyclic, or beat frequency, variation, with a frequency of

$$F_{BEAT} = 6F_{MOTOR} - F_{INV}, \text{ where } 6F_{MOTOR} > F_{INV}$$

$$F_{BEAT} = F_{INV} - 6F_{MOTOR}, \text{ where } 6F_{MOTOR} < F_{INV}.$$

The principal adverse effect of the cycloconverter-inverter interaction is a transient reduction in the duration and width of the inverter diode current pulse. The width of this pulse is the turn-off time available for the SCR anti-parallel to the diode. The short inverter turn-off time problem was eliminated in the 1Ø/3Ø system by the use of a rectifier-capacitor filter placed across the cycloconverter terminals. This filter clipped the transient peaks of the envelope of the cycloconverter input voltage. A method was devised to bleed the capacitor of excess charge, regenerating the bleeder current into the dc supply with very low power loss. This filter and bleeder arrangement are covered in U. S. Patent 3,866,099.

Later in the IR&D effort, the drive concept was changed to 3Ø/3Ø conversion. A full scale 3Ø/3Ø breadboard converter was designed and fabricated. Tests with the 0-75 Hz "workhorse" motor showed that the inverter-cycloconverter interaction was much less severe than with the 1Ø/3Ø system. This eliminated the need for a rectifier-capacitor filter across the cycloconverter input terminals.

Following receipt of the ASDP contract, further system development was conducted with a motor capable of operating to 133 Hz on an overspeed basis. Abnormal inverter-cycloconverter interaction was not observed. This interaction could have been overlooked because testing at the maximum frequency was done only briefly because of safety concerns.

The transient loading on the inverter caused by cycloconverter commutation has two probable primary causes, both related to motor inductance.

The most obvious transient load occurs when motor current commutates from one phase to the next. During the commutation time, which is inversely proportional to the motor leakage inductance, the simultaneous conduction of an SCR in the off-going phase and an SCR in the on-going phase effectively places the two phases in parallel. The impedance seen by the inverter abruptly drops during the motor commutation interval. If this drop in impedance occurs during conduction of an inverter diode, the diode current amplitude and duration may be reduced, thus reducing the turn-off time.

The second probable cause of cycloconverter-inverter interaction is the resonance of the coupling capacitance with motor leakage inductance or with the inductance in series with the coupling capacitors. The latter inductance was added to prevent excessive cycloconverter dV/dt and di/dt during fault conditions. The cycloconverter and inverter commutations excite these resonant circuits in a quasi-random manner except when the inverter frequency is close to six times the motor frequency. The excitation then becomes coherent and this could result in a magnified resonant current response.

The use of cycloconverter input voltage as a cycloconverter timing reference is also a source of inverter turn-off time fluctuation. This is diccussed further in paragraph 6.3.3.3.2. A beat frequency voltage extending to dc (when $F_{INVERTER} = 6F_{MOTOR}$) is superimposed on the normal cycloconverter input voltage. The use of a high pass reference signal stepdown and isolation device, such as the CIRTS transformer, cannot pass

the low frequency beat component of the cycloconverter input voltage and hence gives rise to a cyclic error in SCR gate pulse timing. Some testing was done with cycloconverter SCR gate timing derived from dc coupled photosensors operating on the cycloconverter input voltage. Results were inconclusive because of the limited amount of testing done. It should be noted that some degree of cycloconverter-inverter interaction was observed even with unsynchronized (dc) cycloconverter SCR gating.

Some of the development testing conducted to diagnose the inverter-cycloconverter interaction problem included:

- Frequency modulating or "dithering" the inverter frequency to avoid stationary inverter-cycloconverter beat frequencies. This had no effect on the jitter in the inverter turn-off time.
- Placing various values of capacitance across the field supply transformer secondary. This capacitance was initially added to reduce field excitation transients as discussed in paragraph 6.3.3.3.7. Insofar as inverter-cycloconverter interaction is concerned, the added capacitance had two effects. First, the motor field current increased appreciably as indicated by an increase in CEMF. Second, the transient impedance of the field supply transformer in series with the coupling capacitors decreased, as indicated by a decrease in transient voltage across the transformer primary. The jitter in inverter SCR turn-off time also increased with increased field supply transformer secondary shunt capacitance. Further development testing is necessary to determine if this was due to increased CEMF or to reduced field supply transformer primary impedance.

Recommendations for further development testing for diagnosis of the interaction problem are included in paragraph 7.2.

6.3.3.3.4 Failure of Cycloconverter DSAS Devices

DSAS devices are used in parallel with the cycloconverter SCRs to protect the SCRs from damage by short time duration voltage spikes or transients. These devices, (FMC P/N 7638), which are similar to back-to-back Zener diodes, conduct when the applied voltage exceeds approximately 1500 V. In August, as operation at high speeds and motor currents was verified,

DSAS failures occurred. Investigation showed the devices were being overstressed by large fault currents which randomly occurred at the moment of system shutdown. The source of energy for the transient was found to be the inductance of the motor armature.

The motor armature has an inductance of 600 μH and a resistance of 27 mΩ. The time constant τ = L/R is 22 msec. The fault current in the motor winding frequently exceeds 500 A. The decay of this current is governed by the exponential relationship for a series L-R circuit; i.e.,

$$I(t) = I_o \epsilon^{-t/\tau} .$$

Figure 6.3-27 shows a plot of the rated capability of the DSAS-17 surge suppression device in terms of current level vs time duration. The area below the solid line represents the safe operating area. The four circled points represent the manufacturers data points. The fault current flowing through these DSAS devices, as determined from the above equation, is shown by the dashed line on Figure 6.3-27.

It is obvious that the fault current generally exceeds the dissipation capability of the DSAS device. The ratio by which the applied energy exceeds the rated energy may be obtained by comparing the area beneath the solid curve to the energy stored in the motor inductance. Between 10 μs and infinity, the area under the solid line is found to be 0.218 ampere-second while the area under the motor inductance discharge curve is 11.10 ampere-seconds. The ratio of these two numbers is 50.9 or, in other words, the DSAS devices were being driven to approximately 50 times their rated capability.

The problem may be worked in reverse to obtain the maximum inductance that will allow 500 A and not exceed the DSAS ratings. This inductance is calculated to be 11.8 μH. This amount of inductance may be represented by a pair of #0000 wires, 28 feet long and separated by 6 inches.

One solution to protect the DSAS devices in the laboratory setup was to turn on the dynamic braking phase control SCRs and dump the stored motor energy into the brake grid resistors. This procedure worked a majority of the time but random DSAS failures continued to be experienced. In light of the minimum inductance requirements set forth in the preceding paragraph, it is not surprising in retrospect. The wire run to the brake grid resistors and their own self-inductance exceeded 11.8 μH several times over.

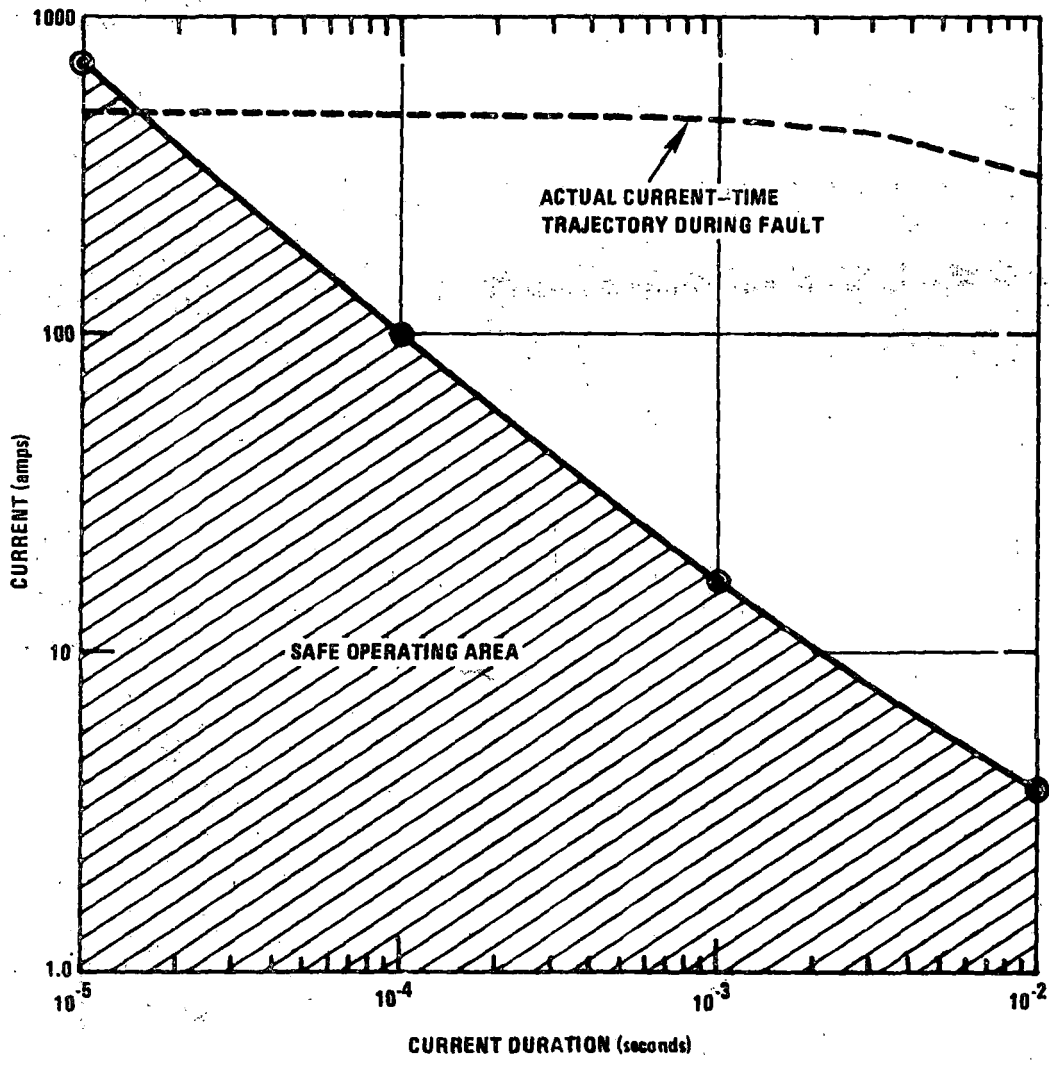

Figure 6.3-27. DSAS Safe Operating Characteristics and Actual Operating Characteristics During Fault Conditions

To avoid the inductance of the brake grid resistors, the regenerative braking SCRs were turned on. This lowered the dump path inductance by taking current back to the input capacitor bank. The inductance of this new circuit path was not measured, but because of random DSAS failures, one might expect that it is still not low enough.

The fault current, if not interrupted through interruption of the braking SCR gating, will ultimately overcharge the input filter capacitors in the event of a rail gap, or cause the railcar to jerk if a great amount of energy is returned to the line. In effect, maximum regenerative braking has been initiated. This operational aspect of the problem was not addressed in the developmental tests performed.

6.3.3.3.5 Excessive Cycloconverter di/dt

The modified Mapham inverter used in the system exhibits a capacitive output impedance at high frequencies. Should a cycloconverter fault occur where two SCRs are turned on line-to-line across the inverter, methods are required to control the SCR di/dt during the ensuing resonating and coupling capacitor discharge. Failure to do so can result in cycloconverter SCR failure. One method of providing this control is through the use of non-saturating inductors (air core) between the cycloconverter and the inverter. The SCR rating is 200A/μs maximum. If the fault occurs when the inverter capacitors are charged to about 900 V, the required value of this inductance is found by

$$L = \frac{V}{di/dt} = \frac{900}{200} \times 10^{-6} = 4.5\ \mu H.$$

This value of inductance was placed in series with the existing 100 μH saturating inductors thereby limiting the SCR di/dt to the specified limit.

The saturating inductors are provided to alleviate another potential problem, which is to reduce the magnitude of the current spikes during 60 degree motor transients. During this time, motor phase current is changing and simultaneous conduction of the "wrong" SCRs can occur in the cycloconverter. The saturating inductors come out of saturation during the current reversals and soften the effect of these current spikes.

6.3.3.3.6 Commutation Problems at Low Inverter Frequency, High Motor Speed

When the motor frequency is greater than approximately 1/6 of the inverter frequency, the cycloconverter output current must be commutated by leading motor power factor to

ensure freedom from faulting. At the maximum motor speed of 5642 rpm, the motor frequency is 188 Hz. Six times the maximum motor frequency is 1128 Hz which is near the maximum inverter frequency. Thus, at high motor speeds, commutation must be effected by leading motor power factor for all inverter frequencies. One additional criteria is that there be adequate field excitation current to cause sufficient CEMF to effect commutation. System test results indicated commutation was not adequate when operating at high speed and low torque. The consequence is potential cycloconverter faulting.

The limits obtainable in torque and speed before cycloconverter faulting may occur are shown in Figure 7.2-1. The primary reason for the faulting is inadequate field excitation current. With a weak rotor field, there is insufficient CEMF to commutate the motor stator current to successive stator phases. The loss of excitation at low inverter frequency is inherent with the use of a current transformer in the stator current path to derive field excitation. Under ideal conditions, field excitation would be proportional to stator current. In the actual system however, there are losses, primarily due to the required magnetization current of the rotary transformer in the motor.

The final automatic PFA configuration incorporated a circuit which provided a fixed advance of 30^{o} when motor current was less than 150 A. This was approximately equal to an inverter frequency of 700 Hz. The increased power factor mitigated the problem of cycloconverter faulting but only to a limited degree. The result was that slightly higher speeds or lower torques were possible before faulting would begin to occur. This low torque, high speed faulting was not considered a high priority problem and, except for the above noted modification to the automatic PFA, no effort was expended on it. Possible solutions are discussed in paragraph 7.2.

6.3.3.3.7 Rotating Rectifier Protection Circuit

Zener Diode Failure and Replacement with Crowbar

The Zener diodes connected across the motor field winding to provide surge protection fail[ed] soon after the initiation of system testing. The first failure occurred on 3/11/77 and subsequent failures occurred on 4/21/77 and 5/2/77. The failure was observed to occur coincident with faulting of the motor commutation due to cycloconverter timing problems. The fault induced current transients in the motor stator were being coupled to

the motor field winding on the rotor through mutual inductance. These transients were expected. In previous systems, they were dissipated by adding resistance in parallel with the field winding. In the ASDP system, Zener diodes replaced the resistors to reduce power dissipation and minimize field excitation power requirements. Failure to dissipate the transients may result in excessive voltage across the excitation bridge rectifier diodes or breakdown of the field winding insulation.

The failures occurred because the energy level of the transients was considerably greater than expected. However, accurate measurement of the transients is not possible without access to the motor rotor. Also, the exact manner in which transients were induced into the rotor was not well understood. Additionally, many scenarios are possible for the transients ranging from a single large transient to recurring smaller transients. Subsequent analysis of one example scenario led to a prediction that 50 joules of energy could be dissipated in the Zeners in the surge protection circuit. The capacity of the Zeners however was only approximately 2 joules (1 joule per device).

Since the failures occurred while operating at low motor power levels, the preliminary analysis clearly indicated the Zener diodes were inadequate. On the other hand, it was not possible to quantitatively specify an adequate circuit. In view of these circumstances, three decisions were made in early May as follows: 1) to replace the ASDP motor with the previously discussed workhorse motor for the continuation of the motor control electronics (MCE) development work. Continued use of the ASDP motor would have resulted in additional Zener failures and excessive laboratory down time for motor repairs; 2) to replace the Zener diode surge protection circuit in the ASDP motor with a "crowbar circuit" which employed SCRs in place of the Zener diodes; and 3) to modify one of the ASDP motors at Delco Products by replacing the rotary transformer (RT) with slip rings and ship the motor to Delco Electronics. The purpose of obtaining the slip ring motor was to permit quantitative measurements of the transients being experienced by the motor field winding.

A simplified diagram of the motor field excitation system and a simplified schematic of the original and the crowbar surge protection circuits are illustrated in Figure 6.3-28. With the original circuit, the transient energy was primarily dissipated in the Zener diodes. The crowbar circuit can tolerate much higher energy levels because it functions to momentarily short circuit the field winding and therefore cause the transient energy to be dissipated in the field winding.

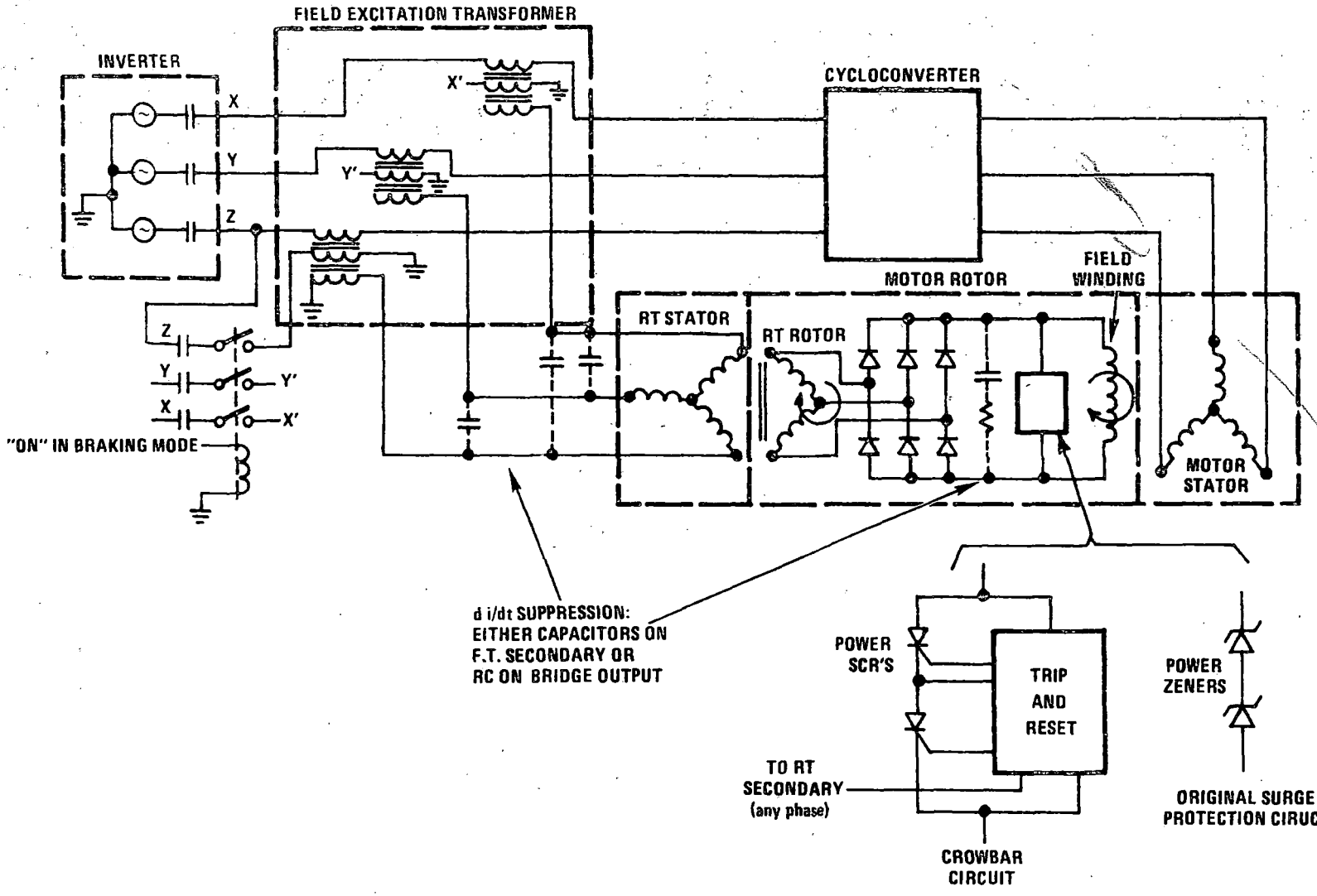

Figure 6.3-28. Field Excitation and Surge Protection

Small signal Zener diodes detect the field voltage as illustrated by Figure 6.3-29 and turn-on the SCRs at approximately 540 V, a voltage somewhat higher than the approximate 400 V point at which the original power Zener's conducted. If one assumes a transient current is introduced into the field, and if decay times are disregarded, then the difference in energy dissipated in the SCRs versus the energy dissipated in the Zener diodes is proportional to the difference in the voltage drop across the respective devices during the conduction period. Since the drop across the SCR is approximately 4V (2V each), an improvement of 100:1 is indicated. The full improvement is not realized however. The period of conduction increases because there is only the IR drop of the field to dampen it. Reset of the SCR, as illustrated by Figure 6.3-29 is accomplished by using the ac voltage from one phase of the rotary transformer secondary to momentarily reverse the polarity across one of the SCRs.

Problems with Crowbar Circuit

There was insufficient confidence that the crowbar circuit would be an adequate solution. Relatively they could tolerate much greater surges (they were rated to 35A continuous and 325A surge). Furthermore, Delco Products had previously used the circuit successfully on other motors and had subjected an ASDP motor to a surge test based on applying 60 cycles to the motor stator and running it as an induction motor.

The reservation about the capability existed because the actual transient currents that could be expected in the ASDP system, in the event of a cycloconverter fault while operating at a high power level, were unknown. The faults which caused the Zener failures had occurred at relatively low power levels. There was also a new potential problem with the crowbar circuit which did not exist with the Zener circuit. This new problem was that, during normal system operation, commutation generated short duration, low energy, high voltage noise transient spikes were developed across the field winding. Similar spikes also result from rectifier diode recovery currents. Should these spikes exceed the 540V trip level of the crowbar circuit, the crowbar would repeatedly trip and thereby shunt the normal field excitation current through the crowbar circuit.

Verification at the ASDP system level of the crowbar surge protection circuit was delayed due to the considerable design time required to incorporate the modification into a motor, as well as to competing priorities in the test laboratory after a motor was available.

SCR CIRCUIT

REQUIREMENT – LIMIT VOLTAGE ACROSS FIELD WINDING TO 600V MAX.
REASON – REVERSE VOLTAGE BREAKDOWN LIMIT OF RECTIFIER DIODES.

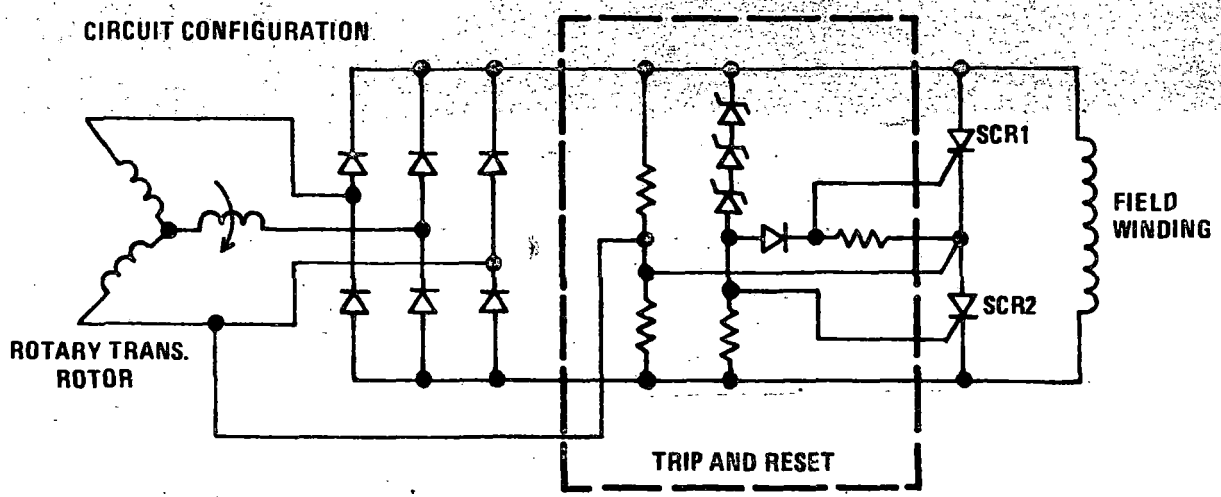

- TRIP LEVEL – 540V +10%
- BLOCK VOLTAGE – 1200V
- CURRENT
  - SURGE – 325A
  - CONTINUOUS – 35A

Figure 6.3-29. Crowbar Trip and Reset

Analytic work and laboratory tests of new circuits and component level tests of the ASDP slip ring motor were performed in the intervening period. In early August measurements were made of transient voltages on the field of the ASDP slip ring motor with the motor operating under cycloconverter control in the motoring mode. These measurements were made at torque levels to 1600 ft-lb but speed was limited to 2000 rev/min since the testing was performed in the B lab. The tentative conclusions drawn from interpretation and extrapolation of the data obtained were: (1) that current transients resulting from cycloconverter faulting would not cause failure of the SCRs in the surge protection circuit, and (2) that there was a high probability the noise spikes would cause "false triggering" of the crowbar circuit and loss of field excitation. Subsequent tests and experience would confirm these tentative conclusions. Figure 6.3-30, a photograph of the voltage across the field winding, was taken during this series of tests.

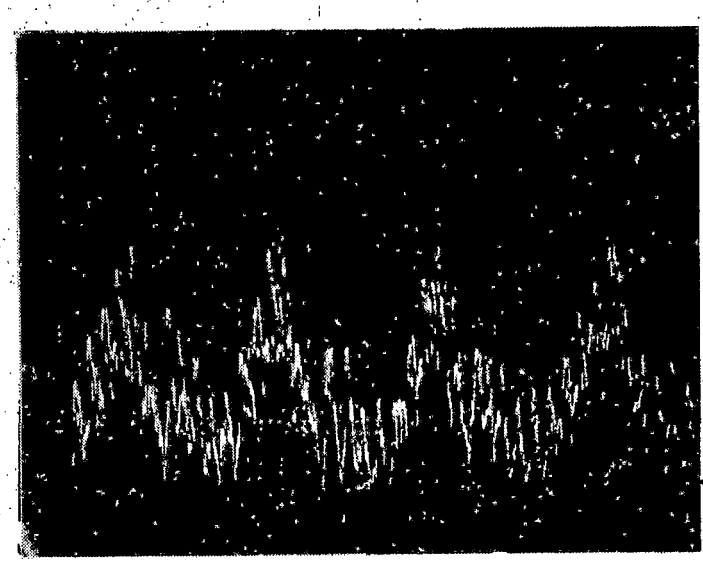

Figure 6.3-30. Voltage Across Field Winding of ASDP Slip Ring Motor

The identification of the potential crowbar false triggering problem led to further investigation into the source of the noise spikes and possible methods of controlling them. An alternate approach of modifying the crowbar circuit to trip at a higher voltage level was not pursued. The reason was that to obtain adequate margins would have required raising the threshold by 50% to 100%, i.e., to the 800 V to 1100 V region. This would have required increasing the reverse voltage rating of the bridge rectifier diodes well above the current

800 V level. The investigation revealed the noise spikes were not the result of the mutual coupling between the motor rotor and stator. As previously discussed, this was the source of the high energy transients which caused failure of the original Zener diode. Also, the voltage transients in the braking mode were not sufficient in magnitude to cause potential false triggering. The reason is that the cycloconverter is inoperative, and field excitation in this mode, as illustrated by Figure 6.3-28, is derived from a voltage source rather than a current source. In the absence of cycloconverter commutation, the inverter output is less distorted and the dV/dt levels at the field transformer secondary are much lower.

Investigation of the noise coupling through the field excitation transformer, current transformer and diode bridge revealed the spikes to be the result of two conditions. One was the rectifier bridge diode recovery currents. As the diodes recover and terminate reverse conduction, the resulting high di/dt develops a high voltage across the diodes. This voltage is reflected through the diode of the conducting phase and appears across the field windings. The left-hand photograph of Figure 6.3-31 shows the recovery transient and the related voltage transient. The photos were taken with the motor rotor locked, therefore motor commutation related transient effects do not appear. The second condition causing transient voltage spikes was the high rate of current change (di/dt) of the inverter output currents. These di/dt's resulted from the cycloconverter commutation of the inverter output and were maximum when simultaneous motor and inverter commutation occurred. Since the field excitation transformer acts as a current transformer in the motoring mode, the di/dt's appeared at the transformer secondary. The transients were coupled through the rotary transformer and diode bridge and appeared as voltage transients across the highly inductive field winding.

Two solutions were developed to suppress the transients coming from the field excitation source. Both are illustrated in Figure 6.3-28. One was to install capacitors across the field transformer secondary. The effectiveness of this solution is illustrated in Figure 6.3-32. The capacitance value for the illustrated data was ten (10) microfarads but related tests showed two (2) microfarads were sufficient to reduce the transients to acceptable levels. The other solution was to install a resistor and capacitor in series across the field winding. Component values of 25 Ω and 0.1 μF provided significant and probably adequate reduction of the transients. Unfortunately, the slip ring motor failed before the investigation of component values was completed. In addition, it was felt that addition of the capacitor across the field transformer was perferred since this approach avoided mounting components on the motor rotor.

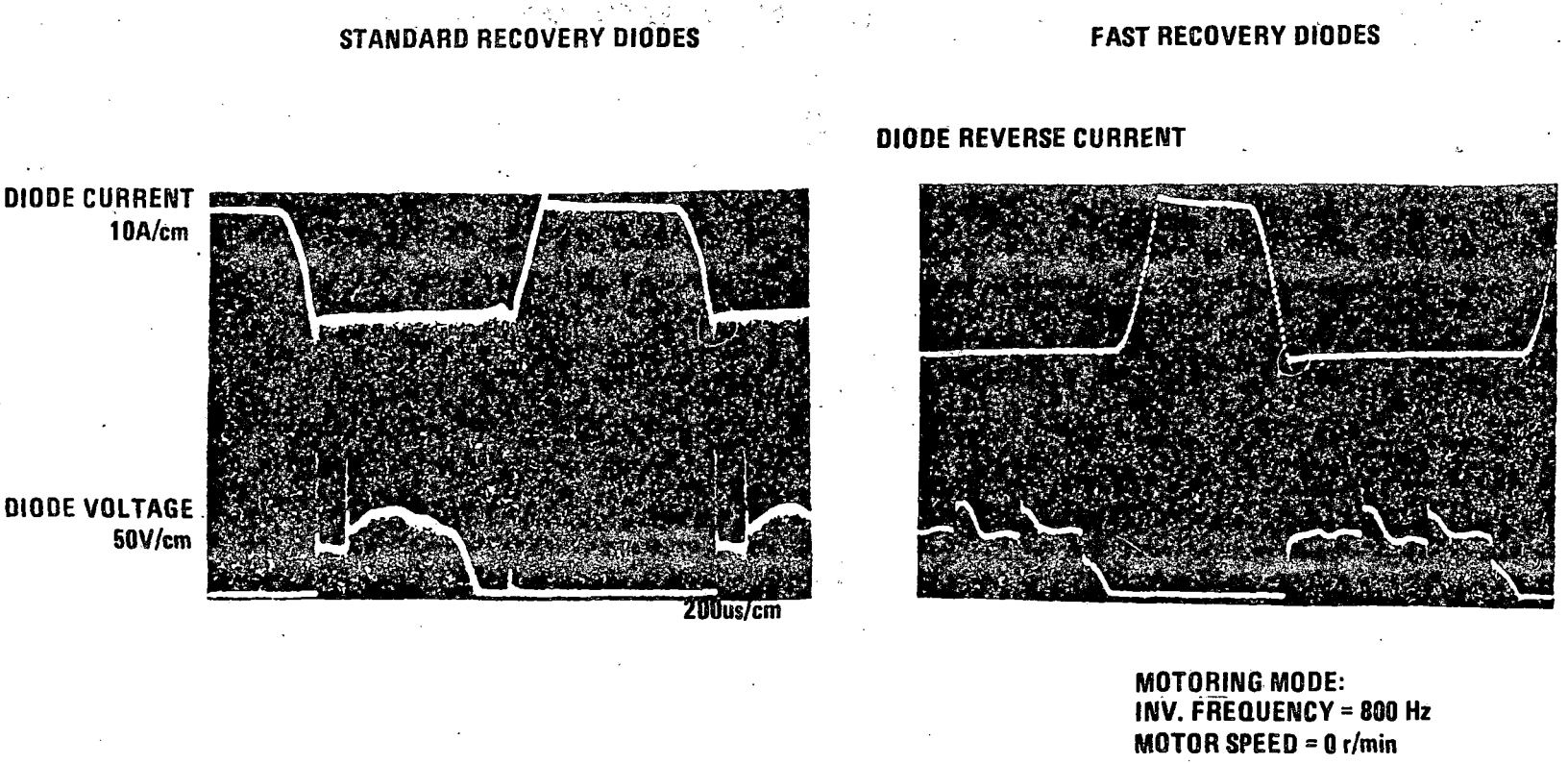

Figure 6.3-31. Field Rectifier Diode Recovery Characteristics

FAST RECOVERY DIODES INSTALLED

ZERO MICROFARADS

ed = 590V-pk

If = 30.9Adc

TEN MICROFARADS

ed = 215V-pk

If = 34.8Adc

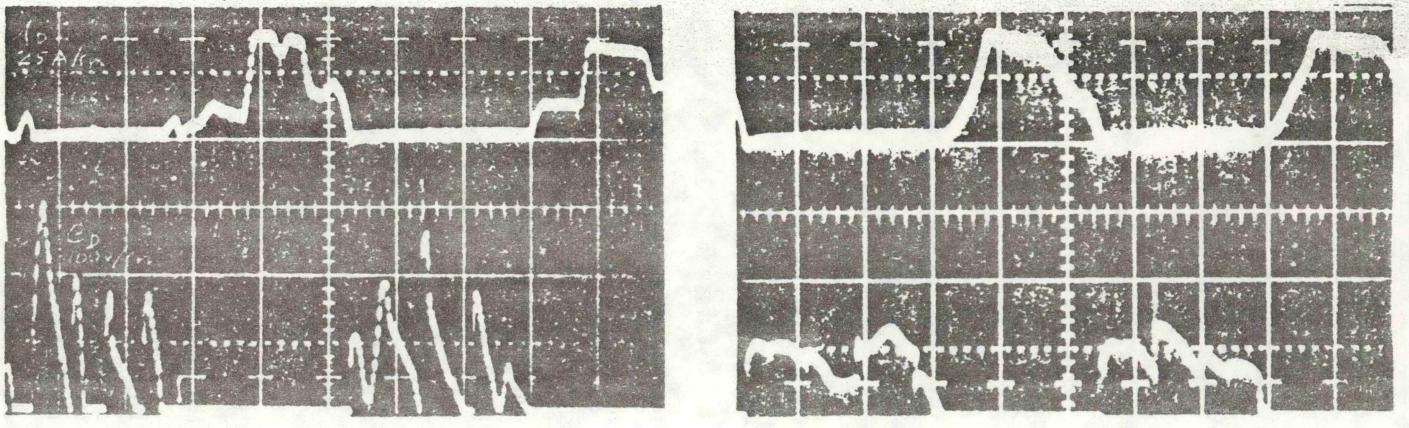

200us/cm

MOTORING MODE:

INV. FREQUENCY = 1000Hz

MOTOR SPEED = 1000r/min

TORQUE ≈1160 ft-lbs

Figure 6.3-32. Effect of Field Supply Transformer Shunt Capacitance on Rotating Rectifier Diode Voltage and Current

Differences in Motor Performance and Inverter Recovery Interrelationships

The series of tests which led to the incorporation of fast recovery diodes and capacitors across the field transformer secondary were conducted in the month of September on the ASDP slip ring motor in the B lab. Since this laboratory was limited in speed capability, testing above 2200 rpm was not performed.

Around mid-September, while operating motor S/N 3 in the A lab, an undesirable side effect of adding the capacitance across the motor field was discovered. The system would automatically shut down or QSD if operated in the region of 4000 r/min with an inverter frequency near 800 Hz. Investigation revealed the cause to be degradation in inverter SCR recovery time. This problem, discussed in paragraphs 6.3.3.3.2 and 6.3.3.3.3, was not new, but the degree of degradation was much more severe with the 20 μF capacitor which had now been added across the field.

Subsequent investigation in the A lab showed the degradation to be a function of the amount of capacitance added and even as little as 2 μF had a significant deleterious effect. The investigation which revealed this undesirable degradation in inverter recovery time was accomplished in late October and early November using ASDP Motor S/N 2B77. These tests also indicated that operation over the full torque-speed range capability of the A lab was possible without the transient suppression capacitors across the field. Earlier tests of Motor S/N 3 in the A lab indicated that noise transient spikes were apparently false triggering the surge protection circuit at some high speed, maximum power operating points. The initial conclusion was that the amplitude of the transients was higher with the slip ring motor and with Motor S/N 3 than with Motor S/N 2B77.

One condition which could have resulted in differences between the motors was found. It was that the damper bars in the rotors were not well terminated electrically. It had the effect of leaving possible discontinuities in the squirrel cage formed by the damper bars. The condition was corrected in Motors S/N 2B77 and S/N 3. The effect of the improved termination on field excitation transients could not be evaluated since Motor S/N 3 was not run in the motoring mode after the termination was improved.

Other early data also suggested differences between the motors – for example, data comparing Motors S/N 2B77 and S/N 3 with respect to torque at identical operating points in terms of speed and VCO frequency. Later, differences were seen day-to-day in data

taken on Motor 2B77. Investigation showed most of the differences to be the result of changes in the dc input voltage to the inverter. Additional apparent differences can reasonably be attributed to errors in instrumentation, differences in operator interpretation of meter indications and changes in instrumentation; e.g., the measurement of a critical voltage or current on a precision Fluke meter rather than on a panel meter. The best judgment that can be made from the available data relative to possible differences in the motors is that, if differences exist, they are minor and subtle. If they affect operation, e.g., noise triggering of surge protection circuit, it is because an already marginal condition exists.

Final System Configuration

There were no surge suppression capacitors across the field excitation transformer for the final series of system performance tests conducted on 9 December 1977, nor for subsequent motor bearing tests. The capacitors were deleted to minimize vulnerability to the incipient QSD problem. It is presumed that further development of the system would mitigate the inverter recovery problem and permit the use of the capacitors across the field transformer to reduce the possibility of transients false triggering the surge protection circuit. The alternative, and the preferred configuration for a new ground-up design, would be to incorporate an RC circuit directly across the field winding.

6.3.3.4 Significance of Motoring Mode Problems

6.3.3.4.1 Inverter-Cycloconverter Interaction

Inverter-cycloconverter Interaction, as discussed in paragraph 6.3.3.3.3, is probably the most important remaining motoring mode problem. This is so more because it represents a fragility or an uncertainty than because it represents a definable capability limitation. During the final phases of testing, as on 12/9/77 and in subsequent motor bearing tests, the interaction did not constrain the system capability in any respect. There was not even an incipient problem with inverter SCR recovery time. The shortest times seen were 170 μs and a system QSD is not effected until the time deteriorates to 50 μs. On the other hand, the condition, although qualitatively understood, cannot currently be analytically modeled or described. Subtle differences in gate control or timing (as discussed in paragraph 6.3.3.3.2), motor characteristics or power system configuration (as discussed in paragraph 6.3.3.3.7) can result in an increase in the level of interaction. Development

tests to further define this phenomena and possible modifications to reduce susceptibility to it are discussed in paragraph 7.2. To the extent that gate timing is improved to minimize the interaction, it also reduces the di/dt seen by the cycloconverter SCRs (see paragraph 6.3.3.3.5).

6.3.3.4.2 Shut-Down Transients

The problem of dissipating the energy stored in the motor at the instant of shutdown also requires further development work. This problem caused the failure of DSAS devices as discussed in paragraph 6.3.3.3.4. It was mitigated by redirecting the energy to the braking circuits, an approach which led to other unsolved system operational problems. Fortunately, the problem can be analytically defined and investigated. Possible solutions are discussed in paragraph 7.2.2.

6.3.3.4.3 High-Speed Cycloconverter Recovery

The inability to operate at high speed and low torque, as discussed in paragraph 6.3.3.3.6, if not resolved would result in limitations to system operation. Fortunately, the reason for the problem is well understood and it is probable that a relatively simple design modification, as discussed in paragraph 7.2.3, will solve the problem.

6.3.3.4.4 Automatic Power Factor Advance (PFA) and RPS ⇔ CEMF Transitioning

The test data recorded on 12/9/77 indicates the related problems of automatic PFA and RPS ⇔ CEMF transitioning to be well in hand. Further optimization via circuit component value changes is possible as discussed in paragraph 7.2.4.

6.3.3.4.5 Rotating Rectifier Surge Protection

The problem of rotating rectifier surge protection is resolved in all but one regard. That is that the addition of capacitance across the field excitation transformer to provide added margin to prevent noise triggering of the crowbar circuit, also has the negative effect of causing increased inverter-cycloconverter interaction. This is discussed in paragraph 6.3.3.3.7. At worst, the solution to this problem, would require the addition of a reasonably small resistor and capacitor across the rotor field.

6.3.4 BRAKING MODE SYSTEM LEVEL TESTS

6.3.4.1 Introduction and Chronological Summary

Braking mode development work and tests were considered lower in priority than motoring mode tests, based on an assumption that open loop operation in the braking mode was simpler and easier to accomplish than in motoring. Subsequent experience would confirm this but it would also uncover significant problems resulting from very high voltages generated in the braking mode.

Significant effort in verification of braking mode operation was initiated in late July 1977. By August 5, modifications to improve the SCR gate drives in the brake control module were completed. These modifications were similar to those previously described for the cycloconverter. In addition, the phase gating delay control circuits for the SCRs were updated from the original design and functionally verified. By late August, minor problems of "arc over" between brake control module feed-through terminals and the case were solved by additional insulation. Successful operation was demonstrated over the full torque range for speeds up to 2000 r/min and at lower torques, limited by dynamometer capability, up to speeds of 3500 r/min. Speeds above 3500 r/min were not attempted because voltages were approaching the 1800 V reverse voltage breakdown limit of the braking module SCRs. Due to the high voltage problem, braking tests were terminated pending the procurement of SCRs rated at 2700 V and the improvement of dV/dt circuits in the braking module. With this modification effort, and the intervention of higher priority motoring mode work, additional braking mode testing work was delayed until mid-October. Between mid-October and mid-November, a final series of braking mode tests was performed. A tabular summary of the tests performed and problems experienced is shown in Table 6.3-IV. In summary, the testing was done in the dynamic braking mode by taking a matrix of data points within the specified torque-speed envelope. One limitation was that maximum torque capability, due to dynamometer limitations, could not be demonstrated at speeds above 2000 r/min. Two basic data sets were taken. In one set, torque at each speed was controlled by varying motor field excitation, i.e., by controlling VCO frequency. In the other, field excitation was maintained at a constant level and phase gating of the braking module SCRs was varied. No testing was accomplished in the regenerative braking mode.

DYNAMIC BRAKING MODE TESTS PERFORMED:

- High speed, torque 850 ft-lb, A lab, S /N 2B77 Motor
- High torque, speed 2000 r/min, B lab, S/N 3 Motor
- Data sets in 500 r/min increments (nominal)
- Test Types
  - Torque versus field excitation (no phase delay)
  - Torque versus phase delay SCR gating (fixed level of field excitation)
- Problems
  - Cycloconverter voltage rating exceeded above 3500 r/min
  - Excessive voltage stress on braking module SCRs
  - Random SCR turn-on at speeds over 4000 r/min (noise problem)
  - Torque pulsations with phase delay gating
  - Overheating of current transformer
  - Instability of TCE current sensors

Table 6.3-IV. Braking Mode Final Tests

Of the problems experienced, the torque pulsations seen with delay gating are considered to be the least serious and probably would not exist in a system on an operational vehicle. That is, they appear to be a phenomenon unique to the gear train of the laboratory dynamometer. It is felt that the problem of random SCR turn-on at speeds over 4000 r/min can be solved by relatively minor modifications of the SCR gating control electronics. The exceeding of the cycloconverter voltage limits is a serious problem which will require modification of the system mechanization. Other minor problems included a current transformer failure due to overtemperature and excessive errors in the outputs of current sensors needed for integration of the system with the train control electronics (TCE).

A summary tabulation and discussion of test results are presented in paragraph 6.3.4.2 which follows. Paragraph 6.3.4.3 then presents a detailed discussion of the problem areas.

6.3.4.2 Summary of Demonstrated Performance Characteristics

Dynamic braking data includes 491 separate data points. Recorded parameters at each point were: torque, r/min, brake grid voltage, brake grid resistance (full or one-third full value), phase delay rectifier gate control voltage, phase gate delay in electrical degrees, line-to-line voltage, phase current, SCR peak voltage, DSAS peak voltage, signals from the Hall

current sensor and transformers used to sense current, motor field excitation (input ac amps to rotary transformer), and inverter frequency.

This data was then processed to correct the torque readings in accordance with a calibration curve, to predict brake grid current, to predict motor current, to calculate brake voltage/resistance and compare to predicted brake grid current, and to calculate dc field amps.

6.3.4.2.1 Dynamic Braking Performance

A composite plot of the maximum dynamic braking torque achieved in laboratory system testing is shown in Figure 6.3-33. The A lab data was obtained using Motor S/N 2B77 and the B lab data was obtained using Motor S/N 3.

The points plotted are the highest torque points tested, but they do not represent the maximum capability of the system. The absence of data in the high torque, high speed corner of the plot was due to A lab dynamometer limitations. Analysis and extrapolation of the data indicates that the full braking torque specified for the system can be realized in the dynamic braking mode throughout the speed range with one possible minor exception. This

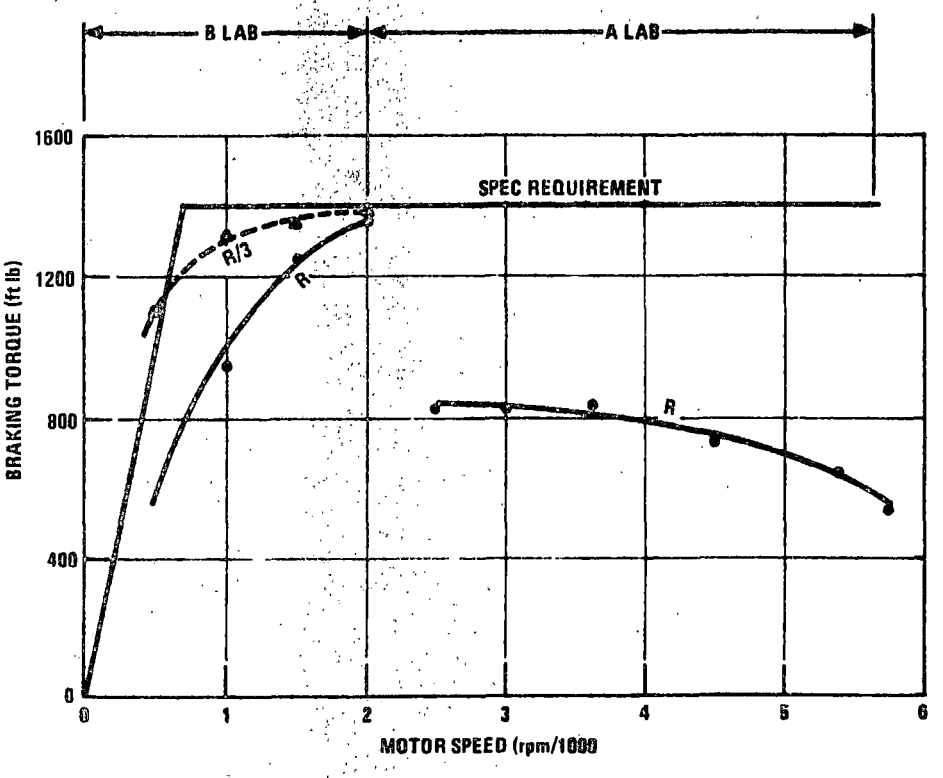

Figure 6.3-33. Dynamic Braking Performance

is a small area in the low speed - high torque corner near the 700 r/min, 1405 ft-lb point. A higher field current than was used in these tests is possible and might provide the specified torque.

The maximum torque obtainable is independent of whether field control or phase gating is used since there is no gating delay when maximum torque is commanded.

6.3.4.2.2 Predicted versus Measured Torque Using Field Control

A three-way comparison of dc field excitation current versus dynamic braking torque was made. Compared were data obtained during motor component level tests by Delco Products, analytical predictions by Delco Electronics, and test data obtained during system level testing. The results are shown in Figure 6.3-34.

The comparisons were made at 2000 r/min since this was a speed at which motor component level test data was available. In general, there is very good correlation. This tends to confirm the validity of the analytical model of the motor for predicting braking performance at operating points where testing was not possible.

3.3.4.2.3 Relationship Between ac and dc Field Currents

The relationship between motor field dc current and the ac current in one phase of the rotary transformer primary is shown in Figure 6.3-35. The ratio of I_{dc} to I_{ac} as determined from the system level tests conducted at Delco Electronics varies from about 0.8 at low current levels to about 1.0 at a current of 50A. The anomalous region around 10 A is the result of resonance between the coupling capacitors and the leakage inductance of the field supply transformer and rotary transformer.

The straight line with a slope of 0.81 on the referenced figure shows the nominal current ratio determined by Delco Products in their motor component level tests. The reason for the difference between the curves is that in the Delco Product tests, excitation was at a fixed frequency of 400 Hz, whereas in the Delco Electronics system level tests, the frequency was varied from 425 Hz to 1200 Hz. A secondary cause could be differences in the form factor of the current since the excitation voltage waveshape at low inverter frequencies is very distorted.

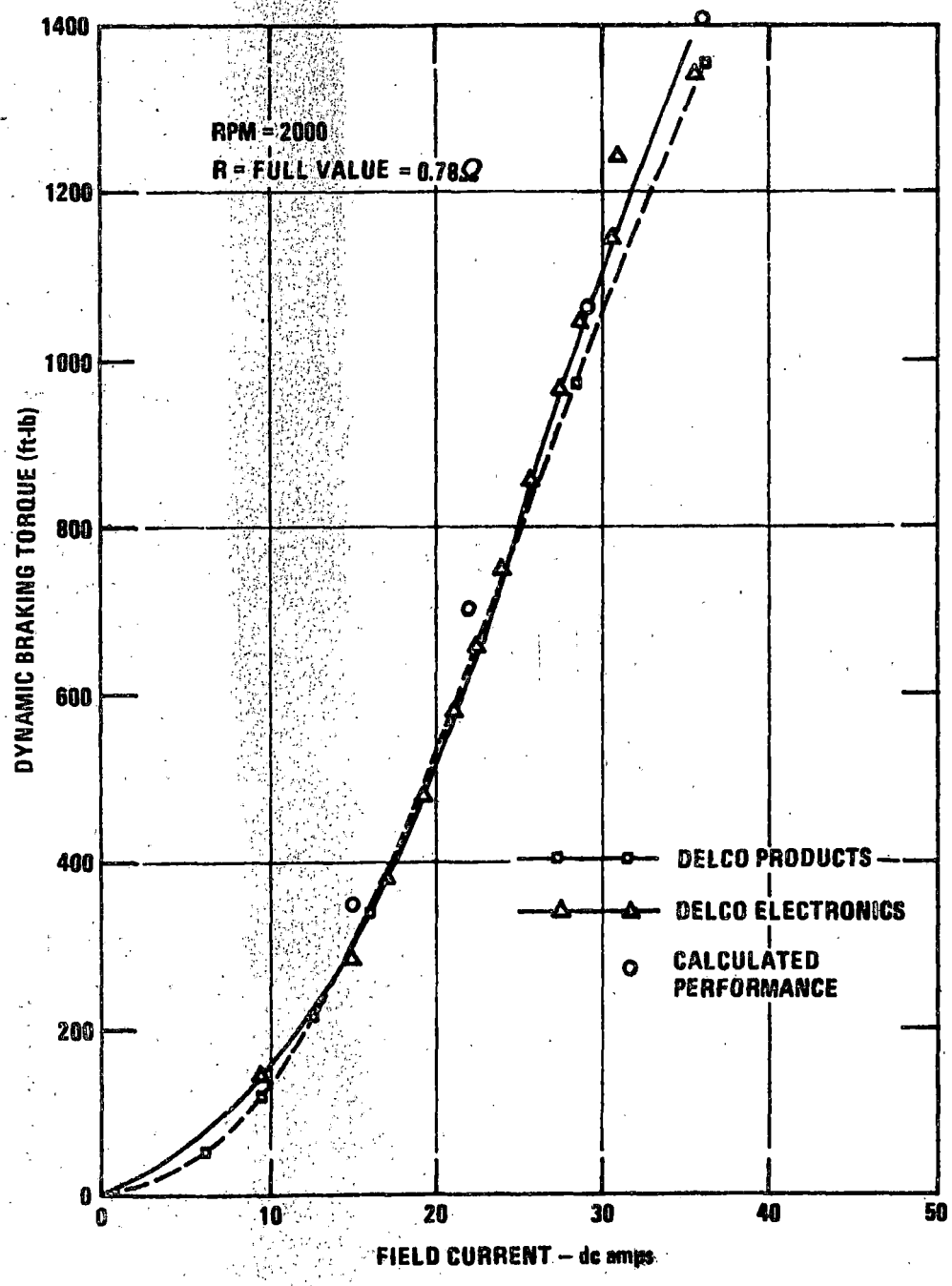

Figure 6.3-34. Field Current Versus Braking Torque — Predicted Versus Test Data

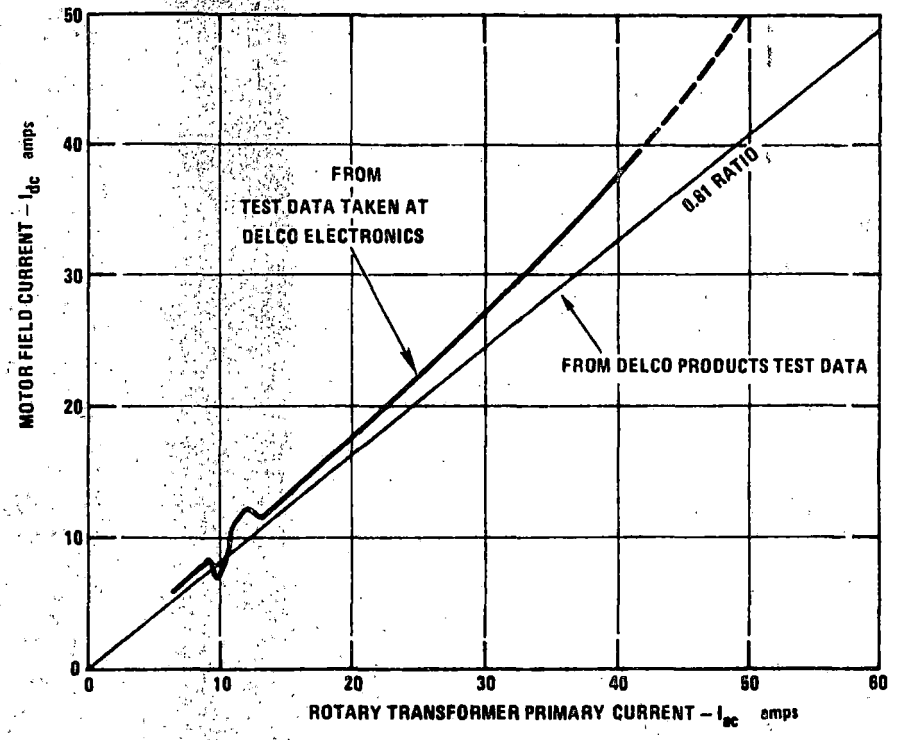

Figure 6.3-35. Relationship Between ac and dc Field Currents

The curve of Figure 6.3-35 was used to derive the dc field currents used in the comparison of predicted versus measured torque shown in Figure 6.3-34.

6.3.4.2.4 Dynamic Braking Resistor Shunting

To maintain maximum commanded dynamic braking capability to the lowest possible speed, it is necessary at some point to change the resistance of the dynamic braking grid resistor from R (0.78 Ω) to R/3 (0.26 Ω). This change is effected by a 10th SCR in the brake module which shunts part of the braking grid. If the SCR is gated at the optimum point relative to motor speed and field current, the transition can be accomplished without a change in torque. This means that the railcar will experience little or no jerk at the time of transition. Based on computer analysis of the test data, the loci for the desired transition is as shown by Figure 6.3-36. In closed-loop operation the data of Figure 6.3-36, after being extended to include the full torque range, would be stored in a look-up table in the TCE microprocessor. The microprocessor would then issue a discrete to the SCR at the desired transition point. The foregoing assumes the use of motor field control only. If phase gating is assumed, an

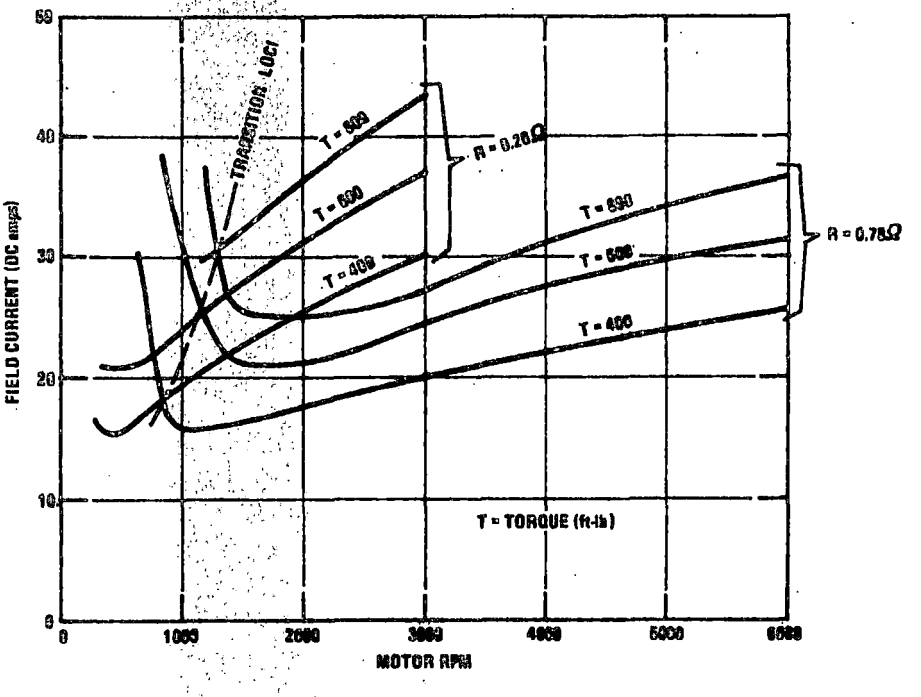

Figure 6.3-36. Dynamic Braking Resistor Shunting — Loci of Transition Points

alternative possibility would be to transition at a specific speed, e.g., 2000 r/min, and use changes in the phase gating angle at the instant of transition to prevent jerk.

6.3.4.2.5 Phase Delay Torque Control

Braking torque control using phase delay gating depends on gating the brake module SCRs at a specific delay angle in degrees of motor voltage. The design objective of the control circuit is that the delay angle be proportional to the control or command voltage and independent of the vehicle speed. The paragraphs following discuss the performance of the circuit which computes the delay angle versus the control voltage and the performance of the propulsion system in the phase delay mode. Performance is described in terms of torque versus phase delay angle at specified levels of field excitation.

Phase Delay versus Control Voltage

It is desired that the computation of SCR gating delay versus control volts be independent of vehicle speed. Since motor frequency is proportional to speed and frequency is inversely proportional to time, it is required that the control circuit compute a time delay which is the inverse of speed. This computation is accomplished by a reset integrator with an input proportional to speed. The control voltage is used as a variable threshold on the integrator output.

The performance of the gate delay computation circuit is plotted in Figure 6.3-37. The data shows complete independence of speed at low speeds and a slight increase in delay angles at high speeds. Since, at the system level, this computation would be inside a closed loop computation of torque, the circuit performance is more than adequate.

Torque versus Phase Delay Angle

The results of system level tests of torque versus phase delay angle are summarized in Figure 6.3-38. Curves are plotted for both the 0.78Ω and 0.26Ω values of dynamic braking resistance. The field current was slightly higher when the lower value of resistance was used, i.e., 44 A versus 42 A, but this small difference is not considered significant in the comparisons being made.

Significant points of interest relative to the data are as follows:

- The torque versus phase delay does not change with speed significantly for motor speeds above 3000 r/min.
- In the 2000 r/min to 3000 r/min speed range, the change in torque resulting from changing load resistance is very low when the phase dealy angle is large. This means there is a wide region where transitioning can be effected.
- The torque at 500 r/min is greater than at 1000 r/min. This is a typical generator characteristic which appears to be magnified by the use of phase delay gating.

The extrapolation of the 3000 to 5000 r/min data is consistent with the extrapolation made on the field control mode data. As previously explained, system test data could not be obtained due to laboratory facility limitations.

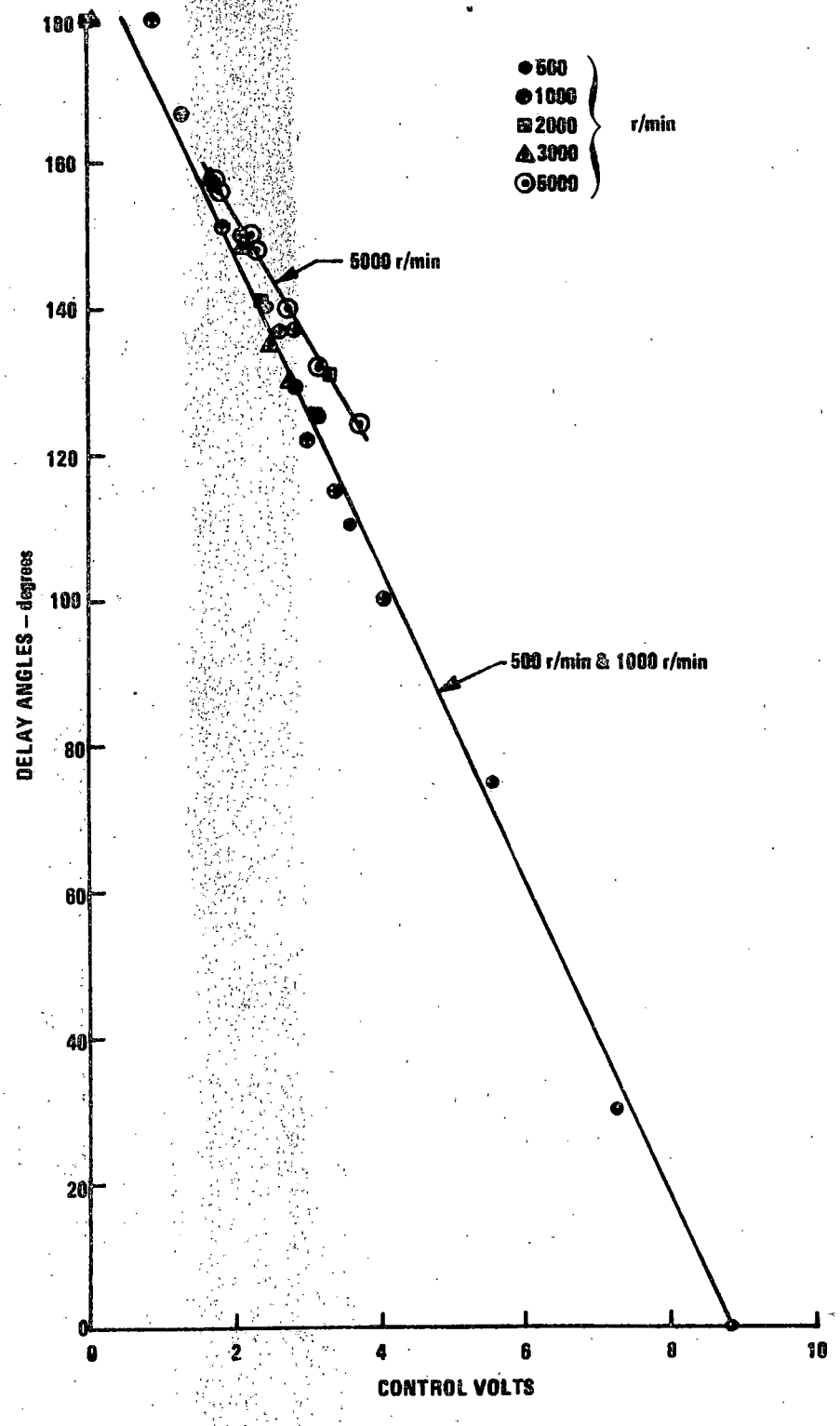

Figure 6.3-37. Phase Delay Angle Versus Control Volts

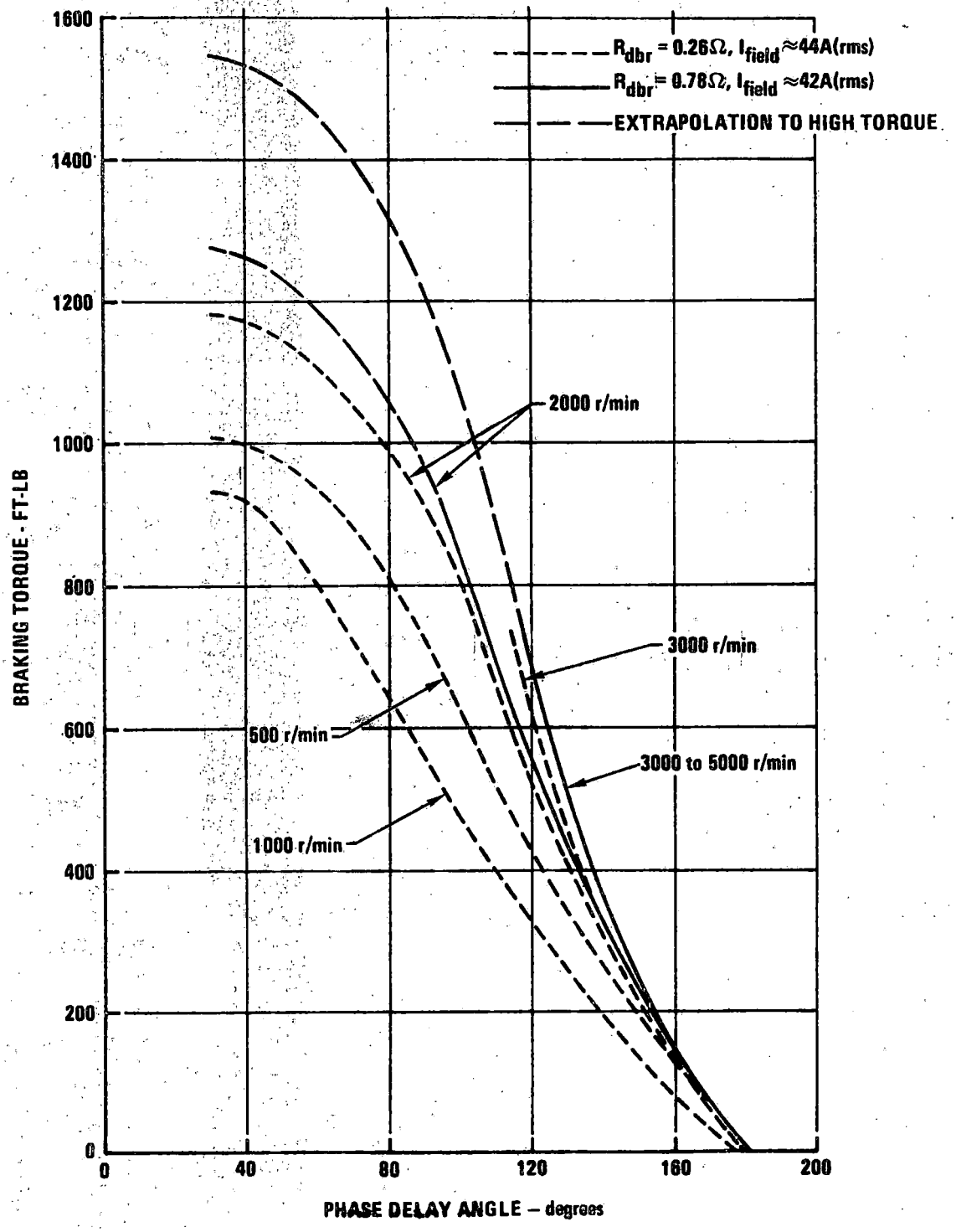

Figure 6.3-38. Braking Torque Versus Phase Delay Angle

6.3.4.3 Braking Mode Problems

6.3.4.3.1 Overvoltage of Cycloconverter SCRs and DSAS Devices

During braking tests in early November, a DSAS shorted, burning out wires connecting it to the cycloconverter and resulting in extensive damage to gate drive logic circuits. These are the same devices which were shorted during motoring tests by large fault currents which randomly occurred at the instant of system shutdown. As noted in the motoring mode discussions, (see paragraph 6.3.3.3.4) the DSAS devices act like high voltage bi-lateral zener diodes. They are in parallel with the cycloconverter SCRs to prevent the SCRs from being damaged by spurious high voltage transients.

Analysis of the braking mode failure showed that the DSAS breakdown voltage of 1700 V was exceeded during phase delay controlled braking at motor speeds above 3800 r/min. This failure, due to excessive voltage, is the result of an oversight. The maximum voltage stress across the inoperative cycloconverter was assumed to be the peak motor voltage. Instead it is the instantaneous sum of the peak motor and peak inverter voltages. Examination of a schematic of the inverter, cycloconverter, and motor will show there are always two pairs of SCR and DSAS devices in series, blocking the motor stator voltage if the cycloconverter SCRs are not gated. Assuming equal voltage division across the series pairs of SCR and DSAS devices, the DSAS voltage can be calculated as follows:

$$\text{DSAS Voltage} = \frac{\text{Peak Inverter Voltage} + \text{Peak Motor Voltage}}{2}$$

The peak DSAS voltage was measured with the system operating at several torque-speed operating points as shown by the data of Table 6.3-V, and compared to that calculated by the above equation. These data indicate that the voltage does not divide equally across the SCR and DSAS pairs. No pattern to the voltage division is seen but the actual voltage across a single DSAS device can approach 2/3 the sum of the peak motor and inverter voltages.

Interpretation of this overvoltage condition relative to the various modes of system operation leads to the following general observations:

1. When phase control is employed in the dynamic braking mode, the DSAS voltage ratings will be exceeded at motor speeds above approximately 3800 r/min.
2. When field control was employed in the dynamic braking mode, the DSAS voltage rating was not exceeded at a speed of 5500 r/min and at 500 ft-lb of torque. The voltage rating probably would be exceeded, however, at the maximum requirements of 5646 r/min and 1405 ft-lb of torque. The latter point could not be tested due to dynamometer limitations.

Motor Speed (r/min)	Torque (ft-lb)	BRAKING MODE	Field Current (I_{ac})	DSAS Peak Volts (Measured)	"Assumes Equal Division" DSAS Peak Voltage $(Inv_{Peak} + Motor_{Peak})/2$
3000	700	Field Control	27.8 amps	950	$\frac{1103 + 495}{2} = 800$
3000	~50	Phase Control	45.0 amps	-	$\frac{1301 + 1041}{2} = 1175$
4000	700	Field Control	30.8 amps	1100	$\frac{1131 + 594}{2} = 862$
4000	~50	Phase Control	45.0 amps	1450	$\frac{1301 + 1400}{2} = 1351$
5000	600	Field Control	32.0 amps	1300	$\frac{1146 + 622}{2} = 890$
5000	~50	Phase Control	45.0 amps	1470	$\frac{1301 + 1748}{2} = 1524$
5500	500	Field Control	30.6 amps	1300	$\frac{1120 + 580}{2} = 850$
5500	~50	Phase Control	45.0 amps	1650	$\frac{1301 + 1973}{2} = 1637$
5640	~50	Phase Control	53.0 amps	-	$\frac{1428 + 2011}{2} = 1720$

Table 6.3-V. DSAS Peak Voltage

3. The regenerative mode was not tested but limitations would be similar to those for the dynamic braking mode.
4. Reverse voltage capacity or derating is required to provide for spurious voltage transients, unequal voltage division ratio, and component degradation.
5. The reverse voltage rating of the cycloconverter SCRs is only 100 V above the DSAS rating (1800 V). To increase the cycloconverter reverse voltage capability requires upgrading of both DSAS devices and SCRs.

This problem significantly limits dynamic and regenerative braking mode capabilities at high speed. Completion of laboratory tests at high speeds was accomplished by circumventing the problem. The solution in the laboratory was to disconnect the cycloconverter from the motor. This did not compromise the validity of the performance characterization data obtained since the cycloconverter is operative in the motoring mode only.

6.3.4.3.2 Voltage Stress on Braking Module SCRs

The maximum predicted peak voltage across the braking module SCRs is 2400 V as shown by Figure 6.3-39. This prediction is based on an extrapolation of data obtained in the series of braking mode tests conducted in August when the maximum motor speed tested was 3500 r/min. Because of the prediction that peak voltage levels would be well over 2000 V, the GE C441 SCRs then in the brake module, which had a peak reverse voltage rating of only 1800 V, were replaced with GE C602LM SCRs having a rating of 2700 V. These higher voltage units were found to be adequate for all voltage conditions experienced during the high-speed tests conducted in November. In addition to changing the SCRs, the voltage rating of the dV/dt capacitors was increased from 2000 V to 3000 V.

This voltage stress condition is not an operational problem. It is only a potential problem to the extent that maximum voltage levels approaching 2400 V are predicted. The limited derating of 300 V could be construed as a reliability problem. If greater derating is desired, SCRs with ratings as high as 3500 V are available. They are larger in size, however, and would require some mechanical redesign of the brake control module to accommodate their use.

6.3.4.3.3 Noise Gating of Braking Module SCRs

During the November series of braking tests, an uncontrolled firing of brake module SCRs

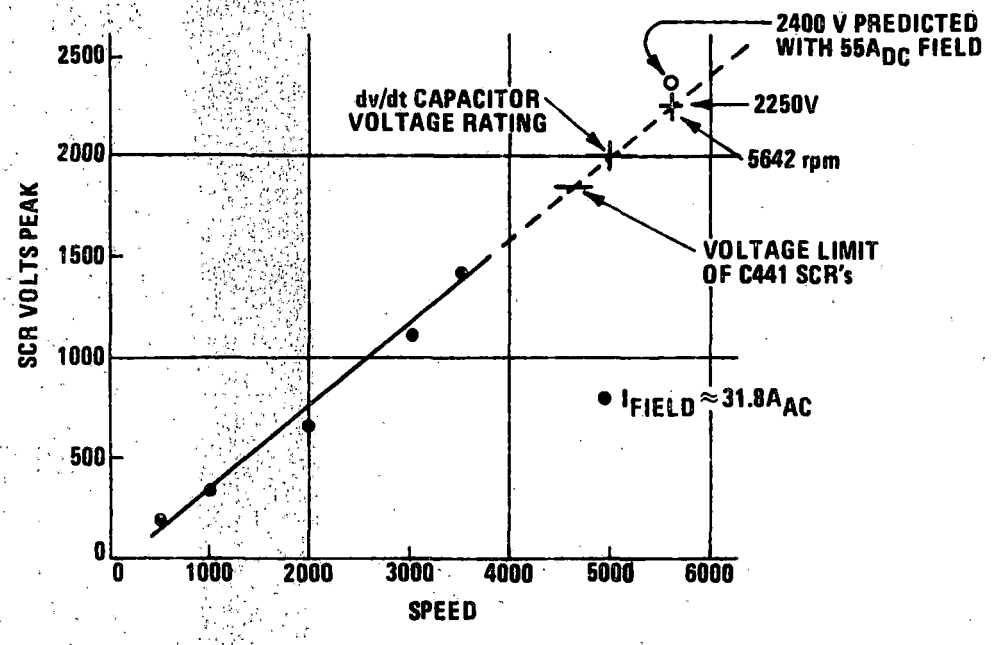

Figure 6.3-39. Brake Module SCR Voltage Capability

occurred under two conditions, as follows:

1. • Maximum gate delay angle (no braking commanded)
   • Inverter at 800 Hz
   • Motor r/min at 3500 to 4500
2. • Maximum gate delay angle (no braking commanded)
   • Inverter above 950 Hz for full field
   • Motor r/min above 5000 (high voltage).

Several tests were conducted to isolate the cause of this false firing. First, the current of the gate drive transistor collectors was monitored while approaching the conditions of false firing and while the false firing occurred. There was no indication of uncommanded current at the gate drive transistor collectors. Secondly, SCR peak voltages were monitored and measured to be approximately 2000 V which is 700 V below their 2700 V rating. It was assumed that overvoltage was not the cause of false firing. Further tests indicated that no false triggering signals were being generated in the MCE logic or gate drive circuitry.

Next, the gate drive input connector was removed from the brake control module, which removes the 30 kHz excitation from the brake module gate drive circuitry. Retesting indicated no false firing of the SCRs.

The findings can be summarized as follows:

1. No false commands generated in logic
2. No extraneous current in gate drive transistors
3. No overvoltage on SCRs
4. Removal of 30 kHz from brake module eliminates the false firing.

Summary Conclusion

The most probable cause of the uncontrolled SCR gating problem is a parasitic path or ground loop for the 30 kHz excitation. This path is apparently shunting the gate drive transistor and enabling a current in the gate drive transformer primary.

Time limitations due to the pending test program termination prevented an engineering investigation in the depth needed to pinpoint the source of the problem and to develop a solution.

Completion of Testing

The completion of the series of dynamic braking tests at speeds up to 5600 r/min was accomplished by isolating the ground side of the dynamic braking resistor from ground. This floating of the load is compatible with the dynamic braking mode of operation and could be a permanent solution if only dynamic braking were considered. It is not compatible with the regenerative braking mode, however, which must operate with the power circuits referenced to ground.

6.3.4.3.4 Torque Pulsations at Light Load

Phase control of braking results in a pulsating torque. When operating at high torque the "p .tion" effect is minimal due to the large SCR conduction angles. As the conduction angle is decreased, the pulsations become more discrete. For most conditions of operation the effect of the pulsations was imperceptible, being evidenced only in differences in the sound of the motor. The pulsations are proportional to motor speed and occur at 3X the motor voltage frequency, which is the SCR gating frequency.

In one operating region, the torque pulsations resulted in severe banging in the reduction gear box between the motor and the dynamometer. This region included speeds between approximately 400 r/min and 1600 r/min and torques of 100 ft-lb to 700 ft-lb. These torques were obtained with SCR conduction angles of 5^{o} to 15^{o}. The "banging" apparently resulted from a momentary reversal of torque in the gear box due to a condition of torsional resonance which amplified the torque pulsations. This phenomenon was experienced only in the A lab which employed a gear reduction between the motor and the dynamometer (load). It was not experienced for identical motor torque-speed conditions in the B lab where the motor was directly connected to the dynamometer.

The resonant condition and "banging" would be very objectionable if it should occur on a rail vehicle. However, it is unlikely that the problem would exist on a rail vehicle since the vehicle drive train is stiff and there is relatively little inertia in the railcar gear train.

6.3.4.3.5 Field Supply Transformer Failure

During the August series of braking tests, the winding of one phase of the field supply current transformer burned out. The other phases showed evidence of overheating. This transformer has a 3-turn primary winding which serves in the motoring mode, a 144-turn primary winding which serves in the braking mode, and a 36-turn secondary winding. In the motoring mode it operates as a "current" transformer, whereas in the braking mode it acts as a "voltage" transformer. The burn-out occurred in one of the braking windings.

Changes were made in the winding design and in reconfiguration of the coolant loop as discussed in paragraph 7.3.5. These changes relieved the problem sufficiently to enable braking with 45A of field current for periods of time up to 12 minutes. Higher currents are possible for shorter periods of time. The braking mode field current profiles have not been sufficiently defined and evaluated to permit a complete assessment to be made of the present capability.

6.3.4.3.6 Current Sensors

Closed loop control of the braking mode requires monitoring of the motor current and obtaining a voltage analog for use by the TCE in computing torque. It is desired that the voltage analog be a function of the true RMS of the motor output. It is also desired that the measurement include all three motor phases. This is difficult in the braking mode

when phase gating is employed due to the large changes in the form factor of the motor current waveshape.

There are two independent sensor systems that monitor motor current. One is a Hall cell and related electronics located in series with the brake grid. Total grid resistor current is seen by this sensor. The other is the three current transformers and related electronics that monitor the current of each motor phase. A detailed study of data obtained by monitoring the sensor circuit outputs shows that neither is adequate in the braking mode from accuracy and stability standpoints. In particular, offsets on the outputs change randomly or vary as a function of certain noise conditions on the system grounds. Also, nonlinearities are large and possible ambiguous. These random offsets and ambiguities preclude the planned use of stored correction tables in the TCE microprocessor to correct for current sensor errors in the computation of torque.

6.3.4.4 Significance of Braking Mode Problems

The problems of cycloconverter DSAS and SCR overvoltage, as discussed in paragraph 6.3.4.3.1, are the most serious of the braking mode problems. These problems limit electrical braking capability at motor speeds above certain limits, depending on operating mode. The greatest limitation is for the case of phase delay control when braking under conditions of low braking torque command. Possible solutions to this problem are discussed in paragraph 7.3.

The noise gating of the braking SCRs, as discussed in paragraph 6.3.4.3.3, and the inadequate accuracy of the current sensors, as discussed in paragraph 6.3.4.3.6, are considered to be detail circuit design problems requiring investigation and probably relatively minor circuit modifications.

The prediction of high voltage stress on braking SCRs, as discussed in paragraph 6.3.4.3.2, and the time limitation on braking mode operation, as discussed in paragraph 6.3.4.3.5, are only potential problems to the extent that greater design margins might be desired. The gear box backlash and resonance problem resulting from torque pulsations, introduced while employing phase gating, would be a serious problem if it were found to exist on a transit car. As discussed in paragraph 6.3.4.3.3, this problem was experienced only in the A lab. The consensus appears to be that a motor driving a transit car would not experience the problem but no modeling or analysis was done to support this conclusion.

SECTION VII

DEVELOPMENTAL SYSTEM - FINAL STATUS

This section of the report contains a description of the changes made (or considered to be still required) to the propulsion system Test Article configuration, the status of the final configuration, a discussion of unresolved problems, and the activities still required in order to arrive at a system configuration suitable for transit service.

7.1 CONFIGURATION CHANGES AND STATUS

The Test Article (TA) designation refers to the configuration of the ASDP propulsion system hardware prior to changes which were made due to problems and deficiencies uncovered during the system level testing discussed in subsection 6.3. The configuration of the hardware at the end of the program is referred to as the " final" configuration.

Extensive modifications have been made to many parts of the propulsion system as a result of system level test effort. These modifications were made in electronic circuits, in electronics packaging, in the traction motors, and in the cooling system. Additional modifications are still required to make the system suitable for transit application.

Some of the changes, such as in the case of the motors, have been developed to a point suitable for vehicle service tests. Other changes, such as those made to the inverter, cycloconverter, and brake control modules, are of a configuration adequate for continued laboratory development work but are not adequate, in terms of mechanical integrity, for vehicle service testing. In still other areas, such as circuit modifications to the motor control electronics (MCE), there are extensive make-shift modifications. In such cases, repackaging is recommended prior to any further development work.

The status of the equipment drawings and specifications, like the status of the hardware, varies from component to component.

The mechanical design drawings and specifications have not been updated to reflect changes [illegible]e Test Article configuration, except in the cases of the truck-mounted equipment. Electrical schematics, however, have been updated to incorporate the changes made during system level testing and do reflect the "final" configuration. A complete drawing list is included in Volume III of this report.

The changes made, and the status of the final configuration of each major component of the system, are discussed in the following paragraphs.

7.1.1 ELECTRONIC CONTROL UNIT (ECU)

Very extensive circuit development work was carried out in the Motor Control Electronics (MCE) portion of the ECU. In contrast, little was done with the Train Control Electronics (TCE). The TCE was functionally verified as described in paragraph 6.2, but the signal interfaces between it and the MCE were not. Also, system level closed loop control was not verified. As a result it is not known what TCE circuit design and electronics packaging changes, if any, may be required. In the case of the MCE, extensive circuit redesign was accomplished and more is required. Furthermore, a complete redesign of the electronics packaging is felt to be required.

7.1.1.1 MCE Modifications

It is recommended that the MCE be repackaged to incorporate the final configuration electronic circuits or refinements thereof prior to further developmental testing of the system. There are two primary reasons for this recommendation. One is that sensitive circuits are not adequately isolated from circuits capable of introducing noise. As an illustration, isolation of gate drive pulses and the 30 kHz carrier circuitry and wiring from the small signal (processing and control) electronics is inadequate. In addition, the isolation of the gate drive signals and grounding paths between the cycloconverter and inverter drive circuits is unsatisfactory. The inadequate 30 kHz isolation causes the carrier and pulse information to appear superimposed on the processing and control electronics signals. The inadequate gate drive isolation results in cross coupling of gate drive pulses between cycloconverter and inverter SCRs. To improve isolation during the system level testing, the 30 kHz circuit was physically removed from the MCE drawer. The inverter and cycloconverter gate drive outputs were separated and wiring to each unit was carried on isolated groups of shielded cables.

The other reason for recommending repackaging is that the MCE chassis now has several new circuits appended to it. There are also inactive circuits on the chassis. These conditions evolve as many modifications were made, as discussed in paragraph 6.3. The appendages and related poor functional partitioning of circuits results in interconnect fragility and excessive noise in sensitive signal circuits.

To reduce the noise susceptibility of sensitive circuits, it is suggested that the motor control electronics be repackaged into five functionally partitioned subassemblies as listed below. Furthermore, appropriate attention should be given to grounding and isolation of the interconnect cables between subassemblies.

Subassembly	Description
1	30 kHz Excitation Circuits
2	Cycloconverter Gate Drive Electronics
3	Inverter Gate Drive Electronics
4	Braking Gate Drive Electronics
5	Low Level RPS, CEMF, PFA Gate Command Signals and Fault Detection Circuits

Only subassembly 5 would contain low level signal processing.

7.1.2 POWER CONVERTER ASSEMBLY CHASSIS

The PCA chassis was not modified during the test program. Changes would eventually be required, however, particularly if the system were to be considered for production. One reason, to be discussed subsequently, is that changes to the inverter, cycloconverter, brake control, and field supply modules may require that the size of these units be increased. Another reason is that the raceway area available for hydraulic and electrical interconnects is marginal. Yet another is the need to add a reservoir to the propulsion power control equipment (PPCE) cooling loop.

The changes made (or considered to be required) to the modules which comprise the power converter assembly are summarized as follows:

7.1.2.1 Inverter Module

The most significant change to the TA inverter module was the redesign of the SCR gate drive circuits. Also, the interconnect wiring from the circuit component board in the inverter to the SCR gate leads was changed to twisted pairs. The new circuit schematic and packaging concept layout is shown on drawing 7561541. As a result of the changes, the unit density is now too high to permit easy component access. It is therefore recommended that the unit be partially redesigned to improve serviceability. The recommended redesign includes changes in the mechanical structure and may result in the volume of the module assembly being increased.

7.1.2.2 Capacitor Module

No changes were made to the TA capacitor module and no need for changes is foreseen.

7.1.2.3 Cycloconverter Module

Changes made to the TA cycloconverter module were as follows:

1. The SCR gate drive circuits were extensively modified and the gate drive transformers were replaced with redesigned units that were larger in size.
2. The interconnect wires between the gate drive circuits and the SCR gate wires were replaced with shielded, twisted wires having double layers of shrink tubing applied for supplemental insulation. The new wires were rerouted for minimum length. This required that the wires be cascaded over the edge of the circuit component board directly down to the respective SCRs.
3. To implement the Item 2 wire routing change, it was necessary to remove side reinforcing structure needed by the module to survive the shock and vibration levels expected on a transit car.

The existing printed circuit component board was retained when the Item 1 changes were incorporated. This required extensive modification and resulted in a configuration not suitable for use other than in laboratory tests. Redesign is therefore required. In addition, redesign and reinstallation of the Item 3 reinforcing structure is required. To accommodate this redesign it is probably necessary either to reroute the Item 2 interconnect wiring or to use a larger module chassis.

7.1.2.4 Field Supply Module

The failure of the field supply transformer as discussed in paragraph 6.3.4.3.5 required modification of the windings for improved cooling. It also indicated that continuous flow of coolant to the module was necessary. In the TA configuration the module acted as a stand-pipe sump in the coolant loop. The loop flow did not pass through it.

To provide the required flow the coolant loop was changed for laboratory tests to the configuration illustrated by the schematic on Figure 7.1-1. In this configuration, the field supply was placed in series with the capacitor module and a large tank was added to act as a sump or reservoir.

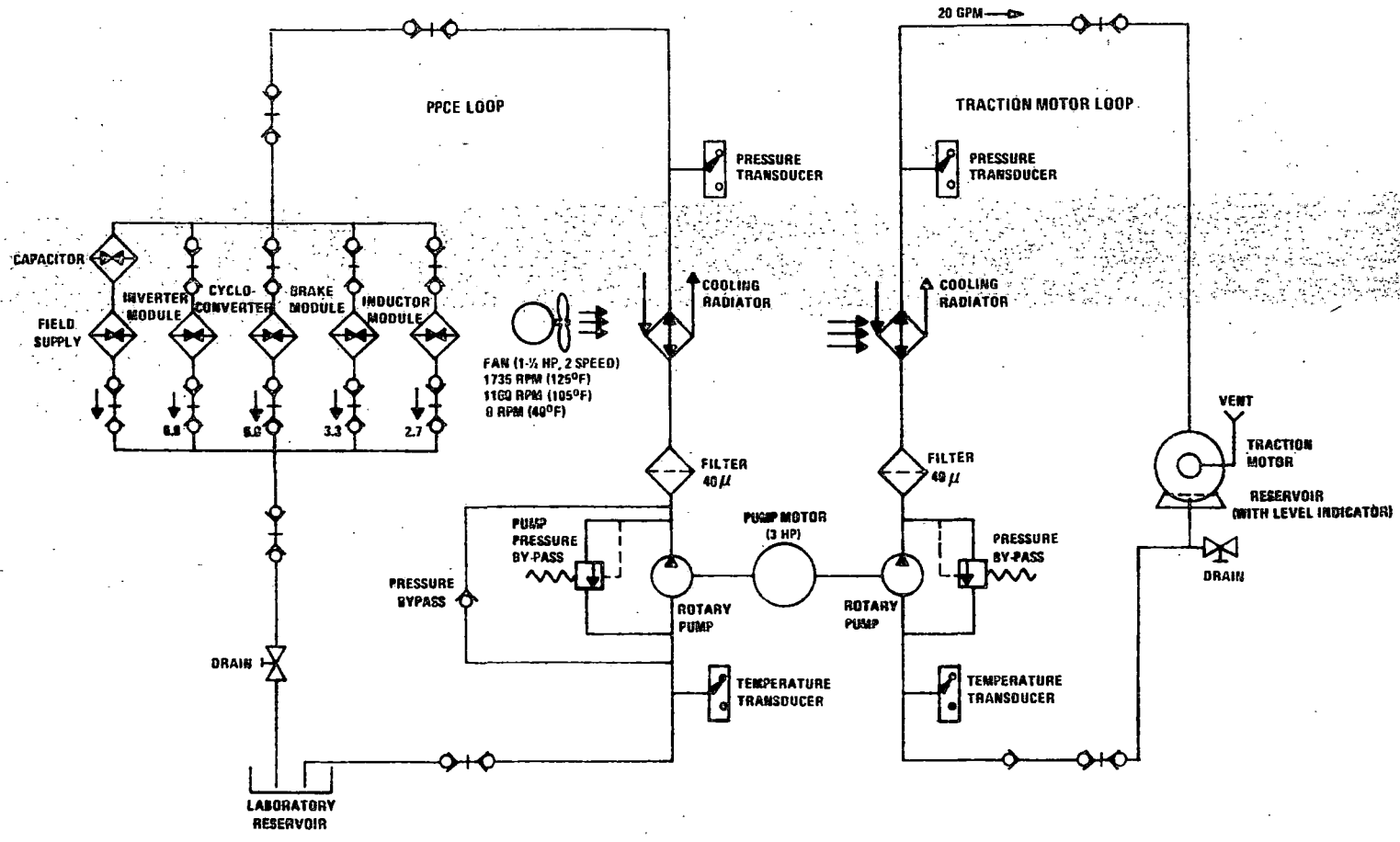

Figure 7.1-1. Schematic — Reconfigured Cooling System

Another field supply problem which affected the coolant loop was the vent valve. This device was intended to act as a low differential pressure, bi-directional venting valve. In use, the valve was found to be unreliable even in the benign laboratory environment. As a result, the cooling system needs an improved venting arrangement which must be relocated to the new sump.

7.1.2.5 Brake Control Module

Several major hardware changes were made to the TA configuration brake control module. Voltages during the braking mode were found to be considerably higher than in other units. This resulted in the addition of insulation barriers around some of the bus strips and all of the terminal feedthroughs. This was accomplished (for the laboratory testing) through the use of heat shrink tubing. New SCR gate drive and dV/dt circuits were also added. A re-layout of the gate drive circuit (which included larger transformers) was necessary to improve drive characteristics and isolation between adjacent interconnect wiring. The dV/dt circuits were added to compensate for voltage rise times in excess of 150 V/μsec. In order to accommodate the dV/dt resistors and capacitors a deeper enclosure (identical to the existing cycloconverter and inverter enclosures) was made. The conceptual layout is shown in Figure 7.1-2. Another change involved electrical modifications to the gate driver circuit. The circuit was also relocated closer to the SCRs to reduce the potential for false gate triggering due to cross talk. This was done by mounting a new terminal board assembly directly to the SCR clamp studs. Circuit-to-SCR interconnect wires were cascaded down to the nearest SCR to minimize potential cross coupling. The wires were arranged in a manner similar to those in the inverter module.

The electrical modifications were incorporated in the brake module with minimum documentation of the packaging design. Also, as with the cycloconverter, support structures were removed. Prior to vehicle service tests, repackaging of this module would be required. The previously mentioned larger module case will fit in the power converter chassis, but if additional space is required for the repackaging it might be necessary to increase the size of the power converter chassis.

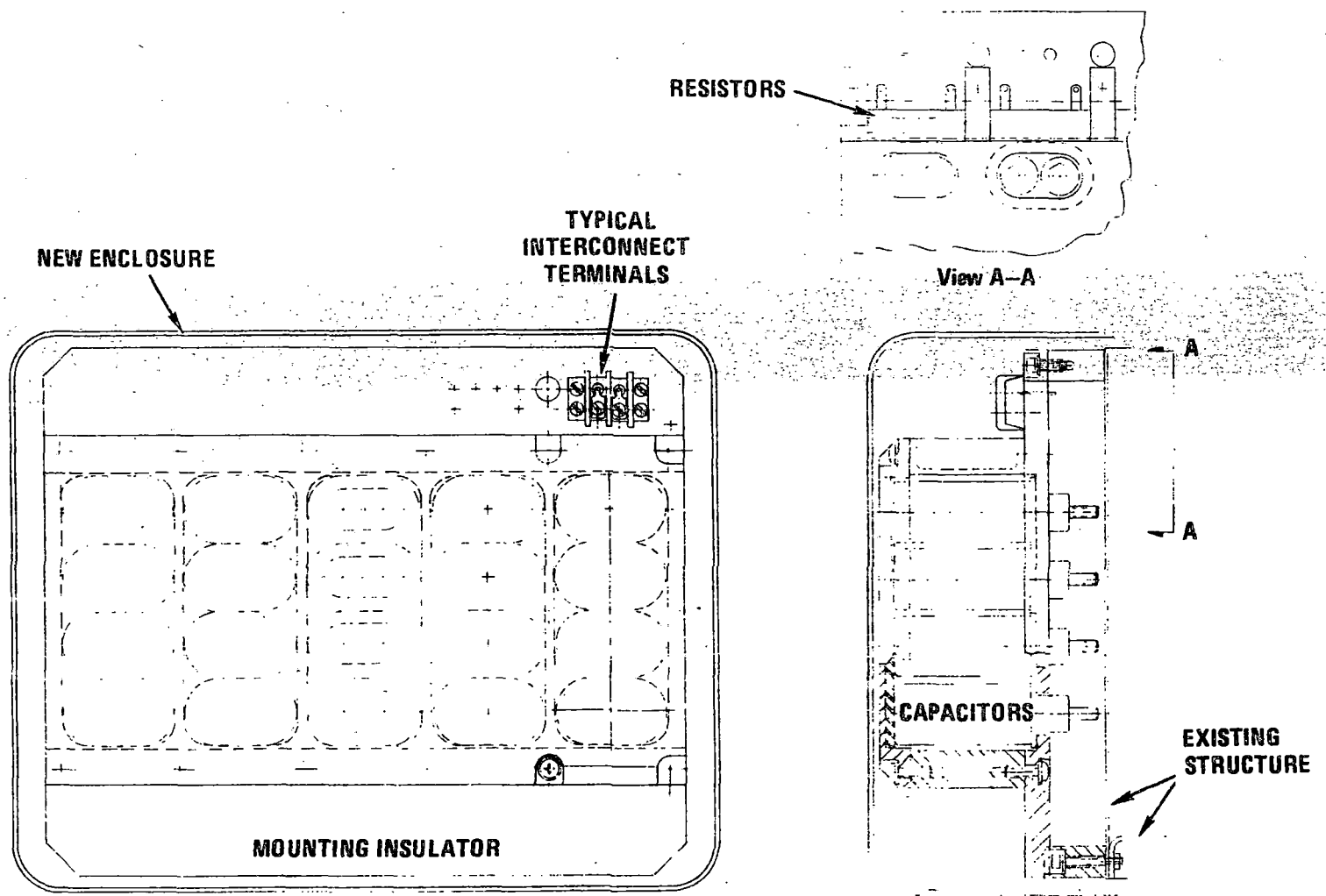

Figure 7.1-2. Layout of dV/dt Circuit in Brake Control Module

7.1.3 INPUT LINE FILTER

In an early system level test it was found that the inrush current through the input filter inductor at turn-on was larger than expected. This resulted in blowing the 60A fuzes in series with the filter capacitors. To alleviate this problem, the current rating of the fuzes was increased and the damping sheets (see paragraph 5.3.3) were removed. Removing the sheets reduced the tendency to blow fuzes, even though the peak, instantaneous value of the inrush current increased. This apparently was because the transient current pulse was much narrower. The current rise time was also slower, apparently due to increased inductance. An undesirable effect of removing the damping plates was that the voltage overshoot across the filter capacitor became excessive.

To circumvent the overshoot problem, a diode was installed across the line filter inductance with the anode on the input side. The diode eliminated the overshoot problem but filter action was no longer bi-lateral, a condition probably not acceptable in an operational environment. Further investigation and development of the input filter was planned but pre-empted by higher priority problems associated with motoring and braking motor control. To avoid the uncertainty relative to having the inductor in the system, it was electrically disconnected and not used in all system testing accomplished after mid July.

The input filter, and especially the inductor, requires further analysis, test, and development. The configuration of the damping plate, prior to its removal, was based on a preliminary best estimate. It was not optomized based on empirical characteristics as originally planned. Also the previously noted contradiction relative to removing the plates, wherein the surge current increased but the tendency to blow fuzes decreased, is not well explained. In addition it was observed that removing the damping plate apparently resulted in an increase in the inductance. This was not analytically predicted.

Part of the reason for the inconsistency may be that the analytic model treats the inductance as linear, whereas it varies considerably with current due to saturation. It is also possible that some of the data is erroneous, since the tests were run early in the program when procedures for use of the instrumentation were not well developed.

In an overview sense, the problem of blowing fuzes in series with the filter capacitor can be overcome by increasing the rating as required, but the problem of transient voltage suppression is more serious. Optimization of the damping plate might provide an adequate solution. If it does not, some type of voltage snubbing device will be required in parallel with the inductors.

7.1.4 RESONATING INDUCTOR MODULE

As a result of a component level test (described in paragraph 6.2.1) which indicated a poor inductor quality factor (Q), the internal support structure of the resonating inductor module had been changed from aluminum to an inert fiberglass material. This is shown by the photograph of Figure 7.1-3. At the same time a change was made in the location of the fuses at the input to the inverter to correct an original circuit design error. This resulted in an extensive revision of the interconnect between the resonating inductor and the inverter module. To accomplish the interconnect change it was necessary, on the resonating inductor front panel, to change the location of feedthroughs and the location of the breather vent. Following these changes, the performance of the resonating inductor was satisfactory and no further changes are considered to be required.

7.1.5 COOLING SYSTEM

Two improvements to the cooling system were incorporated during the TA test program. First, a reservoir was added in the laboratory configuration to permit coolant flow through the field module, which previously had served as the reservoir. This flow was needed to alleviate an overheating problem discussed in paragraphs 6.3.4.3.5 and 7.1.2.4. Second, sound dampening acoustic foam was placed in appropriate areas within the cooling assembly interior to absorb fan and pump noise.

As shown in the schematic of Figure 7.1-1, the reservoir was installed in the return line from PPCE to the cooling assembly. This created a positive pressure in the module enclosures. To prevent the relief valves on the modules from opening, a bypass valve

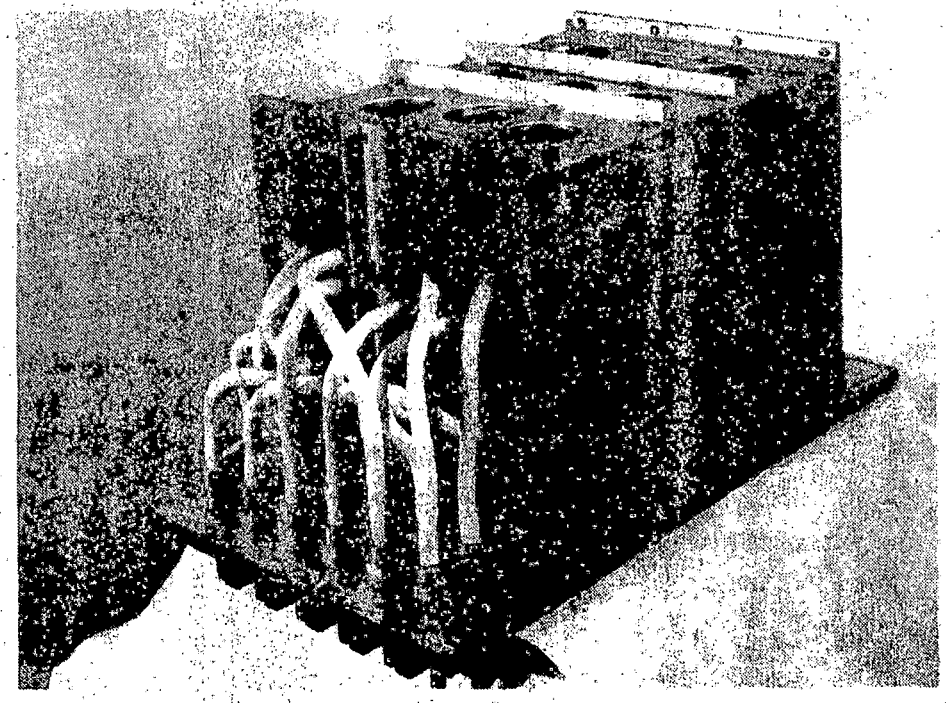

Figure 7.1-3. Resonating Inductor with Fiberglass Frame

assembly was installed on the cooling assembly outlet. The flow was adjusted to the maximum possible without causing the relief valves to open.

Acoustic noise tests were run on the cooling system which indicated that the cooling assembly was exceeding the 65 dBA maximum noise level defined in the Boeing Vertol Specification D239-10000-1 by as much as 22 dBA. To reduce the noise levels, different types of "Soundcoat" sound absorbing foam were placed on the interior faces of various assembly panels. An optimized arrangement resulted in substantially reduced noise levels which were still not considered acceptable. In an attempt to further reduce the noise levels, foam was wrapped around the pump assemblies. This resulted in a worst-case average cooling assembly noise level of 75.4 dBA. The worst-case reading in a transit station, however, would be only 69.4 dBA since the power dissipated, under these circumstances, would be minimal. A summary of the measurements taken are shown in Table 7.1-I.

It is felt that the 69.4 dBA reading is reasonably low and that this can be further reduced with the development of an actual design of a foam encased housing for the pumps.

DATE	CONDITIONS	AVERAGE LEVEL (dBA)
4-2-77	1. Low Speed Fan 2. No Insulation 3. Wind Screen Used*	84.2
	1. High Speed Fan 2. No Insulation 3. Wind Screen Used*	85.9
4-13-77	1. Low Speed Fan 2. Pumps/Panels Insulated 3. Wind Screen Used*	76.0
	1. High Speed Fan 2. Pumps/Panels Insulated 3. Wind Screen Used*	79.2
4-13-77	1. Low Speed Fan 2. Pumps/Panels Insulated 3. No Wind Screen	69.4
	1. High Speed Fan 2. Pumps/Panels Insulated 3. No Wind Screen	75.4

NOTES

*The wind screen is mounted over the Sound Level Meter Receiver. The readings should decrease with its usage. This was not found to be the case.

1. Instrumentation Used:
   - A. Sound Level Meter — Bruel and Kjar Type 2203
   - B. Sound Level Calibrator — Bruel and Kjar Type 4220
   - C. Octave Filter Set — Bruel and Kjar Type 1613
2. Measurements were taken 15 ft from cooling assembly surfaces.

Table 7.1-I. Cooling Assembly Noise Test Results

7.1.6 TRACTION MOTOR

The traction motor development effort is detailed in Delco Electronics Report R78-15. The following discussion encompasses a summary of the problems encountered and their respective solutions. The more important traction motor failures can be categorized into three groups:

1. Zener diode failures in the rotating rectifier assembly
2. Magnetic seal failures
3. Fixed-end traction motor bearing failures.

Another problem area, as discussed in paragraph 6.3.3.3.7, within the traction motor was the unsatisfactory electrical terminations of the rotor damper bars. This problem did not cause motor failure but was suspected of causing differences in characteristics of the various motors. The motors have been reworked but have not been comparison tested.

The rotating rectifier Zener diode circuit was modified to a crowbar circuit after repeated failures and after an analysis had confirmed a design deficiency.

The magnetic seal serves as a rotating seal between the rotor shaft assembly and the bearing cartridge. Investigation revealed that the rotating portion of the seal was forced against a shaft shoulder during assembly and was slipping relative to the shaft. This resulted in the shoulder machining away the metal seal face and eventual complete seal failure. To eliminate the problem, the seal was modified to provide a tighter fit to the rotor shaft. Assuming a proper installation, this removed the possibility of any movement between the rotor assembly shaft and the rotating portion of the seal.

The fixed end bearing problem was not recognized for a time. The cause of failure was originally attributed to silicone fluid contamination of the bearing grease due to the seal failure described above. Later, high speed was considered another possible cause.

Failures had not occurred during a long period of early testing. However, the motor speed during this test phase was quite low (below 4000 r/min) with typically short test durations (less than one hour). As a result, the possibility of a speed related failure was not initially apparent. Once speeds in excess of 4500 r/min were being maintained on a regular basis, the frequency of fixed-end roller bearing failures increased dramatically. It was finally

discovered, through analysis of the failed bearings and data from rotor shaft end load tests that the bearing was failing at high speeds from excessive end loads. Further testing indicated that the coupling was the cause and that the end load increased in a quadratic relationship to the rotational rotor velocity. To increase end load carrying capability a deep groove Conrad type, low precision ball bearing was selected to replace the previously used roller bearing. The specific replacement was a Q3213 New Departure bearing which could be directly substituted for the roller bearing. It was thought that the bearing precision might be lower than desired and that the phenolic retainer might be fragile, but no other bearing could be obtained in time to complete planned bearing verification tests prior to program termination.

Preliminary tests on one motor, in which about 20 hours of running time was accumulated, indicated the solution to be sound. A formal plan was then established to verify the bearing selection. This included a 2-hour run at 4000 r/min and a 2-hour run at 5640 r/min. A new bearing was installed for the tests. The bearing failed and upon teardown showed indications of its possibly being defective. Another new bearing was installed which again resulted in a failure.

In both cases, the bearing retainer appeared to have fractured prior to ball or race degradation. Since this concern had been expressed prior to the bearing selection, a survey of the industry was conducted to locate a more suitable bearing. An SKF bearing was found of the same size and with a machined bronze retainer. This bearing is also a precision 5 bearing which should provide much more repeatable performance. The bearing is scheduled for assembly into the deliverable motors by the end of March 1978. However, no further laboratory testing will be conducted to verify bearing suitability.

7.2 UNRESOLVED MOTORING MODE PROBLEMS

7.2.1 INVERTER-CYCLOCONVERTER INTERACTION AND CYCLOCONVERTER GATE TIMING

The phenomenon of inverter-cycloconverter interaction is discussed in paragraph 6.3.3.3.3 and the problems of SCR gate drive and cycloconverter gate timing control are discussed in paragraph 6.3.3.3.2. In summary, the problems of inadequate gate drive and of inhibiting timing related weak gates are solved. The problems of automatic power factor advance and RPS ⟷ CEMF transitioning are also solved or well in hand.

Lower order problems remain however. These problems interrelate and manifest themselves symptomatically in one of two ways. They result either in degradation of inverter SCR recovery time which in turn results in an inverter initiated system QSD, or they result in an increase in the dV/dt across cycloconverter SCR's. The QSD's are immediately evident. The high dV/dt can only be detected with sophisticated instrumentation. Although the dV/dt's were higher than desired, they did not appear to induce SCR failures.

The problems or conditions which contributed to inverter recovery degradation and dV/dt increases are summarized as follows:

1. CIRTS Input Series Resonance

   When the resonant frequency of the CIRTS input circuit is equal to the inverter-motor beat frequency, inverter gate timing is disrupted. This resonance is analytically described in paragraph 6.3.3.3.3 and illustrated in Figure 6.3-24.

   The resonance problem appears significant only if there is a source of excitation in the system at the beat resonance frequency. The problem did not manifest itself as a QSD and only slight degradation in inverter recovery time was recorded when the final performance data set was taken, as discussed in paragraph 6.3.3.3.2.

2. CIRPS Zero Beat QSD

   CIRTS was replaced by CIRPS to avoid the previous beat problem. It did, but in limited testing it appeared to introduce or aggravate a severe loss of inverter recovery time at the zero beat frequency.

The prevailing engineering judgment is that CIRPS would work if completely developed and verified, but, due to the subtleties of the problem, this cannot be presumed with certainty. Pending program termination prevented completion of the development and verification.

3. Field Supply Circuit Capacitors

As discussed in paragraph 6.3.3.3.7, it was found that capacitors added across the field supply transformer secondary would reduce di/dt to the rotating rectifier circuit and thereby reduce false triggering of the crowbar circuit. These capacitors appeared to be required with Motor S/N 3 but were not required with Motor S/N 2B77, the motor employed for the final data set.

However, a deleterious effect of adding the capacitors was that they caused the degradation in inverter recovery, as discussed in relation to Items 1 and 2 above, to be more severe. It appears that the field transformer isolates cycloconverter developed transients from the inverter and that the added capacitors are reflected across the transformer primary and degrade the isolation.

There are two ways to diagnose problems of this type in a complex system such as the one under discussion. The preferred method is a computer simulation of the inverter, cycloconverter, and motor. Experience has shown that a hybrid analog-digital simulation is the most effective approach. However, this requires a highly sophisticated simulation facility and painstaking development and verification of the analytical model. The alternative to a computer simulation is to conduct an orderly series of developmental investigations. This entails introducing a change into the system and interpreting the results.

In this paragraph, changes are suggested which, in general, pursue one of two objectives. The first is to more quantitatively describe the mechanism of the interaction and to develop c[illegible]uration modifications which will suppress it. The second is to more completely understand the sources of excitation to the interaction in terms of gate timing, PFA unbalance, etc. The suggested procedure is to introduce a change and then to observe and

interpret the effect on the jitter in inverter SCR recovery time while operating throughout the beat frequency region. The changes suggested for evaluation, somewhat in order of priority, are as follows:

1. Modify the PFA circuit to produce a different power factor on one phase. This will indicate if the interaction is sensitive to power factor unbalance.

2. Operate the system using separate field excitation and evaluate the effect of changing the level of motor field excitation. This will indicate the sensitivity of the interaction to the level of field excitation.

3. Remove the linear and saturating inductors between the inverter and cycloconverter. This will indicate if the interaction is sensitive to resonance between the inductor and the inverter output capacitors.

4. Complete the development and evaluation of CIRPS. This circuit obviates problems due to resonance or roll-off in inverter commutation related gate signals. The flat frequency response to dc of this circuit should be ideal. The circuit is still less than ideal, however, in that it derives rather than directly monitors the voltage across the cycloconverter SCR. This is discussed in paragraph 6.3.3.3.2.

   As part of this development, observe the effect of variations and unbalances in the magnitude of the SCR "finger" voltage on the interaction. Interphase differences are of particular interest.

5. As an alternative to the CIRPS and CIRTS circuits, develop and evaluate a set of sensor circuits capable of directly and reliably monitoring the voltage across each cycloconverter SCR. This approach could be carried as a back-up to the above described CIRPS development. It might be more complex due to the detector circuit design problems discussed in paragraph 6.3.3.3.2, as well as to the need for 18 sensors, but it provides maximum assurance of obtaining the desired inverter commutation.

6. Install an interphase inductor between the cycloconverter and the motor. (Locating the inductor between the inverter and the cycloconverter would also work, but this would require interchanging the input and output terminals of the cycloconverter since access to both current polarities on all phases is required.) The interphase inductor will isolate the motor inductance from the inverter output coupling capacitance. If the jitter in inverter SCR turn-off time does not decrease as a result of this isolation, then resonance between the coupling capacitance and the motor inductance is not the cause, and the transient change in cycloconverter input impedance due to motor current commutation is the (most likely) cause of the turn-off time jitter.

In summary, it is felt that the solutions to the inverter recovery time and cycloconverter dV/dt problems reside more in several refinements rather than in any single change or step. The complexity and nonlinearity of the system, and the unique discontinuities introduced by the commutation process, severely limit an attack on the problems by vigorous analytical approaches. The alternative is the proposed laboratory development work.

7.2.2 CYCLOCONVERTER VOLTAGE TRANSIENT PROTECTION

The problem of DSAS failures, as discussed in paragraph 6.3.3.3.4, requires additional study and development work. The solution of turning on the braking SCRs and dumping the stored motor energy into the brake grid is marginally adequate for purposes of laboratory testing and may not be acceptable for transit vehicle service use. The laboratory capability is not completely satisfactory because DSAS devices still occasionally fail at the instant of system shutdown. In transit service, it is possible that a high level of braking could be experienced for up to one second or until the motor field decays. The problem is further complicated by the braking mode problem of excessive voltage being applied to the cycloconverter SCRs and DSAS devices.

For this discussion it is assumed that the braking mode problem is solved by the use of u[illegible]ded SCRs or a mechanical contactor which isolates the inverter from the motor during braking. This permits consideration of the motoring mode problem only.

The analysis of paragraph 6.3.3.3.4 indicates the DSAS devices may be overstressed by a factor of 50. The problem cannot be solved by devices of increased rating because they do not exist. Two approaches to a solution remain.

One approach is to improve on the technique used in the laboratory tests of discharging the energy using the braking circuits. Improvements are required in two areas. One is that line inductance must be reduced either by shorter leads or by capacitive bypassing near the braking SCRs. The other required improvement is in the brake module SCR gate control logic. As presently mechanized, all braking SCRs are gated continuously following a QSD discrete. This is equivalent to transitioning to a "maximum braking mode" until the motor field excitation is lost. The purpose of the improved logic would be to gate the braking SCRs only long enough to allow all cycloconverter SCRs to terminate conduction and to discharge the energy stored in the motor field. This would typically be in one revolution of the motor or less.

An alternate approach would be to turn on the cycloconverter SCRs rather than the braking SCRs. The feasibility and the gate control aspects of this approach have not been completely analyzed but some of the considerations involved are as follows:

- The concept amounts to placing a short circuit across the motor, thereby dissipating the stored energy in the motor stator winding.
- The desired sequence of events is to allow the motor current to increase until motor current limiting occurs and voltages decrease. Then, phase by phase, remove the shorts and transition to open circuits as the motor currents pass through zero.
- Depending on the details of gate control, some or all phases of the inverter may be short circuited. Since the system is in a QSD mode and the inverter is not being gated, the energy stored in the inverter will be dissipated in the motor stator winding.
- On a transient or momentary basis, the motor stator can easily and safely absorb the energy involved. Analysis and/or laboratory tests are required to determine if fuses between the inverter and motor would be blown.
- The cycloconverter gate control logic needed for the desired control sequence had not been developed.

Other approaches to the problem are also possible but the ones suggested have the advantage of requiring minimum changes to the existing system with most of the changes being made to low level gate control circuits.

7.2.3 LOW TORQUE, HIGH SPEED MOTOR COMMUTATION

It is explained in paragraph 6.3.3.3.6 that operation of the system at low inverter frequency and high speed is not possible due to cycloconverter faulting. The onset of incipient faulting can be seen by monitoring one of the motor phase currents. The incipient condition exists if a current transient reappears in a given phase after conduction has been commutated to the next phase.

The region where the problem exists in terms of system torque, speed and inverter frequency is shown by Figure 7.2-1. The curves are based on laboratory data taken as part of data sets recorded on 10/8, 11/28 and 12/9/77, and on related observations of system performance. Since the data points on which the curves are based were limited in number and highly subject to interpreations, the areas described by the curves should be considered as nominal approximations. As indicated by the difference between curves 1 and 2, there is quite a wide region of operation where there is some degradation in commutation but where the probability of faulting is very low.

As previously noted, the faulting is caused by insufficient motor field current. The direct solution therefore is to increase motor field current in the problem area. An indirect approach which relieves the problem somewhat, but does not solve it, is to increase the power factor angle. This was done in laboratory tests both by the use of manual power factor control and by a supplemental circuit in the automatic power factor advanced control. In concept, the PFA was advanced to a fixed 30^{o} angle when motor current was below approximately 150A. This occurred at an inverter frequency of approximately 700 Hz. This approach provides an estimated improvement illustrated by the difference between curve 1 and curve 3. The key point is that PFA helps only if an adequate excitation field exists. The supplemental circuit, i.e., the transition to a fixed 30^{o} PFA was not operat when the final data set for the system was taken on 9 December.

The direct solution to the cycloconverter faulting problem is to increase the motor field excitation current in the faulting region.

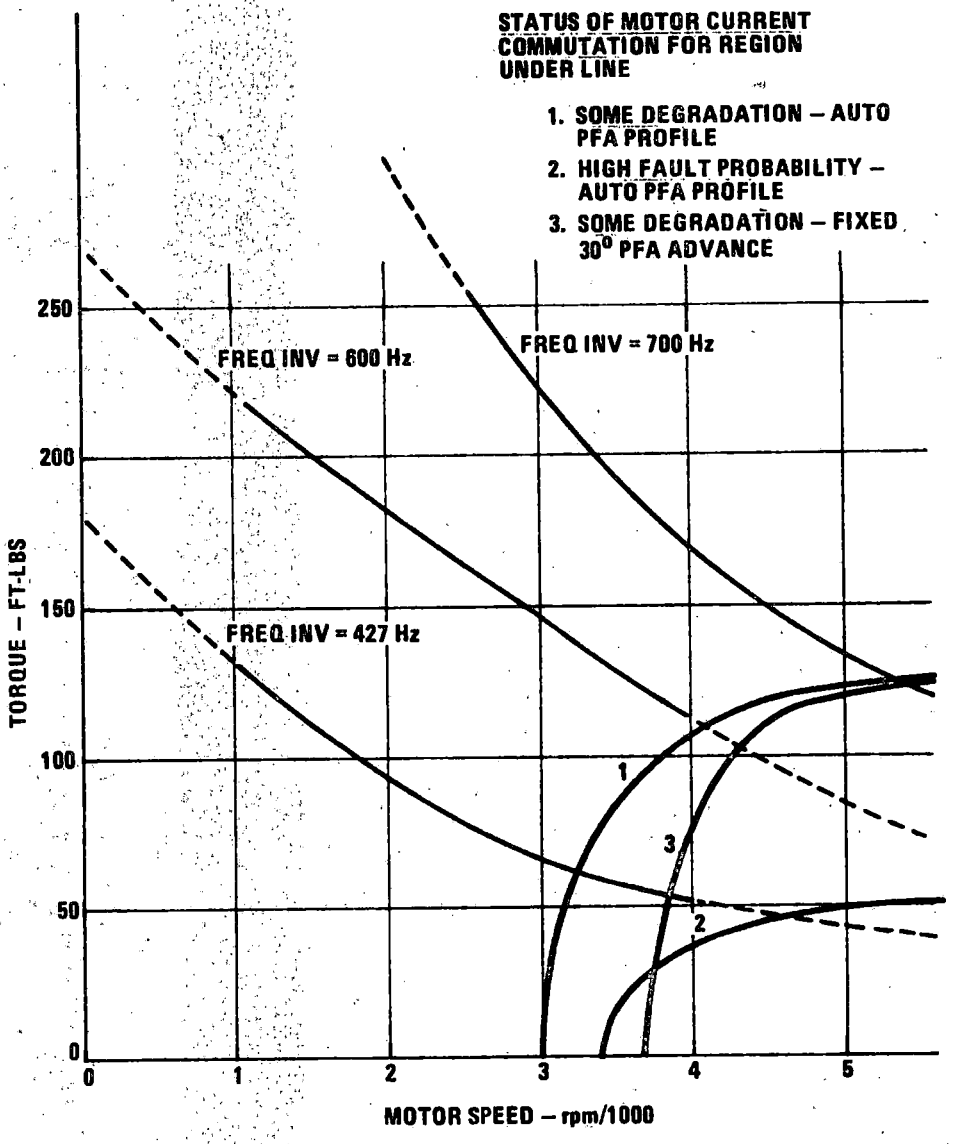

Figure 7.2-1. High Speed Cycloconverter Faulting

An alternate approach is to incorporate into the system a separate controllable dc to dc converter as a programmable field supply for the motor. This more complex and costly approach would provide the capability to control motor excitation under all operating conditions. It also offers other potential advantages as follows:

- It will obviate the previously discussed problem of motor armature current spikes feeding into the field excitation circuit and possibly triggering the crow bar protection circuit.
- It might mitigate or even eliminate the inverter short turn-off problem by programming the field excitation into a manner to decrease the beat coupling feedback to the inverter.

- In braking mode, the main inverter could be turned "off", thereby eliminating the forward voltage component across the cycloconverter DSAS device which has been failing due to excessive voltage stress. This would eliminate the need to disconnect the inverter from the cycloconverter via contactors or SCR's to protect the DSAS device.

A suggested simpler approach is illustrated in Figure 7.2-2. In this concept, the braking winding of the field transformer is used to supplement the motoring mode excitation current when operating at high speed and low inverter frequency. The modification to the system is therefore comprised of additions of a relay, coupling capacitors and a relay control circuit.

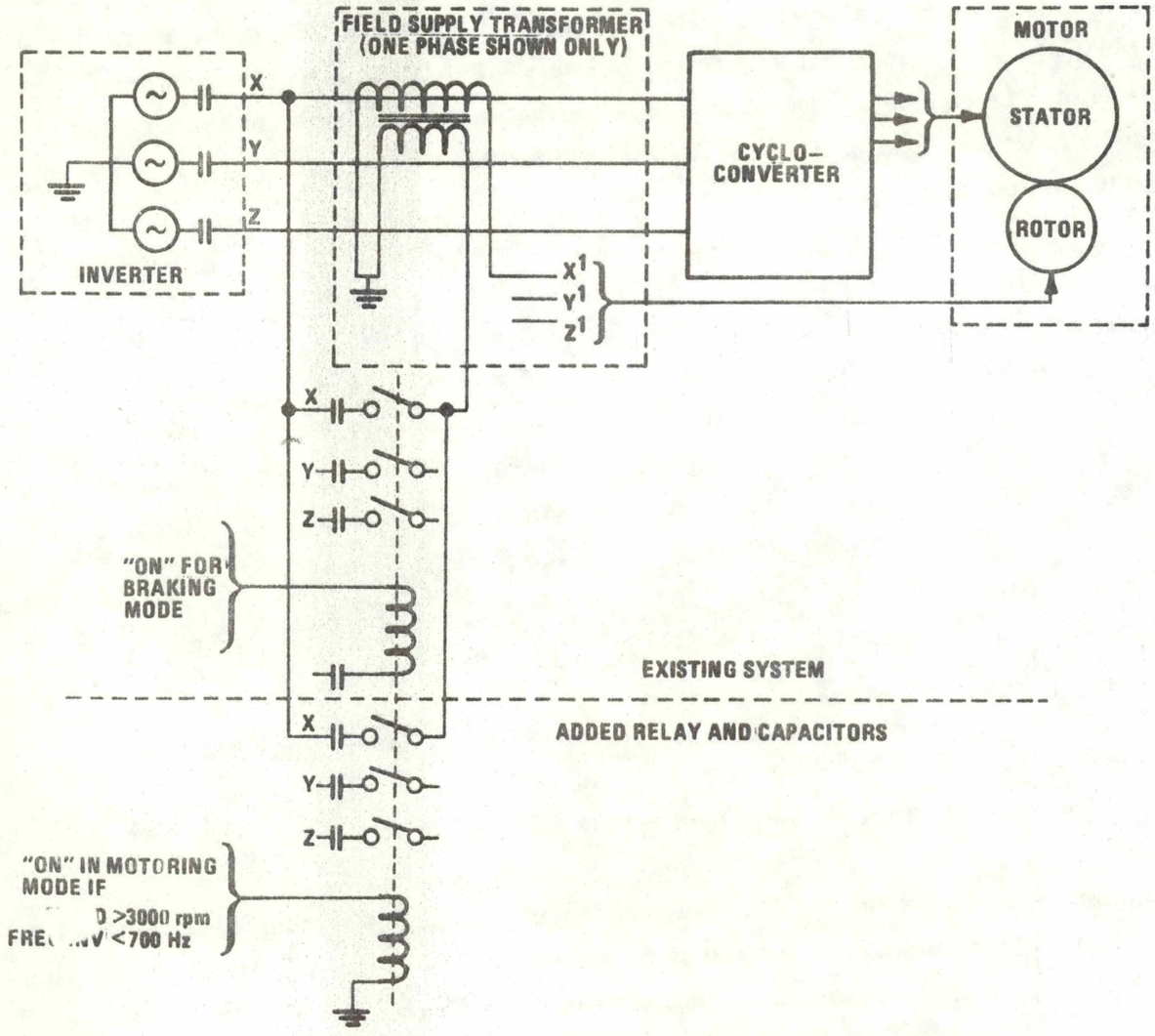

Figure 7.2-2. Supplemental Motoring Mode Field Excitation

Two preliminary steps are recommended to determine the preferred approach. One is to operate the ASDP motor in the laboratory with a separate field supply and map out the optimum field current for a complete family of motor torque, speed, and voltage conditions. The second is to conduct cost tradeoffs of a separate supply vs the cost of the alternatate solutions to all the related problems.

7.2.4 PFA OPTIMIZATION

Motor commutation and therefore motor power factor control transitions from RPS control to CEMF control and vice versa at 2000 r/min in the final configuration of the automatic PFA. This is a discrete change which causes a step change in the motor power factor. Relevant data of the final system tests of 12/9/77, illustrating this step transition in power factor angle and torque, is summarized in Table 7.2-I. It is also shown in the plotted curves of Figure 6.3-4. These data indicate that the transition point has not been optimized. The phase lead of the CEMF signal at the 2000 r/min point of transition is approximately 10^{o} too large.

Hz	TORQUE (ft-lb)		PFA (degrees) ①		PFA (degrees)
INV	RPS	CEMF	RPS	CEMF	CHANGE
427	103	90	+5.8	+10.3	+4.5
500	128	117	+6.0	+10.8	+4.8
600	205	194	-2.8	+17.7	+20.5*
700	330	298	+8.0	+19.3	+11.3
800	492	446	+13.2	+24.0	+10.8
900	700	647	+10.5	+20.4	+9.9
950	843	780	+9.6	+21.5	+11.9

① + = Leading PFA

* Suspect erroneous data. Torque change does not correlate with PFA change.

Table 7.2-I. RPS versus CEMF PFA

To minimize the step changes, it is only necessary to change the component values of the phase shift determining resistors and capacitors in the PFA circuit. Figure 7.2-3 illustrates: as curve 1, the power factor advance profile which was believed to be optimum when the existing circuit was designed; as curve 2, the calculated profile of the existing circuit; and as curve 3, the profile now considered optimum.

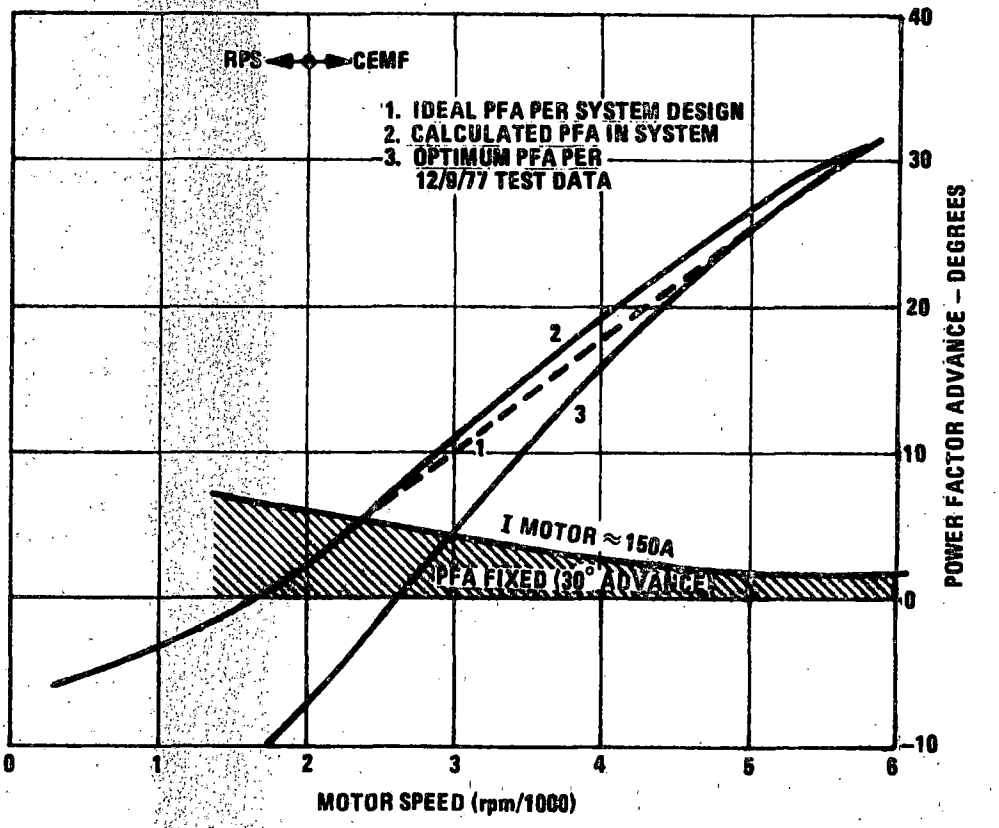

Figure 7.2-3. Power Factor Advance Profiles

An alternative to optimizing the transition at 2000 r/min also exists. It is to add a low pass filter to the CEMF signal and activate it only for speeds below 2000 r/min where noise problems currently prevent use of the CEMF signal. This would permit a gradual blended RPS ⟷ CEMF transition as originally contemplated.

7.3 BRAKING MODE UNRESOLVED PROBLEMS

7.3.1 EXCESSIVE VOLTAGE ACROSS CYCLOCONVERTER

Several conceptual approaches are available to solving the problem of excessive voltage across the cycloconverter during braking operations. One is to use cycloconverter components of increased voltage rating, another is to short circuit the cycloconverter input, and a third is to disconnect the cycloconverter from either the inverter or motor when in the braking mode. The latter was done in the laboratory to obtain high-speed braking data. A fourth approach is to employ a separate field supply converter for both the braking and motoring modes.

The approach of increasing the voltage ratings does not appear attractive because a capability of 3000 to 4000 V is considered necessary. This would require larger and more expensive SCRs, more DSAS devices connected in series, and larger capacitors with higher voltage ratings in the dV/dt circuits. Improvements in feedthroughs, increases in conductor spacing and increases in conductor insulation would also be required in certain areas to prevent arc-overs.

The second approach requires the addition of three SCRs to short circuit the input to the cycloconverter, as illustrated by Figure 7.3-1. An advantage to this approach is that it eliminates the need for the brake control relay, and the 3 μF coupling capacitors. There is also a potential problem in that the Mapham inverter does not work well when loaded by a short circuit. Analysis or test of the field supply current transformer as an adequate load is required.

There are several ways to implement the third approach. All involve the addition of SCRs or mechanical contactors in series with either the cycloconverter input or output. If mechanical contactors are used, three SPST contactors are required. If SCRs are used, six are required due to the bi-directional currents. One approach exists which, at the expense of several mechanical contactors, all operated in parallel, significantly reduces the number of high current, high voltage SCRs required in the system. In this approach, the cycloconverter SCRs also accomplish the functions of the dynamic and regenerative braking SCRs. This means there is a net reduction in the system of 9 SCRs. The contactors and the schematic for implementing this configuration are shown in Figure 7.3-2. For this concept to be practical, it would be necessary to construct a "gang" contactor and to integrate it from a packaging design standpoint with the cycloconverter.

Designs which employ contactors are notoriously unpopular because of their reliability limitations. That consideration should not be significant, however, in any of the identified configurations, since all switching would be of dry circuits at the time of mode transitioning from motoring to braking and vice versa.

Further evaluation is required in order to select a preferred solution to the problem of over-voltage on the cycloconverter during braking. The key elements in the tradeoff will be cost, reliability, and development time. No significant performance differences are seen.

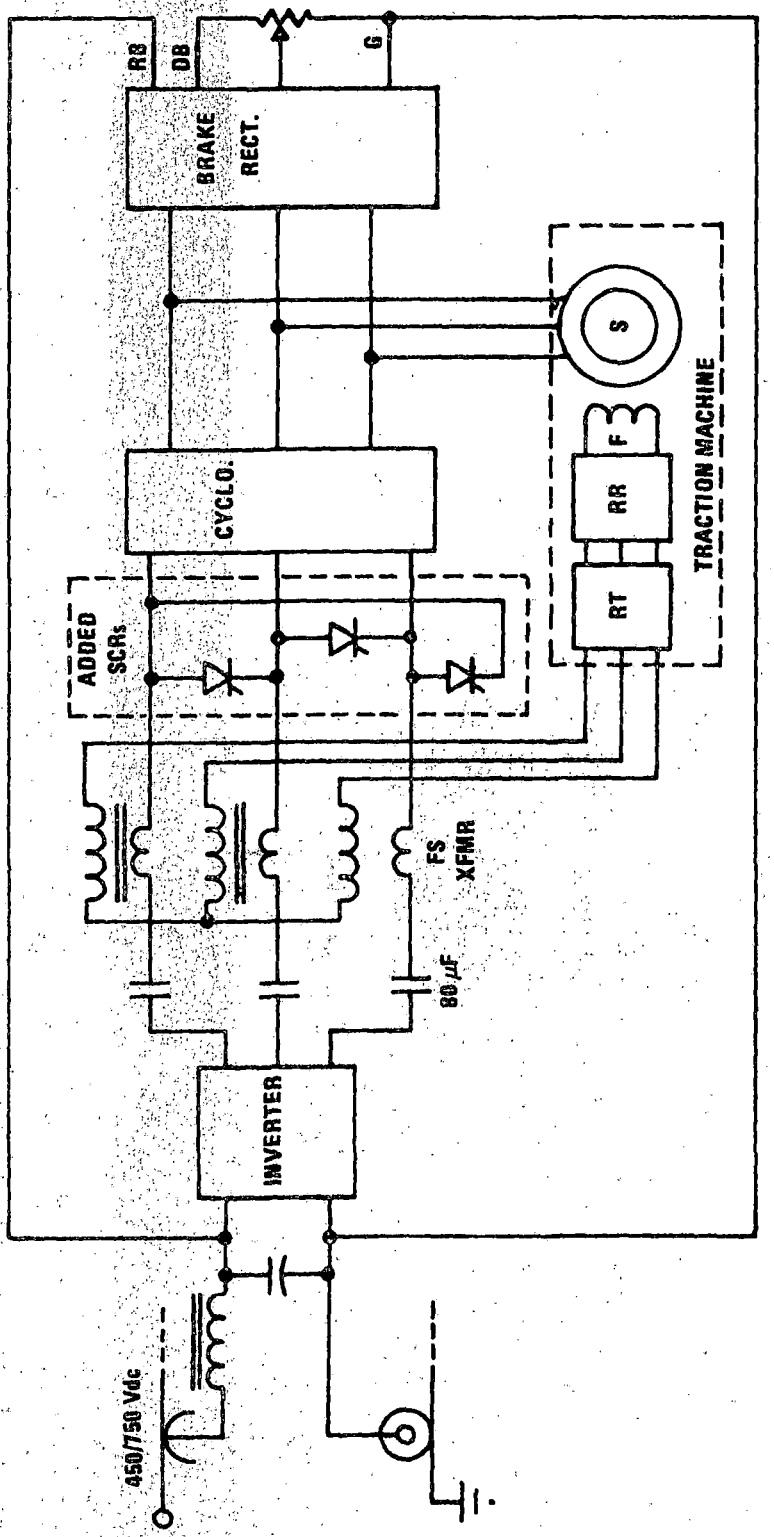

Figure 7.3-1. Cycloconverter Input Short Circuited During Braking

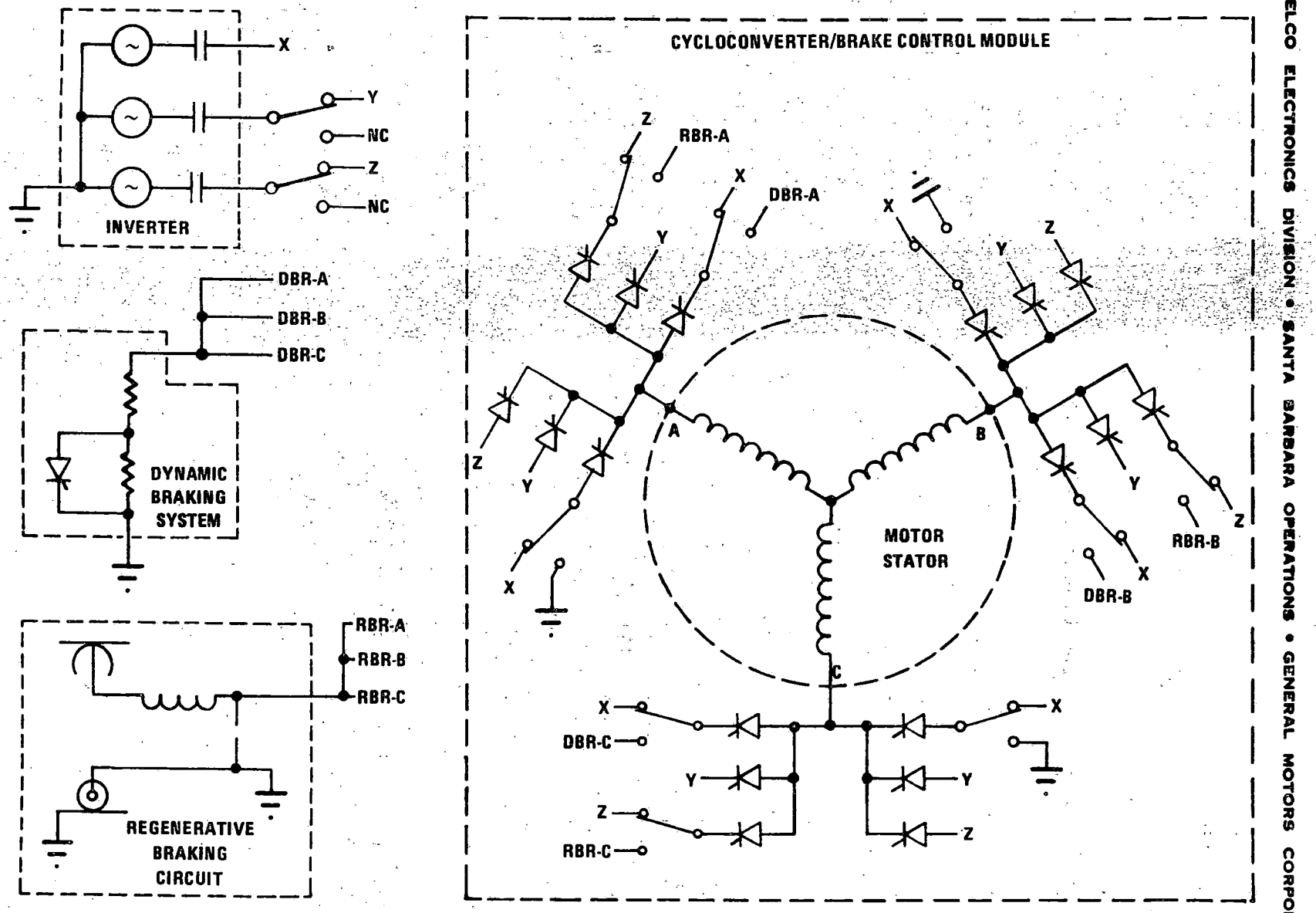

Figure 7.3-2. Combined Cycloconverter/Brake Control Module

7.3.2 IMPROVED CURRENT SENSORS

Circuit design study and development is required to overcome the problems of excessive errors and offsets in the sensors of the braking mode motor stator currents. As discussed in paragraph 6.3.4.3.6, the objective is to obtain an accurate indication of the motor power. The severe distortion caused by phase delay gating of the motor voltage makes accurate computation difficult.

For dynamic braking, power is I^2R and for regenerative braking, power is EI where E is the 3rd rail voltage. There are, in concept, two approaches to determining braking power. One is to multiply the instantaneous values of voltage and current. The other, is to determine the true RMS value of the current.

The circuit presently in the system is based on the latter concept. As a judgment, the circuit appears capable of acceptable performance if detail circuit design problems of grounding and noise rejection at the interfaces are resolved.

7.3.3 BRAKING MODULE SCR VOLTAGE STRESS

The discussion of paragraph 6.3.4.3.2 indicates that the voltage margin on the brake module SCRs may not be as large as desired. The approach selected to ameliorate this concern depends on the requirements seen necessary and the acceptability of certain design tradeoffs. Two possibilities and related tradeoffs are briefly discussed in the following:

1. Use SCRs of Increased Voltage Rating

   SCRs with considerably higher voltage ratings are available. The tradeoff is with size and cost. The higher voltage devices are larger and would require some mechanical redesign of the braking module.

2. Restrict the Use of Phase Delay Gating at High Speeds

   The SCR voltage stress is higher if phase delay gating is used than if field control is used. It is probably possible to operate in the dynamic braking mode without extensive reliance on phase delay gating. It is primarily required for the regeneration braking mode. One way to reduce stress, therefore, is to use only dynamic braking above a certain high speed point, say 65 mph.

7.3.4 LOSS OF CONTROL OF BRAKING SCRs

The reason for loss of control of the braking SCRs is known only in terms of the problem symptoms. These symptoms suggest a ground loop and/or capacitive coupling through the gate drive transformer. Much attention in developing the gate drive circuit modifications was directed to minimzing coupling through the transformer. The problem may involve a defective transformer or an unknown ground loop. This is a detail circuit problem which can only be investigated by tracing the problem to its source in an operating system.

7.3.5 FIELD SUPPLY CURRENT TRANSFORMER

The wire insulation failed on one winding of the field supply transformer during maximum power dynamic braking. Additional detail relative to the failure is included in the discussion of paragraph 6.3.4.3.5. The cause of the failure was attributed to excessive heat.

In the rewinding of a replacement transformer coil, a thermocouple was embedded in the winding to establish safe current limits in future tests. In addition, changes were made to improve the cooling of the transformer. One change was to selectively relieve the winding bobbin as required to allow increased coolant flow near the winding. Another change was to reconfigure the coolant flow loop to provide continuous flow through the unit. Previously, the unit acted as a sump in the coolant loop.

The coolant loop changes were discussed in detail in paragraphs 7.1.2 and 7.1.5. It was determined through monitoring the winding temperature after the changes that it was possible to operate for a maximum of 12 minutes at a field current of 45 amperes. Higher currents were possible for shorter time periods. If the time-temperature limits are exceeded, insulation deterioration and eventually, a repeat of the failure will be experienced.

A detailed duty cycle should be established for the field supply transformer, based on the vehicle duty cycle requirements postulated in paragraph 5.4.2 (which include both motoring and braking), and then a thermal analysis conducted to verify the adequacy of the present design.

7.4 TASKS REQUIRED TO DEVELOP A PRODUCTION CONFIGURATION

The development of a production configuration requires, in general, the completion of the laboratory development and system qualification tests followed by a series of vehicle service tests. The remaining laboratory development tests consist of the following: (1) solving the previously discussed problems and completion of the open-loop characterization of the system for both the motoring and braking modes; (2) integration of the MCE with the TCE and verification of closed loop control of the system for both the motoring and braking modes; (3) verification of mode to mode transitioning and control; (4) resolution of previously identified cooling system and packaging problems; and (5) completion of simulation studies supportive to the development of a closed loop motoring and braking control capability.

Upon completion of laboratory development, qualification tests must be conducted to verify that the equipment meets the established design and performance requirements and to provide a degree of assurance that it is suitable for integration into the modified-SOAC. Some of these tests would be conducted at the major component or assembly level; however, the primary means of qualification would be through system level tests of an integrated propulsion system.

The vehicle service tests would consist of engineering evaluation and acceptance tests of the equipment as installed on the modified-SOAC. These tests would be carried out at the HSGTC at Pueblo, Colorado.

7.4.1 LABORATORY DEVELOPMENT

Specific background and tasks relative to completing the laboratory development phase of the remaining effort is discussed in this paragraph.

7.4.1.1 Motoring Mode

The remaining open-loop motoring mode development work can be divided into two areas, as follows:

1) The development and verification of solutions to the previously discussed motoring mode problems

2) The verification and characterization of motoring mode characteristics and capabilities when the input voltage is varied over the specified range. The input voltage was between 600V and 700V for most of the testing performed.

Upon completion of the open-loop characterization tests, a series of integrated system motoring mode development tests remain. Included are the integration of the train control electronics, including the microprocessor, into the system and the verification of the required signal interfaces between the MCE and the TCE. It is assumed that this integration and verification would be accomplished on a piecemeal basis as various signals and software based computations and controls are needed to perform specific functions.

Specific areas of development work required include the following:

1) The verification of closed loop motoring mode control. This involves placing the inverter VCO under the control of the microprocessor, closing the feedback loop indicating motor output power, and controlling the system via a simulated P-signal. If the microprocessor is verified in a simulation, as discussed in subsection 5.5, little difficulty is foreseen in this development area.

2) The verification and characterization of system operation when subjected to transients and step changes in input voltage. This is a very difficult area in which to conduct evaluation for two primary reasons. One is that the test inputs, i.e., the transients or step changes, are not well defined or specified. The other is that it is extremely difficult in the test laboratory, at the power levels involved, to generate the transients.

   As a minimum, it would be desirable to turn the system "on" and "off" at all specified input voltage levels by the application and removal of input power. This differs from previous testing in which turn "on" was effected by first applying input voltage and then, under manual control, turning-on and bringing up the inverter from the minimum frequency operating point. Turn-off, in previous testing, has been randomly accomplished from a wide range of power levels as QSDs have occurred. Additional turn-off testing should be done over a full range of input voltages and system torque-speed operating points. Shutdowns should also be effected by interrupting the input power.

The input power turn-on and interrupt tests would, to a limited degree, simulate the expected interruption and reapplication of 3rd rail power as it occurs in practice. Interpretation of the results would also afford a good assessment of future system behavior such as when transitioning rail gaps, etc.

The problems of simulating input transients are difficult, with the most difficult being the step changes in 3rd rail voltage which can occur on transit properties and last for hundreds of milliseconds.

Studies are recommended to define possible laboratory development tests and to trade off laboratory tests versus simulation studies versus vehicle service tests.

Prior to accomplishing any of the closed-loop or turn-on, turn-off transient testing, it is necessary that the input filter problem discussed in paragraph 7.1.3 be solved and that the filter be in the system.

7.4.1.2 Braking Mode

7.4.1.2.1 Introduction

The remaining braking mode development work is greater in extent and more difficult to define than that for the motoring mode. Several interrelated reasons for this are identified as follows:

- There are two modes of operation to control: dynamic braking and regenerative braking. In addition, the potential exists for a hybrid mode in which both types of braking are employed simultaneously. The simultaneous mode was not assumed in the baseline design of the system but the concept offers potential advantages.
- It is necessary to transition between the dynamic and regenerative modes without interruption of the braking effort. The transition must be nearly instantaneous (within a few milliseconds) and may be required at any instant because the 3rd rail may become unreceptive and this cannot be anticipated.

- There are two means of controlling braking torque in both the dynamic and regenerative modes: motor field control and braking SCR phase gating control. The criteria for the interrelated use of the two control methods has not been defined. Each has certain advantages or limitations to be discussed later.
- The performance of the system, in terms of torque developed at a given speed, field excitation level, phase delay, etc., cannot be completely predicted analytically. The developmental concept therefore is to predict performance by obtaining empirical characterization data as a multi-dimensional function of all variables of interest.
- The specific development testing required depends to some degree on the specific solution selected for previously discussed braking mode problems. The most important problem in this regard is the cycloconverter over voltage problem as discussed in paragraph 7.3.1.

Of the previously discussed considerations, the greatest difficulty is involved in resolving the use of field control versus phase gating control. The following discussion surveys the relative capabilities and limitations of the control methods, suggests a method for optimizing their use, identifies in concept what approach appears to be the most attractive, and summarizes the required braking mode development work.

7.4.1.2.2 Field Control versus Phase Control

The generalized characteristics of torque control, as effected by controlling the level of motor field excitation, versus torque control via phase delay gating of the braking module SCRs, are summarized as follows:

- Field excitation control effects torque control by varying the output voltage of the motor. Phase control delays the turn-on of the braking module SCRs and thereby controls current.
- Field excitation is prerequisite to phase control. Phase gating can only reduce the torque from some maximum as defined by the field current, the speed, and either brake grid resistance (dynamic braking) or 3rd rail voltage (regenerative mode).

- On a relative basis, phase control is faster by approximately two orders of magnitude than field control; e.g., phase gating can be modified on each cycle of each motor phase (a few milliseconds) while changes in field current, due to the large inductance of the field winding, may require from 0.4 to 2.0 seconds. Response time cannot be characterized by a simple L/R time constant because of field saturation effects.

From a system standpoint, field control is preferred for all conditions except where fast response is required. The advantages of field control are as follows:

1) It minimizes dissipation in the motor field winding since field control implicitly provides minimum current consistent with required braking torque. As a counterpoint, higher motor field currents are possible without overheating the motor. The biggest disadvantage to the higher current is the increased cooling load on the heat exchanger.

2) Phase control results in very high motor voltage, especially when operating at high speed and low braking torque. This condition increases the stress on the braking SCRs as discussed in paragraph 6.3.4.3.1.

3) The torque pulsations discussed in paragraph 6.3.4.3.4 are minimized by using field control. Inversely, operating with high field currents means operating with small conduction angles (the condition when the magnitude of the pulses is greatest) for all conditions of light braking.

There are three operational conditions where the fast response characteristics of phase delay are needed or desired. They are:

1) In the regenerative braking mode to compensate for sudden changes in 3rd rail voltage. If high jerk levels are to be avoided, it is required that the controls react almost as fast as the 3rd rail voltage changes. The exact speed of response required and the exact magnitude of disturbance in braking torque cannot be predicted without completing the characterization of the system and an evaluation of dynamic response characteristics.

2) At the moment of transition from dynamic to regenerative braking and vice versa. In this case, it is assumed that the transition should be made without significantly changing the level of braking torque; i.e., to the vehicle operator or rider, the transition should not be apparent. The level of field excitation current needed for a given torque is different (usually greater) for dynamic braking than for regerative braking. If field control only is used, a change in the braking rate will occur and then braking will slowly recover to the desired level as field excitation is corrected.

3) During slide control to rapidly reduce torque.

It is seen that the regenerative mode of operation may be highly dependent on the fast response characteristics provided by phase delay gating. The primary need for phase delay control in the dynamic braking mode is for slide control.

Possible Control Concepts

The simplest control concept capable of providing quick response when needed is to employ a constant high level of field current and to accomplish all control or reduction in braking torque by using phase delay gating control. This means foregoing the advantages of field control as previously noted. There is a more complex alternative concept which permits partial retention of the advantages of field control. It is to program the field current as a function of speed and the P-signal (tractive effort command). The excitation current would then always be at the minimum value sufficient to satisfy the needs of either the dynamic or regenerative modes. With this control concept, field current would be low at low braking rates (except at very low speeds) and high at high braking rates. Phase control would reduce torque from the level established by the field current based on mode transitioning and slide control requirements, and during regeneration, the requirement to compensate for changes in 3rd rail voltage.

7.4.1.2.3 Braking Mode Development Required

A series of development tasks are required to complete the laboratory phase of the braking mode development effort. These tasks are listed somewhat in sequence but they are highly interrelated and as a result, considerable iteration will be required. The tasks are summarized on the following page.

1) Develop and verify solutions to the braking mode problems discussed in subsection 7.3.

2) Verify operation in the regenerative braking mode in a manner similar to the verification of the dynamic braking mode of operation.

3) Complete the characterization of the system for both the dynamic and regenerative braking modes. The specific system characterization data needed are as follows:

- For the dynamic braking mode: Torque versus Speed versus Field Excitation Current versus Phase Delay.

  This interdependent data is needed for both values of dynamic braking resistance in those areas of the torque-speed profile where either may be used.

  Available data is reasonably complete for a single value of field excitation current only.

- For the regenerative braking mode: Torque versus Speed versus Field Control versus Phase Delay versus Input (3rd rail) Voltage.

  This interdependent data is needed for input voltage levels within the specified range of operating voltages.

4) Measure the system response times for the dynamic and regenerative modes using both field control and phase delay control.

5) Using the characterization data and the dynamic response characteristics, simulate the braking mode in a hybrid computer simulation similar to the simulation of the motoring mode, as discussed in subsection 5.5.

6) Using the simulation, develop control algorithms for both the regenerative and dynamic braking modes. These algorithms would determine the relative use of field control versus SCR phase delay gating control.

7) Develop software, program the TCE microprocessor, and verify the braking mode including mode transitioning on the simulation.

8) Program the microprocessor in the system to duplicate the simulation and verify system level dynamic and regenerative braking mode operation.

7.4.1.3 Mode Transitioning and Operational Sequence Verification

A series of integrated system laboratory tests are required with the objective of verifying sequencing of the system through simulated operational profiles. Key elements will be verification of the capability to transition between the motoring and braking modes and verifying the control of jerk rate throughout the sequences. These tests depend on the completion of the previously discussed motoring mode and braking mode development tests. They also depend on integrated operation of the system under the control of the TCE microprocessor. The basic test procedure would be to vary the P-signal in various profiles, simulating the actions of the train motorman. Concurrently, the torque of the dynamometer would be controlled as required. Two important capabilities required of the dynamometer are: 1) that it be capable of simulating the inertia, weight, etc., of the vehicle; and 2) that it be capable of rapid (and probably automatic) transitioning from the motoring to the braking mode since it must always transition modes inversely to the ASDP propulsion system.

7.4.2 LABORATORY QUALIFICATION TESTS

Qualification testing of the ASDP propulsion system must be accomplished to assure that the equipment will meet the design and performance criteria established in Boeing Specification D239-10000-1. Qualification would be accomplished primarily by subassembly and system laboratory tests and in some cases by analysis and/or similarity to equipment presently used in transit car environments. The ASDP propulsion system qualification matrix is shown in Table 7.4-I.

The general approach would be to qualify the majority of the components and subassemblies at the system level using dynamometer simulation. This approach eliminates complex simulated interfaces with other subassemblies, reduces test duplication, and more comprehensively verifies subsystem integration.

The gear drive and axle coupling assembly has been fully qualified by the vendor and requires no further effort. The acoustic noise and vibration/shock testing would also be accomplished at the subassembly level. The ground brush assembly is a commercially procured component with a long history of use in transit car environment and is therefore, qualified by similarity for ASDP application. EMI/RFI testing is deferred until vehicle system tests due to the difficulty of simulating the effect of the vehicle structure and configuration.

Test Hardware Requirements	Performance Characteristics	Thermal	Vibration and Shock	Acoustic Noise	Transients	EMI-RFI
Electronic Control Unit	SL	S	S	NA	SL	VS
Power Control Switchgear	SL	SL	A	NA	SL	VS
Resonating Inductor	SL	SL	A	Sa	SL	VS
Power Converter Assembly	SL	SL	Sa/A	NA	SL	VS
Traction Motor	Sa/SL	Sa/SL	Sa*/A	Sa	SL	VS
Line Filter Inductor	SL	SL	A	NA	SL	VS
Brake Resistor	SL	SL	S	NA	NA	NA
Cooling Assembly	SL	SL	A	Sa	NA	NA
Speed Sensors	SL	SL	S	NA	NA	NA
Truck Connector Box	S	SL	S	NA	SL	NA
Motor-Gearbox Coupling	SL	SL	S	NA	NA	NA

VS - Vehicle Systems Tests
SL - Propulsion System Laboratory Tests
Sa - Subassembly Test

S - Similarity
A - Analysis
NA - Not Applicable

* Generated Vibration only.

Table 7.4-I. Propulsion System Qualification Matrix

Analysis would be used for qualification of several subassemblies for the vibration and shock environments. The load and stress analysis conducted for these subassemblies gives adequate assurance that these units would survive the relatively mild specified vibration/shock environments. In addition, one of the most critical solid state equipment modules (inverter module) would be subjected to vibration and shock testing.

Testing to verify performance characteristics would be accomplished in system laboratory tests using dynamometer equipment as described in paragraph 6.3.2, to simulate transit car operation. The test articles used in these system qualifi cation tests would be as shown in the hardware family tree of Figure 7.4-1. It should be noted that with the exception of the gear drive assembly, ground brush, and diagnostics unit, all elements of the propulsion system would be included in these tests.

The testing would cover the following:

- Acceleration and Braking Performance
- Continuous Speed and Coast Performance
- Regenerative Braking Capability
- Operation at 400, 450 and 750 Vdc Line Voltage
- Operation Over Rail Gaps
- System Thermal Capability (see duty cycles described in 5.4.2)
- System Control, Functional.

7.4.3 PUEBLO TEST UPDATE

Completion of the modifications and tests discussed in paragraphs 7.3 through 7.4.2 will provide a system ready for simulated transit service testing at the Pueblo HSGTC Test Track. This will also represent a system that is close to a production configuration. Remaining effort will involve the incorporation of modifications required to solve problems uncovered in the field testing and the incorporation of changes and refinements to improve producibility, maintainability, reliability, etc.

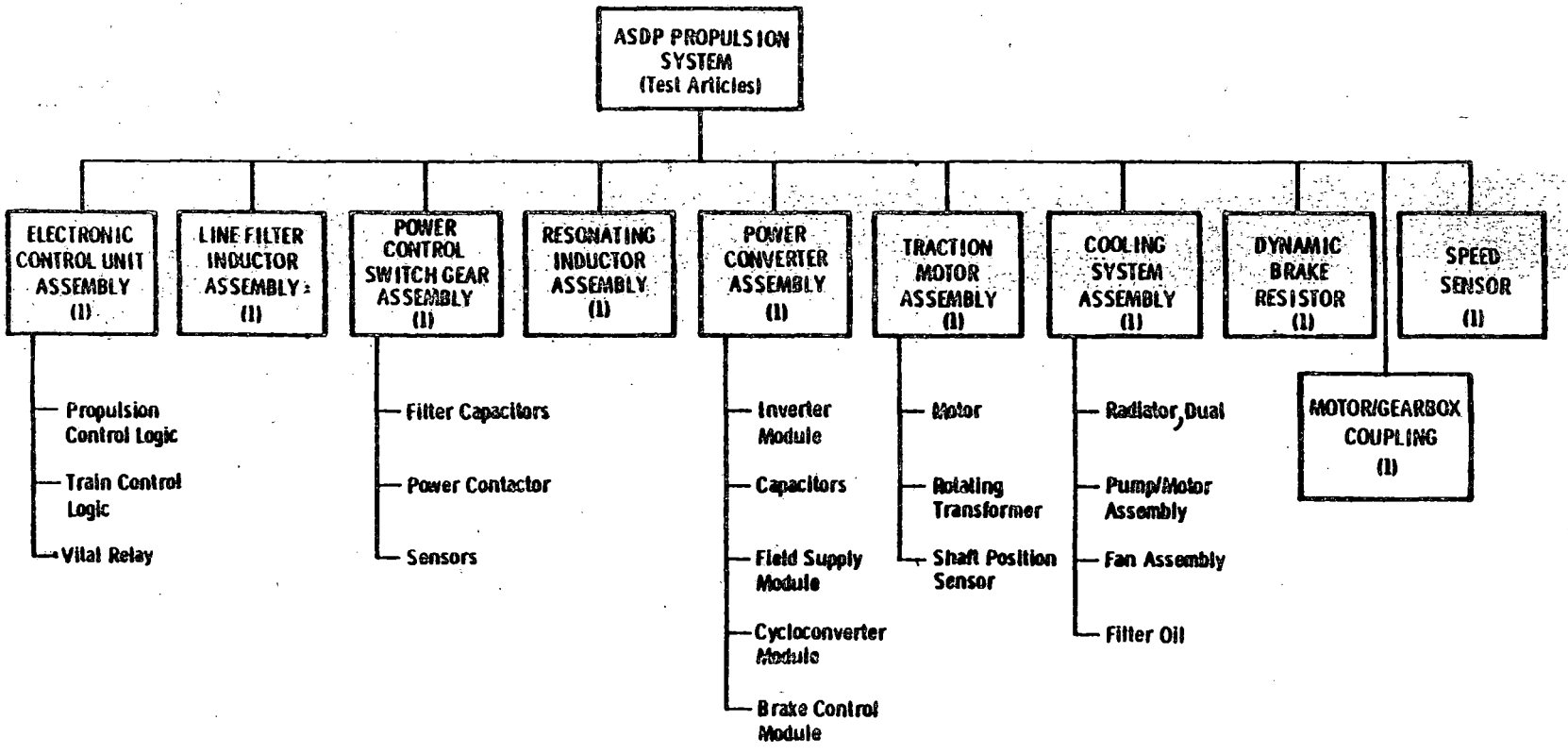

Figure 7.4-1. Test Articles – System Laboratory Tests

LIST OF REFERENCES

1. "Synchronous Motor Power Factor Control", invention disclosure, File D-891
2. "Rotor Position Sensor for a Self-Synchronous Motor", invention disclosure, File 71-390
3. "Improved Commutation Angle Advance Method", invention disclosure, File A 18250
4. "AC Motor Drive Fault Inhibit", invention disclosure, File A 18107
5. "Motor Power Supply System", U. S. Patent No. 3,866,099
6. "Cycloconverter Controlled Rectifier Protection Circuit", U. S. Patent No. 3,942,092
7. "Heat Sink Development" Memo, Bourbeau to Pavlics dated October 4, 1972
8. "Thyristor/Diode Cooling Method", U. S. Patent No. 4,010,489
9. "ASDP Heat Sink Performance Tests" Memo CEM 76-161, P. Ebert to R. Heltmach dated July 13, 1976
10. "Wide Speed Range Cycloconverter — AC Motor Drives Operating from Utility Frequency Power", IEEE paper by F. Bourbeau, presented in Orlando, Fla., March 1977.